2020

Mathematical models for hepatocytic-erythrocytic dynamics and therapeutic control of malaria

Titus Okello Orwa
Strathmore Institute of Mathematical Sciences
Strathmore University

Mathematical Models for Hepatocytic-Erythrocytic Dynamics and Therapeutic Control of Malaria

Titus Okello Orwa

Submitted in total fulfillment of the requirements for the Degree of Doctor of Philosophy in Biomathematics at Strathmore University

Strathmore Institute of Mathematical Sciences
Strathmore University
Nairobi, Kenya

June, 2020

Declaration and Approval

Declaration

I declare that this work has not been previously submitted and approved for the award of a degree by this or any other University. To the best of my knowledge and belief, the thesis contains no material previously published or written by another person except where due reference is made in the thesis itself.

Titus Okello Orwa
Signature .....
Date: 25/10/2019

Approval

The thesis of Titus Okello Orwa was reviewed and approved by the following:

Professor Livingstone Serwadda Luboobi
Strathmore Institute of Mathematical Sciences

Professor Rachel Waema Mbogo
Strathmore Institute of Mathematical Sciences

Mr. Ferdinand Othieno
Dean, Strathmore Institute of Mathematical Sciences

Dr. Bernard Shibwabo
Director, Office of Graduate Studies

Abstract

Malaria is a mosquito-borne infectious disease caused by parasites of the genus *Plasmodium*. Mortality and morbidity due to malaria infection is a serious burden to malaria endemic countries. Despite the many years of prevention and control, malaria cases and mortality are still quite high. In 2018, the World Health Organization (WHO) reported about 219 million cases and 435000 deaths due to malaria globally. The threat of parasite resistance, minimal efficacy of malaria vaccines and the high burden of malaria prevention and control measures offer serious challenge to malaria elimination efforts. Improved therapeutic measures is hence necessary for malaria control and possible eradication.

In this study, deterministic in-host malaria models with therapeutic control measures are extended and mathematically analysed. Effects of antimalarial drugs and malaria vaccines on disease severity are established analytically and numerically. Parasite resistance and the effects of competition between different parasite strains are also investigated numerically. Each model is analysed and vital properties such as positivity, existence of steady states and their stability conditions are precisely determined. By Pontryagin's Maximum Principle, the optimal control therapy measure against *P. falciparum* malaria is determined.

Results indicate that a combination of different malaria vaccine antigens yield better therapeutic outcome compared to individual vaccine antigens. A highly efficacious malaria vaccine (efficacy $> 90\%$) is likely to offer the much needed protection against *P. falciparum* malaria. Multiple-strain infection is likely to increase parasitaemia and hence the severity and cost of malaria control. Malaria therapeutic control efforts should focus on reducing: the parasite invasion rate, the proportions of merozoites that become gametocytes per dying blood schizont, the average number of merozoites released per bursting blood schizonts and the rate of development of resistance during multiple-strain infections. Moreover, a combination of pre-erythrocytic vaccine antigen, blood schizontocide and gametocytocide drugs is likely to offer the best therapeutic control strategy against *P. falciparum* malaria.

In conclusion, future malaria control efforts should consider efficacious malaria vaccines and vaccine combinations. To reduce development of resistance and morbidity, only efficacious antimalarials such as ACT should be used against *P. falciparum* malaria. The administration and use of current antimalarial drugs alongside efficacious malaria vaccines is likely to offer the much needed therapeutic combination against *P. falciparum*. Regular and strict surveillance on quality and standards of antimalarial drugs in medical facilities in malaria endemic countries is therefore very critical. Collectively, results from this study highlights the need for continued investment in malaria drug development and urgent drive to improve the efficacy of malaria vaccine candidates such as RTS,S/AS01.

Table of contents

List of figures

List of tables

List of Abbreviations

ACT	Artemisinin-based Combination Therapy	AL	Artemether-Lumefanthrine
RBC	Red Blood Cells	IRBC	Infected Red Blood Cells
ISM	Inhibit Sporozoite Motility	PEV	Pre-erythrocytic vaccine
BSV	Blood Stage Vaccine	TBV	Transmission Blocking Vaccine
P	Plasmodium	PQ	Primaquine
IPTi	Intermittent Preventive Treatment in infants	IPTp	Intermittent Presumptive Treatment in pregnancy
IRS	Indoor Residual Spraying	ITNs	Insecticide-Treated mosquito Nets
LLIN	Long-Lasting Insecticidal Net	MDG	Millennium Development Goal
MVI	Malaria Vaccine Initiative	CSP	Circumsporozoite Protein
MSP1	Merozoite Surface Protein 1	AMA	Apical Membrane Antigen 1
NGO	Non-Governmental Organization	RBM	Roll Back Malaria
UN	United Nations	Pfs25	Plasmodium falciparum ookinete surface antigen
USAID	United States Agency for International Development	WHO	World Health Organization
LHS	Latin Hypercube Sampling	PRCC	Partial Rank Correlation Coefficient
GTS	Global Technical Strategy for malaria 2016–2030	HIV	Human Immunodeficiency Virus
AIDS	Acquired Immune Deficiency Syndrome	RDT	Rapid Diagnostic Test
G6PD	Glucose-6-Phosphate Dehydrogenase	UHC	Universal Health Coverage

Acknowledgements

My sincere gratitute goes to my supervisors, Prof. Livingstone Serwadda Luboobi and Prof. Rachel Waema Mbogo for their academic guidance, fruitful discussions, careful reading and editing of this thesis. I am thankful to Prof. Luboobi for his patience, humility and timely feedback. These are academic virtues that I hope to embed in my future research activities. I am also inspired by Prof. Vitalis Onyango-Otieno, who offered prayers and couselling during this study period. I am very thankful to you all for your support and priceless wisdom.

This work was supported by funding from the German Academic Exchange Service (DAAD), the National Research Fund (NRF-Kenya) and the Strathmore Institute of Mathematical Sciences (SIMS). I am very grateful to all the funders. Special thanks to DAAD for awarding me the short term research visit scholarship at Tubingen University in Germany. Most importantly, I am thankful to Prof. Dr. Steffen Borrmann for his academic support and for hosting me in his lab at the Institute for Tropical Medicine during my short stay in Tubingen University. This was a very fruitful visit that enabled me to fast track my PhD thesis and publications.

Family support is very important in any academic undertaking. I therefore express my deep and sincere gratitute to my immediate family (Alice[wife], Lezanie and Talia [daughters]) for their love, support and patience. I am also thankful to my parents (Leah and Joshua) and siblings (Jael, Mark, Maurice, Samson and Zack) who have supported me for the many years of my schooling.

Finally, I would like to thank the Strathmore Institute of Mathematical Sciences and Strathmore University for creating an enabling environment characterised by support facilities for the successful completion of this study. Special thanks to Emily Sawe and Fredrick Adika (both of SU Library Services) for their timely response and support during the study period.

Dedication

I dedicate this thesis to the memory of my brother and friend Mark Odhiambo Orwa, who always believed in my ability to be successful in the academic arena. You are gone but your belief in me has made this journey possible.

Publications arising from this study

1. **Orwa, T. O.**, Mbogo, R. W., and Luboobi, L. S. (2018a). Mathematical model for hepatocytic-erythrocytic dynamics of malaria. *International Journal of Mathematics and Mathematical Sciences*, vol. 2018, Article ID 7019868, 18 pages, 2018. https://doi.org/10.1155/2018/7019868.

2. **Orwa, T. O.**, Mbogo, R. W., and Luboobi, L. S. (2018b). Mathematical model for in-host malaria dynamics subject to malaria vaccines. *Letters in Biomathematics*, 5(1), 222-251.

3. **Orwa, T. O.**, Mbogo, R. W., and Luboobi, L. S. (2019a). Uncertainty and sensitivity analysis applied to an in-host malaria model with multiple vaccine antigens. *International Journal of Applied and Computational Mathematics*, 5(73). https://doi.org/10.1007/s40819-019-0658-3.

4. **Orwa, T. O.**, Mbogo, R. W., and Luboobi, L. S. (2019b). Multiple-strain malaria infection and its impacts on Plasmodium falciparum resistance to antimalarial therapy - a mathematical modelling perspective. *Computational and Mathematical Methods in Medicine*, vol. 2019, Article ID 9783986, 26 pages, 2019. https://doi.org/10.1155/2019/9783986.

Conference presentations

1. "*Mathematical model for hepatocytic-erythrocytic dynamics of malaria*", at the Southern Africa Mathematical Sciences Association (SAMSA) conference, Arusha, Tanzania, 20th-23rd November 2017.
2. "*Uncertainty and sensitivity analysis applied to an in-host malaria model with multiple vaccine antigens*", at Seams School 2018 on Dynamical systems and Bifurcation Analysis (DysBa), School of Mathematical Sciences, Universiti Sains Malaysia, Malaysia. 6th-13th August 2018.
3. "*Application of optimal control theory to hepatocytic-erythrocytic dynamics of P. falciparum malaria*.", at Future of Science Conference, AIMS-Rwanda, Kigali, Rwanda, 7th-9th July 2019.
4. "*Mathematical model for in-host malaria dynamics subject to malaria vaccines*", at Strathmore International Mathematics Conference (SIMC), Strathmore University, Kenya, 12th-16th August 2019. .

Glossary

Artemisinin-based combination therapy	A combination of artemisinin derivative and a partner monotherapy drug with a different mode of action
Basic reproduction number	A threshold quantity that represent the average number of secondary cases per infected red blood cells in a completely susceptible human host
Case	A particular instance/occurrence of malaria disease
Chemoprophylaxis	Administration of antimalarials to prevent the development of malaria infection or progression to disease level
Combination therapy	A combination of two or more antimalarial drugs with different modes of action
Diagnosis	The process of establishing the cause of an infection/illness
Drug efficacy	Capacity of an antimalarial drug to achieve the therapeutic objective when administered at a recommended dose
Drug resistance	Ability of a parasite strain to survive despite the administration of antimalarial drugs in recommended or even higher doses
Gametocidal	Antimalarial drug that kills gametocytes, preventing them from infecting a mosquito vector
Monotherapy	Malaria drug with a single active compound or a synergistic combination of two compounds with similar modes of action
Parasitaemia	The presence of malaria parasite in the blood
Recrudescent	Recurrence of asexual parasitemia following antimalarial treatment, owing to incomplete clearance of asexual parasites
Schizontocidal	Antimalarial drug that kills liver and blood stage schizonts
Treatment failure	Inability of antimalarial drug to clear malarial parasitaemia or prevent recrudescence

Chapter 1

Introduction

1.1 Background to the study

Malaria is a mosquito-borne infectious disease caused by protozoa of the genus *Plasmodium (P)*. Since its discovery in 1880, malaria infection has greatly influenced human evolution and history (Carter and Mendis, 2002; Sachs and Malaney, 2002; Snow et al., 2005). Today, nearly half of the world's population is at risk of malaria infection (Whegang et al., 2019). In 2018, the World Health Organization (WHO) reported about 219 million cases and 435000 deaths due to malaria globally. The WHO African region was the most affected. This region accounted for 92% and 93% of reported global malaria cases and deaths, respectively (WHO, 2018f). Majority of the reported global deaths (61%) were from children aged under 5 years. The WHO South-East Asia Region continued to see its incidence rate fall (from 17 (in 2007) to 7 (in 2017)) cases per 1000 population at risk, representing a 59% decline in reported malaria cases (WHO, 2018f). Although it is estimated that malaria cases declined by about 20 million in 2010-2017 period, data for the period 2015-2017 indicates that no significant progress in reducing global malaria cases was made during this period (WHO, 2018f).

The socio-economic burden of malaria has significant negative impacts on individuals, families and governments, especially in the WHO African region (Gallup and Sachs, 2001; Rowe et al., 2006; Sachs and Malaney, 2002), where the disease is most prevalent. In 2017, an estimated US$ 3.1 billion and US$ 2.2 billion was invested in malaria control and elimination efforts globally and in the WHO African region, respectively. Despite stable funding since the year 2010, a lot more funding will be necessary if the Global Technical Strategy for Malaria (GTS) are to be achieved (WHO, 2015a).

Research in malaria control constitutes a significant component of these efforts and budgets. Although funding for malaria vaccine research and development declined in the period 2015-2016, investment in vector control doubled in the same period (US$ 33 million to US$ 61 million) (Zelman et al., 2016). While targeting the highly (malaria) burdened African countries, the WHO has rolled out a new drive called "high burden to high impact" to achieve the much needed global malaria response back (WHO, 2018b). This drive is a partnership of the WHO and the Roll Back Malaria (RBM) initiative. It aims to galvanize national and global political attention to reduce morbidity and mortality due to malaria infections.

Human malaria is caused by five species of *Plasmodium* parasites. They include: *P. falciparum*, *P. vivax*, *P. ovale* and *P. malariae* and *P. knowlesi* (Abdulla et al., 2011). Most malaria infections are caused by the deadly *P. falciparum*, which is predominant in sub-Saharan Africa (see Figure 1.1) (Brazier et al., 2017). The parasite is responsible for the most severe malaria globally. *P. vivax* mainly contributes to malaria's morbidity (Wickramasinghe and Abdalla, 2000). *P. vivax* and *P. ovale* can hide in the liver for prolonged periods as hypnozoites. This can cause relapsing malaria months or even years after the initial infection (Derbyshire et al., 2011). Although human infections are rare, *P. knowlesi* is mainly found in long-tailed and pig-tailed macaques (Cox-Singh et al., 2008). It is primarily zoonotic (Singh and Daneshvar, 2013).

Victims of malaria infection often experience a wide variety of symptoms. Uncomplicated *P. falciparum* malaria is characterised by such symptoms as fever, chills, sweats, headaches, nausea and vomiting, body aches and general malaise (CDC, 2019a). Physical symptoms may include elevated temperatures ($> 38^oC$), perspirations, body weakness, enlarged spleen, mild jaundice, enlarged liver and increased respiratory rate (Bartoloni and Zammarchi, 2012). Severe malaria occur when the infection is complicated and is often characterised by major organ failures or abnormalities in the patients's blood or metabolism. Symptoms of severe malaria include: severe anaemia due to haemolysis, haemoglobuniria, acute respiratory distress syndrome, abnormalities in blood coagulation, low blood pressure due to cardiovascular collapse, hyperparasitaemia ($>$ 100000 per mm^3), metabolic acidosis and hypoglycemia (Weatherall et al., 2002). Severe malaria is a clinico-pathological medical emergency that should be treated immediately and aggressively (CDC, 2019a).

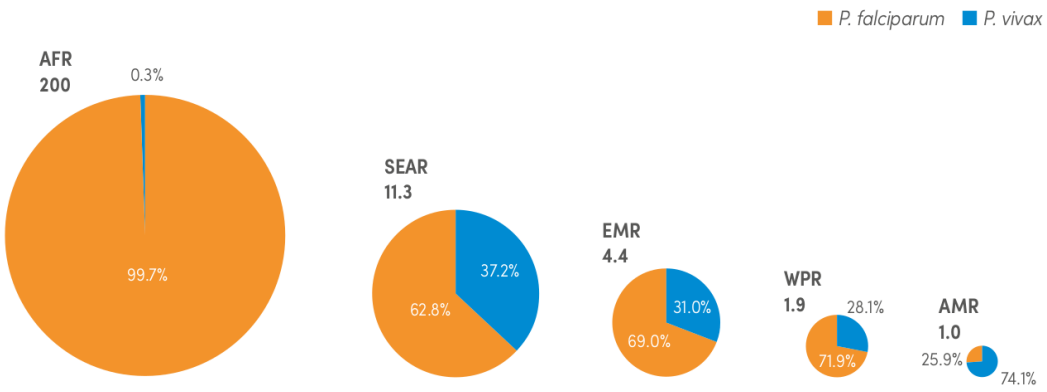

Figure 1.1: Estimated malaria cases (in millions) based on WHO regions for the year 2017. The area of the circle is shown as a percentage of the estimated number of cases in each region. AFR (WHO African region), AMR (WHO region of the Americas), EMR (WHO Eastern Mediterranean region), SEAR (WHO South-East Asia region), WPR (WHO Western Pacific region). Source: WHO (2018f).

1.2 The life cycle of malaria parasite

Plasmodium parasite has a complex life cycle characterised by cyclical sexual and asexual stages between vertebrates and female *Anopheles* mosquitoes. Both sexual and asexual stages occurs within the human host. This is preceded by another sexual phase within the mosquito vectors. These three phases translate into (1) pre-erythrocytic stage (which begins when sporozoites enter the human host, its movement towards and development within the liver hepatocytes), (2) erythrocytic stage (which begins when merozoites are released into blood stream, their invasion of and development within the red blood cells. The third and final phase is the (3) sporogonic cycle (which begins when mosquitos ingest gametocytes (male and female), preceded by fertilization, leading to formation of oocysts that rupture into sporozoites) (Chiyaka, 2010; Li et al., 2011). The life cycle of *P. falciparum* is summarised as shown in Figure 1.2.

Pre-erythrocytic phase kicks off when an infected mosquito transmits haploid sporozoites into the human dermis during its blood meal. The injected sporozoites travel randomly from the skin, through the blood stream, and within 2 hours to the liver. Once in the liver, a sporozoite migrates through several hepatocytes before it settles on a final one (Frevert et al., 2005). Within the hepatocyte, the sporozoites develop, divide and propagate to produce 1500-8000 merozoites that are released into the blood stream from mature schizonts (Sturm et al., 2006). This pre-erythrocytic phase (also called the liver stage) is asymptomatic. The release of

infective merozoites into the host's blood stream marks the beginning of the erythrocytic phase (blood stage) of the parasite life cycle.

The free floating merozoites then begin to invade the host's erythrocytes through a complex multi-stage process that results in the formation of protective parasitophorous vacuole (Koch and Baum, 2016; Paul et al., 2015). A mature blood schizont releases 8-24 daughter merozoites (Lee and Fidock, 2008). The waves of bursting red blood cells and the invasion of fresh red blood cells by the newly released merozoites produce malaria's characteristic symptoms (Miller et al., 2013). The infected erythrocytes develop into trophozoites which mature into schizonts full of merozoites. A single erythrocytic cycle due to *P. falciparum* takes about 48 hours (Reilly et al., 2007). Some of infected erythrocytes develop into sexual forms called gametocytes, which are later taken up by other mosquitoes when they feed on infected blood from infected individuals (Miller et al., 2002). Successive erythrocytic cycles result in an increase in parasitaemia and disease severity. Unless they are brought under control by the host's protective immune responses or antimalarial drug therapy, the human host is likely to undergo severe infection leading to anemia and even death.

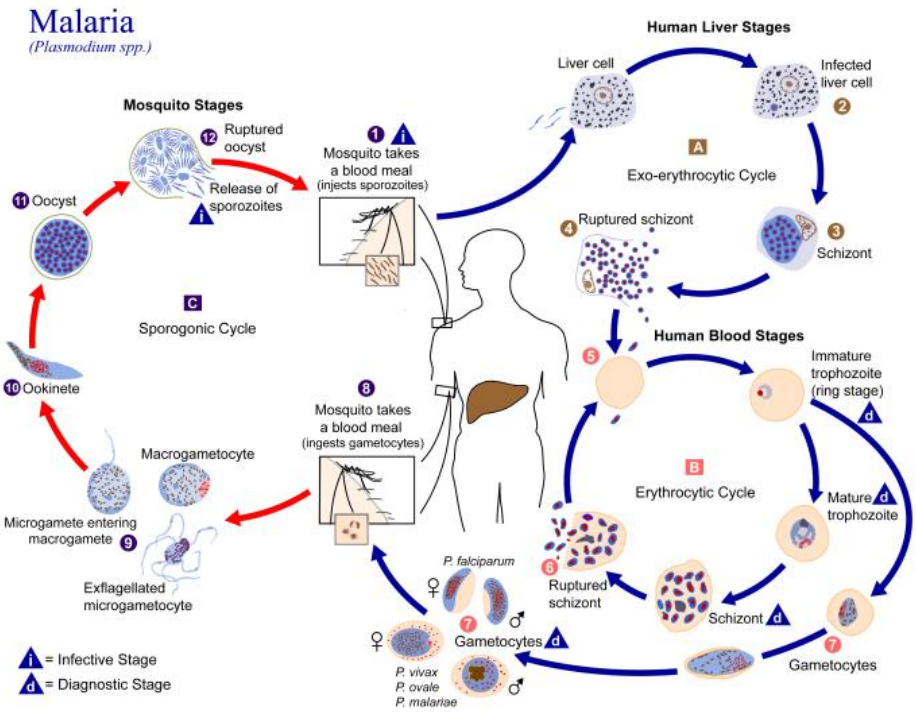

Figure 1.2: Illustration of the life cycles of malaria parasites, *Plasmodium (P)* species. Source: CDC (2017).

In the mosquito midgut, the gametocytes taken up from the human host differentiate into macrogametes and microgametes in response to environment cues (Kengne-Ouafo et al., 2019). Sexual reproduction results in the formation of a motile form called ookinete that migrates through the mosquito gut wall and transforms into an oocyst. In approximately 2 weeks, the oocyst produces and releases thousands of sporozoites that invade the mosquito's salivary glands (Chiyaka et al., 2008; Sidjanski and Vanderberg, 1997). These parasites are then transmitted to human hosts in subsequent blood meals for new infections.

Parasite invasion of susceptible hepatocytes and erythrocytes is described by Cowman et al. (2012) as an ordered three stage process involving initial attachment, reorientation and invasion. The asymptomatic liver stage which the parasite goes through only once in its life time offer a special target for future malaria control (March et al., 2013). The use of highly effective malaria vaccines could interrupt the parasite's life cycle at this stage, eliminating the establishment of clinical infections. In this study, we shall limit our analysis to the dynamics within the human host.

1.3 Malaria diagnosis and treatment

Malaria is both a preventable and treatable disease. Microscopic examination based on Romanovsky stain is the gold standard laboratory confirmation of malaria in sick individuals (CDC, 2019a). Prompt malaria diagnosis and treatment is the best strategy to prevent progression from mild to severe disease and death (Talisuna et al., 2007). The goal of malaria treatment is to ensure total eradication of all infecting parasites from the human host (Lin Ouédraogo et al., 2015). Epidemiologically, treatment is offered to reduce infectious reservoirs (Gerardin et al., 2015; Goncalves, 2017). Additionally, effective malaria treatment therapy limits development of resistance and reduces spread of infection to other susceptible humans and mosquito vector (Talisuna et al., 2007).

Malaria therapeutic interventions are patient-dependent and may vary based on: the species of infecting parasite, the clinical status of the patient, pregnancy status (females), drug allergies or other medications taken by the patient (CDC, 2019b). Most antimalarial drugs are active against blood stage parasites. Some blood schizontocides include: chloroquine, atovaquone-proguanil, artemether-lumefantrine, mefloquine, quinine, quinidine, doxycycline, clindamycin and artesunate. Primaquine is active against the hypnozoites at the liver stage, preventing infection relapses. However, this drug should not be administered to malaria

patients with glucose-6-phosphate dehydrogenase deficiency (G6PD), as they may develop anaemia (Peters and Noorden, 2009).

Currently, artemisin-based combination therapies (ACTs) is the recommended first-line antimalaria drug against uncomplicated *P. falciparum* malaria infections (Heller and Roepe, 2019). ACT is a combination of artemisinin derivative (artemether, artesunate and dehydroartemisinin) and a partner monotherapy drug. Artemisinin derivative reduces the parasite biomass within the first three days of therapy while the partner drug, with longer half-life, eliminates the remaining parasites (Bhatt et al., 2015). The five recommended ACTs by the WHO include: artesunate-amodiaquine (AS+AQ), artesunate-mefloquine (AS+MQ), artemether-lumefantrine (AL), artesunate+sulfadoxine-pyrimethamine (AS+SP) and dihydroartemisinin-piperaquine (DHA+PPQ). Additionally, artesunate-pyronaridine (AS+PY) may be used in regions where ACT treatment response is low (WHO, 2018e).

Access to ACT has been tremendous in the last 8 years; with recorded increases of 122 million procured treatment courses for the period 2010-2016. However, resistance to currently used ACTs have important public health consequences, especially in the WHO African region, where the disease is endemic (White and Pongtavornpinyo, 2003). Effective vector control strategies such as insecticide-treated mosquito nets (ITNs) and indoor residual spraying (IRS) are considered by the WHO as the main ways to prevent and reduce malaria transmission in communities with high malaria prevalence (Homan, 2016). In 2017, half of the population at risk of malaria infection were protected by ITNs (WHO, 2018f). Other vector control measures are presented in Table 1.1.

Women and children are considered the most vulnerable groups in malaria epidemiology. To reduce maternal anaemia, low birth weight and perinatal mortality in sub-Saharan Africa, the WHO recommends the use of intermittent preventive treatment in pregnancy (IPTp) using sulfadoxine-pyrimethamine (SP) (Yaya et al., 2018). For travellers and tourists from malaria-free regions, chemoprophylaxis such as Atovaquone/Proguanil (Malarone) may be taken to prevent possible malaria infection in malaria endemic countries (Dorsey et al., 2000). The combination of vector control, personal protective measures and the use of antimalarial drugs have contributed immensely to the substantial global decline in malaria mortality and morbidity (Nega1 et al., 2016). However, despite the success of the existing malaria prevention and control strategies, reported malaria cases are still quite high (Talapko et al., 2019).

Table 1.1: Malaria vector control strategies. Source: Killeen et al. (2017).

Action	**For individual and family protection**	**For community protection**
Reduction of human-mosquito-contact	Insecticide-treated nets, repellents, protective clothing, screening of houses	Insecticide-treated nets zooprophylaxis
Destruction of adult mosquitoes		Insecticide-treated nets, indoor residual spraying, space spraying, ultra low-volume sprays
Destruction of mosquito larvae	Peri-domestic sanitation	Larviciding of water surfaces, intermittent irrigation, slucing, biological control
Source reduction	Small-scale drainage	Environmental sanitation, water management, drainage
Social protection	Motivation for personal and family protection	Health education, community participation

1.4 Parasite resistance to antimalarial drugs

Artemisinin (partial) resistance is defined as delayed parasite clearance following treatment with an artesunate monotherapy or with an ACT drug (WHO, 2018a). Resistance to antimalaria drugs is associated with the following factors: (i) poor patient treatment services, (ii) inadequate treatment adherence to prescribed malaria drugs, (iii) widespread availability of oral artemisinin-based monotherapies and (iv) substandard antimalarial drugs (Mackinnon, 2005; WHO, 2018a). In the past decade, *P. falciparum* has developed resistance to several antimalarial drugs (Xu et al., 2018). Resistance to chloroquine and sulfadoxine–pyrimethamine led malaria endemic countries to adopt WHO recommended ACTs as a first-and second-line treatment for uncomplicated *P. falciparum* malaria as well as for chloroquine-resistant *P. vivax* malaria (Dondorp et al., 2009).

Several studies conducted in the period 2010-2017 showed that ACT drugs are very effective with a success rates of at least 95% (Whegang et al., 2019). However, as of July 2016,

artemisinin resistance was confirmed in 5 countries of the Greater Mekong subregion (GMS): Cambodia, the Lao People's Democratic Republic, Myanmar, Thailand and Viet Nam (WHO, 2017b). Despite the above reported cases, there has been a massive reduction in malaria cases and deaths in the GMS (WHO, 2018f). Most patients treated with an ACT containing an effective partner drug have however been able to recover.

To prevent global spread of the resistant strain, it is important to identify molecular markers associated with ACT resistance. Results from genome wide association studies (GWAS) have revealed mutations in the $PF3D7\_1343700$ kelch propeller domain ('$K13$-propeller') in artemisinin-resistant parasite from Cambodia (Das et al., 2017). Outside the GMS, treatment failure with ACTs have mainly occurred due to resistance of the parasite to the partner drug (Dondorp et al., 2010; WHO, 2012a). In sub-Saharan Africa, artemisin resistance is yet to be reported. It is important to note that ACTs have been very integral in the recent success of global malaria control. Monitoring their efficacy has resulting in prompt updating of malaria treatment policies in the GMS and globally. It is therefore prudent that multidrug resistance is stopped before it emerges in other parts of the world, especially in sub-Saharan Africa.

1.5 The role of immunity in controlling malaria infection

The presence of malaria parasites in the human body elicits response from numerous immune cells. The innate and the adaptive immune systems form the first and the second lines of defenses, respectively (Augustine et al., 2009). Adaptive immunity, which is acquired naturally in individuals living in malaria-endemic areas following continuous exposure to the parasite, provides protection against future exposures to malaria pathogens. However, this immunity wanes in the absence of ongoing *P. falciparum* exposures (Doolan and Martinez-Alier, 2006). Historic passive transfer studies have demonstrated a key role of the antibodies in controlling blood-stage parasites during natural *P. falciparum* infection and reducing clinical symptoms of malaria (Cohen et al., 1961). Although antibodies are crucial in controlling blood-stages, naturally acquired immunity never results in complete parasite elimination.

Malaria-specific antibodies perform such functions as (i) inhibition of cytoadherence (Newbold et al., 1992) (ii) inhibition of red blood cell invasion (Patiño et al., 1997), and (iii) antibody dependent cytotoxicity and cellular inhibition (Oeuvray et al., 1994). Innate immune cells such as the *P. falciparum* DNA, natural killer cells (NK cells), dendritic cells (DCs), macrophages, natural killer T (NKT) cells and T cells are involved in the clearance

of circulating parasites, infected erythrocytes and infected hepatocytes (Augustine et al., 2009). Subject to parasite strain, the DCs and NK cells may prompt or restrain inflammatory responses (Chen et al., 2014). The NKT cells also help regulate DCs and T cell responses to plasmodium (Augustine et al., 2009).

Additionally, studies by Franklin et al. (2009) have demonstrated that malaria infection induces activation of Toll-like receptors (TLRs): TLR1, TLR2, TLR4 (which are located on the cell surface) and TLR9 which is not expressed on the cell surface. TLR2 and TLR9 are also activated by malarial glycosylphosphatidylinositol (GPI) anchors and parasite-derived DNA bound to hemozoin (Franklin et al., 2009). Cell-mediated immune responses include macrophage activation by NK cell-,$\gamma\delta$T cell- or Th1-derived interferon γ (IFN-γ) for enhanced phagocytosis and killing of infected/parasitised red blood cells (Fritsche et al., 2001), inhibition of sporozoite growth and development within the liver hepatocytes by $CD8^{+}$ cytotoxic and IFN-γ-producing T cells (Tsuji and Zavala, 2003). Unlike the NK cells, the macrophages have been shown to effectively phagocytose malaria-infected red blood cells during the erythrocytic phase (De Back et al., 2014). A part from its ability to wholly ingest infected red blood cells, the macrophages can also selectively extract malaria parasites from recently infected erythrocytes (Chotivanich et al., 2002). The parasite-extraction capability of macrophage therefore leaves the surving erythrocytes to continue to circulate like the other healthy red blood cells.

1.6 Malaria vaccine development

A malaria vaccination strategy is performed to either induce protective immune responses prior to malaria infection or to provide protection in case of malaria attack (Arama and Troye-Blomberg, 2014). There are more than 30 malaria vaccine candidates under development. These vaccines are generally categorised into: (1) pre-erythrocytic vaccines (PEV), (2) blood stage vaccines (BSV) and (3) transmission blocking vaccines (TBV) (Birkett, 2016). The vaccines target the parasite at specific life stages as shown in Figure 1.3.

The PEV induces antibodies that block invasion of hepatocytes by sporozoites and or cell-mediated immune responses that target infected hepatocytes (Duffy et al., 2012). On the other hand, BSV target blood merozoites or infected red blood cells. They elicit anti-invasion and anti-disease responses at the blood stage (Moorthy et al., 2004). They, therefore, lower merozoites density and prevent clinical manifestations and hence severity of malaria infection in humans. Unlike PEV and BSV, TBV are mainly intended to reduce parasite transmission to

secondary hosts. TBV induce antibodies against antigens on gametes, zygotes and ookinetes, blocking ookinete to oocyst transition and hence stopping parasite development within the mosquito mid-gut (Carter et al., 2000). While TBV does not directly protect the person who is vaccinated, it has the potential to stop continued spread of malaria infection within a population.

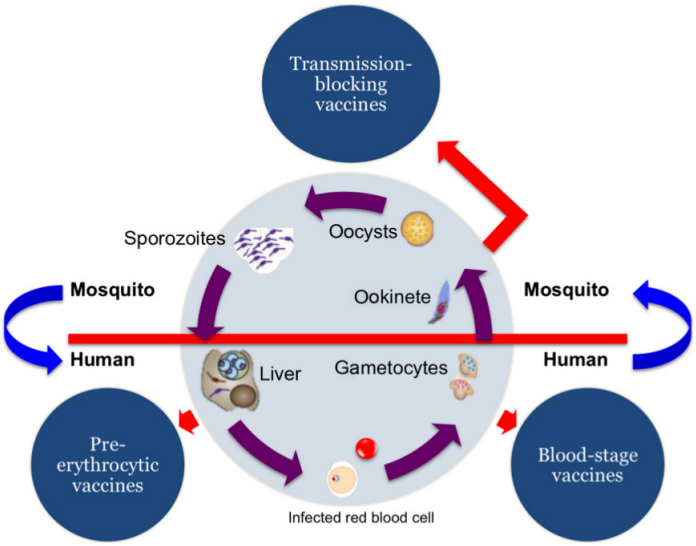

Figure 1.3: Target sites in the malaria life cycle that could be interrupted by: pre-erythrocytic, blood-stage and transmission-blocking vaccines. Source: Arama and Troye-Blomberg (2014).

Currently available malaria vaccines have shown minimal efficacy (Birkett, 2016; Birkett et al., 2013; Miura, 2016). RTS,S/AS01 (also known as Mosquirix) is the only malaria vaccine that has received a positive scientific opinion from the European Medicines Agency (EMA) (EMA, 2015). This pre-erythrocytic vaccine has been evaluated in large phase 3 trial in sub-Saharan Africa. The vaccine showed a 45.7% (95% CI, 41.7 - 49.5) efficacy against all episodes of clinical *P. falciparum* malaria across all sites in the 5-17 month age category (RCTP, 2014). Despite positive assessment from EMA, the World Health Organization (WHO) recommends further evaluation of RTS,S/AS01 in a series of pilot implementations before it can be introduced on a wide scale (WHO, 2018d).

Despite minimal progress, many experts believe that a malaria vaccine is a necessary tool for successful malaria elimination (MVFG, 2018; Ouattara and Laurens, 2014). In this study, we have provided important insights on the impacts of improved vaccine efficacy on the dynamics of clinical malaria infection. We have also analysed a combination of different vaccine antigens in improving their overall efficacies.

1.7 Problem statement

Malaria is one of the most frequently occurring infectious disease worldwide, with almost 0.6 million deaths and an estimated 240 million clinical cases annually. The infectious disease remains a global health priority with over 3 billion people in 97 countries at risk of periodic infections and death (WHO, 2018f). To date, the WHO consider effective vector control strategies such as long-lasting insecticidal nets (ITNs) and indoor residual spraying (IRS) as the main ways to prevent and reduce malaria transmission in communities with high malaria prevalence. Chemoprophylaxis and antimalarial drugs such as chloroquine and artemisinin-based combination therapy (ACT) are currently used to prevent and treat clinical malaria, respectively, in different parts of the world. These strategies have contributed to the substantial global decline in malaria mortality and morbidity.

Despite the global success in malaria control, global malaria cases and mortality are still quite high and malaria remains a global health challenge. The WHO-African region still bears the highest burden of malaria infection. In 2017, the region was home to 92% of global malaria cases and 93% of global deaths caused by malaria infections (WHO, 2018f). Neither artemisinin nor chloroquine is effective against the liver stage infections. The emergence of *P. falciparum* resistance to both artemisinin and partner drugs in some parts of Cambodia and Thailand (WHO, 2012a) is a threat to future therapeutic control against malaria infections. Moreover, vector resistance to insecticides coupled with severity and complex nature of the infective parasite has slowed down malaria control in some regions. Additionally, current malaria vaccines have shown minimal efficacy. The only malaria vaccine that has received a positive scientific opinion from the European Medicines Agency (EMA) (EMA, 2015) is RTS,S/AS01. It showed a 30-50% protection for human trials in Africa. However, the WHO recommends further evaluation of RTS,S/AS01 in a series of pilot implementations before it can be introduced on a wide scale (WHO, 2018d).

Owing to increasing level of drug-resistance with no ready vaccine for public use, a multi-pronged approach to malaria research is imperative. It is therefore important to provide theoretical insights on possible new targets, new drug-combinations that not only kill the infective parasites but also reduce parasite transmission to the next host. Effects of improved malaria vaccines and vaccine combinations alongside effective antimalarial drugs such as ACTs are investigated in this study. We extend existing in-host malaria models to determine effective antimalarial drug and vaccine combination therapies for *P. falciparum* malaria while providing rich insights on parasite dynamics and future therapeutic control measures.

1.8 Research objectives

The main objective of this study is to improve therapeutic strategies against *P. falciparum* malaria by extending and analysing (mathematically) models of in-host malaria dynamics. Specific objectives include:

1. To extend and analyse a mathematical model for in-host malaria infection that incorporate the liver and blood stages of parasite development.
2. To mathematically determine the effectiveness of malaria vaccines at different stages of parasite/disease progression.
3. To determine influential parameters and establish their contributions to in-host malaria disease dynamics and control.
4. To mathematically determine the effects of *P. falciparum* multiple-strain infection on development of parasite resistance and on in-host malaria dynamics and control.
5. To determine an optimal control therapy for in-host *P. falciparum* malaria infection.

1.9 Significance of the study

Although numerous prevention and control techniques have been employed to manage malaria infection, the deadly infectious disease still exerts a heavy toll on susceptible populations around the globe. This study is therefore important in the following aspects:

(i) Contributing to existing knowledge on mathematical modelling of in-host malaria dynamics and control measures. The presented models consider both the liver and blood stages in malaria therapy.

(ii) Improving the understanding of in-host dynamics during malaria infections.

(iii) Shaping policy making processes related to antimalarial drug use within communities and countries.

(iv) Determining optimal therapy combinations for elimination of infectious malaria within human host.

Locally, the findings of this study could be useful to malaria research organisations such as the Kenya Medical Research Institute (KEMRI), Centers for Disease Control and Prevention (CDC-Kenya) and the Ministry of Health in their effort to control malaria in the country. Our

results on the impacts of drug and vaccine combinations could be investigated further through vaccine trials in-vitro in these institutions. Threats caused by parasite resistance offers a unique opportunity to closely monitor use and misuse of antimalarial drugs. Our results call for regular and strict surveillance on antimalarial drugs use in clinics and hospitals in malaria-endemic counties. Moreover, this study highlights gametocyte eradication measures within the human host. This forms an important effort towards the 2030 global malaria eradication goal.

1.10 Outline of the thesis

Chapter 2 gives a review of mathematical models that have been formulated and analysed previously to provide insights on malaria disease transmission and control. Specific reviews are focused on in-host malaria models and key results from such selected models. A review on malaria infection in Kenya and a historical perspective of the disease in Kenya and globally is provided. The subject of optimal control theory and its application to disease interventions and especially malaria infection is also reviewed.

Chapter 3 highlights the general dynamics of malaria infection that spans from the liver stage to the blood stage of the parasite life cycle, in the presence of protective macrophages. The formulated model is analysed mathematically; using theories in Mathematical Biology. Sensitivity analysis based on the normalised forward sensitivity technique is performed to establish influential parameters in the disease progression. Due to non-linearity, the model is solved numerically using Runge Kutta fourth order scheme in Matlab software, to ascertain the long term dynamics of the blood cells, the immune cells and *P. falciparum* parasites.

In Chapter 4, the model (formulated in Chapter 3) is modified to incorporate vaccine control strategy. The vaccines are categorised into: pre-erythrocytic vaccines, erythrocytic vaccines and transmission blocking vaccines. Impact of vaccine efficacy is evaluated and critical efficacy of blood stage vaccine determined. Additionally, the general impact of vaccine combinations on parasitaemia is predicted numerically. Parameter sensitivity to the vaccine reproduction number is also performed. The effects of higher vaccine efficacies and possible vaccine combinations on parasitaemia and disease progression within the human host is investigated.

In Chapter 5, uncertainty that may accompany choices for parameter values for in-host malaria model is investigated. The possible effects of the different model parameter values to the model outcome are explored. Uncertainty in the values of the model parameters are

shown to generate variability in the model's predictive capabilities. Variabilities in model predictions are determined using the Latin Hypercube Sampling / Partial Rank Correlation Coefficient (LHS/PRCC) sensitivity techniques.

In Chapter 6, the effect of multiple-strain *P. falciparum* infection on the human host is studied. The effects of competition between the two parasite strains is also evaluated in reference to severity of infection. The effects of parasite resistance is highlighted in a blood stage only model. The effect of single and multiple-strain infection and its impact on the development of resistance to current malaria therapy is investigated. The formulated model is analysed mathematically and sensitivity analysis pegged on the strain-specific reproduction number established using the normalised forward technique.

In Chapter 7, the theory of optimal control is applied to an in-host malaria model. Control measures in the form of antimalarial drug regimens and malaria vaccine antigens are employed both at the pre-erythrocytic stage and the blood stage. The permissible control measures are assumed to be nonlinear. The optimal control model with constant control strategies is mathematically analysed and its stability conditions determined. Using Pontryagin's maximum principle, the best combination strategy that minimises the population of infected hepatocytes, infected erythrocytes, merozoites and free floating gametocytes is determined.

In Chapter 8, a conclusive summary of the study is provided and some of the recommendations based on the research findings listed.

Chapter 2

Literature review

2.1 Introduction

The biology and life cycle of *Plasmodium* parasite is extremely complicated with numerous unknown dynamics and behaviour straits (Cowman et al., 2016). The parasite alternates between the human host and female *Anopheles* mosquito vector to accomplish its complex infectious life cycles. Additionally, the parasite require the formation of unique zoite forms to invade host cells (Josling and Llinas, 2015). The invasion and transmission of the parasite from humans to mosquito has been under study for several years. Mathematical modelling has provided useful insights in understanding such complicated dynamics.

In this chapter, we review mathematical models that have been formulated and analysed previously to provide insights on malaria disease transmission and control. Specific reviews are focused on in-host malaria models and key results from such selected models. We also review malaria infection in Kenya and provide a historical perspective of disease in Kenya and globally. The subject of optimal control theory and its application to disease interventions and especially malaria infection is also reviewed.

2.2 Historical perspective of malaria

Malaria is one of the most fatal diseases worldwide (see Figures 2.1 and 2.2). The infectious disease mainly affects children under 5 years and pregnant women who are categorised as the most vulnerable groups to the disease (Harrington et al., 2009). Molecular genetic

evidence suggests that the first ancestor of malaria parasite existed at least half a billion years ago (Carter and Mendis, 2002). The cause of malaria was unknown until the year 1880, when Charles Lavran [1854-1925] discovered malaria parasite in the human blood in Africa (Cox, 2010). Eight years later, the discovered protozoan parasite was named *Plasmodium* by Giovanni Grassi [1854-1925]. In 1897 Ronald Ross [1857-1932] demonstrated that the malaria parasite could be transmitted from the infected *Anopheles* mosquito to humans (Packard, 2007). Until 1969, the mono-dimensional dichloro-diphenyl-trichloroethane (DDT) was the only chemical used in malaria control. Emergence and widespread parasite resistance to chloroquine coupled by the long term environmental consequences of DDT worsened global morbidity and mortality due to malaria infections in the 1980's (Packard, 2007).

Interestingly, much of the in-host malaria dynamics was unknown until 1948 when Henry Shortt [1887-1987] and Cyril Garnham [1901-1994] discovered the liver stage in the development of the parasite life cycle (Cox, 2010). The parasites grow and develop within the liver cells before they join the blood stream. However, some of the sporozoites may remain dormant in the liver (as hypnozoites), causing malaria relapse. This phenomenon was discovered in 1982 (Krotoski, 1985). For over a century, research on malaria epidemiology has focused on treatment and control of disease transmission between the mosquito vector and the human host.

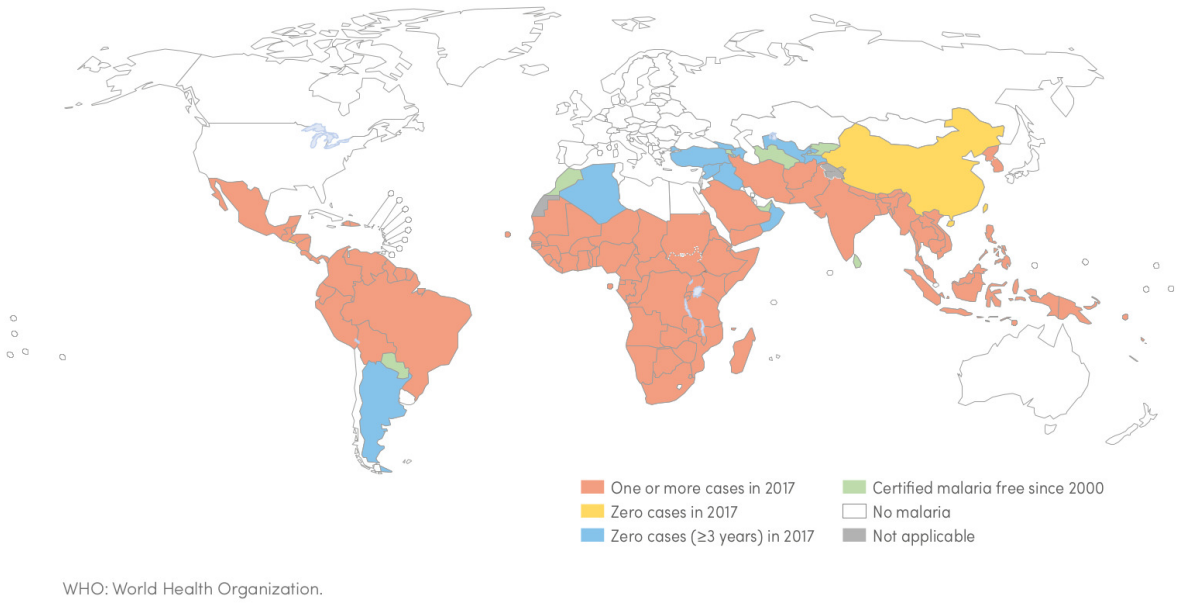

Figure 2.1: Countries with indigenous cases in 2000 and their status by 2017. Only countries in the WHO European region, China and El Salvador reported zero indigenous cases. Source: WHO (2018f).

Recent success in malaria treatment and control has resulted in significant global decline in morbidity and mortality due to malaria infection. However, the estimated cases and deaths due to *P. falciparum* malaria are still quite high, especially in the WHO African region. Figures 2.2a and 2.2b show the global trends in cases and mortality due to malaria infections in the last decade. It is evident that a lot more resources and research activities would be necessary if the 2030 goal of malaria eradication by WHO is to be accomplished (MCGV, 2011).

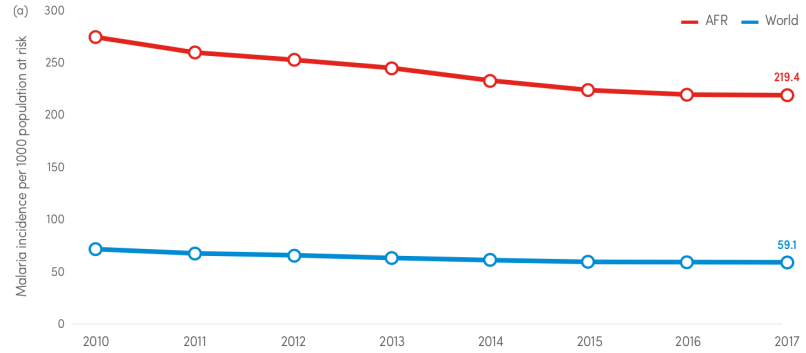

(a)

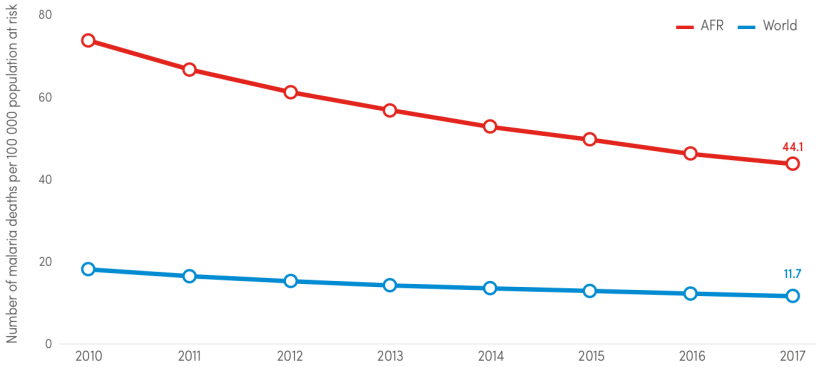

(b)

Figure 2.2: Trends in malaria case incidence rate (cases per 1000 population at risk) and mortality rate (cases per 100000 population at risk) globally (World) verses the WHO Africa region (AFR) for the 2010-2017 period. The cases are displayed in Figure 2.2a while the deaths are in Figure 2.2b. Source: WHO (2018f).

2.2.1 A review of malaria infection in Kenya

Kenya is a country in East Africa with a population of about 47.9 million people (KNBS, 2012; USAID, 2018). In the country's population, children under 5 and under 15 accounts for

16% and 42% of the total population, respectively. Geographically, the country is sub-divided into two major regions: low-land regions (Lake Victoria basin and Coastal areas) and highland regions (along the Great Rift Valley). Majority of the population live along the West-East belt (Lake Victoria basin and Western), Nairobi, Coast and Central highlands. Arid and semi-arid Southern and Northern parts of the country are sparsely populated. Historically, the country experiences seasonal rainfall pattern comprising of long rains (in the months of March/April and May/June) and short rains (in the months of October to November/December).

Malaria prevalence in the country therefore varies across the different geographic regions (see Figure 2.3) and is seasonal (MOH, 2016).

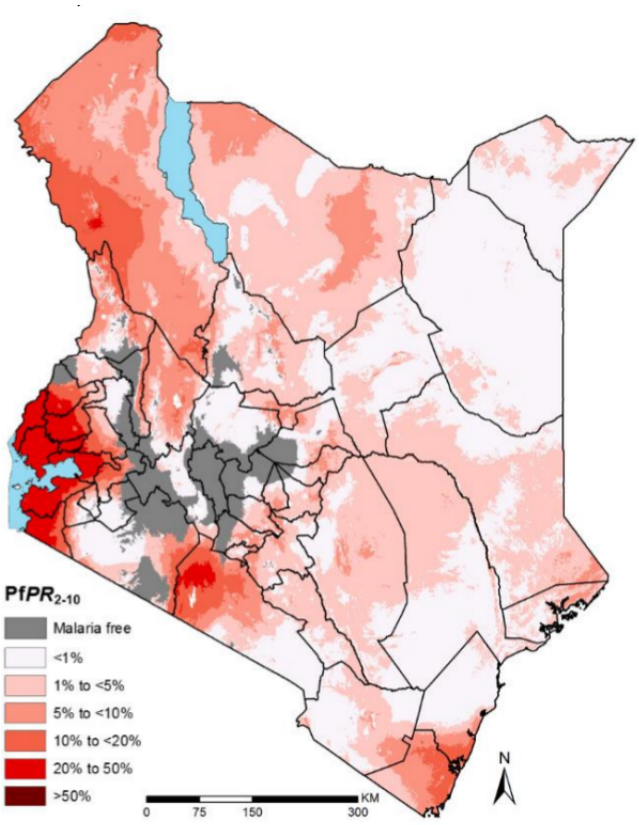

Figure 2.3: Kenya population adjusted *P. falciparum* malaria prevalence ($PAPfPR_{2-10}$) at $1\times$ 1 km spatial by sub-county (2000-2015). Source: USAID (2018).

Despite global and regional success in reducing morbidity and mortality due to malaria, malaria still remains a major public health problem in Kenya. About 4 million malaria cases are reported annually, with about 5.1% mortality rate among patients admitted with severe malaria. Over 99% of all reported cases are due to the deadly *P. falciparum* malaria. The vector species are members of the *Anopheles (An) gambiae* complex: *An. gambiae s.s.*,

An. arabiensis, *An. merus* and *An. funestus* (USAID, 2018). In 2015, malaria infections accounted for 16% of country-wide outpatient consultations in public and private medical facilities in Kenya (USAID, 2018).

A survey report by the Kenya National Bureau of Statistics (KNBS) showed that over three-quarter of the total population is at risk of malaria infections (KNBS, 2017). According to the WHO 2018 malaria report, about 35 million Kenyans live in malaria high transmission zones i.e., those with more than one case per 1000 population (WHO, 2018f). Another 14.8 million live in low transmission areas i.e., those with 0 to 1 case per 1000 population. Of the 50.6 million malaria cases reported in the East and Southern Africa (ESA) region, Kenya accounted for 7% of all cases (3.542 million). Although reported mortality due to malaria declined (by 11%) in the ESA region, malaria cases increased by 3% (from 49.1 million in 2010 to 50.6 million in 2017) (WHO, 2018f).

Malaria transmission and infection risks in the country are largely influenced by altitude, rainfall, vector species and parasite's intensity of biting (MOH, 2016). Temperature is the key determinant of environmental suitability for transmission of human malaria in the country (Gething et al., 2011). A temperature Suitability Index (TSI) for malaria transmission in Kenya indicates that Lake Victoria and Coastal regions have the ambient temperatures suitable for vector survival and hence malaria transmission. Additionally, these regions receive adequate and seasonal rainfall, making them suitable for sustained longer periods of transmission. This partly explains their endemic classification for malaria transmission and infections in the country (MOH, 2016).

In the past 15 years, the Kenyan government with the support of international donors under the Roll Back Malaria Partnership program, have invested millions of shillings in reducing morbidity, mortality and economic burden of malaria in the country (MOH, 2016). Vector control measures such as ITNs, IRS and LLINs and the use of ACTs as a first-line treatment for uncomplicated *P. falciparum* malaria, form the basis for the remarkable decline in malaria cases and deaths in the country. Moreover, in high burden counties (along Lake Victoria and the Coastal region), populations have been covered with IRS. Although these efforts have moved the country towards achieving the Global Technical Strategy (GTS) goal for malaria, the achievements are still a drop in the ocean if the country's vision 2030 of a malaria-free Kenya is to be achieved. To control malaria vector, reduce parasite transmission and provide efficient therapy for malaria, a lot more funding and malaria resources should be provided to the 47 counties in the country. This study highlights the pivotal role played by strict administration of effective ACT drugs in the country to enhance treatment success. The

study also emphasises the need to monitor malaria drug use in clinics and hospitals to reduce development of parasite resistance in the country.

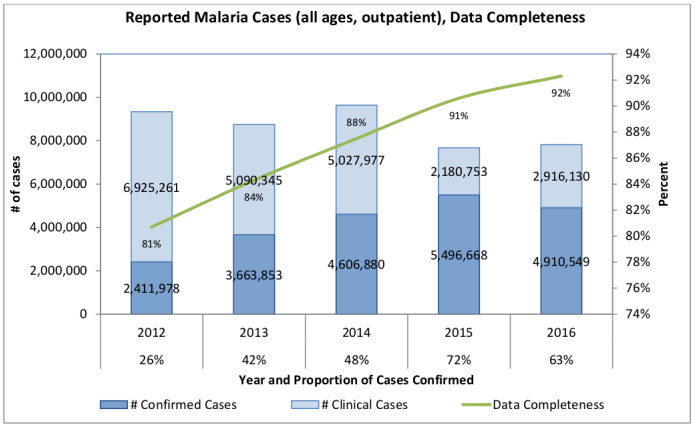

Figure 2.4: Trends in reported malaria cases (all ages, outpatient) in Kenya for the period 2012-2016. Source: USAID (2018).

2.3 Mathematical modelling as a tool to support infectious disease control

Mathematical models (deterministic and stochastic) have evolved together with science (natural sciences and social sciences) and currently have broad applications in engineering, biology, economics among others. It therefore forms an essential and inseparable part of scientific activity (Wainwright and Mulligan, 2013). These models are instrumental in studying the different components of a system and help make predictions of the futuristic behaviours of the system. Moreover, dynamical models have contributed significantly towards the understanding of complex biological phenomenon including pathogen-host invasions and disease transmission. Such models have provided simple and insightful understanding of disease epidemiology and virology. They have been applied in the study of HIV/AIDS, tuberculosis, malaria among other deadly infectious diseases.

Mathematical modelling is the process of using mathematical analysis to describe real world phenomenon, with the goal of generating explanations and solutions to such problems. The subject of mathematical modelling is founded on formulated mathematical models. Such models can broadly be categorised into deterministic and stochastic models. A suitable model should integrate present data and predict with reasonable accuracy the response of the system to planned changes (Carrera et al., 1989).

Unlike stochastic models, deterministic models ignore random variations. Stochastic models are most appropriate when the system under study is characterised by inherent randomness. However, for small data set with exact, repeated and fixed output, a deterministic approach is preferred. Nevertheless, both model forms are characterised by assumptions on inherent variables and parameters. They provide a simplified representation of a real system.

The translation of a real-world problem into a mathematical model begins from conceptualisation and ends with a quantitative model. The conceptual model is often represented using boxes and arrows in many epidemiological models. The boxes typify the state variables whereas the arrows indicate the direction of flow/movement or sometimes interactions between different variables (Mbogo, 2014). The rates of change in a particular process are combined to generate an equation to represent that process. Several processes result into two or more equations or a system of equations called a quantitative model. Such equations can take the form of difference equations (when time is regarded as a discrete variable) or differential equations (when time is regarded as a continuous variable).

Mathematical models have become very essential in infectious disease modelling; that is often characterised by complex disease dynamics. Analytical or numerical technique can be employed to analyse such disease models. The preferred method may varry and depends on the complexity of the formulated model. Several other aspects can be investigated from the model including parameter sensitivity and model fitting to data for prediction purposes.

In this study, we have largely used differential equations in formulating our in-host malaria disease models. Due to complexity and nonlinearity properties, the presented models are analysed mathematically and their solutions presented analytically and numerically. Some of the mathematical concepts and tools used in the qualitative analysis of the mathematical models considered in this study are available in Appendix A.

2.4 In-host malaria models

The earliest in-host malaria model was formulated by Anderson et al. (1989). The model describes the intra-host dynamics of malaria infection; the interactions between the healthy erythrocytes and the merozoites. The model ignores the effects of the immune system and hence describes the worst case scenario of the in-host malaria infection. Their mathematical

model is presented as follows:

$$\left.\begin{aligned}\frac{\mathrm{d}x}{\mathrm{d}t} &= \Lambda - \mu_x x - \beta x m,\\ \frac{\mathrm{d}y}{\mathrm{d}t} &= \beta x m - \alpha y,\\ \frac{\mathrm{d}m}{\mathrm{d}t} &= \alpha r y - d m - \beta x m,\end{aligned}\right\} \tag{2.1}$$

where $x(t), y(t)$ and $m(t)$ are the concentrations of the healthy erythrocytes, infected erythrocytes and merozoites, respectively. The uninfected red blood cells (RBCs) are considered susceptibles and are assumed to enter the blood circulation at a rate Λ. By the law of mass action, the RBCs get infected by merozoites to form parasitised/infected red blood cells (IRBCs) at a rate β. As the parasites grow and multiply, the IRBCs get killed at the rate α. The IRBCs then burst and release merozoites at a rate $r\alpha y$. In the absence of immunity, IRBCs release a total of r merozoites per infected erythrocyte. As a consequence of the bursting IRBCs, the merozoites are replenished at a rate $r\alpha y$. Merozoites are assumed to invade RBCs at the rate β, and die naturally at the rate d.

The simple mathematical model (2.1) was later expanded to include immunological responses against malaria merozoites. The study by Anderson et al. (1989), focused on comparing the effectiveness of immune responses against merozoites and infected (parasitised) red blood cells. A compartment for the immune cells was added to the model system (2.1) so that we have the following model given by system (2.2).

$$\left.\begin{aligned}\frac{\mathrm{d}x}{\mathrm{d}t} &= \Lambda - \mu_x x - \beta x m,\\ \frac{\mathrm{d}y}{\mathrm{d}t} &= \beta x m - \mu_y y - k_y b y,\\ \frac{\mathrm{d}m}{\mathrm{d}t} &= r\mu_y y - \mu_m m - \beta x m - k_m b m,\\ \frac{\mathrm{d}b}{\mathrm{d}t} &= (\rho_y y + \rho_m m) b - \mu_b b\end{aligned}\right\} \tag{2.2}$$

where b is the concentration of immune effectors. The IRBCs are either killed by the parasites at the rate μ_y or by immunity at the rate $k_y b$. Initially, the immune effectors form a small population which then grows at the rate $(\rho_y y + \rho_m m)$ and decays at the rate μ_b. Moreover, the growth of the immune effectors are considered influenced by the presence of both the IRBCs and the merozoites, expressed by the mass-action terms $k_y b y$ and $k_m b m$, respectively. The description of model parameters in system (2.2) are presented in Table 2.1.

Table 2.1: Model parameter descriptions

Parameters	Definition
Λ	Immigration rate of x
β	Effective (invasive) contact rate between m and x
r	Number of merozoites released per IRBCs
ρ_y, ρ_m	Immunogenecity of IRBCs and merozoites, respectively
$\mu_x, \mu_y, \mu_m, \mu_b$	Death rates of the populations identified by the subscripts
k_y, k_m	Immunosensitivity of IRBCs and merozoites, respectively

Results from system (2.2) revealed that the immune response against the merozoites is less effective than the immune response against infected red blood cells. Therefore, vaccines based on IRBCs antigens are likely to be more effective than vaccines based on merozoite antigens. Further analyses and criticism of this model can be found in (Molineaux and Dietz, 1999).

Moreover, the effects of immunological responses targeted at different stages in a malaria parasite's life-cycle is also investigated in Anderson et al. (1989). The focus being on the relative merits of humoral versus cell-mediated immunological responses in suppressing parasite abundance and replication within the human host. It is shown that the effectiveness of a given immunological response is inversely related to the life-expectancy of the target stage in the parasite's developmental cycle. Numerical simulation of the formulated in-human malaria model revealed temporal changes in the total abundance of erythrocytes (healthy and infected erythrocytes) in the human host in the presence of immunological responses, as shown in Figures 2.5a and 2.5b, respectively.

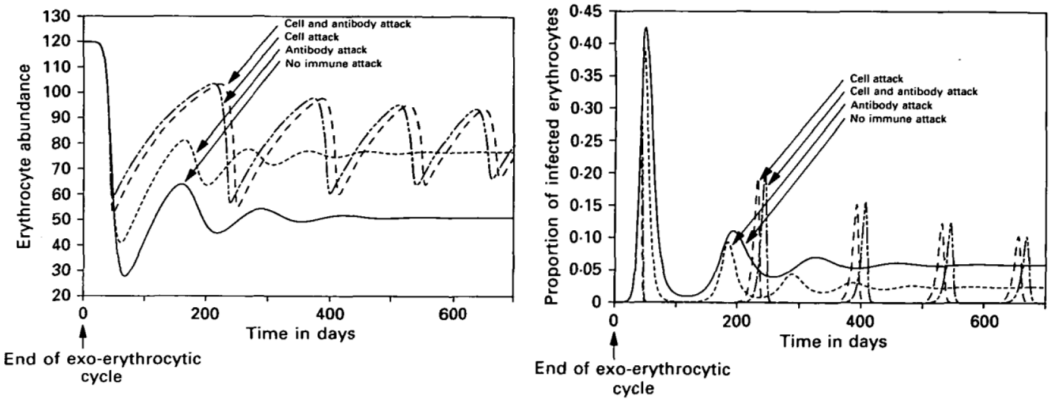

(a) (b)

Figure 2.5: The interaction of the erythrocytic cycle of *P. falciparum* with the human immune system. The model is simulated under four scenarios: full line (no immunological response), dotted line (antibody attack), dashed line (with killing of infected red blood cells) and dotted+dashed line (with immunological responses against merozoites and infected red blood cells). Source: Anderson et al. (1989).

Hetzel and Anderson (1996) extended the model by Anderson et al. (1989) by allowing superinfecting merozoites to invade already infected red blood cells. They assumed that these merozoites are wasted. The growth of the immune effectors is also assumed to be linear in relation to the density of the antigens. This implies that immunity would develop even if immune effectors do not exist. However, at higher effector density, there is a negative feedback.

Further modification of the Anderson et al. (1989) model was done by Hellriegel (1992). In her model, she allowed the gametocytes (g_i) to be generated out of the infected red blood cells (y_i) at a rate r. Moreover, she assumed the existence of two clones that differ in immunogenecity, immunosensitivity, metocytogenesis and rate of invasion of the erythrocytes. Results of her study indicated that in the absence of immunity, the less invasive clone is eliminated by the more invasive clone. The two clones can however coexist in the presence of immunity. The model whose parameters are described in Hellriegel (1992), is presented

as follows:

$$\left.\begin{aligned}
\frac{\mathrm{d}y_i}{\mathrm{d}t} &= \beta_i x s_i - \mu_y y_i - c_i y_i - \left(\sum_{j=1}^{2} k_{ij} I_j\right) y_i, \\
\frac{\mathrm{d}g_i}{\mathrm{d}t} &= c_i y_i - \alpha_g g_i - \left(\sum_{j=1}^{2} l_{ij} I_j\right) g_i, \\
\frac{\mathrm{d}s_i}{\mathrm{d}t} &= \mu_y r y_i - \alpha_s s_i - \beta_i x s_i - \left(\sum_{j=1}^{2} h_{ij} I_j\right) s_i, \\
\frac{\mathrm{d}I_i}{\mathrm{d}t} &= I_i(\sigma_i s_i + \gamma_i y_i + \lambda_i g_i - \mu_I) + \varepsilon/2,
\end{aligned}\right\} \tag{2.3}$$

where, k_{ii}, l_{ii}, h_{ii}, for $i = (1,2)$ represents the genotype-specific and $k_{ij}, l_{ij}, h_{ij} (i \neq j)$ denotes the non-specific genotypes.

Research work by Swinton (1996), restricted immunogenecity and immunosensitivity to infected erythrocytes. Swinton assumed that the growth of the immune effectors is a linear function of the concentration of malaria parasites in the human body. The process of erythropoiesis is also postulated to increase with increase in the death rate of susceptible red blood cells (anaemia).

Austin et al. (1998a) merged a pharmacokinetic and pharmacodynamic models with an intra-host malaria model. This model is basically similar to the model in Hetzel and Anderson (1996). However, they ignored super-infection of IRBCs and assumed that the merozoite density equilibrates instantaneously at all times. Immunogenesity and immunosensitivity is also restricted to the IRBCs only. In order to insert drug action in the model, two key assumptions are made: (1) Antimalarials act exclusively by increasing the death rate of the infected red blood cells; without changing the rate at which they release merozoites and (2) drug action is dose-dependent, saturating at an infected red blood cell death rate $(k\mu_y)$, where the parameter k is drug-specific. According to Molineaux and Dietz (1999), the above key assumptions grossly underestimate the effect of treatment.

The only discrete-time in-host malaria model is that presented by Kwiatkowski and Nowak (1991). They formulated a malaria model based on the association between fever and the rupture of mature schizonts (as shown in system (2.4)). The sensitivity of the IRBCs to fever-like temperatures in vitro was used to modulate the age specific mortality of the IRBCs. Their results showed that a fraction $\exp(-s_i y_1(t))$ of the IRBC of age i survives through the 12 hour interval $(t, t+1)$. The fraction depends on y_i, the density of the youngest IRBCs and on the age specific sensitivity S_i.

$$\left.\begin{aligned} y_1(t+1) =& r(1-h)y_4(t)\exp(-s_4y_1(t)+hy_1(t)\exp(-s_1y_1(t)), \\ y_2(t+1) =& r(1-h)y_{t-1}(t)\exp(-s_{i-1}y_1(t))+\exp(-s_iy_1(t)), \quad i=1,\ldots 4, \end{aligned}\right\} \tag{2.4}$$

where y_i=infected red blood cells, r=number of successful merozoites released per IRBCs, h=fraction staying in the same age-group, s_i=sensitivity of y_i and y_1; t=time (age and time units are 12 hours).

Malaria therapy patients vary by orders of magnitute in the density at which they control their parasitaemia and in the parasite density associated with the first fever (Jeffery et al., 1959). In McKenzie and Bossert (1997), a three intra-host populations of IRBCs (asexual), gametocytes, and immune effectors is considered (as shown in system (2.5)). Contrary to their expectations, all the nine models displayed a domain of parameter space that yields output within the acceptable ranges. Moreover, the peak asexual density decreased monotonuously as the gametocyte conversion rate increased.

$$\left.\begin{aligned} \frac{\mathrm{d}y}{\mathrm{d}t} =& \rho_y y - k_y by - \gamma_A y, \\ \frac{\mathrm{d}g}{\mathrm{d}t} =& \gamma_A y - \mu_g g, \\ \frac{\mathrm{d}b}{\mathrm{d}t} =& \rho_{01} y - \mu_b b - k_y by, \end{aligned}\right\} \tag{2.5}$$

Variables: y=asexual IRBC; g=gametocytes; b=immune effectors. Parameters: ρ_y=net growth rate of y, k_y=immunosensitivity of y; γ_A=rate of gametocytogenesis; μ_g, μ_b=death rates of gametocytes and immune effectors, respectively; ρ_{01}=rate of immunogenesis. The other models of the family are defined by substituting the gametogenesis term γ_Ay by $\gamma_B yb$ or $\gamma_C y^2$, and/or the immunogenesis term $\rho_{01}y$ by $\rho_{02}yb$ or $\rho_{03}y(t-L)$ where L= a time-lag; these options define nine models, labelled $A_1, A_2, A_3, \ldots C_3$, as described and analysed in McKenzie and Bossert (1998).

Some few mathematical models have concentrated on the in-human and in-mosquito malaria dynamics. In Selemani et al. (2016), stability analysis of an in-human and in-mosquito deterministic mathematical model is performed. Using linearisation methodology, it is showed that the malaria-free equilibrium is locally asymptotically stable when $R_0 < 1$. By Metzler matrix theory, the malaria-infection equilibrium (MIE) is found to be globally asymptotically stable provided $R_0 < 1$. However, when $R_0 > 1$, and based on LaSalle's invariance theory, the MIE is shown to be globally asymptotically stable according to Lyapunov functional method.

In Selemani et al. (2017a), the influence of the host's immunity agaist in-host malaria infection is investigated. Immunity is shown to have significant influence in lowering malaria infection at blood and mosquito stages. At the liver stage, however, the immunity was least influential. Severity of malaria infection is shown to decrease with increasing density of defensive immune cells. Although antibodies are very effective at blocking cell invasions by sporozoites and merozoites, the immune cells are shown to be highly effective in suppressing merozoite production at the erythrocytic stages (Selemani et al., 2017a). Moreover, results of sensitivity analysis in Selemani et al. (2017b), revealed that new therapetic intervetions should aim at increasing the death of blood and liver schizonts. This has a direct effect on decreased merozoite densities and hence reduced malaria severity on infected patients.

A thorough review of basic intra-host model of malaria, without immunity is presented by Chiyaka (2010). The paper highlights how concepts in nonlinear dynamics can be used to unravel the underlying dynamical features of an in-host malaria model. The critical role of an intra-host basic reproduction number for a malaria model in controlling malaria infection is highlighted in Chiyaka et al. (2008) and Chiyaka (2010). Bifurcation analysis in Chiyaka (2010), revealed that the model given by system (2.6) has a critical parameter r^c for which the in-host malaria infection persists if $r > r^c$, where r is the average number of merozoites produced per each bursting infected erythrocyte.

The deterministic in-host malaria model is an extension of the original model (2.2) by Anderson et al. (1989). It is established that malaria drugs based on inhibiting parasite production are more effective than those based on inhibiting merozoite invasion of erythrocytes (Chiyaka et al., 2008). Using theories in stability analysis, malaria infection can be eliminated from the infected human host if the drug efficacy level exceeds a certain threshold value and persist otherwise. The mathematical model by Chiyaka et al. (2008), that is only limited to the blood stage of parasite life cycle is presented as follows:

$$\left.\begin{aligned}
\frac{dX}{dt} &= \lambda_x + \sigma Y - \frac{\beta XM}{1+c_0A} - \mu_x X - \omega XMB,\\
\frac{dY}{dt} &= \frac{\beta XM}{1+c_0A} - k_y BY - \mu_y Y,\\
\frac{dM}{dt} &= \frac{r\mu_y Y}{1+c_1B} - \mu_m M - k_m BM - \frac{\beta XM}{1+c_0A},\\
\frac{dB}{dt} &= \lambda_b + B\left(\rho_y \frac{Y}{k_0+Y} + \rho_m \frac{M}{k_1+M}\right) - \mu_b B,\\
\frac{dA}{dt} &= \eta B \frac{M}{k_1+M} - \mu_a A,
\end{aligned}\right\} \tag{2.6}$$

where $X(t)$ and $Y(t)$ are the concentrations of the unparasitised and parasitised erythrocytes, respectively. $M(t)$ are merozoites that infect the healthy RBCs at the rate β. The response of the immune system is captured by the inclusion of the immune cells $B(t)$ and the antibodies $A(t)$ in the system (2.6). Detailed descriptions of the model parameters are as presented by Chiyaka et al. (2008).

2.5 Optimal control measures applied to disease models

In developing response plans to disease outbreaks, decision makers such as government and public health officials are often faced with trade-offs in choosing among various treatment options (Gaff and Schaefer, 2009). Searching for answers to identify the best strategies for intervention prior to what may be an inevitable disease or to an already existing pathogen is not a simple challenge. Diseases such as measles, human papilloma virus and influenza have varied approved medical treatment options as well as available vaccines. Vaccines targeting high burden diseases such as malaria and HIV/AIDS are currently under development, Usually the challenge is to find the optimal response balancing treatment and vaccination that will minimise incidence and disease-related mortality at an affordable cost (Joshi et al., 2006; Omondi et al., 2018).

From the early work by Bernoulli and Blower (2004), and his argument for the advantages of inoculation in controlling smallpox mortality, optimal control theory have broadly found their applications in determining control strategies of diseases (Lenhart and Workman, 2007; Magombedze et al., 2009b), especially in the control of HIV (Adams et al., 2004; Fister et al., 1998; Joshi, 2002; Karrakchou et al., 2006; Kirschner and Webb, 1996; Magombedze et al., 2011b, 2009a; Shiri et al., 2005b) and tuberculosis (Jung et al., 2002; Silva et al., 2016; Silva and Torres, 2012). In these studies, optimal control therapy strategies were explored using Pontryagin's maximum principle on dynamical models (Lenhart and Workman, 2007). Brauer (2006), considered the effect of treatment on some epidemic models. Asymptotically, the complex models and more simple models displayed similar qualitative behaviours. He however advocated for an investigation on the possible trade-off between vaccination and treatment and how the results would be influenced by the complex models.

2.5.1 Optimal control measures applied to malaria disease models

The application of optimal control theory in malaria epidemiology and control has for a long time been limited to population models only (Agusto et al., 2012; Makinde and Okosun, 2011; Mwanga et al., 2015; Okosun et al., 2011). In these models, the goal of the application of optimal control theory is to minimise the number of humans infected with malaria while keeping the costs of control, such as purchase of ITNs and IRS, as low as possible (Mwanga et al., 2015). A study by Okosun et al. (2011), formulated a deterministic model using mass-action form of infection and derived optimal conditions for disease eradication in finite time. Numerical results and cost effectiveness analysis indicate that the optimal strategy to control malaria within a population requires the combination of vaccination and treatment methods. In Makinde and Okosun (2011), a combination of screening of infected immigrants, treatment of infectives and spraying of insecticides against mosquitoes lead to significant decline in new malaria cases and transmissions among susceptible individuals.

In Silva and Torres (2013), optimal supervision and educational campaigns on the use of ITNs are shown to be highly effective in achieveing 75% coverage of the host population within a community. Analyses by Mwanga et al. (2014), revealed that a combination of three control strategies: ITNs, IRS and treatment provides the best control against malaria transmission and infection. Additionally, the use of mosquito-reduction strategies is more effective than personal protection in some cases but not always (Kim et al., 2012). However, a combination of personal protection, treatment and insecticides spray are shown to bear the greatest impact on malaria control (Agusto et al., 2012). In all these dynamical models, optimal control therapy strategies were explored using Pontryagin's maximum principle (Pontryagin, 1987).

That very minimal research work is currently available on the application of optimal control theory to in-host malaria control dynamics is undebatable. This could be explained by the complex dynamics of cell-parasite interactions within the human host. The impact of control measures based on vaccination, anti-malarial drugs and immunological responses targeted at different stages in a malaria parasite is examined by Anderson et al. (1989). Analysis revealed that the influence of a defined control measure on the prevalence or intensity of infection is non-linearly related to the magnitude of control effort. Very high levels of cohort immunisation is required to block transmission for a defined level of coverage. Gametocyte vaccine is also shown to be better with respect to reducing transmission for a defined level of coverage. Sporozoite vaccines are however shown to be very effective in reducing disease morbidity (Anderson et al., 1989).

Although Magombedze et al. (2011a) determined optimal control measures of malaria chemotherapy, their work was limited to the parasite blood stage only. Results of their study indicated that highly toxic drugs with the compensation of high infection suppression have the potential of yielding better treatment results than less toxic drugs with less infection suppression potential or high toxic drugs with less infection suppression potential. It was also observed that a treatment protocol with drugs with high adverse effects and with a high potential of merozoite suppression can be beneficial to patients. However, an optimal control strategy that seeks to maximise immune cells has no potential of improving the treatment of blood stage malaria.

To the best of our knowledge, optimal control study is yet to be applied to a robust in-host malaria model that incorporates the liver and blood stages. In this study, we have considered the important opportunity for malaria control provided by the liver stage. The formulated optimal control methodology aims to reduce severity of infection and/or eradicate infective parasites at a minimal cost. The minimisation function and optimality system is presented in Chapter 7 of this thesis.

In this study, ordinary differential equations are used in the model formulations and extensions. The in-host malaria model by Chiyaka et al. (2008), is extended by adding the liver stage and immune effectors to the in-host malaria dynamics. Model properties including positivity and boundedness of solutions and the prove of the existence of and stability analysis of model equilibrium points are determined. Owing to nonlinearity, the models in this study are solved numerically using Matlab and Python softwares. The deterministic blood stage model by Anderson et al. (1989) is extended to investigate the effects of parasite resistance to antimalarial drugs and the impact of multiple-strain infection on severity of malaria infection. The model is extended by sub-dividing merozoite compartment into drug-sensitive and drug-resistant strains. This division is extended to infected erythrocytes and gametocytes. The severity of infection is investigated in the context of parasite resistance to antimalarial drug therapy.

The next Chapter 3 deals with formulation and analysis of a deterministic, robust, in-host malaria model that illustrates the dynamics and interactions of malaria parasites from the liver stage to the blood stage in the presence of host's immune cells.

Chapter 3

Mathematical model for in-host dynamics of malaria

3.1 Introduction

In this chapter, we develop a mathematical model that describes the dynamics and interactions between the *P. falciparum* parasites, the host's hepatocytes and red blood cells in the presence of immune effectors. The in-host (in-vivo) model is analysed mathematically and solved numerically using Python and Matlab softwares. We compute the in-host basic reproduction number and establish highly sensitive parameters for future therapeutic target and disease control.

3.2 In-host dynamics of malaria

In-host studies are studies aimed at understanding a disease dynamics within a living organism (AIRF, 2012). An in-host malaria model therefore, embodies to describe the dynamics of interactions between the red blood cells, liver hepatocytes, malaria parasitaemia and immune effectors within the human host. The in-host malaria dynamics discussed in this chapter is therefore limited to the liver (pre-erythrocytic phase) and blood (erythrocytic phase) stages of *P. falciparum* parasite life cycle within the human host.

Several studies on mathematical modelling of in-host malaria and its dynamics have been done. Nearly all the earlier mathematical models (see for instance, (Anderson et al., 1989;

Hellriegel, 1992; Swinton, 1996)) focused on improving *P. falciparum* control while focussing on the cyclic blood stage of parasite development and infectivity. These models have been helpful in explaining in-host observations by means of biologically plausible assumptions such as parasite diversity, predicting the impact of interventions or use of antimalarial drugs (Dondorp et al., 2010), and estimating hidden parameter values (White, 2004). Although the models in (Chiyaka et al., 2008; Li et al., 2011; Tumwiine et al., 2008), have considered the impact of immune response and treatment, the modelling is only limited to the blood stage of *P. falciparum* development. In (Selemani et al., 2016, 2017a; Tabo et al., 2017), the liver stage is incorporated in the malaria model. However, the contribution of immune system is ignored in (Selemani et al., 2016; Tabo et al., 2017). Moreover, all the immune cells are assumed to play an active role during malaria infection in (Selemani et al., 2017a). This may not be entirely true. The specific impacts of immune responses to malaria infection are well discussed in (Bate et al., 1988; Elloso et al., 1994; Ganusov et al., 2002; Rouzine and McKenzie, 2003).

3.2.1 Hepatocyte regeneration and repair

Liver hepatocytes are instrumental in the development of malaria parasites. Injected sporozoites travel to the liver of the human host and invade the hepatocytes; crital stage of establishing malaria infection (Silvie et al., 2003). The sources of the hepatocytes vary depending on the growth process. The hepatocytes can be generated from the bone marrow cells (Fausto et al., 2006); this mainly occurs during liver transplants (where they are an important source of nonparenchymal cells, including the kupffer cells and endothelial cells) and often the frequency of hepatocyte proliferation is very low (Fausto, 2004). The replication of existing hepatocytes form the second source of liver hepatocytes. Old hepatocytes are replaced through a process called compensatory hyperplasia (Fausto et al., 2006). A single hepatocyte could replicate 70 or more times in its life-time (Overturf et al., 1997). According to Fausto (2004), replication is the quickest and most efficient way to generate hepatocytes for liver regeneration and repair. This argument is also supported by data in (Weglarz et al., 2000), where diploid, tetraploid and octoploid hepatocytes are reported to have approximately the same capacity to replace damaged liver cells. The third source of hepatocytes are the oval cells. These cells replicate and differentiate into hepatocytes when the replication of mature hepatocytes is delayed or entirely blocked (Fausto, 2004).

3.3 Model formulation

We extended the in-host malaria model by Chiyaka et al. (2008), by incorporating the liver stage of parasite development. The reformulated in-host malaria model focuses on the erythrocytic and hepatocytic stages and describes the dynamics of interactions between the malaria parasites, the liver hepatocytes, the erythrocytes (red blood cells) and the macrophages (immune system cells). Unlike the models in (Selemani et al., 2016, 2017a), we ignored the vector stage of parasite development and assumed a twofold process in the generation of hepatocytes: from the bone marrow and from self-replication of the existing hepatocytes. Again, we assumed that the rate of generation of macrophages and susceptible erythrocytes from the bone marrow increases with increasing density of the infected erythrocytes. However, whatever the densitity of infected erythrocytes, there is a limit on the rate at which cells can be released from the bone marrow.

The compartmental model assumes seven interacting populations of sporozoites $S(t)$, susceptible hepatocytes $H(t)$, infected hepatocytes $H_X(t)$, susceptible erythrocytes $R(t)$, infected erythrocytes $R_X(t)$, merozoites $M(t)$ and macrophages $Z(t)$ at any time t. The dynamics of malaria parasites and host-cell populations in each compartment are described as follows:

Sporozoites (S): The female *Anopheles* mosquito is assumed to inject sporozoites into the human system during blood meal at a constant rate Λ. The sporozoites molt through the blood stream and reach the liver in about 2 hours, where they invade the hepatocytes at the rate β_s. We assume that the sporozoites can die naturally at a rate δ_s.

Susceptible hepatocytes (H): We consider the bone marrow and self-replication as the main sources of the liver hepatocytes in our model. The recruitment of hepatocytes from the bone marrow is assumed to occur at a constant rate λ_h. Just like during liver transplant, (Fausto et al., 2006), we argue that during severe malaria infections, the rate of generation of healthy hepatocytes is likely to increase tremendously and in proportion to the concentrations of the infected hepatocytes (Fausto, 2004). This additional increase is represented by the term $\rho_1 H_X/(\kappa_1 + H_X) = \psi_1(H_X)$, where H_X and ρ_1, respectively, represent the density of infected hepatocytes and their rates of generation. The parameter κ_1 represents the number/concentration of the infected hepatocytes at which the recruitment of the healthy hepatocytes is a half of the maximum rate. Owing to invasion by sporozoites at the rate β_s, susceptible hepatocytes get infected and progress to subpopulation H_X. In addition, hepatocytes in compartment H are assumed to have a natural life expectancy and may hence die naturally at the rate μ_1.

Infected hepatocytes (H_X): Following sporozoite invasion, the healthy hepatocytes get infected leading to formation of infected hepatocytes. The infected hepatocytes mature into liver-stage schizonts. These schizonts burst open, releasing 2000-40000 uninucleate merozoites into the blood stream (Crutcher and Hoffman, 1996). The term $N\mu_2 H_X$ represents the total population of merozoites released upon bursting of infected hepatocytes. The parameter μ_2 represents the death rate of the infected hepatocytes.

Susceptible erythrocytes (R): Similar to malaria models in (Li et al., 2011; Tumwiine et al., 2008) we have assumed that the susceptible red blood cells (RBCs) get recruited at a constant rate λ_r from the bone marrow. We further assume that, during infection, the production rate of erythrocytes is accelerated owing to the presence of infected red blood cells (IRBCs) at the rate ρ_2. This increase is denoted by the term $\rho_2 R_X/(\kappa_2 + R_X) = \psi_2(R_X)$, where κ_2 represents number/concentration of the infected red blood cells at which the recruitment of susceptible red blood cells is a half of the maximum rate. The particular mechanisms involved in this accelerated process is however still poorly understood (Wickramasinghe and Abdalla, 2000). The susceptible RBCs get infected by merozoites at a rate proportional to the contact rate of their density, $\beta_r MR$. The positive constant β_r describes the rate of successful invasion by a malaria merozoite. This process of destruction of the RBCs result in build-up of toxins and debris in the blood. The resultant immune reaction produces side effects which are the common observable symptoms of malaria, such as fever, chills, nausea and aches. The susceptible RBCs die naturally at a rate μ_3.

Infected erythrocytes (R_X) : Upon invasion by merozoite, the healthy RBCs get infected, leading to the formation of infected red blood cells R_X. Although the IRBCs die at a constant rate μ_4, they can also be killed through phagocytosis by the macrophages at the rate η. The parameter η therefore denotes the immunosensitivity of the IRBCs. At maturity, the IRBCs burst open, releasing free merozoites into the blood system, causing secondary invasion and disease progression. During malaria infection, the IRBCs may bind to the endothelial lining of blood vessels in vital organs, such as brain, lung, and heart leading to disease complications and sometimes death (Miller et al., 1994).

Merozoites (M): After 2-15 days, the infected hepatocytes burst open and release merozoites into the blood system. This is represented by the term $N\mu_2 H_X$, where N is the average number of merozoites released per bursting infected hepatocyte. An average of K merozoites are released per each bursting blood schizont. These free parasites suffer a natural death at a rate δ_m, and invade susceptible RBCs at a rate β_r. Within the red blood cells, the merozoites mature either into uninucleate gametocyte or into erythrocytic stage schizont containing 10-36 merozoites (Crutcher and Hoffman, 1996). After about 48-72 hours, the

erythrocytic stage schizont ruptures, releasing more merozoites into blood stream to cause further invasion of healthy RBCs. We assume that a proportion ζ of the merozoites contribute to secondary invasion of the susceptible RBCs. The rest of the merozoites $(1-\zeta)$ transform into gametocytes that are later picked up by female *Anopheles* mosquitoes during feeding. Further depletion of merozoite numbers may arise from destruction by host immunity or from ageing. These two are however not considered in the model presented in this chapter.

Macrophages (Z): The presence of malaria parasites in the human body elicits responses from numerous immune cells: such as the natural killers cells (through contact dependent manner) (Chen et al., 2014), the macrophages (Bate et al., 1988; De Back et al., 2014), the $CD4^+$ T and the $CD8^+$T cells among others (White et al., 2013). Owing to their effectiveness in elimination of infected red blood cells and infective malaria parasites, we have considered the innate macrophage cells as the main part of the immune response in malaria infection. Consequently, we have assumed that macrophage cells are recruited at a constant rate λ_z from the bone marrow. Moreover, they proliferate at a rate ρ_3 at the sites of infection in proportion to the density of IRBCs. This is represented by the term $\rho_3 R_X/(\kappa_3+R_X) = \psi_3(R_X)$, where κ_3 denotes the number/concentration of the infected red blood cells at which the recruitment of the macrophages is a half of the maximum rate. Although macrophages play an important role in promoting erythropoiesis (De Back et al., 2014), and phagocyte on the IRBCs at a rate η, they can also die naturally at a constant rate δ_z.

The variables and parameters that describe the in-host malaria dynamics are presented in Tables 3.1 and 3.2, respectively. The above transmission dynamics of *P. falciparum* malaria are summarised in the compartmental diagram given in Figure 3.1.

Table 3.1: Symbols and definition of state variables considered in the model at time t

Variable	Description
$H(t)$	Population of susceptible hepatocytes
$H_X(t)$	Population of infected hepatocytes
$R(t)$	Population of susceptible erythrocytes (red blood cells)
$R_X(t)$	Population of infected erythrocytes
$Z(t)$	Population of macrophages in the human body
$S(t)$	Population of sporozoites
$M(t)$	Population of merozoites

Table 3.2: Symbols and description of parameters used in the model

Parameter	Description
λ_h	Recruitment rate of susceptible hepatocytes from the bone marrow
Λ	The total rate of injection of sporozoites into liver due to mosquito bites
δ_s	Death rate of sporozoites
μ_1	Natural death rate of susceptible hepatocytes
β_s	The invasion rate of hepatocytes by sporozoites
μ_2	Death rate of infected hepatocytes
λ_r	Recruitment rate of susceptible RBCs from the bone marrow.
μ_3	Natural death rate of susceptible erythrocytes
β_r	The invasion rate of susceptible RBCs by merozoites
μ_4	Death rate of infected erythrocytes
δ_m	Death rate of merozoites
λ_z	Recruitment rate of macrophages from the bone marrow
δ_z	The death rate of a macrophage
η	Elimination rate of IRBCs by macrophages
ρ_1	Production rate of hepatocytes due to presence of infected hepatocytes
ρ_2	Production rate of RBCs due to presence of IRBCs
ρ_3	Immunogenesity of infected red blood cells
κ_1	Number of H_X at which the recruitment of H is a half of the maximum rate.
κ_2	Number of R_X at which the recruitment of R is a half of the maximum rate
κ_3	Number of R_X at which the recruitment of Z is a half of the maximum rate
ζ	The proportion of the merozoites that cause secondary infections
K	The average number of merozoites released per bursting IRBCs
N	The average number of merozoites released per bursting infected hepatocytes

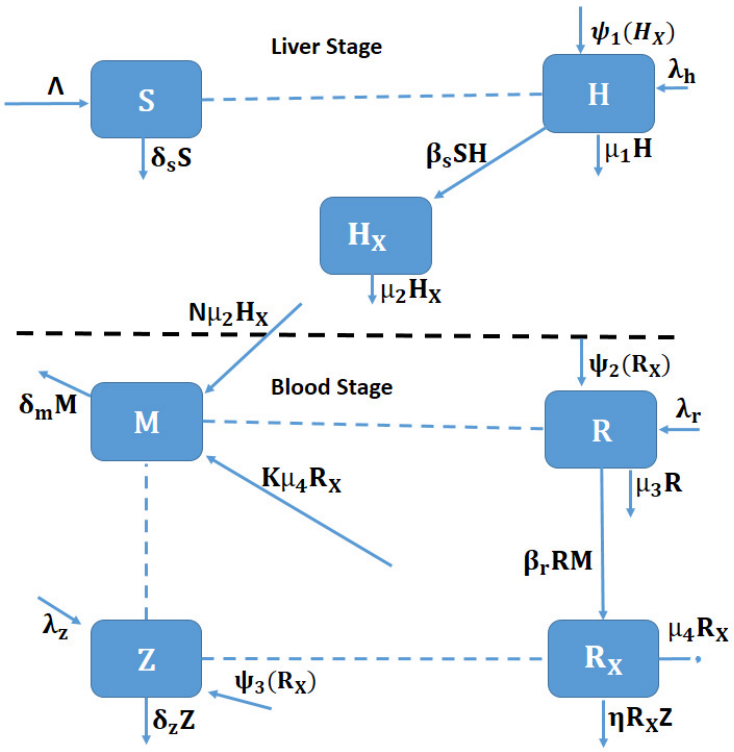

Figure 3.1: Schematic diagram for hepatocytic-erythrocytic and malaria parasite dynamics. The dotted lines without arrows indicate cell-parasite interactions and the solid lines show progression from one compartment to another.

In extending the in-host malaria model by Chiyaka et al. (2008), following model assumptions are made:

1. A total of seven interacting populations are assumed at any given time t. They include susceptible hepatocytes, infected hepatocytes, susceptible red blood cells, infected red blood cells, macrophages, sporozoites and merozoites.
2. Numerous immune cells are elicited during malaria infection. However, only the highly effective macrophages are considered in this model.
3. The red blood cells are recruited at a constant rate from the bone marrow. It is assumed that the background recruitment is accelerated due to the presence of infected red blood cells.
4. Infected red blood cells are eliminated by macrophages
5. Merozoites are generated both from the bursting liver schizonts and blood schizonts.
6. Macrophages are assumed to be recruited at a constant rate from the bone marrow.

7. All model parameters are assumed non-negative.

8. Generation of macrophages is stimulated by the presence of infected red blood cells only.

From the above description of the in-host dynamics of malaria and the representation in Figure 3.1, we derive the following system of ordinary differential equations:

$$\left.\begin{aligned}
\frac{dH}{dt} &= \lambda_h + \frac{\rho_1 H_X}{\kappa_1 + H_X} - \mu_1 H - \beta_s S H, \\
\frac{dH_X}{dt} &= \beta_s S H - \mu_2 H_X, \\
\frac{dR}{dt} &= \lambda_r + \frac{\rho_2 R_X}{\kappa_2 + R_X} - \mu_3 R - \beta_r R M, \\
\frac{dR_X}{dt} &= \beta_r R M - \mu_4 R_X - \eta R_X Z, \\
\frac{dZ}{dt} &= \lambda_z + \frac{\rho_3 R_X}{\kappa_3 + R_X} - \delta_z Z, \\
\frac{dS}{dt} &= \Lambda - \delta_s S - \beta_s S H, \\
\frac{dM}{dt} &= N\mu_2 H_X + K\zeta\mu_4 R_X - \delta_m M - \beta_r R M,
\end{aligned}\right\} \tag{3.1}$$

$$\text{where} \quad H(0) > 0, H_X(0) \geq 0, R(0) > 0, R_X(0) \geq 0, Z(0) > 0, S(0) \geq 0, M(0) \geq 0. \tag{3.2}$$

3.4 Model analysis

In this section, we study whether the formulated model (3.1) is biologically and mathematically meaningful. We establish model equilibrium points and investigate their stability properties.

3.4.1 Well-posedness of the model

For the in-host malaria model (3.1) to be mathematically and biologically meaningful, we need to prove that all the solutions of model (3.1) with nonnegative initial conditions, would remain nonnegative for all time $t \geq 0$. Positivity in the model is shown by proving the following theorem.

Theorem 3.1. *Let the parameters in model (3.1) be positive constants. A nonnegative solution* $(H(t), H_X(t), R(t), R_X(t), Z(t), S(t), M(t))$ *exists for all the state variables with nonnegative initial conditions* $\{H(0) = H_0 \geq 0,\ H_X(0) = H_{X0} > 0,\ R(0) = R_0 > 0,\ R_X(0) = R_{X0} \geq 0,\ Z(0) = Z_0 > 0,\ S(0) = S_0 \geq 0,\ M(0) = M_0 \geq 0\}\ \ \forall t \geq 0.$

Proof: Considering the first equation in system (3.1), let $\psi_1(t) = \rho_1 H_X/(\kappa_1 + H_X)$ so that

$$\frac{\mathrm{d}H}{\mathrm{d}t} = \lambda_h + \psi_1(t) - \mu_1 H - \beta_s SH, \tag{3.3}$$

$$\frac{\mathrm{d}H}{\mathrm{d}t} \geq -(\mu_1 + \beta_s S)H, \tag{3.4}$$

which yields

$$H(t) \geq H(0)\exp\left\{-\left(\int_0^t \beta_s S(s)\, ds + \mu_1 t\right)\right\} > 0. \tag{3.5}$$

Again, from the second equation in system (3.1), we have

$$\frac{\mathrm{d}H_X}{\mathrm{d}t} = \beta_s SH - \mu_2 H_X, \tag{3.6}$$

$$\frac{\mathrm{d}H_X}{\mathrm{d}t} \geq -\mu_2 H_X. \tag{3.7}$$

Upon integrating and applying the initial and conditions in inequality (3.2), we obtain

$$H_X(t) \geq H_X(0)\exp\{-\mu_2 t\} > 0. \tag{3.8}$$

In a similar fashion, this procedure can be applied to all the remaining five equations in system (3.1) so that we have the following solutions:

$$\left.\begin{aligned}
R(t) &\geq R(0)\exp\left\{-\left(\int_0^t \beta_r M(s)\, ds + \mu_3 t\right)\right\} > 0,\\
R_X(t) &\geq R_X(0)\exp\left\{-\left(\int_0^t \eta Z(s)\, ds + \mu_4 t\right)\right\} > 0,\\
Z(t) &\geq Z(0)\exp\{-\delta_z t\} > 0,\\
S(t) &\geq S(0)\exp\left\{-\left(\int_0^t \beta_s H(s)\, ds + \delta_s t\right)\right\} > 0,\\
M(t) &\geq M(0)\exp\left\{-\left(\int_0^t \beta_r R(s)\, ds + \delta_m t\right)\right\} > 0.
\end{aligned}\right\} \tag{3.9}$$

Therefore, the state variables $(H, H_X, R, R_X, Z, S, M)$ of system (3.1) are nonnegative for all time $t > 0$.

3.4.2 Invariant region

System (3.1) describes the dynamics of interaction between the malaria parasites, the hepatocytes, the erythrocytes and macrophages. It is therefore important that it is analysed within a suitable feasible region of biological interest.

Consider the model equations describing hepatocyte dynamics in system (3.1). Let N_H represent the total hepatocyte population, so that $N_H(t) = H(t) + H_X(t)$.

On substituting the derivatives in system (3.1) and simplifying, we have

$$\frac{dN_H}{dt} \leq \lambda_h + \psi_1(t) - \mu_h^* N_H, \tag{3.10}$$

where $\psi_1(t) = \rho_1 H_X/(\kappa_1 + H_X)$ and $\mu_h^* = \min\{\mu_1, \mu_2\}$.

Using integrating factor $e^{\mu_h^* t}$,

$$N_H(t) \leq \frac{\lambda_h}{\mu_h^*} + e^{-\mu_h^* t} \int_0^t \psi_1(\tau) e^{\mu_h^* \tau}\, d\tau + c_1 e^{-\mu_h^* t}, \tag{3.11}$$

where c_1 is a constant of integration. By applying the initial condition $N_H(0) = N_{H0} > 0$ in inequality (3.11), we obtain

$$c_1 = \left(N_H(0) - \frac{\lambda_h}{\mu_h^*}\right) - \int_0^t \psi_1(\tau) e^{-\mu_h^* \tau}\, d\tau. \tag{3.12}$$

Substituting the value of c_1 (in inequality (3.12)) into $N_H(t)$ in inequality (3.11) and simplifying, we get

$$N_H(t) \leq \frac{\lambda_h}{\mu_h^*} + e^{-\mu_h^* t}\left(N_H(0) - \frac{\lambda_h}{\mu_h^*}\right). \tag{3.13}$$

There are two possible cases in analysing the behaviour of $N_H(t)$ in inequality (3.13). In the first case, $N_H(0) > \lambda_h/\mu_h^*$ so that, at time $t = 0$, the right-hand side (RHS) of inequality (3.13) experiences the largest possible value of $N_H(0)$. That is, $N_H(t) \leq N_H(0)$ for all time $t > 0$.

In the second case, we consider $N_H(0) < \lambda_h/\mu_h^*$ so that, the largest possible value of the RHS of inequality (3.13) approaches λ_h/μ_h^* as time t goes to infinity. Thus, $N_H(t) \leq \lambda_h/\mu_h^*$, $\forall t > 0$. From these two cases, we conclude that

$$N_H(t) \leq \max\left\{N_H(0), \frac{\lambda_h}{\mu_h^*}\right\} \quad \text{for all time} \quad t > 0. \tag{3.14}$$

Using the above approach, let the total red blood cells population be $N_R(t)$, so that $N_R(t) = R(t) + R_X(t)$. From the model equations in system (3.1), we have

$$\frac{dN_R}{dt} \leq \lambda_r + \psi_2(t) - \mu_r^* N_R(t), \tag{3.15}$$

where $\psi_2(t) = \rho_2 R_X/(\kappa_2 + R_X)$ and $\mu_r^* = \min\{\mu_3, \mu_4\}$. Upon solving for N_R in inequality (3.15), we have

$$N_R(t) \leq \max\left\{N_R(0), \frac{\lambda_r}{\mu_r^*}\right\} \quad \forall t > 0. \tag{3.16}$$

For the macrophage compartment $Z(t)$, we have

$$\frac{\mathrm{d}Z}{\mathrm{d}t} = \lambda_z + \psi_3(t) - \delta_z Z, \quad \text{for} \quad \psi_3(t) = \frac{\rho_3 R_X}{\kappa_3 + R_X}. \tag{3.17}$$

By integrating factor method, the solution of inequality (3.17) is presented as

$$Z(t) = \frac{\lambda_z}{\delta_z} + e^{-\delta_z t}\int_0^t \psi_3(\tau) e^{\delta_z \tau}\, d\tau + c_2 e^{-\delta_z t}. \tag{3.18}$$

Again, applying the initial conditions in inequality (3.2), the constant of integration c_2 is established to be:

$$c_2 = \left(Z(0) - \frac{\lambda_z}{\delta_z}\right) - \int_0^t \psi_3(\tau) e^{-\delta_z \tau}\, d\tau. \tag{3.19}$$

Therefore,

$$Z(t) \leq \frac{\lambda_z}{\delta_z} + e^{-\delta_z t}\left(Z(0) - \frac{\lambda_z}{\delta_z}\right). \tag{3.20}$$

By employing the same procedure used in inequality (3.13) to equation inequality (3.20), we obtain

$$Z(t) \leq \max\left\{Z(0), \frac{\lambda_z}{\delta_z}\right\} \quad \forall t > 0. \tag{3.21}$$

Finally, let $N_P(t)$ represent the total population of malaria parasites at any time t. That is, $N_P(t) = S(t) + M(t)$ and, from system (3.1),

$$\begin{aligned} \frac{\mathrm{d}N_P}{\mathrm{d}t} &= \Lambda - \delta_s S - \beta_s S H + N\mu_2 H_X + K\zeta\mu_4 R_X - \delta_m M, \\ &\leq \Lambda + N\mu_2 H_X + K\zeta\mu_4 R_X - \delta_p N_P, \quad \text{where} \quad \delta_p = \min\{\delta_s, \delta_m\}. \end{aligned} \tag{3.22}$$

Let $(K\zeta\mu_4 R_X + N\mu_2 H_X) = \psi_4(t)$, so that equation inequality (3.22), becomes

$$\frac{\mathrm{d}N_P}{\mathrm{d}t} \leq \Lambda + \psi_4(t) - \delta_p N_P. \tag{3.23}$$

Upon solving for $N_P(t)$ in inequality (3.23), we get

$$N_p(t) \leq \frac{\Lambda}{\delta_p} + e^{-\delta_p t}\left(N_p(0) - \frac{\Lambda}{\delta_p}\right). \tag{3.24}$$

Clearly, the malaria parasite populations $S(t)$ and $M(t)$ are bounded above. That is,

$$N_P(t) \leq \max\left\{N_P(0), \frac{\Lambda}{\delta_p}\right\} \quad \text{for all time} \quad t > 0. \tag{3.25}$$

Based on this discussion, we have shown the existence of a bounded positive invariant region for system (3.1). Let us denote this region as $\Omega \in \mathbb{R}^7_+$, where

$$\begin{aligned}\Omega = \Bigg\{ &(H, H_X, R, R_X, Z, S, M) \in \mathbb{R}^7_+ : N_P(t) = (S(t) + M(t)) \leq \max\left\{N_P(0), \frac{\Lambda}{\delta_p}\right\}, \\ &N_H(t) = (H(t) + H_X(t)) \leq \max\left\{N_H(0), \frac{\lambda_h}{\mu_h^*}\right\}, Z(t) \leq \max\left\{Z(0), \frac{\lambda_z}{\delta_z}\right\}, \\ &N_R(t) = (R(t) + R_X(t)) \leq \max\left\{N_R(0), \frac{\lambda_r}{\mu_r^*}\right\}\Bigg\}.\end{aligned} \tag{3.26}$$

Moreover, any solution of our system (3.1) which commences in Ω, at any time $t \geq 0$ will always remain confined in that region. We therefore deduce that the region Ω is positively invariant and attracting with respect to malaria model in system (3.1). The in-host malaria model represented by system (3.1) is hence well posed mathematically and biologically.

3.4.3 Existence of disease-free equilibrium point

The disease-free equilibrium point, $\mathscr{E}_0$, is the state in which the human host is free of malaria parasites (or infection). At $\mathscr{E}_0$, the sporozoite recruitment rate, $\Lambda = 0$, and the parasite and host-infected compartments have zero values; that is, $S^* = M^* = R_X^* = H_X^* = 0$. Therefore,

$$\mathscr{E}_0 = (H^*, H_X^*, R^*, R_X^*, Z^*, S^*, M^*) = \left(\frac{\lambda_h}{\mu_1}, 0, \frac{\lambda_r}{\mu_3}, 0, \frac{\lambda_z}{\delta_z}, 0, 0\right). \tag{3.27}$$

3.4.4 In-host basic reproduction number

Epidemiologically, a basic reproduction number is a threshold quantity which represents on average, the number of secondary infections that a single infectious case would generate in a completely susceptible populations over its entire infectious period (Dietz, 1993). A malaria

in-host basic reproduction number is described in Chiyaka et al. (2008) as the number of secondary infected red blood cells produced per primary infected red blood cell in a host at the onset of infection.

Although Molineaux and Dietz (1999) emphasise that basic reproduction number is most meaningful in malaria models describing explicitly infected red blood cells and merozoites populations, the inclusion of the pre-erythrocytic liver stage in the model extends the above description of the in-host basic reproduction number to incorporate the sporozoites populations.

The in-host basic reproduction number, denoted by R_0 is computed using the technique of the next generation matrix approach described in Van den Driessche and Watmough (2002). The analytical computations here are perfomed using Mathematica software (code available in Appendix B). We consider H_X, R_X, S and M as the parasite infested compartments. The subsequent sub-model of system (3.1), is thus given by,

$$\left.\begin{aligned}
\frac{dH_X}{dt} &= \beta_s SH - \mu_2 H_X,\\
\frac{dR_X}{dt} &= \beta_r RM - \mu_4 R_X - \eta R_X Z,\\
\frac{dS}{dt} &= \Lambda - \delta_s S - \beta_s SH,\\
\frac{dM}{dt} &= N\mu_2 H_X + K\zeta\mu_4 R_X - \delta_m M - \beta_r RM.
\end{aligned}\right\} \tag{3.28}$$

Adopting the notations in Van den Driessche and Watmough (2002), we generate two matrices from system (3.28): a nonnegative matrix F of new infections, and a non-singular matrix V, showing the transfer of infections from one compartment to the other. That is,

$$F = \left[\frac{\partial F_i(\mathscr{E}_0)}{\partial x_j}\right] \quad \text{and} \quad V = \left[\frac{\partial V_i(\mathscr{E}_0)}{\partial x_j}\right], \quad \text{for } 1 \leq i, j \leq 4,$$

where,

$$F_i = \begin{pmatrix} \beta_s SH \\ \beta_r RM \\ 0 \\ 0 \end{pmatrix} \quad \text{and} \quad V_i = \begin{pmatrix} \mu_2 H_X \\ \mu_4 R_X + \eta R_X Z \\ -\Lambda + \delta_s S + \beta_s SH \\ -N\mu_2 H_X - K\zeta\mu_4 R_X + \delta_m M + \beta_r RM \end{pmatrix}. \tag{3.29}$$

At disease-free equilibrium point $\mathscr{E}_0$, the matrices F and V are respectively given by

$$F = \begin{pmatrix} 0 & 0 & \beta_s\lambda_h/\mu_1 & 0 \\ 0 & 0 & 0 & \beta_r\lambda_r/\mu_3 \\ 0 & 0 & 0 & 0 \\ 0 & 0 & 0 & 0 \end{pmatrix} \tag{3.30}$$

and

$$V = \begin{pmatrix} \mu_2 & 0 & 0 & 0 \\ 0 & \mu_4+\eta\lambda_z/\delta_z & 0 & 0 \\ 0 & 0 & \delta_s+\beta_s\lambda_h/\mu_1 & 0 \\ -N\mu_2 & -K\zeta\mu_4 & 0 & \delta_m+\beta_r\lambda_r/\mu_3 \end{pmatrix}. \tag{3.31}$$

The inverse of matrix V is hence given by

$$V^{-1} = \begin{pmatrix} \frac{1}{\mu_2} & 0 & 0 & 0 \\ 0 & \frac{\delta_z}{\eta\lambda_z+\delta_z\mu_4} & 0 & 0 \\ 0 & 0 & \frac{1}{\delta_s+\beta_s\lambda_h/\mu_1} & 0 \\ \frac{N\mu_3}{\beta_r\lambda_r+\delta_m\mu_3} & \frac{K\zeta\delta_z\mu_3\mu_4}{(\beta_r\lambda_r+\delta_m\mu_3)(\eta\lambda_z+\delta_z\mu_4)} & 0 & \frac{1}{\delta_m+\beta_r\lambda_r/\mu_3} \end{pmatrix}. \tag{3.32}$$

The next generation matrix G, which is the product of the matrices F and V^{-1}, works out to be

$$G = \begin{pmatrix} 0 & 0 & \frac{\beta_s\lambda_h}{\beta_s\lambda_h+\delta_s\mu_1} & 0 \\ \frac{N\beta_r\lambda_r}{\beta_r\lambda_r+\delta_m\mu_3} & \frac{K\zeta\beta_r\delta_z\lambda_r\mu_4}{(\beta_r\lambda_r+\delta_m\mu_3)(\eta\lambda_z+\delta_z\mu_4)} & 0 & \frac{\beta_r\lambda_r}{\beta_r\lambda_r+\delta_m\mu_3} \\ 0 & 0 & 0 & 0 \\ 0 & 0 & 0 & 0 \end{pmatrix}. \tag{3.33}$$

The in-host basic reproduction number R_0 is the spectral radius of the next generation matrix G. It can clearly be seen that three of the four eigenvalues of matrix G in (3.33) have zero values; that is, $\lambda_1 = \lambda_2 = \lambda_3 = 0$. The fourth and largest nonnegative eigenvalue λ_4 becomes the in-host basic reproduction number. We therefore have

$$\mathrm{R}_0 = \frac{K\beta_r\lambda_r}{(\beta_r\lambda_r+\delta_m\mu_3)}\frac{\zeta\delta_z\mu_4}{(\eta\lambda_z+\delta_z\mu_4)}. \tag{3.34}$$

The terms in R_0 can be interpreted as follows:

(i) The term $K\beta_r\lambda_r/(\beta_r\lambda_r+\delta_m\mu_3)$ represents the expected number of infectious merozoite parasite resulting from bursting blood schizonts at the blood stage of malaria infection.

(ii) The second term $\zeta\delta_z\mu_4/(\eta\lambda_z+\delta_z\mu_4)$ represents the expected proportion of merozoites that participate in the cycle of erythrocytic schizogony.

(iii) Observe that the terms $(\beta_r\lambda_r)/(\beta_r\lambda_r+\delta_m\mu_3)<1$ and $(\delta_z\mu_4)/(\eta\lambda_z+\delta_z\mu_4)<1$. So our $R_0\leq K\zeta$. This implies that the number of secondary infections during malaria infections is largely influenced by the average number of merozoites released K, from a bursting blood schizonts, most of which are responsible for secondary infections at the blood stage.

Despite the inclusion of the liver stage dynamics, it is interesting to observe that the above in-host basic reproduction number and hence the disease progression is heavily driven by the dynamics at the erythrocytic stage. This result is consistent with the current and past malaria chemotherapy research and development, which is heavily inclined towards the symptomatic blood stage of infection.

In the sections that follow, both the local stability and global stability of the disease-free equilibrium point $\mathscr{E}_0$ of system (3.1) are established.

3.4.5 Local stability of the disease-free equilibrium point, $\mathscr{E}_0$

To bring malaria infection under control, there is a need to identify disease transmission parameters that will guarantee the existence of a stable disease-free equilibrium point (Chiyaka et al., 2008). The disease-free equilibrium point $\mathscr{E}_0$ is said to be locally asymptotically stable if the eigenvalues of the Jacobian matrix of system (3.1), evaluated at $\mathscr{E}_0$ have negative real parts.

The Jacobian matrix of system (3.1), evaluated at the disease-free equilibrium point $\mathscr{E}_0$ is given by

$$J_1(\mathscr{E}_0)=\begin{pmatrix} -\mu_1 & 0 & 0 & 0 & 0 & -\frac{\beta_s\lambda_h}{\mu_1} & 0 \\ 0 & -\mu_2 & 0 & 0 & 0 & \frac{\beta_s\lambda_h}{\mu_1} & 0 \\ 0 & 0 & -\mu_3 & \frac{\rho_2}{\kappa_2} & 0 & 0 & -\frac{\beta_r\lambda_r}{\mu_3} \\ 0 & 0 & 0 & -\frac{\eta\lambda_z}{\delta_z}-\mu_4 & 0 & 0 & \frac{\beta_r\lambda_r}{\mu_3} \\ 0 & 0 & 0 & \rho_3/\kappa_3 & -\delta_z & 0 & 0 \\ 0 & 0 & 0 & 0 & 0 & -\frac{\beta_s\lambda_h}{\mu_1}-\delta_s & 0 \\ 0 & N\mu_2 & 0 & K\zeta\mu_4 & 0 & 0 & -\frac{\beta_r\lambda_r}{\mu_3}-\delta_m \end{pmatrix}. \tag{3.35}$$

Clearly, the first eigenvalue of matrix (3.35), $\lambda_1 = -\mu_1 < 0$. Upon deleting the first row and first column, matrix (3.35) is reduced to the following 6×6 matrix:

$$J_2(\mathscr{E}_0) = \begin{pmatrix} -\mu_2 & 0 & 0 & 0 & \frac{\beta_s \lambda_h}{\mu_1} & 0 \\ 0 & -\mu_3 & \frac{\rho_2}{\kappa_2} & 0 & 0 & -\frac{\beta_r \lambda_r}{\mu_3} \\ 0 & 0 & -\frac{\eta \lambda_z}{\delta_z} - \mu_4 & 0 & 0 & \frac{\beta_r \lambda_r}{\mu_3} \\ 0 & 0 & \rho_3/\kappa_3 & -\delta_z & 0 & 0 \\ 0 & 0 & 0 & 0 & -\frac{\beta_s \lambda_h}{\mu_1} - \delta_s & 0 \\ N\mu_2 & 0 & K\zeta\mu_4 & 0 & 0 & -\frac{\beta_r \lambda_r}{\mu_3} - \delta_m \end{pmatrix}. \tag{3.36}$$

Again, it can easily be seen from matrix (3.36) that the second eigenvalue, $\lambda_2 = -\mu_3 < 0$. We further reduce matrix (3.36) by deleting row two and column two. So,

$$J_3(\mathscr{E}_0) = \begin{pmatrix} -\mu_2 & 0 & 0 & \frac{\beta_s \lambda_h}{\mu_1} & 0 \\ 0 & -\frac{\eta \lambda_z}{\delta_z} - \mu_4 & 0 & 0 & \frac{\beta_r \lambda_r}{\mu_3} \\ 0 & \rho_3/\kappa_3 & -\delta_z & 0 & 0 \\ 0 & 0 & 0 & -\frac{\beta_s \lambda_h}{\mu_1} - \delta_s & 0 \\ N\mu_2 & K\zeta\mu_4 & 0 & 0 & -\frac{\beta_r \lambda_r}{\mu_3} - \delta_m \end{pmatrix}. \tag{3.37}$$

From column 3 in matrix (3.37), $\lambda_3 = -\delta_z < 0$. This process continues and the matrix (3.37) is further reduced to J_4 by deleting the elements in row three and column three.

$$J_4(\mathscr{E}_0) = \begin{pmatrix} -\mu_2 & 0 & \frac{\beta_s \lambda_h}{\mu_1} & 0 \\ 0 & -\frac{\eta \lambda_z}{\delta_z} - \mu_4 & 0 & \frac{\beta_r \lambda_r}{\mu_3} \\ 0 & 0 & -\frac{\beta_s \lambda_h}{\mu_1} - \delta_s & 0 \\ N\mu_2 & K\zeta\mu_4 & 0 & -\frac{\beta_r \lambda_r}{\mu_3} - \delta_m \end{pmatrix}. \tag{3.38}$$

From the third row of matrix (3.38), it can easily be seen that $\lambda_4 = -(\beta_s \lambda_h/\mu_1 + \delta_s) < 0$.

Finally, we reduce the matrix (3.38) to J_5, by deleting row three and column three. So,

$$J_5(\mathscr{E}_0) = \begin{pmatrix} -\mu_2 & 0 & 0 \\ 0 & -\frac{\eta \lambda_z}{\delta_z} - \mu_4 & \frac{\beta_r \lambda_r}{\mu_3} \\ N\mu_2 & K\zeta\mu_4 & -\frac{\beta_r \lambda_r}{\mu_3} - \delta_m \end{pmatrix}. \tag{3.39}$$

From row one of matrix (3.39), the fifth eigenvalue $\lambda_5 = -\mu_2 < 0$.

The remaining two eigenvalues of matrix (3.35) can be obtained by reducing matrix (3.39) into the following 2×2 matrix:

$$J_6(\mathscr{E}_0) = \begin{pmatrix} -\frac{\eta\lambda_z}{\delta_z} - \mu_4 & \frac{\beta_r\lambda_r}{\mu_3} \\ K\zeta\mu_4 & -\frac{\beta_r\lambda_r}{\mu_3} - \delta_m \end{pmatrix}. \tag{3.40}$$

Using the variable λ, the characteristic polynomial associated with matrix (3.40) is

$$p(\lambda) = \lambda^2 + B_1\lambda + B_0, \tag{3.41}$$

where

$$B_1 = \delta_m + \frac{\eta\lambda_z}{\delta_z} + \frac{\beta_r\lambda_r}{\mu_3} + \mu_4 \quad \text{and} \tag{3.42}$$

$$B_0 = \frac{\eta\delta_m\lambda_z}{\delta_z} + \frac{\eta\beta_r\lambda_r\lambda_z}{\delta_z\mu_3} + \delta_m\mu_4 + \frac{\beta_r\lambda_r\mu_4}{\mu_3} - \frac{K\zeta\beta_r\lambda_r\mu_4}{\mu_3}. \tag{3.43}$$

The characteristic polynomial (3.41) has negative roots (eigenvalues) if $B_1 > 0$ and $B_0 > 0$. The coefficient B_1 in equation (3.42) is clearly positive ($B_1 > 0$). We now need to show that B_0 in equation (3.43) is strictly positive if $\mathrm{R}_0 < 1$. This is done by expressing the coefficient term B_0 in terms of model R_0 as follows:

$$\begin{aligned} B_0 &= \frac{1}{\delta_z\mu_3}\left[(\mu_4\delta_z + \eta\lambda_z)(\beta_r\lambda_r + \delta_m\mu_3) - K\zeta\beta_r\delta_z\lambda_r\mu_4\right], \\ &= \frac{1}{\delta_z\mu_3}\left[(\mu_4\delta_z + \eta\lambda_z)(\beta_r\lambda_r + \delta_m\mu_3)\left[1 - \frac{K\zeta\beta_r\delta_z\lambda_r\mu_4}{(\mu_4\delta_z + \eta\lambda_z)(\beta_r\lambda_r + \delta_m\mu_3)}\right]\right], \\ &= \frac{(\mu_4\delta_z + \eta\lambda_z)(\beta_r\lambda_r + \delta_m\mu_3)}{\delta_z\mu_3}[1 - \mathrm{R}_0]. \end{aligned} \tag{3.44}$$

It can clearly be seen from equation (3.44) that the coefficient B_0 is positive if and only if $\mathrm{R}_0 < 1$. We have thus established the following result.

Theorem 3.2. *The disease-free equilibrium point $\mathscr{E}_0$ is locally asymptotically stable in Ω if $\mathrm{R}_0 < 1$. If $\mathrm{R}_0 > 1$, then $\mathscr{E}_0$ is unstable.*

Biologically, Theorem 3.2 implies that malaria infection can be eliminated from the human host when $\mathrm{R}_0 < 1$. To ensure that elimination of malaria is independent of the initial sizes of the subpopulations, it is necessary to show that $\mathscr{E}_0$ is globally asymptotically stable in Ω, where the model is mathematically and biologically sensible.

3.4.6 Global asymptotic stability of the disease-free equilibrium point, $\mathscr{E}_0$

Using the results obtained in Kamgang and Sallet (2005), we show that the malaria-free equilibrium point $\mathscr{E}_0$ is globally asymptotically stable when the in-host basic reproduction number is less than unity ($R_0 < 1$). We begin by rewriting system (3.1) in pseudo-triangular form as follows:

$$\begin{aligned}\dot{X}_1 &= A_1(X)(X_1 - X_1^*) + A_2(X)X_2,\\ \dot{X}_2 &= A_3(X)X_2,\end{aligned}$$

where X_1 is the vector representing the state of different compartment of liver and blood cells that are not infected and do not transmit malaria infections. X_2 represents the states of malaria parasites and host's cells that are responsible for disease transmission. Hence,

$$X = (X_1, X_2), X_1 = (H, R, Z), X_2 = (H_X, R_X, S, M) \text{ and } X_1^* = \left(\frac{\lambda_h}{\mu_1}, \frac{\lambda_r}{\mu_3}, \frac{\lambda_z}{\delta_z}\right).$$

From the subsystem X_1, we have

$$A_1(X) = \begin{pmatrix} -\mu_1 & 0 & 0 \\ 0 & -\mu_3 & 0 \\ 0 & 0 & -\delta_z \end{pmatrix} \text{ and } A_2(X) = \begin{pmatrix} \frac{\rho_1}{\kappa_1} & 0 & -\frac{\lambda_h}{\mu_1}\beta_s & 0 \\ 0 & \frac{\rho_2}{\kappa_2} & 0 & -\frac{\lambda_r}{\mu_3}\beta_r \\ 0 & \frac{\rho_3}{\kappa_3} & 0 & 0 \end{pmatrix}.$$

A direct computation indicates that the eigenvalues of matrix $A_1(X)$ are real and negative. This shows that the system $\dot{X}_1 = A_1(X)(X_1 - X_1^*) + A_2(X)X_2$ is globally asymptotically stable at the disease-free equilibrium point, $\mathscr{E}_0$. Similarly, the subsystem $\dot{X}_2$ gives rise to the following matrix $A_3(X)$:

$$A_3(X) = \begin{pmatrix} -\mu_2 & 0 & \beta_s\frac{\lambda_h}{\mu_1} & 0 \\ 0 & -(\eta\frac{\lambda_z}{\delta_z} + \mu_4) & 0 & \beta_r\frac{\lambda_r}{\mu_3} \\ 0 & 0 & -(\beta_s\frac{\lambda_h}{\mu_1} + \delta_s) & 0 \\ N\mu_2 & K\zeta\mu_4 & 0 & -(\beta_r\frac{\lambda_r}{\mu_3} + \delta_m) \end{pmatrix}. \tag{3.45}$$

It can clearly be seen that $A_3(X)$ is a Metzler matrix: all the off-diagonal elements of $A_3(X)$ are nonnegative. In order to establish the global stability of the disease-free equilibrium point, we need to show that the matrix $A_3(X)$ is Metzler stable by providing a proof for the following lemma:

Lemma 3.1. *Let $\mathbb{M}$ be a square Metzler matrix which is block decomposed:*

$$\mathbb{M} = \begin{pmatrix} A & B \\ C & D \end{pmatrix}, \tag{3.46}$$

where A and D are square matrices. The matrix $\mathbb{M}$ is Metzler stable if and only if A and $D - CA^{-1}B$ are Metzler stable.

In our case, matrix $\mathbb{M}$ is represented by matrix A_3 in matrix (3.45) so that,

$$\begin{aligned} A &= \begin{pmatrix} -\mu_2 & 0 \\ 0 & -\left(\eta\frac{\lambda_z}{\delta_z} + \mu_4\right) \end{pmatrix}, \quad B = \begin{pmatrix} \beta_s\frac{\lambda_h}{\mu_1} & 0 \\ 0 & \beta_r\frac{\lambda_r}{\mu_3} \end{pmatrix}, \\ C &= \begin{pmatrix} 0 & 0 \\ N\mu_2 & K\zeta\mu_4 \end{pmatrix} \text{ and } \quad D = \begin{pmatrix} -\left(\beta_s\frac{\lambda_h}{\mu_1} + \delta_s\right) & 0 \\ 0 & -\left(\beta_r\frac{\lambda_r}{\mu_3} + \delta_m\right) \end{pmatrix}. \end{aligned} \tag{3.47}$$

Upon computation in Mathematica software, we obtain

$$D - CA^{-1}B = \begin{pmatrix} -\omega_1 & 0 \\ \omega_2 & -\omega_3 \end{pmatrix}, \tag{3.48}$$

where $\omega_1 = \delta_s + \beta_s(\lambda_h/\mu_1)$, $\omega_3 = \delta_m + \beta_r\lambda_r(\eta\lambda_h + (1-K\zeta)\delta_z\mu_4)/\mu_3(\eta\lambda_z + \delta_z\mu_4)$ and $\omega_2 = N\beta_s\lambda_h/\mu_1$.

For the matrix $D - CA^{-1}B$ to be Metzler stable, ω_3 should be strictly nonnegative. Therefore, the expression in the numerator

$$\beta_r\lambda_r(\eta\lambda_h + (1-K\zeta)\delta_z\mu_4) \geq 0. \tag{3.49}$$

Upon simplification of inequality (3.49),

$$\begin{aligned} K\zeta\beta_r\lambda_r\delta_z\mu_4 &\leq \beta_r\lambda_r(\eta\lambda_h + \delta_z\mu_4), \\ \left(\frac{\beta_r\lambda_r + \delta_m\mu_3}{\beta_r\lambda_r}\right)\left(\frac{K\zeta\beta_r\lambda_r\delta_z\mu_4}{(\beta_r\lambda_r + \delta_m\mu_3)(\eta\lambda_z + \delta_z\mu_4)}\right) &\leq 1, \\ \left(\frac{\beta_r\lambda_r + \delta_m\mu_3}{\beta_r\lambda_r}\right)\mathrm{R}_0 &\leq 1, \\ \mathrm{R}_0 \leq \frac{\beta_r\lambda_r}{\beta_r\lambda_r + \delta_m\mu_3} &\leq 1. \end{aligned}$$

It is clearly seen that the matrix A in system (3.47) is Metzler stable. However, the matrix $D - CA^{-1}B$ is Metzler stable if and only if $\mathrm{R}_0 < 1$. From Lemma 3.1, the following theorem is deduced:

Theorem 3.3. *The malaria-free equilibrium point $\mathscr{E}_0$ of system (3.1) is globally asymptotically stable if the threshold quantity $\mathrm{R}_0 < 1$.*

The above result is quite significant in malaria control. The global stability of the disease-free status would be guaranteed if and only if the in-host basic reproduction number R_0 is less than one. Malaria intervention should therefore focus on eliminating infected erythrocytes and/or malaria merozoites that are responsible for erythropoiesis cycle and invasions at the blood stage.

3.4.7 Endemic equilibrium point analysis

When the in-host basic reproduction number R_0 is greater than one $\mathrm{R}_0 > 1$, the stability of the disease-free equilibrium point $\mathscr{E}_0$ is violated. A different equilibrium state termed the endemic equilibrium point is achieved. By equating to zero the RHS of system (3.1) we have:

$$\lambda_h + \frac{\rho_1 H_X}{\kappa_1 + H_X} - \mu_1 H - \beta_s S H = 0, \tag{3.50}$$

$$\beta_s S H - \mu_2 H_X = 0, \tag{3.51}$$

$$\lambda_r + \frac{\rho_2 R_X}{\kappa_2 + R_X} - \mu_3 R - \beta_r R M = 0, \tag{3.52}$$

$$\beta_r R M - \mu_4 R_X - \eta R_X Z = 0, \tag{3.53}$$

$$\lambda_z + \frac{\rho_3 R_X}{\kappa_3 + R_X} - \delta_z Z = 0, \tag{3.54}$$

$$\Lambda - \delta_s S - \beta_s S H = 0, \tag{3.55}$$

$$N\mu_2 H_X + K\zeta\mu_4 R_X - \delta_m M - \beta_r R M = 0. \tag{3.56}$$

Solving for the state variables R, H, Z, S, M in terms of the infected states H_X and R_X, in equations (3.50)-(3.56), we obtain the endemic state $\mathscr{E}_1 = (H^*, H_X^*, R^*, R_X^*, Z^*, S^*, M^*)$,

where

$$H^* = f_H(H_X^*) = \frac{1}{\mu_1}\left\{\lambda_h + \frac{\rho_1 H_X^*}{\kappa_1 + H_X^*} - \mu_2 H_X^*\right\}, \tag{3.57}$$

$$S^* = f_S(H_X^*) = \frac{\mu_h \mu_2 H_X^*}{\beta_s\left(\lambda_h + \rho_1 H_X^*/(\kappa_1 + H_X^*) - \mu_2 H_X^*\right)}, \tag{3.58}$$

$$R^* = f_R(R_X^*) = \frac{1}{\mu_3}\left\{\lambda_r + \frac{\rho_2 R_X^*}{\kappa_2 + R_X^*} - \mu_4 R_X^*\right\}, \tag{3.59}$$

$$M^* = f_M(R_X^*) = \mu_3\left(R_X^*\mu_4 + \frac{\eta R_X^*\left(\rho_3 R_X^*/(\kappa_3 + R_X^*) + \lambda_z\right)}{\mu_h}\right). \tag{3.60}$$

$$Z^* = f_Z(R_X^*) = \frac{1}{\delta_z}\left\{\lambda_z + \frac{\rho_3 R_X^*}{\kappa_3 + R_X^*}\right\}, \tag{3.61}$$

Substituting equations (3.57) and (3.58) into equation (3.51), and simplifying, we obtain the following cubic equation:

$$\alpha_3 H_X^{*3} + \alpha_2 H_X^{*2} + \alpha_1 H_X^* + \alpha_0 = 0, \tag{3.62}$$

where

$$\begin{aligned}
\alpha_3 =& \mu_2^2 \beta_s > 0,\\
\alpha_2 =& \mu_2\left(\mu_h(-\delta_s) - \beta_s(\lambda_h - \kappa_1\mu_2 + \Lambda + \rho_1)\right),\\
\alpha_1 =& \beta_s\left(\lambda_h(\Lambda - \kappa_1\mu_2) + \Lambda(\rho_1 - \kappa_1\mu_2)\right) - \kappa_1\mu_h\mu_2\delta_s, \quad \text{and}\\
\alpha_0 =& \kappa_1\Lambda\lambda_h\beta_s > 0.
\end{aligned}$$

The number and nature of the roots of equation (3.62) are determined by the following discriminant (Schmidt and Hess, 1988):

$$\Delta = 18\alpha_3\alpha_2\alpha_1\alpha_0 - 4{\alpha_2}^3\alpha_0 + {\alpha_2}^2{\alpha_1}^2 - 4\alpha_3{\alpha_1}^3 - 27{\alpha_3}^2{\alpha_0}^2. \tag{3.63}$$

So

(i) $\Delta = 0$, then equation (3.62) has a multiple real roots and only one endemic equlibrium would exist,

(ii) $\Delta < 0$, then equation (3.62) has 1 real root and a complex conjugate root hence only one endemic equilibrium,

(iii) $\Delta > 0$, then equation (3.62) has 3 distinct real roots and so there are more than one endemic equilibrium point when $R_0 > 1$ for system (3.1).

Analysis under equation (3.63) implies that, in the absence of external interventions in the form of anti-malarial treatment, there will always be some infected hepatocytes during malaria infection. We further proceed to evaluate the possible values of the state variable R_X at equilibrium point by substituting expressions in equations (3.59), (3.60) and (3.61) into equation (3.53). After simplification in Mathematica software, we obtain the following quartic equation:

$$R_X^*(\theta_3 R_X^{*3} + \theta_2 R_X^{*2} + \theta_1 R_X^* + \theta_0) = 0, \tag{3.64}$$

where

$$\begin{aligned}
\theta_3 =& -\mu_4\beta_r(\mu_h\mu_4 + \eta(\rho_3 + \lambda_z)) < 0,\\
\theta_2 =& \eta\rho_3(\beta_r(-\kappa_2\mu_4 + \rho_2 + \lambda_r) - 1) + (\mu_h\mu_4 + \eta\lambda_z)(\beta_r(-(\kappa_2 + \kappa_3)\mu_4 + \rho_2 + \lambda_r) - 1),\\
\theta_1 =& \eta\kappa_2\rho_3(\beta_r\lambda_r - 1) - (\mu_h\mu_4 + \eta\lambda_z)(\kappa_3 + \kappa_2(\beta_r(\kappa_3\mu_4 - \lambda_r) + 1) + \kappa_3(-\beta_r)(\rho_2 + \lambda_r)),\\
\theta_0 =& \kappa_2\kappa_3(\beta_r\lambda_r - 1)(\mu_h\mu_4 + \eta\lambda_z).
\end{aligned}$$

Clearly, $R_X^* = 0$ or

$$\theta_3 R_X^{*3} + \theta_2 R_X^{*2} + \theta_1 R_X^* + \theta_0 = 0. \tag{3.65}$$

The state $R_X^* = 0$ corresponds to a scenario in which there are no parasite infected red blood cells. This could signify the liver stage of parasite development so that an endemic state $(H^*, H_X^*, R^*, 0, 0, S^*, 0)$ exists. Alternatively, $R_X^* = 0$ could correspond to the disease-free equilibrium point $\mathscr{E}_0$ for system (3.1).

The roots of the cubic equation (3.65) are given as

$$R_{X1}^* = -\frac{\kappa_3(\mu_h\mu_4 + \eta\lambda_z)}{\eta\rho_3 + \mu_h\mu_4 + \eta\lambda_z} < 0, \tag{3.66}$$

$$R_{X2,3}^* = \frac{(\beta_r\lambda_r - \kappa_2\mu_4\beta_r + \rho_2\beta_r - 1) \pm \sqrt{\Theta}}{2\mu_4\beta_r}, \tag{3.67}$$

where

$$\Theta = 4\mu_4\beta_r(\kappa_2\beta_r\lambda_r - \kappa_2) + (\beta_r\lambda_r - \kappa_2\mu_4\beta_r + \rho_2\beta_r - 1)^2. \tag{3.68}$$

The root $R_{X1}^* < 0$ should be ignored since all the model state variables are nonnegative for all time $t \geq 0$. This leaves $R_{X2,3}^*$ as the only two possible roots of equation (3.65).

From the above discussion, system (3.1) could experience a single endemic state or multiple states subject to the roots of equations (3.62) and (3.64). If $R_{X2,3}^*$ are real and positive then one or two endemic equilibrium points are possible for system (3.1). It is thus evident that

the explicit form of the endemic equilibrium point for model (3.1) is cumbersome. We shall therefore show its existence numerically based on certain choice of parameter values in subsection 3.5.3. Note that case (iii) of equation (3.63) indicates the possibility of having multiple endemic equilibrium points and hence the likelihood of experiencing a backward bifurcation phenomenon.

3.5 Numerical simulation and discussions

In this section, we provide some numerical simulations to illustrate the behaviour of system (3.1). We carry out model sensitivity analysis and investigate parameter influence on the dynamics of erythrocytes, hepatocytes, macrophages and malaria parasites under different conditions on the in-host basic reproduction number, R_0.

3.5.1 Sensitivity analysis

In epidemic modelling, sensitivity analysis is performed to investigate model parameters with significant influence on R_0, and hence on the transmission and the spread of the disease under study (Chitnis et al., 2008; Okosun and Makinde, 2012; Olaniyi and Obabiyi, 2014). Following Arriola and Hyman (2005), the normalised forward-sensitivity index of a variable, Δ, which depends differentiably on a parameter, α, is defined as

$$\Gamma_{\alpha}^{\Delta} = \frac{\partial \Delta}{\partial \alpha} \times \frac{\alpha}{\Delta}. \tag{3.69}$$

Using the formulation in equation (3.69), and the in-host basic reproduction number R_0 in equation (3.34), we obtain the following expressions for normalised forward sensitivity indices of R_0 relative to model parameters.

$$\left.\begin{aligned}
\Gamma_{K}^{R_0} &= +1, & \Gamma_{\zeta}^{R_0} &= +1,\\
\Gamma_{\beta_r}^{R_0} &= \frac{\mu_3\delta_m}{\mu_3\delta_m+\beta_r\lambda_r}, & \Gamma_{\lambda_r}^{R_0} &= \frac{\mu_3\delta_m}{\mu_3\delta_m+\beta_r\lambda_r},\\
\Gamma_{\mu_4}^{R_0} &= \frac{\eta\lambda_z}{\mu_4\delta_z+\eta\lambda_z}, & \Gamma_{\mu_3}^{R_0} &= -\frac{\mu_3\delta_m}{\mu_3\delta_m+\beta_r\lambda_r},\\
\Gamma_{\delta_z}^{R_0} &= -\frac{\eta\lambda_z}{\mu_4\delta_z+\eta\lambda_z}, & \Gamma_{\lambda_z}^{R_0} &= \frac{\eta\lambda_z}{\mu_4\delta_z+\eta\lambda_z},\\
\Gamma_{\eta}^{R_0} &= -\frac{\eta\lambda_z}{\mu_4\delta_z+\eta\lambda_z}, & \Gamma_{\delta_m}^{R_0} &= -\frac{\mu_3\delta_m}{\mu_3\delta_m+\beta_r\lambda_r}.
\end{aligned}\right\} \tag{3.70}$$

The numerical sensitivity indices (SI) are calculated using Mathematica software and the results summarised in Table 3.3. Note that, due to limited data on in-host dynamics, all the parameter values (see Table 3.4) used in evaluating the sensitivity indices are obtained from literature.

Table 3.3: Sensitivity indices of R_0 to the model parameters

Parameter	SI	Parameter	SI
K	+1.0000	ζ	+1.0000
β_r	+0.920422	μ_3	-0.920422
λ_r	+0.920422	λ_z	-0.998585
μ_4	+0.998585	η	-0.998585
δ_z	+0.998585	δ_m	-0.920422

Table 3.4: Parameter values used in the numerical simulations of system (3.1)

Parameter	Value	Unit	Source
Λ	20	$sporozoites/day$	(Selemani et al., 2016)
δ_z	0.05	day^{-1}	(Selemani et al., 2016)
δ_s	1.2×10^{-11}	day^{-1}	(Selemani et al., 2016)
η	10^{-10}	$cells/\mu l/day$	(Hetzel and Anderson, 1996)
λ_h	3×10^{3}	$cells/\mu l/day$	(Selemani et al., 2016)
ρ_1	2.5×10^{-5}	day^{-1}	(Chiyaka et al., 2008)
μ_1	0.029	day^{-1}	(Selemani et al., 2016)
ρ_2	2.5×10^{-5}	day^{-1}	(Chiyaka et al., 2008)
β_s	1.0×10^{-6}	$sporozoites/day$	(Selemani et al., 2016)
ρ_3	2.5×10^{-5}	day^{-1}	(Chiyaka et al., 2008)
μ_2	0.02	day^{-1}	(Selemani et al., 2016)
κ_1	1	$cells/\mu l$	(Selemani et al., 2017a)
λ_r	4×41500	$cells/\mu l^{-1}/day$	(Li et al., 2011)
ζ	0.726	unitless	(Talman et al., 2004)
μ_3	0.0083	day^{-1}	(Li et al., 2011)
κ_2	1	$cells/\mu l^{-1}$	(Selemani et al., 2017a)
β_r	2.0×10^{-6}	$/merozoites/day$	(Hetzel and Anderson, 1996)
N	10000	Unitless	(Tumwiine et al., 2008)
μ_4	0.025	day^{-1}	(Chiyaka et al., 2008)
κ_3	1	$cells/\mu l^{-1}$	(Selemani et al., 2017a)

Continued on next page

Table 3.4 – *Continued from previous page*

Parameter	Value	Unit	Source
δ_m	48	day^{-1}	(Hetzel and Anderson, 1996)
K	16	Unitless	(Chiyaka et al., 2008)
λ_z	30	$/\mu l^{-1}/day$	(Chiyaka et al., 2008)

A positive sign (+) on the SI indicates that an increase (decrease) in the value of such a parameter increases (decreases) the value of the in-host basic reproduction number R_0 and hence the growth of malaria infection. On the other hand, a negative sign (-) on SI is indicative of a parameter that negatively affects R_0; that is, an increase (decrease) in such a parameter decreases (increases) the value of R_0. In order to eliminate in-host malaria infection, the in-host basic reproduction number should be less that one, that is, $R_0 < 1$.

From Table 3.3, it can clearly be seen that the average number of merozoites released per bursting infected erythrocyte K and the proportion of merozoites that cause secondary invasions at the blood phase ζ, are the two most sensitive parameters in determining model outcomes. They have the highest sensitivity indices of +1.0000. For instance, a 10% increase (decrease) in the value of ζ or K generates a proportional 10% increase (decrease) on in-host basic reproduction number and hence malaria infection.

The parameters λ_z, η, μ_4, δ_z occupy the second rank on influencing the model outcomes. An increase (or decrease) in the parameters μ_4 and δ_z is likely to increase (or decrease) the disease R_0. On the other hand, an increase in λ_z and η has a direct negative influence on disease R_0. Note that a 50% increase (decrease) in the rate of elimination of infected red blood cells at the erythrocytic stage will result into a 49.92925% decrease (increase) in the in-host basic reproduction number and hence the disease progression. Macrophages are highly instrumental in malaria parasite clearance and should be preserved.

The rate of generation of macrophages from the bone marrow, λ_z, together with the rate of phagocytosis of infected red blood cells, η, is likely to decrease proportionally the disease progression when they are increased. With increased λ_z, there would be more macrophages to phagocytose and clear the rapidly growing density of blood schizonts. This would negatively affect the erythrocytic schizogony. Decreased clearance rate by macrophages would only guarantee successful multiplication of the merozoites through the erythrocytic schizogonic cycle. The subsequent result is increased density of merozoites in the host's blood, leading to disease progression to even deadly levels.

The rate of invasion of susceptible erythrocytes by merozoites β_r, and the rate of generation of erythrocytes from the epithelial cells of the host's bone marrow λ_r increased (or decreased) disease R_0 when they are increased (or decreased). Epidemiologically, an improved erythrocyte invasion rate, β_r, is likely to generate even more new blood schizonts. This increases parasitaemia in the human host. A 10% increase (decrease) in β_r would increase (decrease) the threshold parameter R_0 by about +9.2%.

Any therapeutic effort that clears the blood schizonts and the infectious merozoites at the blood stage would definitely guarantee immense reduction in disease R_0. Therefore, an increase in the death rate of infected erythrocytes and that of the merozoites is likely to decrease significantly the in-host basic reproduction number R_0. This can be achieved through the use of effective antimalarials such as ACTs in malaria treatment. Moreover, effective vaccines at the erythrocytic stage could greatly minimize erythrocyte infection rate β_r.

Since the local sensitivity indices are relatively close, we carry out further investigation on parameter influence on disease progression by generating the partial rank correlation coefficients (PRCCs) for each parameter value in disease R_0 in the following section.

3.5.2 Global sensitivity analysis

A global sensitivity analysis (GSA) is performed to examine the response of an epidemic model to parameter variation within a wider range of parameter space (Wu et al., 2013). Applying the approach in Wu et al. (2013), the PRCCs between the in-host basic reproduction number R_0 and each of the parameters in R_0 are derived. Using 1000 simulations per run of the Latin Hypercube Sampling (LHS) scheme (Stein, 1987), the established PRCCs are derived and presented in Figure 3.2.

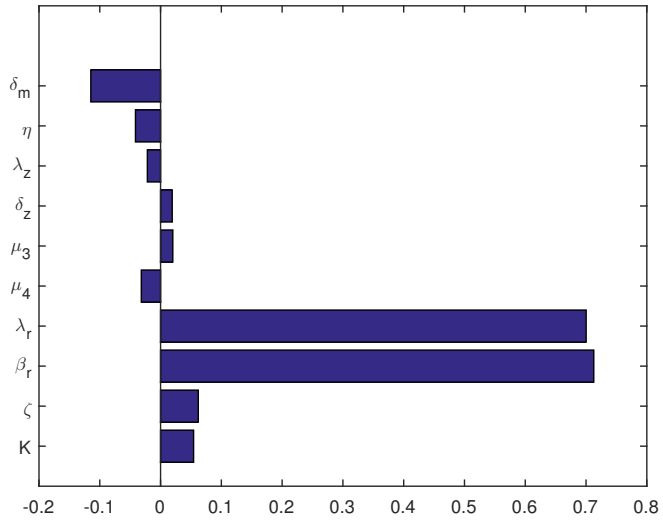

Figure 3.2: Tornado plots of partial rank correlation coefficients (PRCCs) of parameters that influence model R_0 generated using parameter values in Table 3.4. Parameters with $PRCC > 0$ and $PRCC < 0$ increase and decrease disease R_0, respectively.

Parameters with positive PRCC values will increase R_0 when they are increased and vice versa for those with negative PRCC. Unlike the results in Table 3.3, the model parameter with the highest influence on R_0 according to the PRCCs results shown in Figure 3.2 is the rate of invasion of red blood cells by merozoites, β_r. This is followed closely by the recruitment rate of susceptible red blood cells λ_r from the borne marrrow. Both parameters increase R_0 when they are increased. The second set of parameters that also increase (decrease) disease R_0 when they are increased (decreased) are the ζ, K, μ_3 and δ_z, respectively.

The merozoites' death rate δ_m, the death rate of infected red blood cells and the rate of elimination of infected erythrocytes by the macrophages η are shown to have the highest negative influence on disease progression. Although the increase in μ_4 was shown to increase disease progression in Table 3.3, the results from global sensitivity analysis are contradictory. An increase in the death rate of parasitised red blood cells μ_4 decreases parasitaemia and hence disease progression within the human host.

In Figure 3.3, the effects of the two most sensitive parameters (K, ζ) on R_0 are displayed using Monte Carlo simulations (Rubinstein and Kroese, 2016). The results in Figures 3.3 are consistent with those obtained earlier under sensitivity analysis (see Table 3.3). An increase in K, and/or ζ increases R_0 and severity of malaria infection.

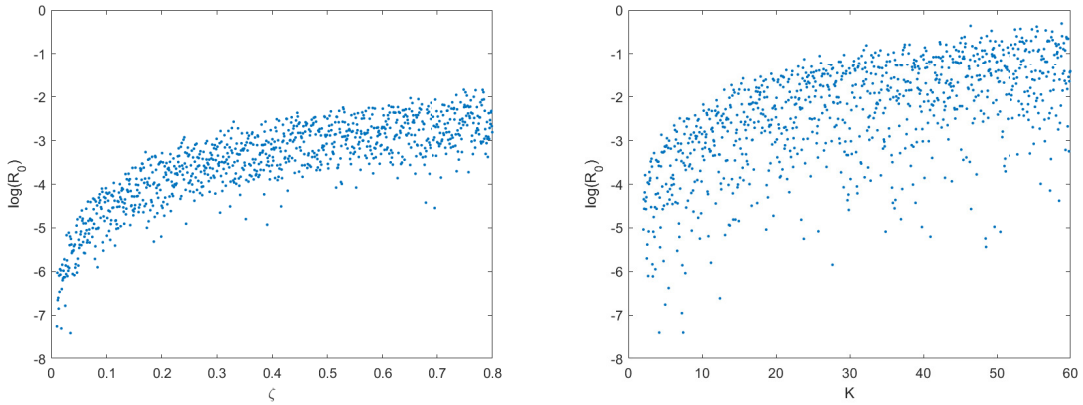

(a) (b)

Figure 3.3: Graphs (a) and (b) show the Monte Carlo simulations for the two parameters with the greatest sensitivity indices in the in-host malaria model (3.1). Parameter values in Table 3.4 and 1,000 simulations per run were used.

Based on these results of sensitivity analysis, we make the following remarks: (1) results of global sensitivity analysis are robust and a lot more realistic for implementation, (2) malaria control should target elimination of merozoites and infected red blood cells, (3) an effective and efficient malaria vaccine that deactivates infectious merozoites could be helpful in limiting erythrocyte invasion rate, and (4) a vaccine that is protective of susceptible erythrocytes could further ensure reduced density of second and future generation of merozoites that are responsible for disease progression.

3.5.3 Numerical results

In this section, numerical simulation of system (3.1) under different values of the threshold parameter R_0 is carried out. The in-host malaria model is solved numerically using the package scipy.integrate.odeint in Python language. A sample code is shown in Appendix B. The simulations are performed to illustrate the possible dynamics of the erythrocytes, the hepatocytes, the malaria parasite and the macrophages when R_0 is less or greater than one. For purposes of these simulations, the initial conditions of the variables are hereby conveniently set. It is noted that different output may be achieved for different initial conditions.

When the in-host basic reproduction number is less than unity ($R_0 < 1$), the dynamics of the different compartments in system (3.1) are as presented in Figures 3.4 and 3.5. At the pre-erythrocytic stage, the density of susceptible hepatocyte initially decline as the density of infected hepatocytes rises due to invasion from malaria sporozoites (see Figure 3.4). The

host's immune system responds to sporozoite invasion by increasing hepatocyte density that levels off at the disease-free equilibrium point $\mathscr{E}_0$ (see Figure 3.4a). As the sporozoites decline to near zero value (see Figure 3.4b), infected hepatocytes decline and stabilise at $\mathscr{E}_0$ in equation (3.27).

At the blood stage, the rising density of infected erythrocytes declines in a similar fashion to that of the infective merozoites when $R_0 < 1$ (see Figure 3.5). The densities of the infected erythrocytes and merozoites approach $\mathscr{E}_0$ asymptotically. On the other hand, it is observed that the density of susceptible red blood cells decreases initially due to infection by merozoites and later rises before it plateaus at $\mathscr{E}_0$ as shown in Figure 3.5.

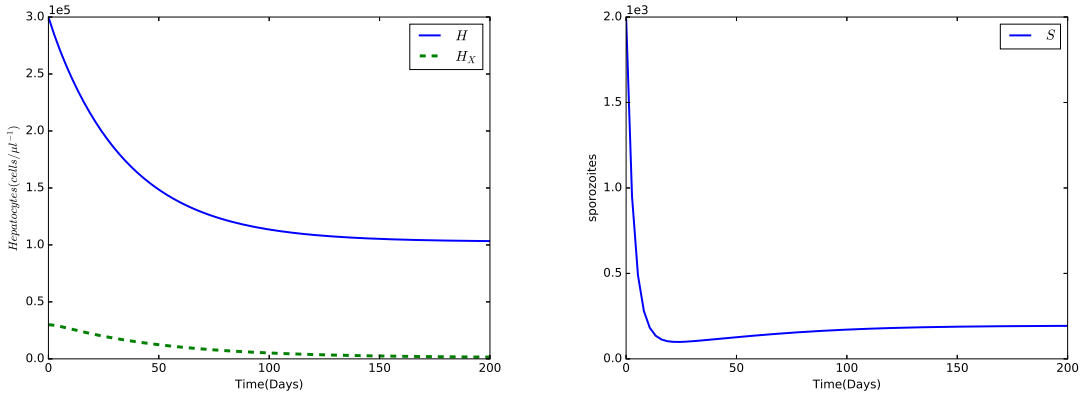

(a) Susceptible and infected hepatocytes

(b) Malaria sporozoites

Figure 3.4: Graphs showing the dynamics of susceptible and infected hepatocytes in the presence of malaria sporozoites when disease $R_0 = 0.8066 < 1$. The initial conditions are: $H0 = 300000$, $H_X0 = 20000$, $R0 = 500000$, $R_X0 = 50$, $Z0 = 300000$, $S0 = 2000$ and $M0 = 70$. Used parameter values are shown in Table 3.4.

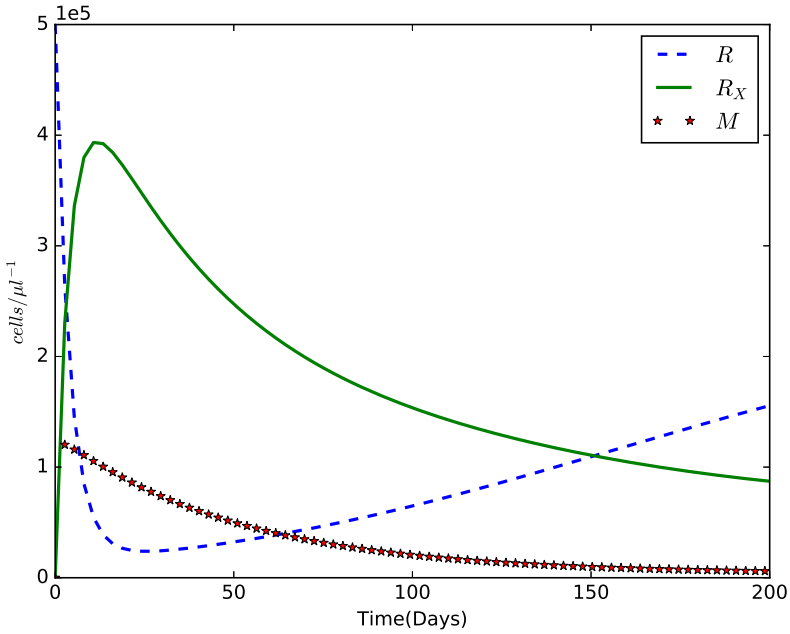

Figure 3.5: Graphs showing the simulation of system 3.1 at the erythrocytic stage when disease $R_0 = 0.8066 < 1$. The chosen initial conditions are $H0 = 300000$, $H_X0 = 20000$, $R0 = 500000$, $R_X0 = 50$, $Z0 = 300000$, $S0 = 2000$, and $M0 = 70$. Model parameter values are shown in Table 3.4.

When $R_0 > 1$, a sharp fall in the density of susceptible hepatocytes in the liver is observed (see Figure 3.6a). This is due to rapid invasion of hepatocytes by the sporozoites. An invasion on susceptible hepatocyte generates a corresponding steady rise in the density of infected hepatocytes (see Figure 3.6b). Owing to natural intervention by the immune cells, the respective decline and rising levels of susceptible and infected hepatocytes level off and remain relatively constant after the third month. More hepatocytes are generated to replace infected ones. There is a steady decline in sporozoite density at the liver stage (see Figure 3.6c). The invaded hepatocytes develop into liver schizonts that burst open to release merozoites and hence the steady decline in sporozoite levels.

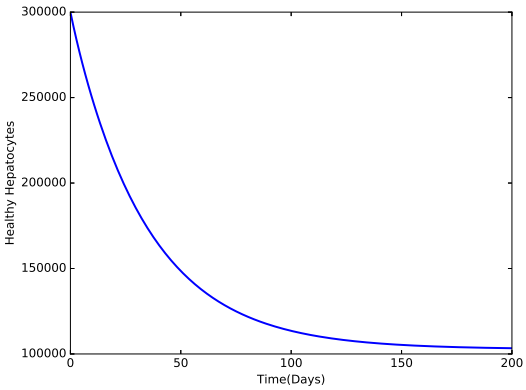

(a) Susceptible hepatocytes

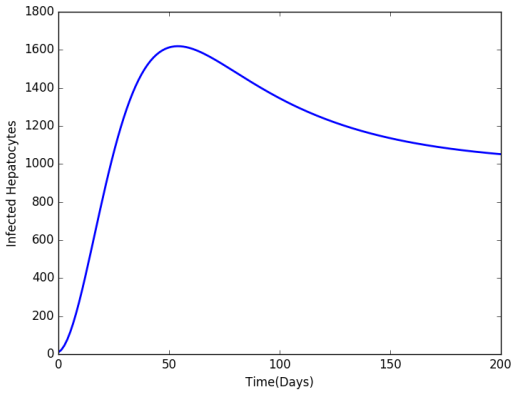

(b) Infected hepatocytes

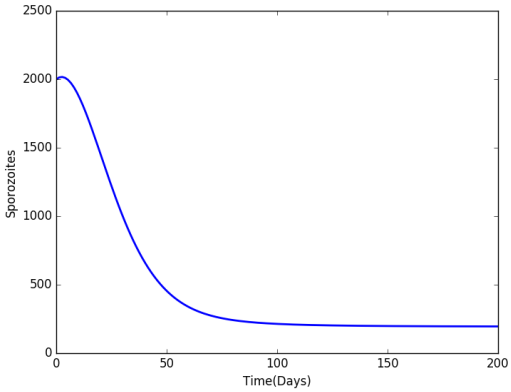

(c) Sporozoites

Figure 3.6: Graphs showing population dynamics at the liver stage when $R_0 = 1.58690 > 1$. Used parameter values are shown in Table 3.4. Chosen initial conditions are: $H0 = 300000$, $H_X0 = 10$, $R0 = 500000$, $R_X0 = 10$, $Z0 = 10$, $S0 = 2000$ and $M0 = 20$.

The severity of malaria infection is most rapid in the first 2 weeks within the host liver as illustrated in Figures 3.6a, 3.6b and 3.6c. This is similar to results in (Selemani et al., 2017a; Tabo et al., 2017). In the absence of clinical intervention, some of the sporozoites remain dormant in the human liver and could cause future malaria infections.

As the liver schizonts release merozoites into the blood stream of the host, a rapid decline in the density of red blood cells is observed (see Figure 3.7a). Merozoites invade susceptible erythrocytes resulting in a corresponding rise in the density of infected erythrocytes as shown in Figure 3.7b.

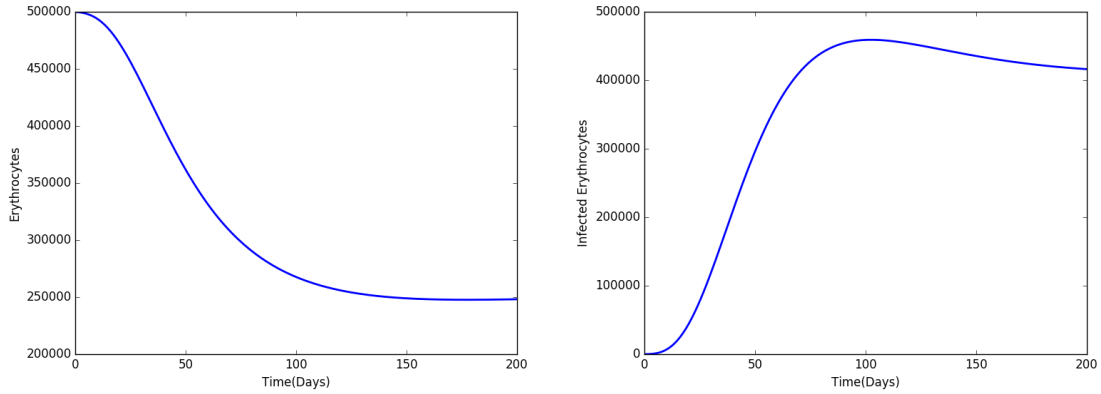

(a) Susceptible erythrocytes

(b) Infected erythrocytes

Figure 3.7: Graphs showing population dynamics of susceptible erythrocytes and infected erythrocytes in the presence of malaria merozoites when $R_0 = 1.58690 > 1$. The values of the mode parameters are shown in Table 3.4.

In Figure 3.8a, there is an early sharp rise in the density of merozoites in the first week of the blood stage. The density remains high for several weeks and does not decline for the entire infection period of one month. A second generation merozoite invades other sets of healthy erythrocyte within minutes, leading to an exponential growth in the density of blood schizonts and hence merozoites in the human blood stream. Without therapeutic intervention, the density of merozoites stabilises several weeks after infection at the endemic equilibrium point. This is consistent with the findings in Chiyaka et al. (2008); Li et al. (2011); Selemani et al. (2016).

The invasion of healthy red blood cells prompts an immune response from host's macrophages. These macrophages phagocyte on the generated blood schizonts. At the onset of erythrocytic infection, several macrophages are generated. The rise in the density of macrophages is proportional to that of infected erythrocytes as shown in Figure 3.8b. This rising density is shown to level off after about 16 days at the endemic equilibrium point. It remains high throughout the infection period.

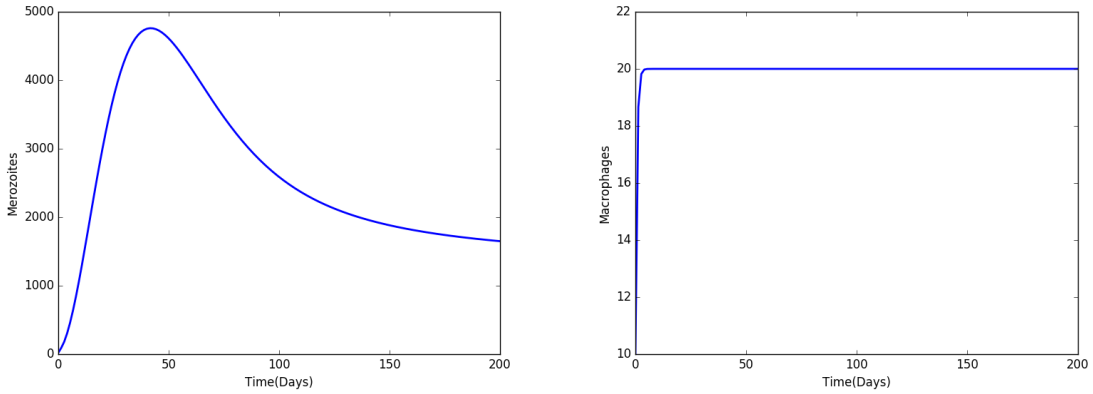

(a) Merozoites (b) Macrophages

Figure 3.8: Graphs showing the population dynamics of (a) merozoites and (b) macrophages during the erythrocytic cycle. $R_0 = 1.58690 > 1$ and the parameter values used are given in Table 3.4.

From these discussions, the following observations are made: (1) if $R_0 < 1$, low level malaria infection can easily be contained by the host's defence mechanism and loss of life is less likely; (2) therapeutically, $R_0 < 1$ may be achieved through quick intervention targeting the blood schizonts and the merozoites responsible for secondary infections during erythrocytic cycle; (3) Figures 3.6, 3.7 and 3.8 shows the existence of in-host malaria endemic equilibrium point.

Hematological parameters such as the density of healthy and infected erythrocytes in malaria hosts have considerable influence on malaria infection and possible impacts (Erhart et al., 2004). According to WHO (WHO, 1990), high hyperparasitaemia causes drastic reduction in concentrations of erythrocytes leading to anaemia among malaria patients (Bashawri et al., 2002; Ekvall, 2003). The impacts of increasing the model parameters δ_m and β_r on healthy and infected red blood cells are as shown in Figures 3.9 and 3.10, respectively.

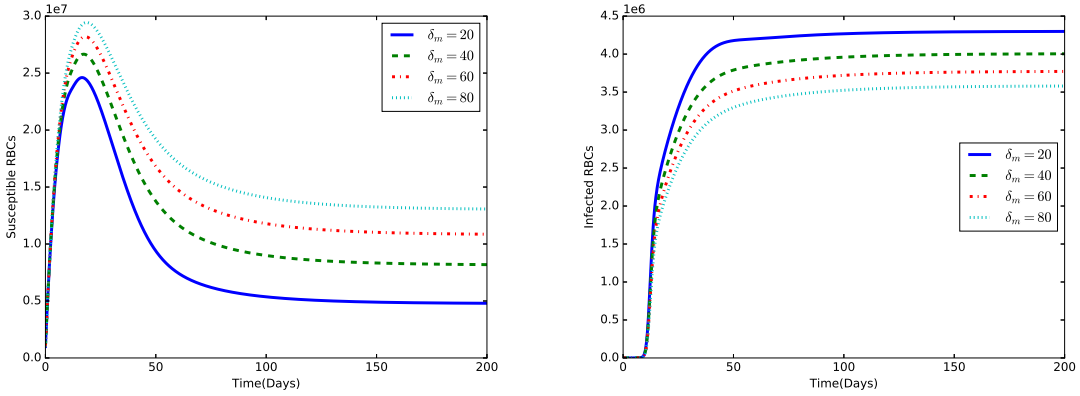

(a) (b)

Figure 3.9: Graphs that show the behaviour of (a) susceptible red blood cells and (b) infected red blood cells. They were obtained by varying the death rate of merozoites δ_m from 20 to 80 in steps of 20, while keeping the other parameters (in Table 3.4) constant.

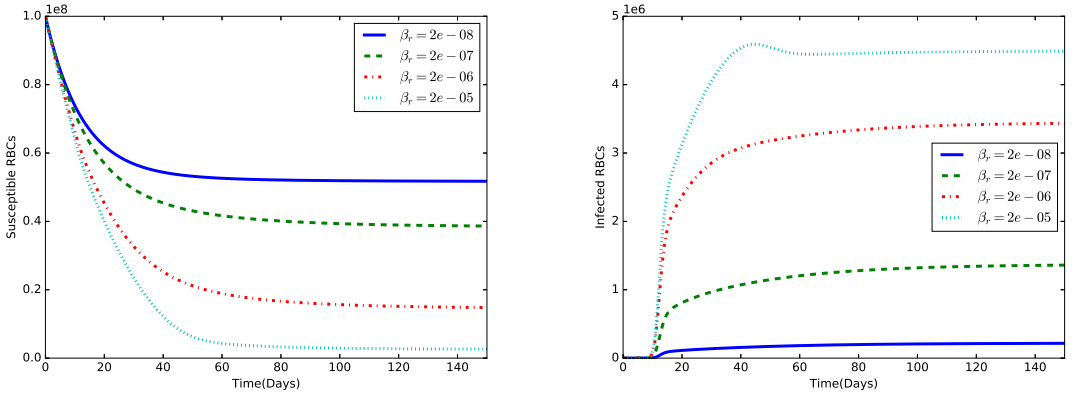

(a) (b)

Figure 3.10: Graphs that show the behaviour of (a) susceptible red blood cells and (b) infected red blood cells. They were obtained by varying the merozoite invasion rate β_r from 2×10^{-8} to 2×10^{-5} in steps of 10^{-1}, while keeping the other parameters (in Table 3.4) constant.

Observe that an increase in the death rate of malaria merozoites δ_m decreases and increases the density of infected erythrocytes and healthy erythrocytes, respectively (see Figures 3.9a and 3.9b). Malaria control should thus target the infectious merozoites at the blood stage. Results in Figure 3.10a indicate that an improved invasion rate by merozoites on susceptible erythrocytes causes more loss in healthy erythrocytes. The reverse effect is observed in Figure 3.10b, where an increase in the rate of infection of healthy erythrocytes produces a

corresponding increase in the density of infected erythrocytes. A keen look at Figure 3.10b reveals that the infected red blood cells (IRBCs) begin to appear after about 10-15 days of initial infection. This is consistent with the incubation period of *P. falciparum* malaria (Collins and Jeffery, 2007).

The severity of malaria infection can easily increase if the density or production of macrophages is compromised (Chiyaka et al., 2008). Figure 3.11b shows a near direct relationship on the density of infected erythrocytes R_X and the death rate of the macrophages δ_z. An increase in the death rate of macrophages would propel erythrocytic schizogony and hence increased merozoite numbers in the blood stream of the human host. A high merozoite density increases the severity of malaria infection. This result is quite vital in malaria intervention, especially with respect to malaria patients who may be suffering from other infections that are deleterious to immune cells. Diseases such as HIV/AIDS greatly weaken the immune system of the patient as important immune cells such as macrophages are destroyed (Honeycutt et al., 2016; Koppensteiner et al., 2012). Macrophages are an important target cells for HIV-1 virus (Shiri et al., 2005a). During malaria infections, such patients often suffer severe malaria and should seek immediate medical attention.

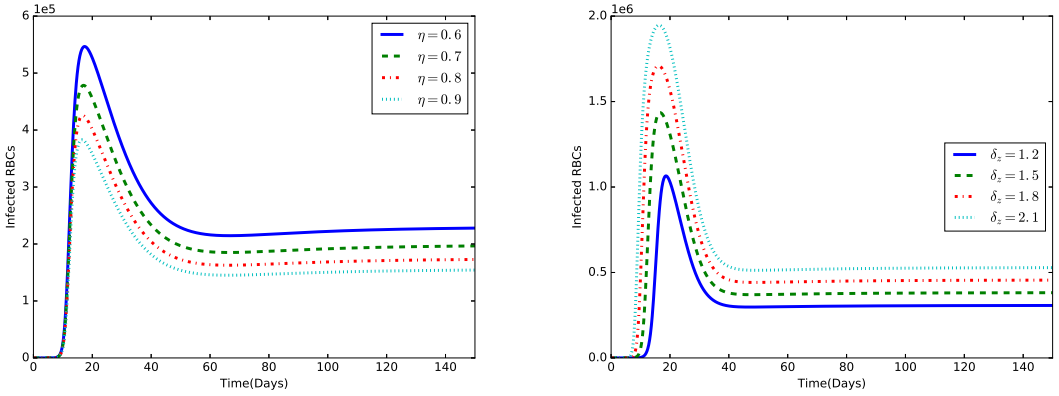

(a) (b)

Figure 3.11: Graphs that show the effect of varying the rate of phagocytosis of infected red blood cells by macrophages, η (in (a)) and the effect of increased decay rate of macrophages δ_z (in (b)), on the dynamics of infected erythrocytes R_X. All parameter values are shown in Table 3.4.

Like the senescent erythrocytes, aberrant infected erythrocytes formed during malaria infection are eliminated phagocytically by the host's macrophage cells in the red pulp of the spleen (Krücken et al., 2005). The phagocytic potential of the spleen is vital at the erythrocytic cycle. The higher the phagocytic behaviour of the macrophage, the lower the density of parasitised

erythrocytes (see Figure 3.11b). Moreover, the severity of malaria infection increases with decreasing ability of the host's phagocytic macrophages to clear infected erythrocytes from circulation during the erythrocytic cycle.

3.6 Conclusion

In this chapter, a mathematical model of in-host malaria infection by Chiyaka et al. (2008) is extended to include the liver stage of parasite development. Unlike the models in Li et al. (2011) and Tumwiine et al. (2008), the macrophages are considered as the most effective innate immune cells in eliminating malaria parasites from blood circulation. In addition, the liver hepatocytes are assumed to be generated from the bone marrow and through a process of self-regeneration from existing hepatocytes. The malaria-free equilibrium point is shown to be locally asymptotically stable when the in-host basic reproduction number is less than unity. The global stability of the malaria-free state is only guaranteed if the threshold quantity R_0 is less than unity.

Numerical simulation results indicate that intervention during malaria infection should focus on minimising merozoite invasion rate on healthy erythrocytes and the density of merozoites in circulation, which are responsible for secondary invasion at the blood stage. In the absence of malaria treatment, the immune cells (macrophages) are shown to be vital in eliminating infected erythrocytes at the blood stage. The higher the rate of phagocytosis of infected erythrocytes by macrophages, the lower the density of infected erythrocytes and hence malaria parasitaemia. Patients suffering from such infections as HIV/AIDS which have deleterous effect on the protective immune cells should seek immediate medical treament when infected with malaria. Their compromised immune system exposes them to severe malaria attacks and possible untimely death.

For quick and timely reduction of parasitaemia, an increased merozoite death rate using antimalarial drugs such as ACT would be necessary. This would further ensure reduced density of infected red blood cells and hence future generation merozoites. By killing a single blood schizont, the production of 16 merozoites at maturity is avoided. Moreover, an appropriate malaria vaccine that targets erythrocyte invasion process may equally guarantee minimal recrudescence.

The next Chapter 4 incorporate malaria vaccines to the model discussed in this chapter. The impacts of efficacious malaria vaccines and vaccine combinations that target the parasites at different stages of their life cycle are evaluated.

Chapter 4

Mathematical model for the in-host malaria dynamics subject to malaria vaccines

4.1 Introduction

To date, the WHO considers effective vector control strategies such as long-lasting insecticidal treated nets (ITNs) and indoor residual spraying (IRS) as the main ways to prevent and reduce malaria transmission in communities with high malaria prevalence (Homan, 2016; WHO, 2017a). Chemoprophylaxis and antimalarial drugs such as chloroquine and artemisinin-based combination therapy (ACT) are currently used to prevent and treat clinical malaria, respectively, in different parts of the world (Bhatt et al., 2015; WHO, 2015d). These strategies have contributed to the substantial global decline in malaria mortality and morbidity (Nega1 et al., 2016). However, despite the success of the existing malaria prevention and control strategies, reported malaria cases globally are still quite high. In 2017, the WHO reported about 219 million malaria cases (WHO, 2017b). The global decline in malaria cases in the period 2015-2017 is however insignificant (WHO, 2018f). A lot more effort is hence necessary to further reduce cases and mortality due to malaria.

Parasite resistance to current antimalarial drugs (Dondorp et al., 2010; Maude et al., 2009; Sidhu et al., 2002; Wellems and Plowe, 2001) and vector insecticides (Alout et al., 2017a,b; Soko et al., 2015) pose a serious threat to malaria control. To defeat the disease, many more tools with the potential to save lives today and in the future are needed (Birkett, 2016;

Greenwood and Targett, 2009; MVI, 2018). An efficacious, safe and affordable malaria vaccine would help to bridge the control gap left by other intervention measures (MVI, 2018). A malaria vaccination strategy is performed to either induce protective immune responses prior to malaria infection or to provide protection in case of malaria attack (Arama and Troye-Blomberg, 2014).

Current malaria vaccines have shown minimal efficacy (Birkett, 2016; Birkett et al., 2013; Miura, 2016). RTS,S/AS01 is the only malaria vaccine that has received a positive scientific opinion from the European Medicines Agency (EMA) (EMA, 2015). However, the WHO recommends further evaluation of RTS,S/AS01 in a series of pilot implementations before it can be introduced on a wide scale (WHO, 2018d).

This chapter reviews malaria vaccine development and explores, using mathematical modelling, the impacts of efficacious malaria vaccines. It also presents analytically and numerically, the probable effects of vaccine combinations in reducing levels of parasitaemia within the human host.

4.2 Malaria vaccines

Malaria parasite has a tendency to undergo morphological changes accompanied with antigenic variations during its transition from the pre-erythrocytic to erythrocytic stages (Hisaeda et al., 2005; Nega1 et al., 2016). This has presented an enormous challenge in malaria vaccine development. Although there is no licensed vaccine against malaria today, many experts believe that a malaria vaccine is a necessary tool for successful malaria elimination (MVFG, 2018; Ouattara and Laurens, 2014). Vaccines against malaria infection can be categorised into three groups based on the targeted stage of the parasite life cycle (Arumugam et al., 2014). These include: pre-erythrocytic vaccines (PEV), blood stage vaccines (BSV) and transmission blocking vaccines (TBV) as shown in Figure 4.1. The development progress and action of some of the most advanced malaria vaccines is presented in the discussions in the following subsections.

4.2.1 Pre-erythrocytic vaccines (PEV)

The most advanced pre-erythrocytic malaria vaccine candidate against *P. falciparum* is called RTS,S/AS01 (Birkett, 2016; Birkett et al., 2013; Nunes et al., 2014). The RTS,S malaria vaccine is both safe and immunogenic (Abdulla et al., 2008; Otieno et al., 2016). This

vaccine is commercially known as 'Mosquirix' and has been developed by the U.S. military at the Walter Reed Army Institute of Research (WRAIR) through a partnership between GlaxoSmithKline (GSK) Biologicals, the Programs for Appropriate Technologies in Health (PATH) and Malaria Vaccine Initiative (MVI) (Nega1 et al., 2016).

The antigen of RTS,S is a recombinant of circumsporozoite protein (CSP), hepatitis B surface antigen (HBsAg) and HBsAg alone (S) (Ballou, 2009). CSP which is highly expressed on the surface of sporozoites is made up of asparagine-alanine-asparagine-proline (NANP) amino acid repeat region (R) and T-cell epitope domain (T).

During the pre-erythrocytic phase, the administered RTS,S target the CSP which mediates the entry of sporozoites into liver hepatocyte (Frevert, 2004; Singh et al., 2007). RTS,S vaccine induces both humoral and cellular immunity, with high antibody titres that can block sporozoite infection of the liver hepatocytes (Nega1 et al., 2016; Nudelman et al., 1989; Plassmeyer et al., 2009). Since the CSP-specific antibodies alone are insufficient to achieve sterile immunity (Edogan et al., 1987), RTS,S is also designed to have CSP T-cell epitopes in addition to the prominent B-cell epitope (Ballou, 2009; Moorthy and Ballou, 2009).

Several clinical trials (Abdulla et al., 2008; Alonso et al., 2004; Bojang et al., 2001; Polhemus et al., 2009) and (RCTP, 2011) have shown the potential of RTS,S to prevent malaria infection and clinical disease in infants and young children living in sub-Saharan Africa. RTS,S showed a 30-50% protection for human trials in Africa (Alonso et al., 2004; RCTP, 2012). However, an efficient pre-erythrocytic vaccine must be effective enough to protect humans with and without natural immunity. Moreover, the period of protection offered by RTS,S is relatively short. To improve its efficacy, more effort should focus on boosting immune responses at the liver stage. RTS,S may also induce protection against clinical malaria at the blood stage by temporarily reducing the density of merozoites that emerge from the bursting infected hepatocytes (Guinovart et al., 2009). This could boost the naturally acquired erythrocytic stage immunity (Arama and Troye-Blomberg, 2014).

A pilot implementation of RTS,S/AS01 is currently ongoing in selected areas in Kenya, Ghana and Malawi to demonstrate feasibility of delivering the schedule to the target age group and assess vaccine's impact on mortality and potential adverse effects of the vaccine (Galactionova et al., 2017).

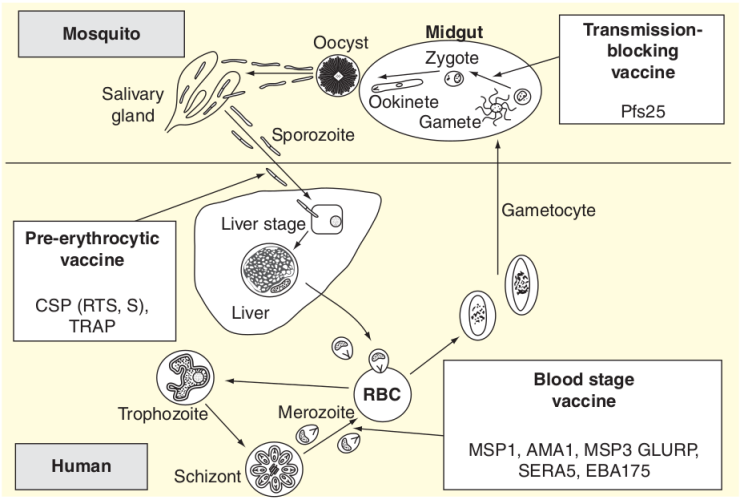

Figure 4.1: Malaria vaccines mapped on the parasite's life cycle: pre-erythrocytic, blood-stage and transmission-blocking vaccines. Source: Arumugam et al. (2014).

4.2.2 Blood stage vaccines (BSV)

BSVs elicit anti-invasion and anti-diseases responses at the blood stage (Moorthy et al., 2004). They, therefore, lower merozoites density and prevent clinical manifestations and hence severity of malaria infection in humans. Due to gene alteration and antigenic variation in malaria merozoites, BSV may not provide complete immunity to the host (Pandey et al., 2013). Nevertheless, BSV are capable of reducing mortality and morbidity due to malaria. At present, merozoite surface protein 3 (MSP3) (Audran et al., 2005) and merozoite surface protein 1 (MSP1) (Ogutu et al., 2009) are the leading blood stage vaccine candidates for plasmodium malaria (Plowe et al., 2009). MSP1 and MSP3 target merozoite to inhibit erythrocyte invasion. Other BSV in clinical trials that have shown the allele-specific protection are: apical membrane antigen 1 (AMA1) (Sagara et al., 2009), erythrocyte-binding antigen-175 (EBA-175) (El Sahly et al., 2010), glutamate-rich protein (GLURP) (Hermsen et al., 2007) and serine repeat antigen 5 (SERA5) (Horii et al., 2010). AMA1 primarily targets the merozoite's invasion apparatus to prevent the infection of the red blood cells.

4.2.3 Transmission blocking vaccines (TBV)

The aim of TBV is to stop subsequent generation of infectious malaria sporozoites from the mosquito vector. While, TBV does not directly protect the person who is vaccinated, it has the potential to stop continued spread of malaria infection in a population. TBVs induce

antibodies against antigens on gametes, zygotes and ookinetes, blocking ookinete to oocyst transition and hence stopping parasite development within the mosquito midgut (Carter et al., 2000). Currently, *P. falciparum* ookinete surface antigens (Pfs25) is the leading malaria vaccine candidate in this category (Arevalo-Herrera et al., 2005; Hisaeda et al., 2000).

To improve its immunogenicity, Pfs25 is chemically cross linked to an Expo-protein A (Pfs25-EPA) and delivered as a nanoparticle. Pfs25-EPA is currently under trials by the US National Institute of Allergy and Infectious Diseases (Shimp Jr et al., 2013). The rest of the TBVs are presently at the preclinical trial and includes: *P. falciparum* surface protein 28, *P. falciparum* surface protein 48, *P. falciparum* surface protein 45 and *P. falciparum* surface protein 230 (Ouattara and Laurens, 2014; WHO, 2018c). Pfs25 and Pfs28 antigens are expressed only after fertilization in the mosquito midgut and are not present in the gametocyte as they circulate in the blood. A key aspect of TBVs is in their potential to reduce the emergence and spread of parasite resistance to other malaria vaccine components and even to antimalarial drugs (Carter et al., 2000). However, the absence of natural boosting following immunisation with TBV might limit their efficacy and hence utilisation (Dinglasan et al., 2013; Vannice et al., 2012).

4.2.4 The role of CD8^+ T cells during malaria infection

Malaria parasites are susceptible to immune mediated control by CD8^+ T-cells, which target intracellular pathogens (Villarino and W Schmidt, 2013). The CD8^+ T-cells have both direct and indirect effector pathways for parasite elimination at the liver stage. The indirect mechanism include the production of IFN-γ and TNF, whereas the direct mechanism involves the release of perforin and granzymes (Nganou-Makamdop et al., 2012). IFN-γ suppresses parasite development through direct impairment of parasite differentiation in hepatocytes (Mellouk et al., 1987). Moreover, IFN-γ increases the expression of nitric oxide synthase which leads to subsequent increase in nitric oxide that confers protection against *P. falciparum* (Seguin et al., 1994). Although CD8^+ T-cells are sufficiently primed during blood stage malaria, they offer minimal contribution to protective immunity. It is thought that vascular endothelial cells that acquire antigen from IRBCs stimulate CD8^+ T-cells to release perforin and granzyme B during blood stage malaria (Villarino and W Schmidt, 2013). The capacity of CD8^+ T-cells to eradicate malaria parasites and infected cells both at the liver and blood stages is therefore considered in this study.

Several research studies on clinical malaria control have been carried out (Austin et al., 1998b; Hellriegel, 1992; Kamangira et al., 2014; Li et al., 2011). Some of these models

(Malaguarnera and Musumeci, 2002) have focussed on the role of the host's immune cells in in-host malaria control. Others (Kamangira et al., 2014; Magombedze et al., 2011a) have targeted the use of antimalaria drugs in controlling clinical malaria. Chiyaka et al. (2008) considered both the immune cells and malaria chemotherapy in malaria control in humans. In (Rouzine and McKenzie, 2003), the role of innate immunity in mediating synchronization between the replication cycles of parasites in different erythrocytes is explored. Kamangira et al. (2014) investigated erythrocytes-malaria parasite dynamics in the presence of immune response and or drug intervention at the erythrocytic stage. Tabo et al. (2017) incorporated the liver stage in their model and investigated treatment as a control strategy for blood stage malaria.

These research studies have been very insightful in understanding in-host malaria dynamics and control, however, none of these investigations has attempted to evaluate the possible impact of malaria vaccines in controlling clinical *P. falciparum* malaria. In this study, therefore, an in-host malaria model that considers parasite-cell interactions at the liver and blood stages, subject to malaria vaccines is formulated and analysed mathematically. The goal of this chapter is to study the cell-parasite dynamics using a mathematical model and to numerically investigate the impact of malaria vaccines and vaccine combinations in the control of *P. falciparum* malaria infection within the human host.

4.3 Model formulation

A mathematical model of in-host *P. falciparum* malaria dynamics in the presence of malaria vaccines is presented. The compartmental model is an extension of the in-host malaria model in Chapter 3 of this thesis. Two more compartments of gametocytes $G(t)$ and $CD8^+$ T cells $W(t)$ are incorporated into the model to capture the effects of the transmission blocking vaccines and the general effects of $CD8^+$ T cells on the density of the infected erythrocytes and hence malaria infection dynamics. Based on their stage of infection, the infected erythrocytes are classified into blood trophozoites (early stage of infection) and blood schizonts (late stage of infection). Therefore, the rest of the populations include susceptible hepatocytes $H(t)$, infected hepatocytes $X(t)$, malaria sporozoites $S(t)$, susceptible erythrocytes $R(t)$, blood trophozoites $T(t)$, blood schizonts $C(t)$ and malaria merozoites $M(t)$.

Susceptible erythrocytes are recruited at a constant rate λ_r from the bone marrow and their density decreases through natural death at the rate μ_r or due to invasion by the merozoites

at the rate β_r. Following merozoite invasion, susceptible erythrocytes move to the class of infected erythrocytes T. The generated blood trophozoites decay naturally at a rate μ_t or progress into blood schizonts C class at the rate γ. Mature blood schizonts burst open to release more merozoites into blood stream. This is represented by the term $P\mu_c C/(1+dW)$, where P denotes the number of merozoites released per bursting blood schizont, μ_c is the decay rate of the blood schizonts and d is the rate of inhibition of immune response.

At the pre-erythrocytic stage, the malaria sporozoites are debilitated by vaccine-induced anti-CSP antibodies (PEV) as they molt through the tissues (Mellouk et al., 1990; Schwenk et al., 2003). The reduced invasion by sporozoites is represented by the term $\beta_s(1-\nu)SH$, where $0<\nu<1$ is the efficacy of the pre-erythrocytic vaccine. Sporozoites that successfully invade the hepatocytes are however, targeted by vaccine-induced CSP-specific $CD8^+$ T cells (PEV). The $CD8^+$ T cells kill the resulting infected hepatocyte (Renia et al., 1991; Sun et al., 2003; White et al., 2013). This reduces the burst size N of the infected hepatocytes to $(1-b)N$, where $0<b<1$ is the probability with which the vaccine inhibits merozoite emergence from infected hepatocyte.

An unbounded bilinear function rEI is considered by Anderson et al. (1989), Niger and Gumel (2011) and Hetzel and Anderson (1996) to model the killing of infected cells I by the $CD8^+$T cells E. The simple mass-action term rEI depends solely on the product of the density of the immune cells E and the density of the infected cells I. However, if the fact that cell proliferation can saturate is taken into account, then the nonlinear bounded Michaelis-Menten-Monod function, presented in equation (4.1) is most reasonable (Agur et al., 1989; Antia et al., 1994).

$$\nabla = \nabla_{\max}\frac{B}{K_b+B}, \tag{4.1}$$

where B is the concentration of substrate, ∇ is the growth rate of the microorganisms B, $\nabla_{\max}$ is the maximum specific growth rate of B and K_b is the half-velocity constant, $\nabla/\nabla_{\max}$.

In Pilyugin and Antia (2000), the nonlinear bounded Michaelis-Menten-Monod function (4.1) is used to model the handling time in immune response and their targets and how it affects the infection. In this study, the nonlinear bounded function $p_1IE/(1+\beta I)$, used in Chiyaka et al. (2008), to describe the killing of infected erythrocytes I by the immune cells E ($CD8^+$ T cells, in our case) is adopted. This formulation has also been used by Cai et al. (2017) and Selemani et al. (2017a). The parameter p_1 describes the rate of removal of I by E and $1/\beta$ is the saturation constant that stimulates the proliferation of the $CD8^+$ T cells to grow at half their maximum rate.

The effects of the BSV on merozoite invasion of the erythrocytes are represented by the term $(1-\varrho)\beta_r RM/(1+dW)$, where $0<\varrho<1$ is the efficacy of the BSV and $1/d$ is a saturation constant that stimulates $CD8^+$ T cells to grow at half their maximum rate. Further, BSV reduces the density of merozoites that are released per bursting blood schizont, so that the burst size P becomes $(1-a)P$, where $0<a<1$ accounts for the vaccine-induced reduction of merozoites released per bursting infected erythrocyte. BSV is further assumed to enhance the production of $CD8^+$T cells at a rate τ, where $\tau>1$. For purposes of simulation, it is assumed that $1<\tau<2$. Administered TBV reduces the sporozoite recruitment rate from Λ to $(1-\chi)\Lambda$, where $0<\chi<1$ is the efficacy of the TBV. Inoculated sporozoites are assumed to die naturally at the rate μ_s.

The immune cells ($CD8^+$ T cells) are recruited at a constant rate λ_w from the thymus. Furthermore, the presence of infected cells such as infected hepatocytes, blood trophozoites and blood schizonts stimulates the production of $CD8^+$ T cells. The increased production of $W(t)$ due to $X(t)$, $T(t)$ and $C(t)$ is also modelled using the nonlinear bounded Michaelis-Menten-Monod function (4.1) and is represented by the terms $\delta_x WX/(1+\varepsilon_0 X)$, $\delta_t WT/(1+\varepsilon_1 T)$ and $\delta_c WC/(1+\varepsilon_2 C)$, respectively. The parameters $\delta_i|i=x,t,c$ represents the immunogenecity of infected hepatocytes, blood trophozoites and blood schizonts, respectively. On the other hand, the phagocytotic effects of $CD8^+$ T cells on infected cells X, T and C are represented by the terms $k_x(1-\nu)WX/(1+\varepsilon_0 X)$, $k_t(1-\varrho)WT/(1+\varepsilon_1 T)$ and $k_c(1-\varrho)WC/(1+\varepsilon_2 C)$, where, $k_j|j=x,t,c$ is the immunosensitivity of X,T and C, respectively.

The density of blood schizonts C decreases when they burst open to release merozoites into the blood stream or when they die naturally at the rate μ_c. A proportion π of the released merozoites develops into gametocytes $G(t)$ whose natural decay rate is denoted by μ_g. Just like the susceptible hepatocytes whose natural mortality is at the rate μ_h, a constant decay rates μ_t and μ_w are assumed for blood trophozoites and the $CD8^+$ T cells, respectively. The descriptions of state variables and parameters used in the model are summarised in Tables 4.1 and 4.2, respectively. The in-host malaria dynamics subject to malaria vaccines is represented in the compartmental flow diagram in Figure 4.2.

Table 4.1: Symbols and definition of state variables considered in the model at time t

Variable	Description
$H(t)$	Population of susceptible hepatocytes
$X(t)$	Population of infected hepatocytes
$R(t)$	Population of susceptible erythrocytes (red blood cells)
$T(t)$	Population of blood trophozoites
$C(t)$	Density of blood schizonts
$S(t)$	Density of sporozoites
$M(t)$	Density of merozoites in blood
$G(t)$	Density of gametocytes in blood
$W(t)$	Concentration of $CD8^+$ T cells

Table 4.2: Description of parameters

Parameter	Description
χ	Efficacy of transmission blocking vaccine
ϱ	Efficacy of blood stage vaccine
ν	Efficacy of pre-erythrocytic stage vaccine
Λ	The rate of injection of sporozoites into liver due to mosquito bites
μ_s, μ_w	Decay rate of sporozoites and $CD8^+$ T cells, respectively
λ_r,λ_h	Rate of production of susceptible RBCs and susceptible hepatocytes from the bone marrow, respectively
μ_h, μ_r, μ_x	Death rate of susceptible hepatocyte, erythrocyte and infected hepatocyte, respectively
π	Proportion of parasites that become gametocytes per dying blood schizont
k_x, k_t, k_c	Immunosensitivity of infected hepatocytes, blood trophozoites and blood schizonts, respectively
$\delta_x, \delta_t, \delta_c$	Immunogenecity of infected hepatocytes, blood trophozoites and blood schizonts, respectively
β_s, β_r	Infection rate of hepatocytes and erythrocytes, respectively
μ_t, μ_c	The rate of decay of blood trophozoites and blood schizonts, respectively
μ_m, μ_g	Decay rate of merozoites and gametocytes, respectively
d	The rate of inhibition of immune response
τ	A parameter that accounts for vaccine-induced enhanced production of $CD8^+$T cells

Continued on next page

Table 4.2 – *Continued from previous page*

Parameter	Description
γ	Rate of progression from blood trophozoite stage to blood schizont stage
λ_w	The rate of production of $CD8^+$ T cells from thymus
$1/\varepsilon_0, 1/\varepsilon_1, 1/\varepsilon_2$	half saturation constants for infected hepatocytes, blood trophozoites and blood schizonts, respectively
b	A parameter that accounts for PEV-induced reduction of merozoites released per bursting liver schizont
a	A parameter that accounts for BSV-induced reduction of merozoites released per bursting blood schizont
P	The average number of merozoites released per bursting blood schizont
N	Number of merozoites released per bursting hepatocyte

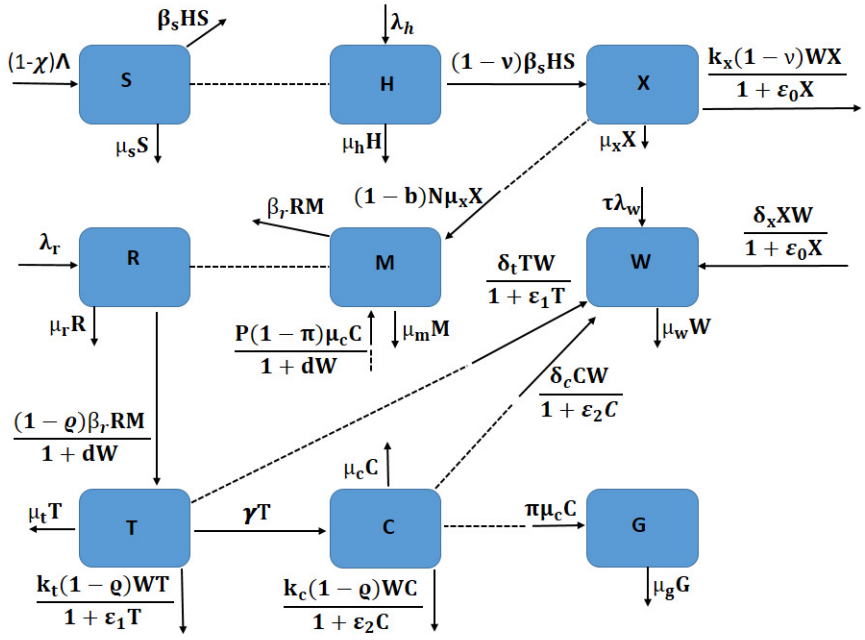

Figure 4.2: Schematic diagram for in-host malaria with vaccine therapy. The dotted lines without arrows indicate cell-parasite interaction and the solid lines show progression from one compartment to another.

The incorporation of malaria vaccine control measures to the in-host malaria model in Chapter 3 lead to the following additional model assumptions:

1. There are nine interacting populations of susceptible hepatocytes, infected hepatocytes, susceptible red blood cells, blood trophozoites, blood schizonts, sporozoites, merozoites, gametocytes and $CD8^+$ T cells, at any given time t.
2. It is assumed that malaria vaccines accelerate the rate of generation of $CD8^+$ T cells.
3. $CD8^+$ T cells are recruited at a constant rate from the thymus.
4. The blood stage vaccine reduces the rate of invasion of the susceptible red blood cells.
5. The pre-erythrocytic vaccine reduces the rate of invasion of the susceptible hepatocytes at the liver stage.
6. The transmission blocking vaccine reduces the recruitment rate of sporozoites into the liver.
7. Infected hepatocytes, blood schizonts and blood trophozoites are eliminated by $CD8^+$ T cells.
8. Merozoites are generated both from the bursting liver schizonts and blood schizonts only.
9. All model parameters are assumed non-negative.
10. Generation of $CD8^+$ T cells is stimulated by the presence of infected hepatocytes, blood schizonts and blood trophozoites.

Based on the above model description and assumptions, the in-host malaria model subject to malaria vaccines is formulated using a system of nonlinear ordinary differential equations

and presented as follows:

$$\left.\begin{aligned}
\frac{\mathrm{d}S}{\mathrm{d}t} &= (1-\chi)\Lambda - \mu_s S - \beta_s HS,\\
\frac{\mathrm{d}H}{\mathrm{d}t} &= \lambda_h - \mu_h H - \beta_s(1-\nu)HS,\\
\frac{\mathrm{d}X}{\mathrm{d}t} &= \beta_s(1-\nu)SH - \mu_x X - \frac{k_x(1-\nu)WX}{1+\varepsilon_0 X},\\
\frac{\mathrm{d}R}{\mathrm{d}t} &= \lambda_r - \frac{(1-\varrho)\beta_r RM}{1+dW} - \mu_r R,\\
\frac{\mathrm{d}T}{\mathrm{d}t} &= \frac{(1-\varrho)\beta_r RM}{1+dW} - \mu_t T - \gamma T - \frac{k_t(1-\varrho)WT}{1+\varepsilon_1 T},\\
\frac{\mathrm{d}C}{\mathrm{d}t} &= \gamma T - \mu_c C - \frac{k_c(1-\varrho)WC}{1+\varepsilon_2 C},\\
\frac{\mathrm{d}M}{\mathrm{d}t} &= (1-b)N\mu_x X + \frac{P(1-\pi)(1-a)\mu_c C}{1+dW} - \mu_m M - \beta_r RM,\\
\frac{\mathrm{d}G}{\mathrm{d}t} &= \pi\mu_c C - \mu_g G,\\
\frac{\mathrm{d}W}{\mathrm{d}t} &= \tau\lambda_w + W\left(\frac{\delta_x X}{1+\varepsilon_0 X} + \frac{\delta_t T}{1+\varepsilon_1 T} + \frac{\delta_c C}{1+\varepsilon_2 C}\right) - \mu_w W.
\end{aligned}\right\} \tag{4.2}$$

It is assumed that all the parameters used in the model are positive and the initial conditions for system (4.2) are: $H(0)>0, X(0)\geq 0, S(0)\geq 0, R(0)>0, T(0)\geq 0, C(0)\geq 0, M(0)\geq 0, G(0)\geq 0, W(0)>0$.

4.4 Model analysis

We aim is to evaluate the effects of the different vaccines on the density of infected hepatocytes and infected erythrocytes. Therefore, the model should be biologically coherent. That is, all the state variables and their solutions must be nonnegative and bounded, respectively, in the region Φ, where

$$\begin{aligned}
\Phi = \Bigg\{ &(H,X,R,T,C,S,M,G,W) \in \mathbb{R}_+^9 : N_r(t) \leq \max\left\{N_r(0), \frac{\lambda_r}{\mu_1^*}\right\},\\
&N_h(t) \leq \max\left\{N_h(0), \frac{\lambda_h}{\mu_2^*}\right\}, N_p(t) \leq \max\left\{N_p(0), \frac{(1-\chi)\Lambda}{\mu_3^*}\right\},\\
&W(t) \leq \max\left\{W(0), \frac{\tau\lambda_w}{\mu_w}\right\}\Bigg\},
\end{aligned} \tag{4.3}$$

and $N_r(t) = R(t) + T(t) + C(t)$, $N_h(t) = H(t) + X(t)$, $N_p(t) = S(t) + M(t) + G(t)$, $\mu_1^* = \min\{\mu_r, \mu_t, \mu_c\}$, $\mu_2^* = \min\{\mu_h, \mu_x\}$ and $\mu_3^* = \min\{\mu_s, \mu_m, \mu_g\}$.

For system (4.2) to be biologically meaningful, the following theorem is proved:

Theorem 4.1. *The region Φ is positively invariant with respect to the in-host malaria model (4.2) and a nonnegative solution $(H(t), X(t), R(t), T(t), C(t), S(t), M(t), G(t), W(t))$ exists $\forall t \geq 0$.*

Proof: From the sporozoite compartment $S(t)$ in system (4.2), it is clear that

$$\frac{\mathrm{d}S}{\mathrm{d}t} = (1-\chi)\Lambda - \mu_s S - \beta_s H S \geq -(\mu_s + \beta_s H)S. \tag{4.4}$$

Integrating inequality (4.4) yields:

$$S(t) \geq S(0)\exp\{-(\mu_s t + \beta_s \int_0^t H(n)\mathrm{d}n)\}. \tag{4.5}$$

This shows that in the absence of malaria interventions, $S(t) \geq 0$ for all time $t \geq 0$.

Using the same argument above, it is easy to see that

$$H(t) \geq H(0)\exp\{-(\mu_h t + \beta_s(1-\nu) \int_0^t S(n)\mathrm{d}n)\}. \tag{4.6}$$

This process can be repeated for all the state variables so that $S(t), H(t)$, $X(t)$, $R(t)$, $T(t)$, $C(t)$, $M(t)$, $G(t)$, $W(t)$ are all positive for all $t \geq 0$. Thus, the solutions of the in-host malaria model remain positive in Φ, $\forall t \geq 0$.

To show that the solutions of system (4.2) are bounded, let N_r be the total population of the red blood cells in the human host, that is $N_r(t) = R(t) + T(t) + C(t)$ and

$$\begin{aligned} \frac{\mathrm{d}N_r}{\mathrm{d}t} &= \lambda_r - \mu_r R - \mu_t T - \mu_c C - \left(\frac{k_t(1-\varrho)WT}{1+\varepsilon_1 T} + \frac{k_c(1-\varrho)WC}{1+\varepsilon_2 C}\right), \\ &\leq \lambda_r - \mu_1^* N_r \quad \text{where} \quad \mu_1^* = \min\{\mu_r, \mu_t, \mu_c\}. \end{aligned} \tag{4.7}$$

Using the initial condition $N_r(0) = N_{r0} > 0$, equation (4.7) is solved by integration into:

$$N_r(t) \leq \frac{\lambda_r}{\mu_1^*} + e^{-\mu_1^* t}\left(N_r(0) - \frac{\lambda_r}{\mu_1^*}\right). \tag{4.8}$$

This implies that at any time t, $N_r(t) \leq \max\{N_r(0), \lambda_r/\mu_1^*\}$. This approach can similarly be applied to the population of hepatocytes $N_h(t) = H(t) + X(t)$, population of parasites

$N_p(t) = S(t) + M(t) + G(t)$ and to the density of CD8$^+$T cells $W(t)$. That is,

$$\begin{aligned} N_h(t) &\leq \max\left\{N_h(0), \frac{\lambda_h}{\mu_2^*}\right\}, \text{ where } \quad \mu_2^* = \min\{\mu_h, \mu_x\}, \\ N_p(t) &\leq \max\left\{N_p(0), \frac{(1-\chi)\Lambda}{\mu_3^*}\right\}, \text{ where } \quad \mu_3^* = \min\{\mu_s, \mu_m, \mu_g\} \quad \text{and} \\ W(t) &\leq \max\left\{W(0), \frac{\tau\lambda_w}{\mu_w}\right\}. \end{aligned} \tag{4.9}$$

The above analysis shows that the region Φ is positively invariant and attracting for system (4.2) and the model is hence well posed for study.

4.4.1 Parasite-free equilibrium point and vaccination reproduction number

The parasite-free equilibrium (PFE), E_v, depicts the absence of malaria parasites from the human host. The PFE of the in-host malaria model depicted in system (4.2) exists and is given by

$$E_v = (H^0, X^0, R^0, T^0, C^0, S^0, M^0, G^0, W^0) = \left(\frac{\lambda_h}{\mu_h}, 0, \frac{\lambda_r}{\mu_r}, 0, 0, 0, 0, 0, \frac{\tau\lambda_w}{\mu_w}\right). \tag{4.10}$$

The vaccination reproduction number (denoted by R_v), on the other hand, is a threshold quantity which governs the spread of the infection. It represents on average the number of new infected erythrocytes (or hepatocytes) generated by a single infectious merozoite (or sporozoites) at the blood (or liver) stage in the presence of malaria vaccines. Using the next generation matrix approach (Diekmann et al., 1990; Van den Driessche and Watmough, 2002), the matrix $\mathscr{F}_1$ which represents the rate of appearance of new infections and the matrix $\mathscr{V}_1$, which denotes the transfer of infections from one compartment to the other are respectively given as:

$$\mathscr{F}_1 = \begin{pmatrix} \beta_s(1-\nu)SH \\ 0 \\ \frac{(1-\varrho)\beta_r RM}{1+dW} \\ 0 \\ 0 \\ 0 \end{pmatrix} \text{ and } \mathscr{V}_1 = \begin{pmatrix} \mu_x X + \frac{k_x(1-\nu)WX}{1+\varepsilon_0 X} \\ -(1-\chi)\Lambda + \mu_s S + \beta_s SH \\ \mu_t T + \gamma T + \frac{k_t(1-\varrho)WT}{1+\varepsilon_1 T} \\ -\gamma T + \mu_c C + \frac{k_c(1-\varrho)WC}{1+\varepsilon_2 C} \\ -(1-b)N\mu_x X - \frac{P(1-\pi)(1-a)\mu_c C}{1+dW} + \mu_m M + \beta_r RM \\ -\pi\mu_c C + \mu_g G \end{pmatrix}. \tag{4.11}$$

Taking partial derivatives of the terms in $\mathscr{F}_1$ and $\mathscr{V}_1$ and evaluating at the parasite-free equilibrium E_v, a nonnegative matrix F_1 and a non-singular matrix V_1 are obtained as follows:

$$\mathrm{F}_1 = \begin{pmatrix} 0 & \frac{(1-\nu)\beta_s\lambda_h}{\mu_h} & 0 & 0 & 0 & 0 \\ 0 & 0 & 0 & 0 & 0 & 0 \\ 0 & 0 & 0 & 0 & \frac{(1-\varrho)\beta_r\lambda_r\mu_w}{\mu_r(d\tau\lambda_w+\mu_w)} & 0 \\ 0 & 0 & 0 & 0 & 0 & 0 \\ 0 & 0 & 0 & 0 & 0 & 0 \\ 0 & 0 & 0 & 0 & 0 & 0 \end{pmatrix} \tag{4.12}$$

and

$$\mathrm{V}_1 = \begin{pmatrix} V_a & 0 & 0 & 0 & 0 & 0 \\ 0 & \frac{\beta_s\lambda_h}{\mu_h}+\mu_s & 0 & 0 & 0 & 0 \\ 0 & 0 & V_b & 0 & 0 & 0 \\ 0 & 0 & -\gamma & \frac{(1-\varrho)\tau k_c\lambda_w}{\mu_w}+\mu_c & 0 & 0 \\ -(1-b)N\mu_x & 0 & 0 & -\frac{(1-a)P(1-\pi)\mu_c}{\frac{d\tau\lambda_w}{\mu_w}+1} & \frac{\beta_r\lambda_r}{\mu_r}+\mu_m & 0 \\ 0 & 0 & 0 & -\pi\mu_c & 0 & \mu_g \end{pmatrix}, \tag{4.13}$$

where $V_a = ((1-\varrho)\tau k_x\lambda_w/\mu_w)+\mu_x$ and $V_b = \gamma+\mu_t+((1-\varrho)\tau k_t\lambda_w)/\mu_w$.

The vaccination reproduction number is the spectral radius of $(\mathrm{F}_1\mathrm{V}_1^{-1})$. That is,

$$\mathrm{R}_v = \frac{P(1-\pi)(1-a)(1-\varrho)\gamma\beta_r\lambda_r\mu_c}{\mu_r\left(\frac{d\tau\lambda_w+\mu_w}{\mu_w}\right)^2\left(\mu_m+\frac{\beta_r\lambda_r}{\mu_r}\right)\left(\frac{(1-\varrho)\tau k_c\lambda_w}{\mu_w}+\mu_c\right)\left(\frac{(1-\varrho)\tau k_t\lambda_w}{\mu_w}+\gamma+\mu_t\right)}. \tag{4.14}$$

In the absence of malaria vaccines ($\chi = \varrho = \nu = a = b = 0, \tau = 1$), the in-host malaria model depicted in system (4.2), has a basic reproduction number R_m given by

$$\mathrm{R}_m = \frac{P(1-\pi)\gamma\beta_r\lambda_r\mu_c}{\mu_r\left(\frac{d\lambda_w+\mu_w}{\mu_w}\right)^2\left(\frac{k_c\lambda_w}{\mu_w}+\mu_c\right)\left(\mu_m+\frac{\beta_r\lambda_r}{\mu_r}\right)\left(\gamma+\frac{k_t\lambda_w}{\mu_w}+\mu_t\right)}. \tag{4.15}$$

Comparing equations (4.14) and (4.15), gives

$$R_m = R_v \times \Theta^{**}, \tag{4.16}$$

where

$$\Theta^{**} = \frac{(1-a)(1-\varrho)\left(\frac{d\lambda_w}{\mu_w}+1\right)(d\lambda_w+\mu_w)\left(\frac{k_c\lambda_w}{\mu_w}+\mu_c\right)\left(\gamma+\frac{k_t\lambda_w}{\mu_w}+\mu_t\right)}{\mu_w\left(\frac{d\tau\lambda_w}{\mu_w}+1\right)^2\left(\frac{(1-\varrho)\tau k_c\lambda_w}{\mu_w}+\mu_c\right)\left(\gamma+\frac{(1-\varrho)\tau k_t\lambda_w}{\mu_w}+\mu_t\right)}.$$

It is observed from equation (4.16) that in the absence of vaccination, $R_v = R_m$. However, the introduction of malaria vaccines reduces the basic reproduction number by a factor of $0 < \Theta^{**} < 1$. The use of efficacious malaria vaccines therefore has a great potential in reducing mortality due to *P. falciparum* malaria disease.

4.4.2 Local stability of parasite-free equilibrium point

The local stability of E_v is investigated as follows. Linearising model system (4.2) around E_v gives the following Jacobian matrix G_1.

$$G_1 = \begin{pmatrix} -\mu_h & 0 & -A_0 & 0 & 0 & 0 & 0 & 0 & 0 \\ 0 & -A_1 & A_2 & 0 & 0 & 0 & 0 & 0 & 0 \\ 0 & 0 & -A_3 & 0 & 0 & 0 & 0 & 0 & 0 \\ 0 & 0 & 0 & -\mu_r & 0 & 0 & -A_4 & 0 & 0 \\ 0 & 0 & 0 & 0 & -A_5 & 0 & A_6 & 0 & 0 \\ 0 & 0 & 0 & 0 & \gamma & -A_7 & 0 & 0 & 0 \\ 0 & A_{11} & 0 & 0 & 0 & A_8 & -A_9 & 0 & 0 \\ 0 & 0 & 0 & 0 & 0 & \pi\mu_t & 0 & -\mu_g & 0 \\ 0 & \frac{\tau\delta_x\lambda_w}{\mu_w} & 0 & 0 & A_{10} & \frac{\tau\delta_c\lambda_w}{\mu_w} & 0 & 0 & -\mu_w \end{pmatrix}, \tag{4.17}$$

where

$$A_0 = \frac{(1-\nu)\beta_s\lambda_h}{\mu_h}, \quad A_1 = \frac{(1-\nu)\tau k_x\lambda_w}{\mu_w} + \mu_x, \quad A_2 = \frac{(1-\nu)\beta_s\lambda_h}{\mu_h},$$
$$A_3 = \frac{\beta_s\lambda_h}{\mu_h} + \mu_s, \quad A_4 = \frac{(1-\varrho)\beta_r\lambda_h}{\mu_h\left(\frac{d\tau\lambda_w}{\mu_w}+1\right)}, \quad A_5 = \gamma + \mu_t + \frac{(1-\varrho)\tau k_t\lambda_w}{\mu_w},$$
$$A_6 = \frac{(1-\varrho)\beta_r\lambda_h}{\mu_h\left(\frac{d\tau\lambda_w}{\mu_w}+1\right)}, \quad A_7 = \frac{(1-\varrho)\tau k_c\lambda_w}{\mu_w} + \mu_c, \quad A_8 = \frac{(1-a)P(1-\pi)\mu_c}{\frac{d\tau\lambda_w}{\mu_w}+1},$$
$$A_9 = \frac{\beta_r\lambda_h}{\mu_h} + \mu_m, \quad A_{10} = \frac{\tau\delta_t\lambda_w}{\mu_w} \quad \text{and} \quad A_{11} = (1-b)N\mu_x.$$

It is clear from matrix G_1, that the first eigenvalue, $\lambda_1 = -\mu_h < 0$. Upon deleting row one and column one from matrix (4.17), a new sub-matrix G_2 is produced.

$$G_2 = \begin{pmatrix} -A_1 & A_2 & 0 & 0 & 0 & 0 & 0 & 0 \\ 0 & -A_3 & 0 & 0 & 0 & 0 & 0 & 0 \\ 0 & 0 & -\mu_r & 0 & 0 & A_4 & 0 & 0 \\ 0 & 0 & 0 & -A_5 & 0 & A_6 & 0 & 0 \\ 0 & 0 & 0 & \gamma & -A_7 & 0 & 0 & 0 \\ A_{11} & 0 & 0 & 0 & A_8 & -A_9 & 0 & 0 \\ 0 & 0 & 0 & 0 & \pi\mu_t & 0 & -\mu_g & 0 \\ \frac{\tau\delta_x\lambda_w}{\mu_w} & 0 & 0 & A_{10} & \frac{\tau\delta_c\lambda_w}{\mu_w} & 0 & 0 & -\mu_w \end{pmatrix}. \tag{4.18}$$

Applying the above procedure to columns 3,7 and 8 and their corresponding rows in matrix (4.18), the next three eigenvalues: $\lambda_2 = -\mu_r < 0$, $\lambda_3 = -\mu_g < 0$ and $\lambda_4 = -\mu_w < 0$ are obtained. The resultant matrix G_3 is given by

$$G_3 = \begin{pmatrix} -A_1 & A_2 & 0 & 0 & 0 \\ 0 & -A_3 & 0 & 0 & 0 \\ 0 & 0 & -A_5 & 0 & A_6 \\ 0 & 0 & \gamma & -A_7 & 0 \\ A_{11} & 0 & 0 & A_8 & -A_9 \end{pmatrix}. \tag{4.19}$$

The rest of the eigenvalues are obtained by solving the characteristic equation of matrix G_3:

$$\lambda^5 + \beta_1\lambda^4 + \beta_2\lambda^3 + \beta_3\lambda^2 + \beta_4\lambda + \beta_5 = 0, \tag{4.20}$$

where

$$\beta_1 = A_1 + A_3 + A_5 + A_7 + A_9 > 0, \tag{4.21}$$

$$\beta_2 = A_1A_3 + A_1A_5 + A_3A_5 + A_1A_7 + A_3A_7 + A_5A_7 + A_1A_9 + A_3A_9 + A_5A_9 + A_7A_9 > 0, \tag{4.22}$$

$$\beta_3 = A_1A_3A_5 + A_1A_3A_7 + A_1A_5A_7 + A_3A_5A_7 + A_1A_3A_9 + A_1A_5A_9 + A_3A_5A_9 + A_1A_7A_9 + A_3A_7A_9 + A_5A_8A_9 \left[(1 - R_v) \left(\frac{A_6^2 A_7 A_8}{\lambda_r} \right) \right], \tag{4.23}$$

$$\beta_4 = A_6A_8(A_1A_8)[(1 - R_v)] + A_1A_3A_5A_7 + A_1A_3A_5A_9 + A_1A_3A_7A_9 + A_1A_5A_7A_9, \tag{4.24}$$

$$\beta_5 = A_1A_3A_5A_7A_9 \left[(1 - R_v) \frac{A_6}{\lambda_r} \right]. \tag{4.25}$$

Equation (4.20) has negative roots (eigenvalues) if all its coefficients terms are positive. That is, $\beta_1 > 0$, $\beta_2 > 0$, $\beta_3 > 0$, $\beta_4 > 0$ and $\beta_5 > 0$. It is clear from equations (4.21) and (4.22) that β_1 and β_2 are positive terms. However, the coefficients β_3, β_4 and β_5 can only be positive if the vaccine reproduction number R_v is less than unity, $\mathrm{R}_v < 1$.

Thus, using Theorem 2 in Van den Driessche and Watmough (2002), the following lemma is established.

Lemma 4.1. *The parasite-free equilibrium E_v is locally asymptotically stable if* $\mathrm{R}_v < 1$ *and unstable if* $\mathrm{R}_v > 1$.

Lemma 4.1 shows that if the malaria parasite is eliminated following malaria infection, then a vaccine or combinations of vaccines that would guarantee the existence of a stable parasite-free equilibrium should be administered. Epidemiologically, when $R_v < 1$, it is expected that the parasites will decay off so that the severity of malaria infection is reduced to near zero or totally eliminated. On the other hand, if $R_v > 1$, the malaria infection persists within the human host; that is, more red blood cells and susceptible hepatocytes are infected. This implies that the vaccines may not be efficacious; their use does not eradicate malaria parasites among infected individuals. The malaria parasites are therefore likely to persist at the erythrocytic stage in an infected individual and subsequently, can be transmitted to other persons in close contact via the mosquito vector.

4.5 Critical efficacy of blood stage vaccine

Definition 4.1. *Vaccine efficacy is interpreted as the proportionate reduction in malaria disease attack rate within a vaccinated person compared to an unvaccinated person (Small et al., 2010).*

Generally, the vaccine efficacy V_E is expressed as follows (Orenstein et al., 1990):

$$V_E = \frac{ARU - ARV}{ARU} \times 100, \tag{4.26}$$

where ARU is the parasite attack rate of unvaccinated individual and ARV is the attack rate for vaccinated people. A critical vaccine efficacy therefore refers to the minimum efficacy value beyond which the vaccine is capable of eradicating the infection from the human host. To establish a critical malaria vaccine efficacy from the vaccine reproduction number (4.14), it is assumed that only the blood stage vaccine is administered to the individual. That is, $\nu = 0, b = 0, \chi = 0$. Solving for ϱ from the equation $R_v = 1$ gives,

$$\frac{P(1-\pi)(1-a)(1-\varrho)\gamma\beta_r\lambda_r\mu_c}{\left(\frac{(1-\varrho)\tau k_c\lambda_w}{\mu_w}+\mu_c\right)\left(\frac{(1-\varrho)\tau k_t\lambda_w}{\mu_w}+\gamma+\mu_t\right)} = \mu_r\left(\frac{d\tau\lambda_w+\mu_w}{\mu_w}\right)^2\left(\mu_m+\frac{\beta_r\lambda_r}{\mu_r}\right). \tag{4.27}$$

By simplification, equation (4.27) reduces to

$$\frac{(1-\varrho)\mu_w^2}{(\mu_c\mu_w+(1-\varrho)\tau k_t\lambda_w)(\mu_w(\gamma+\mu_t)+(1-\varrho)\tau k_c\lambda_w)} = \Delta^{**}, \tag{4.28}$$

where

$$\Delta^{**} = \frac{\mu_r\left(\frac{d\tau\lambda_w}{\mu_w}+1\right)(d\tau\lambda_w+\mu_w)\left(\mu_m+\frac{\beta_r\lambda_r}{\mu_r}\right)}{(1-\pi)(1-a)\gamma P\mu_c\beta_r\lambda_r\mu_w}. \tag{4.29}$$

Upon solving for $(1-\varrho)$ in equation (4.28) using the quadratic formula gives

$$(1-\varrho) = \frac{-\mathscr{B}_1 \pm \sqrt{|\mathscr{B}_1{}^2 - 4(\mathscr{B}_2\mathscr{B}_0)|}}{2\mathscr{B}_2}, \tag{4.30}$$

where

$$\mathscr{B}_0 = -\Delta^{**}\mu_c(\gamma+\mu_t)\mu_w^2, \quad \mathscr{B}_1 = -\mu_w(\Delta^{**}\tau k_c\lambda_w(\gamma+\mu_c+\mu_t)-\mu_w), \text{ and} \tag{4.31}$$

$$\mathscr{B}_2 = -\Delta^{**}(\tau k_c\lambda_w)^2. \tag{4.32}$$

From equation (4.30), the critical efficacy of the blood stage vaccine, $0 < \varrho_c < 1$, is

$$\varrho_c = 1 - \left(\frac{-\mathscr{B}_1 \pm \sqrt{|\mathscr{B}_1{}^2 - 4(\mathscr{B}_2\mathscr{B}_0)|}}{2\mathscr{B}_2} \right), \tag{4.33}$$

where $\mathscr{B}_i$, $i = \{0,1,2\}$ are as defined in equation (4.30). Equation (4.33) implies that for any blood stage vaccine to effectively control clinical malaria, its efficacy must be higher than the stated critical vaccine efficacy.

Differentiating R_v with respect to vaccine efficacy ϱ yields

$$\begin{aligned} \frac{\partial R_v}{\partial\, \varrho} = & -\frac{P(1-\pi)(1-a)\beta_r\lambda_r\mu_c\gamma}{\mu_r\left(\mu_m+\frac{\beta_r\lambda_r}{\mu_r}\right)\left(\frac{(1-\varrho)\tau k_c\lambda_w}{\mu_w}+\mu_c\right)\left(\frac{d\tau\lambda_w}{\mu_w}+1\right)^2\Psi_3} \\ & + \frac{P(1-\pi)(1-a)\beta_r\lambda_r\mu_c\gamma(1-\varrho)\tau\lambda_w k_t}{\mu_r\mu_w\left(\mu_m+\frac{\beta_r\lambda_r}{\mu_r}\right)\left(\frac{(1-\varrho)\tau k_c\lambda_w}{\mu_w}+\mu_c\right)\left(\frac{d\tau\lambda_w}{\mu_w}+1\right)^2{\Psi_3}^2} \\ & + \frac{P(1-\pi)(1-a)\beta_r\lambda_r\mu_c\gamma(1-\varrho)\tau\lambda_w k_c}{\mu_r\mu_w\left(\mu_m+\frac{\beta_r\lambda_r}{\mu_r}\right)\left(\frac{(1-\varrho)\tau k_c\lambda_w}{\mu_w}+\mu_c\right)^2\left(\frac{d\tau\lambda_w}{\mu_w}+1\right)^2\Psi_3}, \end{aligned} \tag{4.34}$$

where $\Psi_3 = ((((1-\varrho)\tau k_t\lambda_w)/\mu_w)+\gamma+\mu_t)$.

The right-hand side of equation (4.34) is simplified by making the following representations: let $\Psi_1 = \mu_r(\mu_m + ((\beta_r\lambda_r)/\mu_r))$, $\Psi_2 = ((((1-\varrho)\tau k_c\lambda_w)/\mu_w)+\mu_c)$ and $\Psi_4 = (1 + ((d\tau\lambda_w)/\mu_w))$. So that,

$$\frac{\partial R_v}{\partial\, \varrho} = \frac{P(1-\pi)(1-a)\beta_r\lambda_r\mu_c\gamma(1-\varrho)\tau\lambda_w k_t k_c}{\Psi_1\Psi_2\Psi_3\Psi_4^2}\left\{\frac{1}{\mu_w k_c\Psi_3}+\frac{1}{\mu_w k_t{\Psi_2}^2}-\Pi^*\right\}, \tag{4.35}$$

where $\Pi^* = (1/((1-\varrho)\tau\lambda_w k_c k_t))$. It is observed that $(\partial R_v/\partial\, \varrho) < 0$ when $\mu_c{\mu_w}^2(\gamma+\mu_t) > \tau k_c k_t{\lambda_w}^2(1-\varrho)$. R_v is therefore a decreasing function of the blood stage vaccine ϱ. This means that an efficacious BSV reduces the density of infected erythrocytes within the human host. Figure 4.4 shows the profiles of the density of blood trophozoites and blood schizonts as a function of the efficacy of the BSV, ϱ. The density of infected erythrocytes decreases with increasing values of ϱ.

4.6 Numerical simulation

4.6.1 Sensitivity analysis

The main concern in the control of infectious diseases is the capacity of the infection to invade the population. The threshold quantity called the vaccine reproduction number, provides a reasonable measure of the ability of the infective malaria parasites to invade the susceptible cell populations (Heesterbeek and Dietz, 1996). When $R_v < 1$, the infective parasites produce less than one new infection per infection period and the disease subsequently dies out. However, when $R_v > 1$, an infective parasite generates several infections leading to disease severity. In light of this, the sensitivity analysis of disease R_v in (4.14) is carried out so as to determine important parameters in the dynamics of *P. falciparum* malaria in the presence of vaccine controls. The normalised forward sensitivity index technique as presented by Arriola and Hyman (2007) is adopted. Using Mathematica software, the sensitivity results for the 17 parameters in R_v are as shown in Table 4.3.

Table 4.3: The sensitivity indices of R_v with respect to model parameters

Parameter	Sensitivity index	Parameter	Sensitivity index
P	+1.0000	π	-0.2500
a	-0.2500	ϱ	-0.770486
γ	+0.293702	β_r	+0.0000663956
λ_r	+0.0000664	μ_c	+0.0000247494
μ_r	-0.000066396	d	-0.0222497
τ	-0.080544	λ_w	-0.080544
μ_w	+0.080	μ_m	-0.00006639
k_c	-0.0000247494	k_t	-0.0582696
μ_t	-0.235433		

The rate of merozoite invasion β_r, the rate of progression of infected red blood cells from the trophozoite state to blood schizonts γ and the average number of merozoites released per bursting blood schizont P increase (or decrease) the vaccine reproduction number when they are increased (or decreased) as shown in Table 4.3. Malaria vaccine development should target these parameters to reduce malaria disease progression in humans. On the other hand, the higher the efficacy of blood stage vaccine e, the lower the value of R_v. A highly efficient erythrocytic vaccine has the potential to eradicate clinical malaria. The proportion

of merozoites that develop into gametocytes π is also shown to decrease the value of R_v when they are increased. The higher the density of gametocytes, the lower the density of merozoites in the host's blood. Although this would minimise secondary and subsequent erythrocytic invasions and hence malaria severity, it has the potential to enhance parasite transmission to the mosquito vector. This is due to increased density of gametocytes per blood sample per mosquito bite.

The number of merozoites released per bursting infected red blood cells and the efficacy of the blood stage vaccine are shown to be the most sensitive parameters in influencing in-host malaria progression. For example, a 10% increase (or decrease) on P, will cause a 10% increase (or decrease) in R_v. These two parameters should hence be carefully estimated (Mikucki, 2012) and clinical malaria control using antimalarial drugs and malaria vaccines should target the two parameters.

4.6.2 Vaccine efficacy

Lemma 4.2. *The vaccination threshold* $R_v < 1$ *whenever* $\varrho > \varrho_c$

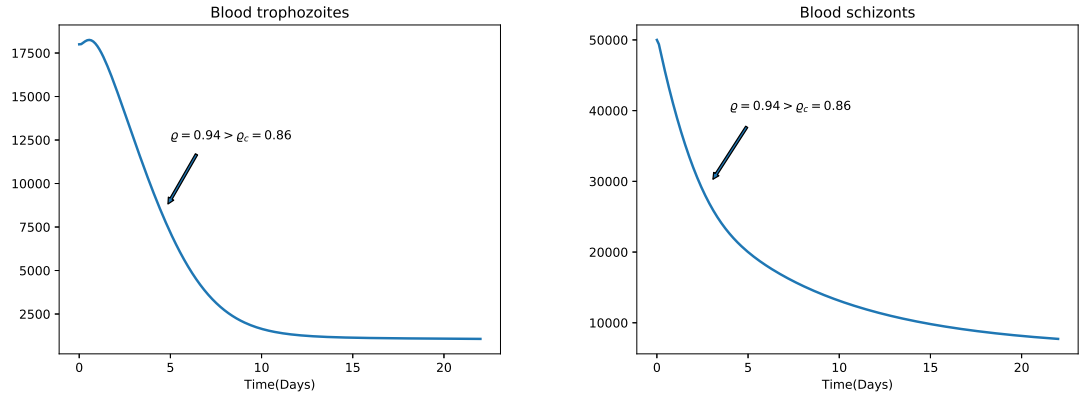

(a) (b)

Figure 4.3: Graphs showing the density of (a) blood trophozoites $T(t)$ and (b) blood schizonts $C(t)$ when the blood stage vaccine efficacy, $\varrho = 0.94 > \varrho_c = 0.86$ and $R_v = 0.58 < 1$. Used parameter values are shown in Table 4.4.

When the efficacy of the BSV (ϱ_c) is higher than the critical vaccine efficacy ϱ_c, the merozoites are eradicated from the blood stream. Under this setting, the capacity of the blood stage vaccine to eradicate malaria parasites in the host's blood stream is guaranteed by Lemma 4.2. The results of Lemma 4.2 are shown graphically in Figures 4.3a and 4.3b using different

values of ϱ. In Figure 4.3, a blood stage vaccine with a minimum efficacy of 94% is needed to control the blood stage parasites. Using the provided parameter values and expression (4.14), it is observed that under this condition, R_v is less that unity. That is $R_v = 0.58 < 1$.

Lemma 4.3. *The vaccination threshold* $R_v > 1$ *whenever* $\varrho < \varrho_c$

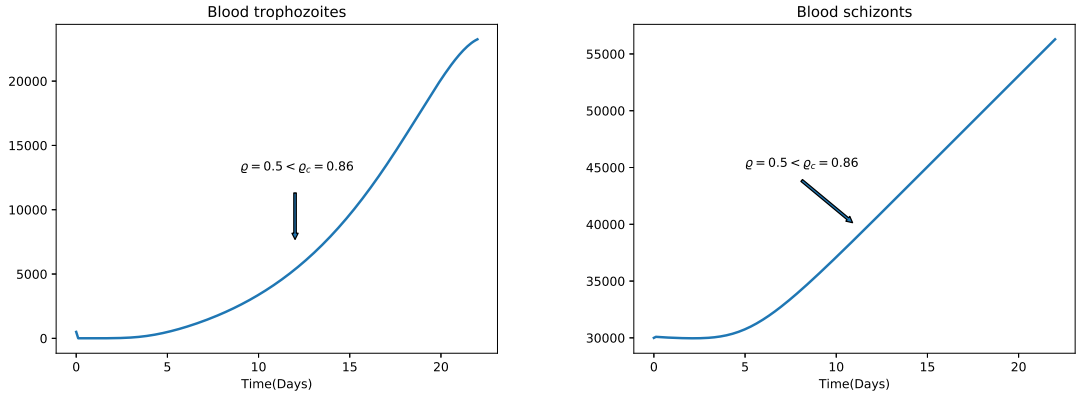

(a) (b)

Figure 4.4: Graphs showing the density of (a) blood trophozoites $T(t)$ and (b) blood schizonts $C(t)$ when the efficacy of blood stage vaccine, $\varrho = 0.5 < \varrho_c = 0.86$ and $R_v = 1.27 > 1$. Used parameters values are shown in Table 4.4.

When the efficacy of the blood stage vaccine is lower than the critical efficacy $(\varrho < \varrho_c)$, the rate of infection of susceptible red blood cells is higher. This leads to increased density of blood trophozoites and blood schizonts as shown in Figure 4.4. Using the parameter values in Table 4.4 and the expression for the vaccine reproduction number, it is observed that the above condition is only guaranteed when R_v is greater than unity. That is, $R_v = 1.27 > 1$.

It is clear, therefore, that only a highly efficacious blood stage vaccine, $(\varrho > 90\%)$ would guarantee the achievement of a parasite-free equilibrium point shown in Figure 4.5. A blood stage vaccine with lower efficacy $(\varrho < 50\%)$ is likely to be less effective in clearing the malaria parasites. A malaria persistent steady state is hence probable (see Figure 4.5).

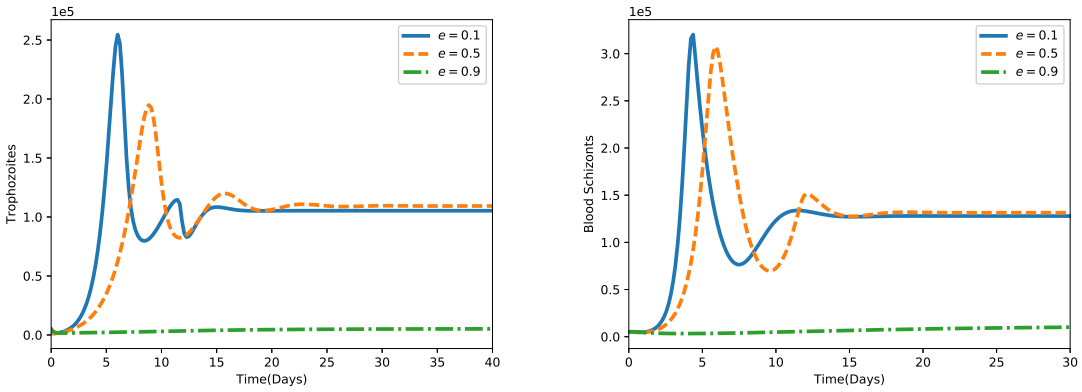

(a) (b)

Figure 4.5: Simulations showing the effect of varying the efficacy of blood stage vaccine (ϱ) on the density of infected red blood cells. All other parameter values are shown in Table 4.4.

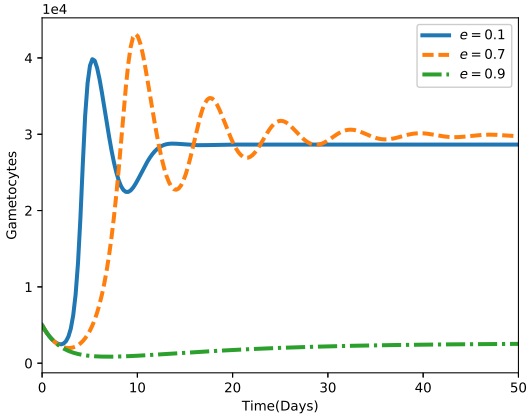

Figure 4.6: Simulations showing the effect of varying the efficacy of blood stage vaccine (ϱ) on the density of gametocytes in blood. All other parameter values are shown in Table 4.4.

The density of gametocytes in the blood stream is indirectly influenced by the blood stage vaccine. Higher vaccine efficacy minimises the density of gametocytes that are later sucked up by feeding anopheles mosquitoes. As the efficacy of blood stage vaccine diminishes, higher density of gametocytes is observed in the blood stream as shown is Figure 4.6.

The effect of BSV-induced reduction of merozoites released per bursting blood schizont is monitored by differentiating R_v with respect to a. This gives

$$\frac{\partial R_v}{\partial a} = -\frac{(1-\pi)\gamma(1-\varrho)P\mu_c\beta_r\lambda_r}{\mu_r\left(\mu_m+\frac{\beta_r\lambda_r}{\mu_r}\right)\left(1+\frac{d\tau\lambda_w}{\mu_w}\right)^2\left(\frac{(1-\varrho)\tau k_c\lambda_w}{\mu_w}+\mu_c\right)\Psi_3} < 0, \tag{4.36}$$

where $\Psi_3 = ((((1-\varrho)\tau k_t\lambda_w)/\mu_w)+\gamma+\mu_t)$.

The following observations are made: the vaccine reproduction number R_v decreases with increasing value of a. As less blood schizonts burst, less merozoites are released and hence less secondary infections that increases the severity of the disease as displayed in Figure 4.7. This leads to the reduction in the vaccine reproduction number and hence the density of infected red blood cells in the blood stream.

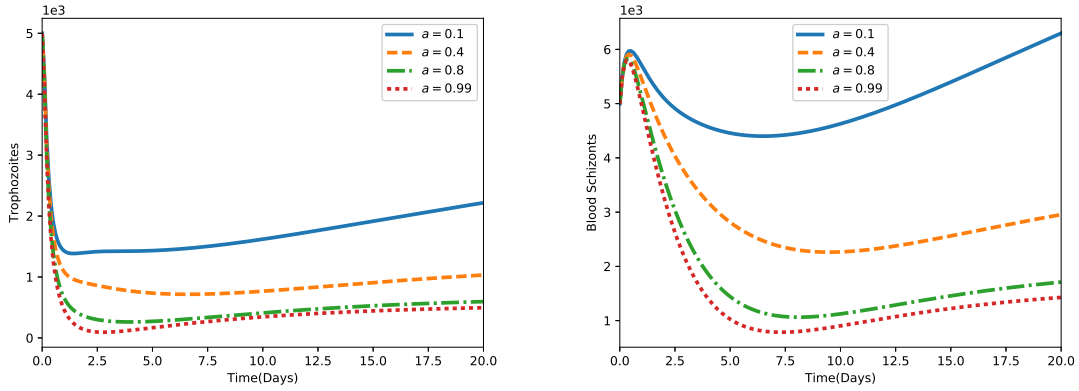

(a) (b)

Figure 4.7: Simulations showing the effect of varying the parameter a on the density of (a) blood trophozoites $T(t)$ and (b) blood schizonts $C(t)$. All other parameter values are shown in Table 4.4.

The effect of the BSV-induced enhanced production of CD8$^+$ T cells is monitored by the partial derivatives of R_v with respect to τ.

$$\begin{aligned}\frac{\partial R_v}{\partial \tau} = &-\frac{(1-\pi)(1-a)\gamma(1-\varrho)^2 P k_c \mu_c \beta_r \lambda_r \lambda_w}{\mu_r \mu_w \left(\frac{d\tau\lambda_w}{\mu_w}+1\right)^2 \left(\mu_m + \frac{\beta_r\lambda_r}{\mu_r}\right)\left(\frac{(1-\varrho)\tau k_c \lambda_w}{\mu_w}+\mu_c\right)^2 \Psi_3} \\ &-\frac{(1-\pi)(1-a)\gamma(1-\varrho)^2 P k_t \mu_c \beta_r \lambda_r \lambda_w}{\mu_r \mu_w \left(\frac{d\tau\lambda_w}{\mu_w}+1\right)^2 \left(\mu_m + \frac{\beta_r\lambda_r}{\mu_r}\right)\left(\frac{(1-\varrho)\tau k_c \lambda_w}{\mu_w}+\mu_c\right) {\Psi_3}^2} \\ &-\frac{2(1-\pi)(1-a)\gamma d(1-\varrho) P \mu_c \beta_r \lambda_r \lambda_w}{\mu_r \mu_w \left(\frac{d\tau\lambda_w}{\mu_w}+1\right)^3 \left(\mu_m + \frac{\beta_r\lambda_r}{\mu_r}\right)\left(\frac{(1-\varrho)\tau k_c \lambda_w}{\mu_w}+\mu_c\right) \Psi_3}\end{aligned} \tag{4.37}$$

where, $\Psi_3 = ((((1-\varrho)\tau k_t \lambda_w)/\mu_w) + \gamma + \mu_t)$.

By applying the algebraic substitutions used in equation (4.35), equation (4.37) simplifies to:

$$\frac{\partial R_v}{\partial \tau} = -\frac{\Theta^*}{\Psi_1 \Psi_2 \Psi_3 \Psi_4^2}\left(\frac{1}{dk_t\Psi_2} + \frac{1}{dk_c\Psi_3} + \frac{2}{(1-\varrho)k_c k_t \Psi_4},\right) < 0, \tag{4.38}$$

where

$$\Theta^* = (1-\pi)(1-a)\gamma P(1-\varrho)^2 d k_c k_t \mu_c \beta_r \lambda_r \lambda_w.$$

It is evident from equation (4.38) that R_v decreases with increasing τ. As more CD8$^+$ T cells are activated, more trophozoites and blood schizonts are killed through phagocytosis, leading to reduction in the severity of malaria infection as shown in Figure 4.8.

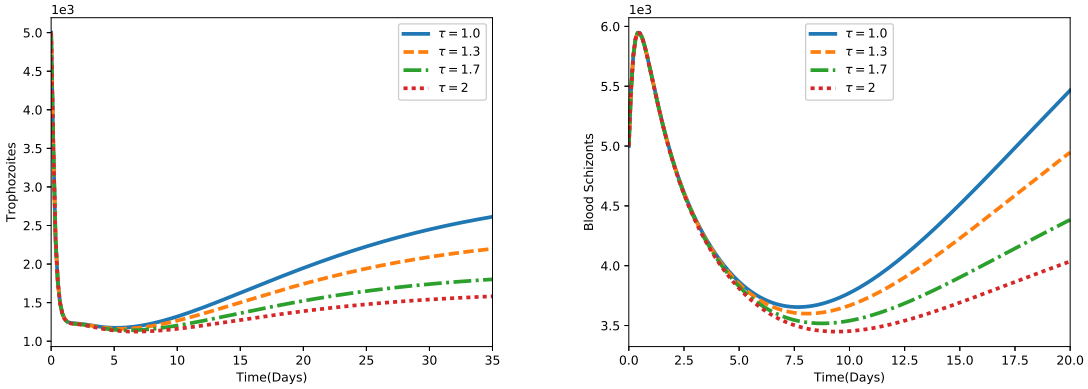

(a) (b)

Figure 4.8: Simulation showing the the density of (a) blood trophozoites $T(t)$ and (b) blood schizonts $C(t)$ for varying values of blood stage vaccine-induced enhanced production parameter τ. All other parameter values are shown in Table 4.4.

The effect of the BSV-induced reduction in the burst size P of infected red blood cells is shown by the following formula:

$$\frac{\partial R_v}{\partial P} = \frac{(1-\pi)(1-a)\gamma(1-\varrho)\mu_c\beta_r\lambda_r\mu_c}{\mu_r\left(\frac{d\tau\lambda_w}{\mu_w}+1\right)(d\tau\lambda_w+\mu_w)\left(\mu_m+\frac{\beta_r\lambda_r}{\mu_r}\right)\left(\frac{(1-\varrho)\tau k_c\lambda_w}{\mu_w}+\mu_c\right)\Psi_3}, \tag{4.39}$$

where $\Psi_3 = ((((1-\varrho)\tau k_t\lambda_w)/\mu_w)+\gamma+\mu_t)$.

Note that $(\partial R_v/\partial P) > 0$ and R_v decreases (increases) with decreasing (increasing) value of P. The higher the density of released merozoites from bursting blood schizonts, the higher the rate of secondary invasions at the blood stage. The density of infected red blood cells in blood is observed to increase with increasing value of P as shown in Figure 4.9. An efficacious malaria vaccine would be necessary in minimising secondary and future invasions that occur at the blood stage of malaria infection.

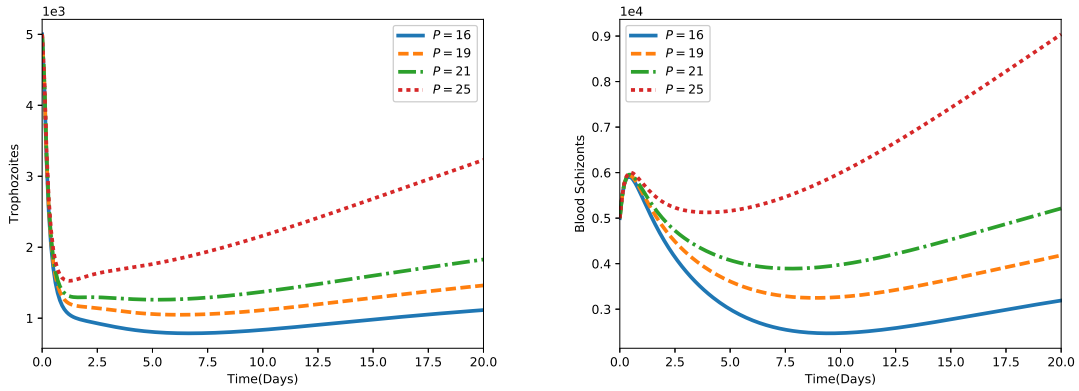

(a) (b)

Figure 4.9: Simulations showing how the infected red blood cell burst size P affects the density of (a) blood trophozoites $T(t)$ and (b) blood schizonts $C(t)$. All other parameter values are shown in Table 4.4.

4.6.3 Threshold analysis and vaccine impact

The Malaria Vaccine Technology Road map updated in November 2013 has two key strategic goals targeting *P. falciparum* and *P. vivax* malaria by the year 2030: (1) to develop vaccines with over 75% protective efficacy against clinical malaria and (2) to develop transmission blocking vaccines thereby reducing new cases of human malaria infections (MVFG, 2018). A combination of malaria vaccines (pre-erythrocytic, blood stage and transmission blocking

vaccines) could help in achieving the over 75% strategic goal (Miura, 2016).

A highly efficacious blood stage vaccine has a potential to significantly reduce the number of gametocytes in the blood stream, thereby minimising parasite transmission to mosquitoes and subsequently to other human beings. In the following section, the possible impact of different malaria vaccine combinations with varying degrees of efficacy is highlighted.

In the absence of malaria vaccines, $\varrho = \chi = \nu = 0$, it is observed from Figure 4.13, that the density of infected red blood cells increases rapidly and settles at the parasite persistent equilibrium point. This trend is also observed with the infected hepatocytes (see Figure 4.10b). The density of infected hepatocytes rises due to invasion by sporozoites for about a week. This is followed by a slight decline in density and subsequent persistent concentration at the liver stage.

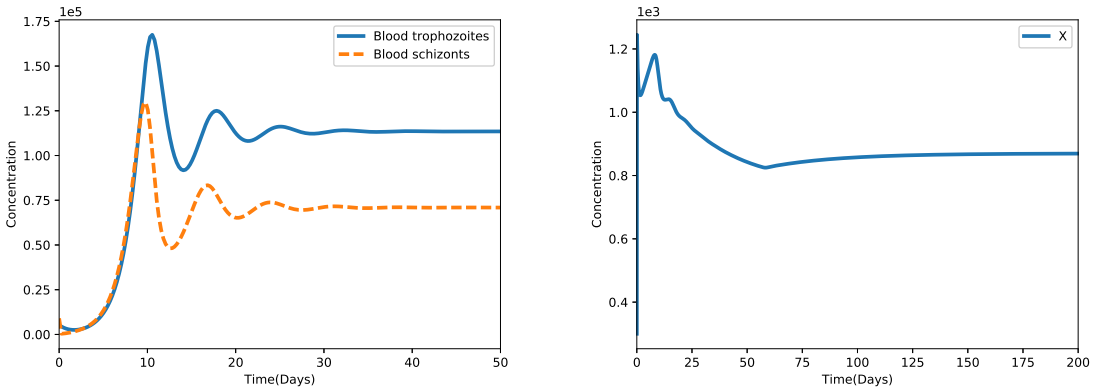

(a) (b)

Figure 4.10: Time profile of the density of (a) infected red blood cells and (b) infected hepatocytes in the absence of malaria vaccines ($\varrho = \chi = \nu = 0$). All parameter values are shown in Table 4.4.

A malaria vaccine with an efficacy of 45% may not be adequate in eliciting sufficient immune response to reduce and clear infection as shown in Figure 4.11. More *Plasmodium* parasites are likely to persist in the blood stream, raising the severity of infections. A combination of blood stage vaccine (efficiency $\geq$ 90%) and transmission blocking vaccine (efficiency $\geq$ 90%) is likely to result in rapid eradication of the infected red blood cells from the human host as displayed in Figure 4.12. Observe that the parasite-free equilibrium is highly probable irrespective of the efficacy of the pre-erythrocytic vaccine in this context.

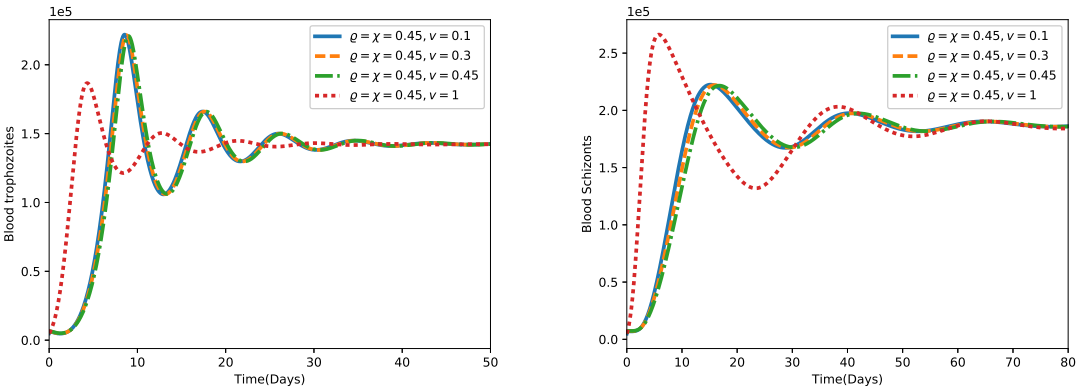

(a) (b)

Figure 4.11: Time profile of the density of (a) blood trophozoites and (b) blood schizonts for $\varrho = \chi = 0.45$ with varying efficacy of pre-erythrocytic vaccine v. Used arameter values are shown in Table 4.4.

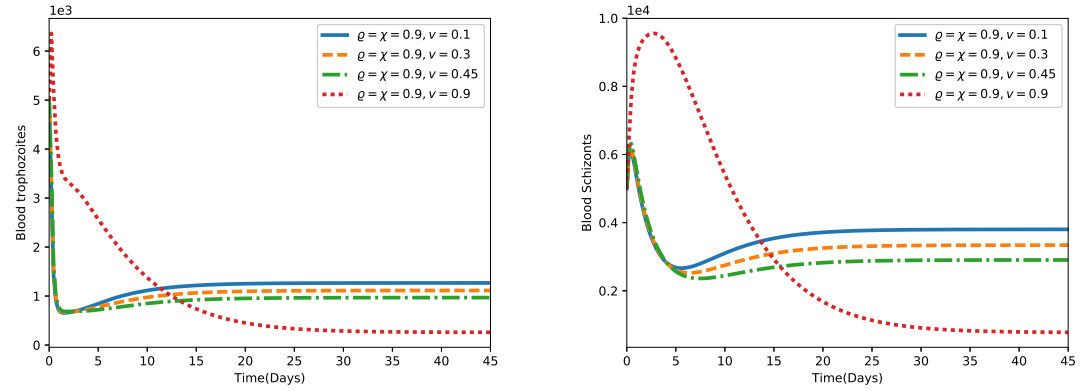

(a) (b)

Figure 4.12: Time profile of the density of (a) blood trophozoites and (b) blood schizonts for $\varrho = \chi = 0.9$ with varying efficacy of pre-erythrocytic vaccine v. The set of parameter values is shown in Table 4.4.

Similarly, the density of gametocytes in the blood stream is observed to diminish quickly in the presence of efficacious malaria vaccine combinations (see Figure 4.13).

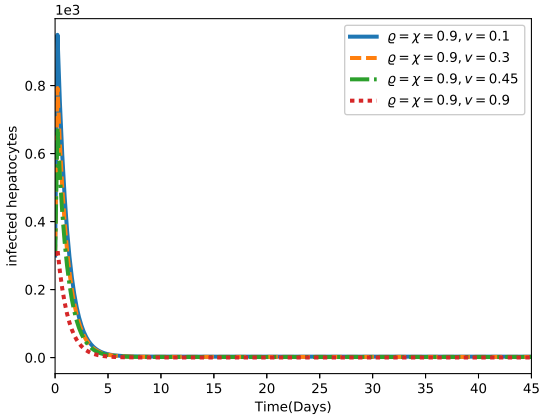

Figure 4.13: Simulation showing the profile of infected hepatocytes in the presence of perfect malaria vaccines ($\varrho = \chi = 0.9$). The efficacy of the pre-erythrocytic vaccine v is varied from 0 to 1. The set of parameter values is shown in Table 4.4.

Table 4.4: Parameter values used in the numerical simulations and sensitivity analysis

Parameter	Value	Range	Units	Source
P	16	(15-20)	Unitless	(Diebner et al., 2000)
k_x	0.01	(0.001-0.9)	/day	(Chiyaka et al., 2008)
k_t	0.01	(0.001-0.9)	/day	(Chiyaka et al., 2008)
k_c	10^{-6}	$(10^{-7} - 0.9)$	/day	(Chiyaka et al., 2008)
μ_r	0.083	(0.05-0.1)	/day	(Anderson et al., 1989)
β_r	2×10^{-1}	(0.07-0.3)	$/mm^3$/day	(Dondorp et al., 2000)
β_s	10^{-3}	(0.001-0.2)	$/mm^3$/day	(Selemani et al., 2016)
π	0.2	(0.1-0.9)	unitless	(Talman et al., 2004)
μ_h	0.029	(0.01-0.5)	/day	Estimated
μ_x	0.02	(0.01-1)	/day	(Selemani et al., 2016)
λ_r	3×10^3	(3E+3–3E+8)	cells/ml/day	(Li et al., 2011)
λ_h	3×10^5	(3E+3–3E+8)	cells/ml/day	(Tumwiine et al., 2008)
λ_w	30	(10-40)	$/\mu l^{-1}$/day	(Chiyaka, 2010)
μ_m	48	(46-50)	/day	(Li et al., 2011)
Λ	30	(18-35)	sporozoites/day	(Selemani et al., 2016)
μ_s	1.2	(1.0-2.4)	/day	(Selemani et al., 2016)
μ_t	0.5	(0.01-0.8)	/day	(Magombedze et al., 2011a)
μ_c	0.5	(0.01-0.9)	/day	(Magombedze et al., 2011a)
μ_g	6.25×10^{-5}	(6E-5–7E-8)	/day	(Selemani et al., 2016)

Continued on next page

Table 4.4 – *Continued from previous page*

Parameter	Value	Range	Units	Source
μ_w	2	(0.05-3)	/day	(Chiyaka, 2010)
δ_x	10^{-5}	$(10^{-4} - 10^{-7})$	mm^{-3}/day	(Chiyaka, 2010)
δ_t	0.05	(0.01-0.08)	mm^{-3}/day	(Chiyaka, 2010)
δ_c	0.05	(0.01-0.08)	mm^{-3}/day	(Chiyaka, 2010)
γ	1.5	(0.1-2)	/day	(Selemani et al., 2016)
χ	0.2	(0-1)	unitless	Assumed
ν	0.3	(0-1)	unitless	Assumed
τ	1.5	(1-2)	unitless	(Niger and Gumel, 2011)
b	0.2	(0-1)	unitless	(Niger and Gumel, 2011)
a	0.2	(0-1)	unitless	(Niger and Gumel, 2011)
d	5×10^{-4}	(5E-5–1E-2)	unitless	(Magombedze et al., 2011a)
N	10^4	$(10^3 - 10^5)$	Unitless	(Tumwiine et al., 2008)
ϱ	0.45	(0-1)	unitless	(Birkett, 2016)

4.7 Discussion

Using numerical simulation, it is observed that the activated $CD8^+$T cells and malaria vaccines have a considerable effects on malaria control. Vaccination reduces the basic reproduction number by a constant factor. A blood stage vaccine, with an efficacy of at least 90% is shown to be effective in controlling in-host *P. falciparum* malaria.

It is further observed that malaria vaccines that minimise the total number of merozoites released per bursting hepatocyte, reduces the density of blood trophozoites and blood schizonts. Similarly, a highly efficacious vaccine greatly reduces the burst size of the blood schizonts, so that less merozoites are released from the infected red blood cells. This has the potential to reduce malaria severity and hence malaria transmission to the mosquito vector.

An efficacious blood stage vaccine should maximise the rate of activation of $CD8^+$T cells. It is noted that the higher the vaccine potential to activate these immune cells, the lower the density of infected red blood cells in the human host. Moreover, different vaccine combinations yield different results. In the absence of vaccine therapy, the density of infected red blood cells (blood trophozoites and blood schizonts) is shown to increase and stabilise at

the parasite persistent equilibrium point. A pre-erythrocytic vaccine with an efficacy of at least 90% is also shown to guarantee the attainment of a parasite-free equilibrium.

Like many other epidemic models, the presented in-host malaria model is formulated based on several model assumptions. The parameter values used in the study are also obtained from past literature. The results of our study should therefore be approached with some discretion. The presented model ignores the biology of $CD8^+$ T activation and assumes constant parameter values. It would therefore be difficult to predict with higher accuracy, the optimal malaria vaccine efficacy. In spite of the stated shortcomings, the presented in-host malaria model provides useful insights on the need to improve the efficacy of current malaria vaccines in development and the need to try vaccine combinations in controlling *P. falciparum* malaria infection.

4.8 Conclusion

In this chapter, a mathematical model for in-host malaria dynamics subject to malaria vaccines has been presented. The analysis of the model provides useful insights into individual and combined vaccine impacts in reducing the severity of clinical *P. falciparum* malaria. The notion of critical vaccine efficacy is key in the development of malaria vaccines with the potential to eliminate *P. falciparum* malaria in individuals that would get infected with the disease.

In order to achieve a substantial reduction in malaria mortality and morbidity, the efficacy of the malaria vaccine should be higher than the corresponding critical vaccine efficacy. For instance, when the efficacy of the blood stage vaccine is lower than the critical efficacy ($\varrho < \varrho_c$), the rate of infection of susceptible red blood cells is higher and clinical malaria persists. However, the density of blood trophozoites and blood schizonts decreases drastically if the efficacy of the blood stage vaccine is higher than the critical blood stage vaccine efficacy. The combined administration of malaria vaccines (Miura, 2016) and antimalarial drugs is likely to provide the much needed therapeutic control against *P. falciparum* malaria.

In the next Chapter 5, uncertainty and sensitivity analysis is performed to establish critical model parameters for therapeutic target and interventions during clinical malaria infections.

Chapter 5

Uncertainty and sensitivity analysis applied to an in-host malaria model subject to vaccines

5.1 Introduction

During disease model formulation, simplifications and assumptions on the model itself and on the parameters that represent the different transitions and interactions in the model are made. Owing to uncertainty in parameter values, it is important to correctly understand the possible effects of such parameter values to the anticipated model outcome (Gomero, 2012; Pereira and Broed, 2006). Uncertainty in the set of parameter values generates variability in the model's predictive capabilities. The lower the number of uncertain parameters in a model, the lower the significance of variability introduced into a model. On the other hand, a higher number of parameters with uncertain values result into a higher variability in model outcome (Gomero, 2012).

In-host malaria transmission models have become very complex. Unlike simple models, complex models may best be understood by numerical analysis (Blower and Dowlatabadi, 1994). Uncertainty and sensitivity analysis are instrumental in analysing the dynamics of such structurally complex models that experiences high levels of uncertainty in the estimation of their input parameter values. The concept of uncertainty analysis enables us to evaluate the variability in the output (Iman and Helton, 1988). Conversely, a sensitivity analysis helps us to discern important parameters in the dynamics of infection under study.

There are three techniques of uncertainty and sensitivity analysis (Iman and Helton, 1988). These include: (i) latin hypercube sampling / partial rank correlation coefficient (LHS/PRCC), (ii) response surface methodology; and (3) differential analysis. The more sophisticated and efficient approach of LHS/PRCC (Blower et al., 1991; Iman and Helton, 1988) that permits synchronous variation of all input variables is considered in this study. LHS/PRCC sensitivity analysis is a synergy of Latin Hypercube Sampling (McKay et al., 1979) and the Partial Rank Correlation Coefficient (Hamby, 1994). It aims to identify and rank pivotal model parameters whose uncertainties contribute to prediction imprecision (Gomero, 2012).

Several research studies (Anderson et al., 1989; Diebner et al., 2000; Diekmann et al., 1990; Gravenor and Kwiatkowski, 1998; Gurarie and McKenzie, 2006; Hetzel and Anderson, 1996; Hoshen et al., 2000; McQueen and McKenzie, 2004; Molineaux et al., 2001; Molineaux and Dietz, 1999; Saul, 1998) have focussed on understanding the dynamics and control of *P. falciparum* infections. Although most of these models have investigated parameter importance in driving malaria infection, this is mainly based on the basic reproduction number of the disease, which often do not have all the model parameters. Sensitivity analysis for the entire parameter space provides the right rigour for parameter evaluation in driving malaria disease progression.

Previous studies (Neilan et al., 2010; Zhong, 2011), used parameter-driven LHS/PRCC procedure to ascertain important parameters and their relative importance in the disease model output. In (Gomero, 2012), LHS/PRCC procedure is coupled with the optimal control numerical procedure to simultaneously examine the effects of all LHS parameters on the objective functional value. In this chapter, the LHS/PRCC uncertainty and sensitivity analysis technique is applied to an in-host *P. falciparum* malaria model with vaccine controls (pre-erythrocytic vaccines, blood stage vaccines and transmission blocking vaccines). Multi-component and multi-stage vaccine combinations are evaluated to establish optimal vaccine combinations.

5.2 Model formulation

The compartmental model in this chapter is an extension of in-most malaria model in Chapter 3. The model is composed of nine compartments: the malaria sporozoites $S(t)$, the susceptible hepatocytes $H(t)$, the infected hepatocytes $X(t)$, the susceptible erythrocytes $R(t)$, the infected erythrocytes $T(t)$, the gametocytes $G(t)$, the merozoites $M(t)$, unactivated $CD8^+$ T cells $W_n(t)$ and activated $CD8^+$ T cells $W_a(t)$. The activation of $CD8^+$ T cells

caused by the presence of infected hepatocytes and infected erythrocytes only. This activation is further assumed to occur at a constant rate λ_w for both infected hepatocytes X and infected erythrocytes T. Unactivated $CD8^+$ T cells are produced at a fixed rate Ω from the thymus.

A proportion q and ρ of infected erythrocytes and infected hepatocytes get eradicated by the $CD8^+$ T cells before they develop to the schizont stages, respectively. The rest of infected hepatocytes develop asexually and burst open to release blood stage merozoites. It is assumed that some of the newly generated merozoites develop into gametocytes. This proportion is denoted by the parameter π. The commitment to gametocytogenesis is presumably made during the immediately preceding cycle of blood schizogy (Diebner et al., 2000). These blood floating gametocytes are transmitted to the mosquito vector during feeding, marking the onset of sporogonic cycle (not considered in this study).

During blood meal, an infected female mosquito injects sporozoites into the blood stream of the human host at a rate Λ. The sporozoites traverse the blood stream and enter the liver where they invade the liver hepatocytes H at the rate β_s to generate infected hepatocytes X at the liver stage. A natural death rate of μ_s for malaria sporozoites is assumed. Susceptible hepatocytes are recruited at a constant rate λ_h from the bone marrow. Both the infected and uninfected hepatocytes experience natural death at the rates μ_x and μ_h, respectively.

Three malaria vaccines are considered in this model to reduce the severity of *P. falciparum* malaria infection. These are: pre-erythrocytic vaccine (PEV) (see, (Birkett, 2016; Birkett et al., 2013; Nunes et al., 2014)), blood stage vaccine (BSV) (see (Audran et al., 2005; Moorthy et al., 2004; Ogutu et al., 2009)), and transmission blocking vaccines (TBV)(see (Arevalo-Herrera et al., 2005; Hisaeda et al., 2000)). The leading PEV, BSV and TBV considered in this study are RTS,S/AS01, merozoite surface protein 3 (MSP3), *P. falciparum* ookinete surface antigens (Pfs25), respectively. The PEV, BSV and TBV vaccines are assumed to possess efficacies denoted by ν, ϱ and χ, respectively. Note that $0 < \nu < 1$, $0 < \varrho < 1$ and $0 < \chi < 1$.

A summary of the descriptions of model parameters and the state variables is presented in Tables 5.1 and 5.2, respectively. The compartmental flow diagram for the in-host malaria model is provided in Figure 5.1. The structural complexity of the in-host malaria model is the motivation to apply LHS/PRCC technique for uncertainty and sensitivity analysis.

Table 5.1: Table showing model parameters and their descriptions

Parameter	Description
P	Number of merozoites released per bursting erythrocyte
Λ	Injection rate of sporozoites
μ_s	Death rate of sporozoites
β_r	Rate of infection of erythrocytes by merozoites
μ_t	Mortality rate of infected erythrocytes
λ_h	The recruitment rate of hepatocytes
λ_r	The recruitment rate of erythrocytes from the bone marrow
μ_h, μ_x	Death rate of susceptible hepatocyte and infected hepatocyte, respectively
π	Proportion of merozoites that develop into gametocytes per dying infected erythrocyte
ρ, q	Immunosensitivity of infected hepatocyte and erythrocyte, respectively
χ	Efficacy of transmisssion blocking vaccine
μ_r	Natural mortality rate of susceptible erythrocytes
d	Inhibition rate of $CD8^+$T cells response
ϱ	Efficacy of blood stage vaccine
λ_w	Immunogenicity of IRBCs and infected hepatocytes
$1/\varepsilon_0, 1/\varepsilon_1$	A saturation (half) constants for infected hepatocytes and infected erythrocytes, respectively
μ_m, μ_g	Death rate of merozoites and gametocytes, respectively
τ	A modification parameter that accounts for vaccine-induced increased generation of activated $CD8^+$T cells
ν	Efficacy of pre-erythrocytic stage vaccine
μ_n, μ_a	Death rates of unactivated and activated $CD8^+$ T cells, respectively
β_s	Infection rate of hepatocytes by sporozoites
Ω	Recruitment rate of unactivated $CD8^+$ T cells from the thymus
b	A modification parameter accounting for PEV-induced reduction of merozoites released per bursting infected hepatocyte,
a	A modification parameter accounting for BSV-induced reduction of merozoites released per bursting erythrocyte
N	The average number of merozoites released per bursting infected-hepatocytes

Table 5.2: Description of the state variables

Variable	Description
$W_n(t)$	Concentration of unactivated CD8$^+$T cells
$W_a(t)$	Concentration of activated CD8$^+$T cells
$H(t)$	Population of susceptible liver hepatocytes
$X(t)$	Population of infected hepatocytes
$S(t)$	Population of malaria sporozoites
$R(t)$	Population of susceptible erythrocytes
$T(t)$	Population of infected erythrocytes
$M(t)$	Population of merozoites
$G(t)$	Density of gametocytes in blood

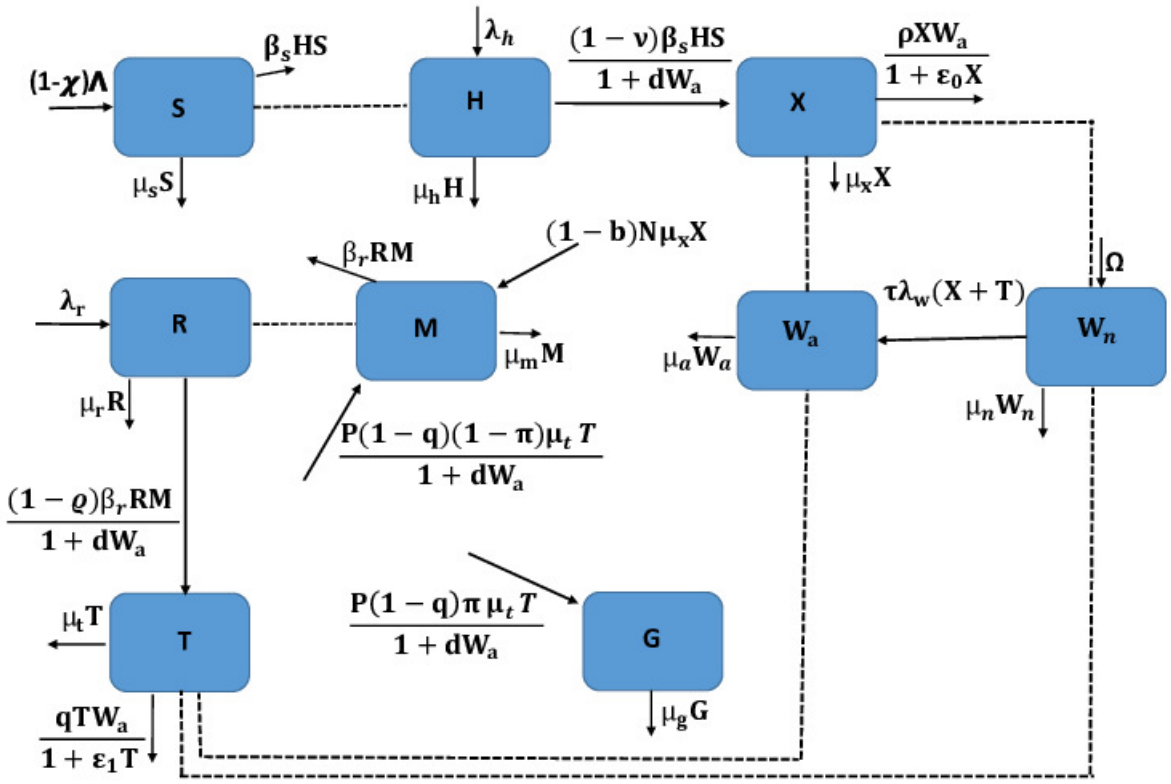

Figure 5.1: A compartmental representation of the dynamics of in-host malaria infection with vaccine control measures.

Based on the dynamics described in Figure 5.1, the following deterministic model describes the dynamics of the in-host malaria infections with multi-stage malaria vaccines:

$$\left.\begin{aligned}
\frac{dS}{dt} &= (1-\chi)\Lambda - \mu_s S - \beta_s SH,\\
\frac{dH}{dt} &= \lambda_h - \mu_h H - \frac{\beta_s(1-\nu)SH}{1+dW_a},\\
\frac{dX}{dt} &= \frac{\beta_s(1-\nu)SH}{1+dW_a} - \mu_x X - \frac{\rho X W_a}{1+\varepsilon_0 X},\\
\frac{dR}{dt} &= \lambda_r - \frac{(1-\varrho)\beta_r RM}{1+dW_a} - \mu_r R,\\
\frac{dT}{dt} &= \frac{(1-\varrho)\beta_r RM}{1+dW_a} - \mu_t T - \frac{qTW_a}{1+\varepsilon_1 T},\\
\frac{dM}{dt} &= \frac{P(1-q)(1-\pi)(1-a)\mu_t T}{1+dW_a} + (1-\rho)(1-b)N\mu_x X - \mu_m M - \beta_r RM,\\
\frac{dG}{dt} &= \frac{P(1-q)(1-a)\pi\mu_t T}{1+dW_a} - \mu_g G,\\
\frac{dW_n}{dt} &= \Omega - \tau\lambda_w(X+T)W_n - \mu_n W_n,\\
\frac{dW_a}{dt} &= \tau\lambda_w(X+T)W_n - \mu_a W_a,
\end{aligned}\right\} \tag{5.1}$$

subject to the following initial conditions:

$S(0) \geq 0, H(0) > 0, X(0) \geq 0, R(0) > 0, T(0) \geq 0, M(0) \geq 0, G(0) \geq 0, W_n(0) > 0, W_a(0) \geq 0$.

Positivity of solutions

The long term behaviour of any dynamical system is instrumental in the understanding of the system. System (5.1) monitors changes in the density of erythrocytes, hepatocytes, malaria parasite and $CD8^+$ T cells. To warrant biological sense, the state variables of system (5.1) should be nonnegative. Specifically, we show that all solutions of system (5.1) with nonnegative initial conditions will remain nonnegative $\forall t \geq 0$.

Theorem 5.1. *Given nonnegative initial conditions* $(S(0) \geq 0, H(0) > 0, X(0) \geq 0, R(0) > 0, T(0) \geq 0, M(0) \geq 0, G(0) \geq 0, W_n(0) > 0, W_a(0) \geq 0)$*, the system* (5.1) *has a nonnegative solution* $(S(t), H(t), X(t), R(t), T(t), M(t), G(t), W_n(t), W_a(t))$*, for all time* $t \geq 0$.

Proof:
From the first equation in system (5.1), it can clearly see that

$$\frac{\mathrm{d}S}{\mathrm{d}t} \geq -(\mu_s + \beta_s H)S. \tag{5.2}$$

Integrating equation (5.2) gives

$$S(t) \geq S_0 \exp\left\{-\int_0^t (\mu_s + \beta_s H(s))\mathrm{d}s\right\}. \tag{5.3}$$

Therefore, $S(t) \geq 0 \quad \forall t \geq 0$.

Similarly, the last equation in system (5.1) yields

$$\frac{\mathrm{d}W_a}{\mathrm{d}t} \geq -\mu_a W_a. \tag{5.4}$$

Integrating the separable inequality (5.4) gives

$$W_a(t) = W_a(0)\exp(-\mu_a t) \geq 0. \tag{5.5}$$

Using the same argument, the rest of the state variables can similarly be shown to be nonnegative for all time $t \geq 0$. That is, $H(t) > 0$, $X(t) \geq 0$, $R(t) > 0$, $T(t) \geq 0$, $M(t) \geq 0$, $G(t) \geq 0$ and $W_n(t) \geq 0 \; \forall t \geq 0$. This completes the proof.

Boundedness of solutions

The nonnegative solutions to system (5.1) must be well posed in regions of biological sense. The proof that the solutions are bounded is as follows:

Let N_r be the total population of susceptible and infected erythrocytes in the host. This gives $N_r(t) = R(t) + T(t)$. Therefore,

$$\begin{aligned}\frac{\mathrm{d}N_r}{\mathrm{d}t} &= \lambda_r - \mu_r R - \mu_t T - qTW_a, \\ &\leq \lambda_r - \bar{\mu}_1 N_r \quad \text{where} \quad \bar{\mu}_1 = \min\{\mu_r, \mu_t\}.\end{aligned} \tag{5.6}$$

Using the initial condition $N_r(0) = N_{r0} > 0$, inequality (5.6) is solved by integrating factor method to obtain

$$N_r(t) \leq \frac{\lambda_r}{\bar{\mu}_1} + e^{-\bar{\mu}_1 t}\left(N_r(0) - \frac{\lambda_r}{\bar{\mu}_1}\right). \tag{5.7}$$

This implies that at any time t, $N_r(t) \leq \max\{N_r(0), \lambda_r/\bar{\mu}_1\}$.

Again, let $N_p(t) = S(t) + M(t) + G(t)$, be the sum of malaria parasites at any time t during clinical *P. falciparum* infection. So that

$$\begin{aligned}
\frac{\mathrm{d}N_p}{\mathrm{d}t} &= (1-\chi)\Lambda + \frac{P(1-q)(1-\pi)(1-a)\mu_t T}{1+dW_a} + (1-\rho)(1-b)N\mu_x X \\
&\quad + \frac{P(1-q)(1-a)\pi\mu_t T}{1+dW_a} - \mu_s S - \mu_m M - \mu_g G - \beta_s SH - \beta_r RM, \\
&\leq (1-\chi)\Lambda + \Psi_1(t) - \bar{\mu}_2 N_p \quad \text{where} \quad \bar{\mu}_2 = \min\{\mu_s, \mu_m, \mu_g\}, \quad \text{and} \qquad (5.8) \\
\Psi_1(t) &= \frac{P(1-q)(1-\pi)(1-a)\mu_t T}{1+dW_a} + (1-\rho)(1-b)N\mu_x X + \frac{P(1-q)(1-a)\pi\mu_t T}{1+dW_a}.
\end{aligned}$$

Solving inequality (5.8) gives

$$N_p(t) \leq \frac{(1-\chi)\Lambda}{\bar{\mu}_2} + e^{-\bar{\mu}_2 t}\int_0^t e^{-\bar{\mu}_2 t}\Psi_1(t)\mathrm{d}t + C_1 e^{-\bar{\mu}_2 t}, \tag{5.9}$$

where the constant of integration C_1 is given by

$$C_1 = \left(N_P(0) - \frac{(1-\chi)\Lambda}{\bar{\mu}_2}\right) - \int_0^s \Psi_1(0)\mathrm{d}s. \tag{5.10}$$

Observe that $N_p(t) \leq \max\left\{N_p(0), ((1-\chi)\Lambda/\bar{\mu}_2)\right\}$. The above procedure can similarly be applied to the total concentrations of the liver hepatocytes $N_l(t) = H(t) + X(t)$ and that of CD8$^+$ T cells $N_w(t) = W_a(t) + W_n(t)$ so that

$$\frac{\mathrm{d}N_l}{\mathrm{d}t} \leq \lambda_h - \bar{\mu}_3 N_l \quad \text{and} \quad \frac{\mathrm{d}N_w}{\mathrm{d}t} \leq \Omega - \bar{\mu}_w N_w, \tag{5.11}$$

where $\bar{\mu}_3 = \min\{\mu_h, \mu_x\}$ and $\bar{\mu}_w = \min\{\mu_a, \mu_n\}$.

Integrating and simplifying the inequalities in system (5.11) gives

$$N_l(t) \leq \max\left\{N_l(0), \frac{\lambda_h}{\bar{\mu}_3}\right\} \quad \text{and} \quad N_w(t) \leq \max\left\{N_w(0), \frac{\Omega}{\bar{\mu}_w}\right\} \quad \text{for all time} \quad t > 0.$$

Therefore, all feasible solutions of system (5.1) enter the region:

$$\begin{aligned}\mathscr{D} = \Bigg\{ (S,H,X,R,T,M,G,W_n,W_a) \in \mathbb{R}_+^9 : N_r(t) \leq \max\left\{N_r(0), \frac{\lambda_r}{\bar{\mu}_1}\right\} \\ N_p(t) \leq \max\left\{N_p(0), \frac{(1-\chi)\Lambda}{\bar{\mu}_2}\right\}, \\ N_l(t) \leq \max\left\{N_l(0), \frac{\lambda_h}{\bar{\mu}_3}\right\}, N_w(t) \leq \max\left\{N_w(0), \frac{\Omega}{\bar{\mu}_w}\right\}\Bigg\},\end{aligned} \tag{5.12}$$

which is a positively invariant set of system (5.1). This implies that all solutions in $\mathscr{D}$ remain in $\mathscr{D}$ $\forall t \geq 0$. It thus suffices to study the dynamics of system (5.1) in $\mathscr{D}$.

5.3 Model analysis

5.3.1 Stability analysis of disease-free equilibrium point, E_0

At E_0, $\Lambda = 0$ and there are no activated CD8$^+$ T cells; that is, $W_a = 0$. Setting the right-hand-side of system (5.1) to zero, gives the following disease-free equilibrium:

$$E_0 = (S^0,H^0,X^0,R^0,T^0,M^0,G^0,W_n^0,W_a^0) = \left(0, \frac{\lambda_h}{\mu_h}, 0, \frac{\lambda_r}{\mu_r}, 0, 0, 0, \frac{\Omega}{\mu_n}, 0\right). \tag{5.13}$$

The disease-free steady state is very crucial in the understanding of in-host malaria infection dynamics. In order to eradicate in-host malaria, it is important to identify and establish necessary conditions for the disease-free equilibrium to be stable. This stability could be achieved through the use of effective antimalarial drugs such as ACT or by using highly efficacious *P. falciparum* malaria vaccines.

The next generation matrix (NGM) approach (see (Diekmann et al., 1990; Van den Driessche and Watmough, 2002) for detailed explanation of the technique) is employed to compute effective reproduction number R_{eff} of system (5.1). The NGM method presumes the local stability of E_0 for $\mathrm{R}_{eff} < 1$ and instability for $\mathrm{R}_{eff} > 1$. R_{eff} is the spectral radius of the next generation matrix ($\mathrm{F}_2\mathrm{V}_2^{-1}$) of system (5.1); that is, $\mathrm{R}_{eff} = \rho(\mathrm{F}_2\mathrm{V}_2^{-1})$. Adopting the matrix notations in (Van den Driessche and Watmough, 2002), the matrices F_2 and V_2 are

respectively given by

$$\mathrm{F}_2 = \begin{pmatrix} 0 & 0 & 0 & 0 & 0 & 0 & 0 \\ 0 & \frac{(1-\nu)\beta_s\lambda_h}{\mu_h} & 0 & 0 & 0 & 0 & 0 \\ 0 & 0 & 0 & \frac{(1-\varrho)\beta_r\lambda_r}{\mu_r} & 0 & 0 & 0 \\ 0 & 0 & 0 & 0 & 0 & 0 & 0 \\ 0 & 0 & 0 & 0 & 0 & 0 & 0 \\ 0 & 0 & 0 & 0 & 0 & 0 & 0 \\ 0 & 0 & 0 & 0 & 0 & 0 & 0 \end{pmatrix} \tag{5.14}$$

and

$$\mathrm{V}_2 = \begin{pmatrix} V_{01} & 0 & 0 & 0 & 0 & 0 & 0 \\ 0 & \mu_x & 0 & 0 & 0 & 0 & 0 \\ 0 & 0 & \mu_t & 0 & 0 & 0 & 0 \\ 0 & -V_{02} & V_{03} & \frac{\beta_r\lambda_r}{\mu_r}+\mu_m & 0 & 0 & 0 \\ 0 & 0 & -P\pi(1-a)(1-q)\mu_t & 0 & \mu_g & 0 & 0 \\ 0 & \frac{\tau\Omega\lambda_w}{\mu_n} & \frac{\tau\Omega\lambda_w}{\mu_n} & 0 & 0 & \mu_n & 0 \\ 0 & -\frac{\tau\Omega\lambda_w}{\mu_n} & -\frac{\tau\Omega\lambda_w}{\mu_n} & 0 & 0 & 0 & \mu_a \end{pmatrix}, \tag{5.15}$$

where $V_{01} = \frac{\beta_s\lambda_h}{\mu_h} + \mu_s$, $V_{02} = (1-\rho)(1-b)N\mu_x$ and $V_{03} = (1-a)P(1-\pi)(1-q)\mu_t$. Thus, the effective reproduction number R_{eff} is given by

$$\mathrm{R}_{eff} = \rho(\mathrm{F}_2\mathrm{V}_2{}^{-1}) = \max\{\mathrm{R}_{01}, \mathrm{R}_{02}\}, \tag{5.16}$$

where

$$\mathrm{R}_{01} = \frac{(1-\nu)\beta_s\lambda_h}{\mu_h\mu_x} \quad \text{and} \quad \mathrm{R}_{02} = \frac{P(1-\pi)(1-a)(1-\varrho)(1-q)\beta_r\lambda_r}{\beta_r\lambda_r + \mu_m\mu_r}. \tag{5.17}$$

Observe that R_{01} is the contribution of new cell invasions at the liver stage due to mortile sporozoites and R_{02} is the contributions of new cell invasions at the blood stage due to merozoite parasites. From equations (5.16) and (5.17), it is evident that new cell invasions occur both at the liver stage (as depicted by R_{01}) and at the blood stage (as depicted by R_{02}). This implies that clinical control of *P. falciparum* malaria should target the parasite at both stages of its life cycle within the human host. An antimalarial drug or drug combinations with the capacity to eradicate the sporozoites at the pre-erythrocytic stage and merozoites at the erythrocytic stage is most recommended. Furthermore, malaria vaccine development should equally focus on both stages of parasite development. A novel malaria vaccine should

begin parasite eradication from the pre-erythrocytic stage and this should continue to the blood stage. This result is very important to the ongoing research and development of malaria vaccines.

Theorem 5.2. *The disease-free equilibrium E_0 of system (5.1) is locally asymptotically stable if $\mathrm{R}_{eff} < 1$ and unstable otherwise.*

Proof: The qualitative matrix stability approach (Abdulrahman et al., 2013) to determine the local stability of the disease-free equilibrium E_0 for system (5.1) is used. Linearisation of the system (5.1) along E_0 gives the following Jacobian matrix

$$\mathrm{J}_2(\mathrm{E}_0) = \begin{pmatrix} -A_2 & 0 & 0 & 0 & 0 & 0 & 0 & 0 & 0 \\ -A_3 & -\mu_h & 0 & 0 & 0 & 0 & 0 & 0 & 0 \\ A_3 & 0 & -\mu_x & 0 & 0 & 0 & 0 & 0 & 0 \\ 0 & 0 & 0 & -\mu_r & 0 & -A_4 & 0 & 0 & 0 \\ 0 & 0 & 0 & 0 & -\mu_t & A_4 & 0 & 0 & 0 \\ 0 & 0 & 0 & 0 & A_0 & -A_5 & 0 & 0 & 0 \\ 0 & 0 & 0 & 0 & A_1 & 0 & -\mu_g & 0 & 0 \\ 0 & 0 & -\frac{\tau\Omega\lambda_w}{\mu_n} & 0 & -\frac{\tau\Omega\lambda_w}{\mu_n} & 0 & 0 & -\mu_n & 0 \\ 0 & 0 & \frac{\tau\Omega\lambda_w}{\mu_n} & 0 & \frac{\tau\Omega\lambda_w}{\mu_n} & 0 & 0 & 0 & -\mu_a \end{pmatrix}, \qquad (5.18)$$

where $A_0 = (1-a)P(1-\pi)(1-q)\mu_t$, $A_1 = (1-a)P\pi(1-q)\mu_t$, $A_2 = ((\beta_s\lambda_h)/\mu_h + \mu_s)$, $A_3 = (((1-\nu)\beta_s\lambda_h)/\mu_h)$, $A_4 = (((1-\varrho)\beta_r\lambda_r)/\mu_r)$ and $A_5 = (\beta_r\lambda_r/\mu_r + \mu_m)$.

To obtain the eigenvalues of matrix (5.18), first transform it into an upper triangular matrix. The required 11 elementary row transformations are performed in the order presented below:

(1) $\frac{-A_3}{A_2} \times \text{row } 1 + \text{row } 2 \to \text{row } 2$

(2) $\frac{A_3}{A_2} \times \text{row } 1 + \text{row } 3 \to \text{row } 3$

(3) $\frac{A_0}{\mu_t} \times \text{row } 5 + \text{row } 6 \to \text{row } 6$

(4) $\frac{A_1}{\mu_t} \times \text{row } 5 + \text{row } 7 \to \text{row } 7$

(5) $\frac{\tau\Omega\lambda_w}{-\mu_x\mu_n} \times \text{row } 3 + \text{row } 8 \to \text{row } 8$

(6) $\frac{\tau\Omega\lambda_w}{\mu_x\mu_n} \times \text{row } 3 + \text{row } 9 \to \text{row } 9$

(7) $\frac{A_1A_4}{-Y_0\mu_t} \times \text{row } 6 + \text{row } 7 \to \text{row } 7$

(8) $\frac{\tau\Omega\lambda_w}{-\mu_t\mu_n} \times \text{row } 5 + \text{row } 8 \to \text{row } 8$

(9) $\frac{\tau\Omega\lambda_w}{\mu_t\mu_n} \times \text{row } 5 + \text{row } 9 \to \text{row } 9$

(10) $\frac{\tau\Omega\lambda_w}{-\mu_g\mu_n} \times \text{row } 7 + \text{row } 8 \to \text{row } 8$

(11) $\frac{\tau\Omega\lambda_w}{\mu_g\mu_n} \times \text{row } 7 + \text{row } 9 \to \text{row } 9$

The resultant upper triangular matrix J_2^* is presented as follows:

$$\mathrm{J}_2^* = \begin{pmatrix} -A_2 & 0 & 0 & 0 & 0 & 0 & 0 & 0 & 0 \\ 0 & -\mu_h & 0 & 0 & 0 & 0 & 0 & 0 & 0 \\ 0 & 0 & -\mu_x & 0 & 0 & 0 & 0 & 0 & 0 \\ 0 & 0 & 0 & -\mu_r & 0 & -A_4 & 0 & 0 & 0 \\ 0 & 0 & 0 & 0 & -\mu_t & A_4 & 0 & 0 & 0 \\ 0 & 0 & 0 & 0 & 0 & Y_0 & 0 & 0 & 0 \\ 0 & 0 & 0 & 0 & 0 & 0 & -\mu_g & 0 & 0 \\ 0 & 0 & 0 & 0 & 0 & 0 & 0 & -\mu_n & 0 \\ 0 & 0 & 0 & 0 & 0 & 0 & 0 & 0 & -\mu_a \end{pmatrix}, \tag{5.19}$$

where

$$Y_0 = (1-a)P(1-\pi)(1-q)\frac{(1-\varrho)\beta_r\lambda_r}{\mu_r} - \left(\frac{\beta_r\lambda_r}{\mu_r} + \mu_m\right). \tag{5.20}$$

The eigenvalues of the transformed row-echelon Jacobian matrix (5.19) are hence given as:

$$\lambda_1 = -\left(\frac{\beta_s\lambda_h}{\mu_h} + \mu_s\right) < 0, \quad \lambda_2 = -\mu_h < 0, \quad \lambda_3 = -\mu_x < 0, \quad \lambda_4 = -\mu_r < 0,$$
$$\lambda_5 = -\mu_t < 0, \quad \lambda_6 = Y_0, \quad \lambda_7 = -\mu_g < 0, \quad \lambda_8 = -\mu_n < 0, \quad \lambda_9 = -\mu_a < 0.$$

It can clearly be seen that $\lambda_1, \lambda_2, \lambda_3, \lambda_4, \lambda_5, \lambda_7, \lambda_8$ and λ_9 are all strictly negative. The disease-free equilibrium is locally asymptotically stable if all the eigenvalues of the Jacobian matrix (5.18) are negative. The conditions necessary for $\lambda_6 = Y_0$ to be strictly negative are established as shown below:

Re-write equation (5.20) as follows:

$$Y_0 = \frac{P(1-a)(1-\pi)(1-q)(1-\varrho)\beta_r\lambda_r}{\mu_r} - \frac{\beta_r\lambda_r + \mu_r\mu_m}{\mu_r}. \tag{5.21}$$

Factorising equation (5.21) gives

$$Y_0 = \frac{\beta_r\lambda_r + \mu_r\mu_m}{\mu_r}\left(\frac{P(1-a)(1-\pi)(1-q)(1-\varrho)\beta_r\lambda_r}{\beta_r\lambda_r + \mu_r\mu_m} - 1\right). \tag{5.22}$$

That is,

$$Y_0 = \frac{\beta_r\lambda_r + \mu_r\mu_m}{\mu_r}\left(\mathrm{R}_{eff} - 1\right). \tag{5.23}$$

where $\mathrm{R}_{eff} = \mathrm{R}_{02}$ as defined in equation (5.17).

Equation (5.23), implies that $Y_0 < 0$ if and only if $\mathrm{R}_{eff} < 1$. Hence, E_0 is locally asymptotically stable if $\mathrm{R}_{eff} < 1$. This completes the proof.

The global stability of the disease-free equilibrium is established using a suitable Lyapunov candidate function (Li and Shu, 2010; Omondi et al., 2018). Consider the following theorem.

Theorem 5.3. *The disease-free equilibrium E_0 is globally asymptotically stable in $\mathbb{R}^9_+$ if $\mathrm{R}_{eff} \leq 1$.*

Proof: Let $V(X,T,S,M,G) = \psi_1 X + \psi_2 T + \psi_3 S + \psi_4 M + \psi_5 G$ be a candidate Lyapunov function for some nonnegative coefficients ψ_1, ψ_2, ψ_3, ψ_4 and ψ_5. The derivative of V with respect to time t is given by

$$\begin{aligned}
\frac{\mathrm{d}V}{\mathrm{d}t} &= \psi_1 \frac{\mathrm{d}X}{\mathrm{d}t} + \psi_2 \frac{\mathrm{d}T}{\mathrm{d}t} + \psi_3 \frac{\mathrm{d}S}{\mathrm{d}t} + \psi_4 \frac{\mathrm{d}M}{\mathrm{d}t} + \psi_5 \frac{\mathrm{d}G}{\mathrm{d}t}, \\
&= \psi_1 \left(\frac{\beta_s(1-\nu)SH}{1+dW_a} - \mu_x X - \frac{\rho X W_a}{1+\varepsilon_0 X} \right) + \psi_2 \left(\frac{(1-\varrho)\beta_r RM}{1+dW_a} - \mu_t T - \frac{qTW_a}{1+\varepsilon_1 T} \right) \\
&\quad + \psi_3 \left((1-\chi)\Lambda - \mu_s S - \beta_s SH \right) + \\
&\quad \psi_4 \left(\frac{P(1-q)(1-\pi)(1-a)\mu_t T}{1+dW_a} + (1-\rho)(1-b)N\mu_x X - \mu_m M - \beta_r RM \right) \qquad (5.24) \\
&\quad + \psi_5 \left(\frac{P(1-q)(1-a)\pi\mu_t T}{1+dW_a} - \mu_g G \right), \\
&= \left(-\mu_x \left(N\psi_4(b(-\rho)+b+\rho-1) + \psi_1 \right) - \frac{\Omega}{\mu_n}(\rho\psi_1 + q\psi_2) \right) X \\
&\quad + \left(-\mu_t \left((a-1)P(q-1)\left((\pi-1)\psi_4 - \pi\psi_5\right) + \psi_2 \right) \right) T \\
&\quad + \left(\psi_3(-\mu_s) - \frac{\lambda_h}{\mu_h}\left((\nu-1)\psi_1 + \psi_3\right)\beta_s \right) S \\
&\quad + \left(\psi_4(-\mu_m) - \frac{\lambda_r}{\mu_r}\left((e-1)\psi_2 + \psi_4\right)\beta_r \right) M \\
&\quad + (-\mu_g \psi_5) G. \qquad (5.25)
\end{aligned}$$

Evaluating the coefficients of the suitable Lyapunov function such that the coefficients of X, T, S, M and G are equal to zero gives

$$\psi_1 = \frac{N(1-b)(1-\rho)\mu_x(1-\varrho)\beta_r\lambda_r\mu_a^2 - q\Omega(\beta_r\lambda_r + \mu_m\mu_r)\mu_a}{(1-\varrho)\beta_r\lambda_r\mu_a(\rho\Omega + \mu_x\mu_a)}\psi_4,$$

$$\psi_3 = \frac{\frac{\lambda_h}{\mu_h}(1-\nu)\beta_s}{\frac{\lambda_h}{\mu_h}\beta_s+\mu_s}\left[\frac{N(1-b)(1-\rho)\mu_x(1-\varrho)\beta_r\lambda_r\mu_a^2 - q\Omega(\beta_r\lambda_r+\mu_m\mu_r)\mu_a}{(1-\varrho)\beta_r\lambda_r\mu_a(\rho\Omega+\mu_x\mu_a)}\right]\psi_4, \quad (5.26)$$

$$\psi_2 = \left[\frac{\frac{\lambda_r}{\mu_r}\beta_r+\mu_m}{(1-\varrho)\frac{\lambda_r}{\mu_r}\beta_r}\right]\psi_4 \quad \text{and} \quad \psi_5 = \frac{\frac{1}{1-\varrho} - P(1-a)(1-\pi)(1-q) + \frac{\mu_m\mu_r}{\beta_r\lambda_r(1-\varrho)}}{\pi P(1-a)(1-q)}\psi_4. \quad (5.27)$$

Using these coefficients, the time derivatives of the Lyapunov function is given as

$$\begin{aligned}\frac{dV}{dt} = &-\frac{(q+(1-b)(1-\varrho)N(1-\rho)\rho)\beta_r\lambda_r+q\mu_m\mu_r)(\mu_a+\mu_n)\mu_x}{(1-\varrho)\beta_r\lambda_r\mu_n(\rho\Omega+\mu_a\mu_x)}X \\ &-\frac{\mu_m\mu_r\mu_t(1+(1-\varrho)^2\lambda_r^2)}{(1-e)\beta_r\lambda_r}T - \frac{\mu_g(1-\varrho)\lambda_r\mu_m\mu_r}{\pi\beta_r(1-a)(1-q)}G(1-\mathrm{R}_{eff}).\end{aligned} \quad (5.28)$$

If $\mathrm{R}_{eff} < 1$ in equation (5.28) then $[\mu_g(1-\varrho)\lambda_r\mu_m\mu_r]/[\pi\beta_r(1-a)(1-q)](1-\mathrm{R}_{eff}) > 0$. This gives $(dV/dt) \leq 0$. Furthermore, $(dV/dt) = 0$ if and only if $T = X = G = 0$. Therefore, V is a Lyapunov function in $\mathscr{D}$. Given that $\mathscr{D}$ is positively invariant and attracting, it follows that the maximum invariant set in $\{(S,H,X,R,T,M,G,W_n,W_a) \in \mathscr{D} : \dot{V} = 0\}$ is the singleton E_0. By LaSalle's invariant principle (LaSalle, 1976), E_0 is globally asymptotically stable in $\mathscr{D}$ provided that $\mathrm{R}_{eff} \leq 1$.

5.3.2 The malaria-persistent steady state

The malaria-persistent equilibrium E_p for system (5.1) in the presence of $CD8^+$ T cells is established by equating the right-hand side of system (5.1) to zero. Using Mathematica software, system (5.1), exhibits a malaria-persistent equilibrium point

$$E_p = (S^*, H^*, X^*, R^*, T^*, M^*, G^*, W_n^*, W_a^*),$$

where

$$H^* = \frac{(1+dW_a^*)\lambda_h}{(1-\nu)\beta_s S^* + (1+dW_a^*)\mu_h}, \quad R^* = \frac{(1+dW_a^*)\lambda_r}{(1-\varrho)\beta_r M^* + (1+dW_a^*)\mu_r}, \quad (5.29)$$

$$W_n^* = \frac{\Omega}{\tau\lambda_w(X^*+T^*)+\mu_n}, \; W_a^* = \frac{\tau\lambda_w(X^*+T^*)W_n^*}{\mu_a} \quad (5.30)$$

$$G^* = \frac{P(1-q)(1-a)\pi\mu_t T^*}{\mu_g(1+dW_a^*)}, \quad (5.31)$$

$$M^* = \frac{(1+dW_a^*)[(1-b)^2(1-\varrho)NX^*\beta_r\mu_m\mu_x - (1+dW_a^*)\mu_r] \pm \sqrt{\Delta}}{2(1-\varrho)(1+dW_a^*)\beta_r}, \quad \text{where} \tag{5.32}$$

$$\begin{aligned}\Delta_m = (1+dW_a^*)\{&(-(e-1)\beta_r(-4(1-\pi)(1-a)P(1-q)T^*\mu_t \\ &+(1-b)^2NX^*(1+dW_a^*)\beta_r\mu_x(4(1+dW_a^*)\lambda_r+(1-b)^2(1-e)NX^*\mu_m^2\mu_x)) \\ &-2(1-b)^2(1-e)NX^*(1+dW_a^*)^2\mu_m\beta_r\mu_r\mu_x+(1+dW_a^*)^3\mu_r^2\},\end{aligned}$$

$$S^* = \frac{1}{-2(1-\nu)\beta_s\nu_s}\left\{-\Delta_s \pm \sqrt{\Delta_s^2+4((1-\nu)\beta_s\mu_s)((1-\chi)\Lambda(1+dW_a^*)\mu_h)}\right\}, \tag{5.33}$$

$$\text{where} \quad \Delta_s = \beta_s(\Lambda(1-\chi)(1-\nu)-(1+dW_a^*)\lambda_h)-(1+dW_a^*)\mu_h\mu_s,$$

$$T^* = \frac{1}{-2\varepsilon_1((1-\varrho)\beta_rM^*+(1+dW_a^*)\mu_r)\mu_t}\left\{-\Delta_t \pm \sqrt{\Delta_T^*}\right\}, \tag{5.34}$$

$$\begin{aligned}&\text{where} \quad \Delta_t = \beta_s(\Lambda(1-\chi)(1-\nu)-(1+dW_a^*)\lambda_h)-(1+dW_a^*)\mu_h\mu_s; \\ &\Delta_T^* = \Delta_t^2+4\varepsilon_1\mu_t((1-\varrho)\beta_rM^*+(1+dW_a^*)\mu_r)(\beta_r\lambda_r(1-\varrho)M^*) \quad \text{and}\end{aligned}$$

$$X^* = \frac{\Delta_x \pm \sqrt{\Delta_x^2+4\varepsilon_0((1-\nu)\beta_sS^*+(1+dW_a^*)\mu_h)\mu_x)(1-\nu)\beta_s\lambda_hS^*}}{2\varepsilon_0((1-\nu)\beta_sS^*+(1+dW_a^*)\mu_h)\mu_x}, \quad \text{where} \tag{5.35}$$

$$\Delta_x = (1-\nu)(\varepsilon_0\lambda_h-\mu_x)\beta_sS^*-d\rho W_a^{*2}\mu_h-\mu_h\mu_x-W_a^*((1-\nu)\rho\beta_sS^*+\mu_h(\rho+d\mu_x)).$$

Based on the formulated model in system (5.1), the activated CD8$^+$ T cells only exist due to the presence of infected red blood cells and infected hepatocytes. Hence, in the absence of malaria infection ($X = T = 0$), $W_a = 0$. Moreover, none of the malaria parasites exists; that is $S^* = M^* = G^* = 0$. It is further observed that when $S^* = M^* = X^* = T^* = W_a^* = 0$, the susceptible erythrocytes, susceptible hepatocytes and the unactivated CD8$^+$ T cells become $H^* = (\lambda_h/\mu_h)$, $R^* = (\lambda_r/\mu_r)$ and $W_n^* = (\Omega/\mu_n)$, respectively. This gives an equilibrium point called the disease-free equilibrium point of system (5.1) illustrated in equation (5.13). From the above computations, it is evident that the analytical expressions of E_p is too complex. The numerical simulation of the equilibrium points is provided in Section 5.6.

Theorem 5.4. *The malaria persistent steady state E_p is locally asymptotically stable if $\mathrm{R}_{eff} > 1$ in the interior of the biologically feasible region $\mathscr{D}$.*

Proof: The stability of the malaria persistent equilibrium E_p (when $\mathrm{R}_{eff} > 1$ but close to 1) is proved using the center manifold theory (CMT) presented by Castillo-Chavez and Song (2004). The notations used therein Castillo-Chavez and Song (2004) and without re-stating

the theorem are adopted to calculate the values of arguments **a** and **b**. The signs (+ or -) of **a** and **b** determine the local dynamics of system (5.1) around E_p (White and Comiskey, 2007).

Suppose β_* is considered to be the bifurcation parameter, then at $\mathrm{R}_{eff} = 1$, $\beta_* = \max\{\beta_s^*, \beta_r^*\}$, where

$$\beta_r^* = \frac{\mu_m \mu_r}{[P(1-q)(1-\pi)(1-\varrho)(1-a)-1]\lambda_r} \quad \text{and} \quad \beta_s^* = \frac{\mu_h \mu_x}{(1-\nu)\lambda_h}. \tag{5.36}$$

The CMT is applied by first transforming the state variables (S,H,X,R,T,M,G,W_n,W_a) into $(x_1,x_2,x_3,x_4,x_5,x_6,x_7,x_8,x_9)$, respectively. The model in system (5.1), is hence represented as $(dg/dt) = g(\mathbf{x})$, where $\mathbf{x} = (x_1,x_2,x_3,x_4,x_5,x_6,x_7,x_8,x_9)$. The model (5.1) thus becomes

$$\left.\begin{aligned}
\dot{x}_1 &= (1-\chi)\Lambda - \mu_s x_1 - \beta_s x_1 x_2,\\
\dot{x}_2 &= \lambda_h - \mu_h x_2 - \frac{\beta_s(1-\nu)x_1 x_2}{1+dx_9},\\
\dot{x}_3 &= \frac{\beta_s(1-\nu)x_1 x_2}{1+dx_9} - \mu_x x_3 - \frac{\rho x_3 x_9}{1+\varepsilon_0 x_3},\\
\dot{x}_4 &= \lambda_r - \frac{(1-\varrho)\beta_r x_4 x_6}{1+dx_9} - \mu_r x_4,\\
\dot{x}_5 &= \frac{(1-\varrho)\beta_r x_4 x_6}{1+dx_9} - \mu_t x_5 - \frac{q x_5 x_9}{1+\varepsilon_1 x_5},\\
\dot{x}_6 &= \frac{P(1-q)(1-\pi)(1-a)\mu_t x_5}{1+dx_9} + (1-\rho)(1-b)N\mu_x x_3 - \mu_m x_6 - \beta_r x_4 x_6,\\
\dot{x}_7 &= \frac{P(1-q)(1-a)\pi\mu_t x_5}{1+dx_9} - \mu_g x_7,\\
\dot{x}_8 &= \Omega - \tau\lambda_w(x_3+x_5)x_8 - \mu_n x_8,\\
\dot{x}_9 &= \tau\lambda_w(x_3+x_5)x_8 - \mu_a x_9,
\end{aligned}\right\} \tag{5.37}$$

such that:

$x_1(0) \geq 0$, $x_2(0) \geq 0$, $x_3(0) \geq 0$, $x_4(0) \geq 0$, $x_5(0) \geq 0$, $x_6(0) \geq 0$, $x_7(0) \geq 0$, $x_8(0) \geq 0$, $x_9(0) \geq 0$.

The new system (5.37) with the bifurcation point β_* has a simple zero eigenvalue. This attribute enables the use of CMT to analyse the stability of system (5.37) near $\beta_* = \max\{\beta_s^*, \beta_r^*\} = \max\{\beta_s, \beta_r\}$.

Therefore, a right eigenvector $w = [w_1, w_2, w_3, w_4, w_5, w_6, w_7, w_8, w_9]^T$ associated with the simple zero eigenvalue is obtained from the linearisation matrix corresponding to the zero

eigenvector as follows:

$$\begin{pmatrix} -A_2 & 0 & 0 & 0 & 0 & 0 & 0 & 0 & 0 \\ -A_3 & -\mu_h & 0 & 0 & 0 & 0 & 0 & 0 & 0 \\ A_3 & 0 & -\mu_x & 0 & 0 & 0 & 0 & 0 & 0 \\ 0 & 0 & 0 & -\mu_r & 0 & -A_4 & 0 & 0 & 0 \\ 0 & 0 & 0 & 0 & -\mu_t & A_4 & 0 & 0 & 0 \\ 0 & 0 & 0 & 0 & A_0 & -A_5 & 0 & 0 & 0 \\ 0 & 0 & 0 & 0 & A_1 & 0 & -\mu_g & 0 & 0 \\ 0 & 0 & -\frac{\tau\Omega\lambda_w}{\mu_n} & 0 & -\frac{\tau\Omega\lambda_w}{\mu_n} & 0 & 0 & -\mu_n & 0 \\ 0 & 0 & \frac{\tau\Omega\lambda_w}{\mu_n} & 0 & \frac{\tau\Omega\lambda_w}{\mu_n} & 0 & 0 & 0 & -\mu_a \end{pmatrix} \begin{pmatrix} w_1 \\ w_2 \\ w_3 \\ w_4 \\ w_5 \\ w_6 \\ w_7 \\ w_8 \\ w_9 \end{pmatrix} = \begin{pmatrix} 0 \\ 0 \\ 0 \\ 0 \\ 0 \\ 0 \\ 0 \\ 0 \\ 0 \end{pmatrix} \tag{5.38}$$

where $A_0, \cdots, A_5$ are as presented in the Jacobian matrix (5.18).

Solving for the right eigenvectors gives

$$\begin{aligned} w_7 &= \frac{-(1-a)P\pi(1-q)\mu_t}{\mu_g} + \frac{\left(\frac{\beta_r\lambda_r}{\mu_r} + \mu_m\right)}{(1-a)P(1-\pi)(1-q)\mu_t}, \quad w_4 = -\frac{(1-\varrho)\beta_r\lambda_r}{\mu_r^2}, \\ w_9 &= -\frac{\tau\Omega\lambda_w}{\mu_a\mu_n}\left(\frac{\beta_r\lambda_r}{\mu_r} + \mu_m\right), \quad w_8 = \frac{\tau\Omega\lambda_w}{(1-a)P(1-\pi)(1-q)\mu_t\mu_n^2}\left(\frac{\beta_r\lambda_r}{\mu_r} + \mu_m\right), \\ w_5 &= \frac{-\left(\frac{\beta_r\lambda_r}{\mu_r} + \mu_m\right)}{(1-a)P(1-\pi)(1-q)\mu_t}, w_6 = 1, \quad w_1 = w_2 = w_3 = 0. \end{aligned} \tag{5.39}$$

Similarly, upon solving for the left eigenvector $v = [v_1, v_2, v_3, v_4, v_5, v_6, v_7, v_8, v_9]^T$ associated with the zero eigenvalue in system (5.37) gives

$$v_1 = v_2 = v_3 = v_4 = 0, \quad v_5 = P(1-a)(1-\pi)(1-q), v_6 = 1, v_7, v_8, v_9 = 0.$$

Next, the values of **a** and **b** as described in Castillo-Chavez and Song (2004) are calculated. That is,

$$\mathbf{a} = \sum_{i,j,k=1}^{9} v_k w_i w_j \frac{\partial^2 g_k(\mathbf{O},0)}{\partial x_i \partial x_j} \quad \text{and} \quad \mathbf{b} = \sum_{i,k=1}^{9} v_k w_i \frac{\partial^2 g_k(\mathbf{O},0)}{\partial x_i \partial \beta_*}. \tag{5.40}$$

The non-zero partial derivatives of $g(x)$ in system (5.37) associated with the argument **a** are given as

$$\begin{aligned}
&\frac{\partial^2 g_1}{\partial x_1 \partial x_2} = -\beta_s, \quad \frac{\partial^2 g_2}{\partial x_1 \partial x_2} = -(1-\nu)\beta_s, \quad \frac{\partial^2 g_2}{\partial x_1 \partial x_9} = d(1-\nu)\frac{\lambda_h}{\mu_h}\beta_s, \\
&\frac{\partial^2 g_4}{\partial x_4 \partial x_6} = -(1-\varrho)\beta_r, \\
&\frac{\partial^2 g_4}{\partial x_6 \partial x_9} = \frac{d(1-\varrho)\beta_r\lambda_r}{\mu_r}, \quad \frac{\partial^2 g_5}{\partial x_5 \partial x_9} = -q, \quad \frac{\partial^2 g_5}{\partial x_4 \partial x_6} = (1-\varrho)\beta_r, \\
&\frac{\partial^2 g_5}{\partial x_6 \partial x_9} = \frac{-d(1-\varrho)\beta_r\lambda_r}{\mu_r}, \\
&\frac{\partial^2 g_6}{\partial x_4 \partial x_6} = -\beta_r, \quad \frac{\partial^2 g_6}{\partial x_5 \partial x_9} = P(1-a)(1-\pi)(1-q)d\mu_t, \\
&\frac{\partial^2 g_7}{\partial x_5 \partial x_9} = P\pi(1-a)(1-q), \quad \frac{\partial^2 g_8}{\partial x_3 \partial x_8} = \frac{\partial^2 g_8}{\partial x_5 \partial x_8} = -\tau\lambda_w, \\
&\frac{\partial^2 g_9}{\partial x_3 \partial x_8} = \frac{\partial^2 g_9}{\partial x_5 \partial x_8} = \tau\lambda_w.
\end{aligned} \tag{5.41}$$

Thus, the expression for **a** is:

$$\begin{aligned}
\mathbf{a} &= v_5 w_5 w_9 \frac{\partial^2 g_5}{\partial x_5 \partial x_9} + v_5 w_4 w_6 \frac{\partial^2 g_5}{\partial x_4 \partial x_6} + v_5 w_6 w_9 \frac{\partial^2 g_5}{\partial x_6 \partial x_9} + v_6 w_4 w_6 \frac{\partial^2 g_6}{\partial x_4 \partial x_6} \\
&\quad + v_6 w_5 w_9 \frac{\partial^2 g_6}{\partial x_5 \partial x_9} \\
&= -\left(\frac{\beta_r\lambda_r}{\mu_r} + \mu_m\right)\left(\frac{d(1-\varrho)\beta_r\lambda_r}{\mu_r}\right)\left(\frac{P(1-a)(1-\pi)(1-q)\mu_t\tau\Omega\lambda_w}{\mu_a\mu_t\mu_n}\right) < 0.
\end{aligned} \tag{5.42}$$

The above procedure in computing the values of **b** is repeated. The non-zero partial derivatives of $g(x)$ associated with **b** are given by

$$\begin{aligned}
&\frac{\partial^2 g_1}{\partial x_1 \partial \beta_*} = -\frac{\lambda_h}{\mu_h}, \quad \frac{\partial^2 g_2}{\partial x_1 \partial \beta_*} = \frac{-(1-\nu)\lambda_h}{\mu_h}, \quad \frac{\partial^2 g_3}{\partial x_1 \partial \beta_*} = \frac{(1-\nu)\lambda_h}{\mu_h}, \\
&\frac{\partial^2 g_4}{\partial x_6 \partial \beta_*} = \frac{-(1-\varrho)\lambda_r}{\mu_r}, \frac{\partial^2 g_5}{\partial x_6 \partial \beta_*} = \frac{(1-\varrho)\lambda_r}{\mu_r}, \quad \frac{\partial^2 g_6}{\partial x_6 \partial \beta_*} = \frac{-\lambda_r}{\mu_r}.
\end{aligned} \tag{5.43}$$

Upon substituting these derivatives into equation (5.40), it follows that

$$\begin{aligned}\mathbf{b} &= v_5 w_6 \frac{\partial^2 g_5}{\partial x_6 \partial \beta_*} + v_6 w_6 \frac{\partial^2 g_6}{\partial x_6 \partial \beta_*} \\ &= \frac{\lambda_r}{\mu_r}\left(P(1-a)(1-\pi)(1-q)(1-\varrho)+1\right) > 0. \end{aligned} \tag{5.44}$$

Thus, $\mathbf{a}$ is positive ($\mathbf{a} > 0$) and $\mathbf{b}$ is negative ($\mathbf{b} < 0$). Based on item (iv) of theorem 2 in (Castillo-Chavez and Song, 2004), the malaria persistent equilibrium E_p is locally asymptotically stable for $\mathrm{R}_{eff} > 1$, but close to 1.

5.4 Uncertainty and sensitivity analysis

5.4.1 Sensitivity analysis of infected and infective states of the in-host malaria model

The in-host malaria model in this chapter has numerous unknown parameters, coupled with limited data. Therefore, there is a considerable uncertainty (Blower et al., 1991) in estimating the values of the 30 transmission parameters in system (5.1). The uncertainty in the input values allows significant variability in the model predictions of the future malaria parasite density within the human host and the concentrations of the infected red blood cells and hence the severity of clinical *P. falciparum* malaria. Consequently, LHS/PRCC sensitivity analysis is performed to evaluate variability in model predictions. With LHS/PRCC technique, it is possible to explore the entire parameter space of system (5.1), with minimal computer simulation.

The effects of the LHS parameters on the two infected state variables are simultaneously examined: the infected liver hepatocytes $X(t)$ and the infected red blood cells $T(t)$ and the three infective parasite states: the sporozoite $S(t)$, the merozoites $M(t)$ and the gametocytes $G(t)$ in model (5.1). The PRCCs are used to identify the key parameters contributing to the imprecision in predicting the future density of infected liver hepatocytes and infected red blood cells (Blower et al., 1991).

5.4.2 Sampling the Latin hypercube sampling (LHS) parameters

The process of performing Latin Hypercube Sampling on disease models consists of the following steps: (1) identifying model of interest, (2) listing all the model parameters together with their estimated or exact values, (3) extracting uncertain parameters from the list of model parameter values; provide baseline values and range values for known and unknown parameters, respectively, (4) for U simulations, the inequality $U > (4/3)Q$, must be true for Q uncertain parameters (McKay et al., 1979). The parameter space is hence defined by Q dimensions. The appropriate sample size U is established from the desired level of significance attached to the PRCC values (Blower and Dowlatabadi, 1994), (5) a probability density function (pdf) for each uncertain parameter is then specified. This may include (i) uniform distribution, (ii) triangular distribution, (iii) multi-modal Weibull distribution and (iv) skewed distribution. Finally, each pdf is then divided into U overlapping equiprobable intervals, which are then randomly sampled once.

Next, define the probability distribution function of parameter p to be $f(p)$, the interval of $f(p)$ to be $F(p)$ and the inverse of $F(p)$ to be $F^{-1}(p)$. If the function is normalized then:

$$[F(p)]_{p_{min}}^{p_{max}} = 1. \tag{5.45}$$

The area under each equiprobable interval is equivalent to $1/U$. That is,

$$1/U = \int_{p_{min}^i}^{p_{max}^i} f(p)\,\mathrm{d}p = F(p_{max}^i) - F(p_{min}^i). \tag{5.46}$$

At the end of step (5), each of the Q uncertain parameters will have U values. This is stored in an $U \times Q$ matrix.

5.4.3 Partial rank correlation coefficient (PRCC) methodology

To perform PRCC, begin by ranking the LHS parameters in the LHS matrix together with the outcome measures. In our case, the outcome measures are the states $T(t)$, $X(t)$, $M(t)$, $G(t)$ and $S(t)$. Two linear regression models are generated in response to each parameter and outcome measure. A Pearson rank correlation coefficient for the residuals from the two regression models gives the PRCC values for that specific parameter. The underlying parameter distributions can be established through expert judgment or based on empirical

evidence (Pereira and Broed, 2006). Due to lack of data on the distribution function, a uniform distribution for all model parameters in Table 5.9 is considered.

The PRCC for each input variable is established as follows: Begin by adding an additional column $Q+1$ (called the outcome vector), to the matrix containing the input parameter values. Secondly, the ranks $1,2,\cdots U$ corresponding to each column is represented by the set of ordinal numbers $\xi_{1i},\xi_{2i},\cdots,\xi_{ki}$, where the index i denotes the run number. The average rank η is given as $\eta=(1+U)/2$. In the event that two or more parameters have the same ranking based on a particular run, then only one of the parameters is considered in the calculation of PRCC (Kendall, 1946). Finally, a symmetric matrix $C=c_{ij}$ of dimension $Q+1$ is defined as follows:

$$C=\frac{\sum_{i=1}^{U}(\xi_{it}-\eta)(\xi_{jt}-\eta)}{\sqrt{\sum_{t=1}^{U}(\xi_{it}-\eta)^2\sum_{s=1}^{U}(\xi_{js}-\eta)^2}},\quad i,j=1,2,3,\cdots,Q. \tag{5.47}$$

Next, let the matrix $D=[d_{ij}]$ be the inverse of matrix C and ρ_{iz} be the PRCC corresponding to the i-th and z-th input parameter and outcome variable, respectively. The PRCC ρ_{iz} is hence given by

$$\rho_{iz}=\frac{-d_{i,Q+1}}{\sqrt{d_{ii}d_{Q+1,Q+1}}}. \tag{5.48}$$

Then test the importance of the non-zero value of the PRCC by deriving t_{iz}, where

$$t_{iz}=\eta_{iz}\sqrt{\frac{U-2}{1-\eta_{iz}}}. \tag{5.49}$$

The above procedure is repeated for a second outcome variable and so on until the PRCCs are obtained for all the input parameters and their corresponding outcome variables.

5.5 Results of analysing the LHS/PRCC for the in-host malaria model

Using 1000 runs of Latin hypercube sampling, the PRCC and p values of the 30 parameters in system (5.1) are computed based on the regression coefficient for outcome measures $T(t)$, $X(t)$, $M(t)$, $G(t)$ and $S(t)$ and summarised in Tables 5.3, 5.4, 5.5, 5.6 and 5.7. The size of PRCC shows the importance of the uncertainty in estimating the value of the specific variable in contributing to the prediction imprecision (Blower et al., 1991). The PRCC sign (+ or -), however, shows the qualitative relationship between the input parameter and the output

variables. Parameters with large PRCC values coupled with a corresponding small p value (p value < 0.05) are considered as the most influential (Gomero, 2012).

A slight change in a highly influential parameter is likely to produce a significant change in the outcome variable. The symbol $(*)$ indicates less influential parameters with p values $<$ 0.05 and PRCC values in the range (-0.1 to -0.49 or 0.1 to 0.49). Further, the symbol $(**)$ is used to indicate moderately critical parameters in prediction imprecision, and have p value $<$ 0.05 and PRCC values in the range (-0.5 to -0.79 or 0.5 to 0.79) . Lastly, the symbol $(***)$ indicates the most critical and likely contributors to uncertainty, with PRCC values in the range (-0.8 to -0.99 or +0.8 to +0.99).

Results displayed in Tables 5.3, 5.4, 5.5, 5.6 and 5.7 indicate that the rate of invasion by merozoites β_r, the rate of invasion of liver hepatocytes by sporozoites β_s, malaria vaccine efficacies (ϱ, ν, and χ) and the recruitment rates for hepatocytes and erythrocytes, λ_h and λ_r, respectively, are statistically significant in determining the variation of concentrations of infected erythrocytes, infected hepatocytes and the density of malaria parasites (sporozoites, merozoites and gametocytes). The number of merozoites P released per bursting infected erythrocytes and the number of merozoites N released per bursting infected hepatocytes are shown to significantly increase the density of the merozoites and the density of infected erythrocytes T. Clinical malaria controls should thus target these infected cells for eradication before they mature to schizont stages.

Moreover, from Tables 5.3 and 5.6, the proportion of merozoites that develop into gametocytes per dying infected erythrocyte π and immunosensitivity of infected erythrocytes q are shown to have significant influence in determining the density of gametocytes and merozoites, respectively, during clinical *P. falciparum* infection. An efficacious blood stage vaccine coupled with a transmission blocking vaccine antigens has the potential of reducing the density of gametocytes during clinical malaria. This reduces parasite transmission to mosquito vector.

It is evident that a highly efficacious pre-erythrocytic vaccine such as RTS,S/SA01 (with efficacy ν) and blood stage vaccine such as MSP3 (with efficacy ε) could effectively help in reducing parasitaemia and malaria severity during clinical *P. falciparum* infections. Sporozoite invasion rate β_s and the merozoite invasion parameter β_r are also shown to increase the disease R_{eff} and hence the severity of the disease within the human host.

Table 5.3: Partial rank correlation coefficients (PRCC) between infected red blood cells T and model parameters. The results are significant at the 0.05 level

Parameter	PRCC	p value	Parameter	PRCC	p value
Λ	0.040124	0.69185	ν	*-0.35423	0.0001255
μ_s	0.092654	0.35921	d	-0.021968	0.82825
λ_h	0.16815	0.094459	λ_w	0.02639	0.79438
λ_r	***0.99993	1.2467E-191	τ	0.028815	0.77596
β_r	** 0.60394	0.0030343	a	-0.033076	0.7439
β_s	-0.072861	0.47128	b	-0.037844	0.70854
μ_h	0.045043	0.65633	P	* 0.28652	0.0038515
μ_x	0.022164	0.82674	N	** 0.50348	0.0003056
π	0.24376	0.14528	ε_0	-0.050167	0.62012
μ_r	** -0.54174	5.8708E-9	ε_1	0.0092028	0.92759
μ_t	-0.043585	0.66677	ρ	0.087162	0.38852
μ_m	-0.08574	0.39634	q	*-0.261905	0.00154063
μ_g	-0.13006	0.19715	μ_n	-0.093091	0.35694
χ	-0.13607	0.17706	μ_a	-0.054864	0.58771
ϱ	-0.30701	0.0018909	Ω	0.041721	0.68024

Table 5.4: Partial rank correlation coefficients (PRCC) between infected hepatocytes X and model parameters. The results are significant at the 0.05 level

Parameter	PRCC	p value	Parameter	PRCC	p value
Λ	-0.034437	0.73375	ν	* -0.307831	0.00093836
μ_s	0.071002	0.48269	d	-0.1442	0.15231
λ_h	*** 0.9749	9.5419E-66	λ_w	-0.094174	0.35135
λ_r	0.06407	0.52654	τ	* -0.20137	0.000044531
β_r	-0.080809	0.42415	a	-0.075135	0.45751
β_s	** 0.53926	0.00016701	b	0.061933	0.54045
μ_h	***-0.87273	2.7908E-23	P	0.076347	0.45026
μ_x	0.14762	0.14273	N	0.10516	0.29776
π	-0.045846	0.6506	ε_0	0.21125	0.034877
μ_r	0.094998	0.34713	ε_1	-0.16583	0.09918
μ_t	0.12588	0.21205	ρ	0.033235	0.74272
μ_m	0.13493	0.18073	q	0.095106	0.34658
μ_g	0.033064	0.74399	μ_n	0.039223	0.69843
χ	-0.28902	0.0035417	μ_a	-0.052237	0.60575
ϱ	-0.061742	0.5417	Ω	0.10411	0.30264

Table 5.5: Partial rank correlation coefficients (PRCC) between merozoites M and model parameters. The results are significant at the 0.05 level

Parameter	PRCC	p value	Parameter	PRCC	p value
Λ	0.013086	0.89718	ν	** -0.61866	6.9194E-12
μ_s	0.12012	0.23389	d	0.12239	0.22509
λ_h	- 0.005884	0.95367	λ_w	-0.30208	0.0022545
λ_r	**-0.78852	2.0731E-22	τ	-0.11155	0.26918
β_r	**0.77199	5.3565E-21	a	0.14416	0.15243
β_s	0.10834	0.28328	b	-0.18907	0.059575
μ_h	0.080773	0.42436	P	* 0.28652	0.0038515
μ_x	* 0.46617	1.0183E-06	N	** 0.50348	0.0003056
π	-0.29849	0.0025577	ε_0	-0.23892	0.01667
μ_r	0.060227	0.55168	ε_1	-0.057548	0.56955
μ_t	-0.05975	0.55485	ρ	-0.25708	0.0098207
μ_m	-0.090522	0.37042	q	-0.047855	0.63635
μ_g	0.18256	0.069072	μ_n	-0.0015737	0.9876
χ	**-0.67251	1.8298E-14	μ_a	0.1363	0.17632
ϱ	-0.024582	0.80818	Ω	-0.12172	0.22769

Table 5.6: Partial rank correlation coefficients (PRCC) between gametocytes G and model parameters. The results are significant at the 0.05 level

Parameter	PRCC	p value	Parameter	PRCC	p value
Λ	0.09861	0.32902	ν	** -0.54919	3.2858E-09
μ_s	-0.18356	0.067537	d	-0.33627	0.00062476
λ_h	0.16929	0.092216	λ_w	-0.14215	0.15831
λ_r	***-0.79454	5.8878E-23	τ	-0.080527	0.42578
β_r	**-0.76958	8.4228E-21	a	-0.16499	0.10092
β_s	-0.021251	0.83378	b	-0.31287	0.0015279
μ_h	0.060337	0.55095	P	0.059063	0.55941
μ_x	* 0.40198	3.3899E-05	N	0.24601	0.013619
π	** 0.698883	0.0032768	ε_0	-0.28727	0.0037563
μ_r	-0.022582	0.82353	ε_1	0.075806	0.45349
μ_t	0.075502	0.45531	ρ	-0.047433	0.63933
μ_m	0.067991	0.50149	q	0.12264	0.22416
μ_g	-0.084857	0.40124	μ_n	-0.12368	0.22021
χ	**-0.55186	2.6601E-09	μ_a	0.17443	0.082611
ϱ	** -0.55799	1.6273E-09	Ω	0.15261	0.12956

Table 5.7: Partial rank correlation coefficients (PRCC) between sporozoites S and each parameter. The results are significant at the 0.05 level

Parameter	PRCC	p value	Parameter	PRCC	p value
Λ	* 0.31314	0.00097533	ν	0.0067811	0.94661
μ_s	** -0.68707	0.0094591	d	0.010905	0.91425
λ_h	-0.012635	0.90071	λ_w	0.0043436	0.96579
λ_r	0.03593	0.72266	τ	0.023508	0.81642
β_r	0.025432	0.80168	a	0.0065303	0.94859
β_s	-0.0091069	0.92835	b	-0.017604	0.86199
μ_h	0.022838	0.82156	P	-0.019561	0.84683
μ_x	0.0056574	0.95545	N	-0.015923	0.87505
π	-0.0047473	0.96261	ε_0	-0.00027845	0.99781
μ_r	0.00025243	0.99801	ε_1	-0.0003386	0.99733
μ_t	-0.011016	0.91338	ρ	-0.031317	0.75709
μ_m	0.0096995	0.9237	q	-0.0037326	0.9706
μ_g	-0.023075	0.81974	μ_n	0.030253	0.7651
χ	*-0.699368	0.0001184	μ_a	-0.0042258	0.96672
ϱ	0.01863	0.85403	Ω	-0.0052564	0.95861

Figures 5.2 and 5.3 illustrates Monte Carlo simulations for some of the parameters with the greatest PRCC values against model R_{eff}.

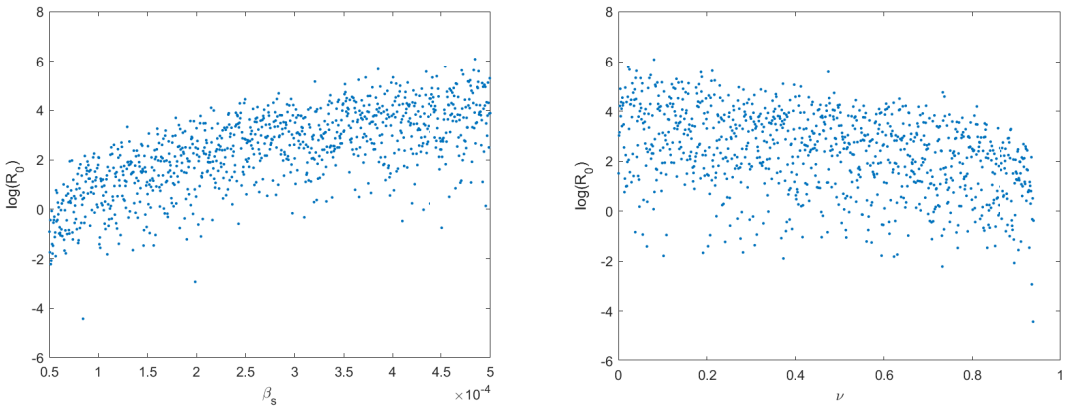

(a) (b)

Figure 5.2: The Monte Carlo simulations for some of the parameters with the greatest partial rank correlation coefficient (PRCC) magnitudes, using values in Table 5.9 and 1000 simulations per run. The parameters are: (a) sporozoite invasion rate β_s and (b) efficacy of pre-erythrocytic vaccine ν.

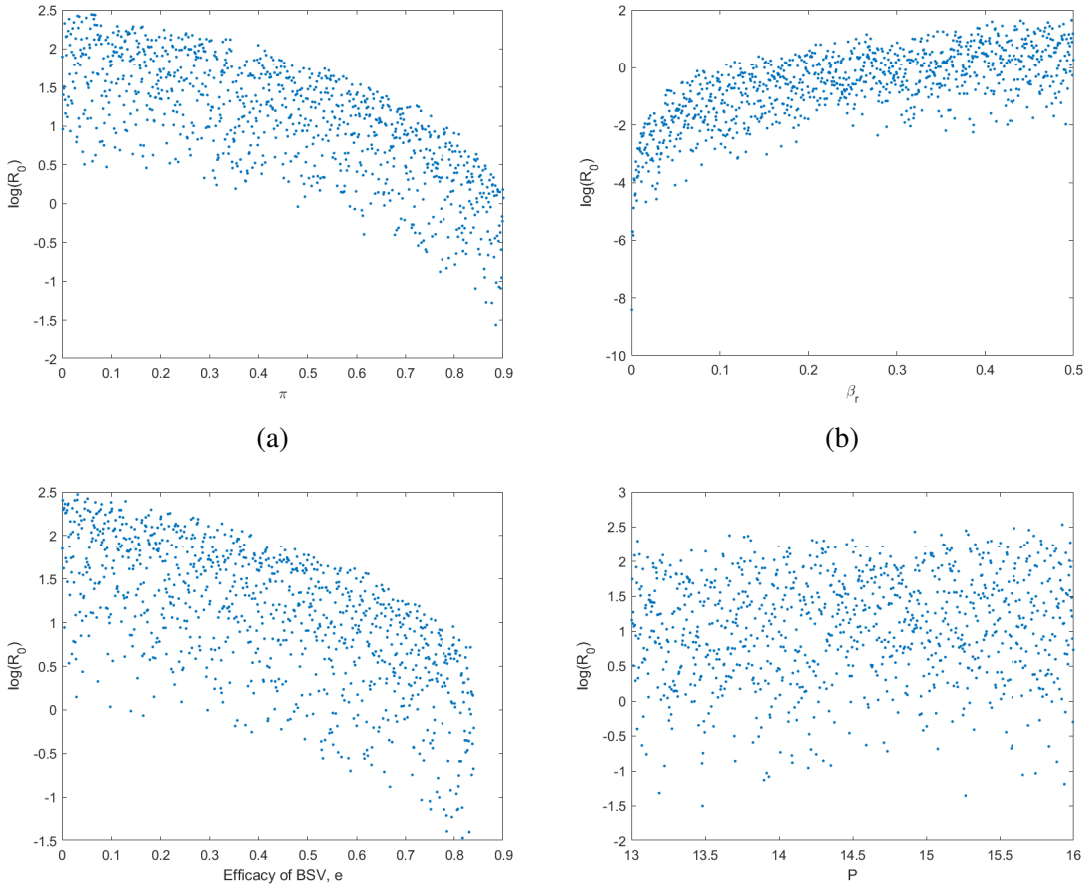

Figure 5.3: The Monte Carlo simulations for some of the parameters with the greatest partial rank correlation coefficients (PRCC) magnitudes, using values in Table 5.9 and 1000 simulations per run. They are: (a) proportion of parasites that become gametocytes π, (b) merozoite invasion rate β_r, (c) efficacy of blood stage vaccine ϱ and (d) the number of merozoites produced per bursting blood schizont P.

It is evident that a highly efficacious pre-erythrocytic vaccine such as RTS,S/SA01 and blood stage vaccine such as MSP3 could effectively help in reducing parasitaemia and malaria severity during clinical *P. falciparum* infections. Sporozoite invasion rate β_s and the merozoite invasion parameter β_r are also shown to increase the model R_{eff} and hence the severity of the disease within the human host.

Although the LHS/PRCC technique is useful in identifying significant parameters in the in-host malaria model, it fails to rank the parameters in order of their contribution to variations and disease progression. This ranking is very crucial in the design of clinical interventions and in the development of malaria vaccines. The normalised forward sensitivity index of

the effective reproduction number in equations (5.16) and (5.17) against LHS parameters in Table 5.9 are considered in the next section.

5.5.1 Sensitivity analysis based on effective reproduction number, R_{eff}

The normalised forward sensitivity (NFS) index technique described by Arriola and Hyman (2005) is adopted to compute the sensitivity indices of the model R_{eff} with respect to input parameters $P, \beta_r, \beta_s, \lambda_h, \lambda_r, \mu_h, \mu_r, \mu_x, \mu_m, \varrho, a, \pi, \nu$. The sensitivity indices are evaluated in Mathematica software based on the baseline parameter values given in Table 5.9 and results presented in Table 5.8.

Table 5.8: Table of sensitivity results

Parameter	SI	Parameter	SI
P	+1.00000	a	-0.785714
β_s	+1.00000	π	-0.785714
λ_h	+1.00000	β_r	+0.62402
μ_h	-1.00000	λ_r	+0.62402
μ_x	-1.00000	μ_m	-0.62406
ϱ	-0.785714	μ_r	-0.62406
ν	-0.785714	q	-0.428571

From Table 5.8, it is observed that the density of merozoites released per bursting blood schizont P, the rate of invasion of healthy hepatocytes β_s and erythrocytes β_r, the rate of recruitment of susceptible hepatocytes λ_h and erythrocytes λ_r have a direct effect on severity of clinical malaria. A 10% increase (or decrease) in the magnitude of P increases (or decreases) model R_{eff} by 10%. Clinical malaria control should aim at reducing these parameters. On the other hand, malaria vaccines (ϱ and ν) are shown to reduce R_{eff} when their efficacies are improved.

An increase (or decrease) in the immunosensitivity of infected red blood cells q is similarly shown to reduce (or increase) the model R_{eff}. The proportion of merozoites that develop into gametocytes π is also shown to decrease the value of R_{eff} when they are increased. By rank, the parameters P, β_s, λ_h are the most influential in model (5.1), followed by the vaccine efficacies ϱ and ν. Clinical considerations should thus favour these parameters in the development of malaria vaccines.

Table 5.9: Parameter values used in the sensitivity analysis and numerical simulations

Paremeter	Value	Min	Max	Unit	Source
Λ	30	20	35	sporozoites/day	(Selemani et al., 2016)
μ_s	1.2	0.8	1.5	/day	(Selemani et al., 2016)
λ_r	3E5	3E3	3E6	cells/ml/day	(Li et al., 2011)
λ_h	3E5	3E3	3E6	cells/μl^{-1}/day	(Tumwiine et al., 2008)
β_r	8E-5	8E-7	8E-3	/mm^3/day	(Dondorp et al., 2000)
β_s	5E-4	5E-5	5E-3	/mm^3/day	(Selemani et al., 2016)
μ_h	0.029	0.01	0.03	/day	(Selemani et al., 2017b)
μ_x	0.02	0.01	0.05	/day	(Selemani et al., 2016)
π	0.2	0.1	0.9	Unitless	(Talman et al., 2004)
μ_r	8.3E-5	8.3E-6	0.0001	/day	(Anderson et al., 1989)
μ_m	48	46	49	/day	(Li et al., 2011)
μ_t	0.7	0.5	0.8	/day	(Magombedze et al., 2011a)
μ_g	0.0625	0.5	0.78	/day	(Selemani et al., 2016)
χ, ϱ, ν	0.6	0	1	Unitless	Assumed
d	5E-4	1E-4	0.001	Unitless	Assumed
τ	1.5	1.2	1.9	Unitless	(Niger and Gumel, 2011)
λ_w	30	25	35	cells/day	(Niger and Gumel, 2011)
a, b	0.17	0.2	0.5	Unitless	(Niger and Gumel, 2011)
P	16	13	20	Unitless	(Diebner et al., 2000)
N	10000	8000	11000	Unitless	(Tumwiine et al., 2008)
$\varepsilon_0, \varepsilon_1$	1E-5	1E-6	1E-4	/day	(Tumwiine et al., 2008)
q	0.01	0.001	0.02	Unitless	(Niger and Gumel, 2011)
ρ	0.3	0.2	0.45	Unitless	(Niger and Gumel, 2011)
μ_n, μ_a	0.4	0.3	0.72	/day	(Li et al., 2011)
Ω	30	24	33	/day	(Magombedze et al., 2011a)

In conclusion, the LHS/PRCC technique is robust and considers the entire parameter space in determining significant parameters in the disease model. However, it fails the ranking test. On the other hand, although the NFS index approach is beneficial in discerning and ranking significant parameters in a model, it fails to explain the considerable uncertainties in estimating parameter values. It therefore fails to uncover parameter effects on particular variables or populations in the model. Due to the importance attached to the significance and

rank of each parameter in the model, it is advisable that both approaches be used in future analysis of parameter uncertainty and sensitivity analysis in disease models.

5.6 Numerical simulation

In this section, the dynamics of the in-host malaria in system (5.1) is numerically illustrated using Python software. When the effective reproduction number R_{eff} is less than unity, clinical *P. falciparum* malaria is observed to die out (see Figures 5.4 and 5.5).

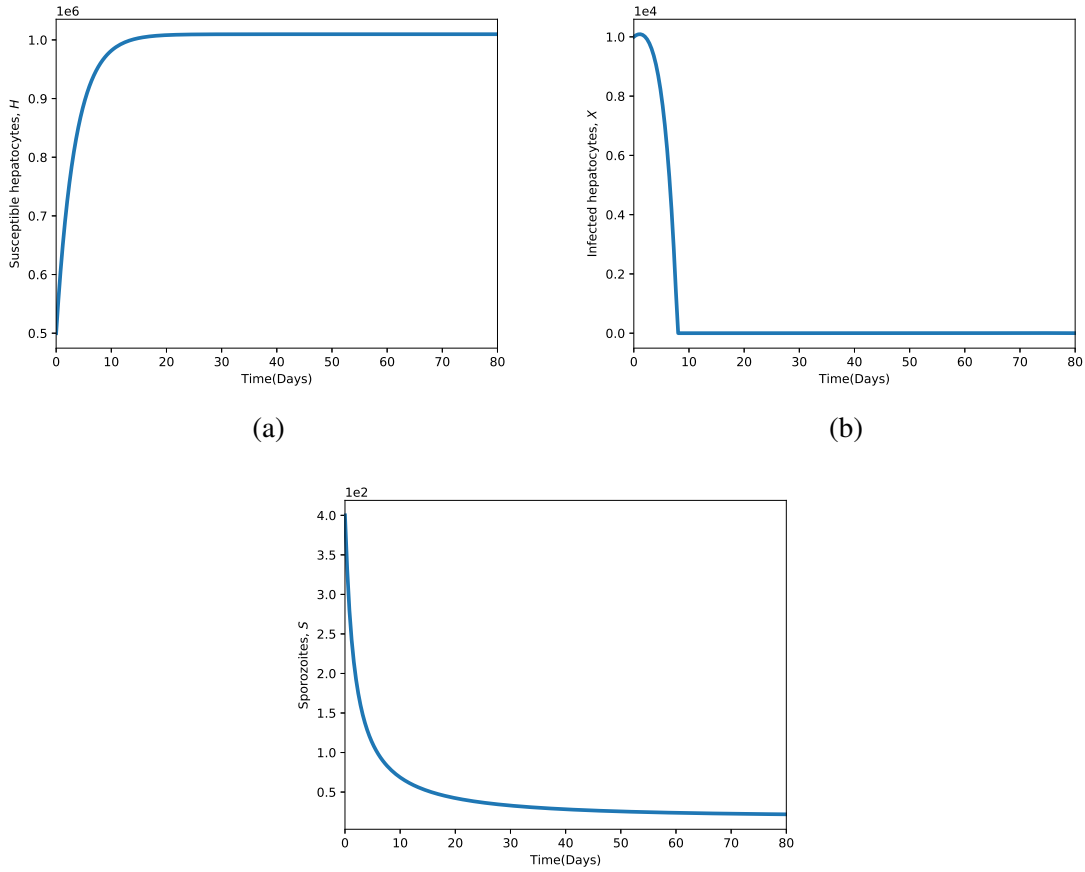

(a) (b)

(c)

Figure 5.4: Population dynamics of the liver hepatocytes and the sporozoites when the effective reproduction number $R_{eff} = 0.8881 < 1$. The parameter values are shown in Table 5.9.

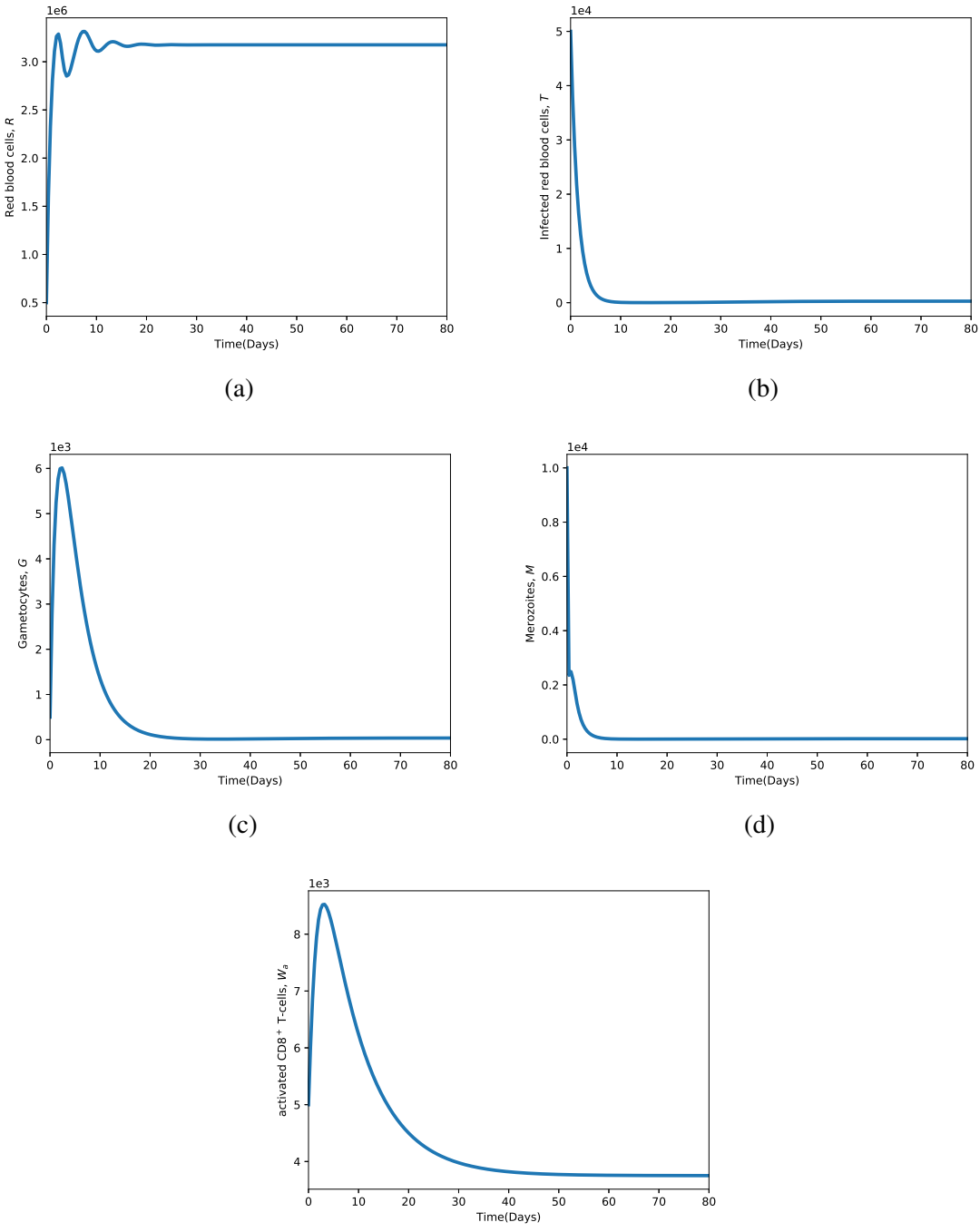

Figure 5.5: The dynamics of system (5.1) when the effective reproduction number $\mathrm{R}_{eff} = 0.8881 < 1$.

The disease-free equilibrium E_0 is globally asymptotically stable. Note that even if R_{eff} is less than unity, some activated $\mathrm{CD8}^{+}$T cells $W_a(t)$ still exist (see Figure 5.5e). This shows

that individual-level acquired immunity against malaria is maintained for some period of time even if all malaria parasites are eradicated from the host. All simulations are performed using parameter values given in Table 5.9.

Similarly, the density of sporozoites declines rapidly when $\mathrm{R}_{eff} = \mathrm{R}_{01} < 1$, leading to a corresponding decrease in the density of infected hepatocytes as shown in Figure 5.4. The malaria-persistent steady state, $E_p = (S^*, H^*, X^*, R^*, T^*, M^*, G^*, W_n^*, W_a^*) = (10^3, 3 \times 10^5, 3 \times 10^3, 5 \times 10^6, 5 \times 10^3, 10^3, 5 \times 10^2, 5 \times 10^3, 5 \times 10^3)$ is shown to be stable when R_{eff} is greater than unity, $\mathrm{R}_{eff} = 1.3364 > 1$ (see Figures 5.7 and 5.6). It is observed that the densities of sporozoites, merozoites, gametocytes, infected hepatocytes and infected erythrocytes grow and persists both at the pre-erythrocytic and blood stages of parasite development.

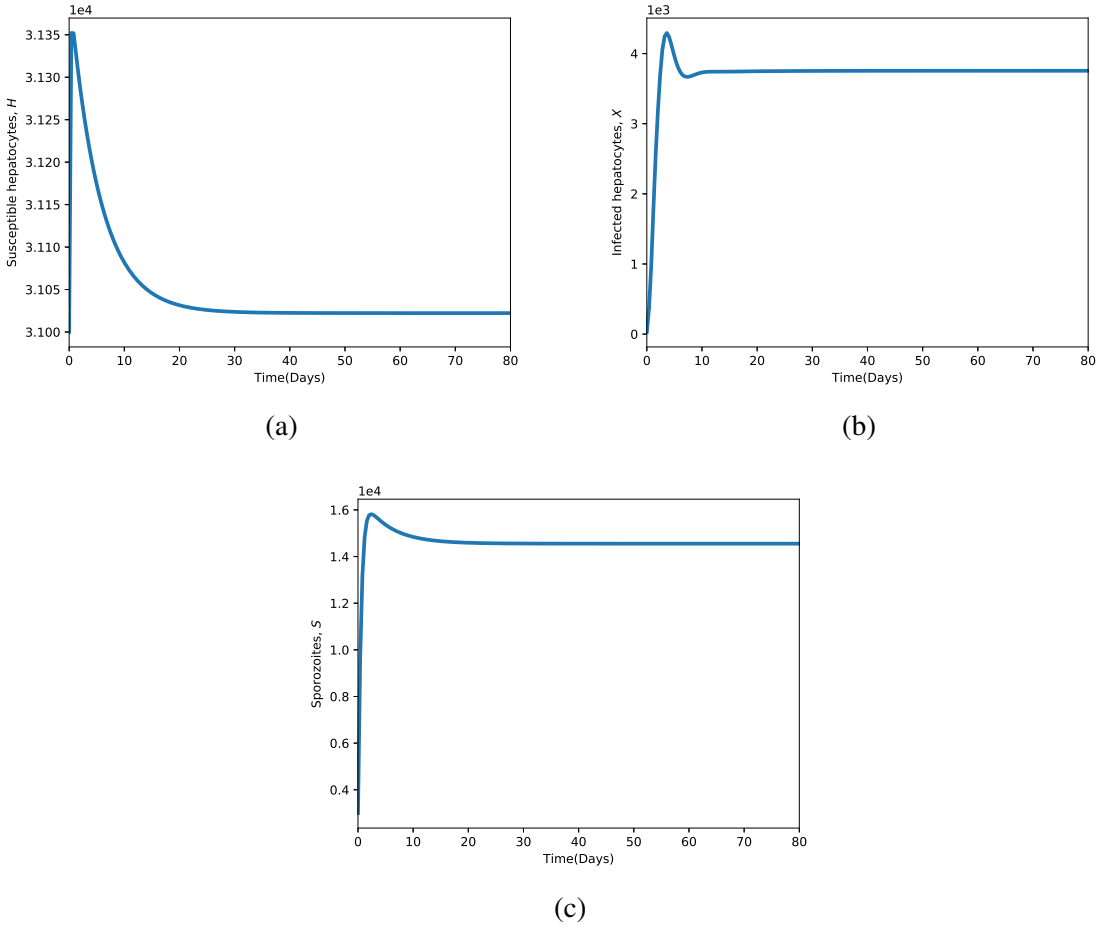

(a) (b)

(c)

Figure 5.6: When the effective reproduction number $\mathrm{R}_{eff} = 1.3364 > 1$, the malaria-persistent equilibrium E_p is stable.

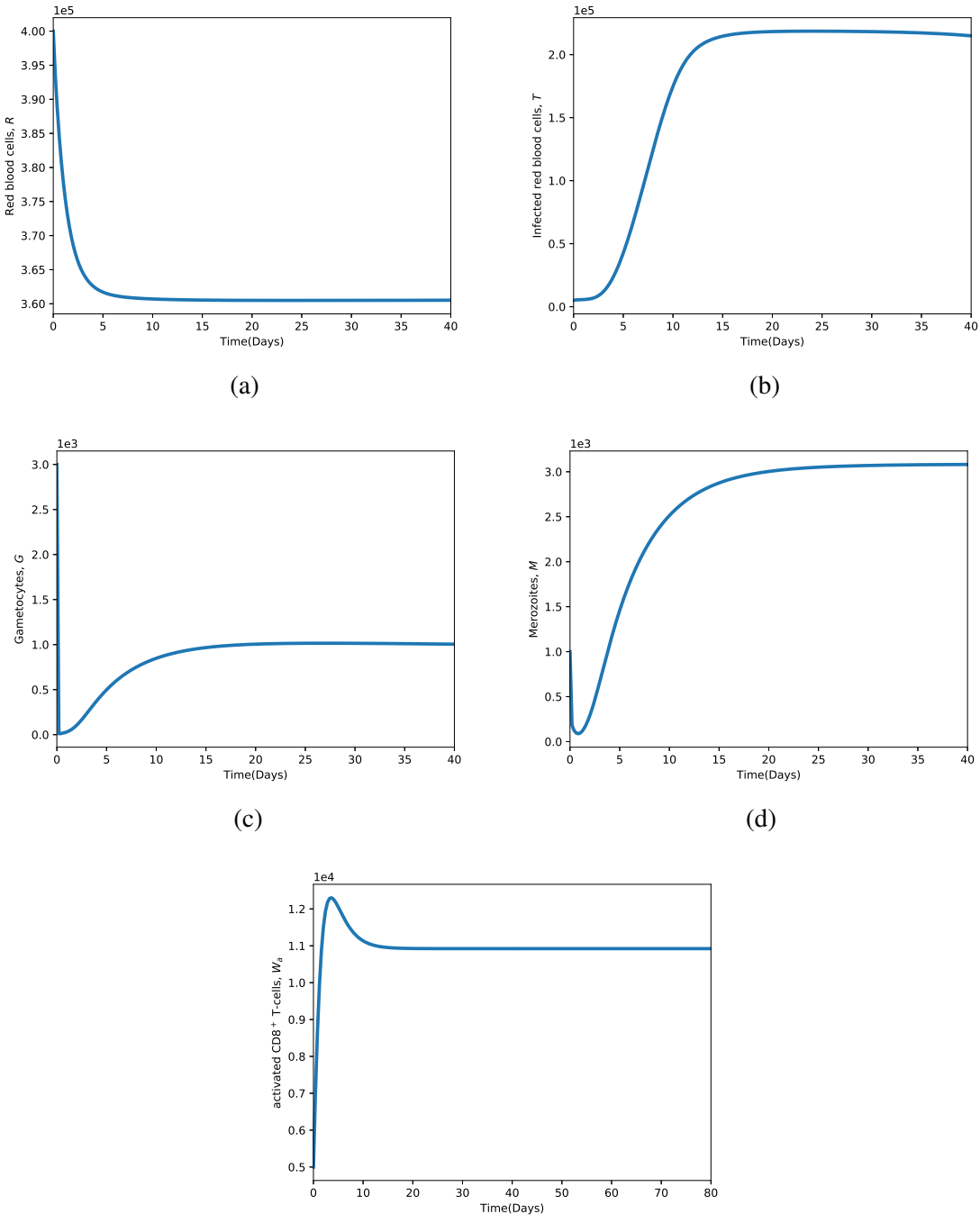

Figure 5.7: When the effective reproduction number $R_{eff} = 1.3364 > 1$, the malaria-persistent equilibrium point E_p is stable for the chosen set of parameter values. The model parameter values are shown in Table 5.9 and $R(0) = 5 \times 10^6$.

5.7 Multi-component and multi-stage vaccine cocktail

The need to develop a multi-component and multi-stage *P. falciparum* malaria vaccine with sufficient prospect to minimise the severity of malaria infection from human host is illustrated. Several strategies have been considered in the development of efficient multi-component and multi-stage *P. falciparum* vaccine formulations (Doolan and Hoffman, 2001; Pan et al., 2004; Rampling et al., 2016; Stoute et al., 1997; Stowers et al., 2002; White and Smith, 2013). A synthetic peptide (SPf66) that combines antigens from the blood stages of malaria linked together with an antigen from the sporozoite stage reduced the number of first attacks with *P. falciparum* by 28% in South America (Graves and Gelband, 2006). High level of sterile efficacy and safety of combining pre-erythrocytic vaccine RTS,S/AS01B with vectored vaccines were reported by Rampling et al. (2016).

P. falciparum chimeric protein 2.9 which is a combination of the C-terminal regions of domain III of AMA-1 and 19-kDa of MSP1 induced both anti-MSP1–19 and anti-AMA-1(III) Abs at levels 11- and 18-fold higher, respectively, than individual components did (Pan et al., 2004). Studies in Faber et al. (2013) have also shown that a combination of multiple vaccine candidates in fusion proteins may lead to improved characteristics of the vaccine.

Synergism from combination of transmission blocking vaccines is shown in (White and Smith, 2013) to confer protection by simultaneously inducing multiple, independent immune responses directed towards *P. falciparum* sporozoites. This ensures high levels of vaccine efficacy against the parasite. The need for multi-stage malaria vaccine is also emphasised in (Doolan and Hoffman, 2001) where DNA vaccines are shown to have high capacity to induce $CD8^+$ cytotoxic T lymphocytes and interferon-gamma responses in humans during *P. falciparum* infection (Tuteja, 2002).

From these studies, it is evident that a multi-stage specific vaccine cocktail has the potential to prevent initial malaria infection at the pre-erythrocytic stage, reduce or eradicate clinical manifestation and prevent the transmission of gametocytes from infected human hosts to susceptible feeding female *Anopheles* mosquitos (Boes et al., 2015). Therefore, effects of malaria vaccine combinations on the severity of *P. falciparum* malaria infection are evaluated numerically. The vaccines are broadly categorised as: pre-erythrocytic vaccines, blood stage vaccines and transmission blocking vaccines. The vaccines are assumed to have an optimal efficacy of 75%. This figure chosen is in consistency with the WHO strategic goal of developing a *P. falciparum* vaccine with atleast 75% efficacy (MVFG, 2018).

Results in Figure 5.8, show the effects of all the three vaccines combined with a constant optimal efficacy of 75%. The simulations here were performed in Matlab software. A sample code is presented in Appendix B. The density of infected erythrocytes T and infected hepatocytes X is shown to fall significantly. The severity of malaria infection is therefore highly reduced when the three efficacious vaccine antigens are combined.

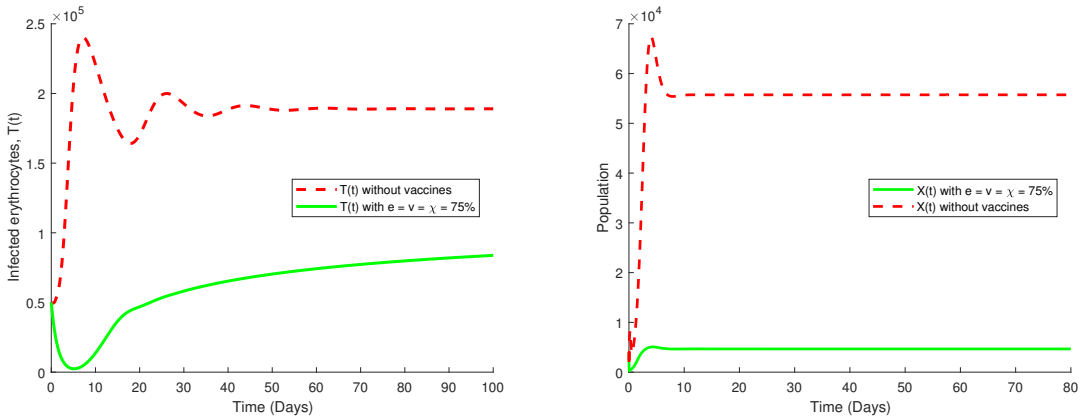

(a) (b)

Figure 5.8: Impact of a 75% efficacious combined malaria vaccines (pre-erythrocytic vaccine, blood stage vaccine and transmission blocking vaccine) on the dynamics of infected erythrocytes T and infected hepatocytes X. The simulations are performed when $R_{01} = 2.564 > 1$, and $R_{02} = 5.564 > 1$.

The use of only one vaccine is shown in Figures 5.9, 5.10 and 5.11 to have minimal effects on the severity of malaria infection.

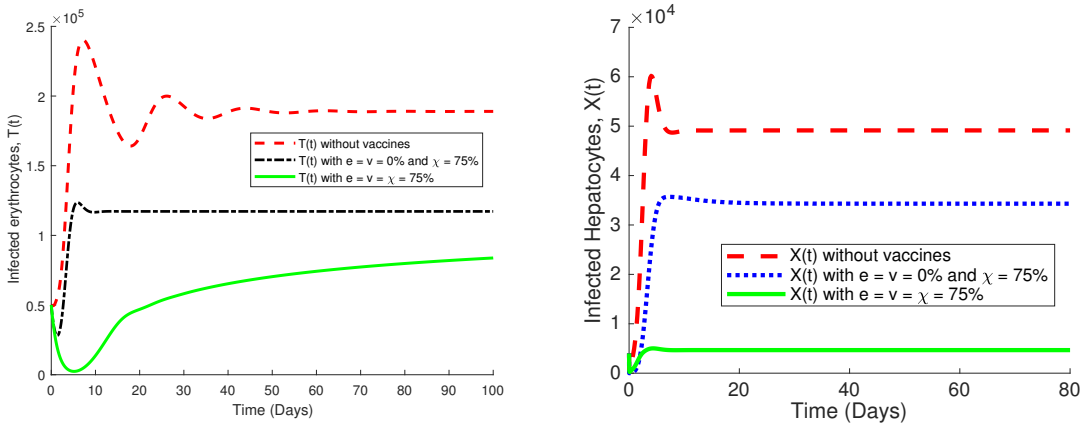

(a) (b)

Figure 5.9: Impact of a 75% efficacious transmission blocking vaccine (TBV) on the dynamics of infected erythrocytes and infected hepatocytes. The simulations are performed when $R_{01} = 2.564 > 1$, and $R_{02} = 5.564 > 1$.

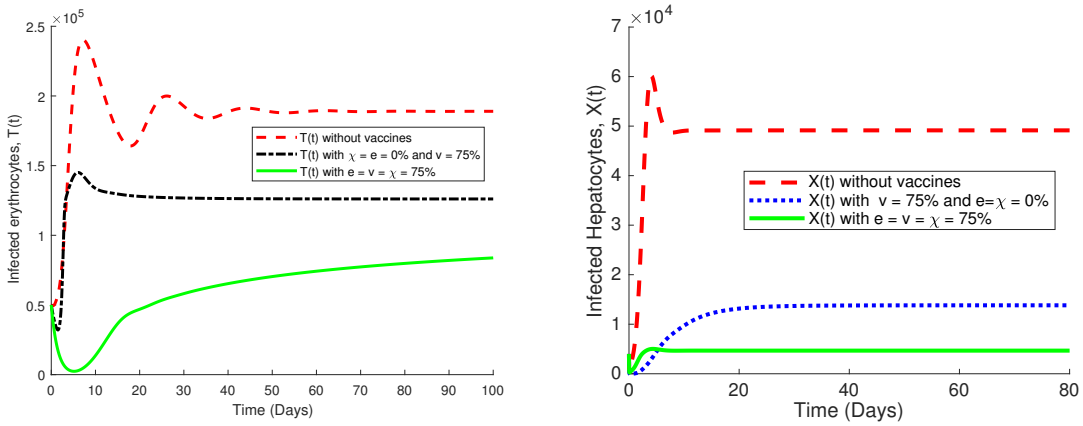

(a) (b)

Figure 5.10: Impact of a 75% efficacious pre-erythrocytic vaccine (PEV) on the dynamics of infected erythrocytes and infected hepatocytes. The simulations are performed when $R_{01} = 2.564 > 1$, and $R_{02} = 5.564 > 1$.

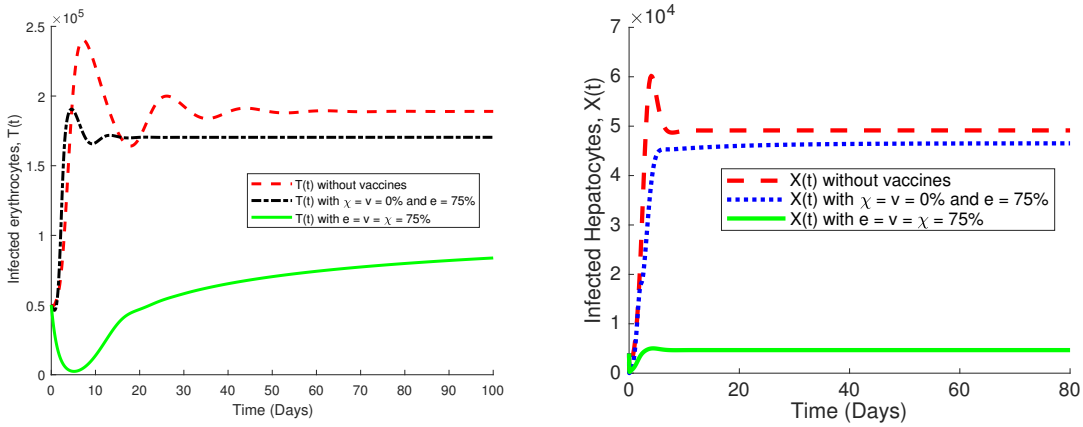

(a) (b)

Figure 5.11: Impact of a 75% efficacious blood stage vaccine (BSV) on the dynamics of infected erythrocytes and infected hepatocytes. The simulations are performed when $R_{01} = 2.564 > 1$, and $R_{02} = 5.564 > 1$.

Finally, a combination of any two vaccines (with different antigens) is likely to moderately reduce the severity of malaria infection. The effects of paired - vaccine combinations are as shown in Figures 5.12, 5.13 and 5.14. Unlike infected hepatocytes, transmission blocking vaccines are shown to have minimal effects on the density of infected red blood cells (see Figure 5.10).

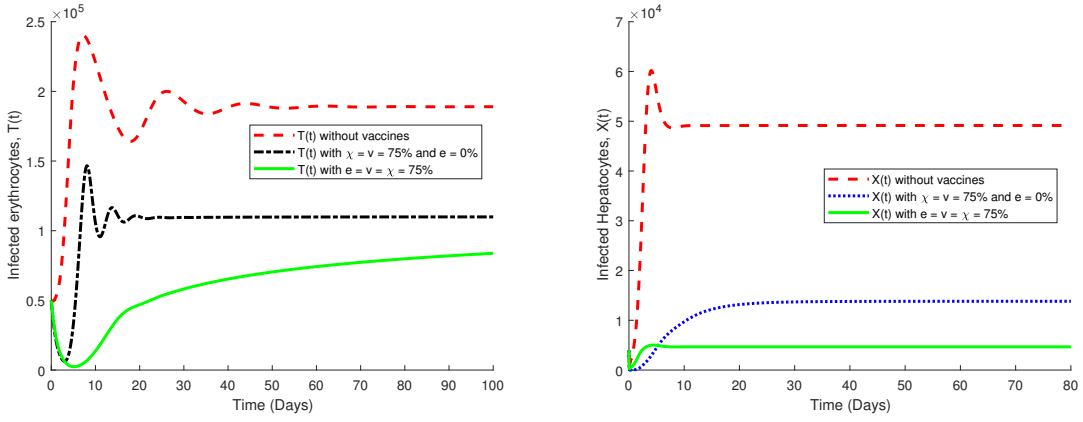

(a) (b)

Figure 5.12: The effect of combining a pre-erythrocytic vaccine (PEV) and a trasmission blocking vaccine (TBV) that are both 75% efficacious on the dynamics of infected erythrocytes and infected hepatocytes. The simulations are performed when $R_{01} = 2.564 > 1$, and $R_{02} = 5.564 > 1$.

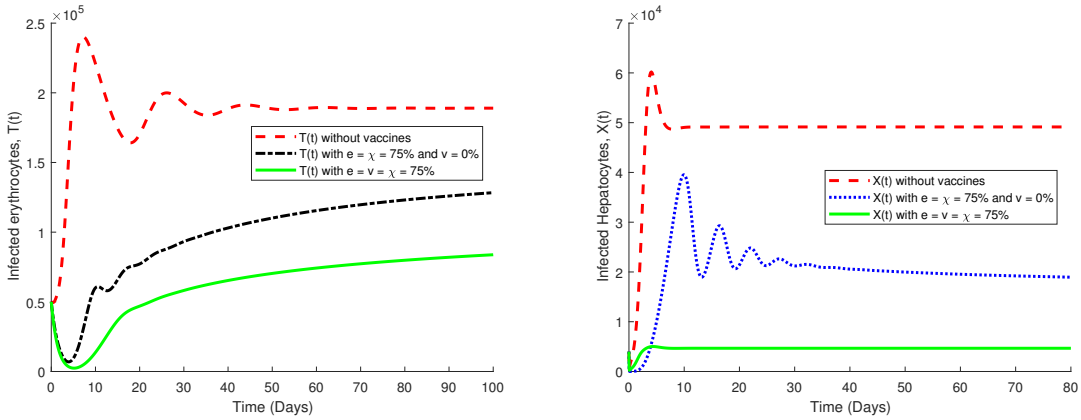

(a) (b)

Figure 5.13: The effect of combining a trasmission blocking vaccine (TBV) and a blood stage vaccine (BSV) that are both 75% efficacious on the dynamics of infected erythrocytes and infected hepatocytes. The simulations are performed when $R_{01} = 2.564 > 1$, and $R_{02} = 5.564 > 1$.

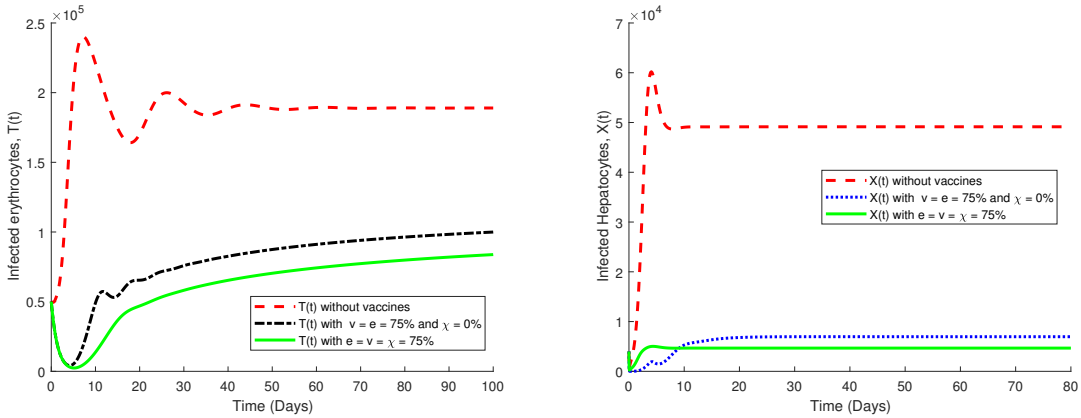

(a) (b)

Figure 5.14: The effect of combining a blood stage vaccine (BSV) and a pre-erythrocytic vaccine (PEV) that are both 75% efficacious on the dynamics of infected erythrocytes and infected hepatocytes. The simulations are performed when $R_{01} = 2.564 > 1$, and $R_{02} = 5.564 > 1$.

A combination of an efficacious pre-erythrocytic vaccine and an effective blood stage vaccine antigens has the potential to significantly reduce malaria severity as shown in Figure 5.14. Moreover, a combination of antigens from transmission blocking vaccine and those of pre-erythrocytic vaccine at the liver stage, as shown in Figure 5.12b, are very effective in suppressing the density of infected hepatocytes in the liver.

5.8 Conclusion

Results of uncertainty and sensitivity analysis have significant epidemiological importance in malaria control. The in-host malaria model presented in system (5.1) is shown to be sensitive to variations in vaccine efficacies χ, ϱ and ν. Only efficacious malaria vaccines have a chance to eradicate *P. falciparum* malaria or to reduce its severity significantly during clinical infection. Sensitivity indices based on the effective reproduction number indicate that the rate of invasion of susceptible erythrocytes by merozoites β_r and the rate of invasion of liver hepatocytes by sporozoites β_s are highly sensitive to malaria disease progression. Malaria vaccines must therefore target and eradicate the infective parasites and infected cells.

Other parameters such as the proportion of merozoites that become gametocytes per dying infected erythrocyte π and the average number of merozoites released per bursting erythrocyte P are also shown to have a considerable impact on R_{eff} and hence the severity of infection.

A highly efficacious blood stage vaccine has a potential to greatly reduce the density of malaria gametocytes in blood. This reduces malaria transmission from the human host to the mosquito vector. Given the protective capacity of liver stage- specific $CD8^+$ T cells (Villarino and W Schmidt, 2013), a lot more research that focuses on developing an efficacious blood stage vaccine that would prime blood trophozoite-specific $CD8^+$ T cells is called for. The parameter τ which accounts for vaccine-induced production of $CD8^+$ T cells is shown to have significant negative effects on the density of infected hepatocytes. The more efficient the pre-erythrocytic vaccine is, the lower the density of released merozoites into the host's blood.

Moreover, a rapid eradication of parasitised liver hepatocytes is likely to result into less infected erythrocytes at the blood stage. An efficacious pre-erythrocytic vaccines has a potential to eradicate infected liver hepatocytes. Such liver stage vaccines may also reduce the overall burst size of an infected hepatocyte, leading to reduced erythrocytic schizogony and hence the severity of clinical *P. falciparum* malaria.

Multiple combination of malaria vaccine antigen has a great potential of reducing the severity of malaria infections due to *P. falciparum*. The synergy of combining pre-erythrocytic vaccines, blood stage vaccines and transmission blocking vaccines antigens induces multiple immune responses with the potential to prevent or eradicate malaria infection. As highlighted in Kumar (2007), this study shows that a highly effective vaccine combination is critical for *P. falciparum* malaria disease elimination goal.

Although efficacious malaria vaccines are shown to be very effective in reducing severity of clinical malaria, the results from this study further confirm the need to combine vaccine with existing antimalarial therapy to achieve a complete eradication of the parasites from the host. Moreover, the LHS/PRCC analysis revealed that the prediction imprecision was mainly due to certain key parameters. Long term precise predictions of the density of infected liver hepatocytes and infected erythrocytes would be difficult until these key parameters are correctly determined. A great understanding of parameter uncertainty and sensitivity analysis of in-host malaria in humans is therefore necessary in order to develop effective vaccines against *P. falciparum* pathogens.

In the next Chapter 6, the impact of multiple-strains of *P. falciparum* infections on the severity of malaria infection within a human host and its effects on development of parasite resistance is investigated.

Chapter 6

Multiple-strain infection and resistance to antimalarial therapy: A mathematical modelling perspective

6.1 Introduction

The emergence of parasite resistance (Dondorp et al., 2010; Maude et al., 2009; Sidhu et al., 2002; Wellems and Plowe, 2001) to antimalarial drugs has contributed significantly to human mortality and morbidity due to malaria infection, worldwide (Smith et al., 2010; Snow et al., 2001; White, 1999). A global malaria control strategy of 1992 (WHO, 1993) that advocated for early diagnosis and prompt treatment has been heavily compromised by the emergence of parasite resistance to antimalarial drugs. The evolution of parasite resistance has been described in Kim and Schneider (2013) as an example of a Darwinian evolution. Parasites undergo mutations in their genome in response to drug-treated human host. These mutations reduce the rate of parasite elimination from the host and increases their survival chances (Kim and Schneider, 2013).

The most extensively used antimalarial drugs against the deadly *P. falciparum* malaria are Chloroquine (CQ) and Sulfadoxine-pyrimethamine (SP) (Talisuna et al., 2004; White and Pongtavornpinyo, 2003). These drugs are cheap, easily available and slowly eliminated from the human body (White and Pongtavornpinyo, 2003). However, the extensive use of CQ and SP resulted into *P. falciparum* resistance. This led to global increase in malaria cases and mortality (Trape et al., 1998). In 2006, the World Health organization (WHO)

recommended the use of artemisinin-based combination therapies (ACTs) as a first-line treatment for uncomplicated *P. falciparum* malaria (WHO, 2015c).

Resistance to ACTs which are currently the standard treatment for uncomplicated *P. falciparum* is likely to cause global health crisis especially in African region where *P. falciparum* malaria is endemic (Ashley et al., 2014; Ouji et al., 2018). The Global Technical Strategy for Malaria 2016-2030 calls on countries and global malaria partners to monitor the efficacy of antimalarial medicines so that the most appropriate treatments can be selected for national policies (WHO, 2018f).

In this chapter, the effects of parasite resistance to antimalarial drugs are investigated by extending the in-host malaria model by Anderson et al. (1989). The malaria parasites are categorised into drug-sensitive strain and drug-resistant strain. The impact of multi-strain infection on severity of the disease is investigated in the context of parasite resistance.

6.1.1 Parasite resistance to antimalarial drugs

The emergence of parasite resistance to malaria therapy dates back to the 19th century. Quinine (introduced in 1820) was the first-line antimalarial drug against *P. falciparum* (Dobson, 2001). High mortality cases coupled with high parasite resistance led to the introduction of a second drug, chloroquine (CQ) in 1934 (Thompson and Leslie, 1972). A decade later, CQ was considered the first-line antimalarial drug by several countries until 1957, when the first foci of *P. falciparum* resistance was detected along Thai-Cambodia border (Harinasuta et al., 1965). In Africa, CQ resistance to *P. falciparum* was first discovered among travelers from Kenya to Tanzania (Fogh et al., 1979). By 1983, CQ resistance had spread to Sudan, Uganda (Onori, 1984), Zambia (Ekue et al., 1983) and Malawi (David et al., 1984).

CQ was replaced for the first time with Sulfadoxine-pyrimethamine (SP) as a first line antimalarial drug in Thailand in 1967. Several other countries in Asia and South America followed thereafter (Talisuna et al., 2004). Resistance to SP was however reported the same year (Wernsdorfer and Payne, 1991) in the region. In 1988, CQ was replaced for the first time in Africa. South Africa replaced CQ with SP (Bredenkamp et al., 2001). In 1993, Malawian government changed the treatment policy from CQ to SP. Other African countries followed thereafter: Kenya, South Africa and Botswana (in 1998); Cameroon, Tanzania (in 2001) and Zimbabwe (in 2000) (Bloland et al., 1993). The effectiveness of SP was equally undermined

by resistance. Unlike CQ, *P. falciparum* resistance to SP was mainly attributed to the long half-life of the drug (Foote and Cowman, 1994).

Confirmed resistance to the artemisinin derivatives was first reported in Cambodia and Mekong regions (CMR) in 2008 (WHO, 2016a). The number of ACTs with high failure rates in CMR is presented in Figure 6.1. Artemisinin resistance is characterised by slow parasite clearance (WHO, 2018f). To leverage on parasite resistance, cost of treatment and burden of malaria infection to communities and governments, the WHO recommends the use of artemisinin-based combination therapy (ACTs) as the first and second-line treatment drugs for uncomplicated *P. falciparum* malaria (WHO, 2016a). ACT is a combination of artemisinin derivative and a partner monotherapy drug. Artemisinin derivatives include artemether, artesunate and dehydroartemisinin. These derivatives reduce the parasite biomass within the first three days of therapy while the partner drug, with longer half-life, eliminates the remaining parasites (WHO, 2018e).

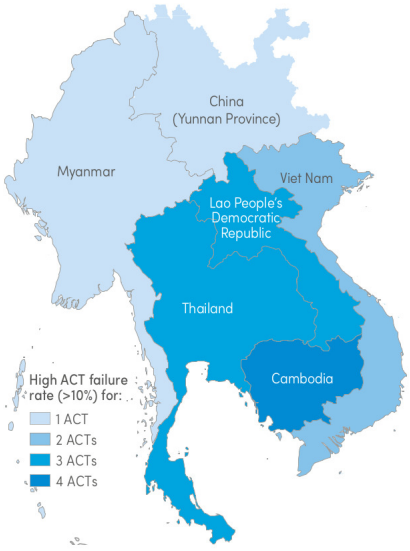

Figure 6.1: Number of artemisinin-based combination therapies (ACTs) with high failure rates in the treatment of *P. falciparum* infections. Source: WHO (2018f).

Currently, WHO recommends five different ACTs: (1) Artesunate-amodiaquine (AS+AQ), (2) artesunate-mefloquine (AS+MQ), (3) artesunate+sulfadoxine-pyrimethamine (AS+SP), (4) artemether-lumefantrine (AM-LM) and (5) dihydroartemisinin-piperaquine (DHA+PPQ). Additionally, artesunate-pyronaridine (AS+PY) which has received a positive scientific opinion from the European Medicines Agency (EMA) maybe used in regions where ACT treatment response is low (WHO, 2018e). Access to ACT has been tremendous in the last 8 years; with recorded increases of 122 million procured treatment courses for the

period 2010-2016. However, resistance to currently used ACTs have important public health consequences, especially in the African region, where resistant *P. falciparum* is predominant.

Numerous cross-sectional studies (Bushman et al., 2016; Harrington et al., 2009) have revealed the possible impact of multiple-strains of *P. falciparum* in the development of resistance to ACTs. In Bushman et al. (2018) and citations therein, drug-sensitive parasites are shown to strongly suppress the growth and transmission of drug-resistant *P. falciparum* parasites. Although high transmission settings such as sub-Saharan Africa account for about 90% of all global malaria deaths, resistance to antimalarial drugs have been shown to emerge from low transmission settings, such as Southeast Asia and South America (Bushman et al., 2018).

Causes of parasite resistance to ACTs are diverse. Historical studies (Mita et al., 2009; Vinayak et al., 2010) indicate that antimalarial-resistant parasites could emerge from a handful of lineages. It is argued elsewhere (Hastings and Watkins, 2005; Talisuna et al., 2003) that recombination during sexual reproduction in the mosquito vector could be responsible for the delayed appearance of multi-locus resistance in high-transmission regions. Moreover, owing to repeated exposure for many years, individuals in high-transmission settings are likely to develop clinical immunity to malaria, leading to stronger selection for resistance (Klein et al., 2008). Studies in Bushman et al. (2018) also support the hypothesis that in-host competition between drug-sensitive and drug-resistant parasites could inhibit the spread of resistance in high transmission settings. Owing to their integral role in the recent success of global malaria control, the protection of efficacy of ACTs should be a global health priority (WHO, 2017b).

Mathematical models of in-host malaria epidemiology and control constitute important tools in guiding strategies for malaria control (McKenzie, 2000; McKenzie and Samba, 2004) and the associated financial planning (Coleman et al., 2004). While some researchers have focussed on probabilistic models (Hastings, 1997; Mackinnon, 2005), others have investigated the effects of drug treatment and resistance development using deterministic models (Aneke, 2002; Koella and Antia, 2003). A deterministic model by Esteva et al. (2009) monitored the impact of drug resistance on the transmission dynamics of malaria in a human population. In Bushman et al. (2018), the impacts of within-host parasite competition is shown to inhibit the spread of resistance (Klein et al., 2012; Legros and Bonhoeffer, 2016). On the contrary, some models (Hastings, 1997; Wargo et al., 2007) have suggested that within-host competition is likely to speed up the spread of resistance in high-transmission settings due to a phenomenon called ‘competitive release’. In this chapter, theoretical insights

using mathematical modelling of the impact of multiple-strain infections on resistance, dynamics and antimalarial control of *P. falciparum* malaria are provided.

6.2 Model formulation

To investigate the effects of parasite resistance to antimalarial drugs and the impact of multiple-strain infection on severity of the disease, the deterministic blood stage malaria model by Anderson et al. (1989) is extended. This model considers the co-infection and competition between the drug-sensitive (dss) and the drug-resistant (drs) *P. falciparum* strains in the presence of antimalarial therapy. The drs arise presumably from the dss. The rare mechanism here could possibly be due to single point mutation (zur Wiesch et al., 2011). Both drs and dss initiate immune responses that follow density-dependent kinetics.

The model is composed of eight compartments: susceptible/healthy/unparasitised erythrocytes $X(t)$, parasitised/infected erythrocytes ($Y_r(t)$ and $Y_s(t)$), merozoites ($M_s(t)$ and $M_r(t)$), gametocytes ($G_s(t)$ and $G_r(t)$) and immune cells $W(t)$. The healthy red blood cells (RBCs) make up the resource for competition between the drug-resistant strain and the drug-sensitive strain. The infected red blood cells (IRBCs) and the different erythrocytic parasite life cycles are categorised based on the strain of infecting parasite. The merozoites are therefore categorised into drug-sensitive strain and drug-resistant strain, denoted by $M_s(t)$ and $M_r(t)$, respectively. The merozoites invade the healthy erythrocytes during erythrocytic stage leading to formation of infected erythrocytes. The variable $Y_s(t)$ denotes the red blood cells (RBCs) infected with drug-sensitive merozoites, whereas, $Y_r(t)$ refers to the RBCs infected with drug-resistant merozoites. Similarly, the variables $G_s(t)$ and $G_r(t)$ represent drug-sensitive and drug-resistant gametocytes, respectively. Owing to saturation in cell and parasite growth, the nonlinear Michaelis-Mented-Monod function described in Agur et al. (1989); Antia et al. (1994) and used in Cai et al. (2017); Chiyaka et al. (2008); Pilyugin and Antia (2000); Selemani et al. (2017a), is considered to model the reductive effects of the immune cells on the parasite and infected-cell populations.

The density of the healthy RBCs is increased at the rate λ_x per healthy RBC from the host's bone marrow and die naturally at a rate μ_x. Following parasite invasion by free floating merozoites, the healthy erythrocytes get infected by both drug-sensitive and drug-resistant merozoite strains at the rates β and $\delta_r\beta$, respectively. The parameter δ_r (with $0 < \delta_r < 1$) accounts for the reduced fitness (infectiousness) of the resistant parasite strains in relation to the drug-sensitive strain. The destruction of the healthy red blood cells is however limited

by the adaptive immune cells W. This is represented by the term $1/(1+\gamma W)$, where γ is a measure of the efficacy of the immune cells. The equation that governs the evolution of the healthy RBCs is hence given by

$$\frac{\mathrm{d}X}{\mathrm{d}t} = \lambda_x - \mu_x X - \frac{\beta X}{1+\gamma W}(M_s + \delta_r M_r). \tag{6.1}$$

The infected red blood cells are generated through mass action contact (invasion) between the healthy erythrocytes X and the blood floating merozoites (M_r and M_s). The merozoites subdivide mitotically, within the infected erythrocytes, into thousands of other merozoites leading to cell-burst and emergence of malaria characteristic symptoms. Additionally, a single infected erythrocyte undergoes hemolysis at the rate μ_{ys} to produce P secondary merozoites, sustaining the erythrocytic cycle. The drug-sensitive IRBCs (Y_s) burst open to generate more drug-sensitive merozoites or drug-sensitive gametocytes at the rate σ_s.

Similar dynamics are observed with the drug-resistant IRBCs, where the drug-resistant gametocytes are generated at the rate σ_r from IRBCs. Treatment with ACT is assumed to inhibit the development of the merozoite within the infected erythrocyte. The drug-infested erythrocytes are hence likely to die faster. This is represented by the term $(1-\omega_s)^{-1}$, where $0 < \omega_s < 1$ represents the antimalarial-specific treatment efficacy. In this chapter and for purposes of illustration and simulations, ω_s, corresponds to the efficacy of artemether-lumefantrine (AL), which is the recommended first-line antimalarial ACT drug for *P. falciparum* infection in Kenya. It is assumed that no treatment is available for erythrocytes infected with the resistant parasite strain. The time rate of change for Y_s and Y_r takes the form:

$$\frac{\mathrm{d}Y_s}{\mathrm{d}t} = \frac{\beta X M_s}{1+\gamma W} - \frac{k_y Y_s W}{1+aY_s} - \frac{1}{1-\omega_s}\mu_{ys} Y_s - \sigma_s Y_s, \tag{6.2}$$

$$\frac{\mathrm{d}Y_r}{\mathrm{d}t} = \frac{\delta_r \beta X M_r}{1+\gamma W} - \frac{k_y Y_r W}{1+aY_r} - \mu_{yr} Y_r - \sigma_r Y_r. \tag{6.3}$$

The drug-resistant merozoites M_r and the drug-resistant gametocytes G_r die naturally at the rates μ_{mr} and μ_{gr}, respectively. It is further assumed that drug sensitive merozoites M_s and gametocytes G_s may develop into drug-resistant merozoites M_r and gametocytes G_r at the rates Ψ_1 and Ψ_2, respectively. The cost of resistance associated with AL is represented by the parameter α_s. Parasite resistance to antimalarial drugs exacerbates the erythrocytic cycle and increases the cost of treatment (De Roode et al., 2004; Hayward et al., 2005). The higher the resistance to antimalarial therapy, the higher the density of malaria parasites in blood. Therefore, this decline in drug effectiveness is modelled by re-scaling the density of

merozoites released per bursting infected erythrocyte P by the factor $(1-\alpha_s)$, where $\alpha_s = 1$ implies no resistance, that is, the ACT is highly effective in eradicating the parasites. $\alpha_s = 0$ corresponds to maximum resistance; and the used ACT drug is least effective in treating the infection. The converse of these descriptions applies to the drug-resistant *P. falciparum* parasite strain. The equations that govern the rate of change of the infected red blood cells and the merozoites takes the form:

$$\frac{dM_s}{dt} = (1-\alpha_s)P\mu_{ys}Y_s - \frac{\beta M_s X}{1+\gamma W} - \frac{k_m M_s W}{1+aM_s} - (\Psi_1 + \mu_{ms} + \zeta)M_s, \tag{6.4}$$

$$\frac{dM_r}{dt} = (1-\alpha_r)P\mu_{yr}Y_r + \Psi_1 M_s - \frac{\delta_r \beta M_r X}{1+\gamma W} - \frac{k_m M_r W}{1+aM_r} - \mu_{mr}M_r, \tag{6.5}$$

$$\frac{dG_s}{dt} = \sigma_s Y_s - \frac{k_g W G_s}{1+aG_s} - (\Psi_2 + \mu_{gs} + \eta)G_s, \tag{6.6}$$

$$\frac{dG_r}{dt} = \sigma_r Y_r + \Psi_2 G_s - \frac{k_g W G_r}{1+aG_r} - \mu_{gr}G_r. \tag{6.7}$$

Antimalarial therapy increases the rate of elimination of drug-sensitive merozoites and gametocytes. This is represented by the nonnegative enhancement parameters ζ and η, respectively. Although the innate immunity is faster, it is often limited by the on and off rates in its response to invading pathogens (Doolan et al., 2009; Liehl et al., 2015). The adaptive immunity on the contrary, is very slower at the beginning but lasts long enough to ensure no parasite growth in subsequent infections (Bushman et al., 2016). It is assumed that the immune cells are independent of the invading parasite strain. For simplicity, we consider the adaptive immune system, which is mainly composed of the $CD8^+$T cells (Villarino and W Schmidt, 2013).

The assumption that the background recruitment of immune cells is constant (at the rate λ_w) is adopted. Additionally, the production of the immune cells is assumed to be boosted by the infective and infected cells (G_r, G_s), (M_r, M_s) and (Y_r, Y_s) at constant rates h_g, h_m and h_y, respectively. Circulating gametocytes, infective merozoites and infected erythrocytes are thus removed phagocytotically by the immune cells at the rates $k_g W$, $k_m W$ and $k_y W$, respectively. The immune cells also get depleted through natural death at the rate μ_w. The equation for the immune cells takes the following form:

$$\frac{dW}{dt} = \lambda_w + \left\{ \frac{h_g(G_s+G_r)}{G_s+G_r+e_g} + \frac{h_y(Y_s+Y_r)}{Y_s+Y_r+e_y} + \frac{h_m(M_s+M_r)}{M_s+M_r+e_m} \right\} W - \mu_w W. \tag{6.8}$$

Following invasion by the merozoites, the IRBCs either produce merozoites or differentiate into gametocytes upon bursting. The total erythrocyte population at any time t, denoted by

$C(t)$ is therefore given by

$$C(t) = X(t) + Y_s(t) + Y_r(t). \tag{6.9}$$

Similarly, the sum total of *P. falciparum* parasites, denoted by $L(t)$ within the host at any time t is described by the following equation:

$$L(t) = M_s(t) + M_r(t) + G_s(t) + G_r(t). \tag{6.10}$$

The above dynamics can be represented by the schematic diagram shown in Figure 6.2. The list of model variables and parameters are provided in Tables 6.1 and 6.3, respectively.

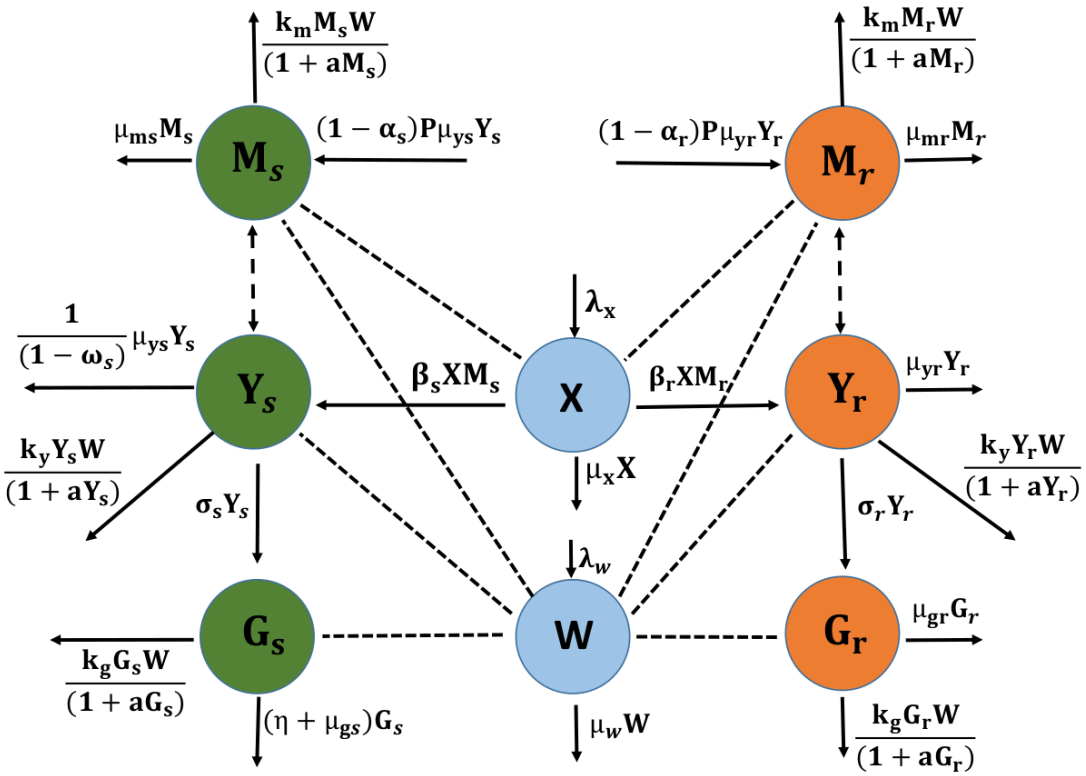

Figure 6.2: A model flow diagram. Drug-sensitive variables are shown in green colours while the drug-resistant variables are indicated in orange colours. Non-strain specific variables like susceptible red blood cells (RBCs) and immune cells are shown in blue colour. Solid lines indicate the movement of populations from one compartment to another. Dotted lines show possible interactions between the different populations.

Table 6.1: Description of the state variables of model (6.11).

Variable	Description
X	Population of uninfected/unparasitised red blood cells (erythrocytes)
Y_s	Population of red blood cells infected by drug-sensitive merozoites
Y_r	Population of red blood cells infected by drug-resistant merozoites
M_s	Population of drug-sensitive merozoites
M_r	Population of drug-resistant merozoites
G_s	Population of drug-sensitive gametocytes
G_r	Population of drug-resistant gametocytes
W	Population of strain-independent immune cell

Table 6.2: Description of model parameters

Parameter	Description
λ_x	The rate of recruitment of red blood cells
ω_s	Antimalarial treatment efficacy
α_s	Fitness cost associated with drug-sensitive merozoites M_s
α_r	Fitness cost associated with drug-resistant merozoites M_r
λ_w	Background recruitment rate of immune cells
e_g, e_m, e_y	Hill parameters in G_i, M_i and Y_i dynamics $(i = s, r)$
μ_x	Per capita natural mortality rate of unparasitised erythrocytes
μ_{ys}	Natural mortality rate of drug-sensitive IRBCs
μ_{yr}	Natural death rate of drug-resistant IRBCs
ζ	Rate of eradication of drug-sensitive merozoites by antimalarial drugs
η	Rate of eradication of drug-sensitive gametocytes by antimalarial drugs
μ_{ms}	Death rate of drug-sensitive merozoites
μ_{mr}	Mortality rate of drug-resistant merozoites
μ_{gs}	Per capita mortality rate of drug-sensitive gametocytes
μ_{gr}	Mortality rate of drug-resistant gametocytes
μ_w	Natural mortality rate of immune cells ($CD8^+$T cells)
β	The rate of infection of susceptible RBCs by blood floating merozoites
σ_r, σ_s	Rate of formation of gametocytes from the infected RBCs
P	Number of merozoites produced per dying infected RBC
h_y	Immune cells proliferation rate due to IRBCs
h_m	Immune cells proliferation rate due to asexual merozoites
h_g	Immune cells proliferation rate due to gametocytes

Continued on next page

Table 6.2 – *Continued from previous page*

Parameter	Description
k_y	Phagocytosis rate of IRBCs by immune cells
k_m	Phagocytosis rate of merozoites by immune cells
k_g	Phagocytosis rate of gametocytes by immune cells
Ψ_1	Rate of development of resistance by drug-sensitive merozoites
Ψ_2	Rate of development of resistance by drug-sensitive gametocytes
δ_r	Accounts for the reduced fitness of the resistant parasite strain
γ	Efficiency of immune effector to inhibit merozoite infection
$1/a$	Half-saturation constant for $Y(t)$, $M(t)$ and $G(t)$

In extending the deterministic blood stage malaria model by Anderson et al. (1989), following model assumptions are made:

1. There are eight interacting populations of susceptible red blood cells, drug-sensitive merozoites, drug-resistant merozoites, red blood cells infected with drug-sensitive merozoites, red blood cells infected with drug-resistant merozoites, drug-sensitive gametocytes, drug-resistant gametocytes and immune cells, at any given time t.
2. The drug-resistant strains of merozoites and gametocytes are assumed to arise presumably from the drug-sensitive strains of merozoites and gametocytes, respectively.
3. Red blood cell infection is merozoite-strain dependent. The infected red blood cells are hence categorised based on the infecting merozoite strain.
4. It is assumed that the drug-resistant merozoites have a lower rate of infection compared to their drug-sensitive competitors.
5. The invasion of the red blood cells is limited by the adaptive immune cells.
6. Treatment using the ACT drug is assumed to inhibit merozoite development within infected red blood cells.
7. Only drug-sensitive merozoites are targeted by antimalarial treatment.
8. The immune cells are assumed to be recruited at a constant rate from the bone marrow.
9. All model parameters are assumed non-negative.

10. Generation of immune cells is stimulated by the presence of infected red blood cells, merozoites and gametocytes.

Based on the above model descriptions, model assumptions and the schematic diagram shown in Figure 6.2, the model in this chapter consists of the following system of nonlinear differential equations:

$$\left.\begin{aligned}
\frac{dX}{dt} &= \lambda_x - \mu_x X - \frac{\beta X}{1+\gamma W}(M_s + \delta_r M_r),\\
\frac{dY_s}{dt} &= \frac{\beta X M_s}{1+\gamma W} - \frac{k_y Y_s W}{1+aY_s} - \frac{1}{1-\omega_s}\mu_{ys} Y_s - \sigma_s Y_s,\\
\frac{dY_r}{dt} &= \frac{\delta_r \beta X M_r}{1+\gamma W} - \frac{k_y Y_r W}{1+aY_r} - \mu_{yr} Y_r - \sigma_r Y_r,\\
\frac{dM_s}{dt} &= (1-\alpha_s)P\mu_{ys} Y_s - \frac{\beta M_s X}{1+\gamma W} - \frac{k_m M_s W}{1+aM_s} - (\Psi_1 + \mu_{ms} + \zeta)M_s,\\
\frac{dM_r}{dt} &= (1-\alpha_r)P\mu_{yr} Y_r + \Psi_1 M_s - \frac{\delta_r \beta M_r X}{1+\gamma W} - \frac{k_m M_r W}{1+aM_r} - \mu_{mr} M_r,\\
\frac{dG_s}{dt} &= \sigma_s Y_s - \frac{k_g W G_s}{1+aG_s} - (\Psi_2 + \mu_{gs} + \eta)G_s,\\
\frac{dG_r}{dt} &= \sigma_r Y_r + \Psi_2 G_s - \frac{k_g W G_r}{1+aG_r} - \mu_{gr} G_r,\\
\frac{dW}{dt} &= \lambda_w + \left\{\frac{h_g(G_s+G_r)}{G_s+G_r+e_g} + \frac{h_y(Y_s+Y_r)}{Y_s+Y_r+e_y} + \frac{h_m(M_s+M_r)}{M_s+M_r+e_m}\right\} W - \mu_w W,
\end{aligned}\right\} \tag{6.11}$$

subject to the following initial conditions

$$X(0) > 0, Y_i(0) \geq 0, M_i(0) \geq 0, G_i(0) \geq 0, W(0) > 0, \quad \text{for} \quad i = s, r.$$

6.3 Model analysis

6.3.1 Positivity and uniqueness of solutions

The consonance between a formulated epidemiological model and its biological reality is key to its usefulness. Given that all the model parameters and variables are nonnegative, it is only sound that the model solutions be positive at any future time $t \geq 0$ within a given biological space.

Theorem 6.1. *The region $\mathbb{R}^8_+$ with solutions of system (6.11) is positively invariant under the flow induced by system (6.11).*

Proof: We need to show that every trajectory from the region $\mathbb{R}^8_+$ will always remain within it. By contradiction, assume $\exists t^*$ (where t^* refers to time) in the interval $[0,\infty)$, such that $X(t^*)=0$, $X'(t^*)<0$ but for $0<t<t^*$, $X(t)>0$, and $Y_i>0$, $M_i>0$, $G_i>0$, and $W_i>0$ for $i=\{r,s\}$. Notice that at $t=t^*$, $X(t)$ is declining from the original zero value. If such as X exists, then it should satisfy the system (6.11). That is,

$$\begin{aligned}\frac{\mathrm{d}X}{\mathrm{d}t} &= \lambda_x - \mu_x X(t^*) - \frac{\beta X(t^*)}{1+\gamma W(t^*)}(M_s(t^*)+\delta_r M_r(t^*)),\\ &= \lambda_x > 0. \end{aligned} \tag{6.12}$$

This is a contradiction i.e. $X'(t^*)>0$. It shows the nonexistence of such t^*. This argument can be extended to all the remaining seven variables $(Y_s,Y_r,M_s,M_r,G_s,G_r,W)$. The process of verification is however simpler. The steps as presented in Chiyaka et al. (2009) are followed. Let the total erythrocyte population $C(t)$ evolve according to the following formulation:

$$\begin{aligned}\frac{\mathrm{d}C}{\mathrm{d}t} &= \lambda_x - \mu_c C - (\sigma_s Y_s + \sigma_r Y_r) - k_y W\left(\frac{Y_s}{1+aY_s}+\frac{Y_r}{1+aY_r}\right),\\ &\leq \lambda_x - \mu_c C, \end{aligned} \tag{6.13}$$

where $\mu_c = \min\{\mu_x,\mu_{ys},\mu_{yr}\}$. Similarly, the total density of malaria parasites $L(t)$ is described by

$$\frac{\mathrm{d}L}{\mathrm{d}t} \leq P\{(1-\alpha_s)\mu_{ys}Y_s + (1-\alpha_r)\mu_{yr}Y_r\} + \sigma_s Y_s + \sigma_r Y_r - \mu_p L, \tag{6.14}$$

where $\mu_p = \min\{\mu_{ms},\mu_{mr},\mu_{gs},\mu_{gr}\}$.

The solution of the last equation in system (6.11) together with those of equations (6.13) and (6.14) are respectively given as

$$W(t) \leq \frac{\lambda_w}{\mu_w} + \left(W(0) - \frac{\lambda_w}{\mu_w}\right)e^{-\mu_w t}, \quad C(t) \leq \frac{\lambda_x}{\mu_c} + \left(C(0) - \frac{\lambda_x}{\mu_c}\right)e^{-\mu_c t} \tag{6.15}$$

and

$$L(t) \leq \frac{\sigma_s\int_0^t Y_s(t)\Delta_{IF}\mathrm{d}t + \sigma_r\int_0^t Y_r(t)\Delta_{IF}\mathrm{d}t}{\Delta_{IF}} + \left(L(0) - \frac{(\sigma_s+\sigma_r)\mu_p}{P\{(1-\alpha_s)\mu_{ys}+(1-\alpha_r)\mu_{yr}\}}\right)\frac{1}{\Delta_{IF}}, \tag{6.16}$$

where

$$\Delta_{IF} = \exp\left\{-\left(P(1-\alpha_s)\mu_{ys}\int_0^t Y_s(t)\mathrm{d}t + P(1-\alpha_r)\mu_{yr}\int_0^t Y_r(t)\mathrm{d}t\right) - \int_0^t \mu_p \mathrm{d}t\right\}.$$

Here, $C(0) = X(0) + Y_s(0) + Y_r(0)$ and $L(0) = M_s(0) + M_r(0) + G_s(0) + G_r(0)$ represents the initial total populations of erythrocytes and malaria parasites, respectively. It is observed that the solutions of W (in system (6.11)), C (in inequality (6.13)) and P (in inequality (6.14)) remain nonnegative for all future time $t \geq 0$. Moreover, the total populations are bounded: $0 \leq C(t) \leq \max\{C(0), (\lambda_x/\mu_c)\}$, $\quad 0 \leq W(t) \leq \max\{W(0), \lambda_w/\mu_w)\}$ and $L(t) \leq \max\{L(0), (((\sigma_s + \sigma_r)\mu_p)/((P(1-\alpha_s)\mu_{ys} + P(1-\alpha_r)\mu_{yr}))\}$. Thus, all the state variables of system (6.11) and all their corresponding solutions are nonnegative and bounded in the phase space φ, where

$$\begin{aligned}\varphi = \big\{&(X, Y_s, Y_r, M_s, M_r, G_s, G_r, W) \in \mathbb{R}^8_+ : C(t) \leq \max\{C(0), (\lambda_x/\mu_c)\},\\ &W(t) \leq \max\{W(0), \lambda_w/\mu_w)\} \quad \text{and}\\ &L(t) \leq \max\left(L(0), \frac{(\sigma_s + \sigma_r)\mu_p}{P(1-\alpha_s)\mu_{ys} + P(1-\alpha_r)\mu_{yr}}\right)\Big\}. \end{aligned} \tag{6.17}$$

It is obvious that φ is twice continuously differentiable function. That is, $\varphi_i \in \mathbb{C}^2$. This is because its components $\varphi_i, 1 \leq i \leq 8$ are rational functions of state variables that are also continuously differentiable functions. In conclusion, the domain φ is positively invariant. It is therefore feasible and biologically meaningful to study system (6.11).

Theorem 6.2. *The system* (6.11) *has a unique solution*

Proof: Let $\mathbf{x} = (X, Y_s, Y_r, M_s, M_r, G_s, G_r, W)^T \in \mathbb{R}^8_+$, so that $\mathbf{x}_1 = X$ and $\mathbf{x}_2 = Y_s$ as presented in system (6.11). Similarly, let $\mathbf{g}(\mathbf{x}) = (\mathbf{g}_i(\mathbf{x}), i = 1, \cdots, 8)^T$ be a vector defined in $\mathbb{R}^8_+$. The system (6.11) can hence be written as

$$\frac{\mathrm{d}\mathbf{x}}{\mathrm{d}t} = \mathbf{g}(\mathbf{x}), \quad \mathbf{x}(0) = \mathbf{x}_0, \tag{6.18}$$

where $\mathbf{x} : [0, \infty) \to \mathbb{R}^8_+$ denotes a column vector of state variables and $\mathbf{g} : \mathbb{R}^8_+ \to \mathbb{R}^8_+$ represents the right-hand side (RHS) of system (6.11). The result is as follows.

Lemma 6.1. *The function* $\boldsymbol{g}$ *is continuously differentiable in* $\boldsymbol{x}$

Proof: All the terms in $\mathbf{g}$ are either linear polynomials or rational functions of nonvanishing polynomials. Since the state variables $(X, Y_s, Y_r, M_s, M_r, G_s, G_r, W)$ are all continuously differentiable functions of t, it follows that all the elements of vector $\mathbf{g}$ are continuously

differentiable. Moreover, let $V(\mathbf{x},\mathbf{n},\theta) = \{\mathbf{x}+\theta(\mathbf{n}-\mathbf{x}): \quad 0 \leq \theta \leq 1\}$. By mean value theorem,

$$||\mathbf{g}(\mathbf{n}) - \mathbf{g}(\mathbf{x})||_\infty = ||\mathbf{g}'(\mathbf{m},\mathbf{n}-\mathbf{x})||_\infty, \tag{6.19}$$

where $\mathbf{m} \in V(\mathbf{x},\mathbf{n},\theta)$ denotes the mean value point and $\mathbf{g}'$ the directional derivative of the function $\mathbf{g}$ at $\mathbf{m}$. However,

$$\begin{aligned} ||\mathbf{g}'(\mathbf{m},\mathbf{n}-\mathbf{x})||_\infty &= \left\| \sum_{i=1}^{8} (\nabla \mathbf{g}_i(\mathbf{m}).(\mathbf{n}-\mathbf{x}))e_i \right\|_\infty \\ &\leq \left\| \sum_{i=1}^{8} (\nabla \mathbf{g}_i(\mathbf{m}) \right\|_\infty ||\mathbf{n}-\mathbf{x}||_\infty, \end{aligned} \tag{6.20}$$

where e_i is the i^{th} coordinate unit in $\mathbb{R}^8_+$. It is easy to see that all the partial derivatives of $\mathbf{g}$ are bounded and that there exists a nonnegative M, such that

$$\left\| \sum_{i=1}^{8} (\nabla \mathbf{g}_i(\mathbf{m}) \right\|_\infty \leq M \quad \text{for all} \quad \mathbf{m} \in V. \tag{6.21}$$

Therefore, there exists $M > 0$ such that

$$||\mathbf{g}(\mathbf{n}) - \mathbf{g}(\mathbf{x})||_\infty \leq M||\mathbf{n}-\mathbf{x}||_\infty. \tag{6.22}$$

This shows that the function $\mathbf{g}$ is Lipschitz continuous. Since $\mathbf{g}$ is Lipschitz continuous, it follows that system (6.11) has a unique solution by uniqueness theorem of Picard (Hale, 1969).

6.3.2 Stability analysis of the parasite-free equilibrium point (PFE)

The in-host malaria dynamics are investigated by studying the behaviour of the model at the different model equilibrium points. Knowledge of model equilibrium points is useful in establishing parameters that drive the infection to different stability points. System (6.11) has a parasite-free equilibrium point $\mathbb{E}_0$ given by

$$\mathbb{E}_0 = (X^0, Y_s^0, Y_r^0, M_s^0, M_r^0, G_s^0, G_r^0, W^0) = \left(\frac{\lambda_x}{\mu_x}, 0,0,0,0,0,0, \frac{\lambda_w}{\mu_w}\right). \tag{6.23}$$

Using the next generation operator method by Van den Driessche and Watmough (2002) and the matrix notations therein, a nonsingular matrix Q showing the terms of transitions from

one compartment to the other and a nonnegative matrix F of new infection terms is obtained as follows:

$$F = \begin{pmatrix} 0 & 0 & \frac{\beta\lambda_x\mu_w}{(\gamma\lambda_w+\mu_w)\mu_x} & 0 & 0 & 0 \\ 0 & 0 & 0 & \frac{\delta_r\beta\lambda_x\mu_w}{(\gamma\lambda_w+\mu_w)\mu_x} & 0 & 0 \\ 0 & 0 & 0 & 0 & 0 & 0 \\ 0 & 0 & 0 & 0 & 0 & 0 \\ 0 & 0 & 0 & 0 & 0 & 0 \\ 0 & 0 & 0 & 0 & 0 & 0 \end{pmatrix} \tag{6.24}$$

and

$$Q = \begin{pmatrix} v_1 & 0 & 0 & 0 & 0 & 0 \\ 0 & v_2 & 0 & 0 & 0 & 0 \\ -P(1-\alpha_s)\mu_{ys} & 0 & v_3 & 0 & 0 & 0 \\ 0 & -P(1-\alpha_r)\mu_{yr} & -\Psi_1 & v_4 & 0 & 0 \\ -\sigma_s & 0 & 0 & 0 & v_5 & 0 \\ 0 & -\sigma_r & 0 & 0 & -\Psi_2 & v_6 \end{pmatrix}, \tag{6.25}$$

where $v_1 = ((k_y\lambda_w/\mu_w) + \sigma_s + \mu_{ys}/(1-\omega_s))$, $v_2 = ((k_y\lambda_w/\mu_w) + \sigma_r + \mu_{yr})$, $v_3 = (\zeta + \mu_{ms} + \Psi_1 + (k_m\lambda_w/\mu_w) + (\beta\lambda_x\mu_w/(\gamma\lambda_w+\mu_w)\mu_x))$ $v_4 = (\mu_{mr} + (k_m\lambda_w/\mu_w) + (\delta_r\beta\lambda_x\mu_w/(\gamma\lambda_w+\mu_w)\mu_x)$, $v_5 = (\eta + \mu_{gs} + (k_g\lambda_w/\mu_w) + \Psi_2)$ and $v_6 = (\mu_{gr} + (k_g\lambda_w/\mu_w))$.

The effective reproduction number R_E associated with the parasite-free equilibrium is the spectral radius of the next generation matrix FQ^{-1}, where

$$Q^{-1} = \begin{pmatrix} \frac{1}{v_1} & 0 & 0 & 0 & 0 & 0 \\ 0 & \frac{1}{v_2} & 0 & 0 & 0 & 0 \\ \frac{P(1-\alpha_s)\mu_{ys}}{v_1v_3} & 0 & \frac{1}{v_3} & 0 & 0 & 0 \\ \frac{P(1-\alpha_s)\mu_{ys}\Psi_1}{v_1v_3v_4} & \frac{P(1-\alpha_r)\mu_{yr}}{v_2v_4} & 0 & \frac{1}{v_4} & 0 & 0 \\ \sigma_s/v_1v_5 & 0 & 0 & 0 & \frac{1}{v_5} & 0 \\ \sigma_s\Psi_2/v_1v_5v_6 & \frac{\sigma_r}{v_2v_6} & 0 & 0 & \Psi_2/v_5v_6 & \frac{1}{v_6} \end{pmatrix}. \tag{6.26}$$

It follows that

$$R_E = \rho(FQ^{-1}) = \max\{R_s, R_r\}, \tag{6.27}$$

where

$$R_s = \frac{P(1-\alpha_s)\mu_{ys}\beta\lambda_x\mu_w}{\left(\frac{k_y\lambda_w}{\mu_w} + \sigma_s + \frac{\mu_{ys}}{1-\omega_s}\right)\left(\zeta + \mu_{ms} + \frac{k_m\lambda_w}{\mu_w} + \Psi_1 + \frac{\beta\lambda_x\mu_x}{(\gamma\lambda_w+\mu_w)\mu_x}\right)(\gamma\lambda_w+\mu_w)\mu_x} \tag{6.28}$$

and

$$R_r = \frac{P(1-\alpha_r)\mu_{yr}\delta_r\beta\lambda_x\mu_w}{\left(\frac{k_y\lambda_w}{\mu_w}+\sigma_r+\mu_{yr}\right)\left(\mu_{mr}+\frac{k_m\lambda_w}{\mu_w}+\frac{\delta_r\beta\lambda_x\mu_w}{(\gamma\lambda_w+\mu_w)\mu_x}\right)(\gamma\lambda_w+\mu_w)\mu_x}. \tag{6.29}$$

From equation (6.27), it is evident that in a multiple-strain *P. falciparum* malaria infection, the progression of the disease depends on the effective reproduction numbers of the different parasite strain. If the threshold quantity $R_s > R_r$, the drug-sensitive parasite strain will dominate the drug-resistant strain. To manage the infection in this case, the patient should be given antimalarials that can eradicate the drug-sensitive parasites. Conversely, if $R_r > R_s$, the infection is mainly driven by the drug-resistant parasite strain. In this scenario, the used antimalarial drugs should be highly efficacious and effective enough to kill both the drug-resistant strain and the drug-sensitive parasite strain in the blood of the human host. This result is quite instrumental in improving antimalarial therapy for *P. falciparum* infections. The best antimalarials should be sufficient enough to eradicate both drug-sensitive and drug-resistant parasite strain within the human host.

The following lemma is based on Theorem 2 in Vannice et al. (2012).

Lemma 6.2. *The parasite-free equilibrium point $\mathbb{E}_0$ is locally asymptotically stable if $R_E < 1$ ($R_s < 1$ and $R_r < 1$) and unstable otherwise.*

The Jacobian matrix associated with system (6.11) at $\mathbb{E}_0$ is given by

$$J_{\mathbb{E}_0} = \begin{pmatrix} -\mu_x & 0 & 0 & \frac{-\beta\lambda_x\mu_w}{(\gamma\lambda_w+\mu_w)\mu_x} & \frac{-\delta_r\beta\lambda_x\mu_w}{(\gamma\lambda_w+\mu_w)\mu_x} & 0 & 0 & 0 \\ 0 & -v_1 & 0 & \frac{\beta\lambda_x\mu_w}{(\gamma\lambda_w+\mu_w)\mu_x} & 0 & 0 & 0 & 0 \\ 0 & 0 & -v_2 & 0 & \frac{\beta\lambda_x\mu_w}{(\gamma\lambda_w+\mu_w)\mu_x} & 0 & 0 & 0 \\ 0 & P(1-\alpha_s)\mu_{ys} & 0 & -v_3 & 0 & 0 & 0 & 0 \\ 0 & 0 & P(1-\alpha_r)\mu_{yr} & \Psi_1 & -v_4 & 0 & 0 & 0 \\ 0 & \sigma_s & 0 & 0 & 0 & -v_5 & 0 & 0 \\ 0 & 0 & \sigma_r & 0 & 0 & \Psi_2 & -v_6 & 0 \\ 0 & \frac{h_y\lambda_w}{e_y\mu_w} & \frac{h_y\lambda_w}{e_y\mu_w} & \frac{h_m\lambda_w}{e_m\mu_w} & \frac{h_m\lambda_w}{e_m\mu_w} & \frac{h_g\lambda_w}{e_g\mu_w} & \frac{h_g\lambda_w}{e_g\mu_w} & -\mu_w \end{pmatrix}, \tag{6.30}$$

where the terms $v_1, \cdots v_6$ are as defined in matrix (6.25). It is clear from matrix (6.30) that the first four eigenvalues are $-\mu_x$ (from column 1), $-\mu_w$ (from column 8), $-(\mu_{gr}+\frac{k_g\lambda_w}{\mu_w}) = -v_6$ (from column 7), $-(\eta+\mu_{gs}+\frac{k_g\lambda_w}{\mu_w}) = -v_5$ (from column 6). They are all negative. The remaining four eigenvalues are obtained from the roots of the following quartic equation:

$$P(\lambda) = \lambda^4 + p_1\lambda^3 + p_2\lambda^2 + p_3\lambda + p_4, \tag{6.31}$$

where

$$p_1 = (v_1 + v_2 + v_3 + v_4) > 0, \tag{6.32}$$

$$p_2 = v_3v_4 + v_2(v_3 + v_4) + v_1(v_2 + v_3 + v_4) - \frac{P\beta\lambda_x\mu_w}{(\gamma\lambda_w + \mu_w)\mu_x}((1-\alpha_s)\mu_{\text{ys}} - (1-\alpha_r)\mu_{\text{yr}}\delta_r), \tag{6.33}$$

$$p_3 = \frac{1}{K}[v_3(v_2v_4K - P(1-\alpha_r)\mu_{yr}\delta_r\beta\lambda_x\mu_w)] - \frac{1}{K}[P(1-\alpha_s)\mu_{ys}\beta\lambda_x\mu_w(v_2+v_4) + \frac{v_1}{K}[(v_3v_4) + v_2(v_3+v_4)]K - P(1-\alpha_r)\mu_{yr}\delta_r\beta\lambda_x\mu_w)] \quad \text{and} \tag{6.34}$$

$$p_4 = \frac{(v_2v_4K - P(1-\alpha_r)\mu_{\text{yr}}\delta_r\beta\lambda_x\mu_w)(v_1v_3K - P(1-\alpha_s)\mu_{\text{ys}}\beta\lambda_x\mu_w)}{K}. \tag{6.35}$$

Due to complexity in the coefficients of the characteristic (6.31), the Routh-Hurwitz stability criterion (Allen, 2007) provides sufficient condition for the existence of the roots of the given polynomial on the left half of the plane.

Definition 6.1. *The solutions of the characteristic equation* (6.31) *are negative or have negative real parts provided that the determinants of all Hurwitz matrices are positive (Allen, 2007).*

Based on the Routh-Hurwitz criterion, the system of inequalities that describe stability region $\mathbb{E}_0$ is presented as follows:

(i) $p_1 > 0$, (ii) $p_3 > 0$, (iii) $p_4 > 0$, and (iv) $p_1p_2p_3 > p_3^2 + p_1^2p_4$.

From equation (6.32), it is clear that $p_1 > 0$. Upon simplifying p_2 in equation (6.33), then

$$p_2 = v_3v_4 + v_2v_3 + v_1v_2 + v_1v_4 + \left(v_1v_3 + \frac{\lambda_x\mu_w\beta B_1}{K}\right) + \left(v_2v_4 + \frac{\lambda_x\mu_w\delta_r\beta B_2}{K}\right), \tag{6.36}$$

where $B_1 = -P(1-\alpha_s)\mu_{ys}$ and $B_2 = -P(1-\alpha_r)\mu_{yr}$.Thus,

$$p_2 = v_3v_4 + v_2v_3 + v_1v_2 + v_1v_4 + v_1v_3\left[1 - \frac{B_1\beta\lambda_x\mu_w}{v_1v_3K}\right] + v_2v_4\left[1 - \frac{B_2\delta_r\beta\lambda_x\mu_w}{v_2v_4K}\right] \tag{6.37}$$

$$= (v_1+v_3)(v_2+v_4) + v_1v_3[1-R_s] + v_2v_4[1-R_r] > 0 \quad \text{if and only if} \quad R_s, R_r < 1.$$

Similarly, the expression for p_4 in equation (6.35) can be rewritten as follows:

$$\begin{aligned} p_4 &= \left[v_1v_3 + \frac{B_1\beta\lambda_x\mu_x}{K}\right]\left[v_2v_4 + \frac{B_2\delta_r\beta\lambda_x\mu_w}{K}\right] \\ &= v_1v_3\left[1 + \frac{B_1\beta\lambda_x\mu_w}{v_1v_3K}\right]v_2v_4\left[1 + \frac{B_2\delta_r\beta\lambda_x\mu_w}{v_2v_4K}\right] \\ &= v_1v_3[1-R_s]v_2v_4[1-R_r] > 0 \quad \text{if and only if} \quad R_s, R_r < 1. \end{aligned} \tag{6.38}$$

Simplifying equation (6.34) gives

$$\begin{aligned} p_3 &= v_2v_3v_4 + v_1v_3v_4 + v_1v_2(v_3+v_4) + \frac{\beta B_1\lambda_x\mu_w(v_2+v_4)}{K} + \frac{\delta_r\beta B_2\lambda_x\mu_w(v_1+v_3)}{K}, \\ &= v_1v_2v_3v_4\left[\frac{1}{v_4}\left(1 + \frac{\beta B_1\lambda_x\mu_w}{v_1v_3K}\right) + \frac{1}{v_2}\left(1 + \frac{\beta B_1\lambda_x\mu_w}{v_1v_3K}\right) + \frac{1}{v_1}\left(1 + \frac{\delta_r\beta B_2\lambda_x\mu_w}{v_2v_4K}\right)\right. \\ &\left. + \frac{1}{v_3}\left(1 + \frac{\delta_r\beta B_2\lambda_x\mu_w}{v_2v_4K}\right)\right] \\ &= v_1v_2v_3v_4\left[\frac{v_2+v_4}{v_2v_4}(1-R_s) + \frac{v_1+v_3}{v_1v_3}(1-R_r)\right] \\ &= v_1v_3(v_2+v_4)[1-R_s] + v_2v_4(v_1+v_3)[1-R_r] > 0, \text{ if and only if } R_s, R_r < 1. \end{aligned} \tag{6.39}$$

Since all the coefficients of the characteristic equation (6.31) are nonnegative, all its roots are therefore negative or have negative real parts. Hence, the Jacobian matrix (6.30) has negative eigenvalues or eigenvalues with negative real parts if and only if the effective reproduction number R_E is less than unity. The equilibrium point $\mathbb{E}_0$ is therefore locally asymptotically stable when $R_E < 1$ (when both $R_s < 1$ and $R_r < 1$). This implies that an effective antimalarial drug would cure the co-strain infected human host, provided that the drug reduces the effective reproduction number to less than 1.

Lemma 6.2 shows that *P. falciparum* malaria can be eradicated/controlled within the human host if the initial parasite and cell populations are within the basin of attraction of the trivial equilibrium point $\mathbb{E}_0$. To be certain to eliminate the infection irrespective of the initial parasite and cell populations, it is necessary to prove the global stability of the parasite-free equilibrium point. This is presented in the following subsection.

6.3.3 Global asymptotic stability analysis of the PFE point

Following the work by Kamgang and Sallet (2005), the system (6.11) is rewritten in pseudo-triangular form:

$$\left.\begin{aligned}\dot{X}_1 &= D_1(X)(X - X_1^*) + D_2(X)X_2\\ \dot{X}_2 &= D_3(X)X_2,\end{aligned}\right\} \tag{6.40}$$

where X_1 is a vector representing the densities of noninfective population groups (unparasitised erythrocytes and immune cells) and X_2 represents the densities of infected/infective groups (infective *P. falciparum* parasites and/or infected host cells) that are responsible for disease transmission. For purposes of clarity, $(X_1, 0)$ is represented with X_1 and $(0, X_2)$ with X_2 in $\mathbb{R}_+^8 \times \mathbb{R}_+^8$. Assume the existence of a parasite-free equilibrium in $\varphi : X^* = (X_1^*, 0)$.

Thus,

$$X = (X_1, X_2), \quad X_1 = (X, W), \quad X_2 = (Y_s, Y_r, M_s, M_r, G_s, G_r), \tag{6.41}$$

$$X_1^* = \left(\frac{\lambda_x}{\mu_x}, \frac{\lambda_w}{\mu_w}\right). \tag{6.42}$$

System (6.40) is analysed based on the assumption that it is positively invariant and dissipative in φ. Moreover, the subsystem X_1 is globally asymptotically stable at X_1^* on the projection of φ on $\mathbb{R}_+^8$. This implies that whenever there are no infective malaria parasites, all cell populations will settle at the parasite-free equilibrium point $\mathbb{E}_0$. Finally, D_2 in system (6.40) is a Metzler matrix that is irreducible for any $X \in \varphi$. It is assumed that adequate interactions between and among different parasites and cell compartments exist in the model.

The matrices $D_1(X)$ and $D_2(X)$ are easily computed from subsystem $\dot{X}_1$ in system (6.40) so that we have

$$D_1(X) = \begin{pmatrix} -\mu_x & 0 \\ 0 & -\mu_w \end{pmatrix} \quad \text{and} \tag{6.43}$$

$$D_2(X) = \begin{pmatrix} 0 & 0 & \frac{-\beta\lambda_x\mu_w}{(\gamma\lambda_w+\mu_w)\mu_x} & \frac{-\delta_r\beta\lambda_x\mu_w}{(\gamma\lambda_w+\mu_w)\mu_x} & 0 & 0 \\ \frac{h_y\lambda_w}{e_y\mu_w} & \frac{h_y\lambda_w}{e_y\mu_w} & \frac{h_m\lambda_w}{e_m\mu_w} & \frac{h_m\lambda_w}{e_m\mu_w} & \frac{h_g\lambda_w}{e_g\mu_w} & \frac{h_g\lambda_w}{e_g\mu_w} \end{pmatrix}. \tag{6.44}$$

It is easily seen that the eigenvalues of matrix D_1 are both real and negative ($-\mu_x < 0$, $-\mu_w < 0$). This shows that the subsystem $\dot{X}_1 = D_1(X)(X - X_1^*) + D_2(X)X_2$ is globally asymptotically stable at the trivial equilibrium X_1^*. Additionally, from subsystem $\dot{X}_2 =$

$D_3(X)X_2$, the following matrix is obtained.

$$D_3(X) = \begin{pmatrix} -v_1 & 0 & \frac{\beta\lambda_x\mu_w}{(\gamma\lambda_w+\mu_w)\mu_x} & 0 & 0 & 0 \\ 0 & -v_2 & 0 & \frac{\beta\lambda_x\mu_w}{(\gamma\lambda_w+\mu_w)\mu_x} & 0 & 0 \\ P(1-\alpha_s)\mu_{ys} & 0 & -v_3 & 0 & 0 & 0 \\ 0 & P(1-\alpha_r)\mu_{yr} & \Psi_1 & -v_4 & 0 & 0 \\ \sigma_s & 0 & 0 & 0 & -v_5 & 0 \\ 0 & \sigma_r & 0 & 0 & \Psi_2 & -v_6 \end{pmatrix}. \quad (6.45)$$

Notice that all the off-diagonal entries of $D_3(X)$ are nonnegative (equal to or greater than zero), showing that $D_3(X)$ is a Metzler matrix. To show the global stability of the parasite-free equilibrium $\mathbb{E}_0$, it is necessary to show that the square matrix $D_3(X)$ in (6.45) is a Metzler stable. We therefore need to prove the following lemma.

Lemma 6.3. *Let K be a square Metzler matrix that is block decomposed:*

$$K = \begin{pmatrix} K_{11} & K_{12} \\ K_{21} & K_{22} \end{pmatrix}, \quad (6.46)$$

where K_{11} and K_{22} are square matrices. The matrix K is Metzler stable if and only if K_{11} and $K_{22} - K_{21}K_{11}^{-1}K_{12}$ are Metzler stable.

Proof:

The matrix K in Lemma 6.3 refers to D_3 in this case. Let

$$K_{11} = \begin{pmatrix} -v_1 & 0 & \frac{\beta\lambda_x\mu_w}{(\gamma\lambda_w+\mu_w)\mu_x} \\ 0 & -v_2 & 0 \\ P(1-\alpha_s)\mu_{ys} & 0 & -v_3 \end{pmatrix}, \quad K_{12} = \begin{pmatrix} 0 & 0 & 0 \\ \frac{\beta\lambda_x\mu_w}{(\gamma\lambda_w+\mu_w)\mu_x} & 0 & 0 \\ 0 & 0 & 0 \end{pmatrix}, \quad (6.47)$$

$$K_{21} = \begin{pmatrix} 0 & P(1-\alpha_r)\mu_{yr} & \Psi_1 \\ \sigma_s & 0 & 0 \\ 0 & \sigma_r & 0 \end{pmatrix}, \quad K_{22} = \begin{pmatrix} -v_4 & 0 & 0 \\ 0 & -v_5 & 0 \\ 0 & \Psi_2 & -v_6 \end{pmatrix}. \quad (6.48)$$

Results from analytical computations based on Mathematica software give

$$K_{11}^{-1} = \begin{pmatrix} \frac{-v_3(\gamma\lambda_w+\mu_w)\mu_x}{(\gamma\lambda_w+\mu_w)\mu_x v_1 v_3+P\beta(\alpha_s-1)\lambda_x\mu_w\mu_{ys}} & 0 & -\frac{\beta\lambda_x\mu_w}{v_1 v_3(\gamma\lambda_w+\mu_w)\mu_x+P\beta(\alpha_s-1)\lambda_x\mu_w\mu_{ys}} \\ 0 & -\frac{1}{v_2} & 0 \\ \frac{P(\alpha_s-1)(\gamma\lambda_w+\mu_w)\mu_x\mu_{ys}}{v_1 v_3(\gamma\lambda_w+\mu_w)\mu_x+P\beta(\alpha_s-1)\lambda_x\mu_w\mu_{ys}} & 0 & \frac{-v_1(\gamma\lambda_w+\mu_w)\mu_x}{(\gamma\lambda_w+\mu_w)\mu_x v_1 v_3+P\beta(\alpha_s-1)\lambda_x\mu_w\mu_{ys}} \end{pmatrix} \quad (6.49)$$

and

$$K_{22}-K_{21}K_{11}^{-1}K_{12}=\begin{pmatrix}-v_4 & 0 & 0\\ 0 & -v_5 & 0\\ 0 & \Psi_2 & -v_6\end{pmatrix}, \tag{6.50}$$

where $v_4=(\mu_{mr}+(k_m\lambda_w/\mu_w)+(\delta_r\beta\lambda_x\mu_w/(\gamma\lambda_w+\mu_w)\mu_x))$, $v_5=(\eta+\mu_{gs}+k_g\lambda_w/\mu_w+\Psi_2)$ and $v_6=(\mu_{gr}+k_g\lambda_w/\mu_w)$.

From equation (6.50), it is evident that all the diagonal elements of matrix $K_{22}-K_{21}K_{11}^{-1}K_{12}$ are negative and the rest of the elements in the matrix are nonnegative. This shows that matrix $K_{22}-K_{21}K_{11}^{-1}K_{12}$ is Metzler stable, and the parasite-free equilibrium point $\mathbb{E}_0$ is globally asymptotically stable in the biologically feasible region φ of system (6.11). Epidemiologically, the above result implies that when there is no malaria infection, the different cell populations under consideration will stabilise at the parasite-free equilibrium. However, if there exists a *P. falciparum* infection, then an appropriate control in form of effective antimalarial drugs would be necessary to clear the parasites from the human blood and restore the system to the stable parasite-free equilibrium state.

6.3.4 Coexistence parasite-persistant equilibrium point

The existence of a nontrivial equilibrium point represents a scenario in which the *P. falciparum* parasites are present within the host and the following conditions hold: $X^*>0, Y_s^*\geq 0, Y_r^*\geq 0, M_s^*\geq 0, M_r^*\geq 0, G_s^*\geq 0, G_r^*\geq 0, W^*>0$. Equating the right-hand side of system (6.11) to zero and solving for the state variables gives the parasite-persistent equilibrium point $\mathbb{E}_1=(X^*,Y_s^*,Y_r^*,M_s^*,M_r^*,G_s^*,G_r^*,W^*)$, where

$$X^*=\frac{(1+\gamma W^*)\lambda_x}{\beta(M_s^*+\delta_r M_r^*)+(1+\gamma W^*)\mu_x},\quad Y_s^*=\frac{\bar{b}+\sqrt{\bar{b}^2-4\bar{a}\bar{c}}}{-2\bar{a}},$$

$$Y_r^*=\frac{\underline{b}+\sqrt{\underline{b}^2-4\underline{a}\underline{c}}}{-2\underline{a}} \tag{6.51}$$

$$\bar{a} = -a\left((1-\omega_s)\sigma_s + \mu_{\text{ys}}\right)\left(\beta M_s^* + \beta M_r^* \delta_r + (\gamma W^* + 1)\mu_x\right) < 0, \tag{6.52}$$

$$\begin{aligned}\bar{b} = &-\beta M_s^*\left(-a(1-\omega_s)\lambda_x - \omega_s\sigma_s + \sigma_s + \mu_{\text{ys}}\right) - W^*(1-\omega_s)k_y\left(\beta M_s^* + \beta M_r^*\delta_r\right.\\ &\left.+\gamma W^*\mu_x + \mu_x\right) + \left((1-\omega_s)\sigma_s + \mu_{\text{ys}}\right)\left(-\left(\beta M_r^*\delta_r + (\gamma W^*+1)\mu_x\right)\right),\end{aligned} \tag{6.53}$$

$$\bar{c} = \beta M_s^*(1-\omega_s)\lambda_x > 0, \tag{6.54}$$

$$\underline{a} = -a\left(\sigma_2 + \mu_{\text{yr}}\right)\left(\beta M_s^* + \beta M_r^*\delta_r + (\gamma W^*+1)\mu_x\right) < 0, \tag{6.55}$$

$$\begin{aligned}\underline{b} = &\beta M_r^*\delta_r\left(a\lambda_x - \sigma_2 - \mu_{\text{yr}}\right) - W^* k_y\left(\beta M_s^* + \beta M_r^*\delta_r + \gamma W^*\mu_x + \mu_x\right)\\ &-\left(\sigma_2 + \mu_{\text{yr}}\right)\left(\beta M_s^* + \gamma W^*\mu_x + \mu_x\right),\end{aligned} \tag{6.56}$$

$$\underline{c} = \beta M_r^*\delta_r\lambda_x > 0. \tag{6.57}$$

$$G_s^* = \frac{b_1 + \sqrt{b_1^2 - 4a_1c_1}}{-2a_1} \quad \text{and} \quad G_r^* = \frac{b_2 + \sqrt{b_2^2 - 4a_2c_2}}{-2a_2} \quad \text{where} \tag{6.58}$$

$$\begin{aligned}a_1 = &-a\left(\eta + \mu_{\text{g1}} + \Psi_2\right) < 0, \quad b_1 = a\sigma_1 Y_s^* - W^* k_g - \eta - \mu_{\text{g1}} - \Psi_2\\ &\text{and} \quad c_1 = \sigma_1 Y_s^* > 0.\end{aligned} \tag{6.59}$$

$$\begin{aligned}a_2 = &-a\mu_{\text{g2}} < 0, \quad b_2 = aG_1\Psi_2 + a\sigma_2 Y_r^* - W^* k_g - \mu_{\text{g2}}\\ &\text{and} \quad c_2 = G_1\Psi_2 + \sigma_2 Y_r^* > 0.\end{aligned} \tag{6.60}$$

$$M_s^* = \frac{b_3 + \sqrt{b_3^2 - 4a_3c_3}}{-2a_3} \quad \text{and} \quad M_r^* = \frac{b_4 + \sqrt{b_4^2 - 4a_4c_4}}{-2a_4} \quad \text{where} \tag{6.61}$$

$$\begin{aligned}a_3 = &-\left(a\beta M_r^*\delta_r(\zeta + \mu_{\text{ms}} + \Psi_1) + a\gamma W^*\mu_{\text{ms}}\mu_x + a\mu_{\text{ms}}\mu_x + a\beta P(1-\alpha_s)\mu_{\text{ys}}Y_s^*\right.\\ &+\Psi_1\left(a(\gamma W^*+1)\mu_x + \beta\right) + a\gamma\zeta W^*\mu_x + a\beta\lambda_x + a\zeta\mu_x + \beta\zeta\\ &\left.+\beta W^* k_m + \beta\mu_{\text{ms}}\right) < 0,\end{aligned} \tag{6.62}$$

$$\begin{aligned}b_3 = &-\beta M_r^*\delta_r\left(a(\alpha_s - 1)PY_s^*\mu_{\text{ys}} + \zeta + W^* k_m + \mu_{\text{ms}} + \Psi_1\right) - (\alpha_s - 1)\beta PY_s^*\mu_{\text{ys}}\\ &-\beta\lambda_x - (\gamma W^*+1)\mu_x\left(a(\alpha_s - 1)PY_s^*\mu_{\text{ys}} + \zeta + W^* k_m + \mu_{\text{ms}} + \Psi_1\right),\end{aligned} \tag{6.63}$$

$$c_3 = P(1-\alpha_s)Y_s^*\mu_{\text{ys}}\left(\beta M_r^*\delta_r + (\gamma W^*+1)\mu_x\right) > 0, \tag{6.64}$$

$$\begin{aligned} a_4 =& -\left(a\beta M_s^*\left(\Psi_1\delta_r+\mu_{\text{mr}}\right)+\mu_{\text{mr}}\left(a(\gamma W^*+1)\mu_x+\beta\delta_r\right)+a\left(1-\alpha_r\right)\beta PY_2\delta_r\mu_{\text{y2}}\right.\\ &\left.+\beta W^* k_m\delta_r\right) < 0, \end{aligned} \tag{6.65}$$

$$\begin{aligned} b_4 =& M_s^*\left(-\beta\left(a\delta_r\lambda_x+\mu_{\text{mr}}\right)+a\left(1-\alpha_r\right)\beta PY_2\mu_{\text{y2}}+\Psi_1\left(a(\gamma W^*+1)\mu_x+\beta\delta_r\right)\right)\\ &+\left(1-\alpha_r\right)PY_2\mu_{\text{y2}}\left(a(\gamma W^*+1)\mu_x+\beta\delta_r\right)-W^*k_m\left(\beta M_s^*+(\gamma W^*+1)\mu_x\right)\\ &-\mu_{\text{mr}}(\gamma W^*+1)\mu_x+a\beta M_s^{*2}\Psi_1, \end{aligned} \tag{6.66}$$

$$\begin{aligned} c_4 =& \beta M_s^{*2}\Psi_1+M_s^*\left((1-\alpha_r)\beta PY_2\mu_{\text{y2}}+\beta\delta_r\lambda_x+\Psi_1(\gamma W^*+1)\mu_x\right)\\ &+\left(1-\alpha_r\right)PY_2(\gamma W^*+1)\mu_x\mu_{\text{y2}} > 0. \end{aligned} \tag{6.67}$$

and

$$W^* = \frac{\triangle_0}{\mu_w\triangle_0-\left(h_g(G_s^*+G_r^*)+h_m(M_s^*+M_r^*)+h_y(Y_s^*+Y_r^*)\right)} \tag{6.68}$$

where $\triangle_0 = (e_g+G_s^*+G_r^*)(e_m+M_s^*+M_r^*)(e_y+Y_s^*+Y_r^*)$.

Using Descartes' "Rule of Signs" (Wang, 2004), it is evident that irrespective of the sign of $\bar{b}$ in (6.53), $\underline{b}$ in (6.56), b_1 in (6.59), b_2 in (6.60), b_3 in (6.63) and b_4 in (6.66), the state variables Y_s^*, Y_r^*, M_s^*, M_r^*, G_s^* and G_r^* can only have one real positive root. This shows that the model (6.11) has a unique parasite-persistent equilibrium point $\mathbb{E}_1$.

6.3.5 Stability of the coexistence parasite-persistent equilibrium point

Here, we shall prove that the coexistence parasite-persistent equilibrium $\mathbb{E}_1$ is local asymptotically stable when $R_E > 1$ (or when $R_s > 1$ and $R_r > 1$). The methodology followed is by Esteva and Vargas (2000) and is based on Krasnoselskii technique (Krasnoselskii, 1964). This methodology requires to prove that the linearisation of system (6.11) about the coexistence parasite-persistent equilibrium, does not have a solution of the form

$$\bar{S}(t) = \bar{S}_0 e^{\xi t}, \tag{6.69}$$

where $\bar{S}_0 = (S_1, S_2, \cdots, S_7)$, $(S_i, \xi) \in \mathbb{C}$ and the real part of ξ is nonnegative, $(\text{Re}(\xi) \geq 0)$. Note that $\mathbb{C}$ is the set of complex numbers.

Substituting a solution of the form of equation (6.69) into the linearised system (6.11) about the coexistence parasite-persistent equilibrium $\mathbb{E}_1$ gives

$$\left.\begin{aligned}
\xi S_1 =& -\left(\frac{\beta M_s}{1+\gamma W}+\frac{k_y W}{1+\gamma W}+\frac{\mu_{ys}}{1-\omega_s}+\sigma_s\right)S_1-\frac{\beta M_s}{1+\gamma W}S_2+\frac{\beta(C^*-Y_s-Y_r)}{1+\gamma W}S_3,\\
\xi S_2 =& -\frac{\delta_r\beta M_r}{1+\gamma W}S_1-\left(\frac{\delta_r\beta M_r}{1+\gamma W}+\frac{k_y W}{1+aY_r}+\mu_{yr}+\sigma_r\right)S_2+\frac{\delta_r\beta(C^*-Y_s-Y_r)}{1+\gamma W}S_4,\\
\xi S_3 =& -\left(\frac{\beta M_s}{1+\gamma W}+P(1-\alpha_s)\mu_{ys}\right)S_1+\frac{\beta M_s}{1+\gamma W}S_2\\
&-\left(\frac{k_m W}{1+aM_s}+\frac{\beta(C^*-Y_s-Y_r)}{1+\gamma W}+k_1\right)S_3,\\
\xi S_4 =& \Psi_1 S_3+\left(\frac{\delta_r\beta M_r}{1+\gamma W}+P(1-\alpha_r)\mu_{yr}\right)S_2+\frac{\delta_r\beta M_r}{1+\gamma W}S_1\\
&-\left(\frac{\delta_r\beta(C^*-Y_s-Y_r)}{1+\gamma W}+\frac{k_m W}{1+aM_r}+\mu_{mr}\right)S_4,\\
\xi S_5 =& \sigma_s S_1-\left(\frac{k_g W}{1+aG_s}+k_2\right)S_5,\\
\xi S_6 =& \sigma_r S_2+\Psi_2 S_4-\left(\frac{k_g W}{1+aG_r}+\mu_{gr}\right)S_5,\\
\xi S_7 =& \lambda+\left(\frac{h_g(G_s+G_r)}{G_s+G_r+e_g}+\frac{h_y(Y_s+Y_r)}{Y_s+Y_r+e_y}+\frac{h_m(M_s+M_r)}{M_s+M_r+e_m}\right)S_7-\mu_w S_7,
\end{aligned}\right\} \tag{6.70}$$

where $(C^*-Y_s-Y_r)=X$, $k_1=(\Psi_1+\mu_{ms}+\zeta)$ and $k_2=(\Psi_2+\mu_{gs}+\eta)$.

Simplifying the equations in (6.70) gives

$$\begin{aligned}
&\left[1+\frac{(1+\gamma W)(1+aY_s)(1-\omega_s)}{\Delta_1}\xi\right]S_1=\frac{\Delta_5}{\Delta_1}\left(-\frac{\beta M_s}{1+\gamma W}S_2+\frac{\beta(C^*-Y_s-Y_r)}{1+\gamma W}S_3\right),\\
&\left[1+\frac{\xi(1+\gamma W)(1+aY_r)}{\Delta_2}\right]S_2=\frac{\Delta_6}{\Delta_2}\left(-\frac{\delta_r\beta M_r}{1+\gamma W}S_1+\frac{\delta_r\beta(C^*-Y_s-Y_r)}{1+\gamma W}S_4\right),\\
&\left[1+\frac{(1+\gamma W)(1+aM_s)}{\Delta_3}\xi\right]S_3=\frac{\Delta_7}{\Delta_3}\left(\frac{\beta M_s}{1+\gamma W}+P(1-\alpha_s)\mu_{ys}S_1+\frac{\beta M_s}{1+\gamma W}S_2\right),\\
&\left[1+\frac{\xi(1+\gamma W)(1+aM_r)}{\Delta_4}\right]S_4=\frac{\Delta_8}{\Delta_4}\left(\Psi_1 S_3+\left(\frac{\delta_r\beta M_r}{1+\gamma W}+P(1-\alpha_r)\mu_{yr}\right)S_2+\frac{\delta_r\beta M_r}{1+\gamma W}S_4\right),\\
&\left[1+\frac{(1+aG_s)}{k_g W+k_2}\xi\right]S_5=\frac{\sigma_s(1+aG_s)}{k_g W+k_2}S_1,\\
&\left[1+\frac{(1+aG_r)}{k_g W+\mu_{gr}}\xi\right]S_6=\frac{(1+aG_r)}{k_g W+\mu_{gr}}\left\{\sigma_r S_2+\Psi_2 S_4\right\},\\
&\left[1+\frac{1}{\mu_w}\xi\right]S_7=\frac{\lambda_w}{\mu_w}+\frac{W}{\mu_w}\left(\frac{h_g(S_5+S_6)}{G_s+G_r+e_g}+\frac{h_y(S_1+S_2)}{Y_s+Y_r+e_y}+\frac{h_m(S_3+S_4)}{M_s+M_r+e_m}\right),
\end{aligned} \tag{6.71}$$

where

$$\begin{aligned}
\Delta_1 =&\beta M_s(1+aY_s)(1-\omega_s)+k_yW(1-\omega_s)(1+\gamma W)+\mu_{ys}(1+aY_s)(1+\gamma W)\\
&+\sigma_s(1+aY_s)(1-\omega_s)(1+\gamma W), \quad \Delta_6=(1+\gamma W)(1+aY_r),\\
\Delta_2 =&\delta_r\beta M_r(1+aY_r)+k_yW(1+\gamma W)+(\mu_{yr}+\sigma_r)(1+aY_r)(1+\gamma W),\\
\Delta_3 =&(1+aM_s)(\beta(C^*-Y_s-Y_r))+k_mW(1+\gamma W)+k_1(1+aM_s)(1+\gamma W),\\
\Delta_4 =&(1+aM_r)(\delta_r\beta(C^*-Y_s-Y_r))+k_mW(1+\gamma W)+\mu_{mr}(1+aM_r)(1+\gamma W),\\
\Delta_5 =&(1+\gamma W)(1+aY_s)(1-\omega_s), \quad \Delta_7=(1+\gamma W)(1+aM_s),\\
\Delta_8 =&(1+\gamma W)(1+aM_r).
\end{aligned} \tag{6.72}$$

Separating the negative terms gives the following system:

$$[1+F_j(\xi)]S_j=(\mathscr{H}\bar{S})_j \quad \text{for } j=1,2,\cdots,7 \tag{6.73}$$

where

$$\left.\begin{aligned}
F_1(\xi)&=\frac{(1+\gamma W)(1+aY_s)(1-\omega_s)}{\Delta_1}\xi, \quad F_2(\xi)=\frac{\xi(1+\gamma W)(1+aY_r)}{\Delta_2},\\
F_3(\xi)&=\frac{(1+\gamma W)(1+aM_s)}{\Delta_3}\xi, \quad F_4(\xi)=\frac{\xi(1+\gamma W)(1+aM_r)}{\Delta_4},\\
F_5(\xi)&=\frac{(1+aG_s)}{k_gW+k_2}\xi, \quad F_6(\xi)=\frac{(1+aG_r)}{k_gW+\mu_{gr}}\xi, \quad F_7(\xi)=\frac{1}{\mu_w}\xi,
\end{aligned}\right\} \tag{6.74}$$

with

$$\mathscr{H}=\begin{pmatrix}
0 & 0 & \frac{\beta\ C^*}{1+\gamma w} & 0 & 0 & 0 & 0\\
0 & 0 & 0 & \frac{\delta_r\beta C^*}{1+\gamma W} & 0 & 0 & 0\\
P(1-\alpha_s)\mu_{ys} & 0 & \frac{\beta C^*}{1+\gamma W}+k_1 & 0 & 0 & 0 & 0\\
0 & P(1-\alpha_r)\mu_{yr} & \Psi_1 & 0 & 0 & 0 & 0\\
\sigma_s & 0 & 0 & 0 & 0 & 0 & 0\\
0 & \sigma_r & 0 & 0 & 0 & 0 & 0\\
0 & 0 & \lambda_w & 0 & 0 & 0 & 0
\end{pmatrix}. \tag{6.75}$$

Note that $X^*=C^*-Y_s^*-Y_r^*$ and all the elements in the square matrix $\mathscr{H}$ are nonnegative. The coordinates of $\mathbb{E}_1$ are all positive and the j^{th} coordinate of the vector $\mathscr{H}(\bar{S})$ is described by the notation $\mathscr{H}(\bar{S})_j$ for $j=1,\cdots,7$. Additionally, the equilibrium $\mathbb{E}_1=(Y_s^*,Y_r^*,M_s^*,M_r^*,G_s^*,G_r^*,W^*)$ satisfies $\mathbb{E}_1=\mathscr{H}\mathbb{E}_1$. Assume, for example that system (6.73) has a solution of the form $\bar{S}$, then there exists a small positive real number ε, such that

$|\bar{S}| \leq \varepsilon \mathbb{E}_1$, where $|\bar{S}| = (|S_1|, |S_2|, \cdots, |S_7|)$. Note also that $|.|$ is a norm in the field of complex numbers.

Next, it is important to show that $\mathrm{Re}(\xi) < 0$. To do so, proof by contradiction is applied. Let $\xi = 0$ and $\xi \neq 0$. For the case when $\xi = 0$, the determinant (∇) of system(6.70) is given by

$$\nabla = \frac{v_5 v_6 \mu_w \{v_2 v_4 \nabla_* \mu_x + P\beta(1-\alpha_r)\lambda_x \mu_w \mu_{yr}\}\{v_1 v_3 \nabla_* \mu_x + P\beta(1-\alpha_s)\lambda_x \mu_w \mu_{ys}\}}{(\gamma\lambda_x + \mu_w)^2 \mu_x^2}, \quad (6.76)$$

where the positive terms $v_1, \cdots, v_6$ are as defined in matrix (6.25).

It is clear that the above determinant is nonnegative $(\nabla > 0)$. Consequently, the system (6.70) can only have the trivial solution $\bar{S} = (0,0,0,0,0,0,\frac{\lambda_w}{\mu_w})$. On the contrary, for $\xi \neq 0$, it is assumed that $\mathrm{Re}(\xi) \geq 0$. Defining $F(\xi) = \min|1 + F_j(\xi)|$, $j = 1,2,\cdots,7$ implies that $F(\xi) > 1$ and $\varepsilon/F(\xi) < \varepsilon$. The minimality of ε means that $|\bar{S}| > \varepsilon/F(\xi)\mathbb{E}_1$. While considering the non-negativity property of $\mathscr{H}$, if the norms on the two sides of system (6.73) are assumed, then

$$F(\xi)|\bar{S}| \leq \mathscr{H}|\bar{S}| \leq \varepsilon \mathscr{H} \mathbb{E}_1 = \varepsilon \mathbb{E}_1. \quad (6.77)$$

This implies that $|\bar{S}| \leq \varepsilon/F(\xi)\mathbb{E}_1 \leq \varepsilon \mathbb{E}_1$, which is a contradiction. Therefore, $\mathrm{Re}(\xi) < 0$ and $\mathbb{E}_1$ is locally asymptotically stable when $R_E > 1$.

6.4 Numerical simulations

6.4.1 Boundary equilibrium points

In this subsection, it is shown by means of numerical simulation, the existence and stability of a positive parasite-persistent equilibrium point that involves only one of the parasite strains under study.

Drug-sensitive-only persistent-equilibrium point E_s

This is an equilibrium point where only the drug-sensitive parasite strain is present in the infected human host. That is, the drug-resistant populations $Y_r = M_r = G_r = 0$. This steady state is only feasible if no resistant parasites emerge from infected red blood cells and the use of antimalarial treatment does not lead to resistance development; that is $\Psi_1 = \Psi_2 = 0$.

The previous system (6.11) is thus reduced to:

$$\left.\begin{aligned}
\frac{dX}{dt} &= \lambda_x - \mu_x X - \frac{\beta X M_s}{1+\gamma W},\\
\frac{dY_s}{dt} &= \frac{\beta X M_s}{1+\gamma W} - \frac{k_y Y_s W}{1+aY_s} - \frac{1}{1-\omega_s}\mu_{ys} Y_s - \sigma_s Y_s,\\
\frac{dM_s}{dt} &= (1-\alpha_s)P\mu_{ys} Y_s - \frac{\beta M_s X}{1+\gamma W} - \frac{k_m M_s W}{1+aM_s} - (\mu_{ms}+\zeta)M_s,\\
\frac{dG_s}{dt} &= \sigma_s Y_s - \frac{k_g W G_s}{1+aG_s} - (\mu_{gs}+\eta)G_s,\\
\frac{dW}{dt} &= \lambda_w + \left\{\frac{h_g(G_s)}{G_s+e_g} + \frac{h_y(Y_s)}{Y_s+e_y} + \frac{h_m(M_s)}{M_s+e_m}\right\} W - \mu_w W.
\end{aligned}\right\} \tag{6.78}$$

Numerically, this equilibrium point is illustrated as shown in Figure 6.3.

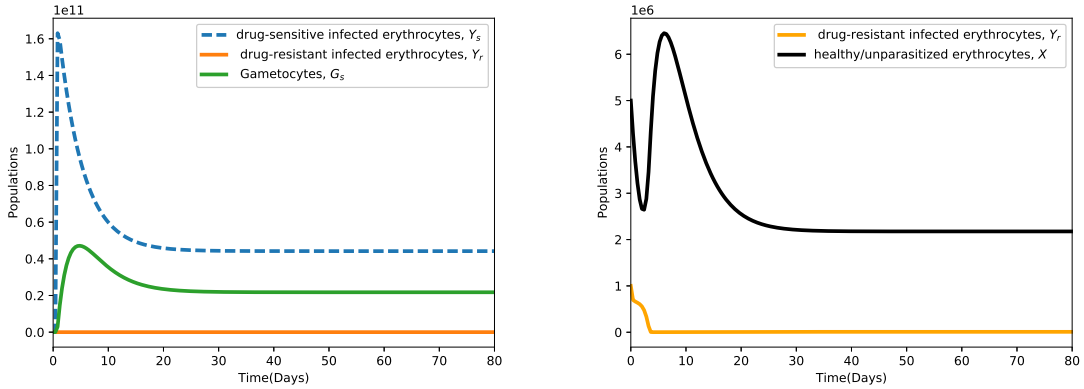

(a) (b)

Figure 6.3: Simulations of system (6.11) showing the existence of drug-sensitive-only equilibrium point. All other parameter values are shown in Table 6.3.

Drug-resistant-only persistent-equilibrium point E_r

In this case, the population of the drug-sensitive parasite strain declines to zero as the density of the resistant strain grows and stabilises at an optimal population size. This is also illustrated numerically as shown in Figure 6.4.

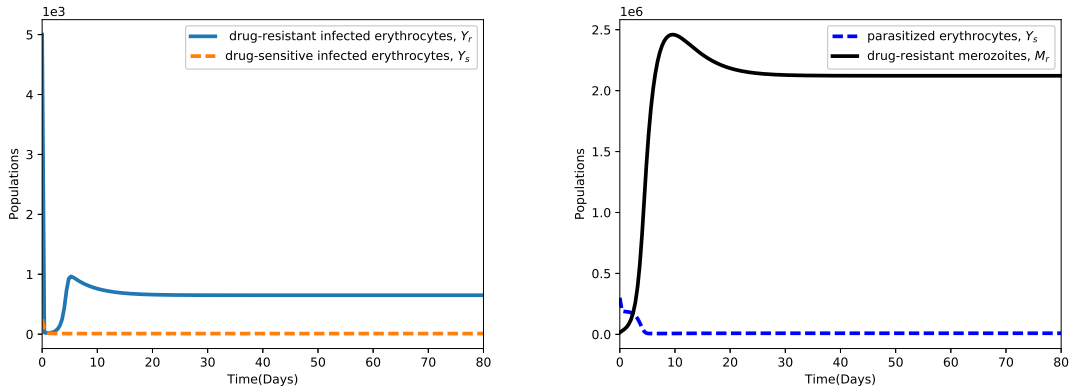

(a) (b)

Figure 6.4: Simulations of system (6.11) showing the existence of drug-resistant-only equilibrium point. Used parameter values are shown in Table 6.3.

Table 6.3: Baseline values and range for parameters of model (6.11)

Parameter	Value	Range	Units	Source
λ_w	30	(10-40)	Cells/μl/day	(Chiyaka, 2010)
ω_s	0.5	(0-1)	Unitless	Assumed
α_s	0.4	(0.1-1)	Unitless	Assumed
α_r	0.2	(0.01-1)	Unitless	Assumed
e_g, e_m, e_y	10^4	$(10^3 - 10^5)$	Unitless	(Colijn and Cohen, 2015)
λ_x	3×10^3	(3E+2-3E+8)	cells/μl/day	(Li et al., 2011)
μ_x	1/120	(0.05-0.1)	day^{-1}	(Chiyaka, 2010)
μ_{ys}	0.5	(0.3-0.8)	day^{-1}	(Mohammed et al., 2013)
μ_{yr}	0.3	(0.3-0.8)	day^{-1}	Assumed
μ_{ms}, μ_{mr}	48	(46-50)	day^{-1}	(Li et al., 2011)
μ_{gs}, μ_{gr}	0.0625	(0.05-0.1)	day^{-1}	(Ofosu-Okyere et al., 2001)
μ_w	0.05	(0.02-0.08)	day^{-1}	(Ofosu-Okyere et al., 2001)
δ_r	0.7	(0.01-0.99)	Unitless	Assumed
ζ, η	0.5	(0-1)	/day	(Mohammed et al., 2013)
P	16	(15-20)	Unitless	(Klein et al., 2008)
β	6.5×10^{-7}	(4.8-6.8)E-7	Merozoites/day	(Hellriegel, 1992)
σ_r, σ_s	0.02	(0.01-0.03)	day^{-1}	(Hellriegel, 1992)
h_y, h_m, h_g	0.05	(0.01-0.08)	mm^{-3}/day	(Chiyaka, 2010)
k_y, k_m, k_g	0.000001	(0.001-0.9)	day^{-1}	(Chiyaka et al., 2008)
Ψ_1	0.2	(0.01-2.2)	day^{-1}	Assumed

Continued on next page

Table 6.3 – *Continued from previous page*

Parameter	Value	Range	Units	Source
Ψ_2	0.01	(0.001-0.1)	day^{-1}	Assumed
δ_r	0.3	(0-1)	Unitless	Assumed
γ	0.5	(0-1)	Immune cells/μl	Assumed
$1/a$	0.2	(0-1)	Unitless	(Niger and Gumel, 2011)

6.4.2 Within-host competition between parasite strains

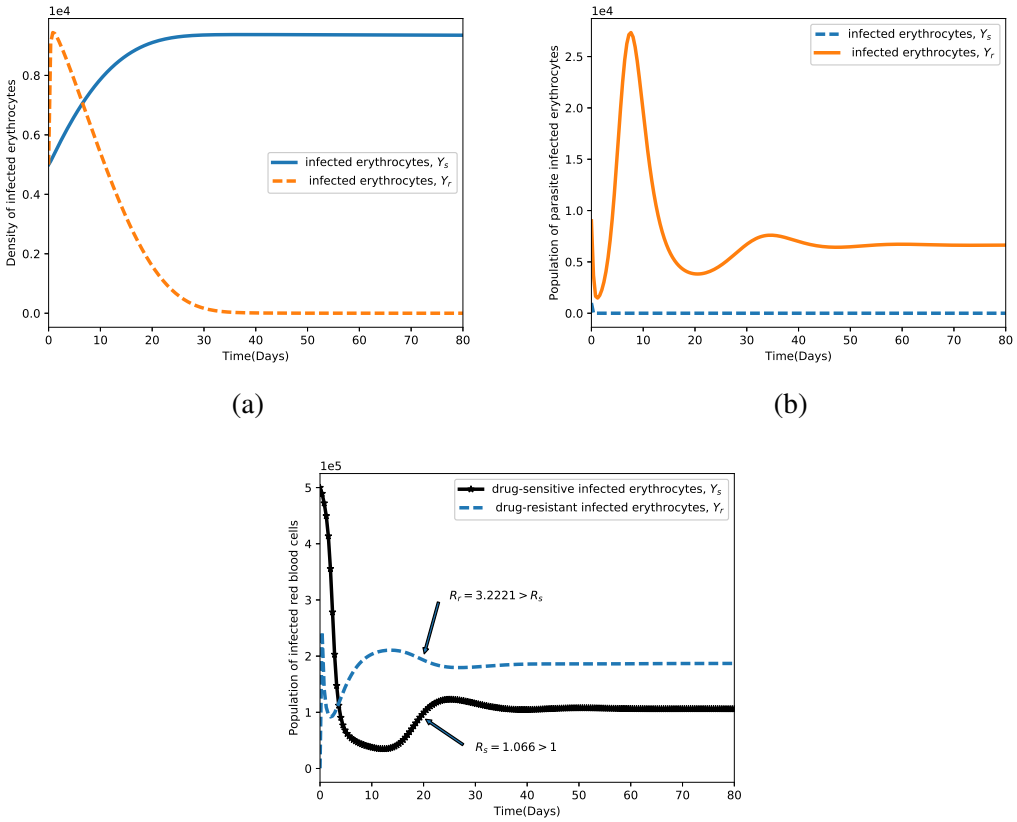

(a) (b)

(c)

Figure 6.5: Simulations of system (6.11). The figures show the dynamics of drug-sensitive and drug-resistant infected red blood cells under different conditions of the threshold values R_s and R_r. In Figure 6.5a, $R_s > R_r$. In Figure 6.5b, $R_r > R_s$, $\Psi_1 = 0$. All other parameter values are shown in Table 6.3.

The competitive exclusion principle is investigated by simulating the system (6.11) under different values of the threshold quantities R_s and R_r in equation (6.27). System (6.11) is simulated so that $R_s = 4.022$ and $R_r = 0.3131$, and a convergence to the drug-sensitive-only endemic equilibrium point E_s, as shown in Figure 6.5a is achieved. Again, using the parameter values in Table 6.3 with $\Psi_1 = 0.9$ and ($R_s = 0.022$; $R_r = 3.0098$), the solutions of Y_s and Y_r converge to the drug-resistant-only endemic equilibrium point E_r (Figure 6.5b).

Provided that both R_s and R_r are greater than 1 (as shown in Figure 6.5c), the parasite-infected erythrocytes persist in the human host. This implies that the merozoites (both drug-sensitive and drug-resistant) continue to multiply in the absence of antimalarial therapy, $\omega_s = 0$, or in the presence of ineffective antimalarial drugs. Similar results are observed in the dynamics of merozoites (M_s and M_r) as shown in Figure 6.6. It should be noted that the dominant merozoite strain is likely to drive the infection under these conditions. As the density of one strain increases, the population of the other strain is likely to decrease due to a phenomenon known as competitive exclusion principle (Hardin, 1960). The most fit parasite strain survives as the weaker competitor dies out, as shown in Figure 6.5a. Both drug-sensitive and drug-resistant merozoite would remain persistent if poor-quality antimalarial drugs are administered to *P. falciparum* malaria patients. Thus, in the absence of efficacious antimalarial drugs like ACTs with the potential to eradicate resistant merozoites, an exponential growth in the density of drug-resistant merozoites as shown in Figure 6.5b is most likely. This may lead to severe malaria and eventual death of the patient.

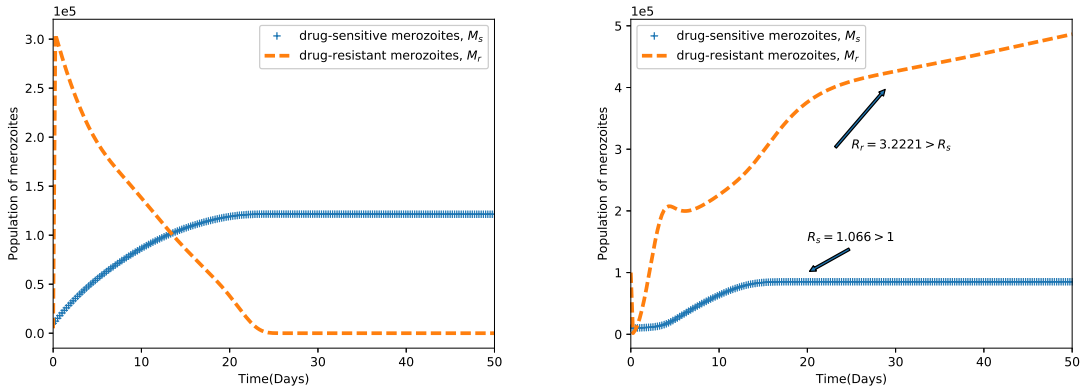

(a) (b)

Figure 6.6: Simulations of system (6.11). The figures show the dynamics of the merozoites under different conditions of the threshold values R_s and R_r. Competitive exclusion among the parasite strains is shown in Figure 6.6a. In Figure 6.6b, both parasite strains coexist and $R_r > R_s$, $\Psi_1 = 0$. Other parameter values are shown in Table 6.3.

The bifurcation analysis of both scenarios is presented in Figure 6.7 (with and without competition between the parasite strains). When there is competition between the parasite strains as shown in Figure 6.7(a), it is observed that the strain with a higher threshold quantity R_E would exclude the other strain. A decrease in the population of the drug-sensitive strain would pave way for a surge in the population of the drug-resistant strain and vice versa. This is despite the fact that drug-resistant strain emerge from the drug-sensitive strain as a result of mutation (Ashley et al., 2014). In Figure 6.7(b), coexistence of the strains is observed. Like the resistance strain, the sensitive strain is only present when their threshold quantity, R_s is greater than unity. Both strains are however present when $R_r > 1$ and $R_s > 1$. Additionally, when $R_r < 1$ and $R_s < 1$, the parasite-free equilibrium (PFE) point as shown in Figures 6.7(a) and 6.7(b) is achieved.

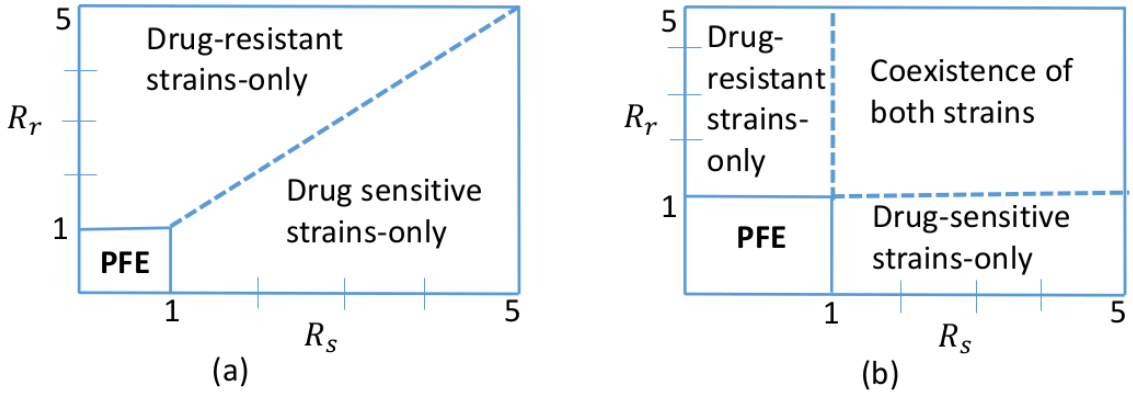

Figure 6.7: Bifurcation diagrams showing competitive exclusion (a) and coexistence equilibrium (b) for the drug-sensitive strain and drug-resistant *P. falciparum* parasite strain under different values of threshold quantities R_s and R_r. Both parasite strains coexist when $R_s > 1$ and $R_r > 1$ (see Figure 6.7(b)).

6.4.3 Antimalarial drug effects and parasite clearance

The effects of antimalarial drug treatment is monitored by establishing first and foremost that

$$\frac{\partial R_s}{\partial \omega_s} = -\frac{\beta\mu_1\mu_2 P(1-\alpha_s)\mu_w\lambda_x}{(1-\omega_s)^2\mu_x(\gamma\lambda_w+\mu_w)\left(\frac{k_v\lambda_w}{\mu_w}+\frac{\mu_2}{1-\omega_1}+\sigma_s\right)^2\left(\zeta+\frac{k_m\lambda_w}{\mu_w}+\mu_{\text{ms}}+\frac{\beta\lambda_x\mu_x^2}{\gamma\lambda_w+\mu_w}+\Psi_1\right)} < 0. \tag{6.79}$$

Thus, R_s is a decreasing function of ω_s (the efficacy of antimalarial drug used). Therefore, using a highly efficient antimalarial drug could lead to a scenario where $R_s < 1$ and $R_r < 1$ (disease-free state shown in Figure 6.8c). In Figure 6.8a, system (6.11) is simulated by

varying the efficacy of the antimalarial drug ω_s and other model parameters chosen such that $R_r = 3.221$ and $R_s = 2.221$. The higher the efficacy of the used antimalarial, the lower the density of infected erythrocytes. Thus, governments and ministry of health officers should only roll out or permit the administration of antimalarials or ACTs that can eradicate (totally) both the drug-resistant strain and the drug-sensitive strain of *P. falciparum* parasites.

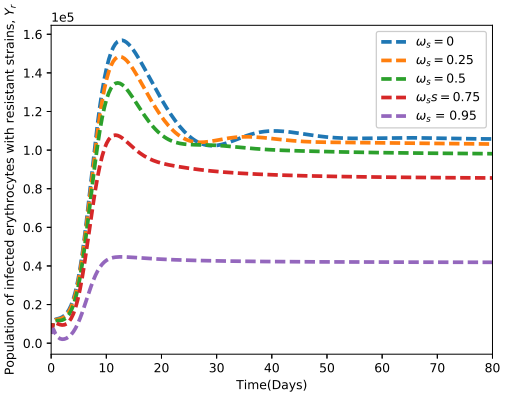

(a)

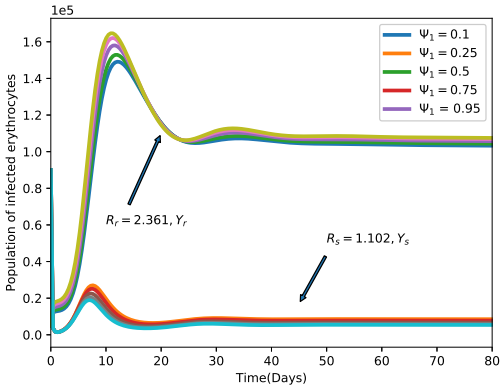

(b)

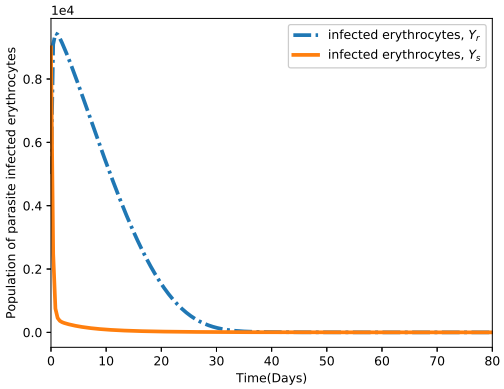

(c)

Figure 6.8: The figures depict the effect of varying the efficacy of antimalarial drug used ω_s and the rate of development of resistance by the drug-sensitive merozoites Ψ_1, on the density of infected erythrocytes (Y_s, Y_r). The value of ω_s ranges from 0 to 1. The rest of the parameter values are shown in Table 6.3.

The rate of development of resistance by the drug-sensitive merozoites, Ψ_1 is shown to have minimal impact on the dynamics of infected red blood cells Y_r as long as $R_r > 1$ and $R_r > 1$ (see Figure 6.8b). Nevertheless, analytical results indicate that the higher the rate of development of resistance, the lower the severity of future malaria infections. This is

presented as

$$\frac{\partial R_s}{\partial \Psi_1} = -\frac{\beta \mu_1 P (1-\alpha_s) \mu_w \lambda_x}{\mu_x (\gamma \lambda_w + \mu_w) \left(\frac{k_y \lambda_w}{\mu_w} + \frac{\mu_2}{1-\omega_1} + \sigma_s\right) \left(\zeta + \frac{k_m \lambda_w}{\mu_w} + \mu_{\text{ms}} + \frac{\beta \lambda_x \mu_x^2}{\gamma \lambda_w + \mu_w} + \Psi_1\right)^2} < 0. \tag{6.80}$$

Further simulations based on contour plots (see (Lane, 2003) for the theory on contour plots) are used to ascertain the relational effects of selected pairs of model parameters on the disease threshold quantities R_s and R_r. In Figure 6.9a, both β and μ_w increases the reproduction number due to drug-sensitive *P. falciparum* parasite strain. A direct relationship exists between the two parameters: the higher the decay rate of the immune cells, the higher the rate of infection of healthy erythrocytes.

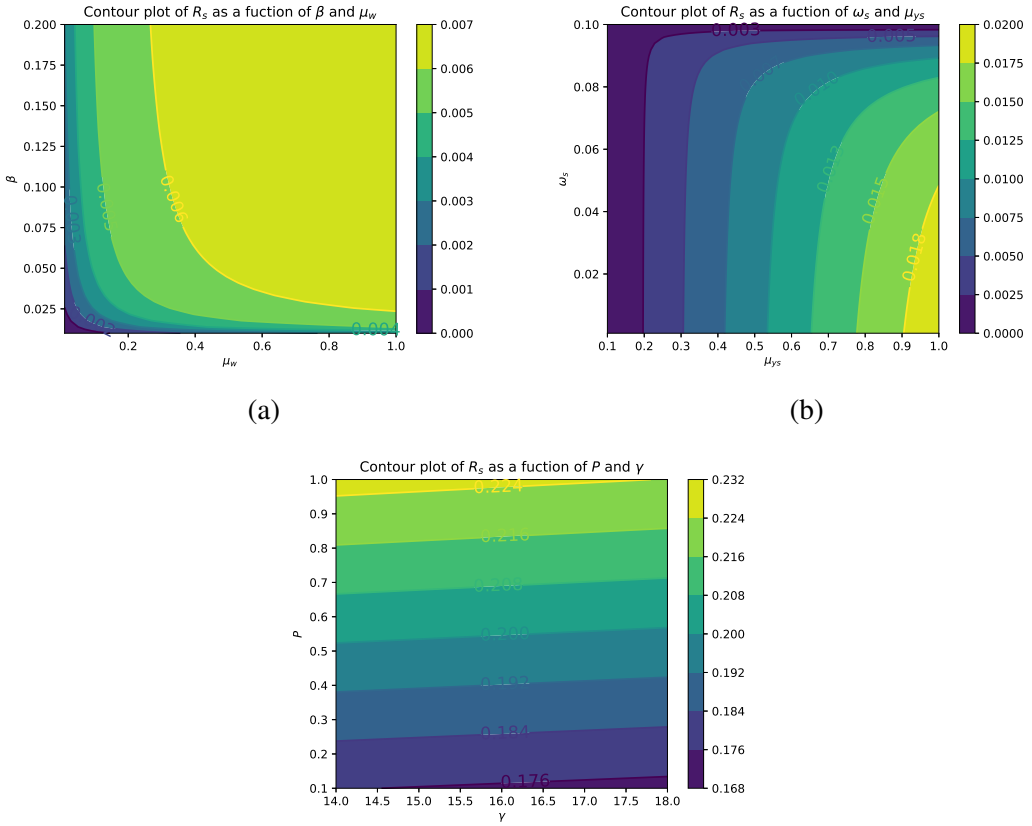

(a) (b)

(c)

Figure 6.9: Contour plot of R_s as a function of (a) β and μ_w, (b) ω_s and μ_{ys}, (c) P and γ

In Figure 6.9b, the least increase in R_s with respect to an increase in ω_s relative to μ_{ys} is observed. Antimalarial therapy is shown to be very effective in reducing the severity of

P. falciparum infection. Conversely, the number of merozoites produced per dying blood schizont, P, is shown in Figure 6.9c to have a very high positive impact on R_s and hence on the severity of malaria infection due to drug-sensitive parasite strain. Clinical control should target and eradicate infected red blood cells to diminish the erythrocytic cycles of infections.

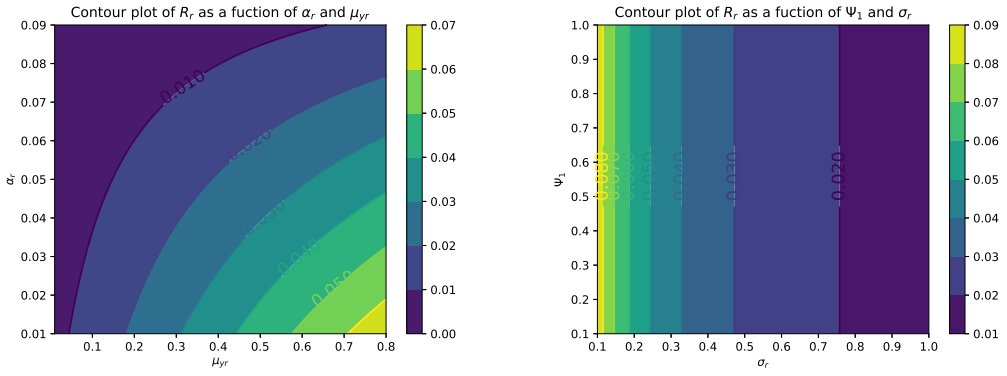

(a) (b)

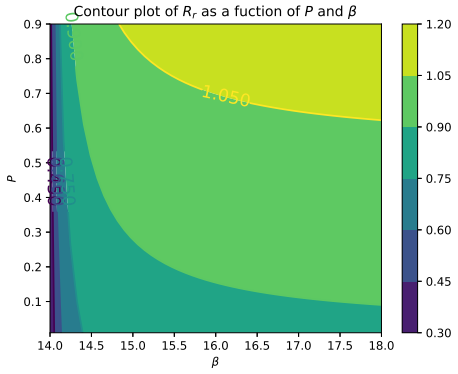

(c)

Figure 6.10: Contour plot of R_r as a function of (a) α_r and μ_{yr}, (b) Ψ_1 and σ_r, (c) P and β .

It is observed in Figure 6.10b that the rate at which merozoites develop resistance due to treatment failure has no resultant effects on the rate of formation of gametocytes that undergo sexual reproduction within the mosquito vector. The higher the value of R_r, the higher the cost of resistance as shown in Figure 6.10a. The higher the density of drug-resistant parasite strain, the higher the level of resistance and hence the cost of disease control. Unfortunately, highly effective antimalarial drugs (such as ACTs) that can eradicate both parasite strains are often slightly expensive in several *P. falciparum* malaria endemic regions (Gelband et al., 2004). Like the parameter P, the parasite infection rate β is shown to have a direct positive effect on the threshold quantity R_r (Figure 6.10c) due to drug-resistant parasite strain.

Effective antimalarials should hence target new cell infections and eliminate recrudescence (by killing already infected erythrocytes).

6.5 Effects of multiple - strain infection and fitness cost on parasite clearance

Numerous studies (Babiker et al., 2009; Bushman et al., 2016) have suggested the negative impacts of drug-resistance on the fitness and ability of the parasite to dominate *P. falciparum* infection. Resistance to antimalarial drugs imposes fitness cost on the drug-resistant parasite. The drug-resistant parasite strain is thought to experience impaired growth within the human host (Bushman et al., 2018). The cost of resistance is further exacerbated due to competition between parasite strains within an infected human-host. In Figure 6.11a, the area under the curve for the drug-resistant strain or the number of infected erythrocytes is lower than that of the drug-sensitive strain. However, in a multiple-strain infection (Figure 6.11b), the area difference is much bigger. This implies that competition between the parasite strains within the human host could result in elimination of one of the parasite-strains provided that both R_s and R_r are less than unity.

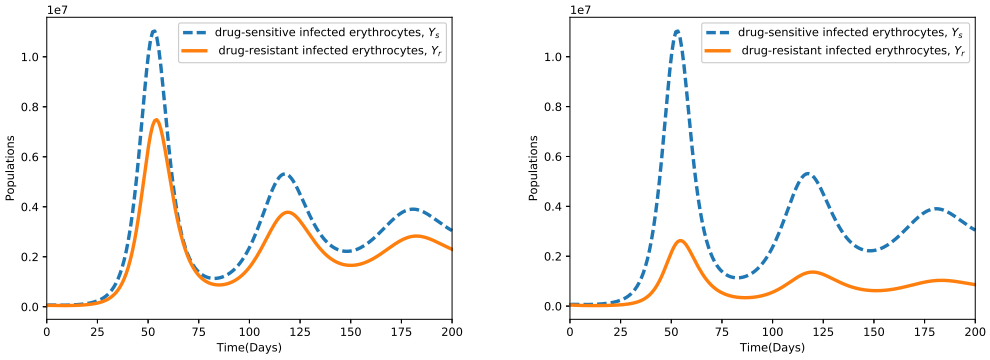

(a) (b)

Figure 6.11: Dynamics of drug-sensitive (blue) and drug-resistant (orange) strains in a single infection (a) and in a multiple-infection (b) in a naive human-host with no antimalarial drug treatment ($\omega_s = 0$). The rest of the parameter values are shown in Table 6.3.

The presence of multiple-strains of *P. falciparum* parasites is likely to complicate and worsen the severity of malaria disease infection in humans. Figures 6.12 and 6.13 show

the simulated model (6.11) for single and multiple-strain infections, in the absence of pre-existing immunity and antimalarial drugs. The persistence of gametocytes in Figures 6.12c and 6.13c is consistent with the actual observations of human malaria infection in the absence of antimalarial therapy (see Teun et al. (2010)). Acquired immunity is shown in Figure 6.12c to increase and eventually level-off at higher levels to contain future infections.

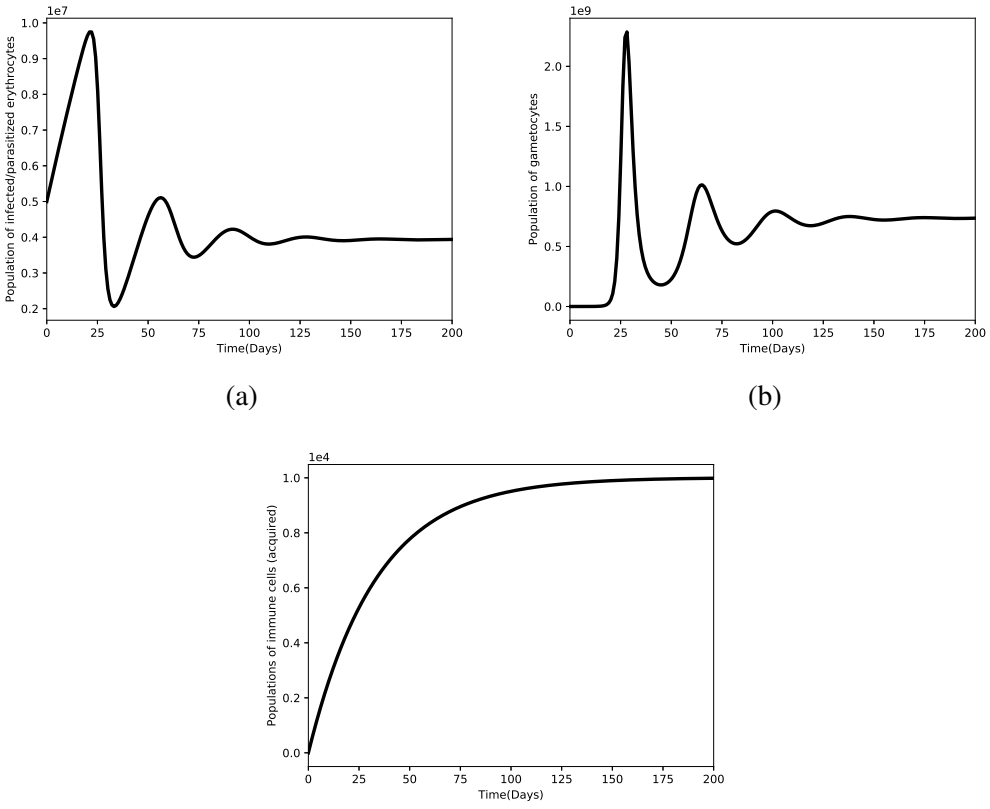

(a) (b)

(c)

Figure 6.12: Dynamics of infected red blood cells, gametocytes and the immune cells with a single strain *P. falciparum* infection. Here, there is no pre-existing immunity. The rest of the parameter values are shown in Table 6.3.

Although the aspect of timing is key in these multiple-strain infections, it is assumed here that the two strains are introduced at the same time. In the long run, it is evident in Figures 6.11b and 6.13c that the sensitive strain overtakes the resistant strain. This could be as a result of strain-specific adaptive responses that symmetrically affects the sensitive parasites.

Unlike single-strain *P. falciparum* parasite infections, data on multiple-strain infections are not readily available. Nevertheless, a multiple-strain infection (drug-sensitive and drug-

resistant) as presented in this chapter is biologically reasonable and consistent with that of *P. Chabaudi* described by De Roode et al. (2005).

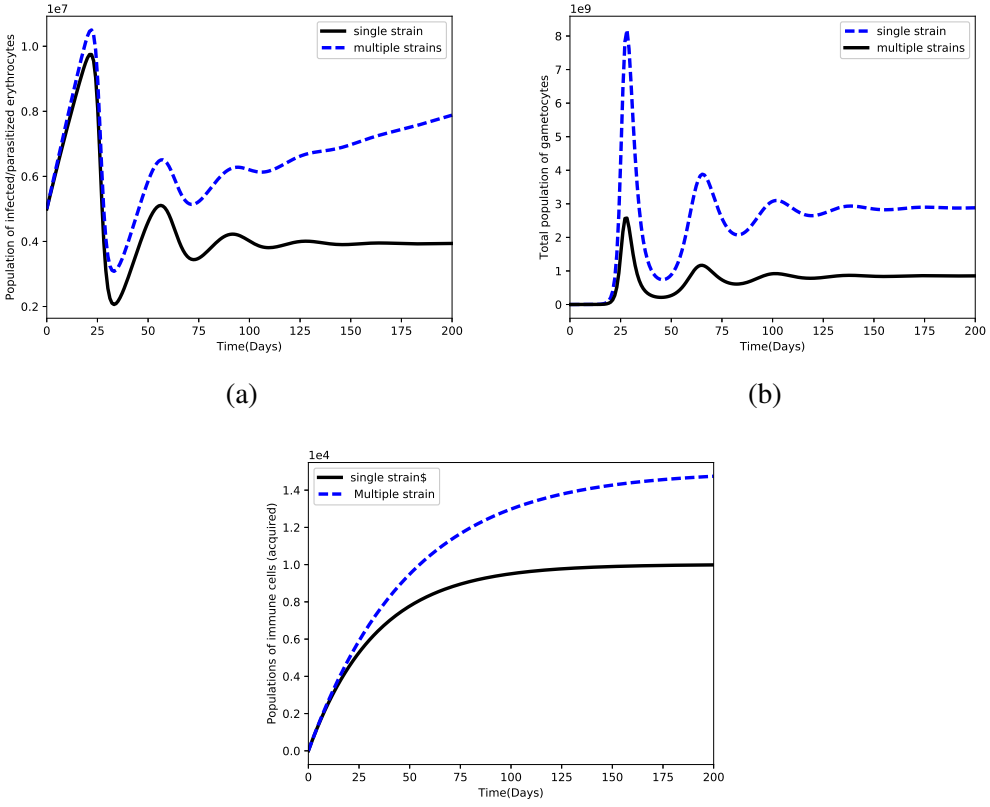

Figure 6.13: Within-human dynamics of single and multiple-strain dynamics of infected red blood cells, gametocytes and the immune cells in the absence pre-existing immunity and with no antimalarial treatment ($\omega_s = 0$). Other parameter values are shown in Table 6.3.

6.5.1 Sensitivity analysis

In this subsection, the primary model output of interest for the sensitivity analysis are the infected erythrocytes (Y_s, Y_r). However, the effective reproduction number R_E is a threshold quantity which represents on overage the number of secondary infected erythrocytes due to merozoite invasions. This therefore measure the sensitivity indices of the effective reproduction number relative to model parameters. Using the normalised forward sensitivity index technique (Arriola and Hyman, 2007) and parameter values in Table 6.3, the sensitivity indices of all the parameters in R_E are as presented in Table 6.4. Observe that the rate of infection of healthy erythrocytes by the merozoites β, the density of merozoites generated per

bursting blood schizonts P, the efficacy of antimalarial drug used ω_s, and the rate at which drug-sensitive merozoites develop resistance Ψ_1 are the four most influential parameters, in determining the disease dynamics as presented in system (6.11).

Table 6.4: Sensitivity indices of R_E relative to the model parameters

Parameter	SI	Parameter	SI
β	+0.9988	Ψ_1	-0.77534
P	+1.0000	μ_{ys}	-0.492
ω_s	-0.87513	λ_w	-0.3471
λ_x	+0.7199	ζ	-0.0041
μ_x	-0.0016	δ_r	+0.0023
k_y	-0.02701	k_m	-0.0020
σ_s	-0.7619	σ_r	-0.541872
γ	-0.3333	α_r	-0.1111
μ_{mr}	-0.433	α_s	-0.09891
μ_{ms}	-0.52123	μ_w	0.3716
μ_{yr}	-0.232		

Results from sensitivity analysis emphasise the use of highly efficacious antimalarial drugs such as ACTs in malaria endemic regions. This would mitigate the many cases of malaria in the region and further help to reduce emerging cases of parasite resistance to existing therapies. Drugs with a higher parasite clearance rate would greatly reduce resistance, which is associated with longer parasite exposure to antimalarial drugs. It is imperative therefore, that government and ministry of health personnel in malaria endemic countries enforce the use of efficient antimalarial drugs that not only cure infected malaria patients but also eliminate the chance of *P. falciparum* parasites to develop resistance to existing therapy.

6.6 Conclusion

In this chapter, a deterministic model of multiple-strain *P. falciparum* malaria infection has been formulated and analysed. The parasite strains are categorised as either drug-sensitive or drug-resistant. The infected erythrocytes and the malaria gametocytes are similarly grouped according to the strain of the parasite responsible for their existence. The immune cells are incorporated to reduce the invasive characteristic of the malaria merozoites. Antimalarial

therapy is applied to the model but only targets red blood cells infected with drug-sensitive merozoites. Based on the computed effective reproduction number R_E, it is evident that the success of *P. falciparum* infection in the presence of multiple parasite strains is directly dependent on the ability of the individual parasite strains to drive the infection. The parasite strain with a higher threshold value, R_E is likely to dominate the infection. Prescribed antimalarial drugs should therefore be effective enough to eradicate both drug-sensitive and drug-resistant parasite strains within the human host.

The use of antimalarial treatment may eradicate one parasite strain so that either a drug-sensitive-only persistent equilibrium point or a drug-resistant-only persistent equilibrium point is attained. To assess the impacts of the different parasite strains to disease dynamics, the model is simulated for different values of the threshold quantities R_s and R_r. It is observed that when $R_r > 1$ and $R_s > 1$, both parasite strains are persistent and the infection becomes severe. If $R_r > 1$ and $R_s < 1$, then the drug-sensitive parasites would decline to zero as the drug-resistant strain continue to multiply and remain persistent, increasing the severity of infections. On the other hand, if $R_s > 1$ and $R_r < 1$, then the drug-resistant parasite strain would be eradicated. Moreover, provided that the threshold quantities R_s and R_r are less than unity, the use of an efficacious antimalarial drug would help eradicate *P. falciparum* infection.

The efficacy of antimalarial drug is shown to have direct negative impact on the density of infected red blood cells. This result is consistent with that in Filipe et al. (2007). The efficacy of antimalarial drug is however shown to have least effect on the population of drug-resistant infected erythrocytes. The rate of development of resistance by drug-sensitive parasites is also shown to drive the infection due to resistant parasite strain. Using contour plots and results from sensitivity analysis, it is observed that the efficacy of antimalarial drug used ω_s, the density of blood floating merozoites produced per infected erythrocyte P, the rate of development of resistance Ψ_1, and the rate of infection by merozoites β are the most important parameters in the disease dynamics and control. Although the drug-resistant strain is shown to be less fit, the presence of both strains in the human host has a huge impact on the cost and success of antimalarial treatment. To reduce the emergence of resistant strain, it is vital that only effective antimalarial drugs are administered to patients in hospitals, especially in malaria endemic regions. The results from this study call for regular and strict surveillance on antimalarial drugs in clinics and hospitals in malaria-endemic countries.

In the next Chapter 7, optimal control theory is applied to establish an appropriate combination therapy against clinical *P. falciparum* malaria.

Chapter 7

Application of optimal control theory to hepatocytic-erythrocytic dynamics of *P. falciparum* malaria

7.1 Introduction

In this chapter, optimal control theory is applied to an in-host malarial model that is characterised by a combination of antimalarial drugs and different vaccine antigens. The analysis of the model with constant vaccine therapy is available in Chapter 4 of this thesis. Time-dependent vaccine and antimalarial drug control therapies are incorporated into the model. The objective of this study is to establish an appropriate combination therapy for clinical *P. falciparum* malaria.

7.2 Antimalarial drugs and drug combinations

Currently, artemisinin-based combination therapy (ACTs) is the standard of care for uncomplicated *P. falciparum* malaria. The five WHO recommended ACTs include: (i) artemether + lumefantrine, (ii) artesunate + amodiaquine, (iii) artesunate + mefloquine and (iv) dihydroartemisinin + piperaquine, (v) artesunate + sulfadoxine–pyrimethamine (SP) (WHO, 2015c). Drug resistance against 4-aminoquinolines and sulpha compounds has remained one of the greatest challenge to malaria chemotherapy development (Visser et al., 2014). *P. falciparum* resistance to artesunate in Western Cambodia was characterised by slow parasite

clearance as shown in Figure 7.1. Further evidence of resistance to artemisinins (Dondorp et al., 2009; Noedl et al., 2008) highlights the need for continuous investment in the development of alternative anti-malarial drugs and vaccines.

The combination of anti-malarial drugs have achieved tremendous success in malaria treatment and transmission reduction (NIH, 2019; Visser et al., 2014). Administration of two or more antimalarials with different targets and modes of action has been shown to be highly effective compared to monotherapy drugs (WHO, 2015c). A rapidly acting artemisinin drug in ACTs exhibit an extremely short half-life. It is hence combined with a longer-acting monotherapy (partner drug) to limit recrudescence and achieve higher clinical response. The artemisinin component reduces parasite numbers by a factor of about 10^4 in each 48-hour asexual cycle (Hodel et al., 2016). Further, it is active against gametocytes that mediate onward transmission to mosquito vector. The longer-acting monotherapy drug, eradicates the remaining parasites. This further reduces the possible occurrence of resistance due to mutations during treatment. Additionally, the long-acting drug may provide a period of post-treatment prophylaxis (WHO, 2015c).

According to Okell et al. (2008), a combination of an ACT partner drug and a nonartemisinin regimen with longer prophylactic times is destined to achieve a greater impact in higher-transmission settings. The addition of artesunate to amodiaquine reduced gametocyte carriage and did not adversely affect tolerability in *P. falciparum* patients (Osorio et al., 2007). Elsewhere (Smithuis et al., 2010), artesunate-mefloquine provided the greatest post-treatment suppression of malaria in Myanmar and the addition of a single dose of primaquine substantially reduced transmission potential.

Although antimalaria drugs and insecticides have helped reduce malaria cases and deaths globally, these two interventions are vulnerable to development of resistance (Chitnis et al., 2015). The availability of effective malaria vaccines is a critical tool for sustainable control and elimination (Abdulla et al., 2011). Unfortunately, malaria vaccine development has been hindered by the extreme complexity of malaria parasite biology. The parasites have a diverse genome which enables them to evade immune system and complete their intricate infection cycle (Mahmoudi and Keshavarz, 2018).

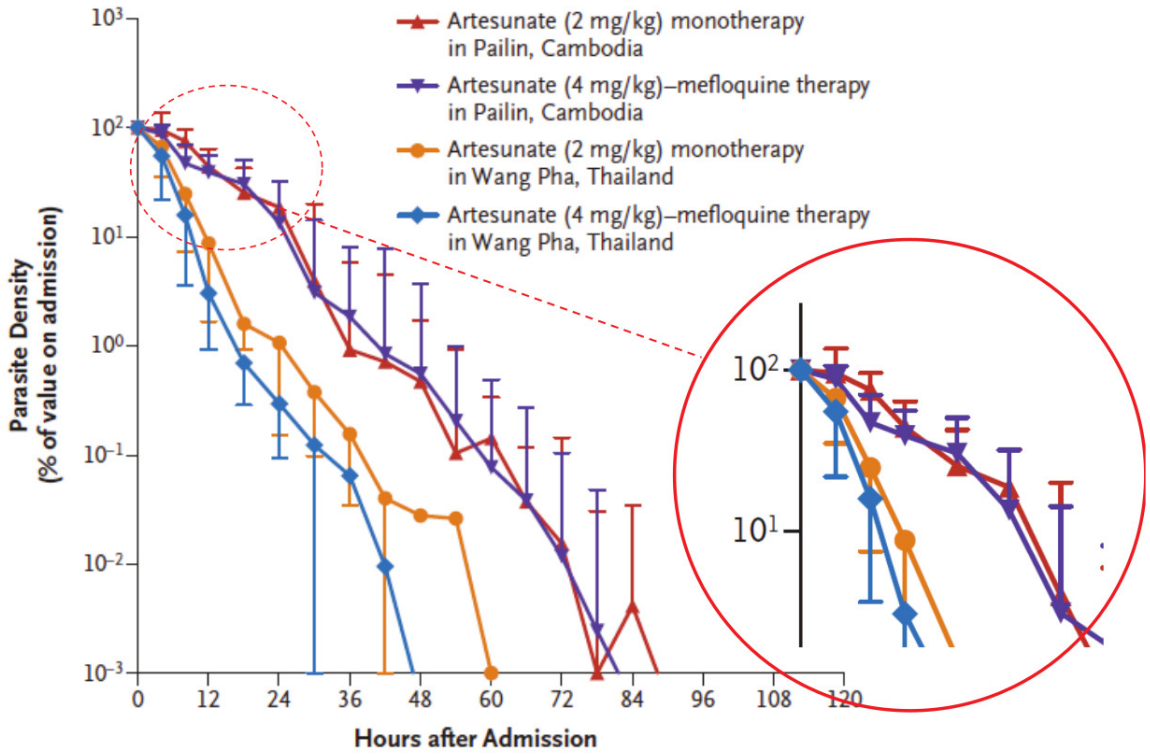

Figure 7.1: Normalised *P. falciparum* parasite clearance curves showing the fraction of initial parasitaemia versus time in patients treated with artesunate in Western Cambodia and Western Thailand. Parasite clearance was significantly slower in Western Cambodia. Source: Dondorp et al. (2009).

7.2.1 The need to combine different vaccine antigens

Several clinical and pre-clinical studies (Bauza et al., 2016; Mahmoudi and Keshavarz, 2018; Sherrard-Smith et al., 2018) have demonstrated the significant benefit of combining two or more malaria vaccine antigens. Recombinant PfMSP-1_{42} formulated with AS02A elicited high antibody titres among young children in Western Kenya (Ogutu et al., 2009). JAIVAC-1 formulated with Montanide ISA720 elicited balanced antibody responses against both PfF2 and PfMSP-1_{19} and exhibited significant growth inhibitory activity against *P. falciparum* (Chitnis et al., 2015). Adenovirus-CSP prime combined with a protein-CSP boost regime provided 100% protection in C57BL/6 mice (Bauza et al., 2016). Moreover, a combined efficacy of 90.8% (86.7-94.2%) was observed in the pre-erythrocytic vaccines (PEV) + transmission-blocking vaccine (TBV) antibody group; 7.8% higher than the estimated efficacy if the two antibodies acted independently (Sherrard-Smith et al., 2018). These studies have

shown that a combination of two or more malaria vaccine antigens is synergistic and is likely to achieve better results in the control of in-host malaria infections.

7.2.2 Optimal control theory applied to malaria models

Optimal control theory (Lenhart and Workman, 2007) has been very helpful in identifying optimal control measures against particular diseases. In malaria epidemiology, the application of optimal control theory has for a long time been limited to population level models (Agusto et al., 2012; Makinde and Okosun, 2011; Mwanga et al., 2015; Okosun et al., 2011). In most of these models, the main objective has been to minimise the population of humans infected with malaria while keeping the costs of control, such as purchase of insecticide-treated bed nets (ITNs), indoor residual spraying (IRS) and antimalarial drugs, as low as possible (Mwanga et al., 2015). In all these dynamical models, optimal control therapy strategies were explored using Pontryagin's maximum principle (Pontryagin, 1987).

A combination of different vaccine antigens are shown by Orwa et al. (2018) to be highly effective in reducing parasitaemia and severity of clinical *P. falciparum* malaria. In addition, a combination of two malaria drugs, fosmidomycin and piperaquine was also established to have higher efficacy, safety and well tolerated (Mombo-Ngoma et al., 2017). Elsewhere (Pukrittayakamee et al., 2004), a combination of artesunate and primaquine (PQ) resulted in significantly shorter gametocyte clearance times. In Pukrittayakamee et al. (2004), artesunate is shown to inhibit gametocyte development whereas primaquine accelerates gametocyte clearance in *P. falciparum* malaria (see Figure 7.3). It is argued that a combination of efficient antimalarial drugs and efficacious malaria vaccines present the best therapeutic strategy to achieving malaria elimination.

7.3 The optimal control model

The model presented in this study is an extension of the in-host malaria model subject to vaccine interventions in Chapter 4 of this thesis. The model describes the interactions of (i) sporozoites (S), (ii) uninfected hepatocytes (H), (iii) infected hepatocytes (X), (iv) uninfected red blood cells (R), (v) early stage infected red blood cells (Blood trophozoites, T), (vi) mature infected red blood cells (blood schizonts, C), (vii) merozoites (M), (viii) gemetocytes (G) and (ix) $CD8^+$ T cells (Z). The only two vaccines considered in this chapter are: pre-erythrocytic vaccine (PEV) and blood stage vaccine (BSV), which offer direct protection

to the recipient human host. The specific vaccines are: RTS,S/AS01 (Birkett, 2016) and merozoite surface protein 3 (Miura, 2016), respectively. The model is extended by adding antimalarial drug therapy: artemether-lumefantrine (a blood schizontocide)(Ogutu, 2013) and primaquine (a gametocytocide) (WHO, 2012b). The combined chemotherapy not only target rapid parasite clearance but also reduced parasite transmissibility to mosquito vector. It is clear that the four interventions considered here, target different sites within the complex malaria dynamics.

The gametocytocide considered in this study is a single dose 0.25 mg base/kg of primaquine. This WHO recommended drug, mainly targets the blood stage gametocytes. It kills the gametocytes irrespective of their stages of development (Recht et al., 2014). This reduces the probability of parasite transmission to the mosquito vector and hence disease morbidity. The lower dose of 0.25mg base/kg of primaquine is considered by WHO as safer and as effective as higher doses (see Figure 7.2) in reducing transmissibility (Eziefula et al., 2014; White et al., 2012; WHO, 2012b). In Figure 7.3, a combination of quinine and the lower dose of 0.25mg base/kg of primaquine is shown to be highly effective in timely eradication of parasitaemia. However, pregnant women and infants aged 6 months or below are exempted from this additinal dose in endemic regions. Moreover, higher doses of PQ could be harmful to those with glucose-6-phosphate dehydrogenase (G6PD) deficiency (Graves et al., 2014).

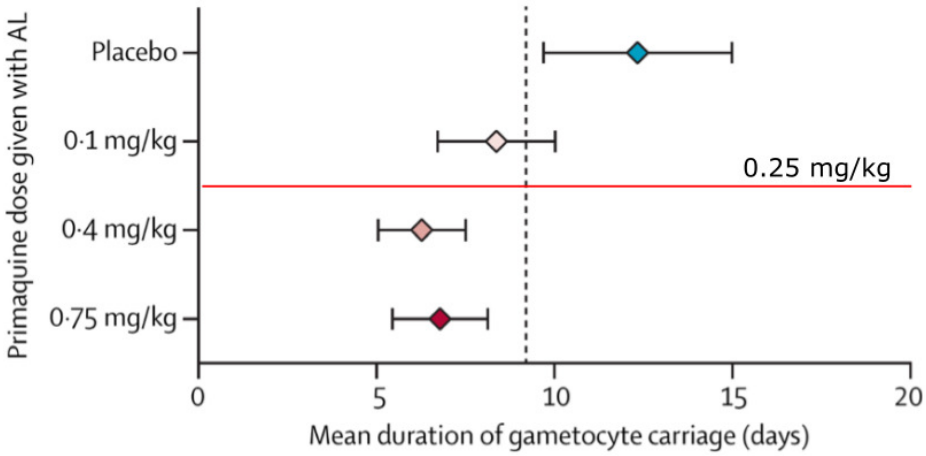

Figure 7.2: Mean duration of female gametocyte carriage in children with *P. falciparum* malaria treated with artemether-lumefantrine (AL) and different doses of primaquine. The dashed line indicates the set threshold for non-inferiority compared with the 0·75 mg/kg reference group. Source: Eziefula et al. (2014).

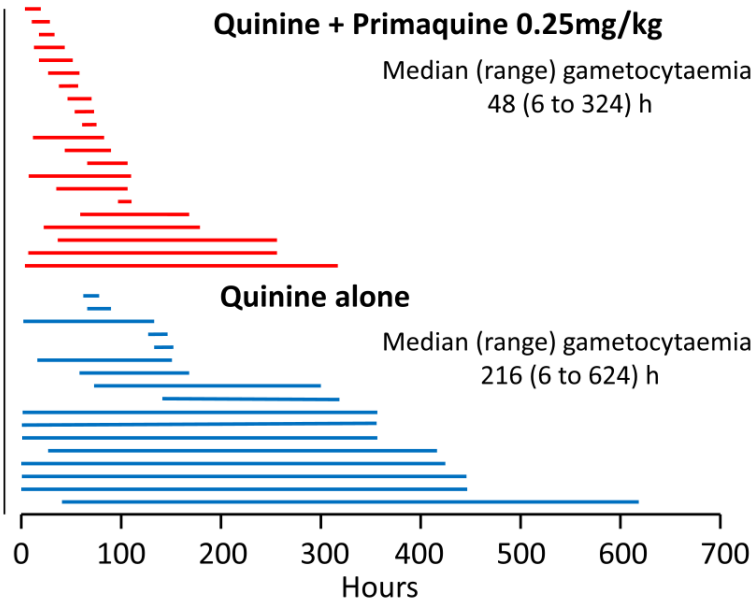

Figure 7.3: The comparison of durations of *P. falciparum* gametocytaemia following quinine alone compared with quinine plus 0.25 mg base/kg of primaquine. Source: Pukrittayakamee et al. (2004).

The Pontryagin's maximum principle is used to minimise the population of infected hepatocytes X, infected erythrocytes T, infective blood stage merozoites M and the gametocytes G. RTS,S/AS01 and MSP3 reduces the rates of invasion of healthy hepatocytes and healthy erythrocytes, respectively. The hepatocyte invasion rate β_s and the erythrocyte invasion rates β_r are hence, reduced to $(1-u_1(t))\beta_s$ and $(1-u_2(t))\beta_r$, respectively. The time dependent controls u_1 and u_2, therefore represent the efficacies of the pre-erythrocytic vaccine and the blood stage vaccine, respectively. The use of primaquine reduces the burst size N of liver schizonts to $(1-u_3(t))N$, where $u_3(t)$ is the normalised primaquine dosage efficacy as a function of time. Similarly, the administration of AL, reduces the burst size P of infected erythrocytes to $(1-u_4(t))P$, where $u_4(t)$ is the normalised AL dosage efficacy as a function of time. The in-host model of *P. falciparum* malaria subject to antimalarial drugs and malaria

vaccines is hence presented as follows:

$$\left.\begin{aligned}
\frac{\mathrm{d}S}{\mathrm{d}t} &= \Lambda - \mu_s S - \beta_s SH, \\
\frac{\mathrm{d}H}{\mathrm{d}t} &= \lambda_h - \mu_h H - (1-u_1(t))\beta_s SH, \\
\frac{\mathrm{d}X}{\mathrm{d}t} &= (1-u_1(t))\beta_s SH - \mu_x X - \frac{k_x ZX}{1+\varepsilon_0 X}, \\
\frac{\mathrm{d}R}{\mathrm{d}t} &= \lambda_r - \frac{(1-u_2(t))\beta_r RM}{1+\alpha Z} - \mu_r R, \\
\frac{\mathrm{d}T}{\mathrm{d}t} &= \frac{(1-u_2(t))\beta_r RM}{1+\alpha Z} - \mu_t T - \gamma T - \frac{k_t ZT}{1+\varepsilon_1 T}, \\
\frac{\mathrm{d}C}{\mathrm{d}t} &= \gamma T - \mu_c C - \frac{k_c ZC}{1+\varepsilon_2 C}, \\
\frac{\mathrm{d}M}{\mathrm{d}t} &= (1-u_3(t))N\mu_x X + \frac{(1-u_4(t))P(1-\pi)\mu_c C}{1+\alpha Z} - \mu_m M - \beta_r RM, \\
\frac{\mathrm{d}G}{\mathrm{d}t} &= \pi\mu_c C - (u_3(t)+\mu_g)G, \\
\frac{\mathrm{d}Z}{\mathrm{d}t} &= \lambda_z + Z\left(\frac{\delta_x X}{1+\varepsilon_0 X} + \frac{\delta_t T}{1+\varepsilon_1 T} + \frac{\delta_c C}{1+\varepsilon_2 C}\right) - \mu_Z Z,
\end{aligned}\right\} \tag{7.1}$$

subject to the following initial conditions:

$$S(0) \geq 0, H(0) > 0, X(0) \geq 0, R(0) > 0, T(0) \geq 0, C(0) \geq 0, M(0) \geq 0, G(0) \geq 0, Z(0) > 0. \tag{7.2}$$

A brief description of model parameters are as presented in Table 7.1.

Table 7.1: Description of model parameters

Parameter	Description
Λ	The rate of injection of sporozoites into liver due to mosquito bites
μ_s	Death rate of sporozoites
β_s	Rate of invasion of hepatocytes by sporozoites
λ_h	Rate of supply of hepatocytes from the bone marrow
λ_r	Rate of supply of erythrocytes from the bone marrow
μ_h, μ_x	Death rate of susceptible hepatocyte and infected hepatocyte, respectively
π	Proportion of parasites that become gametocytes per bursting blood schizont C
k_x, k_t, k_c	Immunosensitivity of X, T and C, respectively

Continued on next page

Table 7.1 – *Continued from previous page*

Parameter	Description
$\delta_x, \delta_t, \delta_c$	Immunogenecity of X, T and C, respectively
μ_r	Natural mortality rate of healthy RBC
β_r	Rate of infection of RBCs by merozoites
μ_t, μ_c	Rate of decay of blood trophozoites and blood schizonts, respectively
μ_m, μ_g	Rate of decay of merozoites and gametocytes, respectively
P	Average number of merozoites released per bursting blood schizont
N	The average number of merozoites released per bursting infected hepatocytes
γ	Rate of progression from blood trophozoite to schizont stages
α	Rate of inhibition of immune response
λ_z	Rate of production of $CD8^+$ T-cells
$1/\varepsilon_0, 1/\varepsilon_1, 1/\varepsilon_2$	Half saturation constants for X, T and C, respectively
μ_z	Rate of decay of $CD8^+$ T-cells

7.4 Formulation of optimal control problem

We endeavor to reduce malaria disease severity within the human host by reducing parasite invasion of the healthy hepatocytes and erythrocytes. To curtail further transmission, we also aim to reduce the density of sexual gametocytes within the host's blood stream. To achieve these two, we set out to establish the most effective control strategy drawn from a combination of malaria vaccine antigens and antimalarial drugs regimens. The policies under consideration are $u_1(t)$, $u_2(t)$, $u_3(t)$ and $u_4(t)$ described in Section 7.3. Therefore, the objective function J defined over a feasible set of controls (u_1, u_2, u_3, u_4) over a finite time interval $[0, t_f]$ is given by

$$J(u_1,u_2,u_3,u_4) = \int_0^{t_f} (A_1X + A_2T + A_3M + A_4G) + \frac{1}{2}(B_1u_1^2 + B_2u_2^2 + B_3u_3^2 + B_4u_4^2), \quad (7.3)$$

subject to system (7.1).

In system (7.3), A_1, A_2, A_3 and A_4 are the costs associated with minimising the infected hepatocyte, infected erythrocytes, the merozoites and gametocytes, respectively. The parameter

t_f denotes the time period of intervention. The quantities B_1, B_2, B_3 and B_4 represent the weight constants for pre-erythrocytic vaccine, blood stage vaccine, blood schizontocide and gametocytocide, respectively. The weight constants accounts for the relative importance pre-assigned by the modeller to the contributing terms in the objective function (Lee et al., 2010). Additionally, we endeavour to minimise the social costs related to resources needed for pre-erythrocytic vaccines $\frac{1}{2}B_1u_1^2$, blood stage vaccine $\frac{1}{2}B_2u_2^2$, blood schizontocide $\frac{1}{2}B_3u_3^2$ and gametocytocide $\frac{1}{2}B_4u_4^2$.

As in other epidemic models (Joshi et al., 2006; Okosun et al., 2011), the costs associated with using antimalarial drugs and malaria vaccines are directly proportional to the rates at which these controls are implemented. Therefore, the coefficients A_1X, A_2T, A_3M and A_4G are linear functions. On the other hand, the cost of implementing the suggested control strategies, $\frac{1}{2}B_1u_1^2$, $\frac{1}{2}B_2u_2^2$, $\frac{1}{2}B_3u_3^2$ and $\frac{1}{2}B_4u_4^2$ are proportional to the square of the corresponding control function. They are hence nonlinear and take quadratic forms.

Numerically, an optimal control set $(u_1^*, u_2^*, u_3^*, u_4^*)$ which minimises the objective function J (7.3) is sought such that

$$J(u_1^*, u_2^*, u_3^*, u_4^*) = \min_U J(u_1, u_2, u_3, u_4), \tag{7.4}$$

where $U = \{(u_1, u_2, u_3, u_4)$ such that $\{u_1, u_2, u_3, u_4\}$ is a Lebeque measurable control set with $0 \leq u_i(t) \leq 1,\ i = 1, \cdots, 4,$ for $t \in [0, t_f]\}$.

7.4.1 Existence of optimal solutions to the control problem

An optimal control solution is said to exist if the five necessary conditions that define the optimal solutions $J(u_1^*, u_2^*, u_3^*, u_4^*) = \min_{(u_1,u_2,u_3,u_4)\in U} J(u_1, u_2, u_3, u_4)$ of problem in system (7.1) are satisfied. The resulting optimality problem is solved based on Pontryagin's Maximum Principle (Pontryagin, 1987).

Theorem 7.1. *Consider an optimal problem $\mathcal{N}(t, Y(t), u_i(t))$ of system (7.1), subject to initial conditions of state variable $Y(t) \in \mathbb{R}_+^9$ and boundary condition of control variables $u_i(t) \in U$ for $i = 1, \cdots, 4$. There exists an optimal solution $J(u_1^*, u_2^*, u_3^*, u_4^*)$ such that $J(u_1^*, u_2^*, u_3^*, u_4^*) = \min_{(u_1,u_2,u_3,u_4)\in U} J(u_1, u_2, u_3, u_4)$ if the following necessary conditions are satisfied (Chuma et al., 2019):*

(i) Control set U and the corresponding state variables are nonempty,

(ii) Control set U is convex and closed,

(iii) The right hand side of the state system is bounded by the linear function in the state and control variables,

(iv) The integrand of the objective function is convex,

(v) There exist constant numbers q_1, $q_2 > 0$ and $\xi > 1$ such that the integrand of the objective function is bounded below by $q_1(|u_1|+|u_2|+|u_3|+|u_4|)^{\xi/2} - q_2$.

Proof: The existence of an optimal control is verified by conditions stated by Fleming and Rishel (1975). From the optimal problem $\mathcal{N}(t, Y(t), u_i(t))$ of system (7.1), the set of all state variables $Y(t) \in \mathbb{R}^9_+$ and the control variables $\{u_i(t) \in U | 0 \leq u_i(t) \leq 1\}, t \in [0, t_f]$ are non-negative. The first condition is hence satisfied. By definition, the optimal solution $u_i(t)$ is convex and bounded in U. Hence, the second condition is satisfied (Mlay et al., 2015; Mpeshe et al., 2014).

The optimal system (7.1) is bounded which determines the compactness needed for the existence of the optimal control (Athithan and Ghosh, 2015). The third condition therefore holds. Moreover, the integrand in the objective function in equation (7.3) is clearly convex on the control set U. This proves the fourth condition. It is clear that the state variables are bounded in system (7.1). Following the work by Mlay et al. (2015), the integrand in (7.3) is also bounded below by

$$A_1X(t) + A_2T(t) + A_3M(t) + A_4G(t) + \frac{1}{2}\left(\sum_{i=1}^{4} B_i u_i^2\right) \geq q_1 \left(\sum_{i=1}^{4} |u_i(t)|\right)^{\xi/2} - q_2 \tag{7.5}$$

for $i = 1, \cdots, 4$. This proves condition five. The above five conditions are hence satisfied. Therefore, there exist control variables $u_1^*(t)$, $u_2^*(t)$, $u_3^*(t)$ and $u_4^*(t)$ such that

$$J(u_1^*, u_2^*, u_3^*, u_4^*) = \min_U J(u_1, u_2, u_3, u_4). \tag{7.6}$$

7.4.2 Characterisation of the optimal control

The Pontryagin's Maximum Principle (Pontryagin, 1987) is used in solving the stated optimal control problem. This principle converts the optimality system (7.1), (7.3) and (7.4) into a problem of minimising a pointwise Hamiltonian H_a, with respect to controls u_1, u_2, u_3 and u_4. The Lagrangian of the optimal control problem is given by

$$L = A_1X + A_2T + A_3M + A_4G + \frac{1}{2}(B_1u_1^2 + B_2u_2^2 + B_3u_3^2 + B_4u_4^2). \tag{7.7}$$

Clearly, the second derivative of L in equation (7.7) with respect to $u_i, i = 1, \cdots, 4$, are positive, indicating that the optimal control problem is a minimum at controls u_1^*, u_2^*, u_3^* and u_4^*. The aim is to obtain the Lagrangian minimum value. This is accomplished by defining a Hamiltonian function H_a for the control problem as follows:

$$
\begin{aligned}
H_a &= L(X,T,M,G,u_1,u_2,u_3,u_4) \\
&\quad + \Upsilon_1\dot{S} + \Upsilon_2\dot{H} + \Upsilon_3\dot{X} + \Upsilon_4\dot{R} + \Upsilon_5\dot{T} + \Upsilon_6\dot{C} + \Upsilon_7\dot{M} + \Upsilon_8\dot{G} + \Upsilon_9\dot{Z} \\
&\quad = A_1X + A_2T + A_3M + A_4G + \frac{1}{2}(B_1u_1^2 + B_2u_2^2 + B_3u_3^2 + B_4u_4^2) \\
&\quad + \Upsilon_1\left[\Lambda - \mu_sS - \beta_sSH\right] \\
&\quad + \Upsilon_2\left[\lambda_h - \mu_hH - (1-u_1(t))\beta_sSH\right] \\
&\quad + \Upsilon_3\left[(1-u_1(t))\beta_sSH - \mu_xX - \frac{k_xZX}{1+\varepsilon_0X}\right] \\
&\quad + \Upsilon_4\left[\lambda_r - \frac{(1-u_2(t))\beta_rRM}{1+\alpha Z} - \mu_rR\right] \\
&\quad + \Upsilon_5\left[\frac{(1-u_2(t))\beta_rRM}{1+\alpha Z} - \mu_tT - \gamma T - \frac{k_tZT}{1+\varepsilon_1T}\right] \\
&\quad + \Upsilon_6\left[\gamma T - \mu_cC - \frac{k_cZC}{1+\varepsilon_2C}\right] \\
&\quad + \Upsilon_7\left[(1-u_3(t))N\mu_xX + \frac{(1-u_4(t))P(1-\pi)\mu_cC}{1+\alpha Z} - \mu_mM - \beta_rRM\right] \\
&\quad + \Upsilon_8\left[\pi\mu_cC - (u_3(t)+\mu_g)G\right] \\
&\quad + \Upsilon_9\left[\lambda_z + Z\left(\frac{\delta_xX}{1+\varepsilon_0X} + \frac{\delta_tT}{1+\varepsilon_1T} + \frac{\delta_cC}{1+\varepsilon_2C}\right) - \mu_ZZ\right],
\end{aligned}
\tag{7.8}
$$

where Υ_i, for $i = 1,2,3,\cdots,9$, are the adjoints or co-state variables.

Theorem 7.2. *Let $S^*, H^*, X^*, R^*, T^*, C^*, M^*, G^*$ and Z^* be the solutions of the corresponding optimal control problem in system (7.1) and (7.4) associated with the optimal control*

solutions $(u_1^*, u_2^*, u_3^*, u_4^*)$. *Then there exists adjoint variables* Υ_i, $i = 1, 2, \cdots, 9$ *satisfying*

$$\left.\begin{aligned}
\frac{d\Upsilon_1}{dt} &= (\Upsilon_2 - \Upsilon_3)(1-u_1)\beta_s H + \Upsilon_1(\mu_s + \beta_s H),\\
\frac{d\Upsilon_2}{dt} &= (\Upsilon_1 + (\Upsilon_2 - \Upsilon_3)(1-u_1))\beta_s + \Upsilon_2\mu_h,\\
\frac{d\Upsilon_3}{dt} &= \frac{(\Upsilon_3 k_x - \Upsilon_9\delta_x)Z}{(1+\varepsilon_0 X)^2} - A_1 + (\Upsilon_3 - \Upsilon_7 N(1-u_3))\mu_x,\\
\frac{d\Upsilon_4}{dt} &= \frac{\beta_r((1+\alpha Z)\Upsilon_7 + (1-u_2)(\Upsilon_4 - \Upsilon_5))M}{(1+\alpha Z)} + \Upsilon_4\mu_r,\\
\frac{d\Upsilon_5}{dt} &= \frac{(\Upsilon_5 k_t - \Upsilon_9\delta_t)Z}{(1+\varepsilon_1 T)^2} + \Upsilon_5(\gamma + \mu_t) - (A_2 + \gamma\Upsilon_6),\\
\frac{d\Upsilon_6}{dt} &= \Upsilon_6\left(\frac{k_c Z}{(1+\varepsilon_2 C)^2} + \mu_c\right) - \frac{\Upsilon_9\delta_c Z}{(1+\varepsilon_2 C)} - \pi\Upsilon_8\mu_c - \frac{(1-u_4)(1-\pi)P\Upsilon_7\mu_c}{(1+\alpha Z)},\\
\frac{d\Upsilon_7}{dt} &= \Upsilon_7(\beta_r R + \mu_m) - A_3 + \frac{(\Upsilon_4 - \Upsilon_5)(1-u_2)\beta_r R}{1+\alpha Z},\\
\frac{d\Upsilon_8}{dt} &= \Upsilon_8(u_3 + \mu_g) - A_4,\\
\frac{d\Upsilon_9}{dt} &= \frac{\Upsilon_3 k_x X}{1+\varepsilon_0 X} + \frac{\Upsilon_6 k_c C}{1+\varepsilon_2 C} - \frac{\Upsilon_4(1-u_2)\alpha\beta_r MR}{(1+\alpha Z)^2} + \frac{\Upsilon_7(1-\pi)P(1-u_4)\alpha\mu_c C}{(1+\alpha Z)^2}\\
&\quad - \Upsilon_9\left(\frac{\delta_x X}{1+\varepsilon_0 X} + \frac{\delta_t T}{1+\varepsilon_1 T} + \frac{\delta_c C}{1+\varepsilon_2 C} - \mu_z\right) + \Upsilon_5\left(\frac{k_t T}{1+\varepsilon_1 T} + \frac{(1-u_2)\alpha\beta MR}{(1+\alpha Z)^2}\right),
\end{aligned}\right\} \tag{7.9}$$

with transversality conditions (or boundary conditions)

$$\Upsilon_i(t_f) = 0, \quad for \quad i = 1, 2, 3, \cdots, 9, \tag{7.10}$$

expressed as

$$u_i^* = \begin{cases} 0 & if \;\; u_i \le 0,\\ u_i & if \;\; 0 < u_i < 1,\\ 1 & if \;\; u_i \ge 1. \end{cases} \tag{7.11}$$

Additionally, in the interior of the control set U, the control functions u_1^*, u_2^*, u_3^* and u_4^* are given by

$$u_1^* = \max\left\{\min\left\{\frac{\beta_s(\Upsilon_3-\Upsilon_2)S^*H^*}{B_1},1\right\},0\right\} \tag{7.12}$$

$$u_2^* = \max\left\{\min\left\{\frac{\beta_r(\Upsilon_5-\Upsilon_4)R^*M^*}{(1+\alpha Z)B_2},1\right\},0\right\} \tag{7.13}$$

$$u_3^* = \max\left\{\min\left\{\frac{\Upsilon_8 G^*+\Upsilon_7\mu_x NX^*}{B_3},1\right\},0\right\} \tag{7.14}$$

$$u_4^* = \max\left\{\min\left\{\frac{\Upsilon_7\mu_c(1-\pi)PC^*}{(1+\alpha Z)B_4},1\right\},0\right\}. \tag{7.15}$$

Proof: The form of the adjoint system and the transversality conditions therein are standard results from the Pontryagin's Maximum Principle (Pontryagin, 1987). To obtain the differential equations governing the adjoint or co-state variables, we first set $S=S^*$, $H=H^*$, $X=X^*$, $R=R^*$, $T=T^*$, $C=C^*$, $M=M^*$, $G=G^*$ and $Z=Z^*$, and differentiate (partially) the Hamiltonian function H_a in equation (7.8) with respect to each of the state variables (S,H,X,R,T,C,M,G and Z). Thus,

$$\frac{\mathrm{d}\Upsilon_1}{\mathrm{d}t} = -\frac{\partial H_a}{\partial X}; \quad \Upsilon_1(t_f)=0, \tag{7.16}$$

$$\frac{\mathrm{d}\Upsilon_2}{\mathrm{d}t} = -\frac{\partial H_a}{\partial H}; \quad \Upsilon_2(t_f)=0, \tag{7.17}$$

$$\vdots$$

$$\frac{\mathrm{d}\Upsilon_9}{\mathrm{d}t} = -\frac{\partial H_a}{\partial Z}; \quad \Upsilon_9(t_f)=0. \tag{7.18}$$

To obtain the optimality equations (7.12)-(7.15), first carry out partial derivative of the Hamiltonian H_a with respect to the controls (u_1,u_2,u_3,u_4) and then solve for u_i^* (optimal control) where the derivative vanishes. Thus,

$$\left.\frac{\partial H_a}{\partial u_1}\right|_{u_1^*} = \beta_s(\Upsilon_2-\Upsilon_3)S^*H^*+B_1u_1^* = 0. \tag{7.19}$$

Making u_1^* the subject of the formula in equation (7.19) gives

$$u_1^*(t) = \frac{\beta_s(\Upsilon_3-\Upsilon_2)S^*H^*}{B_1}. \tag{7.20}$$

This procedure can be applied to the remaining three controls such that

$$u_2^* = \frac{\beta_r(\Upsilon_5 - \Upsilon_4)R^*M^*}{(1+\alpha Z)B_2}, \quad u_3^* = \frac{\Upsilon_8 G^* + \Upsilon_7 \mu_x N X^*}{B_3}, \quad u_4^* = \frac{\Upsilon_7 \mu_c (1-\pi) P C^*}{(1+\alpha Z)B_4}. \tag{7.21}$$

$$u_1^* = \begin{cases} 0 & \text{if} \quad \frac{\beta_s(\Upsilon_3 - \Upsilon_2)S^*H^*}{B_1} \leq 0, \\ \frac{\beta_s(\Upsilon_3 - \Upsilon_2)S^*H^*}{B_1} & \text{if} \quad 0 < u_1 < 1, \\ 1 & \text{if} \quad \frac{\beta_s(\Upsilon_3 - \Upsilon_2)S^*H^*}{B_1} \geq 1. \end{cases} \tag{7.22}$$

The solution u_1^* is therefore expressed as

$$u_1^* = \max\left\{\min\left\{\frac{\beta_s(\Upsilon_3 - \Upsilon_2)S^*H^*}{B_1}, 1\right\}, 0\right\}. \tag{7.23}$$

Similarly, the optimal controls u_2^*, u_3^* and u_4^* are given as

$$u_2^* = \max\left\{\min\left\{\frac{\beta_r(\Upsilon_5 - \Upsilon_4)R^*M^*}{(1+\alpha Z)B_2}, 1\right\}, 0\right\} \tag{7.24}$$

$$u_3^* = \max\left\{\min\left\{\frac{\Upsilon_8 G^* + \Upsilon_7 \mu_x N X^*}{B_3}, 1\right\}, 0\right\} \tag{7.25}$$

$$u_4^* = \max\left\{\min\left\{\frac{\Upsilon_7 \mu_c (1-\pi) P C^*}{(1+\alpha Z)B_4}, 1\right\}, 0\right\}. \tag{7.26}$$

Utilising the characteristic functions (7.12)-(7.15), the following optimality system (7.27)-(7.28) characterises the optimal control:

$$\left.\begin{aligned}
\frac{\mathrm{d}S}{\mathrm{d}t} &= \Lambda - \mu_s S - \beta_s S H, \\
\frac{\mathrm{d}H}{\mathrm{d}t} &= \lambda_h - \mu_h H - \left(1 - \max\left\{\min\left\{\frac{\beta_s(\Upsilon_3 - \Upsilon_2)S^*H^*}{B_1}, 1\right\}, 0\right\}\right)\beta_s S H, \\
\frac{\mathrm{d}X}{\mathrm{d}t} &= \left(1 - \max\left\{\min\left\{\frac{\beta_s(\Upsilon_3 - \Upsilon_2)S^*H^*}{B_1}, 1\right\}, 0\right\}\right)\beta_s S H - \mu_x X - \frac{k_x Z X}{1+\varepsilon_0 X}, \\
\frac{\mathrm{d}R}{\mathrm{d}t} &= \lambda_r - \frac{\left(1 - \max\left\{\min\left\{\frac{\beta_r(\Upsilon_5 - \Upsilon_4)R^*M^*}{(1+\alpha Z)B_2}, 1\right\}, 0\right\}\right)\beta_r R M}{1+\alpha Z} - \mu_r R, \\
\frac{\mathrm{d}T}{\mathrm{d}t} &= \frac{\left(1 - \max\left\{\min\left\{\frac{\beta_r(\Upsilon_5 - \Upsilon_4)R^*M^*}{(1+\alpha Z)B_2}, 1\right\}, 0\right\}\right)\beta_r R M}{1+\alpha Z} - \mu_t T - \gamma T - \frac{k_t Z T}{1+\varepsilon_1 T}, \\
\frac{\mathrm{d}C}{\mathrm{d}t} &= \gamma T - \mu_c C - \frac{k_c Z C}{1+\varepsilon_2 C},
\end{aligned}\right\} \tag{7.27}$$

$$
\begin{aligned}
\frac{\mathrm{d}M}{\mathrm{d}t} &= \left(1-\max\left\{\min\left\{\frac{\Upsilon_8 G^* + \Upsilon_7 \mu_x N X^*}{B_3}, 1\right\}, 0\right\}\right) N\mu_x X \\
&\quad + \frac{\left(1-\max\left\{\min\left\{\frac{\Upsilon_7 \mu_c (1-\pi) P C^*}{(1+\alpha Z) B_4}, 1\right\}, 0\right\}\right) P(1-\pi)\mu_c C}{1+\alpha Z} - \mu_m M - \beta_r R M, \\
\frac{\mathrm{d}G}{\mathrm{d}t} &= \pi\mu_c C - \left(\left(\max\left\{\min\left\{\frac{\Upsilon_8 G^* + \Upsilon_7 \mu_x N X^*}{B_3}, 1\right\}, 0\right\}\right) + \mu_g\right) G, \\
\frac{\mathrm{d}Z}{\mathrm{d}t} &= \lambda_z + Z\left(\frac{\delta_x X}{1+\varepsilon_0 X} + \frac{\delta_t T}{1+\varepsilon_1 T} + \frac{\delta_c C}{1+\varepsilon_2 C}\right) - \mu_Z Z, \\
\frac{\mathrm{d}\Upsilon_1}{\mathrm{d}t} &= (\Upsilon_2 - \Upsilon_3)\left(1-\max\left\{\min\left\{\frac{\beta_s(\Upsilon_3-\Upsilon_2)S^* H^*}{B_1}, 1\right\}, 0\right\}\right)\beta_s H + \Upsilon_1(\mu_s + \beta_s H), \\
\frac{\mathrm{d}\Upsilon_2}{\mathrm{d}t} &= (\Upsilon_1 + (\Upsilon_2 - \Upsilon_3)\left(1-\max\left\{\min\left\{\frac{\beta_s(\Upsilon_3-\Upsilon_2)S^* H^*}{B_1}, 1\right\}, 0\right\}\right))\beta_s + \Upsilon_2\mu_h, \\
\frac{\mathrm{d}\Upsilon_3}{\mathrm{d}t} &= \frac{(\Upsilon_3 k_x - \Upsilon_9\delta_x)Z}{(1+\varepsilon_0 X)^2} - A_1 + \left(\Upsilon_3 - \Upsilon_7 N\left(1-\max\left\{\min\left\{\frac{\Upsilon_8 G^* + \Upsilon_7\mu_x N X^*}{B_3}, 1\right\}, 0\right\}\right)\right)\mu_x, \\
\frac{\mathrm{d}\Upsilon_4}{\mathrm{d}t} &= \frac{\beta_r((1+\alpha Z)\Upsilon_7 + \left(1-\max\left\{\min\left\{\frac{\beta_r(\Upsilon_5-\Upsilon_4)R^* M^*}{(1+\alpha Z)B_2}, 1\right\}, 0\right\}\right)(\Upsilon_4 - \Upsilon_5))M}{(1+\alpha Z)} + \Upsilon_4\mu_r, \\
\frac{\mathrm{d}\Upsilon_5}{\mathrm{d}t} &= \frac{(\Upsilon_5 k_t - \Upsilon_9\delta_t)Z}{(1+\varepsilon_1 T)^2} + \Upsilon_5(\gamma + \mu_t) - (A_2 + \gamma\Upsilon_6), \\
\frac{\mathrm{d}\Upsilon_6}{\mathrm{d}t} &= \Upsilon_6\left(\frac{k_c Z}{(1+\varepsilon_2 C)^2} + \mu_c\right) - \frac{\left(1-\max\left\{\min\left\{\frac{\Upsilon_7\mu_c(1-\pi)PC^*}{(1+\alpha Z)B_4}, 1\right\}, 0\right\}\right)(1-\pi)P\Upsilon_7\mu_c}{(1+\alpha Z)} \\
&\quad - \frac{\Upsilon_9\delta_c Z}{(1+\varepsilon_2 C)} - \pi\Upsilon_8\mu_c, \\
\frac{\mathrm{d}\Upsilon_7}{\mathrm{d}t} &= \Upsilon_7(\beta_r R + \mu_m) - A_3 + \frac{(\Upsilon_4 - \Upsilon_5)\left(1-\max\left\{\min\left\{\frac{\beta_r(\Upsilon_5-\Upsilon_4)R^* M^*}{(1+\alpha Z)B_2}, 1\right\}, 0\right\}\right)\beta_r R}{1+\alpha Z}, \\
\frac{\mathrm{d}\Upsilon_8}{\mathrm{d}t} &= \Upsilon_8\left(\left(\max\left\{\min\left\{\frac{\Upsilon_8 G^* + \Upsilon_7\mu_x N X^*}{B_3}, 1\right\}, 0\right\}\right) + \mu_g\right) - A_4, \\
\frac{\mathrm{d}\Upsilon_9}{\mathrm{d}t} &= \frac{\Upsilon_3 k_x X}{1+\varepsilon_0 X} + \frac{\Upsilon_6 k_c C}{1+\varepsilon_2 C} - \frac{\Upsilon_4\left(1-\max\left\{\min\left\{\frac{\beta_r(\Upsilon_5-\Upsilon_4)R^* M^*}{(1+\alpha Z)B_2}, 1\right\}, 0\right\}\right)\alpha\beta_r M R}{(1+\alpha Z)^2} \\
&\quad + \frac{\Upsilon_7(1-\pi)P\left(1-\max\left\{\min\left\{\frac{\Upsilon_7\mu_c(1-\pi)PC^*}{(1+\alpha Z)B_4}, 1\right\}, 0\right\}\right)\alpha\mu_c C}{(1+\alpha Z)^2} \\
&\quad - \Upsilon_9\left(\frac{\delta_x X}{1+\varepsilon_0 X} + \frac{\delta_t T}{1+\varepsilon_1 T} + \frac{\delta_c C}{1+\varepsilon_2 C} - \mu_z\right) \\
&\quad + \Upsilon_5\left(\frac{k_t T}{1+\varepsilon_1 T} + \frac{\left(1-\max\left\{\min\left\{\frac{\beta_r(\Upsilon_5-\Upsilon_4)R^* M^*}{(1+\alpha Z)B_2}, 1\right\}, 0\right\}\right)\alpha\beta M R}{(1+\alpha Z)^2}\right),
\end{aligned}
\tag{7.28}
$$

where $\Upsilon_i(t_f) = 0$, for $i = 1,2,3,\cdots,9$ and $S(0) \geq 0, H(0) > 0, X(0) \geq 0, R(0) > 0, T(0) \geq 0, C(0) \geq 0, M(0) \geq 0, G(0) \geq 0, Z(0) > 0$.

7.4.3 Uniqueness of the optimality system

Given that the state variables and the adjoint functions are bounded and satisfy Lipschitz conditions, the uniqueness of the optimal controls can easily be derived using the technique explained by Kim et al. (2012). Thus, the following theorem is stated.

Theorem 7.3. *The bounded solutions to the optimality system are unique.*

Proof: Suppose $(S,H,X,R,T,C,M,G,Z,\Upsilon_1,\Upsilon_2,\Upsilon_3,\Upsilon_4,\Upsilon_5,\Upsilon_6,\Upsilon_7,\Upsilon_8,\Upsilon_9)$ and $(\bar{X},\bar{H},\bar{S},\bar{R},\bar{T},\bar{C},\bar{M},\bar{G},\bar{Z},\bar{\Upsilon}_1,\bar{\Upsilon}_2,\bar{\Upsilon}_3,\bar{\Upsilon}_4,\bar{\Upsilon}_5,\bar{\Upsilon}_6,\bar{\Upsilon}_7,\bar{\Upsilon}_8,\bar{\Upsilon}_9)$ are two different solutions of our optimality system. Let $S = e^{\Upsilon t}v_1$, $H = e^{\Upsilon t}v_2$, $X = e^{\Upsilon t}v_3$, $R = e^{\Upsilon t}v_4$, $T = e^{\Upsilon t}v_5$, $C = e^{\Upsilon t}v_6$, $M = e^{\Upsilon t}v_7$, $G = e^{\Upsilon t}v_8$, $Z = e^{\Upsilon t}v_9$, $\Upsilon_1 = e^{-\Upsilon t}w_1$, $\Upsilon_2 = e^{-\Upsilon t}w_2$, $\Upsilon_3 = e^{-\Upsilon t}w_3$, $\Upsilon_4 = e^{-\Upsilon t}w_4$, $\Upsilon_5 = e^{-\Upsilon t}w_5$, $\Upsilon_6 = e^{-\Upsilon t}w_6$, $\Upsilon_7 = e^{-\Upsilon t}w_7$, $\Upsilon_8 = e^{-\Upsilon t}w_8$ and $\Upsilon_9 = e^{-\Upsilon t}w_9$. Similarly, let $\bar{S} = e^{\Upsilon t}\bar{v}_1$, $\bar{H} = e^{\Upsilon t}\bar{v}_2$, $\bar{X} = e^{\Upsilon t}\bar{v}_3$, $\bar{R} = e^{\Upsilon t}\bar{v}_4$, $\bar{T} = e^{\Upsilon t}\bar{v}_5$, $\bar{C} = e^{\Upsilon t}\bar{v}_6$, $\bar{M} = e^{\Upsilon t}\bar{v}_7$, $\bar{G} = e^{\Upsilon t}\bar{v}_8$, $\bar{Z} = e^{\Upsilon t}\bar{v}_9$, $\bar{\Upsilon}_1 = e^{-\Upsilon t}\bar{w}_1$, $\bar{\Upsilon}_2 = e^{-\Upsilon t}\bar{w}_2$, $\bar{\Upsilon}_3 = e^{-\Upsilon t}\bar{w}_3$, $\bar{\Upsilon}_4 = e^{-\Upsilon t}\bar{w}_4$, $\bar{\Upsilon}_5 = e^{-\Upsilon t}\bar{w}_5$, $\bar{\Upsilon}_6 = e^{-\Upsilon t}\bar{w}_6$, $\bar{\Upsilon}_7 = e^{-\Upsilon t}\bar{w}_7$, $\bar{\Upsilon}_8 = e^{-\Upsilon t}\bar{w}_8$ and $\bar{\Upsilon}_9 = e^{-\Upsilon t}\bar{w}_9$. Further, we let

$$u_1^*(t) = \max\left\{\min\left\{\frac{\beta_s(w_3 - w_2)v_1v_2e^{\Upsilon t}}{B_1}, 1\right\}, 0\right\},$$
$$\bar{u}_1^*(t) = \max\left\{\min\left\{\frac{\beta_s(\bar{w}_3 - \bar{w}_2)\bar{v}_1\bar{v}_2e^{\Upsilon t}}{B_1}, 1\right\}, 0\right\} \quad \text{and}$$

$$|u_1^*(t) - \bar{u}_1^*(t)| \leq \frac{e^{\Upsilon t}\beta_s}{B_1}\left|((w_3 - w_2)v_1v_2 - (\bar{w}_3 - \bar{w}_2)\bar{v}_1\bar{v}_2)\right|; \tag{7.29}$$

$$u_2^*(t) = \max\left\{\min\left\{\frac{\beta_r(w_5 - w_4)v_5v_4e^{\Upsilon t}}{(1 + \alpha e^{\Upsilon t}v_9)B_2}, 1\right\}, 0\right\},$$
$$\bar{u}_2^*(t) = \max\left\{\min\left\{\frac{\beta_r(\bar{w}_5 - \bar{w}_4)\bar{v}_5\bar{v}_4e^{\Upsilon t}}{(1 + \alpha e^{\Upsilon t}\bar{v}_9)B_2}, 1\right\}, 0\right\} \quad \text{and}$$

$$|u_2^*(t) - \bar{u}_2^*(t)| \leq \frac{e^{\Upsilon t}\beta_r}{B_2}\left|\frac{(w_5 - w_4)v_5v_4(1 + \alpha e^{\Upsilon t}\bar{v}_9) - (\bar{w}_5 - \bar{w}_4)\bar{v}_5\bar{v}_4(1 + \alpha e^{\Upsilon t}v_9)}{(1 + \alpha e^{\Upsilon t}v_9)(1 + \alpha e^{\Upsilon t}\bar{v}_9)}\right|; \tag{7.30}$$

$$u_3^*(t) = \max\left\{\min\left\{\frac{w_8v_8 + w_7v_3\mu_x N}{B_3}, 1\right\}, 0\right\},$$
$$\bar{u}_3^*(t) = \max\left\{\min\left\{\frac{\bar{w}_8\bar{v}_8 + \bar{w}_7\bar{v}_3\mu_x N}{B_3}, 1\right\}, 0\right\}$$

and

$$|u_3^*(t) - \bar{u}_3^*(t)| \leq \frac{1}{B_3}\left|(w_8v_8 - \bar{w}_8\bar{v}_8) + \mu_x N(w_7v_3 - \bar{w}_7\bar{v}_3)\right|; \tag{7.31}$$

$$u_4^*(t) = \max\left\{\min\left\{\frac{w_7\mu_c(1-\pi)Pv_6}{(1+\alpha e^{\Upsilon t}v_9)B_4}, 1\right\}, 0\right\},$$
$$\bar{u}_4^*(t) = \max\left\{\min\left\{\frac{\bar{w}_7\mu_c(1-\pi)P\bar{v}_6}{(1+\alpha e^{\Upsilon t}\bar{v}_9)B_4}, 1\right\}, 0\right\}$$

and

$$|u_4^*(t) - \bar{u}_4^*(t)| \leq \frac{\mu_c(1-\pi)P}{B_4}\left|\frac{w_7v_6(1+\alpha e^{\Upsilon t}\bar{v}_9) - \bar{w}_7\bar{v}_6(1+\alpha e^{\Upsilon t}v_9)}{(1+\alpha e^{\Upsilon t}v_9)(1+\alpha e^{\Upsilon t}\bar{v}_9)}\right|. \tag{7.32}$$

Substituting $S = e^{\Upsilon t}v_1$ into the first equation of system (7.1), $(\mathrm{d}S/\mathrm{d}t)$, the state equation becomes

$$e^{\Upsilon t}(\dot{v}_1 + \Upsilon v_1) = \Upsilon - \mu_s v_1 e^{\Upsilon t} - \beta_s v_2 v_1 e^{2\lambda t}. \tag{7.33}$$

Similarly, substituting $\Upsilon_1 = e^{-\Upsilon t}w_1$ into the first equation of system (7.9), $(\mathrm{d}\Upsilon_1/\mathrm{d}t)$, the adjoint equation becomes

$$e^{-\Upsilon t}(\dot{w}_1 - \Upsilon w_1) = (w_2 - w_3)(1 - u_1^*(t))\beta_s v_2 + \mu_s w_1 e^{-\Upsilon t} + \beta_s w_1 v_2. \tag{7.34}$$

Now, subtracting the equations for S and $\bar{S}$ in equation (7.33), Υ_1 and $\bar{\Upsilon}_1$ in equation (7.34) gives

$$\Upsilon(v_1 - \bar{v}_1) + (\dot{v}_1 - \dot{\bar{v}}_1) = -\mu_s(v_1 - \bar{v}_1) - \beta_s e^{\Upsilon t}(v_1v_2 - \bar{v}_1\bar{v}_2) \quad \text{and} \tag{7.35}$$
$$\Upsilon(w_1 - \bar{w}_1) + (\dot{w}_1 - \dot{\bar{w}}_1) = (1 - u_1^*)\beta_s e^{\Upsilon t}\{v_2(w_2 - w_3) - \bar{v}_2(\bar{w}_2 - \bar{w}_3)\} + \mu_s(w_1 - w_1)$$
$$+ \beta_s e^{\Upsilon t}(w_1v_2 - \bar{w}_1\bar{v}_2). \tag{7.36}$$

Then multiply each equation by the appropriate difference of functions ($(v_1-\bar{v}_1)$ and $(w_1-\bar{w}_1)$, respectively) and integrate from 0 to t_f. This gives (for case of equation (7.35))

$$\frac{1}{2}(v_1-\bar{v}_1)^2+\Upsilon\int_0^{t_f}(v_1-\bar{v}_1)^2dt$$
$$=-\mu_s\int_0^{t_f}(v_1-\bar{v}_1)^2dt-\beta_s e^{\Upsilon t}\int_0^{t_f}(v_1v_2-\bar{v}_1\bar{v}_2)(v_1-\bar{v}_1)dt. \tag{7.37}$$

Following the same procedure for the remaining state variables and adjoint variables (for H and $\bar{H}$, X and $\bar{X}$, R and $\bar{R}$, T and $\bar{T}$, C and $\bar{C}$, M and $\bar{M}$, G and $\bar{G}$, Z and $\bar{Z}$), the following equations are obtained:

$$\frac{1}{2}(v_2-\bar{v}_2)^2+\Upsilon\int_0^{t_f}(v_2-\bar{v}_2)^2dt$$
$$=-\mu_h\int_0^{t_f}(v_2-\bar{v}_2)^2dt-\beta_s\int_0^{t_f}(1-u_1^*)(v_1v_2-\bar{v}_1\bar{v}_2)(v_2-\bar{v}_2)e^{\Upsilon t}dt, \tag{7.38}$$

$$\frac{1}{2}(v_3-\bar{v}_3)^2+\Upsilon\int_0^{t_f}(v_3-\bar{v}_3)^2dt$$
$$=-\mu_x\int_0^{t_f}(v_3-\bar{v}_3)^2dt+\beta_s\int_0^{t_f}(1-u_1^*)(v_1v_2-\bar{v}_1\bar{v}_2)(v_3-\bar{v}_3)e^{\Upsilon t}dt$$
$$-k_x\int_0^{t_f}\left(\frac{v_3v_9}{1+\varepsilon_0e^{\Upsilon t}v_3}-\frac{\bar{v}_3\bar{v}_9}{1+\varepsilon_0e^{\Upsilon t}\bar{v}_3}\right)(v_3-\bar{v}_3)e^{\Upsilon t}dt, \tag{7.39}$$

$$\frac{1}{2}(v_4-\bar{v}_4)^2+\Upsilon\int_0^{t_f}(v_4-\bar{v}_4)^2\,dt$$
$$=-\beta_r\int_0^{t_f}(1-u_2^*)\left(\frac{v_4v_7}{1+\alpha e^{\Upsilon t}v_9}-\frac{\bar{v}_4\bar{v}_7}{1+\alpha e^{\Upsilon t}\bar{v}_9}\right)(v_4-\bar{v}_4)e^{\Upsilon t}dt$$
$$-\mu_r\int_0^{t_f}(v_4-\bar{v}_4)^2\,dt, \tag{7.40}$$

$$\frac{1}{2}(v_5-\bar{v}_5)^2+\Upsilon\int_0^{t_f}(v_5-\bar{v}_5)^2dt$$
$$=\beta_r\int_0^{t_f}(1-u_2^*)\left(\frac{v_4v_7}{1+\alpha e^{\Upsilon t}v_9}-\frac{\bar{v}_4\bar{v}_7}{1+\alpha e^{\Upsilon t}\bar{v}_9}\right)(v_5-\bar{v}_5)e^{\Upsilon t}\,dt$$
$$-k_t\int_0^{t_f}\left(\frac{v_5v_9}{1+\varepsilon_1e^{\Upsilon t}v_5}-\frac{\bar{v}_5\bar{v}_9}{1+\varepsilon_1e^{\Upsilon t}\bar{v}_5}\right)(v_5-\bar{v}_5)e^{\Upsilon t}\,dt$$
$$-(\mu_t+\gamma)\int_0^{t_f}(v_5-\bar{v}_5)^2\,dt, \tag{7.41}$$

$$\frac{1}{2}(v_6-\bar{v}_6)^2+\Upsilon\int_0^{t_f}(v_6-\bar{v}_6)^2dt$$
$$=\gamma\int_0^{t_f}(v_5-\bar{v}_5)(v_6-\bar{v}_6)\,dt-\mu_c\int_0^{t_f}(v_6-\bar{v}_6)^2\,dt$$
$$-k_c\int_0^{t_f}\left(\frac{v_6v_9}{1+\varepsilon_2e^{\Upsilon t}v_6}-\frac{\bar{v}_6\bar{v}_9}{1+\varepsilon_2e^{\Upsilon t}\bar{v}_6}\right)(v_6-\bar{v}_6)e^{\Upsilon t}\,dt, \tag{7.42}$$

$$\frac{1}{2}(v_7-\bar{v}_7)^2+\Upsilon\int_0^{t_f}(v_7-\bar{v}_7)^2dt$$
$$=\mu_xN\int_0^{t_f}(1-u_3^*)(v_3-\bar{v}_3)(v_7-\bar{v}_7)\,dt$$
$$-(1-\pi)P\mu_c\int_0^{t_f}(1-u_4^*)\left(\frac{v_6}{1+\alpha e^{\Upsilon t}v_9}-\frac{\bar{v}_6}{1+\alpha e^{\Upsilon t}\bar{v}_9}\right)(v_7-\bar{v}_7)\,dt$$
$$-\mu_m\int_0^{t_f}(v_7-\bar{v}_7)\,dt-\beta_r\int_0^{t_f}(v_4v_7-\bar{v}_4\bar{v}_7)(v_7-\bar{v}_7)\,dt, \tag{7.43}$$

$$\frac{1}{2}(v_8-\bar{v}_8)^2+\Upsilon\int_0^{t_f}(v_8-\bar{v}_8)^2dt$$
$$=\pi\mu_c\int_0^{t_f}(v_6-\bar{v}_6)(v_8-\bar{v}_8)\,dt-\int_0^{t_f}(u_3^*-\mu_g)(v_8-\bar{v}_8)^2\,dt, \tag{7.44}$$

$$\frac{1}{2}(v_9-\bar{v}_9)^2+\Upsilon\int_0^{t_f}(v_9-\bar{v}_9)^2dt$$
$$=\delta_x\int_0^{t_f}\left(\frac{v_3}{1+\varepsilon_0e^{\Upsilon t}v_3}-\frac{\bar{v}_3}{1+\varepsilon_0e^{\Upsilon t}\bar{v}_3}\right)(v_9-\bar{v}_9)e^{\Upsilon t}\,dt$$
$$\delta_t\int_0^{t_f}\left(\frac{v_5}{1+\varepsilon_1e^{\Upsilon t}v_5}-\frac{\bar{v}_5}{1+\varepsilon_1e^{\Upsilon t}\bar{v}_5}\right)(v_9-\bar{v}_9)e^{\Upsilon t}\,dt$$
$$\delta_c\int_0^{t_f}\left(\frac{v_6}{1+\varepsilon_2e^{\Upsilon t}v_6}-\frac{\bar{v}_6}{1+\varepsilon_2e^{\Upsilon t}\bar{v}_6}\right)(v_9-\bar{v}_9)e^{\Upsilon t}\,dt$$
$$-\mu_z\int_0^{t_f}(v_9-\bar{v}_9)^2\,dt. \tag{7.45}$$

Note that

$$
\begin{aligned}
(i)\quad & k_x \int_0^{t_f} \left(\frac{v_3 v_9}{1+\varepsilon_0 e^{\Upsilon t} v_3} - \frac{\bar{v}_3 \bar{v}_9}{1+\varepsilon_0 e^{\Upsilon t} \bar{v}_3} \right) (v_3 - \bar{v}_3) e^{\Upsilon t}\, dt \\
& = k_x \int_0^{t_f} \left(\frac{v_3 v_9 - \bar{v}_3 \bar{v}_9}{(1+\varepsilon_0 e^{\Upsilon t} v_3)(1+\varepsilon_0 e^{\Upsilon t} \bar{v}_3)} \right) (v_3 - \bar{v}_3) e^{\Upsilon t}\, dt \\
& + \varepsilon_0 k_x \int_0^{t_f} \left(\frac{v_3 v_9 \bar{v}_3 - \bar{v}_3 \bar{v}_9 v_3}{(1+\varepsilon_0 e^{\Upsilon t} v_3)(1+\varepsilon_0 e^{\Upsilon t} \bar{v}_3)} \right) (v_3 - \bar{v}_3) e^{2\Upsilon t}\, dt \\
& \leq (C_1 e^{\Upsilon t_f} + C_2 e^{2\Upsilon t_f}) \int_0^{t_f} [(v_3 - \bar{v}_3)^2 + (v_9 - \bar{v}_9)^2]\, dt
\end{aligned} \tag{7.46}
$$

and

$$
\begin{aligned}
(ii)\quad & \beta_s \int_0^{t_f} (1-u^*)(v_1 v_2 - \bar{v}_1 \bar{v}_2)(v_3 - \bar{v}_3)\, dt \\
& \leq C_3 e^{\Upsilon t_f} \int_0^{t_f} [(v_1 - \bar{v}_1)^2 + (v_2 - \bar{v}_2)^2 + (v_3 - \bar{v}_3)^2]\, dt.
\end{aligned} \tag{7.47}
$$

Upon combining the integrals in equations (7.37)-(7.45) gives

$$
\begin{aligned}
& \frac{1}{2}(v_1 - \bar{v}_1)^2(t_f) + \frac{1}{2}(v_2 - \bar{v}_2)^2(t_f) + \frac{1}{2}(v_3 - \bar{v}_3)^2(t_f) + \frac{1}{2}(v_4 - \bar{v}_4)^2(t_f) + \frac{1}{2}(v_5 - \bar{v}_5)^2(t_f) \\
& + \frac{1}{2}(v_6 - \bar{v}_6)^2(t_f) + \frac{1}{2}(v_7 - \bar{v}_7)^2(t_f) + \frac{1}{2}(v_8 - \bar{v}_8)^2(t_f) + \frac{1}{2}(v_9 - \bar{v}_9)^2(t_f) \\
& + \frac{1}{2}(w_1 - \bar{w}_1)^2(0) + \frac{1}{2}(w_2 - \bar{w}_2)^2(0) + \frac{1}{2}(w_3 - \bar{w}_3)^2(0) + \frac{1}{2}(w_4 - \bar{w}_4)^2(0) \\
& + \frac{1}{2}(w_5 - \bar{w}_5)^2(0) + \frac{1}{2}(w_6 - \bar{w}_6)^2(0) + \frac{1}{2}(w_7 - \bar{w}_7)^2(0) + \frac{1}{2}(w_8 - \bar{w}_8)^2(0) \\
& + \frac{1}{2}(w_9 - \bar{w}_9)^2(0) + \Upsilon \int_0^{t_f} [(v_1 - v_1)^2 + (v_2 - v_2)^2 + (v_3 - v_3)^2 + (v_4 - v_4)^2 \\
& + (v_5 - v_5)^2 + (v_6 - v_6)^2 + (v_7 - v_7)^2 + (v_8 - v_8)^2 + (v_9 - v_9)^2 + (w_1 - w_1)^2 \\
& + (w_2 - w_2)^2 + (w_3 - w_3)^2 + (w_4 - w_4)^2 + (w_5 - w_5)^2 + (w_6 - w_6)^2 \\
& + (w_7 - w_7)^2 + (w_8 - w_8)^2 + (w_9 - w_9)^2]\, \mathrm{d}t
\end{aligned} \tag{7.48}
$$

$$
\begin{aligned}
& \leq (\Upsilon - \bar{D}_1 - \bar{D}_2 e^{3\Upsilon t_f}) \\
& \times \left\{ \int_0^{t_f} [(v_1 - v_1)^2 + (v_2 - v_2)^2 + (v_3 - v_3)^2 + (v_4 - v_4)^2 + (v_5 - v_5)^2 + (v_6 - v_6)^2 \right. \\
& + (v_7 - v_7)^2 + (v_8 - v_8)^2 + (v_9 - v_9)^2] + \int_0^{t_f} [(w_1 - w_1)^2 + (w_2 - w_2)^2 \\
& + (w_3 - w_3)^2 + (w_4 - w_4)^2 + (w_5 - w_5)^2 + (w_6 - w_6)^2 + (w_7 - w_7)^2 \\
& \left. + (w_8 - w_8)^2 + (w_9 - w_9)^2] \right\},
\end{aligned} \tag{7.49}
$$

where $\bar{D}_1$ and $\bar{D}_2$ depend on the coefficients and the bounds of v_i and w_i, $i = 1, \cdots, 9$. If Υ is chosen such that $\Upsilon > (\bar{D}_1 + \bar{D}_2)$ and $t_f < (1/3\Upsilon)\ln((\Upsilon - \bar{D}_1)/\bar{D}_2)$, then $v_1 = \bar{v}_1$, $v_2 = \bar{v}_2$, $v_3 = \bar{v}_3$, $v_4 = \bar{v}_4$, $v_5 = \bar{v}_5$, $v_6 = \bar{v}_6$, $v_7 = \bar{v}_7$, $v_8 = \bar{v}_8$, $v_9 = \bar{v}_9$, $w_1 = \bar{w}_1$, $w_2 = \bar{w}_2$, $w_3 = \bar{w}_3$, $w_4 = \bar{w}_4$, $w_5 = \bar{w}_5$, $w_6 = \bar{w}_6$, $w_7 = \bar{w}_7$, $w_8 = \bar{w}_8$, $w_9 = \bar{w}_9$. Hence, the solution is unique for small time t_f.

The non-linear optimal controls are obtained by solving the optimality system (7.27)-(7.28), which combines the state system (7.1), the adjoint system (7.9), the initial conditions (7.2), boundary conditions (7.10) and the characteristics of the optimal functions (7.12)-(7.15). In order to solve the optimality system, the initial and transversality conditions are used alongside the characterisation of the optimal control (u_1, u_2, u_3, u_4) given in equations (7.12)-(7.15). We therefore obtain optimal control measures through numerical simulations, in the next section. The optimal control set $u_i^*, i = 1, \cdots, 4$ gives an optimal control strategy against in-host *P. falciparum* malaria infection.

7.5 Numerical simulations

In this section, we study the numerical results obtained from the optimal control model (7.1). The backward-forward sweep (BFS) algorithm (Lenhart and Workman, 2007) and the fourth-order Runge-kutta scheme in Matlab (Ince, 1943) are applied to solve the optimality system. The BFS algorithm has been implemented in several research studies (Joshi et al., 2006; Nakakawa et al., 2017; Namawejje et al., 2014; Okosun et al., 2011; Omondi et al., 2018). The optimal control code presented by Lenhart and Workman (2007) is modified to solve the optimality system (7.27). The initial conditions S_0, H_0, X_0, R_0, T_0, C_0, M_0, G_0, Z_0, and $\bar{u}_i$ are used to solve for the state variables $\bar{x} = (S, H, X, R, T, C, M, G, Z)$ forward in time using Runge-kutta fourth-order scheme in Matlab. The adjoint system $\bar{\Upsilon}_i, i = 1, \cdots, 9$ is solved backward in time using the transversality condition $\Upsilon_i(t_f) = 0$ and the values of $\bar{x}$ and $\bar{u}$. The control variables $\bar{u}$ are then updated in the second iteration by entering the new values of the state and adjoint variables. This process is repeated until convergence is achieved.

The parameter values used in the simulations are obtained from existing literature on in-host malaria modelling and control. These are as presented in Table 7.2. Other parameter values are however assumed. The retail price of ACTs in sub-Saharan Africa is roughly 5-7 US dollars ($) (Palafox et al., 2015). The median price of AL (the blood schizontocide) is $5.26 in Uganda, $6.03 in Benin, $4.58 in DRC, $5.36 in Nigeria and $5.36 in Zambia (Palafox et al., 2015). A cross-sectional study on the availability and retail prices of antimalarial drugs

in rural Western Kenya (Kioko et al., 2016), revealed that the mean price (range) of an adult treatment course for AL was $4.5 ($0.35–5) while DHA-PPQ was $4.39 ($0.71–7.06). Penny et al. (2016), estimated the cost per dose of RTS,S/AS01 to be $6.52 ($2.69 –$12.9). In this study, the average retail price of $5 for AL and PQ per dose are assumed. Additionally, the pre-erythrocytic vaccine (RTS,S/AS01) is considered highly cost-effective and is estimated to assume a mid-range cost of $5 per dose under a four-dose schedule (Winskill et al., 2017b). This implies a unit cost of $39.25 is incurred per fully vaccinated child (Penny et al., 2016; Winskill et al., 2017b). It is further assumed that the blood-stage vaccine would bear a similar cost of $5 ($\approx$ Kshs. 500) per dose. Therefore, the costs $A_1 = A_2 = \$39.25\,(\approx Kshs.3925)$. Similarly, $A_3 = A_4 = \$5\,(\approx Kshs.500)$.

Malaria treatment using ACTs have made a significant contribution to current success in malaria control efforts. For the period 2014-2017, WHO spent about US $11.71, $13.70, $12.53 and $14.18 per malaria cases averted, respectively. The 2015 World malaria report showed that about 663 million malaria cases were averted for the period 2001-2015 (WHO, 2016b); of these cases, 21% (17%, 29%) were averted due to ACT use. Therefore, an average of US $11.90 was spent per year on malaria cases averted by ACTs in the period 2014-2017. Additionally, a report by the President's Malaria Initiative (PMI), estimated that about US $94 (95% CI: $51, $166) was spent per disability adjusted life year (DALY) averted for the period 2005-2017 (Winskill et al., 2017a). This represents about US $7.80 per cases averted per year. Unlike the efficacies of antimalarial drugs (95%), the vaccines considered in this study have a moderate efficacy of 75%. The weight constants B_1, B_2, B_3 and B_4 are hence assigned a slighly lower average value of US $7.5 ($\approx$ Kshs. 750). That is, $B_1 = B_2 = B_3 = B_4 = 750$.

In Figures 7.4 - 7.15, the coefficients $A_1 = A_2 = 3925$, $A_3 = A_4 = 500$ and $B_i = 750, i = 1, \cdots, 4$. The initial conditions $S(0) = 3000$, $H(0) = 3 \times 10^5$, $X(0) = 5 \times 10^2$, $R(0) = 5 \times 10^6$, $T(0) = 5 \times 10^3$, $C(0) = 5000$, $M(0) = 9000$, $G(0) = 5000$, $Z(0) = 3000$ are used to illustrate the effects of various control strategies against in-host *P. falciparum* malaria infections. Arbitrary initial conditions were chosen because the presented model (with constant vaccine control) exhibits global stability behaviour (see Chapter 4). Note that all the possible set of control combinations were considered in this study. However, only those that gave substantial decrease in the populations pre-defined in the objective function (7.4) are presented. To simplify the analyses, the four controls are grouped into the following six categories:

- Strategy 1: A combination of two controls
  - (1A) A combination of blood schizontocide and gametocytocide only: $u_1 = 0, u_2 = 0, u_3 \neq 0, u_4 \neq 0$.

  - (1B) A combination of pre-erythrocytic and blood stage vaccine antigens only: $u_1 \neq 0, u_2 \neq 0, u_3 = 0, u_4 = 0,$.
  - (1C) A combination of pre-erythrocytic vaccine and blood schizontocide drugs only: $u_1 \neq 0, u_2 = 0, u_3 \neq 0, u_4 = 0$.
- Strategy 2: A combination of three controls
  - (2A) Pre-erythrocytic vaccine antigen, blood stage vaccine antigen and blood schizontocide only: $u_1 \neq 0, u_2 \neq 0, u_3 \neq 0, u_4 = 0$.
  - (2B) Pre-erythrocytic vaccine antigen, blood schizontocide and gametocytocide only: $u_1 \neq 0, u_2 = 0, u_3 \neq 0, u_4 \neq 0$.
- Strategy 3: A combination of all the four controls (pre-erythrocytic vaccine antigen, blood stage vaccine antigen, blood schizontocide and gametocytocide) : $u_1 \neq 0, u_2 \neq 0, u_3 \neq 0, u_4 \neq 0$.

Table 7.2: Table showing parameter values used for model simulations

Parameter	Value	Range	Units	Source
P	16	(15-20)	Unitless	(Diebner et al., 2000)
k_x	0.01	(0.001-0.9)	/day	(Chiyaka et al., 2008)
k_t	0.02	(0.003-0.9)	/day	(Chiyaka et al., 2008)
k_c	0.001	(0.001-0.9)	/day	(Chiyaka et al., 2008)
μ_r	0.083	(0.05-0.1)	/day	(Anderson et al., 1989)
β_r	0.02	(0.01-0.3)	$/mm^3$/day	(Dondorp et al., 2000)
β_s	0.001	(0.0001-0.2)	$/mm^3$/day	(Selemani et al., 2016)
π	0.2	(0.1-0.9)	Unitless	(Talman et al., 2004)
μ_h	0.029	(0.01-0.5)	/day	Estimated
μ_x	0.02	(0.01-1)	/day	(Selemani et al., 2016)
λ_r	3000	$(300 - 3 \times 10^5)$	cells/ml/day	(Li et al., 2011)
λ_h	3000	$(3 \times 10^5 - 3 \times 10^8)$	cells/μl^{-1}/day	(Tumwiine et al., 2008)
λ_z	30	(10-40)	/μl^{-1}/day	(Chiyaka, 2010)
μ_m	48	(46-50)	/day	(Li et al., 2011)
Λ	30	(18-35)	sporozoites/day	(Selemani et al., 2016)
μ_s	1.2	$(1.0 - 2.4)$	/day	(Selemani et al., 2016)
μ_t	0.27	(0.01-0.8)	/day	(Magombedze et al., 2011a)
μ_c	0.7	(0.1-0.9)	/day	(Magombedze et al., 2011a)

Continued on next page

Table 7.2 – *Continued from previous page*

Parameter	Value	Range	Units	Source
μ_g	6.3×10^{-5}	$(6.0 - 7.0) \times 10^{-5}$	/day	(Selemani et al., 2016)
μ_z	2	(0.5-3)	/day	(Chiyaka, 2010)
δ_x	10^{-5}	(10^{-4}-10^{-7})	mm^{-3}/day	(Chiyaka, 2010)
δ_t	10^{-6}	(10^{-5}-10^{-7})	mm^{-3}/day	(Chiyaka, 2010)
δ_c	10^{-4}	(10^{-3}-10^{-7})	mm^{-3}/day	(Chiyaka, 2010)
γ	1.5	(0.1-2)	/day	(Selemani et al., 2016)
ε_0	1E-5	(1E-6, 1E-4)	/day	(Tumwiine et al., 2008)
ε_1	1E-4	(1E-6, 1E-4)	/day	(Tumwiine et al., 2008)
ε_2	1E-6	(1E-7, 1E-4)	/day	(Tumwiine et al., 2008)
α	5E-4	(5E-5-2E-2)	Unitless	(Magombedze et al., 2011a)
N	10^4	(8E+3-2E+5)	Unitless	(Tumwiine et al., 2008)

7.5.1 Simulation results

The impact of employing strategy (1A) (a combination of blood schizontocide and gametocytocide only) in the control of *P. falciparum* infection in humans is as presented in Figure 7.4. It is evident that an antimalarial drug with such a combination is highly effective in eradicating the merozoites and infected red blood cells as shown in Figures 7.4b and 7.4c, respectively. However, this combination strategy offers little effect on the population of infected hepatocytes as shown in Figure 7.4d. This is because these drugs are not active against the liver stage parasites or schizonts. Moreover, a moderate decrease in the population of gametocytes is also observed (see Figure 7.4a). Besides effective antimalarial drugs, it is clear that other therapeutic measures may be necessary to eradicate all parasites and infected cells during *P. falciparum* malaria infections. The control profile of strategy (1A) is shown in Figure 7.5.

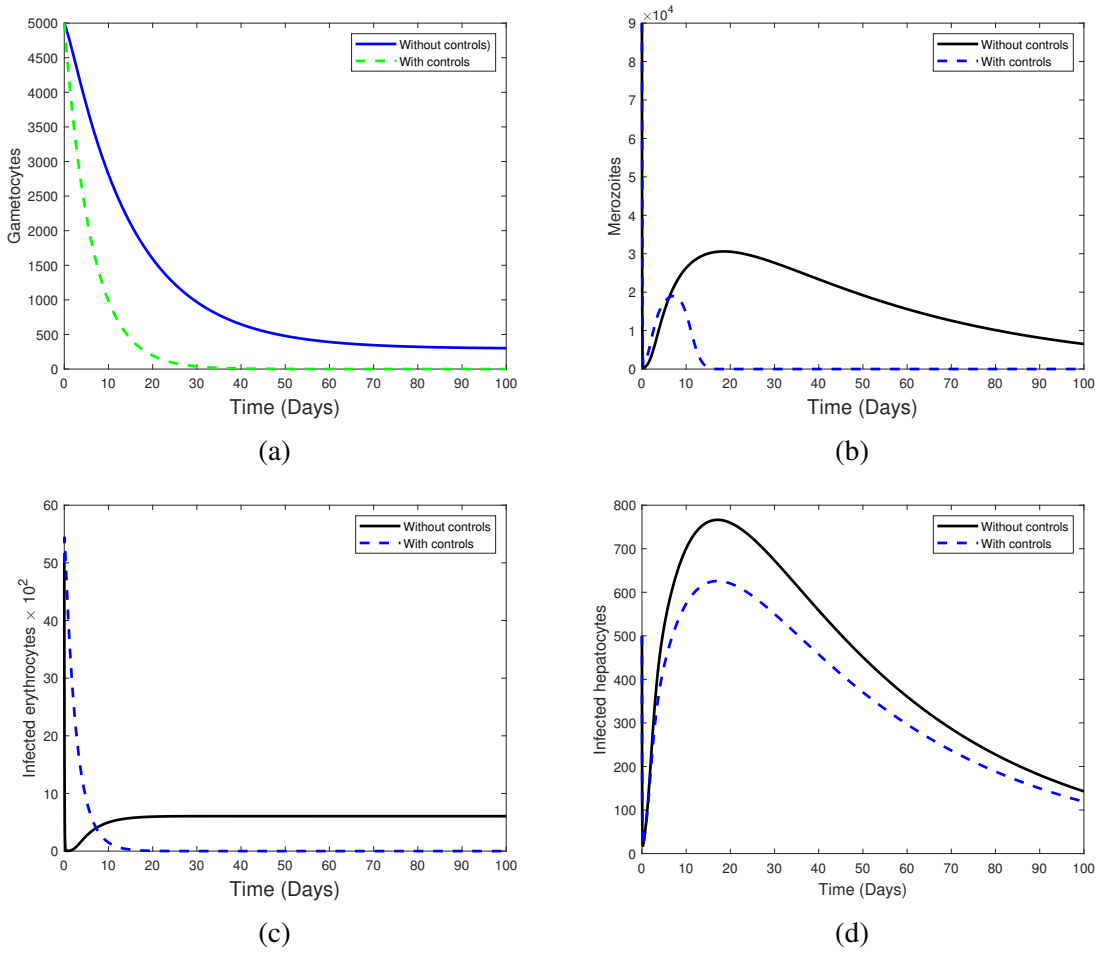

Figure 7.4: Simulations of system (7.1), showing the impact of a combination of blood schizontocide u_3 and a gametocitocide u_4 only during clinical *P. falciparum* malaria infection. Used parameter values are shown in Table 7.2.

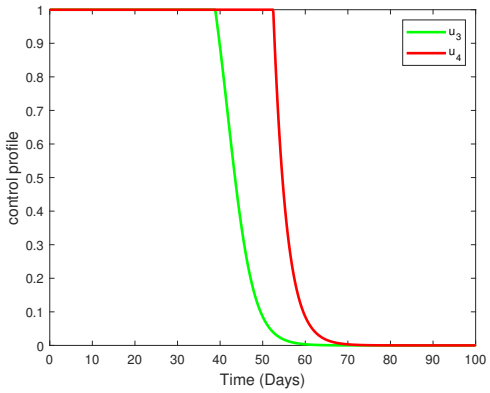

Figure 7.5: Profiles of blood schizontocide u_3 and gametocytocide u_4. Here, $u_1 = 0$, $u_2 = 0$.

In Figure 7.6, a combination of malaria vaccine antigens is considered. This corresponds to strategy (1B). The combination of pre-erythrocytic vaccine antigen u_1 and blood-stage vaccine antigen u_2 is shown to be very effective in decreasing the populations of infected erythrocytes (Figure 7.6c) and infected hepatocytes (Figure 7.6d). Although the merozoites are eradicated, this takes a slightly longer time, due to low vaccine efficacies (see Figure 7.6b). A 100% efficacy of PEV would, however, not require augmenting with BSV. Nevertheless, the efficacies of PEV and BSV is still likely to drop over time as the antibodies decay (Sherrard-Smith et al., 2018). The control profile under this strategy is presented in Figure 7.7. It is observed that the efficacies of the vaccines should be maintained high for the entire period of intervention.

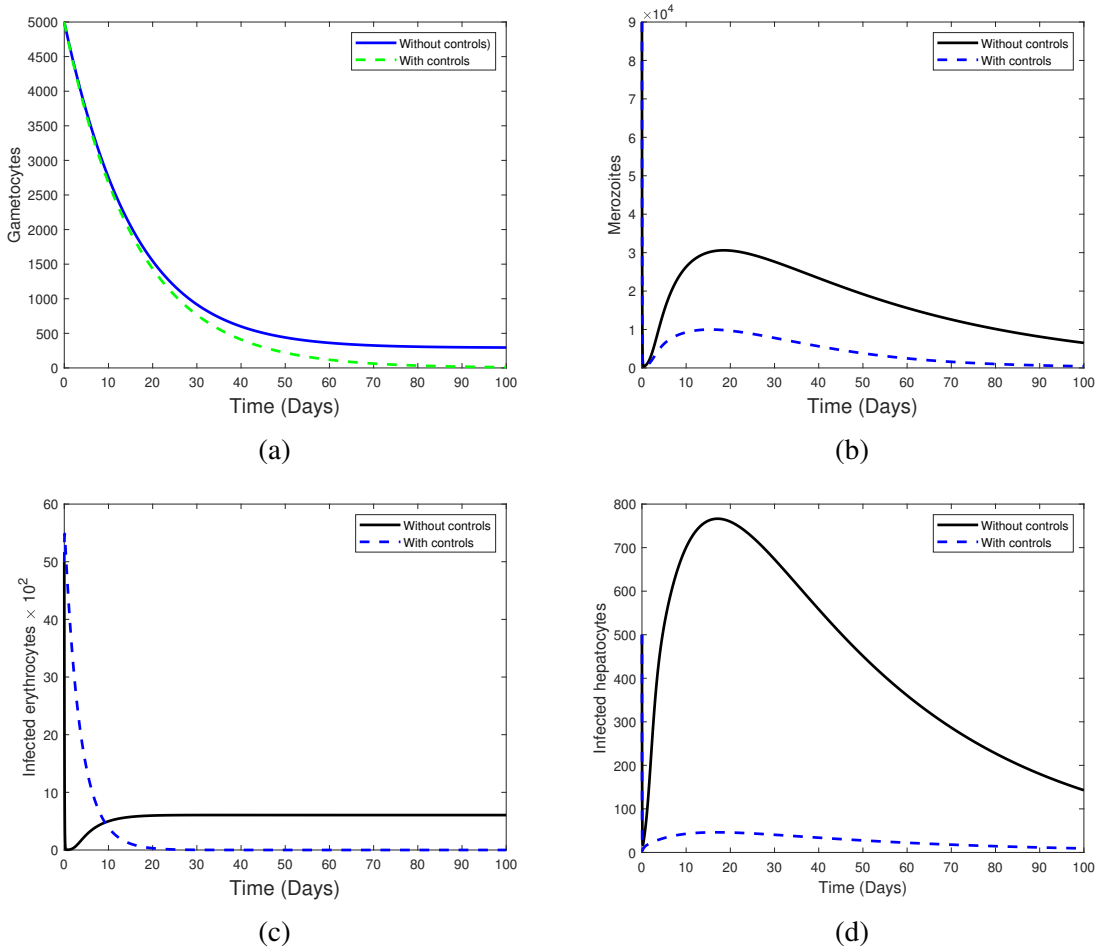

Figure 7.6: Simulations of system (7.1), showing the impact of a combination of pre-erythrocytic vaccine antigens u_1 with blood stage vaccine antigens u_2 only. Used parameter values are shown in Table 7.2.

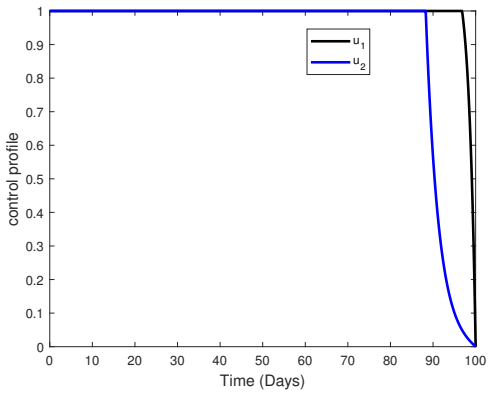

Figure 7.7: Profiles of pre-erythrocytic vaccine antigen u_1 and blood stage vaccine antigens u_2. Here, $u_3 = 0$, $u_4 = 0$.

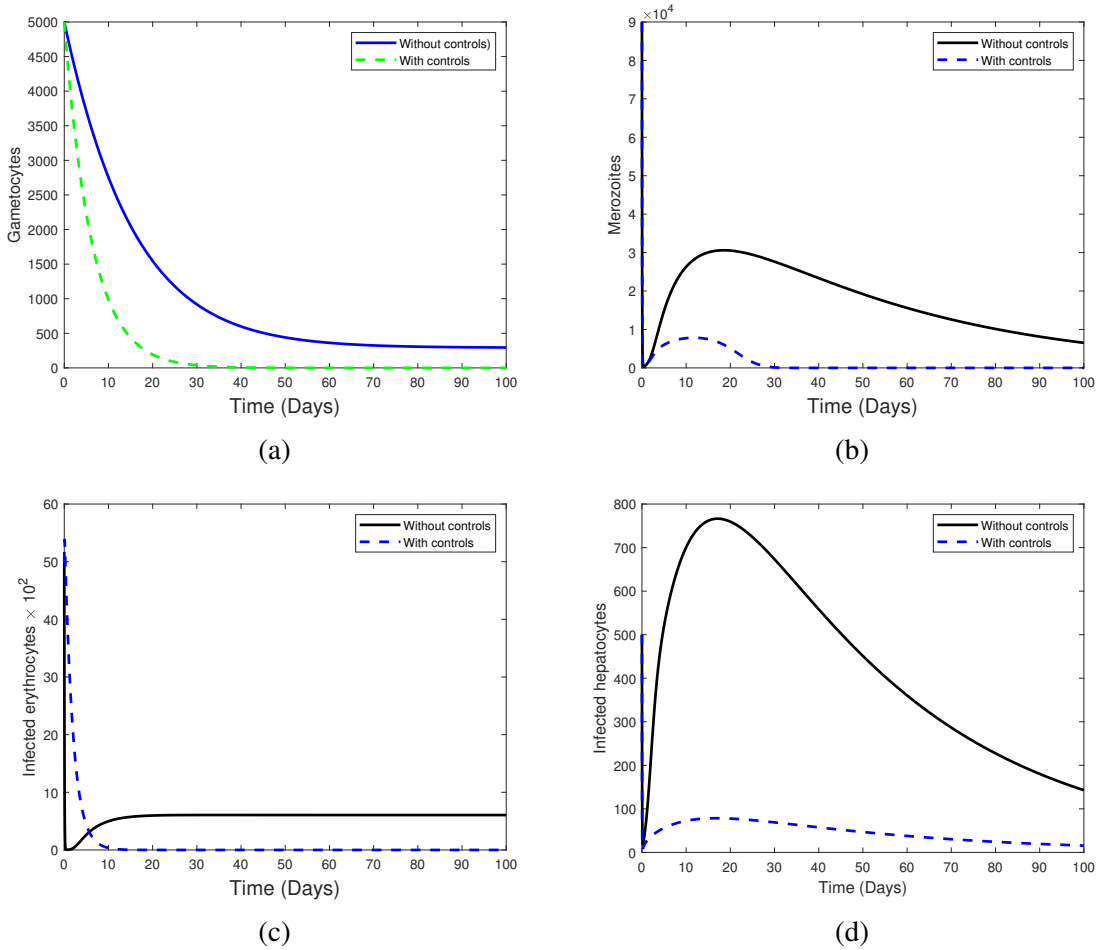

Figure 7.8: Simulations of system (7.1), showing the impact of a combining pre-erythrocytic malaria vaccine u_1 and blood schizontocides u_3 only in the control of within-human *P. falciparum* infection. Used parameter values are shown in Table 7.2.

The combined use of pre-erythrocytic vaccine and blood schizontocide, strategy (1C), is shown to greatly decrease the population of infected erythrocytes and infected hepatocytes in Figures 7.8c and 7.8d, respectively. Unlike strategies (1A) and (1B), this third strategy (IC) is slightly more effective; it eradicates the merozoites and gametocytes within 30 days of infection (see Figures 7.8a and 7.8b). Additionally, this strategy has a maximum duration of 11 days before it eradicates all infected erythrocytes from the host. To guarantee total eradication of all infected cells and infective parasites, the used antimalarial drug should be highly effective (efficacy $> 95\%$). The moderate effect of this strategy on the gametocyte population means that the treated malaria patients would facilitate parasite transmission to the mosquito vector, increasing future malaria cases and mortality. Figure 7.9 shows the profile of the control measures in this strategy. The efficacy of the pre-erythrocyte vaccine (u_1) should be maintained throughout the control period. Similarly, the effectiveness of blood schizontocide (u_3) should remain high for at least half of the intervention period.

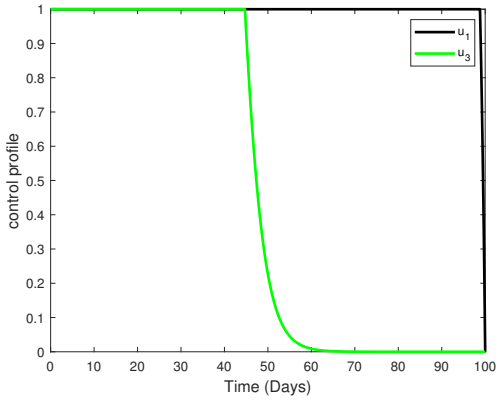

Figure 7.9: Profiles of pre-erythrocytic vaccine antigen u_1 and blood schizontocide drug u_3. Here, $u_2 = 0$, $u_4 = 0$.

If two or more vaccines and antimalarial drugs are combined, then different outcomes are observed as presented in Figures 7.10-7.15. In Figure 7.10, blood schizontocide u_3 is used to treat malaria patients who have received a combination of pre-erythrocytic vaccine antigens u_1 and blood stage vaccine antigens u_2. This defines strategy (2A). The control profiles of $u_1 \neq 0$, $u_2 \neq 0$ and $u_3 \neq 0$ are presented in Figure 7.11. Although there is a general decrease in the populations of infected cells and infective parasite, the rate of decline is moderate and the clearance of gametocytes lasts longer than 20 days. A better result is however, presented in Figure 7.12. In this strategy (2B), a combination of blood schizontocide u_3 and gametocytocides u_4 is administered to a malaria patient who is already on a pre-erythrocytic vaccine u_1. A rapid rate of decline in populations of infected erythrocytes,

infected hepatocytes, merozoites and gametocytes is observed. The density of gametocytes fall exponentially; within 15 days of blood stage malaria. It is also noted that total eradication of merozoite parasites from the human host occurs within two weeks of infection. The profiles of the three control measures are displayed in Figure 7.13.

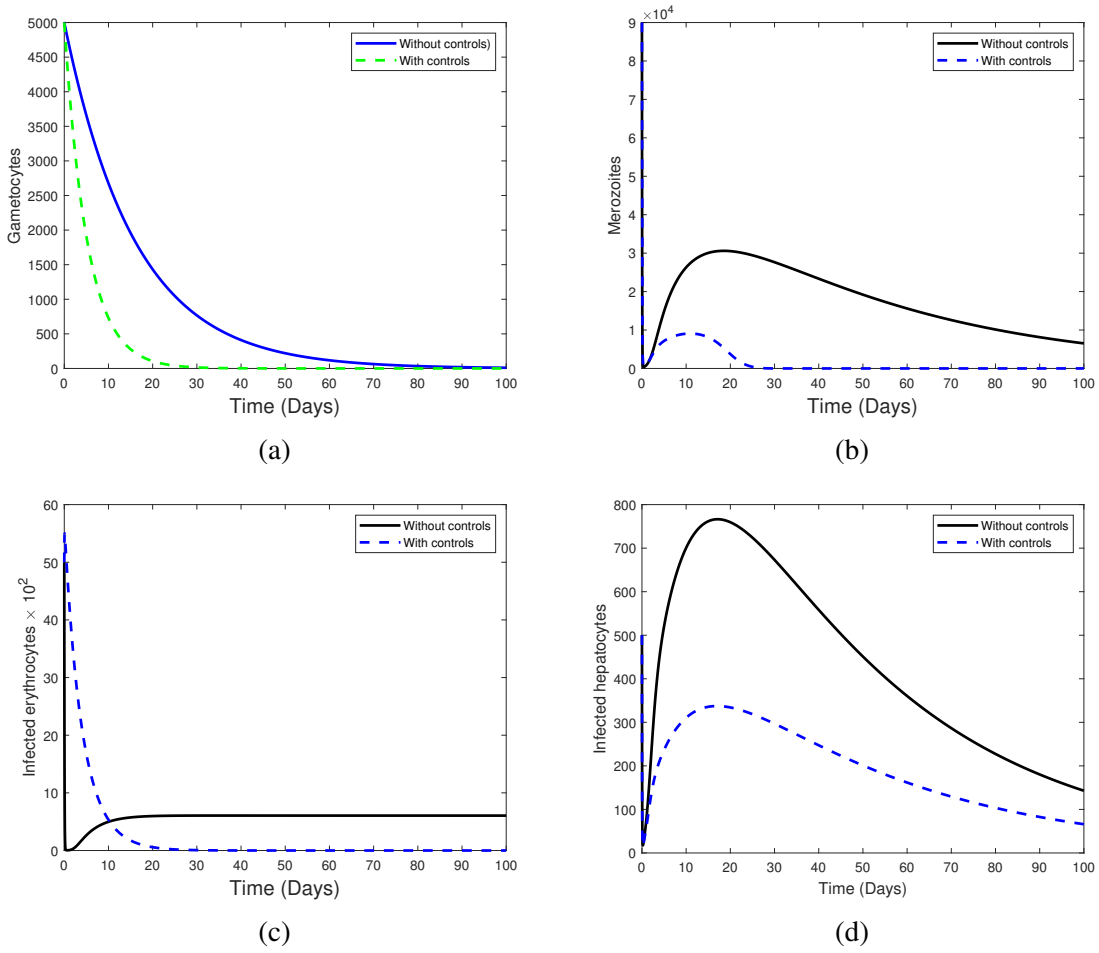

Figure 7.10: Simulations of system (7.1), showing the impact of a combination of pre-erythrocytic vaccine antigens u_1, blood stage vaccine antigens u_2 and blood schizontocide u_3 only. Used parameter values are shown in Table 7.2.

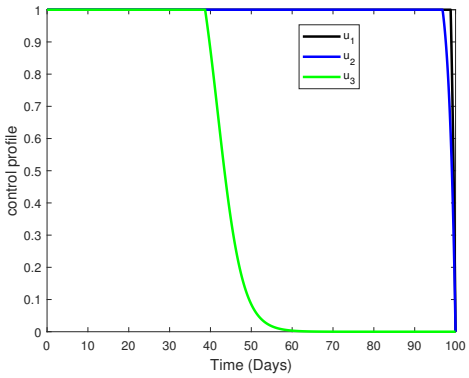

Figure 7.11: Profiles of pre-erythrocytic vaccine antigen u_1, blood stage vaccine antigen u_2 and blood schizontocide u_3. Here, $u_4 = 0$.

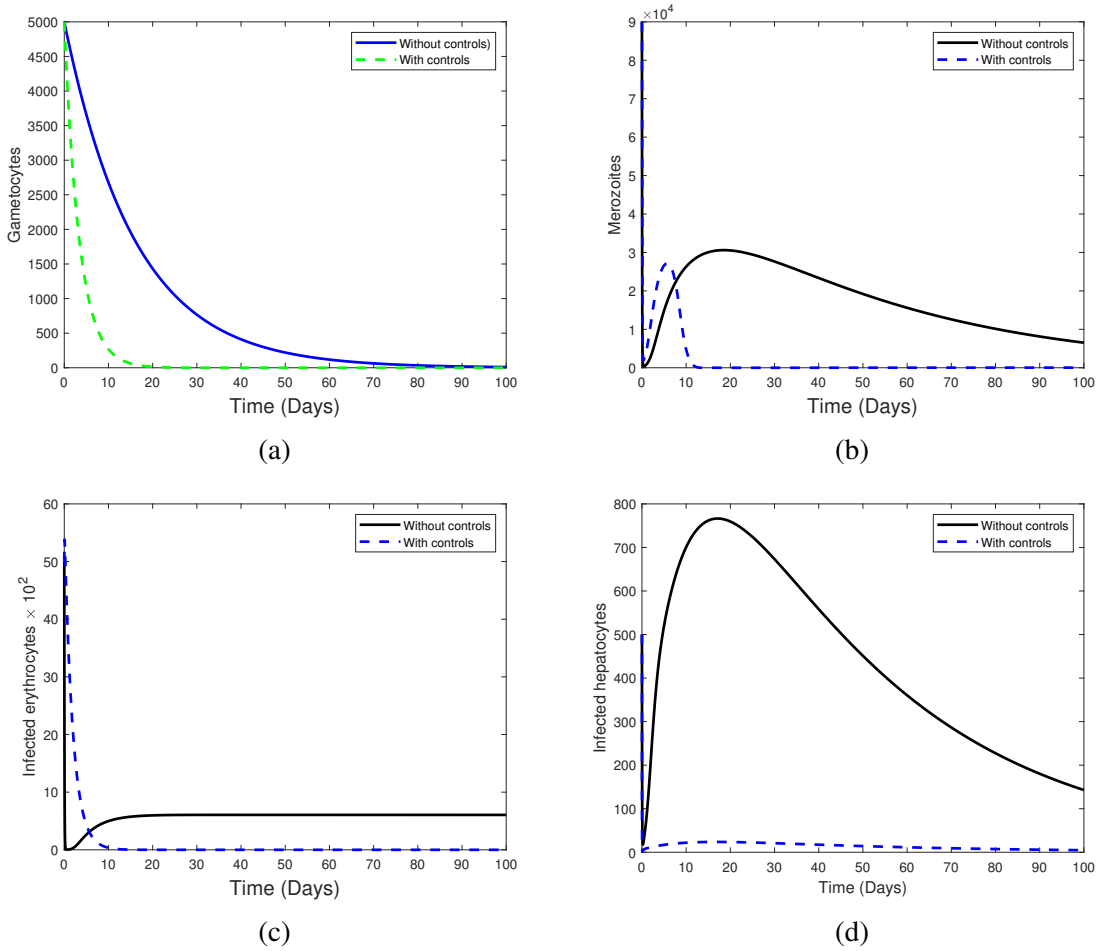

Figure 7.12: Simulations of system (7.1), showing the impact of a combination of pre-erythrocytic vaccine u_1, blood schizontocide u_3 and gametocitocidal drug u_4. Used parameter values are shown in Table 7.2.

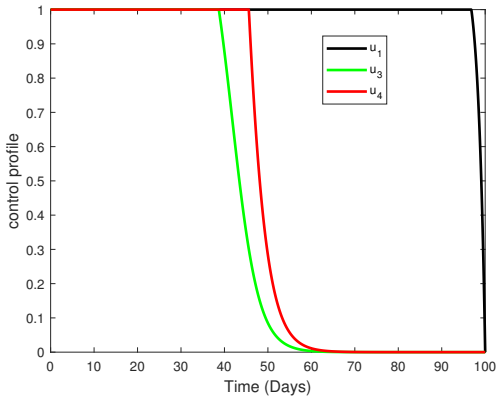

Figure 7.13: Profiles of pre-erythrocytic vaccine antigen u_1, blood schizontocide u_3 and gametocytocide u_4. Here $u_2 = 0$.

Finally, in Figure 7.14, all the four control efforts are employed (strategy 3). Here, anti-malarial drugs consisting of blood schizontocides and gametocytocides are administered to malaria patients who are equally on a combined pre-erythrocytic and blood stage vaccine antigens. Just like in strategy (2B), tremendous decline is observed in the populations of gametocytes, merozoites, infected hepatocytes and infected erythrocytes when all the control measures are employed. It takes a much shorter time to eradicate the malaria parasites from the blood of the human host. Both the merozoites and infected red blood cells get eradicated within 12 days of infection. It is clear that both strategy (2B) and strategy 3 offer the best control options in controlling in-host *P. falciparum* malaria. Moreover, the simulations results in Figures 7.12 and 7.14 reveal that the emergence of clinical malaria would be least likely if either of these control strategies is implemented correctly. Nevertheless, strategy (2B) only needs one highly efficacious malaria vaccine to achieve the same result as that in strategy 3. Additionally, strategy (2B) is likely to be less costly compared to strategy 3, which incorporates all the four control measures. In conclusion, the optimal control strategy against *P. falciparum* malaria is strategy (2B): a combination of efficacious pre-erythrocytic vaccine, effective blood schizontocide and a gametocytocide.

In Figure 7.15, the control profiles for each of the four controls employed in strategy 3 are presented. It is observed that the control profiles of the pre-erythrocytic vaccine (u_1) and blood stage vaccines antigens (u_2) are maintained at highest levels of efficacy (75% in our case) to ensure maximum eradication of asexual sporozoites and infected erythrocytes, respectively. Similarly, the concentrations of blood schizontocides (u_3) and gametocytocides (u_4) should be maintained at the highest levels to maximise eradication of asexual merozoites and infected erythrocytes, respectively. Like in other control strategies already discussed, the

effectiveness of the antimalarial drugs is likely to fall after day 45 and this remains lowest till the end of the intervention period.

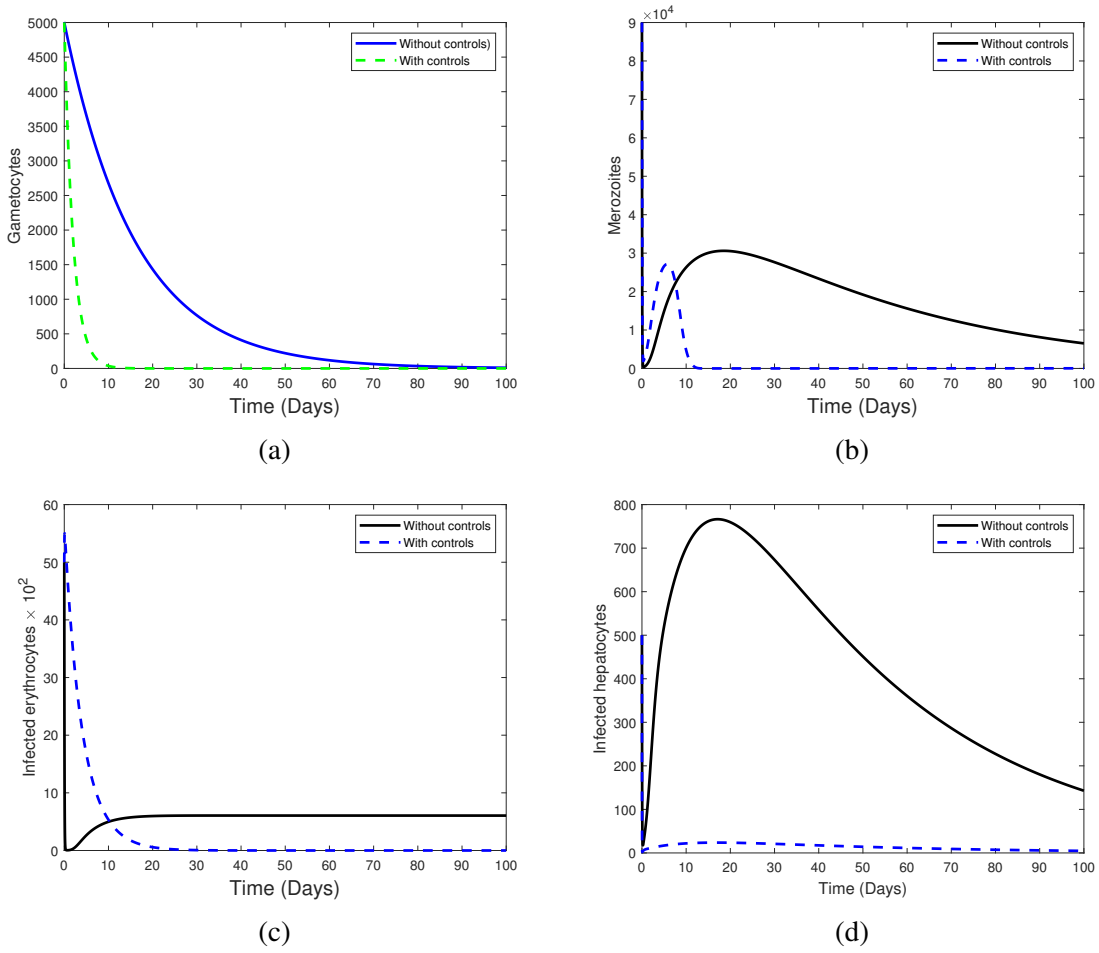

Figure 7.14: Simulations of system (7.1), showing the impact of combining antigens of pre-erythrocytic vaccine and blood stage vaccine together with the administration of combined blood schizontocide and gametocitocidal drugs. Used parameter values are shown in Table 7.2. Here, $u_1 \neq 0$, $u_2 \neq 0$, $u_3 \neq 0$, $u_4 \neq 0$.

The best control strategy of an in-host malaria infection should eradicate all infective merozoites, infected hepatocytes and infected red blood cells within the shortest time possible at a minimal cost. Epidemiologically, the best control strategy should ensure no gametocyte parasites are available for transmission to the mosquito vector. Although strategy (2B) is the optimal strategy in this study, it should be implemented alongside existing vector control measures such as ITNs and IRS if malaria elimination goal is to be achieved (WHO, 2015b). This result is crucial for malaria drug development and highlights the urgent need for a highly efficacious pre-erythrocytic malaria vaccine to complement existing ACTs.

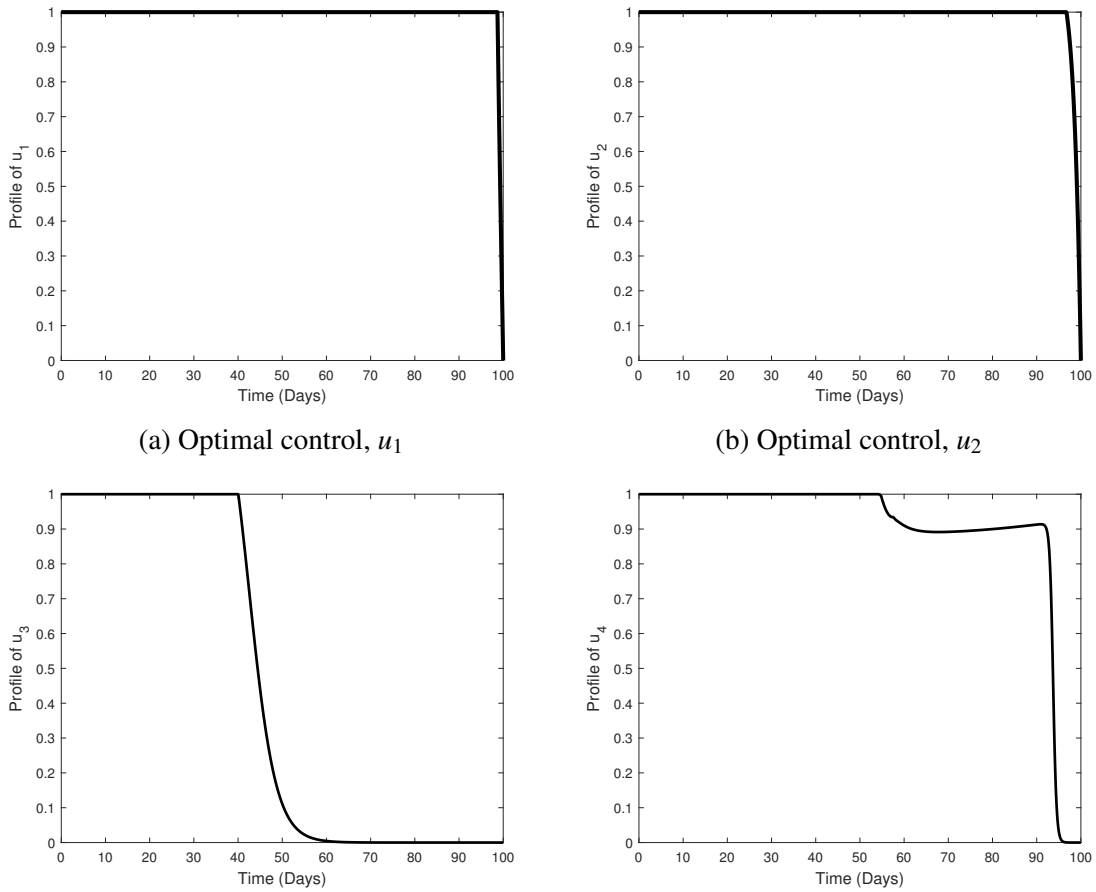

(a) Optimal control, u_1

(b) Optimal control, u_2

(c) Optimal control, u_3

(d) Optimal control, u_4

Figure 7.15: Plots showing the profiles of pre-erythrocytic vaccine antigen u_1, blood stage vaccine antigen u_2, blood schizontocide u_3 and gametocytocide u_4.

7.6 Conclusion

In this chapter, optimal control theory has been applied to a deterministic in-host malaria model. The model incorporates antimalarial drugs and malaria vaccines as control strategies during clinical *P. falciparum* malaria. The objective was to establish the best combination strategy involving (1) a blood schizontocide (2) a gametocytocide (3), a pre-erythrocytic vaccine antigen and (4) blood stage vaccine antigen against *P. falciparum* malaria. The drug and vaccine combinations are categorised into: (i) strategy (1A): a combination of a blood schizontocide and gametocytocide, (ii) strategy (1B): a combination of pre-erythrocytic and blood stage vaccine antigens, (iii) strategy (1C): a combination of pre-erythrocytic vaccine and blood schizontocide drug, (iv) strategy (2A): a combination of pre-erythrocytic

vaccine antigen, blood stage vaccine antigen and blood schizontocide, (v) strategy (2B): a combination of pre-erythrocytic vaccine antigen, blood schizontocide and gametocytocide and (vi) strategy 3: a combination of all the four control options (pre-erythrocytic vaccine antigen, blood stage vaccine, blood schizontocide and gametocytocide).

The Pontryagin's Maximum Principle was used to characterise and discuss control strategies that substantially reduced the populations of infected erythrocytes, infected hepatocytes and malaria parasites. The necessary conditions were derived and analysed for the existence of the optimal control of malaria infection. For sufficiently small values of intervention time, we proved the uniqueness of the optimality system. From the analysis, it was found out that eradication of in-host malaria will be possible if highly efficacious vaccines are used in combination with antimalaria drug therapy. Numerical results showed that a combination of pre-erythrocytic vaccine, blood schizontocide and gametocytocide drugs would offer the best control strategy against clinical *P. falciparum* malaria. A combination of all the four control measures equally gave a comparatively good results, however, it may be too expensive. Nonetheless, the synergy of malaria vaccine antigens and antimalarial drug regimens is crucial for future malaria chemotherapy control.

It is important to note that the parameter values and weights used in this analysis are estimated for illustration purposes. More realistic results would be feasible if data on the costs of implementation of the four controls are available. However, the results presented in this chapter give insights on the need to combine effective antimalarial drugs and to use them alongside efficacious malaria vaccine antigens to control *P. falciparum* malaria infections.

This study is concluded in the next Chapter 8. It summarises the results of the study and list some recommendations for future research activities.

Chapter 8

Conclusion and Recommendations

8.1 Conclusion and discussion

Despite the renewed optimism regarding the achievement of malaria elimination goal, the current antimalarial measures offer little in the way of novel strategies (Sinha, 2014). Malaria cases are strangely on the rise in the top ten high burden African countries (Nigeria, Burkina Faso, Ghana, Niger, Mali, Guinea, Benin, Côte d'Ivoire, Togo and Sierra Leone). It is on record that 3.5 million more cases were reported in 2017 in these countries (WHO, 2018f). The appearance of parasite resistance to currently recommended antimalarial drugs (ACTs) in Thailand and Cambodia and the possible risk of spreading to other malaria endemic regions has generated global concern for future malaria control and elimination measures. Progress in malaria control is currently hampered with inadequate investment (WHO, 2018f). With minimal progress in malaria vaccine development and the absence of alternative drugs in the pipeline, the need to discover and develop newer malaria therapeutic strategies cannot be overemphasised (WHO, 2018f). This study was aimed at formulating and analysing mathematical models of in-host malaria dynamics with the goal of improving malaria vaccine and therapeutic strategies.

In this study, the dynamics and interactions of malaria parasites, the erythrocytes (red blood cells), the liver hepatocytes and the immune cells are represented using a system of nonlinear ordinary differential equations. The extended models are subject to therapeutic conditions of antimalarial drugs and malaria vaccines. The specific control efforts of the immune cells is highlighted in all the formulated models. Parasite resistance and the effects of competition between different parasite strains are also discussed. Based on the next generation matrix

method, the basic/effective reproduction numbers are computed. Optimal control theory is also applied to establish the best therapeutic combination strategy against in-host *falciparum* malaria infection.

The first model in this study is a deterministic model of in-host malaria infection without therapeutic interventions The model incorporates parasite and cell dynamics at the liver and blood stages within the human host. Innate immune cells called macrophages are deployed to eliminate infected red blood cells and malaria parasites from blood circulation. In addition, the liver hepatocytes are assumed to be generated from the bone marrow and through a process of self-regeneration from existing hepatocytes. The malaria-free equilibrium point is shown to be locally asymptotically stable when the in-host reproduction number is less than unity. The global stability of the malaria-free state is only guaranteed if the basic reproduction number R_0 is less than unity.

Results based on numerical simulation show that intervention during malaria infection should target the merozoite invasion rate on healthy erythrocytes and the density of merozoites in circulation that are responsible for secondary invasion at the blood stage. In the absence of malaria treatment, the macrophages are shown to be vital in eliminating infected erythrocytes at the blood stage. The higher the rate of phagocytosis of infected erythrocytes by macrophages, the lower the density of infected red blood cells and hence malaria parasitaemia. For quick and timely reduction of parasitaemia, an increased merozoite death rate using antimalarial drugs such as ACT would be necessary. This would further ensure reduced density of infected red blood cells and hence decreased recrudescence. Moreover, erythrocyte invasion-avoidance vaccine would minimise the density of infected erythrocytes and hence malaria disease severity. This intervention could help terminate the erythrocytic schizony, leading to minimal parasite transmission to mosquito vector.

The potential role of efficacious malaria vaccines in in-host malaria control and eradication is presented in the second model in this study. The in-host malaria model incorporates pre-erythrocytic vaccine (PEV), blood stage vaccine (BSV) and transmission blocking vaccine (TBV). The model is mathematically analysed to provide useful insights on individual and combined vaccine impacts in reducing the severity of *P. falciparum* malaria. It was established that a highly efficacious malaria vaccine (efficacy $> 90\%$) is likely to offer the much needed protection against *P. falciparum* malaria. This estimate should however be treated with some discretion due to 'not so accurate' parameter values. Additionally,the critical vaccine efficacy necessary in the development of future malaria vaccines was established. To achieve a substantial reduction in mortality and morbidity due to malaria infections, the efficacy of the malaria vaccines should be higher than the corresponding critical vaccine efficacies. For

instance, when the efficacy of the blood stage vaccine is lower than the critical efficacy, the rate of infection of susceptible erythrocytes is higher and clinical malaria persists. However, the concentration of blood trophozoites and blood schizonts decreases drastically if the efficacy of the blood stage vaccine is higher than the critical blood stage vaccine efficacy. A combination of different malaria vaccine antigens yields better therapeutic results compared to individual vaccine antigens. Vaccine combinations induce multiple immune responses with the potential to prevent or eradicate malaria infection. Analysis of the model here shows that a highly effective vaccine combination is critical for *P. falciparum* malaria elimination goal.

Due to uncertainties that may accompany choices for parameter values, it is important to correctly understand the possible effects of the parameter values to the model outcome. The more sophisticated and efficient sensitivity analysis approach of LHS/PRCC is applied to the third in-host malaria model subject to vaccine control measures. The model is shown to be highly sensitive to variations in malaria vaccine efficacies. Only efficacious malaria vaccines have a chance to eliminate *P. falciparum* malaria or to reduce its severity during infection. Sensitivity indices based on the basic reproduction number indicates that the parasite invasion rates are highly sensitive to disease progression. Licensed malaria vaccines must therefore be efficacious enough for quick and rapid eradication of all infective parasites. Other parameters such as the proportion of merozoites that become gametocytes per dying blood schizont and the average number of merozoites released per bursting blood schizonts are also shown to have a considerable impact on the severity of malaria infection.

A highly effectious blood stage vaccine is also effective in reducing the density of malaria gametocytes. This is likely to reduce malaria transmission from the human host to the mosquito vector. The protective capacity of liver stage- specific $CD8^+$ T cells is a motivation for developing a blood stage vaccine that would boost the production of blood trophozoite-specific $CD8^+$ T cells. It is observed that the more efficient the pre-erythrocytic vaccine is, the lower the density of released merozoites into the host's blood stream. Moreover, a rapid clearance of infected hepatocytes is likely to result into less infected erythrocytes at the blood stage. An efficacious pre-erythrocytic vaccine has a potential to eliminate all infected liver hepatocytes. Such vaccines may also reduce the overall burst size of an infected hepatocyte, leading to reduced erythrocytic schizonogy.

The synergy of combining pre-erythrocytic vaccines, blood stage vaccines and transmission blocking vaccines antigens induces multiple immune responses with the potential to prevent malaria infection. Although efficacious malaria vaccines are shown to be effective in reducing severity of clinical malaria, the results further confirm the need to combine malaria vaccines

with existing antimalarial therapy to achieve a complete clearance of the parasites from the human host. Moreover, from the LHS/PRCC analysis, it is observed that long term precise predictions of the density of infected liver hepatocytes and infected erythrocytes would be difficult until certain sensitive parameters are correctly determined.

The effects of parasite resistance under single and multiple-strain parasite infection is also investigated in this study. The parasites are categorised as either drug-sensitive strain (dss) or drug-resistant strain (drs). The immune cells are incorporated to reduce the invasive characteristic of the malaria merozoites. The dynamics here are strictly limited to the blood stage of malaria infection. Antimalarial therapy is applied to the model but only targets erythrocytes infected with drug-sensitive merozoites. The results show that the success of *P. falciparum* infection in the presence of multiple parasite strain is directly dependent on the ability of the individual parasite strains to dominate the infection. The parasite strain with a higher threshold value, R_E is likely to dominate the infection. Prescribed antimalarial drugs should therefore be effective enough to eradicate both drug-sensitive and drug-resistant parasite strains.

To assess the impacts of the different parasite strains to disease dynamics, the model is simulated for different values of the threshold quantities R_s and R_r. It is observed that when $R_r > 1$ and $R_s > 1$, then both parasite strains are persistent and the infection becomes severe. If $R_r > 1$ and $R_s < 1$, then the drug-sensitive parasites would decline to zero as the drug-resistant strain continue to multiply and remain persistent, increasing the severity of infections. On the other hand, if $R_s > 1$ and $R_r < 1$, then the drug-resistant parasite strains would be eradicated. Moreover, provided that the threshold quantities R_s and R_r are less than unity, the use of an efficacious antimalarial drug would help clear *P. falciparum* infection from the human host.

The efficacy of antimalarial drug is shown to have direct negative impact on the density of infected erythrocytes. The higher the efficacy of administered antimalarial drug, the lower the population of infective merozoites and the smaller the density of infected erythrocytes. This ensures prompt recovery from malaria infection. The efficacy of antimalarial drug is however shown to have least effect on the population of drug-resistant infected erythrocytes. Using contour plots and results from sensitivity analysis, it is observed that the efficacy of antimalarial drug used, the density of blood floating merozoites produced per infected erythrocyte, the rate of development of resistance and the rate of infection by merozoites are the most important parameters in blood-stage *P. falciparum* malaria infection and control efforts.

Although the drug-resistant strain is shown to be less fit, the presence of both strains in the human host has a huge impact on the cost and success of antimalarial treatment. To reduce the emergence of resistant strains, it is vital that only effective antimalarial drugs are administered to patients in hospitals, especially in malaria endemic regions. Similarly, to improve malaria therapy and reduce cases of parasite resistance to existing therapy, our results call for regular and strict surveillance on antimalarial drug use in clinics and hospitals in malaria-endemic countries.

The theory of optimal control is applied to the in-host malaria model in this study. The model incorporates antimalarial drug regimens and malaria vaccine antigens as control strategies against clinical *P. falciparum* malaria. The goal of using this model is to establish the best combination strategy involving a pre-erythrocytic vaccine antigen, a blood stage vaccine antigen, a blood schizontocide and a gametocytocide against in-host *P. falciparum* malaria infection. The drug and vaccine combinations are categorised into: (i) a combination of blood schizontocide and gametocytocide only (strategy 1A), (ii) a combination of pre-erythrocytic and blood stage vaccine antigens only (strategy 1B), (iii) a combination of pre-erythrocytic vaccine antigen and blood schizontocide drug only (strategy 1C), (iv) a combination of pre-erythrocytic vaccine antigen, blood stage vaccine antigen and blood schizontocide only (strategy 2A), (v) a combination of pre-erythrocytic vaccine antigen, blood schizontocide and gametocytocide only (strategy 2B) and (vi) a combination of all the four control options (pre-erythrocytic vaccine antigen, blood stage vaccine antigen, blood schizontocide and gametocytocide), (strategy 3).

The Pontryagin's Maximum Principle was used to characterise and discuss control strategies that substantially reduced the populations of infected erythrocytes, infected hepatocytes and malaria parasites. The necessary conditions were derived and analysed for the existence of the optimal control therapy for malaria infection. For sufficiently small values of intervention time, the uniqueness of the optimality system was proved. Numerical results showed that a combination of pre-erythrocytic vaccine antigen, blood schizontocide and gametocytocide drugs offers the best control strategy against *P. falciparum* malaria infection.

8.2 Policy recommendations based on this study

Despite global and regional success in reducing morbidity and mortality due to malaria, malaria still remains a major public health problem in Kenya. About 4 million malaria cases are reported annually, with about 5.1% mortality rate among patients admitted with severe

malaria. Over 99% of all reported cases are due to the deadly *P. falciparum* malaria. Research findings from this study could be useful to malaria research organisations such as the Kenya Medical Research Institute (KEMRI), Centers for Disease Control and Prevention (CDC-Kenya) and the Ministry of Health in their effort to prevent and control malaria infections in the country. Specific policy recommendations include the following:

1. For quick and timely treatment of uncomplicated *P. falciparum* malaria, treatment using efficacious ACTs such as artemether-lumefantrine (AL) is necessary.
2. Malaria vaccine minimises the density of infected erythrocytes and hence malaria disease severity. Vaccines such as RTS,S/AS01, should be used alongside existing antimalarial drugs to control *P. falciparum* malaria infections in the country.
3. Threats caused by parasite resistance offer a unique opportunity to closely monitor use and misuse of antimalarial drugs. Regular and strict surveillance on quality and standards of antimalarial drugs in medical facilities in the country is therefore very critical.
4. To reduce mortality and morbidity, only qualified medical officers should be permitted to diagnose and administer antimalarial treatment to malaria patients in the country.
5. Patients suffering from such infections as HIV/AIDS or tuberculosis which have deleterous effect on the protective immune cells should seek immediate medical treament when infected with malaria. Their compromised immune system exposes them to severe malaria attacks and possible untimely death.
6. Individuals presenting malaria symptoms should also be tested for other infections such as HIV/AIDS and tuberculosis.

8.3 Limitations and future work

This study uses mathematical modelling and analyses to provide useful and rich insights necessary for understanding in-host malaria dynamics and for improving vaccine and therapeutic control measures against *P. falciparum* malaria. Like many other epidemic models, the in-host malaria models presented here have numerous model assumptions. These assumptions help to minimise model complexities and maintain systems with manageable analytical sizes. However, the malaria parasite life cycle is extremely complex with several biological functions that are largely unknown. Some of the assumptions in this study could be dropped to improve model outcome. For example, the presented model ignores the biology of $CD8^+$

T activation and assumes constant rate of production of the immune cells during malaria parasite invasion. Secondly, the formation of gametocytes is another mystery in the malaria parasite life cycle. The actual rate of commitment of merozoites to form gametocytes is largely unknown and highly speculated. This process has been highlighted in some studies (Bechtsi and Waters, 2017) as a random process that would best be captured using a stochastic model. Nevertheless, the actual process is still unclear with only a small proportion of the parasites per erythrocytic cycle committing to gametocytogenesis (Josling and Llinas, 2015).

It is important to note that the values of the parameters used in this study were either obtained from existing literature or simply assumed. This is partly occasioned by lack of data and also due to some unknown dynamics within the complex malaria parasite life cycle. Availability of clinical data on *P. falciparum* malaria dynamics with and without vaccine and antimalarial drugs could be very helpful in estimating model parameter values for even better results. It would therefore be difficult to predict with higher accuracy, the optimal malaria vaccine efficacy. Time delay from invasion to schizont rupture is not captured in this study. This is another key area that could improve the results presented here. A time-dependent delay parameter would be a plausible addition to future in-host malaria models. In addition, this study acknowledges that the parasite invasion rates may not necessarily be constant throughout the infection period.

Finally, model validation is a very powerful step in disease modelling. Another possible extension of the models considered in this study can be implemented by carrying out model validation based on valid data on in-host *P. falciparum* malaria dynamics and therapeutic control. Note that the weights used in the optimal control analysis are estimated for illustration purposes. More realistic results would be feasible if data on the costs of implementation of the four controls are available.

In spite of the stated shortcomings, the presented models and analyses performed in this study provide useful insights on in-host malaria dynamics and therapeutic control measures against *P. falciparum* malaria. The results from this study call for continued investment in malaria drug development and urgent drive to improve the efficacy of malaria vaccines such as RTS,S/AS01. The administration of effective antimalarial drugs alongside malaria vaccine antigen combinations present a noble strategy with the potential to malaria eradication in malaria endemic regions.

References

Abdulla, S., Agre, P., Alonso, P., Arevalo-Herrera, M., Bassat, Q., Binka, F., Chitnis, C., Corradin, G., Cowman, A., and Culpepper, J. (2011). A research agenda for malaria eradication: vaccines. *PloS One*, 8(1). e1000398. https://doi.org/10.1371/journal.pmed.1000398.

Abdulla, S., Oberholzer, R., Juma, O., Kubhoja, S., Machera, F., Membi, C., Omari, S., Urassa, A., Mshinda, H., Jumanne, A., Salim, N., Shomari, M., Aebi, T., Schellenberg, D. M., Carter, T., Villafana, T., Demoitié, M.-A., Dubois, M.-C., Leach, A., Lievens, M., Vekemans, J., Cohen, J., Ballou, R., and Tanner, M. (2008). Safety and immunogenicity of RTS, S/AS02D malaria vaccine in infants. *New England Journal of Medicine*, 359(24):2533–2544.

Abdulrahman, S., Akinwande, N. I., Awojoyogbe, O. B., and Abubakar, U. Y. (2013). Sensitivity analysis of the parameters of a mathematical model of Hepatitis B virus transmission. *Universal Journal of Applied Mathematics*, 1(4):230–241.

Adams, B., Banks, H., Kwon, H.-D., and Tran, H. T. (2004). Dynamic multidrug therapies for HIV: Optimal and STI control approaches. *Mathematical Biosciences and Engineering*, 1(2):223–241.

Agur, Z., Abiri, D., and Van der Ploeg, L. (1989). Ordered appearance of antigenic variants of African trypanosomes explained in a mathematical model based on a stochastic switch process and immune-selection against putative switch intermediates. *Proceedings of the National Academy of Sciences of the United States of America*, 86(23):9626–9630.

Agusto, F. B., Marcus, N., and Okosun, K. O. (2012). Application of optimal control to the epidemiology of malaria. *Bulletin of Mathematical Biology*, 2012(81):1–22.

AIRF (2012). Differences between in vitro, in vivo and in silico studies. The marshall protocol knowledge base. Autoimmunity Research Foundation (AIRF). Retrieved from https://mpkb.org/home/patients/assessing_literature/in_vitro_studies#in_vivo_studies. Accessed September 2017.

Allen, L. J. (2007). *Introduction to mathematical biology*. Pearson/Prentice Hall, USA.

Alonso, P. L., Sacarlal, J., Aponte, J. J., Leach, A., Macete, E., Milman, J., Mandomando, I., Spiessens, B., Guinovart, C., and Espasa, M. (2004). Efficacy of the RTS, S/AS02A vaccine against plasmodium falciparum infection and disease in young African children: randomised controlled trial. *The Lancet*, 364(9443):1411–1420.

Alout, H., Labbé, P., Chandre, F., and Cohuet, A. (2017a). Malaria vector control still matters despite insecticide resistance. *Trends in Parasitology*, 33(8):610–618.

Alout, H., Roche, B., Dabiré, R. K., and Cohuet, A. (2017b). Consequences of insecticide resistance on malaria transmission. *PLoS Pathogens*, 13(9):e1006499. https://doi.org/10.1371/journal.ppat.1006499.

Anderson, R., May, R., and Gupta, S. (1989). Non-linear phenomena in-host parasite interactions. *Parasitology*, 99(S1):S59–S79.

Aneke, S. (2002). Mathematical modelling of drug resistant malaria parasites and vector populations. *Mathematical Methods in the Applied Sciences*, 25(4):335–346.

Antia, R., Levin, B. R., and May, R. M. (1994). Within-host population dynamics and the evolution and maintenance of microparasite virulence. *The American Naturalist*, 144(3):457–472.

Arama, C. and Troye-Blomberg, M. (2014). The path of malaria vaccine development: challenges and perspectives. *Journal of Internal Medicine*, 275(5):456–466.

Arevalo-Herrera, M., Solarte, Y., Yasnot, M. F., Castellanos, A., Rincon, A., Saul, A., Mu, J., Long, C., Miller, L., and Herrera, S. (2005). Induction of transmission-blocking immunity in aotus monkeys by vaccination with a plasmodium vivax clinical grade PVS25 recombinant protein. *The American Journal of Tropical Medicine and Hygiene*, 73(5):32–37.

Arriola, L. and Hyman, J. (2005). Lecture notes, forward and adjoint sensitivity analysis: with applications in dynamical systems. *Linear Algebra and Optimisation Mathematical and Theoretical Biology 414 Institute, Summer 2005.*

Arriola, L. M. and Hyman, J. M. (2007). Being sensitive to uncertainty. *Computing in Science & Engineering*, 9(2):10–20.

Arumugam, T. U., Ito, D., Takashima, E., Tachibana, M., Ishino, T., Torii, M., and Tsuboi, T. (2014). Application of wheat germ cell-free protein expression system for novel malaria vaccine candidate discovery. *Expert Review of Vaccines*, 13(1):75–85.

Ashley, E. A., Dhorda, M., Fairhurst, R. M., Amaratunga, C., Lim, P., Suon, S., Sreng, S., Anderson, J. M., Mao, S., Sam, B., Chuor, C., Nguon, C., Sovannaroth, S., Pukrittayakamee, S., Jittamala, P., Chotivanich, K., Chutasmit, K., Suchatsoonthorn, C., Runcharoen, R., Hien, T., Thuy-Nhien, N., Thanh, N., Phu, N., Htut, Y., Han, K.-T., Aye, K., Mokuolu, O., Olaosebikan, R., Folaranmi, O., Mayxay, M., Khanthavong, M., Hongvanthong, B., Newton, P., Onyamboko, M., Fanello, C., Tshefu, A., Mishra, N., Valecha, N., Phyo, A., F., Nosten, Yi, P., Tripura, R., Borrmann, S., Bashraheil, M., Peshu, J., Faiz, M., Ghose, A., Hossain, M., Samad, R., Rahman, M., Hasan, M., Islam, A., Miotto, O., Amato, R., MacInnis, B., Stalker, J., Kwiatkowski, D., Bozdech, Z., Jeeyapant, A., Cheah, P., Sakulthaew, T., Chalk, J., Intharabut, B., Silamut, K., Lee, S., Vihokhern, B., Kunasol, C., Imwong, M., Tarning, J., Taylor, W., Yeung, S., Woodrow, C., Flegg, J., Das, D., Smith, J., Venkatesan, M., Plowe, C., Stepniewska, K., Guerin, P., Dondorp, A., Day, N., , and White, N. (2014). Spread of artemisinin resistance in plasmodium falciparum malaria. *New England Journal of Medicine*, 371(5):411–423.

Athithan, S. and Ghosh, M. (2015). Stability analysis and optimal control of a malaria model with larvivorous fish as biological control agent. *Applied Mathematics & Information Sciences*, 9(4):1893–1913.

Audran, R., Cachat, M., Lurati, F., Soe, S., Leroy, O., Corradin, G., Druilhe, P., and Spertini, F. (2005). Phase I malaria vaccine trial with a long synthetic peptide derived from the merozoite surface protein 3 antigen. *Infection and Immunity*, 73(12):8017–8026.

Augustine, A. D., Hall, B. F., Leitner, W. W., Mo, A. X., Wali, T. M., and Fauci, A. S. (2009). NIAID workshop on immunity to malaria: addressing immunological challenges. *Nature Immunology*, 10(7):673–678.

Austin, D., White, N., and Anderson, R. (1998a). The dynamics of drug action on the within-host population growth of infectious agents: melding pharmacokinetics with pathogen population dynamics. *Journal of Theoretical Biology*, 194(3):313–339.

Austin, D., White, N., and Anderson, R. (1998b). The dynamics of drug action on the within-host population growth of infectious agents: melding pharmacokinetics with pathogen population dynamics. *Journal of Theoretical Biology*, 194(3):313–339.

Babiker, H. A., Hastings, I. M., and Swedberg, G. (2009). Impaired fitness of drug-resistant malaria parasites: evidence and implication on drug-deployment policies. *Expert Review of Anti-infective Therapy*, 7(5):581–593.

Ballou, W. (2009). The development of the RTS,S malaria vaccine candidate: challenges and lessons. *Parasite Immunology*, 31(9):492–500.

Bartoloni, A. and Zammarchi, L. (2012). Clinical aspects of uncomplicated and severe malaria. *Mediterranean Journal of Hematology and Infectious Diseases*, 4(1):e2012026. http://www.mjhid.org/article/view/10109.

Bashawri, L. A., Mandil, A. A., Bahnassy, A. A., and Ahmed, M. A. (2002). Malaria: hematological aspects. *Annals of Saudi Medicine*, 22(5-6):372–376.

Bate, C., Taverne, J., and Playfair, J. (1988). Malarial parasites induce TNF production by macrophages. *Immunology*, 64(2):227–231.

Bauza, K., Atcheson, E., Malinauskas, T., Blagborough, A. M., and Reyes-Sandoval, A. (2016). Tailoring a combination pre-erythrocytic malaria vaccine. *Infection and Immunity*, 84(3):622–634.

Bechtsi, D. and Waters, A. (2017). Genomics and epigenetics of sexual commitment in plasmodium. *International Journal for Parasitology*, 47(7):425–434.

Bernoulli, D. and Blower, S. (2004). An attempt at a new analysis of the mortality caused by smallpox and of the advantages of inoculation to prevent it. *Reviews in Medical Virology*, 14(5):275–288.

Bhatt, S., Weiss, D., Cameron, E., Bisanzio, D., Mappin, B., Dalrymple, U., Battle, K., Moyes, C., Henry, A., Eckhoff, Wenger, E. A., Briet, Penny, M. A., Smith, T. A., Bennett, A., Yukich, J., Eisele, T. P., Griffin, J. T., Fergus, C. A., Lynch, M., Lindgren, F., Cohen, J. M., Murray, C. L. J., Smith, D. L., Hay, S. I., Cibulskis, R. E., and Gething, P. W. (2015).

The effect of malaria control on plasmodium falciparum in Africa between 2000 and 2015. *Nature*, 526(7572):207–2011.

Birkett, A. J. (2016). Status of vaccine research and development of vaccines for malaria. *Vaccine*, 34(26):2915–2920.

Birkett, A. J., Moorthy, V. S., Loucq, C., Chitnis, C. E., and Kaslow, D. C. (2013). Malaria vaccine R&D in the decade of vaccines: breakthroughs, challenges and opportunities. *Vaccine*, 31(2):B233–B243.

Bloland, P. B., Lackritz, E. M., Kazembe, P. N., Were, J. B., Steketee, R., and Campbell, C. C. (1993). Beyond chloroquine: implications of drug resistance for evaluating malaria therapy efficacy and treatment policy in Africa. *Journal of Infectious Diseases*, 167(4):932–937.

Blower, S. M. and Dowlatabadi, H. (1994). Sensitivity and uncertainty analysis of complex models of disease transmission: an HIV model, as an example. *International Statistical Review/Revue Internationale de Statistique*, 62(2):229–243.

Blower, S. M., Hartel, D., Dowlatabadi, H., Anderson, R. M., and May, R. M. (1991). Drugs, sex and HIV: a mathematical model for New York City. *Philosophical Transactions: Biological Sciences*, 331(1260):171–187.

Boes, A., Spiegel, H., Voepel, N., Edgue, G., Beiss, V., Kapelski, S., Fendel, R., Scheuermayer, M., Pradel, G., Bolscher, J. M., Marije, C. B., Koen, J. D., Cornelus, C. H., Robert, W. S., Stefan, S., Andreas, R., and Rainer, F. (2015). Analysis of a multi-component multistage malaria vaccine candidate-tackling the cocktail challenge. *PloS one*, 10(7):e0131456. doi:10.1371/journal.pone.0131456.

Bojang, K. A., Milligan, P. J., Pinder, M., Vigneron, L., Alloueche, A., Kester, K. E., Ballou, W. R., Conway, D. J., Reece, W. H. H., Gothard, P., Yamuah, L., Delchambre, M., Voss, G., Greenwood, B. M., Hill, A., McAdam, K. P. W. J., Tornieporth, Nadia Cohen, J. D., and Doherty, T. (2001). Efficacy of RTS, S/AS02 malaria vaccine against plasmodium falciparum infection in semi-immune adult men in The Gambia: a randomised trial. *The Lancet*, 358(9297):1927–1934.

Brauer, F. (2006). Some simple epidemic models. *Mathematical Biosciences and Engineering*, 3(1):1–15.

Brazier, A. J., Avril, M., Bernabeu, M., Benjamin, M., and Smith, J. D. (2017). Pathogenicity determinants of the human malaria parasite plasmodium falciparum have ancient origins. *mSphere*, 2(1):e00348–16. doi: 10.1128/mSphere.00348-16.

Bredenkamp, B., Sharp, B. L., Mthembu, S. D., Durrheim, D. N., and Barnes, K. I. (2001). Failure of sulphadoxine-pyrimethamine in treating plasmodium falciparum malaria in KwaZulu-Natal. *South African Medical Journal= Suid-Afrikaanse tydskrif vir geneeskunde*, 91(11):970–972.

Bushman, M., Antia, R., Udhayakumar, V., and de Roode, J. C. (2018). Within-host competition can delay evolution of drug resistance in malaria. *PLoS Biology*, 16(8):e2005712. https://doi.org/10.1371/journal.pbio.2005712.

Bushman, M., Morton, L., Duah, N., Quashie, N., Abuaku, B., Koram, K. A., Dimbu, P. R., Plucinski, M., Gutman, J., Lyaruu, P., Kachur, P. S., de Roode, J. C., and Udhayakumar, V. (2016). Within-host competition and drug resistance in the human malaria parasite plasmodium falciparum. *Proceedings of the Royal Society of London. Series B: Biological Sciences*, 283(1826):20153038. doi: 10.1098/rspb.2015.3038.

Cai, L., Tuncer, N., and Martcheva, M. (2017). How does within-host dynamics affect population-level dynamics? Insights from an immuno-epidemiological model of malaria. *Mathematical Methods in the Applied Sciences*, 40(18):6424–6450.

Carrera, J., Medina, A., Heredia, J., Vives, L., Ward, J., and Walters, G. (1989). Parameter estimation in groundwater modelling: From theory to application. In G., J., J., B., Y.Y., H., and F., W., editors, *Groundwater Contamination: Use of Models in Decision-Making*, pages 151–169. Springer, Dordrecht.

Carter, R. and Mendis, K. N. (2002). Evolutionary and historical aspects of the burden of malaria. *Clinical Microbiology Reviews*, 15(4):564–594.

Carter, R., Mendis, K. N., Miller, L. H., Molineaux, L., and Saul, A. (2000). Malaria transmission-blocking vaccines - how can their development be supported? *Nature Medicine*, 6(3):241–244.

Castillo-Chavez, C. and Song, B. (2004). Dynamical models of tuberculosis and their applications. *Mathematical Biosciences and Engineering*, 1(2):361–404.

CDC (2017). Malaria biology. Technical report, Center for Disease Control and Prevention. Retrieved from https://www.cdc.gov/malaria/about/biology/. Accessed January 2017.

CDC (2019a). Malaria disease. Centers for Disease Control and Prevention. Retrieved from https://www.cdc.gov/malaria/about/disease.html. Accessed February 2019.

CDC (2019b). Malaria treatment. Centers for Disease Control and Prevention. Retrieved from https://www.cdc.gov/malaria/diagnosis$_$treatment/treatment.html. Accessed February 2019.

Chen, Q., Amaladoss, A., Ye, W., Liu, M., Dummler, S., Kong, F., Wong, L. H., Loo, H. L., Loh, E., and Tan, S. Q. a. (2014). Human natural killer cells control plasmodium falciparum infection by eliminating infected red blood cells. *Proceedings of the National Academy of Sciences of the United States of America*, 111(4):1479–1484.

Chitnis, C. E., Mukherjee, P., Mehta, S., Yazdani, S. S., Dhawan, S., Shakri, A. R., Bharadwaj, R., Gupta, P. K., Hans, D., and Mazumdar, S. (2015). Phase I clinical trial of a recombinant blood stage vaccine candidate for plasmodium falciparum malaria based on MSP1 and EBA175. *PloS One*, 10(4):e0117820.doi:10.1371/journal.pone.0117820.

Chitnis, N., Hyman, J. M., and Cushing, J. M. (2008). Determining important parameters in the spread of malaria through the sensitivity analysis of a mathematical model. *Bulletin of Mathematical Biology*, 70(5):1272–1296.

Chiyaka, C. (2010). Using mathematics to understand malaria infection during erythrocytic stages. *Zimbabwe Journal of Science and Technology*, 5(2010):1–11.

Chiyaka, C., Garira, W., and Dube, S. (2008). Modelling immune response and drug therapy in human malaria infection. *Computational and Mathematical Methods in Medicine*, 9(2):143–163.

Chiyaka, C., Garira, W., and Dube, S. (2009). Effects of treatment and drug resistance on the transmission dynamics of malaria in endemic areas. *Theoretical Population Biology*, 75(1):14–29.

Chotivanich, K., Udomsangpetch, R., McGready, R., Proux, S., Newton, P., Pukrittayakamee, S., Looareesuwan, S., and White, N. J. (2002). Central role of the spleen in malaria parasite clearance. *Journal of Infectious Diseases*, 185(10):1538–1541.

Chuma, F., Mwanga, G. G., and Masanja, V. G. (2019). Application of optimal control theory to newcastle disease dynamics in village chicken by considering wild birds as reservoir of disease virus. *Journal of Applied Mathematics*, vol. 2019. Article ID 3024965, 14 pages. https://doi.org/10.1155/2019/3024965.

Cohen, S., McGregor, I., and Carrington, S. (1961). Gamma-globulin and acquired immunity to human malaria. *Nature*, 192(192):733–737.

Coleman, P. G., Morel, C., Shillcutt, S., Goodman, C., and Mills, A. J. (2004). A threshold analysis of the cost-effectiveness of artemisinin-based combination therapies in sub-Saharan Africa. *The American Journal of Tropical Medicine and Hygiene*, 71(2):196–204.

Colijn, C. and Cohen, T. (2015). How competition governs whether moderate or aggressive treatment minimizes antibiotic resistance. *Elife*, 4:e10559. https://doi.org/10.7554/eLife.10559.001.

Collins, W. E. and Jeffery, G. M. (2007). Plasmodium malariae: parasite and disease. *Clinical Microbiology Reviews*, 20(4):579–592.

Cowman, A. F., Berry, D., and Baum, J. (2012). The cellular and molecular basis for malaria parasite invasion of the human red blood cell. *Journal of Cell Biology*, 198(6):961–971.

Cowman, A. F., Healer, J., Marapana, D., and Marsh, K. (2016). Malaria: biology and disease. *Cell*, 167(3):610–624.

Cox, F. E. (2010). History of the discovery of the malaria parasites and their vectors. *Parasites & Vectors*, 3(1):3–5.

Cox-Singh, J., Davis, T. M., Lee, K.-S., Shamsul, S. S., Matusop, A., Ratnam, S., Rahman, H. A., Conway, D. J., and Singh, B. (2008). Plasmodium knowlesi malaria in humans is widely distributed and potentially life threatening. *Clinical Infectious Diseases*, 46(2):165–171.

Crutcher, J. and Hoffman, S. (1996). *Malaria*. Medical Microbiology, University of Texas Medical Branch at Galveston, USA, 4th edition.

Das, M. K., Kalita, M. C., Chetry, S., and Dutta, P. (2017). K13 kelch propeller domain and mdr1 sequence polymorphism in field isolates from northeast region, India. *Human Parasitic Diseases*, 2017(9):1–9.

David, O., van den Wall Bake AW, PC, S., and van der Kaay HJ (1984). Chloroquine-resistant falciparum malaria from Malawi. *Tropical and Geographical Medicine*, 36(1):71–72.

De Back, D. Z., Kostova, E. B., van Kraaij, M., van den Berg, T. K., and Van Bruggen, R. (2014). Of macrophages and red blood cells; a complex love story. *Frontiers in Physiology*, 5(9). doi: 10.3389/fphys.2014.00009.

De Roode, J. C., Culleton, R., Bell, A. S., and Read, A. F. (2004). Competitive release of drug resistance following drug treatment of mixed plasmodium chabaudi infections. *Malaria Journal*, 3(33). https://doi.org/10.1186/1475-2875-3-33.

De Roode, J. C., Helinski, M. E., Anwar, M. A., and Read, A. F. (2005). Dynamics of multiple infection and within-host competition in genetically diverse malaria infections. *The American Naturalist*, 166(5):531–542.

Derbyshire, E. R., Mota, M. M., and Clardy, J. (2011). The next opportunity in anti-malaria drug discovery: the liver stage. *PLoS Pathogens*, 7(9):e1002178. doi: 10.1371/journal.ppat.1002178.

Diebner, H. H., Eichner, M., Molineaux, L., Collins, W. E., Jeffery, G. M., and Dietz, K. (2000). Modelling the transition of asexual blood stages of plasmodium falciparum to gametocytes. *Journal of Theoretical Biology*, 202(2):113–127.

Diekmann, O., Heesterbeek, J. A. P., and Metz, J. A. (1990). On the definition and the computation of the basic reproduction ratio R0 in models for infectious diseases in heterogeneous populations. *Journal of Mathematical Biology*, 28(4):365–382.

Dietz, K. (1993). The estimation of the basic reproduction number for infectious diseases. *Statistical Methods in Medical Research*, 2(1):23–41.

Dinglasan, R., Armistead, J., Nyland, J., Jiang, X., and Mao, H. (2013). Single-dose microparticle delivery of a malaria transmission-blocking vaccine elicits a long-lasting functional antibody response. *Current Molecular Medicine*, 13(4):479–487.

Dobson, S. R. M. J. (2001). The history of antimalarial drugs. In *Antimalarial Chemotherapy: Mechanisms of Action, Resistance, and New Directions in Drug Discovery*, pages 15–25. Humana Press, Totowa, NJ. School of Medicine, University of California San Francisco, USA.

Dondorp, A. M., Kager, P. A., Vreeken, J., and White, N. J. (2000). Abnormal blood flow and red blood cell deformability in severe malaria. *Parasitology Today*, 16(6):228–232.

Dondorp, A. M., Nosten, F., Yi, P., Das, D., Phyo, A. P., Tarning, J., Lwin, K. M., Ariey, F., Hanpithakpong, W., Lee, S. J., Ringwald, P., Silamut, K., Imwong, M., Chotivanich, K., Lim, P., Herdman, T., An, S. S., Yeung, S., Singhasivanon, P., Day, N. P., Lindegardh, N., Socheat, D., , and White, N. J. (2009). Artemisinin resistance in plasmodium falciparum malaria. *New England Journal of Medicine*, 361(5):455–467.

Dondorp, A. M., Yeung, S., White, L., Nguon, C., Day, N. P., Socheat, D., and Von Seidlein, L. (2010). Artemisinin resistance: current status and scenarios for containment. *Nature Reviews Microbiology*, 8(4):272–280.

Doolan, D. and Martinez-Alier, N. (2006). Immune response to pre-erythrocytic stages of malaria parasites. *Current Molecular Medicine*, 6(2):169–185.

Doolan, D. L., Dobaño, C., and Baird, J. K. (2009). Acquired immunity to malaria. *Clinical Microbiology Reviews*, 22(1):13–36.

Doolan, D. L. and Hoffman, S. L. (2001). DNA-based vaccines against malaria: status and promise of the Multi-Stage Malaria DNA Vaccine Operation. *International Journal for Parasitology*, 31(8):753–762.

Dorsey, G., Gandhi, M., Oyugi, J. H., and Rosenthal, P. J. (2000). Difficulties in the prevention, diagnosis, and treatment of imported malaria. *Archives of Internal Medicine*, 160(16):2505–2510.

Duffy, P. E., Sahu, T., Akue, A., Milman, N., and Anderson, C. (2012). Pre-erythrocytic malaria vaccines: identifying the targets. *Expert Review of Vaccines*, 11(10):1261–1280.

Edogan, J. E., Weber, J. L., Ballou, W. R., Hollingdale, M. R., Majarian, W. R., Gordon, D. M., Maloy, W. L., Hoffman, S. L., Wirtz, R. A., Schneider, I., Woollett, G. R., Young, J. F., and Hockmeyer, W. T. (1987). Efficacy of murine malaria sporozoite vaccines: implications for human vaccine development. *Science*, 236(4800):453–456.

Ekue, J., Ulrich, A.-M., and Njelesani, E. (1983). Plasmodium malaria resistant to chloroquine in a Zambian living in Zambia. *British Medical Journal (Clinical Research Ed.)*, 286(6374):1315–1316.

Ekvall, H. (2003). Malaria and anemia. *Current Opinion in Hematology*, 10(2):108–114.

El Sahly, H., Patel, S., Atmar, R., Lanford, T., Dube, T., Thompson, D., Sim, B., Long, C., and Keitel, W. (2010). Safety and immunogenicity of a recombinant nonglycosylated erythrocyte binding antigen 175 Region II malaria vaccine in healthy adults living in an area where malaria is not endemic. *Clinical and Vaccine Immunology*, 17(10):1552–1559.

Elloso, M. M., Van Der Heyde, H., Vande Waa, J., Manning, D. D., and Weidanz, W. P. (1994). Inhibition of plasmodium falciparum in vitro by human gamma delta T cells. *The Journal of Immunology*, 153(3):1187–1194.

EMA (2015). First malaria vaccine receives positive scientific opinion from EMA. European Medicines Agency. Retrieved from https://www.ema.europa.eu/en/news/first-malaria-vaccine-receives-positive-scientific-opinion-ema. Accessed March 2019.

Erhart, L. M., Yingyuen, K., Chuanak, N., Buathong, N., Laoboonchai, A., Miller, R. S., Meshnick, S. R., Gasser Jr, R. A., and Wongsrichanalai, C. (2004). Hematologic and clinical indices of malaria in a semi-immune population of western Thailand. *The American Journal of Tropical Medicine and Hygiene*, 70(1):8–14.

Esteva, L., Gumel, A. B., and De LeóN, C. V. (2009). Qualitative study of transmission dynamics of drug-resistant malaria. *Mathematical and Computer Modelling*, 50(3-4):611–630.

Esteva, L. and Vargas, C. (2000). Influence of vertical and mechanical transmission on the dynamics of dengue disease. *Mathematical Biosciences*, 167(1):51–64.

Eziefula, A. C., Bousema, T., Yeung, S., Kamya, M., Owaraganise, A., Gabagaya, G., Bradley, J., Grignard, L., Lanke, K. H., Wanzira, H., Samuel, N., Nicholas, J. W., Emily, L. W., Sarah, G. S., and Chris, D. (2014). Single dose primaquine for clearance of plasmodium falciparum gametocytes in children with uncomplicated malaria in Uganda: a randomised, controlled, double-blind, dose-ranging trial. *The Lancet Infectious Diseases*, 14(2):130–139.

Faber, B. W., Younis, S., Remarque, E. J., Garcia, R. R., Riasat, V., Walraven, V., van der Werff, N., van der Eijk, M., Cavanagh, D. R., Holder, A. A., Thomas, W. A., and Kockena, H. M. C. (2013). Diversity covering AMA1-MSP119 fusion proteins as malaria vaccines. *Infection and Immunity*, 81(5):1479–1490.

Fausto, N. (2004). Liver regeneration and repair: hepatocytes, progenitor cells, and stem cells. *Hepatology*, 39(6):1477–1487.

Fausto, N., Campbell, J. S., and Riehle, K. J. (2006). Liver regeneration. *Hepatology*, 43(51):S45–S53.

Filipe, J. A., Riley, E. M., Drakeley, C. J., Sutherland, C. J., and Ghani, A. C. (2007). Determination of the processes driving the acquisition of immunity to malaria using a mathematical transmission model. *PLoS Computational Biology*, 3(12):e255. doi:10.1371/journal.pcbi.0030255.

Fister, K. R., Lenhart, S., and McNally, J. S. (1998). Optimizing chemotherapy in an HIV model. *Electronic Journal of Differential Equations*, 1998(32):1–12.

Fleming, W. and Rishel, R. (1975). *Optimal Deterministic and Stochastic Control*. Applications of Mathematics, Springer, Berlin, Germany.

Fogh, S., Jepsen, S., and Effersøe, P. (1979). Chloroquine-resistant plasmodium falciparum malaria in Kenya. *Transactions of the Royal Society of Tropical Medicine and Hygiene*, 73(2):228–229.

Foote, S. J. and Cowman, A. F. (1994). The mode of action and the mechanism of resistance to antimalarial drugs. *Acta Tropica*, 56(2-3):157–171.

Franklin, B. S., Parroche, P., Ataíde, M. A., Lauw, F., Ropert, C., de Oliveira, R. B., Pereira, D., Tada, M. S., Nogueira, P., and da Silva, L. H. P. (2009). Malaria primes the innate immune response due to interferon-γ induced enhancement of toll-like receptor expression and function. *Proceedings of the National Academy of Sciences USA*, 106(14):5789–5794.

Frevert, U. (2004). Sneaking in through the back entrance: the biology of malaria liver stages. *Trends in Parasitology*, 20(9):417–424.

Frevert, U., Engelmann, S., Zougbédé, S., Stange, J., Ng, B., Matuschewski, K., Liebes, L., and Yee, H. (2005). Intravital observation of plasmodium berghei sporozoite infection of the liver. *PLoS Biology*, 3(6):e192. https://doi.org/10.1371/journal.pbio.0030192.

Fritsche, G., Larcher, C., Schennach, H., and Weiss, G. (2001). Regulatory interactions between iron and nitric oxide metabolism for immune defense against plasmodium falciparum infection. *The Journal of Infectious Diseases*, 183(9):1388–1394.

Gaff, H. and Schaefer, E. (2009). Optimal control applied to vaccination and treatment strategies for various epidemiological models. *Mathematical Biosciences and Engineering: MBE*, 6(3):469–492.

Galactionova, K., Tediosi, F., Camponovo, F., Smith, T. A., Gething, P. W., and Penny, M. A. (2017). Country specific predictions of the cost-effectiveness of malaria vaccine RTS,S/AS01 in endemic Africa. *Vaccine*, 35(1):53–60.

Gallup, J. L. and Sachs, J. D. (2001). The economic burden of malaria. *The American Journal of Tropical Medicine and Hygiene*, 64(1):85–96.

Ganusov, V. V., Bergstrom, C. T., and Antia, R. (2002). Within-host population dynamics and the evolution of microparasites in a heterogeneous host population. *Evolution*, 56(2):213–223.

Gelband, H., Panosian, C. B., and Arrow, K. J. (2004). *Saving lives, buying time: economics of malaria drugs in an age of resistance*. National Academies Press, USA.

Gerardin, J., Ouédraogo, A. L., McCarthy, K. A., Eckhoff, P. A., and Wenger, E. A. (2015). Characterization of the infectious reservoir of malaria with an agent-based model calibrated to age-stratified parasite densities and infectiousness. *Malaria Journal*, 14(231). doi: 10.1186/s12936-015-0751-y.

Gething, P. W., Van Boeckel, T. P., Smith, D. L., Guerra, C. A., Patil, A. P., Snow, R. W., and Hay, S. I. (2011). Modelling the global constraints of temperature on transmission of P. falciparum and P. vivax. *Parasites & Vectors*, 4(92). https://doi.org/10.1186/1756-3305-4-92.

Gomero, B. (2012). Latin hypercube sampling and partial rank correlation coefficient analysis applied to an optimal control problem. Master's thesis, The university of Tennessee Knoxville.

Goncalves, B. (2017). *The human infectious reservoir of falciparum malaria*. PhD thesis, London School of Hygiene & Tropical Medicine.

Gravenor, M. and Kwiatkowski, D. (1998). An analysis of the temperature effects of fever on the intra-host population dynamics of plasmodium falciparum. *Parasitology*, 117(2):97–105.

Graves, P. M. and Gelband, H. (2006). Vaccines for preventing malaria (spf66). *Cochrane Database of Systematic Reviews*, 1(2):59–66.

Graves, P. M., Gelband, H., and Garner, P. (2014). Primaquine or other 8-aminoquinoline for reducing p. falciparum transmission. *Cochrane Database of Systematic Reviews*, 30(6):CD008152. doi: 10.1002/14651858.CD008152.pub3.

Greenwood, B. and Targett, G. (2009). Do we still need a malaria vaccine? *Parasite Immunology*, 31(9):582–586.

Guinovart, C., Aponte, J. J., Sacarlal, J., Aide, P., Leach, A., Bassat, Q., Macete, E., Dobaño, C., Lievens, M., Loucq, C., Ballou, W. R., Cohen, J., and Alonso, P. L. (2009). Insights into long-lasting protection induced by RTS, S/AS02A malaria vaccine: further results from a phase iib trial in Mozambican children. *PLoS One*, 4(4):e5165. https://doi.org/10.1371/journal.pone.0005165.

Gurarie, D. and McKenzie, F. E. (2006). Dynamics of immune response and drug resistance in malaria infection. *Malaria Journal*, 5(86). doi: 10.1186/1475-2875-5-86.

Hale, J. K. (1969). *Ordinary Differential Equations*. John Wiley & Sons New York, NY, USA.

Hamby, D. (1994). A review of techniques for parameter sensitivity analysis of environmental models. *Environmental Monitoring and Assessment*, 32(2):135–154.

Hardin, G. (1960). The competitive exclusion principle. *Science*, 131(3409):1292–1297.

Harinasuta, T., Suntharasamai, P., and Viravan, C. (1965). Chloroquine-resistant falciparum malaria in Thailand. *Lancet*, 2(7414):657–660.

Harrington, W., Mutabingwa, T., Muehlenbachs, A., Sorensen, B., Bolla, M., Fried, M., and Duffy, P. (2009). Competitive facilitation of drug-resistant plasmodium falciparum malaria parasites in pregnant women who receive preventive treatment. *Proceedings of the National Academy of Sciences of the United States of America*, 106(22):9027–9032.

Hastings, I. (1997). A model for the origins and spread of drug-resistant malaria. *Parasitology*, 115(2):133–141.

Hastings, I. M. and Watkins, W. M. (2005). Intensity of malaria transmission and the evolution of drug resistance. *Acta Tropica*, 94(3):218–229.

Hayward, R., Saliba, K. J., and Kirk, K. (2005). pfmdr1 mutations associated with chloroquine resistance incur a fitness cost in plasmodium falciparum. *Molecular Microbiology*, 55(4):1285–1295.

Heesterbeek, J. and Dietz, K. (1996). The concept of R0 in epidemic theory. *Statistica Neerlandica*, 50(1):89–110.

Heller, L. E. and Roepe, P. D. (2019). Artemisinin-based antimalarial drug therapy: Molecular pharmacology and evolving resistance. *Tropical medicine and infectious disease*, 4(2):89–101.

Hellriegel, B. (1992). Modelling the immune response to malaria with ecological concepts: short-term behaviour against long-term equilibrium. *Proceedings of the Royal Society of London. Series B: Biological Sciences*, 250(1329):249–256.

Hermsen, C. C., Verhage, D. F., Telgt, D. S., Teelen, K., Bousema, J. T., Roestenberg, M., Bolad, A., Berzins, K., Corradin, G., Leroy, O., Theisen, M., and Sauerweina, R. W. (2007). Glutamate-rich protein (GLURP) induces antibodies that inhibit in vitro growth of plasmodium falciparum in a phase 1 malaria vaccine trial. *Vaccine*, 25(15):2930–2940.

Hetzel, C. and Anderson, R. (1996). The within-host cellular dynamics of bloodstage malaria: theoretical and experimental studies. *Parasitology*, 113(1):25–38.

Hisaeda, H., Stowers, A. W., Tsuboi, T., Collins, W. E., Sattabongkot, J. S., Suwanabun, N., Torii, M., and Kaslow, D. C. (2000). Antibodies to malaria vaccine candidates Pvs25 and Pvs28 completely block the ability of plasmodium vivax to infect mosquitoes. *Infection and Immunity*, 68(12):6618–6623.

Hisaeda, H., Yasutomo, K., and Himeno, K. (2005). Malaria: immune evasion by parasites. *The international Journal of Biochemistry & Cell Biology*, 37(4):700–706.

Hodel, E. M., Kay, K., and Hastings, I. M. (2016). Incorporating stage-specific drug action into pharmacological modeling of antimalarial drug treatment. *Antimicrobial Agents and Chemotherapy*, 60(5):2747–2756.

Homan, T. (2016). *Impact of odour-baited mosquito traps for malaria control*. PhD thesis, Wageningen University.

Honeycutt, J. B., Wahl, A., Baker, C., Spagnuolo, R. A., Foster, J., Zakharova, O., Wietgrefe, S., Caro-Vegas, C., Madden, V., and Sharpe, G. (2016). Macrophages sustain HIV replication in vivo independently of T cells. *The Journal of Clinical Investigation*, 126(4):1353–1366.

Horii, T., Shirai, H., Jie, L., Ishii, K. J., Palacpac, N. Q., Tougan, T., Hato, M., Ohta, N., Bobogare, A., Arakaki, Arakaki, N., Matsumoto, Y., Namazue, J., Ishikawab, T., Ueda, S., and Takahashi, M. (2010). Evidences of protection against blood-stage infection of plasmodium falciparum by the novel protein vaccine SE36. *Parasitology International*, 59(3):380–386.

Hoshen, M., Heinrich, R., Stein, W., and Ginsburg, H. (2000). Mathematical modelling of the within-host dynamics of plasmodium falciparum. *Parasitology*, 121(3):227–235.

Iman, R. L. and Helton, J. C. (1988). An investigation of uncertainty and sensitivity analysis techniques for computer models. *Risk Analysis*, 8(1):71–90.

Ince, E. L. (1943). *Integration of ordinary differential equations*. University mathematical texts. Oliver and Boyd.

Jeffery, G. M., Young, M. D., Burgess, R. W., and Eyles, D. E. (1959). Early activity in sporozoite-induced plasmodium falciparum infections. *Annals of Tropical Medicine & Parasitology*, 53(1):51–58.

Joshi, H. R. (2002). Optimal control of an HIV immunology model. *Optimal Control Applications and Methods*, 23(4):199–213.

Joshi, H. R., Lenhart, S., Li, M. Y., and Wang, L. (2006). Optimal control methods applied to disease models. *Contemporary Mathematics*, 410(7):187–208.

Josling, G. A. and Llinas, M. (2015). Sexual development in plasmodium parasites: knowing when it's time to commit. *Nature Reviews Microbiology*, 13(9):573–587.

Jung, E., Lenhart, S., and Feng, Z. (2002). Optimal control of treatments in a two-strain tuberculosis model. *Discrete and Continuous Dynamical Systems Series B*, 2(4):473–482.

Kamangira, B., Nyamugure, P., and Magombedze, G. (2014). A theoretical mathematical assessment of the effectiveness of coartemether in the treatment of plasmodium falciparum malaria infection. *Mathematical Biosciences*, 256:28–41.

Kamgang, J. C. and Sallet, G. (2005). Global asymptotic stability for the disease free equilibrium for epidemiological models. *Comptes Rendus Mathematique*, 341(7):433–438.

Karrakchou, J., Rachik, M., and Gourari, S. (2006). Optimal control and infectiology: application to an HIV/AIDS model. *Applied Mathematics and Computation*, 177(2):807–818.

Kendall, M. G. (1946). *The advanced theory of statistics.*, volume 57. Wiley, London, UK.

Kengne-Ouafo, J. A., Sutherland, C. J., Binka, F. N., Awandare, G. A., Urban, B. C., and Dinko, B. (2019). Immune responses to the sexual stages of plasmodium falciparum parasites. *Frontiers in Immunology*, 10(136). doi: 10.3389/fimmu.2019.00136.

Killeen, G. F., Tatarsky, A., Diabate, A., Chaccour, C. J., Marshall, J. M., Okumu, F. O., Brunner, S., Newby, G., Williams, Y. A., Malone, D., Lucy, T., and Roland, G. (2017). Developing an expanded vector control toolbox for malaria elimination. *BMJ global health*, 2(2):e000211.

Kim, B. N., Nah, K., Chu, C., Ryu, S. U., Kang, Y. H., and Kim, Y. (2012). Optimal control strategy of plasmodium vivax malaria transmission in Korea. *Osong Public Health and Research Perspectives*, 3(3):128–136.

Kim, Y. and Schneider, K. A. (2013). Evolution of drug resistance in malaria parasite populations. *Nature Education Knowledge*, 4(8):6–16.

Kioko, U., Riley, C., Dellicour, S., Were, V., Ouma, P., Gutman, J., Kariuki, S., Omar, A., Desai, M., and Buff, A. M. (2016). A cross-sectional study of the availability and price of anti-malarial medicines and malaria rapid diagnostic tests in private sector retail drug outlets in rural western kenya, 2013. *Malaria Journal*, 15(359). https://doi.org/10.1186/s12936-016-1404-5.

Kirschner, D. and Webb, G. F. (1996). A model for treatment strategy in the chemotherapy of AIDS. *Bulletin of Mathematical Biology*, 58(2):367–390.

Klein, E. Y., Smith, D. L., Boni, M. F., and Laxminarayan, R. (2008). Clinically immune hosts as a refuge for drug-sensitive malaria parasites. *Malaria Journal*, 7(67). https://doi.org/10.1186/1475-2875-7-67.

Klein, E. Y., Smith, D. L., Laxminarayan, R., and Levin, S. (2012). Superinfection and the evolution of resistance to antimalarial drugs. *Proceedings of the Royal Society of London B: Biological Sciences*, 279(1743):3834–3842.

KNBS (2012). 2009 Kenya Population and Housing Census, Volume XIV:Population Projections. Technical report, Kenya National Bureau of Statistics (KNBS), Nairobi. Retrieved from https://www.knbs.or.ke/download/266/analytical-reports/2381/analytical-report-on-population-projections-volume-xiv.pdf. Accessed February 2019.

KNBS (2017). Economic Survey, 2017. Technical report, Kenya National Bureau of Statistics (KNBS), Nairobi. Retrieved from https://www.knbs.or.ke/download/economic-survey-highlights-2017/. Accessed February 2019.

Koch, M. and Baum, J. (2016). The mechanics of malaria parasite invasion of the human erythrocyte–towards a reassessment of the host cell contribution. *Cellular Microbiology*, 18(3):319–329.

Koella, J. and Antia, R. (2003). Epidemiological models for the spread of anti-malarial resistance. *Malaria Journal*, 2(3). https://doi.org/10.1186/1475-2875-2-3.

Koppensteiner, H., Brack-Werner, R., and Schindler, M. (2012). Macrophages and their relevance in Human Immunodeficiency Virus Type I infection. *Retrovirology*, 9(1):82–91.

Krasnoselskii, M. (1964). *Positive Solutions of Operator Equations*. Groningen: Noordhoff, Netherlands.

Krotoski, W. A. (1985). Discovery of the hypnozoite and a new theory of malarial relapse. *Transactions of the Royal Society of Tropical Medicine and Hygiene*, 79(1):1–11.

Krücken, J., Mehnert, L. I., Dkhil, M. A., El-Khadragy, M., Benten, W. P. M., Mossmann, H., and Wunderlich, F. (2005). Massive destruction of malaria-parasitized red blood cells despite spleen closure. *Infection and Immunity*, 73(10):6390–6398.

Kumar, N. (2007). A vaccine to prevent transmission of human malaria: a long way to travel on a dusty and often bumpy road. *Current Science*, pages 1535–1544.

Kwiatkowski, D. and Nowak, M. (1991). Periodic and chaotic host-parasite interactions in human malaria. *Proceedings of the National Academy of Sciences of the United States of America*, 88(12):5111–5113.

Lane, D. (2003). Online statistics education: A multimedia course of study. In *EdMedia: World Conference on Educational Media and Technology*, pages 1317–1320. Association for the Advancement of Computing in Education (AACE), Rice University, Houston, Texas.

LaSalle, J. (1976). The stability of dynamical systems, volume 25 of regional conference series in applied mathematics. *SIAM, Philadelphia, PA*.

Lee, M. C. and Fidock, D. A. (2008). Arresting malaria parasite egress from infected red blood cells. *Nature Chemical Biology*, 4(3):161–162.

Lee, S., Jung, E., and Castillo-Chavez, C. (2010). Optimal control intervention strategies in low-and high-risk problem drinking populations. *Socio-Economic Planning Sciences*, 44(4):258–265.

Legros, M. and Bonhoeffer, S. (2016). A combined within-host and between-hosts modelling framework for the evolution of resistance to antimalarial drugs. *Journal of the Royal Society Interface*, 13(117). 20160148. DOI: 10.1098/rsif.2016.0148.

Lenhart, S. and Workman, J. T. (2007). *Optimal control applied to biological models*. Chapman and Hall/CRC, USA.

Li, M. Y. and Shu, H. (2010). Global dynamics of an in-host viral model with intracellular delay. *Bulletin of Mathematical Biology*, 72(6):1492–1505.

Li, Y., Ruan, S., and Xiao, D. (2011). The within-host dynamics of malaria infection with immune response. *Mathematical Biosciences and Engineering*, 8(4):999–1018.

Liehl, P., Meireles, P., Albuquerque, I. S., Pinkevych, M., Baptista, F., Mota, M. M., Davenport, M. P., and Prudêncio, M. (2015). Innate immunity induced by plasmodium liver infection inhibits malaria reinfections. *Infection and Immunity*, 83(3):1172–1180.

Lin Ouédraogo, A., Gonçalves, B. P., Gnémé, A., Wenger, E. A., Guelbeogo, M. W., Ouédraogo, A., Gerardin, J., Bever, C. A., Lyons, H., Pitroipa, X., Pitroipa, X., Verhave, J. P., Eckhoff, P. A., Drakeley, C., Sauerwein, R., Luty, A. J. F., Kouyate, B., and Bousema, T. (2015). Dynamics of the human infectious reservoir for malaria determined by mosquito feeding assays and ultrasensitive malaria diagnosis in Burkina Faso. *The Journal of Infectious Diseases*, 213(1):90–99.

Mackinnon, M. (2005). Drug resistance models for malaria. *Acta Tropica*, 94(3):207–217.

Magombedze, G., Chiyaka, C., and Mukandavire, Z. (2011a). Optimal control of malaria chemotherapy. *Nonlinear Analysis: Modelling and Control*, 16(4):415–434.

Magombedze, G., Garira, W., Mwenje, E., and Bhunu, C. P. (2011b). Optimal control for HIV-1 multi-drug therapy. *International Journal of Computer Mathematics*, 88(2):314–340.

Magombedze, G., Mukandavire, Z., Chiyaka, C., and Musuka, G. (2009a). Optimal control of a sex-structured HIV/AIDS model with condom use. *Mathematical Modelling and Analysis*, 14(4):483–494.

Magombedze, G., Tchuenche, J., and Chiyaka, C. (2009b). With-in host modelling: Their complexities and limitations. *Infectious Disease Modelling Research Progress, Series: Public Health in the 21st Century, JM Tchuenche and C. Chiyaka, eds., Nova Science Publishers, New York*, pages 253–260.

Mahmoudi, S. and Keshavarz, H. (2018). Malaria vaccine development: The need for novel approaches: A review article. *Iranian Journal of Parasitology*, 13(1):1–10.

Makinde, O. D. and Okosun, K. O. (2011). Impact of chemo-therapy on optimal control of malaria disease with infected immigrants. *BioSystems*, 104(1):32–41.

Malaguarnera, L. and Musumeci, S. (2002). The immune response to plasmodium falciparum malaria. *The Lancet Infectious Diseases*, 2(8):472–478.

March, S., Ng, S., Velmurugan, S., Galstian, A., Shan, J., Logan, D. J., Carpenter, A. E., Thomas, D., Sim, B. K. L., Mota, M. M., Mota, M. M., Hoffman, S. L., and Bhatia1, S. N. (2013). A microscale human liver platform that supports the hepatic stages of plasmodium falciparum and vivax. *Cell Host & Microbe*, 14(1):104–115.

Maude, R. J., Pontavornpinyo, W., Saralamba, S., Aguas, R., Yeung, S., Dondorp, A. M., Day, N. P., White, N. J., and White, L. J. (2009). The last man standing is the most resistant: eliminating artemisinin-resistant malaria in Cambodia. *Malaria Journal*, 8(31). https://doi.org/10.1186/1475-2875-8-31.

Mbogo, R. W. (2014). *Intra-Host stochastic models for HIV dynamics and management*. PhD thesis, Strathmore University Library.

MCGV (2011). A research agenda for malaria eradication: vaccines. The malERA Consultative Group on Vaccines (MCGV). *PLoS Medicine*, 8(1). e1000398. https://doi.org/10.1371/journal.pmed.1000398.

McKay, M. D., Beckman, R. J., and Conover, W. J. (1979). Comparison of three methods for selecting values of input variables in the analysis of output from a computer code. *Technometrics*, 21(2):239–245.

McKenzie, F. E. (2000). Why model malaria? *Parasitology Today*, 16(12):511–516.

McKenzie, F. E. and Bossert, W. H. (1997). The dynamics of plasmodium falciparum blood-stage infection. *Journal of Theoretical Biology*, 188(1):127–140.

McKenzie, F. E. and Bossert, W. H. (1998). A target for intervention in plasmodium falciparum infections. *The American journal of Tropical Medicine and Hygiene*, 58(6):763–767.

McKenzie, F. E. and Samba, E. M. (2004). The role of mathematical modeling in evidence-based malaria control. *The American Journal of Tropical Medicine and Hygiene*, 71(2):94–96.

McQueen, P. G. and McKenzie, F. E. (2004). Age-structured red blood cell susceptibility and the dynamics of malaria infections. *Proceedings of the National Academy of Sciences of the United States of America*, 101(24):9161–9166.

Mellouk, S., Berbiguier, N., Druilhe, P., Sedegah, M., Galey, B., Yuan, L., Leef, M., Charoenvit, Y., Paul, C., Hoffman, S., and Beaudoin, R. (1990). Evaluation of an in vitro assay aimed at measuring protective antibodies against sporozoites. *Bulletin of the World Health Organization*, 68(Suppl):52–59.

Mellouk, S., Maheshwari, R. K., Rhodes-Feuillette, A., Beaudoin, R. L., Berbiguier, N., Matile, H., Miltgen, F., Landau, I., Pied, S., and Chigot, J. P. (1987). Inhibitory activity of interferons and interleukin 1 on the development of plasmodium falciparum in human hepatocyte cultures. *The Journal of Immunology*, 139(12):4192–4195.

Mikucki, M. A. (2012). *Sensitivity analysis of the basic reproduction number and other quantities for infectious disease models*. PhD thesis, Colorado State University Library.

Miller, L. H., Ackerman, H. C., Su, X.-z., and Wellems, T. E. (2013). Malaria biology and disease pathogenesis: insights for new treatments. *Nature Medicine*, 19(2):156–167.

Miller, L. H., Baruch, D. I., Marsh, K., and Doumbo, O. K. (2002). The pathogenic basis of malaria. *Nature*, 415(6872):673–679.

Miller, L. H., Good, M. F., and Milon, G. (1994). Malaria pathogenesis. *Science*, 264(5167):1878–1883.

Mita, T., Tanabe, K., and Kita, K. (2009). Spread and evolution of plasmodium falciparum drug resistance. *Parasitology international*, 58(3):201–209.

Miura, K. (2016). Progress and prospects for blood-stage malaria vaccines. *Expert Review of Vaccines*, 15(6):765–781.

Mlay, G. M., Luboobi, L., Kuznetsov, D., and Shahada, F. (2015). Optimal treatment and vaccination control strategies for the dynamics of pulmonary tuberculosis. *International Journal of Advances in Applied Mathematics and Mechanics*, 2(3):196–207.

MOH (2016). The epidemiology and control profile of malaria in Kenya: reviewing the evidence to guide the future vector control. Technical report, Ministry of Health. Government of Kenya. Retrieved from https://virtual.lshtm.ac.uk/wp-content/uploads/2016/11/Kenya-Epidemiological-Profile.pdf. Accessed March 2019.

Mohammed, A., Ndaro, A., Kalinga, A., Manjurano, A., Mosha, J. F., Mosha, D. F., van Zwetselaar, M., Koenderink, J. B., Mosha, F. W., Alifrangis, M., Reyburn, H., Roper, C., and Kavishe, R. A. (2013). Trends in chloroquine resistance marker, Pfcrt-K76T mutation ten years after chloroquine withdrawal in Tanzania. *Malaria Journal*, 12(415). doi:10.1186/1475-2875-12-415.

Molineaux, L., Diebner, H., Eichner, M., Collins, W., Jeffery, G., and Dietz, K. (2001). Plasmodium falciparum parasitaemia described by a new mathematical model. *Parasitology*, 122(4):379–391.

Molineaux, L. and Dietz, K. (1999). Review of intra-host models of malaria. *Parassitologia*, 41(1/3):221–232.

Mombo-Ngoma, G., Remppis, J., Sievers, M., Zoleko Manego, R., Endamne, L., Kabwende, L., Veletzky, L., Nguyen, T. T., Groger, M., Felix, L., Johannes, M., Lena, F., Johanna, K., Chiara, C., David, H., Stephan, D., Joerg, M., Thirumalaisamy, P. V., Bertrand, L., Michael, R., Ayola, A. A., Mordmueller, B., and Kremsner, P. G. (2017). Efficacy and safety of fosmidomycin–piperaquine as nonartemisinin-based combination therapy for uncomplicated falciparum malaria: A single-arm, age de-escalation proof-of-concept study in gabon. *Clinical Infectious Diseases*, 66(12):1823–1830.

Moorthy, V. S. and Ballou, W. R. (2009). Immunological mechanisms underlying protection mediated by RTS,S: a review of the available data. *Malaria Journal*, 8(312). https://doi.org/10.1186/1475-2875-8-312.

Moorthy, V. S., Good, M. F., and Hill, A. V. (2004). Malaria vaccine developments. *The Lancet*, 363(9403):150–156.

Mpeshe, S. C., Luboobi, L. S., and Nkansah-gyekye, Y. (2014). Optimal control strategies for the dynamics of Rift Valley Fever. *Communications in Optimization Theory*, 26(3):385–402.

MVFG (2018). Malaria vaccine technology roadmap. Malaria vaccine funders group. Autoimmunity Research Foundation. Retrieved from http://www.who.int/immunization/topics/malaria/$vaccine_roadmap$/en/. Accessed April 2018.

MVI (2018). Accelerating malaria vaccine development. Malaria Vaccine Initiative. Retrieved from http://www.malariavaccine.org/malaria-and-vaccines/need-vaccine. Accessed February 2018.

Mwanga, G. G., Haario, H., and Capasso, V. (2015). Optimal control problems of epidemic systems with parameter uncertainties: application to a malaria two-age-classes transmission model with asymptomatic carriers. *Mathematical Biosciences*, 261(2015):1–12.

Mwanga, G. G., Haario, H., and Nannyonga, B. (2014). Optimal control of malaria model with drug resistance in presence of parameter uncertainty. *Applied Mathematical Sciences*, 8(55):2701–2730.

Nakakawa, J., Mugisha, J. Y., Shaw, M. W., Tinzaara, W., and Karamura, E. (2017). Banana xanthomonas wilt infection: The role of debudding and roguing as control options within a mixed cultivar plantation. *International Journal of Mathematics and Mathematical Sciences*, 2017. Article ID 4865015, 13 pages. https://doi.org/10.1155/2017/4865015.

Namawejje, H., Luboobi, L. S., Kuznetsov, D., and Wobudeya, E. (2014). Modeling optimal control of rotavirus disease with different control strategies. *Journal of Mathematical and Computational Science*, 4(5):892–914.

Nega1, D., Alemu, A., and Tasew, G. (2016). Malaria vaccine development: Recent advances alongside the barriers. *Journal of Bacteriology and Parasitology*, 7(6). DOI: 10.4172/2155-9597.1000300.

Neilan, R. L. M., Schaefer, E., Gaff, H., Fister, K. R., and Lenhart, S. (2010). Modeling optimal intervention strategies for cholera. *Bulletin of Mathematical Biology*, 72(8):2004–2018.

Newbold, C., Pinches, R., Roberts, D., and Marsh, K. (1992). Plasmodium falciparum: the human agglutinating antibody response to the infected red cell surface is predominantly variant specific. *Experimental Parasitology*, 75(3):281–292.

Nganou-Makamdop, K., van Gemert, G.-J., Arens, T., Hermsen, C. C., and Sauerwein, R. W. (2012). Long term protection after immunization with p. berghei sporozoites correlates with sustained ifnγ responses of hepatic cd8+ memory t cells. *PloS One*, 7(5):e36508. https://doi.org/10.1371/journal.pone.0036508.

Niger, A. M. and Gumel, A. B. (2011). Immune response and imperfect vaccine in malaria dynamics. *Mathematical Population Studies*, 18(2):55–86.

NIH (2019). Clinical Trials. US national library of medicine. Retrieved from https://clinicaltrials.gov/ct2/results?cond=Malaria%2CFalciparum&term=vaccine+combinations&cntry=&state=&city=&dist=. Accessed April 2019.

Noedl, H., Se, Y., Schaecher, K., Smith, B. L., Socheat, D., and Fukuda, M. M. (2008). Evidence of artemisinin-resistant malaria in western Cambodia. *New England Journal of Medicine*, 359(24):2619–2620.

Nudelman, S., Renia, L., Charoenvit, Y., Yuan, L., Miltgen, F., Beaudoin, R., and Mazier, D. (1989). Dual action of anti-sporozoite antibodies in vitro. *The Journal of Immunology*, 143(3):996–1000.

Nunes, J. K., Woods, C., Carter, T., Raphael, T., Morin, M. J., Diallo, D., Leboulleux, D., Jain, S., Loucq, C., and Kaslow, D. C. (2014). Development of a transmission-blocking malaria vaccine: progress, challenges, and the path forward. *Vaccine*, 32(43):5531–5539.

Oeuvray, C., Bouharoun-Tayoun, H., Gras-Masse, H., Bottius, E., Kaidoh, T., Aikawa, M., Filgueira, M.-C., Tartar, A., and Druilhe, P. (1994). Merozoite surface protein-3: a malaria protein inducing antibodies that promote plasmodium falciparum killing by cooperation with blood monocytes. *Blood*, 84(5):1594–1602.

Ofosu-Okyere, A., Mackinnon, M., Sowa, M., Koram, K., Nkrumah, F., Osei, Y., Hill, W., Wilson, M., and Arnot, D. (2001). Novel plasmodium falciparum clones and rising clone multiplicities are associated with the increase in malaria morbidity in Ghanaian children during the transition into the high transmission season. *Parasitology*, 123(2):113–123.

Ogutu, B. (2013). Artemether and lumefantrine for the treatment of uncomplicated plasmodium falciparum malaria in sub-Saharan Africa. *Expert Opinion on Pharmacotherapy*, 14(5):643–654.

Ogutu, B. R., Apollo, O. J., McKinney, D., Okoth, W., Siangla, J., Dubovsky, F., Tucker, K., Waitumbi, J. N., Diggs, C., Wittes, J., Malkin, E., Leach, A., Soisson, L. A., Milman, J. B., Otieno, L., Holland, C. A., Polhemus, M., Remich, S. A., Ockenhouse, C. F., Cohen, J., Ballou, W. R., Martin, S. K., Angov, E., Stewart, V. A., Lyon, J. A., Jr, D. G. H., and R, M. (2009). Blood stage malaria vaccine eliciting high antigen-specific antibody concentrations confers no protection to young children in Western Kenya. *PloS One*, 4(3):e4708. doi:10.1371/journal.pone.0004708.

Okell, L. C., Drakeley, C. J., Bousema, T., Whitty, C. J., and Ghani, A. C. (2008). Modelling the impact of artemisinin combination therapy and long-acting treatments on malaria transmission intensity. *PLoS Medicine*, 5(11):e226. https://doi.org/10.1371/journal.pmed.0050226.

Okosun, K. O. and Makinde, O. D. (2012). On a drug-resistant malaria model with susceptible individuals without access to basic amenities. *Journal of Biological Physics*, 38(3):507–530.

Okosun, K. O., Ouifki, R., and Marcus, N. (2011). Optimal control analysis of a malaria disease transmission model that includes treatment and vaccination with waning immunity. *Biosystems*, 106(2-3):136–145.

Olaniyi, S. and Obabiyi, O. S. (2014). Qualitative analysis of malaria dynamics with nonlinear incidence function. *Applied Mathematical Sciences*, 8(78):3889–3904.

Omondi, E. O., Orwa, T. O., and Nyabadza, F. (2018). Application of optimal control to the onchocerciasis transmission model with treatment. *Mathematical Biosciences*, 297(2018):43–57.

Onori, E. (1984). The problem of plasmodium falciparum drug resistance in Africa South of the Sahara. *Bulletin of the World Health Organization*, 62(Suppl):55–62.

Orenstein, W. A., Wassilak, S. G., Strebel, P. M., Bernier, R. H., and Blackwelder, W. C. (1990). Efficacy of pertussis vaccine. *The Journal of Pediatrics*, 117(3):508–508.

Orwa, T. O., Mbogo, R. W., and Luboobi, L. S. (2018). Mathematical model for the in-host malaria dynamics subject to malaria vaccines. *Letters in Biomathematics*, 5(1):222–251.

Osorio, L., Gonzalez, I., Olliaro, P., and Taylor, W. R. (2007). Artemisinin-based combination therapy for uncomplicated *Plasmodium falciparum* malaria in Colombia. *Malaria Journal*, 6(25). https://doi.org/10.1186/1475-2875-6-25.

Otieno, L., Oneko, M., Otieno, W., Abuodha, J., Owino, E., Odero, C., Mendoza, Y. G., Andagalu, B., Awino, N., Ivinson, K., Heerwegh, D., Otsyula, N., Oziemkowska, M., Usuf, E. A., Otieno, A., Otieno, K., Leboulleux, D., Leach, A., and Hamel, M. J. (2016). Safety and immunogenicity of RTS, S/AS01 malaria vaccine in infants and children with WHO stage 1 or 2 HIV disease: a randomised, double-blind, controlled trial. *The Lancet Infectious Diseases*, 16(10):1134–1144.

Ouattara, A. and Laurens, M. B. (2014). Vaccines against malaria. *Clinical Infectious Diseases*, 60(6):930–936.

Ouji, M., Augereau, J.-M., Paloque, L., and Benoit-Vical, F. (2018). Plasmodium falciparum resistance to artemisinin-based combination therapies: A sword of damocles in the path toward malaria elimination. *Parasite*, 25(24). doi: 10.1051/parasite/2018021.

Overturf, K., Al-Dhalimy, M., Ou, C.-N., Finegold, M., and Grompe, M. (1997). Serial transplantation reveals the stem-cell-like regenerative potential of adult mouse hepatocytes. *The American Journal of Pathology*, 151(5):1273–1280.

Packard, R. M. (2007). *The making of a tropical disease: a short history of malaria*. JHU Press.

Palafox, B., Patouillard, E., Tougher, S., Goodman, C., Hanson, K., Kleinschmidt, I., Torres Rueda, S., Kiefer, S., O'Connell, K., Zinsou, C., Phok, S., Akulayi, L., Arogundade, E., Buyungo, P., Mpasela, F., Poyer3, S., and Chavasse, D. (2015). Prices and mark-ups on antimalarials: evidence from nationally representative studies in six malaria-endemic countries. *Health Policy and Planning*, 31(2):148–160.

Pan, W., Huang, D., Zhang, Q., Qu, L., Zhang, D., Zhang, X., Xue, X., and Qian, F. (2004). Fusion of two malaria vaccine candidate antigens enhances product yield, immunogenicity, and antibody-mediated inhibition of parasite growth in vitro. *The Journal of Immunology*, 172(10):6167–6174.

Pandey, A. K., Reddy, K. S., Sahar, T., Gupta, S., Singh, H., Reddy, E. J., Asad, M., Siddiqui, F. A., Gupta, P., Singh, B., More, K. R., Mohmmed, A., Chitnis, C. E., Chauhan, V. S., and Gaur, D. (2013). Identification of a potent combination of key plasmodium falciparum merozoite antigens that elicit strain-transcending parasite-neutralizing antibodies. *Infection and Immunity*, 81(2):441–451.

Patiño, J. A. G., Holder, A. A., McBride, J. S., and Blackman, M. J. (1997). Antibodies that inhibit malaria merozoite surface protein–1 processing and erythrocyte invasion are blocked by naturally acquired human antibodies. *Journal of Experimental Medicine*, 186(10):1689–1699.

Paul, A. S., Egan, E. S., and Duraisingh, M. T. (2015). Host-parasite interactions that guide red blood cell invasion by malaria parasites. *Current Opinion in Hematology*, 22(3):220–226.

Penny, M. A., Verity, R., Bever, C. A., Sauboin, C., Galactionova, K., Flasche, S., White, M. T., Wenger, E. A., Van de Velde, N., Pemberton-Ross, P., Griffi, J. T., Smith, T. A., Eckhoff, P. A., Muhib, F., Jit, M., and Ghani, A. C. (2016). Public health impact and cost-effectiveness of the RTS,S/AS01 malaria vaccine: a systematic comparison of predictions from four mathematical models. *The Lancet*, 387(10016):367–375.

Pereira, A. and Broed, R. (2006). Methods for uncertainty and sensitivity analysis: review and recomendations for implementation in ecolego. Stockholm: Fysikum. Retrieved from http://urn.kb.se/resolve?urn=urn:nbn:se:su:diva-1079. Accessed April 2019.

Peters, A. L. and Noorden, C. J. V. (2009). Glucose-6-phosphate dehydrogenase deficiency and malaria: cytochemical detection of heterozygous G6PD deficiency in women. *Journal of Histochemistry & Cytochemistry*, 57(11):1003–1011.

Pilyugin, S. S. and Antia, R. (2000). Modeling immune responses with handling time. *Bulletin of Mathematical Biology*, 62(5):869–890.

Plassmeyer, M. L., Reiter, K., Shimp, R. L., Kotova, S., Smith, P. D., Hurt, D. E., House, B., Zou, X., Zhang, Y., and Hickman, M. (2009). Structure of the plasmodium falciparum circumsporozoite protein, a leading malaria vaccine candidate. *Journal of Biological Chemistry*, 284(39):26951–26963.

Plowe, C. V., Alonso, P., and Hoffman, S. L. (2009). The potential role of vaccines in the elimination of falciparum malaria and the eventual eradication of malaria. *The Journal of Infectious Diseases*, 200(11):1646–1649.

Polhemus, M. E., Remich, S. A., Ogutu, B. R., Waitumbi, J. N., Otieno, L., Apollo, S., Cummings, J. F., Kester, K. E., Ockenhouse, C. F., Stewart, A., Anyinam, O. O., Ramboer, I., Cahill, C. P., Lievens, M., Dubois, M.-C., Marie-Ange, Demoitie, Leach, A., Cohen, J., Ballou, W. R., and D. Gray Heppner, J. (2009). Evaluation of RTS, S/AS02A and RTS, S/AS01B in adults in a high malaria transmission area. *PloS One*, 4(7):e6465. https://doi.org/10.1371/journal.pone.0006465.

Pontryagin, L. S. (1987). *Mathematical theory of optimal processes*. CRC Press.

Pukrittayakamee, S., Chotivanich, K., Chantra, A., Clemens, R., Looareesuwan, S., and White, N. J. (2004). Activities of artesunate and primaquine against asexual-and sexual-stage parasites in falciparum malaria. *Antimicrobial Agents and Chemotherapy*, 48(4):1329–1334.

Rampling, T., Ewer, K. J., Bowyer, G., Bliss, C. M., Edwards, N. J., Wright, D., Payne, R. O., Venkatraman, N., de Barra, E., and Snudden, C. M. (2016). Safety and high level efficacy of the combination malaria vaccine regimen of RTS, S/AS01B with chimpanzee adenovirus 63 and modified vaccinia ankara vectored vaccines expressing ME-TRAP. *The Journal of Infectious Diseases*, 214(5):772–781.

RCTP (2011). First results of phase 3 trial of RTS, S/AS01 malaria vaccine in African children. RTS,S Clinical Trials Partnership (rctp). *New England Journal of Medicine*, 365(20):1863–1875.

RCTP (2012). A phase 3 trial of RTS, S/AS01 malaria vaccine in African infants. RTS,S Clinical Trials Partnership (rctp). *New England Journal of Medicine*, 367(24):2284–2295.

RCTP (2014). Efficacy and safety of the RTS, S/AS01 malaria vaccine during 18 months after vaccination: a phase 3 randomized, controlled trial in children and young infants at 11 African sites. RTS,S Clinical Trials Partnership (rctp). *PLoS Medicine*, 11(7):e1001685. doi: 10.1371/journal.pmed.1001685.

Recht, J., Ashley, E., and White, N. (2014). *Safety of 8-aminoquinoline antimalarial medicines*. World Health Organization, Geneva.

Reilly, H. B., Wang, H., Steuter, J. A., Marx, A. M., and Ferdig, M. T. (2007). Quantitative dissection of clone-specific growth rates in cultured malaria parasites. *International Journal for Parasitology*, 37(14):1599–1607.

Renia, L., Marussig, M. S., Grillot, D., Pied, S., Corradin, G., Miltgen, F., Del Giudice, G., and Mazier, D. (1991). In vitro activity of CD4+ and CD8+ T lymphocytes from mice immunized with a synthetic malaria peptide. *Proceedings of the National Academy of Sciences of the United States of America*, 88(18):7963–7967.

Rouzine, I. M. and McKenzie, F. E. (2003). Link between immune response and parasite synchronization in malaria. *Proceedings of the National Academy of Sciences of the United States of America*, 100(6):3473–3478.

Rowe, A. K., Rowe, S. Y., Snow, R. W., Korenromp, E. L., Schellenberg, J. R. A., Stein, C., Nahlen, B. L., Bryce, J., Black, R. E., and Steketee, R. W. (2006). The burden of malaria mortality among African children in the year 2000. *International Journal of Epidemiology*, 35(3):691–704.

Rubinstein, R. Y. and Kroese, D. P. (2016). *Simulation and the Monte Carlo method*, volume 10. John Wiley & Sons.

Sachs, J. and Malaney, P. (2002). The economic and social burden of malaria. *Nature*, 415(6872):680–685.

Sagara, I., Dicko, A., Ellis, R. D., Fay, M. P., Diawara, S. I., Assadou, M. H., Sissoko, M. S., Kone, M., Diallo, A. I., Saye, R., Guindo, M. A., Kante, O., Niambele, M. B., Miura, K., Mullen, G. E., Pierce, M., Martin, L. B., Dolo, A., Diallo, D. A., Doumbo, O. K., Miller, L. H., and Saul, A. (2009). A randomized controlled phase 2 trial of the blood stage AMA1-C1/Alhydrogel malaria vaccine in children in Mali. *Vaccine*, 27(23):3090–3098.

Saul, A. (1998). Models for the in-host dynamics of malaria revisited: errors in some basic models lead to large over-estimates of growth rates. *Parasitology*, 117(5):405–407.

Schmidt, J. W. and Hess, W. (1988). Positivity of cubic polynomials on intervals and positive spline interpolation. *BIT Numerical Mathematics*, 28(2):340–352.

Schwenk, R., Asher, L. V., Chalom, I., Lanar, D., Sun, P., White, K., Keil, D., Kester, K. E., Stoute, J., Heppner, D. G., and Krzych, U. (2003). Opsonization by antigen-specific antibodies as a mechanism of protective immunity induced by plasmodium falciparum circumsporozoite protein-based vaccine. *Parasite Immunology*, 25(1):17–25.

Seguin, M. C., Klotz, F. W., Schneider, I., Weir, J. P., Goodbary, M., Slayter, M., Raney, J. J., Aniagolu, J. U., and Green, S. J. (1994). Induction of nitric oxide synthase protects against malaria in mice exposed to irradiated plasmodium berghei infected mosquitoes: involvement of interferon gamma and cd8+ t cells. *Journal of Experimental Medicine*, 180(1):353–358.

Selemani, M. A., Luboobi, L. S., and Nkansah-Gyekye, Y. (2016). On stability of the in-human host and in-mosquito dynamics of malaria parasite. *Asian Journal of Mathematics and Applications*, 2016. Article ID ama0353, 23 pages. ISSN 2307-7743.

Selemani, M. A., Luboobi, L. S., and Nkansah-Gyekye, Y. (2017a). The in-human host and in-mosquito dynamics of malaria parasites with immune responses. *New Trends in Mathematical Sciences*, 5(3):182–207.

Selemani, M. A., Luboobi, L. S., and Nkansah-Gyekye, Y. (2017b). Modelling of the in-human host and in mosquito dynamics of parasite. *Journal of Mathematical and Computational Science*, 7(3):430–455.

Sherrard-Smith, E., Sala, K. A., Betancourt, M., Upton, L. M., Angrisano, F., Morin, M. J., Ghani, A. C., Churcher, T. S., and Blagborough, A. M. (2018). Synergy in anti-malarial pre-erythrocytic and transmission-blocking antibodies is achieved by reducing parasite density. *Elife*, 7. e35213 DOI: 10.7554/eLife.35213.

Shimp Jr, R. L., Rowe, C., Reiter, K., Chen, B., Nguyen, V., Aebig, J., Rausch, K. M., Kumar, K., Wu, Y., Jin, A. J., David, S. J., and Narum, D. L. (2013). Development of a Pfs25-EPA malaria transmission blocking vaccine as a chemically conjugated nanoparticle. *Vaccine*, 31(28):2954–2962.

Shiri, T., Garira, W., and Musekwa, S. D. (2005a). A two-strain HIV-1 mathematical model to assess the effects of chemotherapy on disease parameters. 2(4):811–832.

Shiri, T., Hove-Musekwa, S. D., and Garira, W. (2005b). Optimal control of combined therapy in a single strain HIV-1 model. *Electronic Journal of Differential Equations*, 2005(52):1–22.

Sidhu, A. B. S., Verdier-Pinard, D., and Fidock, D. A. (2002). Chloroquine resistance in plasmodium falciparum malaria parasites conferred by pfcrt mutations. *Science*, 298(5591):210–213.

Sidjanski, S. and Vanderberg, J. P. (1997). Delayed migration of plasmodium sporozoites from the mosquito bite site to the blood. *The American Journal of Tropical Medicine and Hygiene*, 57(4):426–429.

Silva, C. J., Maurer, H., and Torres, D. F. (2016). Optimal control of a tuberculosis model with state and control delays. *Mathematical Biosciences and Engineering*, 14(1):321–337.

Silva, C. J. and Torres, D. F. (2012). Optimal control strategies for tuberculosis treatment: a case study in Angola. *Numerical Algebra, Control and Optimization*, 2(3):601–617.

Silva, C. J. and Torres, D. F. (2013). An optimal control approach to malaria prevention via insecticide-treated nets. In *Conference Papers in Science*, volume 2013. Hindawi.

Silvie, O., Rubinstein, E., Franetich, J.-F., Prenant, M., Belnoue, E., Rénia, L., Hannoun, L., Eling, W., Levy, S., Boucheix, C., and Mazier, D. (2003). Hepatocyte cd81 is required for plasmodium falciparum and plasmodium yoelii sporozoite infectivity. *Nature Medicine*, 9(1):93–96.

Singh, A. P., Buscaglia, C. A., Wang, Q., Levay, A., Nussenzweig, D. R., Walker, J. R., Winzeler, E. A., Fujii, H., Fontoura, B. M., and Nussenzweig, V. (2007). Plasmodium circumsporozoite protein promotes the development of the liver stages of the parasite. *Cell*, 131(3):492–504.

Singh, B. and Daneshvar, C. (2013). Human infections and detection of plasmodium knowlesi. *Clinical Microbiology Reviews*, 26(2):165–184.

Sinha, A. (2014). *Molecular basis of gametocytogenesis in malaria parasites*. PhD thesis, University of Glasgow.

Small, D. S., Cheng, J., and Ten Have, T. R. (2010). Evaluating the efficacy of a malaria vaccine. *The International Journal of Biostatistics*, 6(2):4–26.

Smith, D. L., Klein, E. Y., McKenzie, F. E., and Laxminarayan, R. (2010). Prospective strategies to delay the evolution of anti-malarial drug resistance: weighing the uncertainty. *Malaria Journal*, 9(217). https://doi.org/10.1186/1475-2875-9-217.

Smithuis, F., Kyaw, M. K., Phe, O., Win, T., Aung, P. P., Oo, A. P. P., Naing, A. L., Nyo, M. Y., Myint, N. Z. H., Imwong, M., Ashley, E., Lee, S. J., and White, N. J. (2010). Effectiveness of five artemisinin combination regimens with or without primaquine in uncomplicated falciparum malaria: an open-label randomised trial. *The Lancet Infectious Diseases*, 10(10):673–681.

Snow, R. W., Guerra, C. A., Noor, A. M., Myint, H. Y., and Hay, S. I. (2005). The global distribution of clinical episodes of plasmodium falciparum malaria. *Nature*, 434(7030):214–217.

Snow, R. W., Trape, J.-F., and Marsh, K. (2001). The past, present and future of childhood malaria mortality in Africa. *Trends in Parasitology*, 17(12):593–597.

Soko, W., Chimbari, M. J., and Mukaratirwa, S. (2015). Insecticide resistance in malaria-transmitting mosquitoes in Zimbabwe: a review. *Infectious Diseases of Poverty*, 4(1):46–58.

Stein, M. (1987). Large sample properties of simulations using latin hypercube sampling. *Technometrics*, 29(2):143–151.

Stoute, J. A., Slaoui, M., Heppner, D. G., Momin, P., Kester, K. E., Desmons, P., Wellde, B. T., Garçon, N., Krzych, U., and Marchand, M. (1997). A preliminary evaluation of a recombinant circumsporozoite protein vaccine against plasmodium falciparum malaria. *New England Journal of Medicine*, 336(2):86–91.

Stowers, A. W., Kennedy, M. C., Keegan, B. P., Saul, A., Long, C. A., and Miller, L. H. (2002). Vaccination of monkeys with recombinant plasmodium falciparum apical membrane antigen 1 confers protection against blood-stage malaria. *Infection and Immunity*, 70(12):6961–6967.

Sturm, A., Amino, R., Van de Sand, C., Regen, T., Retzlaff, S., Rennenberg, A., Krueger, A., Pollok, J.-M., Menard, R., and Heussler, V. T. (2006). Manipulation of host hepatocytes by the malaria parasite for delivery into liver sinusoids. *Science*, 313(5791):1287–1290.

Sun, P., Schwenk, R., White, K., Stoute, J. A., Cohen, J., Ballou, W. R., Voss, G., Kester, K. E., Heppner, D. G., and Krzych, U. (2003). Protective immunity induced with malaria vaccine, RTS,S, is linked to plasmodium falciparum circumsporozoite protein-specific CD4+ and CD8+ T cells producing IFN-γ. *The Journal of Immunology*, 171(12):6961–6967.

Swinton, J. (1996). The dynamics of blood-stage malaria: Modelling strain specific and strain transcending immunity. In Isham, V. and Medley, G., editors, *Models for Infectious Human Diseases: Their Structure and Relation to Data*, volume 2010, pages 210–212. Cambridge University Press, Cambridge, UK.

Tabo, Z., Luboobi, L. S., and Ssebuliba, J. (2017). Mathematical modelling of the in-host dynamics of malaria and the effects of treatment. *Journal of Mathematics and Computer Science*, 17(1):1–21.

Talapko, J., Skrlec, I., Alebic, T., Jukic, M., and Vcev, A. (2019). Malaria: The past and the present. *Microorganisms*, 7(6):PMC6617065. https://doi:10.3390/microorganisms7060179.

Talisuna, A. O., Bloland, P., and d'Alessandro, U. (2004). History, dynamics, and public health importance of malaria parasite resistance. *Clinical Microbiology Reviews*, 17(1):235–254.

Talisuna, A. O., Langi, P., Mutabingwa, T. K., Van Marck, E., Speybroeck, N., Egwang, T. G., Watkins, W. W., Hastings, I. M., and D'Alessandro, U. (2003). Intensity of transmission and spread of gene mutations linked to chloroquine and sulphadoxine-pyrimethamine resistance in falciparum malaria. *International Journal for Parasitology*, 33(10):1051–1058.

Talisuna, A. O., Okello, P. E., Erhart, A., Coosemans, M., and D'Alessandro, U. (2007). Intensity of malaria transmission and the spread of plasmodium falciparum–resistant malaria: a review of epidemiologic field evidence. In *Defining and Defeating the Intolerable Burden of Malaria III: Progress and Perspectives: Supplement to Volume 77 (6) of American Journal of Tropical Medicine and Hygiene*. American Society of Tropical Medicine and Hygiene.

Talman, A. M., Domarle, O., McKenzie, F. E., Ariey, F., and Robert, V. (2004). Gametocytogenesis: the puberty of plasmodium falciparum. *Malaria Journal*, 3(24). doi: 10.1186/1475-2875-3-24.

Teun, B., Lucy, O., Seif, S., Jamie, T. G., Sabah, O., Patrick, S., Collins, S., Robert, S., Azra, C. G., and Chris, D. (2010). Revisiting the circulation time of plasmodium falciparum gametocytes: molecular detection methods to estimate the duration of gametocyte carriage and the effect of gametocytocidal drugs. *Malaria Journal*, 9(136). http://www.malariajournal.com/content/9/1/136.

Thompson, P. E. and Leslie, W. (1972). *Antimalarial agents: chemistry and phamacology*, volume In G. deStevens (ed.), Medicinal chemistry. Academic Press, Inc., New York.

Trape, J.-F., Pison, G., Preziosi, M.-P., Enel, C., du Loû, A. D., Delaunay, V., Samb, B., Lagarde, E., Molez, J.-F., and Simondon, F. (1998). Impact of chloroquine resistance on malaria mortality. *Comptes Rendus de l'Académie des Sciences-Series III-Sciences de la Vie*, 321(8):689–697.

Tsuji, M. and Zavala, F. (2003). T cells as mediators of protective immunity against liver stages of plasmodium. *Trends in Parasitology*, 19(2):88–93.

Tumwiine, J., Mugisha, J., and Luboobi, L. (2008). On global stability of the intra-host dynamics of malaria and the immune system. *Journal of Mathematical Analysis and Applications*, 341(2):855–869.

Tuteja, R. (2002). DNA vaccine against malaria: a long way to go. *Critical Reviews in Biochemistry and Molecular Biology*, 37(1):29–54.

USAID (2018). President's malaria initiative Kenya: Malaria operational plan FY 2018. Technical report, United States Agency for International Development.

Van den Driessche, P. and Watmough, J. (2002). Reproduction numbers and sub-threshold endemic equilibria for compartmental models of disease transmission. *Mathematical Biosciences*, 180(1):29–48.

Vannice, K. S., Brown, G. V., Akanmori, B. D., and Moorthy, V. S. (2012). MALVAC 2012 scientific forum: accelerating development of second-generation malaria vaccines. *Malaria Journal*, 11(372). doi: 10.1186/1475-2875-11-372.

Villarino, N. and W Schmidt, N. (2013). CD8+ T cell responses to plasmodium and intracellular parasites. *Current Immunology Reviews*, 9(3):169–178.

Vinayak, S., Alam, M. T., Mixson-Hayden, T., McCollum, A. M., Sem, R., Shah, N. K., Lim, P., Muth, S., Rogers, W. O., Fandeur, T., Barnwell, J. W., Escalante, A. A., Wongsrichanalai, C., Ariey, F., Meshnick, S. R., and Udhayakumar, V. (2010). Origin and evolution of sulfadoxine resistant plasmodium falciparum. *PLoS Pathogens*, 6(3):e1000830. https://doi.org/10.1371/journal.ppat.1000830.

Visser, B. J., van Vugt, M., and Grobusch, M. P. (2014). Malaria: an update on current chemotherapy. *Expert Opinion on Pharmacotherapy*, 15(15):2219–2254.

Wainwright, J. and Mulligan, M. (2013). *Environmental Modelling: Finding Simplicity in Complexity, Second Edition*. Wiley, UK.

Wang, X. (2004). A simple proof of descartes's rule of signs. *The American Mathematical Monthly*, 111(6):525. DOI: 10.2307/4145072.

Wargo, A. R., Huijben, S., De Roode, J. C., Shepherd, J., and Read, A. F. (2007). Competitive release and facilitation of drug-resistant parasites after therapeutic chemotherapy in a rodent malaria model. *Proceedings of the National Academy of Sciences of the United States of America*, 104(50):19914–19919.

Weatherall, D. J., Miller, L. H., Baruch, D. I., Marsh, K., Doumbo, O. K., Casals-Pascual, C., and Roberts, D. J. (2002). Malaria and the red cell. *Hematology*, 2002(1):35–57.

Weglarz, T. C., Degen, J. L., and Sandgren, E. P. (2000). Hepatocyte transplantation into diseased mouse liver: kinetics of parenchymal repopulation and identification of the proliferative capacity of tetraploid and octaploid hepatocytes. *The American Journal of Pathology*, 157(6):1963–1974.

Wellems, T. E. and Plowe, C. V. (2001). Chloroquine-resistant malaria. *The Journal of Infectious Diseases*, 184(6):770–776.

Wernsdorfer, W. H. and Payne, D. (1991). The dynamics of drug resistance in plasmodium falciparum. *Pharmacology & Therapeutics*, 50(1):95–121.

Whegang, Y. S., Andreas, C., and K, B. L. (2019). Monitoring the efficacy and safety of artemisinin-based combination therapies: A review and network meta-analysis of antimalarial therapeutic efficacy trials in Cameroon. *Drugs in R&D*, 19(1):1–14.

White, E. and Comiskey, C. (2007). Heroin epidemics, treatment and ODE modelling. *Mathematical Biosciences*, 208(1):312–324.

White, M. T., Bejon, P., Olotu, A., Griffin, J. T., Riley, E. M., Kester, K. E., Ockenhouse, C. F., and Ghani, A. C. (2013). The relationship between RTS,S vaccine-induced antibodies, CD4+ T cell responses and protection against plasmodium falciparum infection. *PLOS One*, 8(4):e61395. https://doi.org/10.1371/journal.pone.0061395.

White, M. T. and Smith, D. L. (2013). Synergism from combinations of infection-blocking malaria vaccines. *Malaria Journal*, 12(280). https://doi.org/10.1186/1475-2875-12-280.

White, N. (1999). Delaying antimalarial drug resistance with combination chemotherapy. *Parassitologia*, 41(1-3):301–308.

White, N. and Pongtavornpinyo, W. (2003). The de novo selection of drug–resistant malaria parasites. *Proceedings of the Royal Society of London B: Biological Sciences*, 270(1514):545–554.

White, N. J. (2004). Antimalarial drug resistance. *The Journal of Clinical Investigation*, 113(8):1084–1092.

White, N. J., Qiao, L. G., Qi, G., and Luzzatto, L. (2012). Rationale for recommending a lower dose of primaquine as a plasmodium falciparum gametocytocide in populations where G6PD deficiency is common. *Malaria Journal*, 11(418). doi: 10.1186/1475-2875-11-418.

WHO (1990). Severe and complicated malaria. *Transactions of the Royal Society of Tropical Medicine and Hygiene*, 84(2):1–65.

WHO (1993). A global strategy for malaria control. World Health Organization. Retrieved from http://www.who.int/malaria/publications/atoz/9241561610/en/. Accessed November 2018.

WHO (2012a). Question and answer on artemisinin resistance. World Health Organization. Retrieved from http://www.who.int/malaria/media/artemisinin_resistance_qa/en/. Accessed March 2019.

WHO (2012b). Single dose primaquine as a gametocytocide in plasmodium falciparum malaria; updated WHO policy recommendation. World Health Organization. Retrieved from https://www.who.int/malaria/publications/atoz/who_pq_policy_recommendation/en/. Accessed April 2019.

WHO (2015a). Global technical strategy for malaria 2016-2030. World Health Organization. Retrieved from https://apps.who.int/iris/bitstream/handle/10665/176712/9789241564991_eng.pdf?sequence=1. Accessed May 2019.

WHO (2015b). Global technical strategy for malaria 2016-2030. World Health Organization. Retrieved from https://apps.who.int/iris/bitstream/handle/10665/176712/9789241564991_eng.pdf?sequence=1. Accessed June 2019.

WHO (2015c). Guidelines for the treatment of malaria. Third edition April 2015. World Health Organization. Retrieved from https://www.who.int/malaria/publications/atoz/9789241549127/en/. Accessed April 2019.

WHO (2015d). World malaria report 2015. World Health Organization. Retrieved from https://www.who.int/malaria/publications/world-malaria-report-2015/report/en/. Accessed January 2019.

WHO (2016a). Artemisinin and artemisinin-based combination therapy resistance. World Health Organization. Retrieved from http://apps.who.int/iris/bitstream/handle/10665/250294/WHO-HTM-GMP-2016.11-eng.pdf;jsessionid=7A41F6784CE6C16FA0431F64953BE653?sequence=1. Accessed November 2018.

WHO (2016b). World malaria report 2016. World Health Organization. Retrieved from https://www.who.int/malaria/publications/world-malaria-report-2016/report/en/. Accessed November 2018.

WHO (2017a). Malaria fact sheet; 2017. World Health Organization, Geneva. Retrieved from http://www.who.int/mediacentre/factsheets/fs094/en/. Accessed February 2017.

WHO (2017b). World malaria report 2017. World Health Organization. Retrieved from https://www.who.int/malaria/publications/world-malaria-report-2017/en/. Accessed February 2019.

WHO (2018a). Artemisinin resistance and artemisinin-based combination therapy efficacy: status report. World Health Organization. Retrieved from http://www.who.int/iris/handle/10665/274362. Accessed March 2019.

WHO (2018b). High burden to high impact: getting back on track to end malaria. Geneva: World Health Organization. Retrieved from www.who.int/malaria/publications/atoz/high-impact-response/en/. Accessed May 2019.

WHO (2018c). Malaria vaccine rainbow tables. Autoimmunity Research Foundation. Retrieved from http://www.who.int/vaccine_research/links/Rainbow/en/index.html. Accessed April 2018.

WHO (2018d). Malaria vaccine: WHO position paper, January 2016–recommendations. *Vaccine*, 36(25):3576–3577.

WHO (2018e). Questions and answers on artemisinin resistance. World Health Organization. Retrieved from https://www.who.int/malaria/media/artemisinin_resistance_qa/en/. Accessed November 2018.

WHO (2018f). World malaria report 2018. World Health Organization. Retrieved from https://www.who.int/malaria/publications/world-malaria-report-2018/en/. Accessed April 2019.

Wickramasinghe, S. N. and Abdalla, S. H. (2000). Blood and bone marrow changes in malaria. *Best Practice & Research Clinical Haematology*, 13(2):277–299.

Winskill, P., Slater, H. C., Griffin, J. T., Ghani, A. C., and Walker, P. G. (2017a). The us president's malaria initiative, plasmodium falciparum transmission and mortality: A modelling study. *PLoS Medicine*, 14(11). e1002448. https://doi.org/10.1371/journal.pmed.1002448.

Winskill, P., Walker, P. G., Griffin, J. T., and Ghani, A. C. (2017b). Modelling the cost-effectiveness of introducing the rts, s malaria vaccine relative to scaling up other malaria interventions in sub-Saharan Africa. *BMJ Global Health*, 2(1). e000090. doi:10.1136/bmjgh-2016-000090.

Wu, J., Dhingra, R., Gambhir, M., and Remais, J. V. (2013). Sensitivity analysis of infectious disease models: methods, advances and their application. *Journal of The Royal Society Interface*, 10(86):20121018. https://doi.org/10.1098/rsif.2012.1018.

Xu, C., Wei, Q., Yin, K., Sun, H., Li, J., Xiao, T., Kong, X., Wang, Y., Zhao, G., Zhu, S., Kou, J., Yan, G., and Huang, B. (2018). Surveillance of antimalarial resistance pfcrt, pfmdr1, and pfkelch13 polymorphisms in African plasmodium falciparum imported to Shandong Province, China. *Nature*, 8(1):12951. doi:10.1038/s41598-018-31207-w.

Yaya, S., Uthman, O., Amouzou, A., and Bishwajit, G. (2018). Use of intermittent preventive treatment among pregnant women in sub-Saharan Africa: Evidence from malaria indicator surveys. *Tropical Medicine and Infectious Disease*, 3(1):18. doi:10.3390/tropicalmed3010018.

Zelman, B., Melgar, M., Larson, E., Phillips, A., and Shretta, R. (2016). Global fund financing to the 34 malaria-eliminating countries under the new funding model 2014–2017: an analysis of national allocations and regional grants. *Malaria Journal*, 15(118). DOI:10.1186/s12936-016-1171-3.

Zhong, P. (2011). *Optimal Theory Applied in Integrodifference Equation Models and in a Cholera Differential Equation Model*. PhD thesis, The university of Tennessee Knoxville.

zur Wiesch, P. A., Kouyos, R., Engelstädter, J., Regoes, R. R., and Bonhoeffer, S. (2011). Population biological principles of drug-resistance evolution in infectious diseases. *The Lancet Infectious Diseases*, 11(3):236–247.

Appendix A

Mathematical preliminaries

Definition A.1. ***Linearisation***. *In mathematics, linearisation refers to the process of finding a linear approximation to a function at a given point.*

The concept of linearisation is very important in the study of dynamical systems. It enables us to assess the local stability of the equilibrium point(s) of a non-linear dynamical system. The process of linearing such a system is presented as follows:

Consider a compartmental model of n state variables (populations): $y_1(t), y_2(t), \cdots, y_n(t)$. The argument t is the independent time variable. This system can be modelled using autonomous n first order differential equations as follows.

$$\left.\begin{aligned} y_1' &= G_1(y_1, y_2, \cdots, y_n), \\ y_2' &= G_2(y_1, y_2, \cdots, y_n), \\ &\vdots \\ y_n' &= G_n(y_1, y_2, \cdots, y_n). \end{aligned}\right\} \tag{A.1}$$

Definition A.2. ***Equilibrium point***. *We define the equilibrium point (or critical or stationary or rest point) of the system* (A.1) *as a solution* $(y_1^*, y_2^*, \cdots, y_n^*)$ *such that*

$$\left.\begin{aligned} G_1(y_1^*, y_2^*, \cdots, y_n^*) &= 0, \\ G_2(y_1^*, y_2^*, \cdots, y_n^*) &= 0, \\ &\vdots \\ G_n(y_1^*, y_2^*, \cdots, y_n^*) &= 0. \end{aligned}\right\} \tag{A.2}$$

A small perturbation ε on the steady state $(y_1^*, y_2^*, \cdots, y_n^*)$ gives

$$\left.\begin{aligned} y_1(t) &= y_1^* + \varepsilon \bar{y}_1(t), \\ y_2(t) &= y_2^* + \varepsilon \bar{y}_2(t), \\ &\vdots \\ y_n(t) &= y_n^* + \varepsilon \bar{y}_n(t). \end{aligned}\right\} \tag{A.3}$$

Substituting (A.3) into (A.1), the differential equations become

$$\left.\begin{aligned} y_1' &= G_1(y_1^* + \varepsilon \bar{y}_1, y_2^* + \varepsilon \bar{y}_2, \cdots, y_n^* + \varepsilon \bar{y}_n), \\ y_2' &= G_2(y_1^* + \varepsilon \bar{y}_1, y_2^* + \varepsilon \bar{y}_2, \cdots, y_n^* + \varepsilon \bar{y}_n), \\ &\vdots \\ y_n' &= G_n(y_1^* + \varepsilon \bar{y}_1, y_2^* + \varepsilon \bar{y}_2, \cdots, y_n^* + \varepsilon \bar{y}_n). \end{aligned}\right\} \tag{A.4}$$

Using a Taylor's expansion for several variables, we have

$$\left.\begin{aligned} \varepsilon \frac{\mathrm{d}\bar{y}_1}{\mathrm{d}t} &= G_1(y_1^*, y_2^*, \cdots, y_n^*) + \varepsilon \left.\frac{\partial G_1}{\partial y_1}\right|_{(y_1^*, y_2^*, \cdots, y_n^*)} \bar{y}_1 + \varepsilon \left.\frac{\partial G_1}{\partial y_2}\right|_{(y_1^*, y_2^*, \cdots, y_n^*)} \bar{y}_2 + \cdots \\ &\quad + \varepsilon \left.\frac{\partial G_1}{\partial y_n}\right|_{(y_1^*, y_2^*, \cdots, y_n^*)} \bar{y}_n + O(y, t), \\ \varepsilon \frac{\mathrm{d}\bar{y}_2}{\mathrm{d}t} &= G_2(y_1^*, y_2^*, \cdots, y_n^*) + \varepsilon \left.\frac{\partial G_2}{\partial y_1}\right|_{(y_1^*, y_2^*, \cdots, y_n^*)} \bar{y}_1 + \varepsilon \left.\frac{\partial G_2}{\partial y_2}\right|_{(y_1^*, y_2^*, \cdots, y_n^*)} \bar{y}_2 + \cdots \\ &\quad + \varepsilon \left.\frac{\partial G_2}{\partial y_n}\right|_{(y_1^*, y_2^*, \cdots, y_n^*)} \bar{y}_n + O(y, t), \\ \varepsilon \frac{\mathrm{d}\bar{y}_n}{\mathrm{d}t} &= G_n(y_1^*, y_2^*, \cdots, y_n^*) + \varepsilon \left.\frac{\partial G_n}{\partial y_1}\right|_{(y_1^*, y_2^*, \cdots, y_n^*)} \bar{y}_1 + \varepsilon \left.\frac{\partial G_n}{\partial y_2}\right|_{(y_1^*, y_2^*, \cdots, y_n^*)} \bar{y}_2 + \cdots \\ &\quad + \varepsilon \left.\frac{\partial G_n}{\partial y_n}\right|_{(y_1^*, y_2^*, \cdots, y_n^*)} \bar{y}_n + O(||\bar{y}_1, \bar{y}_2, \cdots, \bar{y}_n||), \end{aligned}\right\} \tag{A.5}$$

where $O(||\bar{y}_1, \bar{y}_2, \cdots, \bar{y}_n||)$ represents the higher order terms of the expression.

Since $(y_1^*, y_2^*, \cdots, y_n^*)$ is a steady state, then

$$G_1(y_1^*, y_2^*, \cdots, y_n^*) = G_2(y_1^*, y_2^*, \cdots, y_n^*) = \cdots = G_n(y_1^*, y_2^*, \cdots, y_n^*) = 0. \tag{A.6}$$

Neglecting higher order terms of (A.5), the linearisation of system (A.1) is given by

$$\left.\begin{aligned}
\varepsilon \frac{\mathrm{d}\bar{y}_1}{\mathrm{d}t} &= \varepsilon \frac{\partial G_1}{\partial y_1}\bigg|_{(y_1^*, y_2^*, \cdots, y_n^*)} \bar{y}_1 + \varepsilon \frac{\partial G_1}{\partial y_2}\bigg|_{(y_1^*, y_2^*, \cdots, y_n^*)} \bar{y}_2 + \cdots + \varepsilon \frac{\partial G_1}{\partial y_n}\bigg|_{(y_1^*, y_2^*, \cdots, y_n^*)} \bar{y}_n, \\
\varepsilon \frac{\mathrm{d}\bar{y}_2}{\mathrm{d}t} &= \varepsilon \frac{\partial G_2}{\partial y_1}\bigg|_{(y_1^*, y_2^*, \cdots, y_n^*)} \bar{y}_1 + \varepsilon \frac{\partial G_2}{\partial y_2}\bigg|_{(y_1^*, y_2^*, \cdots, y_n^*)} \bar{y}_2 + \cdots + \varepsilon \frac{\partial G_2}{\partial y_n}\bigg|_{(y_1^*, y_2^*, \cdots, y_n^*)} \bar{y}_n, \\
\varepsilon \frac{\mathrm{d}\bar{y}_n}{\mathrm{d}t} &= \varepsilon \frac{\partial G_n}{\partial y_1}\bigg|_{(y_1^*, y_2^*, \cdots, y_n^*)} \bar{y}_1 + \varepsilon \frac{\partial G_n}{\partial y_2}\bigg|_{(y_1^*, y_2^*, \cdots, y_n^*)} \bar{y}_2 + \cdots + \varepsilon \frac{\partial G_n}{\partial y_n}\bigg|_{(y_1^*, y_2^*, \cdots, y_n^*)} \bar{y}_n.
\end{aligned}\right\} \tag{A.7}$$

In matrix form, system (A.7) can be written as

$$\begin{pmatrix} \bar{y}'_1 \\ \bar{y}'_2 \\ \vdots \\ \bar{y}'_n \end{pmatrix} = \begin{pmatrix} \frac{\partial G_1}{\partial y_1} & \frac{\partial G_1}{\partial y_2} & \cdots & \frac{\partial G_1}{\partial y_n} \\ \frac{\partial G_2}{\partial y_1} & \frac{\partial G_2}{\partial y_2} & \cdots & \frac{\partial G_2}{\partial y_n} \\ \vdots & & \ddots & \\ \frac{\partial G_n}{\partial y_1} & \frac{\partial G_n}{\partial y_2} & \cdots & \frac{\partial G_n}{\partial y_n} \end{pmatrix} \begin{pmatrix} \bar{y}_1 \\ \bar{y}_2 \\ \vdots \\ \bar{y}_n \end{pmatrix} \tag{A.8}$$

where

$$\begin{pmatrix} \frac{\partial G_1}{\partial y_1} & \frac{\partial G_1}{\partial y_2} & \cdots & \frac{\partial G_1}{\partial y_n} \\ \frac{\partial G_2}{\partial y_1} & \frac{\partial G_2}{\partial y_2} & \cdots & \frac{\partial G_2}{\partial y_n} \\ \vdots & & \ddots & \\ \frac{\partial G_n}{\partial y_1} & \frac{\partial G_n}{\partial y_2} & \cdots & \frac{\partial G_n}{\partial y_n} \end{pmatrix} \tag{A.9}$$

is the **Jacobian matrix** of system (A.1), evaluated at the steady state $(y_1^*, y_2^*, \cdots, y_n^*)$.

The equilibrium point $y^* = (y_1^*, y_2^*, \cdots, y_n^*)$ is said to be **stable** if all the eigenvalues of the Jacobian matrix (A.9) evaluated at y^*, have negative real parts. The equilibrium point is **unstable** if at least one of the eigenvalues has a positive real part.

Appendix B

Samples of used simulation codes

B.1 (Python Code): Numerical simulations, model 3.1, section 3.6

```
''' Required packages'''
import scipy
import numpy as np
import scipy.integrate
from pylab import * # for plotting commands
import pylab as pl

''' Declaring the fixed parameters '''
betar=2.0*10**(-5); betas=1.6*10**(-6); mu1=0.029
mu2=0.02; mu3=0.0083; mu4=0.025; deltam=48; zeta=0.726
lambdar=4*10**3; lambdah=3*10**3
K=16; deltaz=1.5; deltas=1.2*10**(-11)
eta=10**(-10); lambdaz=30; rho1=2.5*10**(-5)
rho2=2.5*10**(-5); rho3=2.5*10**(-5)
kappa1=1; kappa2=1; kappa3=1; Lambda=20; N=10000

# basic reproduction number R0
RNum=(betar*lambdar*K*zeta*deltaz*mu4);
RDen=((betar*lambdar+deltam*mu3)*(eta*lambdaz+deltaz*mu4));
Rnote= RNum/RDen;
print(Rnote)
```

```
''' Initial conditions'''
H0  = 3*10**5; HX0 = 2*10**4; R0  = 5*10**5; RX0 = 50;
Z0 = 3*10**5; S0 = 2000; M0 = 70

''' Numerical solution of the model'''
def odesystem(X,t): # return derivatives of the array y
  return scipy.array([
  lambdah+(rho1*X[1])/(kappa1+X[1]) - mu1*X[0]-betas*X[5]*X[0],
   betas*X[5]*X[0]-mu2*X[1],
   lambdar+(rho2*X[3])/(kappa2+X[3]) - mu3*X[2]-betar*X[2]*X[6],
   betar*X[2]*X[6]-mu4*X[3]-eta*X[3]*X[4],
   lambdaz+(rho3*X[3])/(kappa3+X[3]) - deltaz*X[4],
   Lambda-deltas*X[5]-betas*X[5]*X[0],
   N*mu2*X[1]-K*zeta*mu4*X[3]-deltam*X[6]-betar*X[2]*X[6]])

'''   Time span over which the integration is done '''
time = scipy.linspace(0, 200, 150) # 1000 plotting points
X0 = scipy.array([H0, HX0, R0, RX0, Z0, S0, M0])

''' The integration of the ODEs '''
Xs = scipy.integrate.odeint(odesystem,X0,time)
'''Plotting'''
p1=pl.plot(time,Xs[:,0],'b',lw = 2)  #H
P2=pl.plot(time,Xs[:,1],'g--',lw = 2)  #HX

'''Plot labels'''
pl.xlabel('Time(Days)')
pl.ylabel('Hepatocytes')
#xlim(0,200)
#''' The plot legend'''
pl.legend(('H', 'H_X'), loc="top left")
pl.show()
```

B.2 (Matlab Code): Vaccine combinations, model 5.1, section 5.7

```
% Part A:

function y2dot=y2combineddot(t3,y2) %defining the function

% Parameter values
Lambda=2500000; mus=0.002; lambdah=3*10^5; lambdar=3*10^5;
betar=2.0*10^(-4); betas=3.0*10^(-5); muh=0.2; mux=0.2;
pi=0.2; kx=0.01; kt=0.01; kc=0.0000001; dx= 0.00001;
dt= 0.00001; dc= 0.00001; mur=0.000083; mut=0.27; muc=0.7;
mum=48; mug=0.0000625; gamma=1.5; chi=0;e=0.75; v=0; d=0.0005;
lambdaw=30; tau=1.5; muw=2; b=0.2; a=0.2; P=16; N=10000;

% Basic reproduction number
% z(1)=H, z(2)=X, z(3)=S, z(4)=R, z(5)=T, z(6)=C, z(7)=M, z(8)=G,
z(9)=W
RO1 = ((1-v)* betas* lambdah)/(muh*mur)
%Model R01 due to pre-erythrocytic infection
RO2 = (P*(1-pi)* (1-a)*(1-e)*betar* lambdar)/(betar* lambdar+mum*mur)
%Model R01 due to erythrocytic infection
%Model system of equations
y2dot(1)=lambdah - muh * y2(1)-betas * (1-v) * y2(3) *
y2(1);
y2dot(2)=betas * (1-v) * y2(3) * y2(1)-mux * y2(2)-kx * (1-v)
* y2(9)* y2(2);
y2dot(3)=Lambda * (1-chi)-mus * y2(3)-betas * y2(3) * y2(1);
y2dot(4)=lambdar-((1-e) * betar * y2(4) * y2(7)) - mur * y2(4);
y2dot(5)=((1-e) * betar * y2(4) * y2(7)) - mut * y2(5)-gamma * y2(5)
-(kt * (1-e) * y2(9) * y2(5));
y2dot(6)=gamma * y2(5)-muc * y2(6)-(kc * (1-e) * y2(9) * y2(6));
y2dot(7)=(1-b) * N * mux * y2(2)+(P * (1-pi) * (1-a) * muc * y2(6))
-mum* y2(7)
-betar * y2(4) * y2(7);
y2dot(8)=pi * muc * y2(6)- mug * y2(8);
y2dot(9)=tau * lambdaw + y2(9)*(dx * y2(2) + dt * y2(5) + dc * y2(6))
```

```
-muw * y2(9);
y2dot=[y2dot(1) y2dot(2) y2dot(3) y2dot(4)
y2dot(5) y2dot(6) y2dot(7) y2dot(8) y2dot(9)]';

% PART B

clear;
to = 0; %Initial time in years.
tf =80; %Final time in years.

%Initial conditions
yo = [3*10^5 4*10^3 1000 5*10^4 4*10^1 50000 1000 5000 20000];
% yo = [H0, X0, S0, R0, T0, C0, M0, G0, W0];
[t1 y]= ode45('ycombineddot',[to tf],yo); %
[t5 z4]= ode45('z4combineddot',[to tf],yo); %
[t2 z]= ode45('zcombineddot',[to tf],yo); %

figure(1)
hold on
plot(t1,y(:,2),'--r','LineWidth',2.2) % No vaccine at all
plot(t5,z4(:,2),':b','LineWidth',2.2) % 75% for v, v=chi=0
plot(t2,z(:,2),'g','LineWidth',2.2) % perfect vaccine 75% efficacious
legend('X(t) without vaccines','X(t) with  v = e = 75% and
\chi = 0%','X(t) with e = v = \chi = 75%','Location','East')
xlabel('Time (Days)')
ylabel('Infected Hepatocytes, X(t)')
```

B.3 (Mathematica Code): Reproduction number, model 3.2, section 3.4.4

f1 = $\beta_s SH$

$HS\beta_s$

D[f1,S]/.{H->λ_h/μ_h,H_X->0,R->λ_r/μ_r,R_X->0,Z->λ_z/δ_z,S->0,M->0}

$\frac{\beta_s \lambda_h}{\mu_1}$

$$\mathbf{f2} = \boldsymbol{\beta_r RM}$$

$$RM\beta_r$$

$$\boldsymbol{D[\mathrm{f2}, M]/.\{H->\lambda_h/\mu_h, H_X->0, R->\lambda_r/\mu_r, R_X->0, Z->\lambda_z/\delta_z, S->0, M->0\}}$$

$$\frac{\beta_r \lambda_r}{\mu_3}$$

$$\mathbf{v1} = \boldsymbol{\mu_2 H_X}$$

$$H_X \mu_2$$

$$\boldsymbol{D[\mathrm{v1}, H_X]/.\{H->\lambda_h/\mu_h, H_X->0, R->\lambda_r/\mu_r, R_X->0, Z->\lambda_z/\delta_z, S->0, M->0\}}$$

$$\mu_2$$

$$\mathbf{v2} = \boldsymbol{\mu_4 R_X + \eta R_X Z}$$

$$R_X \mu_4 + R_X Z \eta$$

$$\boldsymbol{D[\mathrm{v2}, R_X]/.\{H->\lambda_h/\mu_h, H_X->0, R->\lambda_r/\mu_r, R_X->0, Z->\lambda_z/\delta_z, S->0, M->0\}}$$

$$\mu_4 + \eta \lambda_z/\delta_z$$

$$\mathbf{v3} = \boldsymbol{(-\Lambda + \delta_s S + \beta_s SH)}$$

$$-\Lambda + S\delta_s + HS\beta_s$$

$$\boldsymbol{D[\mathrm{v3}, S]/.\{H->\lambda_h/\mu_h, H_X->0, R->\lambda_r/\mu_r, R_X->0, Z->\lambda_z/\delta_z, S->0, M->0\}}$$

$$\delta_s + \beta_s \lambda_h/\mu_1$$

$$\mathbf{v4} = \boldsymbol{-N\mu_2 H_X - K\zeta \mu_4 R_X + \delta_m M + \beta_r RM}$$

$$-H_X Z \mu_2 - R_X K \zeta \mu_4 + M\delta_m + MR\beta_r$$

$$\boldsymbol{D[\mathrm{v4}, M]/.\{H->\lambda_h/\mu_h, H_X->0, R->\lambda_r/\mu_r, R_X->0, Z->\lambda_z/\delta_z, S->0, M->0\}}$$

$$\delta_m + \beta_r \lambda_r/\mu_3$$

$$\mathbf{mat} = \{\{\mu_2, 0, 0, 0\}, \{0, \mu_4 + (\eta\lambda_z/\delta_z), 0, 0\}, \{0, 0, \delta_s + (\beta_s\lambda_s/\mu_1), 0\},$$
$$\{-N\mu_2, -K\zeta\mu_4, 0, \delta_m + (\beta_r\lambda_r/\mu_3), 0\}\}$$

$$v = \mathbf{MatrixForm}[\mathrm{mat}]$$

$$\begin{pmatrix} \mu_2 & 0 & 0 & 0 \\ 0 & \mu_4 + (\eta\lambda_z/\delta_z) & 0 & 0 \\ 0 & 0 & \delta_s + (\beta_s\lambda_h/\mu_1) & 0 \\ -N\mu_2 & -K\zeta\mu_4 & 0 & \delta_m + (\beta_r\lambda_r/\mu_3) \end{pmatrix}$$

$$V = \mathbf{FullSimplify}[\mathbf{Inverse}[\mathrm{mat}]]$$

$$\mathbf{MatrixForm}[V]$$

$$\begin{pmatrix} \frac{1}{\mu_2} & 0 & 0 & 0 \\ 0 & \frac{\delta_z}{\eta\lambda_z + \delta_z\mu_4} & 0 & 0 \\ 0 & 0 & \frac{1}{\delta_s + \frac{\beta_s\lambda_h}{\mu_1}} & 0 \\ \frac{N\mu_3}{\beta_r\lambda_r + \delta_m\mu_3} & \frac{K\zeta\mu_3\mu_4}{(\beta_r\lambda_r + \delta_m\mu_3)(\eta\lambda_z + \delta_z\mu_4)} & 0 & \frac{1}{\delta_m + \frac{\beta_r\lambda_r}{\mu_3}} \end{pmatrix}$$

$$\mathbf{F} = \left\{\{0, 0, \frac{\beta_s\lambda_h}{\mu_1}, 0\}, \left\{0, 0, 0, \frac{\beta_r\lambda_r}{\mu_3}\right\}, \{0, 0, 0, 0\}, \{0, 0, 0, 0\}\right\}$$

$$\mathbf{MatrixForm}[\mathbf{F}]$$

$$\begin{pmatrix} 0 & 0 & \frac{\beta_s\lambda_h}{\mu_1} & 0 \\ 0 & 0 & 0 & \frac{\beta_r\lambda_r}{\mu_3} \\ 0 & 0 & 0 & 0 \\ 0 & 0 & 0 & 0 \end{pmatrix}$$

$$G = \mathbf{FullSimplify}[\mathbf{F.V}]$$

$$\mathbf{Eigenvalues}[G]$$

$$\left\{0, 0, 0, \frac{K\zeta\beta_r\lambda_r\delta_z\mu_4}{(\beta_r\lambda_r + \delta_m\mu_3)(\eta\lambda_z + \delta_z\mu_4)}\right\}$$

Appendix C

Publications

Hindawi
International Journal of Mathematics and Mathematical Sciences
Volume 2018, Article ID 7019868, 18 pages
https://doi.org/10.1155/2018/7019868

Research Article

Mathematical Model for Hepatocytic-Erythrocytic Dynamics of Malaria

Titus Okello Orwa, Rachel Waema Mbogo, and Livingstone Serwadda Luboobi

Institute of Mathematical Sciences, Strathmore University, P.O. Box 59857-00200, Nairobi, Kenya

Correspondence should be addressed to Titus Okello Orwa; torwa@strathmore.edu

Received 23 October 2017; Accepted 20 May 2018; Published 2 July 2018

Academic Editor: Niansheng Tang

Human malaria remains a major killer disease worldwide, with nearly half (3.2 billion) of the world's population at risk of malaria infection. The infectious protozoan disease is endemic in tropical and subtropical regions, with an estimated 212 million new cases and 429,000 malaria-related deaths in 2015. An in-host mathematical model of *Plasmodium falciparum* malaria that describes the dynamics and interactions of malaria parasites with the host's liver cells (hepatocytic stage), the red blood cells (erythrocytic stage), and macrophages is reformulated. By a theoretical analysis, an in-host basic reproduction number R_0 is derived. The disease-free equilibrium is shown to be locally and globally asymptotically stable. Sensitivity analysis reveals that the erythrocyte invasion rate β_r, the average number of merozoites released per bursting infected erythrocyte K, and the proportion of merozoites that cause secondary invasions at the blood phase ζ are the most influential parameters in determining the malaria infection outcomes. Numerical results show that macrophages have a considerable impact in clearing infected red blood cells through phagocytosis. Moreover, the density of infected erythrocytes and hence the severity of malaria are shown to increase with increasing density of merozoites in the blood. Concurrent use of antimalarial drugs and a potential erythrocyte invasion-avoidance vaccine would minimize the density of infected erythrocytes and hence malaria disease severity.

1. Introduction

Human malaria remains a major killer disease worldwide, with nearly half (3.2 billion) of the world's population at risk of malaria infection [1]. The infectious disease is endemic in tropical and subtropical regions, with an estimated 212 million new cases (uncertainty range: 148–304 million) and 429,000 malaria-related deaths (range: 235,000–639,000) in 2015 [2]. 92% of the deaths and 90% of the cases occurred in sub-Saharan Africa. 70% of the reported deaths occurred among children below the age of five. Despite existing vector control measures and tremendous progress in the development of antimalarial therapy accompanied with worldwide decline in incidence rate (fell by 21% in 2015) and mortality rate (fell by 29% in 2015), malaria remains one of the greatest global health challenges to date [2].

The protozoan disease is caused by parasites of the genus *Plasmodium* which are transmitted to humans by the bite of female *Anopheles* mosquito. *Plasmodium falciparum*, which is predominant in sub-Saharan Africa, New Guinea, and Haiti [3], is the major cause of malaria infections. The other *Plasmodium* species that cause malaria are *P. vivax*, *P. ovale*, *P. malariae*, and *P. knowlesi* [4]. *P. vivax* and *P. ovale* can hide in the liver for prolonged periods as hypnozoites, causing relapsing malaria months or even years after the initial infection [5]. *P. vivax* has the greatest geographical range of the disease and hence is the main contributor to worldwide malaria morbidity [3]. Our study focuses on the dynamics of *Plasmodium falciparum* in the human host.

During their obligatory blood meals, infected female *Anopheles* mosquitoes inject sporozoites belonging to *Plasmodium falciparum* species into the human dermis [6]. The motile sporozoites travel through the blood vessels and enter the host's liver. Hepatocyte invasion is accompanied by the formation of parasitophorous vacuole (PV) around the sporozoite [7]. They form preerythrocytic schizonts and multiply by schizogony, culminating in the production of 8–24 first generation merozoites that are released into the

blood when the liver schizonts burst open [8]. The released merozoites invade susceptible erythrocytes and undergo another phase of schizogony, which is relatively faster compared to that at the exoerythrocytic stage [9].

Within a period of two days, the infected red blood cells rupture to release about 16 daughter merozoites [10]. Most of the released merozoites quickly invade susceptible erythrocytes, leading to another cycle of infections. The waves of bursting erythrocytes and the invasion of fresh erythrocytes by the newly released merozoites increase parasitemia and produce malaria's characteristic symptoms [11]. In the absence of adequate protective immune response or antimalarial therapy, the host is likely to suffer severe anaemia or even die [12]. The rest of the daughter merozoites develop into sexual forms called gametocytes [10]. These gametocytes are later taken up by other female *Anopheles* mosquitoes during feeding [13]. This marks the beginning of the sporogenic cycle that occurs within the mosquito vector.

The presence of the malaria parasites in the human body elicits response from numerous immune cells. The innate immune system and the adaptive immune system form the first and the second lines of defence, respectively [14]. Adaptive immune system further provides protection against future exposures to malaria pathogens. Innate immune cells such as the *Plasmodium falciparum* DNA, natural killer cells (NK cells), dendritic cells (DCs), macrophages, natural killer T (NKT) cells, and T cells are involved in the clearance of circulating parasites, infected erythrocytes, and infected hepatocytes [14]. Subject to parasite strain, the DCs and NK cells may prompt or restrain inflammatory responses [15]. The NKT cells also help regulate DCs and T cell responses to *Plasmodium* [14]. Moreover, studies in [16] have demonstrated that malaria infection induces activation of Toll-like receptors (TLRs): TLR1, TLR2, TLR4 (which are located on the cell surface), and TLR9 which is not expressed on the cell surface. TLR2 and TLR9 are also activated by malarial glycosylphosphatidylinositol (GPI) anchors and parasite-derived DNA bound to hemozoin [16].

Unlike the NK cells, the macrophages have been shown to effectively phagocytose malaria-infected red blood cells during the erythrocytic phase [17]. A part from its ability to wholly ingest infected red blood cells, the macrophages can also selectively extract malaria parasites from recently infected erythrocytes [18]. The parasite-extraction capability of macrophage therefore leaves the surviving erythrocytes to continue circulating like the other healthy red blood cells.

The rest of the paper is organized as follows: in Section 2, we formulate the in-host malaria model and state the invariant region in which the model is defined. In Section 3, we compute and describe the model in-host reproduction number. The results on model equilibrium points (disease-free equilibrium and endemic equilibrium points) and the stability of the disease-free equilibrium point are also considered in Section 3. Section 4 is devoted to numerical solution of the in-host model under different conditions of the threshold parameter (in-host reproduction number). Parameter sensitivity analysis and the effects of parameter variation on different populations are investigated in Section 4. A conclusion and discussion complete the paper in Section 5.

2. In-Host Malaria Model

Several studies on mathematical modelling of in-host malaria and its dynamics within the human host have been done. Nearly all the earlier mathematical models (see, e.g., [25–27]) focused on improving *Plasmodium falciparum* control while focusing on the blood stage of parasite development. These models have been found to be useful in explaining in-host observations by means of biologically plausible assumptions such as parasite diversity, predicting the impact of interventions or the use of antimalarials [28], and estimating hidden parameter values [29]. Although the models in [19, 21, 23, 30] have considered the impact of immune response and treatment, the modelling is only limited to the blood stage of *Plasmodium falciparum* development. In [20, 22, 31], the liver stage is incorporated in the malaria model. However, the contribution of immune system is ignored in [20, 31]. Moreover, all the immune cells are assumed to play an active role during malaria infection in [22]. This may not be entirely true. The specific impacts of immune responses to malaria infection are well discussed in [32–36].

In the following sections, we extended the model in [21] by incorporating the liver stage of parasite development. The reformulated in-host malaria model focuses on the erythrocytic and hepatocytic stages and describes the dynamics of interactions between the malaria parasites, the liver hepatocytes, the red blood cells, and the macrophages (immune system cells). Unlike the work in [20, 22], we ignored the vector stage of parasite development and assumed a twofold process in the generation of hepatocytes: from the bone marrow and from self-replication of the existing hepatocytes. Again, we have assumed that the generation of macrophages and the susceptible red blood cells from the bone marrow increase with increasing density of the infected erythrocytes. However, whatever density of the infected erythrocytes, there is a limit on the rate at which cells can be released from the bone marrow.

2.1. Model Formulation. The hepatocytic-erythrocytic malaria model describes the dynamics of *Plasmodium falciparum* parasite during the hepatocytic and erythrocytic stages and their interactions with the host's red blood cells, liver hepatocytes, and the macrophages. The compartmental model assumes seven interacting populations of sporozoites $S(t)$, susceptible hepatocytes $H(t)$, infected hepatocytes $H_X(t)$, susceptible red blood cells (RBCs) $R(t)$, infected red blood cells (IRBCs) $R_X(t)$, merozoites $M(t)$, and macrophages $Z(t)$ at any time t. The dynamics of malaria parasites and host-cell populations in each compartment are described as follows.

Sporozoites (S). The female *Anopheles* mosquito is assumed to inject sporozoites into the human system during blood meal at a constant rate Λ. The sporozoites molt through the blood stream and reach the liver in about 2 hours, where they invade the hepatocytes at the rate β_s. We assume that the sporozoites can die naturally at a rate δ_s.

Susceptible Hepatocytes (H). We consider the bone marrow and self-replication as the main sources of the liver hepatocytes. The recruitment of hepatocytes from the bone marrow is assumed to occur at a constant rate λ_h. Just like during liver transplant [37], we argue that, during severe malaria infections, the rate of generation of healthy hepatocytes is likely to increase tremendously and in proportion to the concentrations of the infected liver cells [38]. This additional increase is represented by the term $\rho_1 H_X/(\kappa_1 + H_X) = \psi_1(H_X)$, where H_X and ρ_1, respectively, represent the concentration of infected hepatocytes and their rates of generation. The parameter κ_1 represents the number/concentration of the infected hepatocytes at which the recruitment of the healthy hepatocytes is a half of the maximum rate. Owing to invasion by sporozoites at the rate β_s, susceptible hepatocytes get infected and progress to subpopulation H_X. In addition, hepatocytes in compartment H are assumed to have a natural life expectancy and may hence die naturally at the rate μ_1.

Infected Hepatocytes (H_X). Infected hepatocytes mature into liver-stage schizonts. These schizonts burst open releasing 2000–40000 uninucleate merozoites into the blood stream [39]. The term $N\mu_2 H_X$ represents the total population of merozoites released upon bursting of infected hepatocytes. The parameter μ_2 represents the death rate of the infected hepatocytes.

Susceptible Red Blood Cells (R). Similar to malaria models in [21, 23, 30], we have assumed that the susceptible RBCs get recruited at a constant rate λ_r from the bone marrow. We further assume that, during infection, the erythrocyte production is accelerated owing to the presence of IRBCs at the rate ρ_2. This increase is denoted by the term $\rho_2 R_X/(\kappa_2 + R_X) = \psi_2(R_X)$, where κ_2 represents number/concentration of the infected red blood cells at which the recruitment of susceptible red blood cells is a half of the maximum rate. The particular mechanisms involved in this accelerated process are, however, still poorly understood [40]. The susceptible RBCs get infected by merozoites at a rate proportional to the contact rate of their density, $\beta_r MR$. The positive constant β_r describes the rate of successful invasion by a malaria merozoite. The susceptible RBCs die naturally at a rate μ_3.

Infected Red Blood Cells (R_X). Upon invasion by merozoites, the healthy RBCs get infected, leading to the formation of infected red blood cells R_X. Although the RBCs die at a constant rate μ_4, they can similarly be killed through phagocytosis by the macrophages at the rate η. At maturity, the IRBCs burst open, releasing free merozoites into the blood system, causing secondary invasion and disease progression.

Merozoites (M). After 2–15 days, the infected hepatocytes burst open and release merozoites into the blood system. This is represented by the term $N\mu_2 H_X$, where N is the average number of merozoites released per bursting infected hepatocytes. An average of K merozoites is released per each bursting IRBC. These free parasites suffer a natural death at a rate δ_m and invade susceptible RBCs at a rate β_r. Within the red blood cells, the merozoites mature either into uninucleate

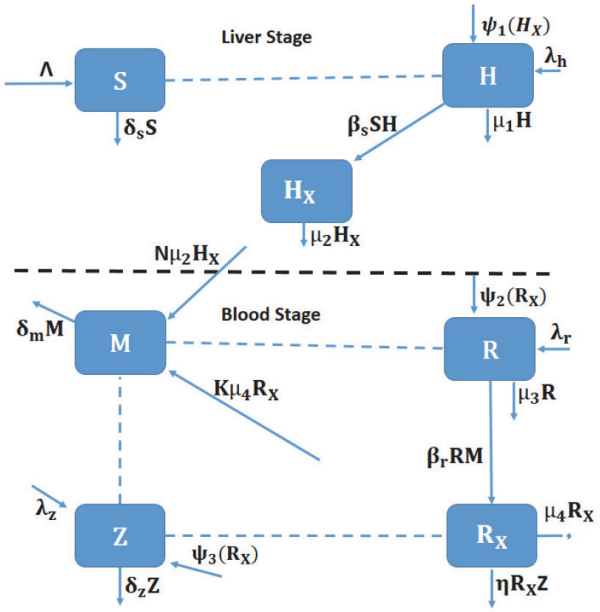

FIGURE 1: Schematic diagram for hepatocytic-erythrocytic and malaria parasite dynamics. The dotted lines without arrows indicate cell-parasite interaction and the solid lines show progression from one compartment to another.

gametocyte or into erythrocytic stage schizont containing 10–36 merozoites [39]. After about 48–72 hours, the erythrocytic stage schizont ruptures, releasing more merozoites into blood stream to cause further invasion of healthy RBCs. We assume that a proportion ζ of the merozoites contribute to secondary invasion of the susceptible RBCs. The rest of the merozoites $(1 - \zeta)$ transform into gametocytes that are later picked up by female *Anopheles* mosquitoes during feeding.

Macrophages (Z). Owing to their effectiveness in elimination of infected erythrocytes and infective malaria parasites, we have considered the innate macrophage cells as the main part of the immune response in malaria infection. Consequently, we have assumed that the macrophage cells are recruited at a constant rate λ_z from the bone marrow. Moreover, they proliferate at a rate ρ_3 in the sites of infection in proportion to the density of IRBCs. This is represented by the term $\rho_3 R_X/(\kappa_3 + R_X) = \psi_3(R_X)$, where κ_3 denotes the number/concentration of the infected red blood cells at which the recruitment of the macrophages is a half of the maximum rate. We further assume that they can die naturally at a constant rate δ_z.

The variables and parameters that describe in-host malaria dynamics are as in Tables 1 and 2, respectively.

The above transmission dynamics of malaria are summarised in the compartmental diagram in Figure 1.

From the above description of the in-host dynamics of malaria and the representation in Figure 1, we derive the following system of ordinary differential equations:

$$\frac{dH}{dt} = \lambda_h + \frac{\rho_1 H_X}{\kappa_1 + H_X} - \mu_1 H - \beta_s SH,$$

Table 1: Symbols and definition of state variables considered in the model.

Variable	Description
$H(t)$	The population of susceptible hepatocytes at time t
$H_X(t)$	The population of infected hepatocytes at time t
$R(t)$	The population of susceptible red blood cells (erythrocytes) at time t
$R_X(t)$	The population of infected red blood cells at time t
$Z(t)$	The density of macrophages in the human body at time t
$S(t)$	The population of sporozoites at time t
$M(t)$	The population of merozoites at time t

Table 2: Symbols and description of parameters used in the model.

Parameter	Description
Λ	The total rate of injection of sporozoites into liver due to mosquito bites
δ_s	The death rate of sporozoites
λ_h	Recruitment rate of susceptible hepatocytes from the bone marrow
μ_1	Natural death rate of susceptible hepatocytes
β_s	The invasion rate of hepatocytes by sporozoites
μ_2	Death rate of infected hepatocytes
λ_r	Recruitment rate of susceptible RBCs by the bone marrow
μ_3	The natural death rate of RBCs
β_r	The invasion rate of RBCs by merozoites
μ_4	Death rates of IRBCs
δ_m	The death rate of merozoites
λ_z	Recruitment rate of macrophages from the bone marrow
δ_z	The death rate of a macrophage
η	Elimination rate of IRBCs by macrophages
ρ_1	Production rate of hepatocytes due to presence of infected hepatocytes
ρ_2	Production rate of RBCs due to presence of IRBCs
ρ_3	Immunogenicity of IRBCs
κ_1	Number of H_X at which the recruitment of H is a half of the maximum rate
κ_2	Number of R_X at which the recruitment of R is a half of the maximum rate
κ_3	Number of R_X at which the recruitment of Z is a half of the maximum rate
ζ	The proportion of the merozoites that cause secondary infections
K	The average number of merozoites released per bursting IRBCs
N	The average number of merozoites released per bursting infected hepatocytes

$$\begin{aligned}
\frac{dH_X}{dt} &= \beta_s SH - \mu_2 H_X,\\
\frac{dR}{dt} &= \lambda_r + \frac{\rho_2 R_X}{\kappa_2 + R_X} - \mu_3 R - \beta_r RM,\\
\frac{dR_X}{dt} &= \beta_r RM - \mu_4 R_X - \eta R_X Z,\\
\frac{dZ}{dt} &= \lambda_z + \frac{\rho_3 R_X}{\kappa_3 + R_X} - \delta_z Z,\\
\frac{dS}{dt} &= \Lambda - \delta_s S - \beta_s SH,\\
\frac{dM}{dt} &= N\mu_2 H_X + K\zeta\mu_4 R_X - \delta_m M - \beta_r RM,
\end{aligned} \tag{1}$$

where $H(0) \geq 0$, $H_X(0) \geq 0$, $R(0) \geq 0$, $R_X(0) \geq 0$, $Z(0) \geq 0$, $S(0) \geq 0$, and $M(0) \geq 0$.

3. Model Analysis

3.1. Basic Properties. In this section, we study whether the formulated model (1) is biologically and mathematically meaningful. We establish model equilibrium points and investigate their stability properties.

3.1.1. Well-Posedness of the Model. For the in-host malaria model (1) to be mathematically and biologically meaningful, we need to prove that all the solutions of model system (1) with nonnegative initial conditions would remain nonnegative for all time $t \geq 0$. Positivity in the model is shown by proving the following theorem.

Theorem 1. *Let the parameters in model (1) be positive constants. A nonnegative solution* $(H(t), H_X(t), R(t), R_X(t), Z(t), S(t), M(t))$ *exists for all the state variables with nonnegative initial conditions* $\{H(0) = H_0 \geq 0,\ H_X(0) = H_{X0} \geq 0,\ R(0) = R_0 \geq 0,\ R_X(0) = R_{X0} \geq 0,\ Z(0) = Z_0 \geq 0,\ S(0) = S_0 \geq 0,\ M(0) = M_0 \geq 0\} \forall t \geq 0$.

Proof. Considering the first equation in system (1), let $\psi_1(t) = \rho_1 H_X/(\kappa_1 + H_X)$, so that

$$\begin{aligned} \frac{\mathrm{d}H}{\mathrm{d}t} &= \lambda_h + \varphi(t) - \mu_1 H - \beta_s S H, \\ \frac{\mathrm{d}H}{\mathrm{d}t} &\geq -(\mu_1 + \beta_s S) H, \end{aligned} \tag{2}$$

which yields

$$H(t) \geq H(0) \exp\left\{-\left(\int_0^t \beta_s S(s)\, ds + \mu_1 t\right)\right\} > 0. \tag{3}$$

In a similar fashion, this procedure can be applied to all the remaining six equations in model system (1), so that we have the following solutions:

$$\begin{aligned} H_X(t) &\geq H_X(0) \exp\{-\mu_2 t\} > 0, \\ R(t) &\geq R(0) \exp\left\{-\left(\int_0^t \beta_r M(s)\, ds + \mu_3 t\right)\right\} > 0, \\ R_X(t) &\geq R_X(0) \exp\left\{-\left(\int_0^t \eta Z(s)\, ds + \mu_4 t\right)\right\} > 0, \\ Z(t) &\geq Z(0) \exp\{-\delta_z t\} > 0, \\ S(t) &\geq S(0) \exp\left\{-\left(\int_0^t \beta_s H(s)\, ds + \delta_s t\right)\right\} > 0, \\ M(t) &\geq M(0) \exp\left\{-\left(\int_0^t \beta_r R(s)\, ds + \delta_m t\right)\right\} > 0. \end{aligned} \tag{4}$$

Therefore, state variables $(H, H_X, R, R_X, Z, S, M)$ of model system (1) are nonnegative for all time $t > 0$. □

3.1.2. Invariant Region. Let $N_H(t)$ represent the total hepatocyte population, so that $N_H(t) = H(t) + H_X(t)$.

On substituting the derivatives in system (1) and simplifying, we have

$$\frac{dN_H}{dt} \leq \lambda_h + \psi_1(t) - \mu_h N_H, \tag{5}$$

where $\psi_1(t) = \rho_1 H_X/(\kappa_1 + H_X)$ and $\mu_h = \min\{\mu_1, \mu_2\}$.

Using integrating factor $e^{\mu_h t}$,

$$N_H(t) \leq \frac{\lambda_h}{\mu_h} + e^{-\mu_h t} \int_0^t \psi_1(\tau) e^{\mu_h \tau} d\tau + c_1 e^{-\mu_h t}, \tag{6}$$

where c_1 is a constant of integration. By applying the initial condition $N_H(0) = N_{H0} > 0$ in (6), we obtain

$$c_1 = \left(N_H(0) - \frac{\lambda_h}{\mu_h}\right) - \int_0^t \psi_1(\tau) e^{-\mu_h \tau} d\tau. \tag{7}$$

Substituting the value of c_1 into $N_H(t)$ in (6) and simplifying, we get

$$N_H(t) \leq \frac{\lambda_h}{\mu_h} + e^{-\mu_h t}\left(N_H(0) - \frac{\lambda_h}{\mu_h}\right). \tag{8}$$

There are two possible cases in analyzing the behaviour of $N_H(t)$ in (8). In the first case, we consider $N_H(0) > \lambda_h/\mu_h$ so that, at time $t = 0$, the right-hand side (RHS) of (8) experiences the largest possible value of $N_H(0)$. That is, $N_H(t) \leq N_H(0)$ for all time $t > 0$.

In the second case, we consider $N_H(0) < \lambda_h/\mu_h$, so that the largest possible value of the RHS of (8) approaches λ_h/μ_h as time t goes to infinity. Thus, $N_H(t) \leq \lambda_h/\mu_h$, $\forall t > 0$. From these two cases, we conclude that $N_H(t) \leq \max\{N_H(0), \lambda_h/\mu_h\}$ for all time $t > 0$.

Using the above approach, let the total red blood cells population be $N_R(t)$, so that $N_R(t) = R(t) + R_X(t)$. From the model equations in system (1), we have

$$\frac{dN_R}{dt} \leq \lambda_r + \psi_2(t) - \mu_r N_R(t), \tag{9}$$

where $\psi_2(t) = \rho_2 R_X/(\kappa_2 + R_X)$ and $\mu_r = \min\{\mu_3, \mu_4\}$. Upon solving for N_R in (9), we have $N_R(t) \leq \max\{N_R(0), \lambda_r/\mu_r\}$, $\forall t > 0$.

For the macrophage compartment $Z(t)$, we have

$$\frac{\mathrm{d}Z}{\mathrm{d}t} = \lambda_z + \psi_3(t) - \delta_z Z, \quad \text{for } \psi_3(t) = \frac{\rho_3 R_X}{\kappa_3 + R_X}. \tag{10}$$

By integration, the solution of (10) is presented as

$$Z(t) \leq \frac{\lambda_z}{\delta_z} + e^{-\delta_z t}\left(Z(0) - \frac{\lambda_z}{\delta_z}\right). \tag{11}$$

By inspection, $Z(t) \leq \max\{Z(0), \lambda_z/\delta_z\}$ for all time $t > 0$.

Finally, let $N_P(t)$ represent the total population of malaria parasites at any time t. That is, $N_P(t) = S(t) + M(t)$ and, from system (1),

$$\begin{aligned} \frac{\mathrm{d}N_P}{\mathrm{d}t} &= \Lambda - \delta_s S - \beta_s S H + N\mu_2 H_X + K\zeta\mu_4 R_X \\ &\quad - \delta_m M, \leq \Lambda + (K\zeta\mu_4 R_X + N\mu_2 H_X) - \delta_p N_p, \\ &\quad \text{where } \delta_p = \min\{\delta_s, \delta_m\}. \end{aligned} \tag{12}$$

Let $(K\zeta\mu_4 R_X + N\mu_2 H_X) = \psi_4(t)$, so that on solving for $N_P(t)$ we get

$$N_p(t) \leq \frac{\Lambda}{\delta_p} + e^{-\delta_p t}\left(N_p(0) - \frac{\Lambda}{\delta_p}\right) \tag{13}$$

Clearly, the malaria parasite populations $S(t)$ and $M(t)$ are bounded above. That is,

$N_P(t) \leq \max\{N_P(0), \Lambda/\delta_p\}$ for all time $t > 0$.

Based on this discussion, we have shown the existence of a bounded positive invariant region for our model system (1). Let us denote this region as $\Omega \in \mathbb{R}_+^7$, where

$$\begin{aligned}\Omega = \Bigg\{ & \left(H, H_X, R, R_X, Z, S, M\right) \in \mathbb{R}_+^7 : N_P(t) \\ & \leq \max\left\{N_P(0), \frac{\Lambda}{\delta_p}\right\}, N_H(t) \\ & \leq \max\left\{N_H(0), \frac{\lambda_h}{\mu_h}\right\}, N_R(t) \\ & \leq \max\left\{N_R(0), \frac{\lambda_r}{\mu_r}\right\}, Z(t) \leq \max\left\{Z(0), \frac{\lambda_z}{\delta_z}\right\}\Bigg\}.\end{aligned} \tag{14}$$

Moreover, any solution of our system (1) which commences in Ω at any time $t \geq 0$ will always remain confined in that region. We therefore deduce that the region Ω is positively invariant and attracting with respect to malaria model (1). Our in-host malaria model (1) is hence well posed mathematically and biologically.

3.1.3. Disease-Free Equilibrium Point. The disease-free equilibrium point, $\mathscr{E}_0$, is the state in which the human host is free of malaria infection. At $\mathscr{E}_0$, the sporozoite recruitment rate, $\Lambda = 0$, and parasite and host-infected compartments have zero values; that is, $S^* = M^* = R_X^* = H_X^* = 0$. Therefore,

$$\begin{aligned}\mathscr{E}_0 &= \left(H^*, H_X^*, R^*, R_X^*, Z^*, S^*, M^*\right) \\ &= \left(\frac{\lambda_h}{\mu_1}, 0, \frac{\lambda_r}{\mu_3}, 0, \frac{\lambda_z}{\delta_z}, 0, 0\right).\end{aligned} \tag{15}$$

3.1.4. In-Host Basic Reproduction Number. The in-host reproduction number of model (1) denoted by R_0 is computed using the technique of the next-generation matrix approach described in [41]. We consider H_X, R_X, S, and M as the parasite infested compartments. Adopting the notations in [41], we generate a nonnegative matrix F of new infections and a nonsingular matrix V, showing the transfer of infections from one compartment to the other as follows:

$$F = \begin{pmatrix} 0 & 0 & \frac{\beta_s \lambda_h}{\mu_1} & 0 \\ 0 & 0 & 0 & \frac{\beta_r \lambda_r}{\mu_3} \\ 0 & 0 & 0 & 0 \\ 0 & 0 & 0 & 0 \end{pmatrix} \tag{16}$$

and

$$V = \begin{pmatrix} \mu_2 & 0 & 0 & 0 \\ 0 & \mu_4 + \frac{\eta \lambda_z}{\delta_z} & 0 & 0 \\ 0 & 0 & \delta_s + \frac{\beta_s \lambda_h}{\mu_1} & 0 \\ -N\mu_2 & -K\zeta\mu_4 & 0 & \delta_m + \frac{\beta_r \lambda_r}{\mu_3} \end{pmatrix}. \tag{17}$$

The inverse of matrix V is hence given by

$$V^{-1} = \begin{pmatrix} \frac{1}{\mu_2} & 0 & 0 & 0 \\ 0 & \frac{\delta_z}{\eta\lambda_z + \delta_z\mu_4} & 0 & 0 \\ 0 & 0 & \frac{1}{\delta_s + \beta_s\lambda_h/\mu_1} & 0 \\ \frac{N\mu_3}{\beta_r\lambda_r + \delta_m\mu_3} & \frac{K\zeta\delta_z\mu_3\mu_4}{\left(\beta_r\lambda_r + \delta_m\mu_3\right)\left(\eta\lambda_z + \delta_z\mu_4\right)} & 0 & \frac{1}{\delta_m + \beta_r\lambda_r/\mu_3} \end{pmatrix}. \tag{18}$$

The next-generation matrix G, which is the product of matrices F and V^{-1}, works out to be

$$G = \begin{pmatrix} 0 & 0 & \frac{\beta_s\lambda_h}{\beta_s\lambda_h + \delta_s\mu_1} & 0 \\ \frac{N\beta_r\lambda_r}{\beta_r\lambda_r + \delta_m\mu_3} & \frac{K\zeta\beta_r\delta_z\lambda_r\mu_4}{\left(\beta_r\lambda_r + \delta_m\mu_3\right)\left(\eta\lambda_z + \delta_z\mu_4\right)} & 0 & \frac{\beta_r\lambda_r}{\beta_r\lambda_r + \delta_m\mu_3} \\ 0 & 0 & 0 & 0 \\ 0 & 0 & 0 & 0 \end{pmatrix}. \tag{19}$$

The in-host basic reproduction number R_0 is the spectral radius of the next-generation matrix G. It can clearly be seen that three of the four eigenvalues of matrix G in (19) have zero values; that is, $\lambda_1 = \lambda_2 = \lambda_3 = 0$. The fourth and largest nonnegative eigenvalue λ_4 becomes the in-host model reproduction number. We therefore have

$$R_0 = \frac{K\beta_r\lambda_r}{(\beta_r\lambda_r + \delta_m\mu_3)} \cdot \frac{\zeta\delta_z\mu_4}{(\eta\lambda_z + \delta_z\mu_4)}. \tag{20}$$

The terms in model R_0 can be interpreted as follows:

(1) The term $K\beta_r\lambda_r/(\beta_r\lambda_r + \delta_m\mu_3)$ represents the expected number of infectious merozoite parasites resulting from bursting blood schizonts at the blood stage of malaria infection.

(2) The second term $\zeta\delta_z\mu_4/(\eta\lambda_z + \delta_z\mu_4)$ represents the expected proportion of merozoites that participate in the cycle of erythrocytic schizogony.

(3) Observe that the terms $(\beta_r\lambda_r)/(\beta_r\lambda_r + \delta_m\mu_3) < 1$ and $(\delta_z\mu_4)/(\eta\lambda_z + \delta_z\mu_4) < 1$. So our $R_0 \leq K\zeta$. This implies that the number of secondary infections during malaria infections is largely influenced by the average number of merozoites released K, from a bursting blood schizont, most of which are responsible for secondary infections at the blood stage.

Despite the inclusion of the liver stage dynamics, it is interesting to observe that the above in-host reproduction number and hence the disease progression are heavily driven by the dynamics at the erythrocytic stage.

In the sections that follow, we shall establish both the local stability and global stability of disease-free equilibrium point (15) of model system (1).

3.1.5. Local Stability of the Disease-Free Equilibrium Point, $\mathscr{E}_0$. The Jacobian matrix of model system (1) evaluated at the disease-free equilibrium $\mathscr{E}_0$ is given by

$$J_1(\mathscr{E}_0) = \begin{pmatrix} -\mu_1 & \frac{\rho_1}{\kappa_1} & 0 & 0 & 0 & -\frac{\beta_s\lambda_h}{\mu_1} & 0 \\ 0 & -\mu_2 & 0 & 0 & 0 & \frac{\beta_s\lambda_h}{\mu_1} & 0 \\ 0 & 0 & -\mu_3 & \frac{\rho_2}{\kappa_2} & 0 & 0 & -\frac{\beta_r\lambda_r}{\mu_3} \\ 0 & 0 & 0 & -\frac{\eta\lambda_z}{\delta_z} - \mu_4 & 0 & 0 & \frac{\beta_r\lambda_r}{\mu_3} \\ 0 & 0 & 0 & \frac{\rho_3}{\kappa_3} & -\delta_z & 0 & 0 \\ 0 & 0 & 0 & 0 & 0 & -\frac{\beta_s\lambda_h}{\mu_1} - \delta_s & 0 \\ 0 & N\mu_2 & 0 & K\zeta\mu_4 & 0 & 0 & -\frac{\beta_r\lambda_r}{\mu_3} - \delta_m \end{pmatrix}. \tag{21}$$

It is clear from the first, third, and fifth columns of matrix (21) that the Jacobian matrix has negative eigenvalues $\lambda_1 = -\mu_1, \lambda_2 = -\mu_3$, and $\lambda_3 = -\delta_z$. Upon deleting the first, third, and fifth rows and columns, matrix (21) is reduced to the following 4×4 matrix:

$$J_2(\mathscr{E}_0) = \begin{pmatrix} -\mu_2 & 0 & \frac{\beta_s\lambda_h}{\mu_1} & 0 \\ 0 & -\frac{\eta\lambda_z}{\delta_z} - \mu_4 & 0 & \frac{\beta_r\lambda_r}{\mu_3} \\ 0 & 0 & -\frac{\beta_s\lambda_h}{\mu_1} - \delta_s & 0 \\ N\mu_2 & K\zeta\mu_4 & 0 & -\frac{\beta_r\lambda_r}{\mu_3} - \delta_m \end{pmatrix}. \tag{22}$$

From row three in (22), $\lambda_4 = -\beta_s\lambda_h/\mu_1 - \delta_s$. We further reduce matrix (22) by deleting row three and column three. So,

$$J_3(\mathscr{E}_0) = \begin{pmatrix} -\mu_2 & 0 & 0 \\ 0 & -\frac{\eta\lambda_z}{\delta_z} - \mu_4 & \frac{\beta_r\lambda_r}{\mu_3} \\ N\mu_2 & K\zeta\mu_4 & -\frac{\beta_r\lambda_r}{\mu_3} - \delta_m \end{pmatrix}. \tag{23}$$

Note from row one of (23) that the fifth eigenvalue $\lambda_5 = -\mu_2 < 0$.

The remaining two eigenvalues can be obtained by reducing matrix (23) into the following 2×2 matrix:

$$J_6(\mathscr{E}_0) = \begin{pmatrix} -\frac{\eta\lambda_z}{\delta_z} - \mu_4 & \frac{\beta_r\lambda_r}{\mu_3} \\ K\zeta\mu_4 & -\frac{\beta_r\lambda_r}{\mu_3} - \delta_m \end{pmatrix}. \tag{24}$$

Using the variable λ, the characteristic polynomial associated with matrix (24) is

$$p(\lambda) = \lambda^2 + A\lambda + B, \tag{25}$$

where

$$A = \delta_m + \frac{\eta\lambda_z}{\delta_z} + \frac{\beta_r\lambda_r}{\mu_3} + \mu_4 \text{ and} \tag{26}$$

$$B = \frac{\eta\delta_m\lambda_z}{\delta_z} + \frac{\eta\beta_r\lambda_r\lambda_z}{\delta_z\mu_3} + \delta_m\mu_4 + \frac{\beta_r\lambda_r\mu_4}{\mu_3} - \frac{K\zeta\beta_r\lambda_r\mu_4}{\mu_3}. \tag{27}$$

The characteristic polynomial (25) has negative roots (eigenvalues) if $A > 0$ and $B > 0$. The coefficient A in (26) is clearly positive. We now need to show that B in (27) is strictly positive if $R_0 < 1$. This is done by expressing the coefficient term B in terms of model R_0 as follows:

$$\begin{aligned} B &= \frac{1}{\delta_z\mu_3}\left[\left(\mu_4\delta_z + \eta\lambda_z\right)\left(\beta_r\lambda_r + \delta_m\mu_3\right) - K\zeta\beta_r\delta_z\lambda_r\mu_4\right], \\ &= \frac{1}{\delta_z\mu_3}\left[\left(\mu_4\delta_z + \eta\lambda_z\right)\left(\beta_r\lambda_r + \delta_m\mu_3\right) \cdot \left[1 - \frac{K\zeta\beta_r\delta_z\lambda_r\mu_4}{\left(\mu_4\delta_z + \eta\lambda_z\right)\left(\beta_r\lambda_r + \delta_m\mu_3\right)}\right]\right], \\ &= \frac{\left(\mu_4\delta_z + \eta\lambda_z\right)\left(\beta_r\lambda_r + \delta_m\mu_3\right)}{\delta_z\mu_3}\left[1 - R_0\right]. \end{aligned} \tag{28}$$

It can clearly be seen from (28) that the coefficient B is positive if and only if $R_0 < 1$. We have thus established the following result.

Theorem 2. *The disease-free equilibrium $\mathscr{E}_0$ is locally asymptotically stable in Ω if $R_0 < 1$. If $R_0 > 1$, then $\mathscr{E}_0$ is unstable.*

Biologically, Theorem 2 implies that malaria infection can be eliminated from the human host when $R_0 < 1$. To ensure that elimination of malaria is independent of the initial sizes of the subpopulations, it is necessary to show that $\mathscr{E}_0$ is globally asymptotically stable in Ω, where the model is mathematically and biologically sensible.

3.1.6. Global Asymptotic Stability of the Disease-Free Equilibrium. Using the results obtained in [42], we show that the malaria-free equilibrium state $\mathscr{E}_0$ is globally asymptotically stable when $R_0 < 1$. We begin by rewriting the model system (1) in pseudotriangular form as follows:

$$\begin{aligned} \dot{X}_1 &= A_1(X)\left(X_1 - X_1^*\right) + A_2(X)X_2, \\ \dot{X}_2 &= A_3(X)X_2, \end{aligned} \tag{29}$$

where X_1 is the vector representing the state of different compartment of liver and blood cells that are not infected and do not transmit malaria infections. X_2 represents the states of malaria parasites and host's cells that are responsible for disease transmission. Hence,

$$\begin{aligned} X &= \left(X_1, X_2\right), \\ X_1 &= \left(H, R, Z\right), \\ X_2 &= \left(H_X, R_X, S, M\right) \text{ and} \\ X_1^* &= \left(\frac{\lambda_h}{\mu_1}, \frac{\lambda_r}{\mu_3}, \frac{\lambda_z}{\delta_z}\right). \end{aligned} \tag{30}$$

From the subsystem X_1, we have

$$A_1(X) = \begin{pmatrix} -\mu_1 & 0 & 0 \\ 0 & -\mu_3 & 0 \\ 0 & 0 & -\delta_z \end{pmatrix} \text{ and}$$

$$A_2(X) = \begin{pmatrix} \frac{\rho_1}{\kappa_1} & 0 & -\frac{\lambda_h}{\mu_1}\beta_s & 0 \\ 0 & \frac{\rho_2}{\kappa_2} & 0 & -\frac{\lambda_r}{\mu_3}\beta_r \\ 0 & \frac{\rho_3}{\kappa_3} & 0 & 0 \end{pmatrix}. \tag{31}$$

A direct computation indicates that the eigenvalue of matrix $A_1(X)$ is real and negative. This shows that the system $\dot{X}_1 = A_1(X)(X_1 - X_1^*) + A_2(X)X_2$ is globally asymptotically stable at the disease-free equilibrium, $\mathscr{E}_0$. Similarly, the subsystem X_2 gives rise to the following matrix $A_3(X)$:

$$A_3(X) = \begin{pmatrix} -\mu_2 & 0 & \beta_s\frac{\lambda_h}{\mu_1} & 0 \\ 0 & -\left(\eta\frac{\lambda_z}{\delta_z} + \mu_4\right) & 0 & \beta_r\frac{\lambda_r}{\mu_3} \\ 0 & 0 & -\left(\beta_s\frac{\lambda_h}{\mu_1} + \delta_s\right) & 0 \\ N\mu_2 & K\zeta\mu_4 & 0 & -\left(\beta_r\frac{\lambda_r}{\mu_3} + \delta_m\right) \end{pmatrix}. \tag{32}$$

It can clearly be seen that $A_3(X)$ is a Metzler matrix: all the off-diagonal elements of $A_3(X)$ are nonnegative.

In order to establish the global stability of the disease-free equilibrium, we need to show that the matrix $A_3(X)$

is Metzler stable by providing a proof of the following lemma.

Lemma 3. *Let M be a square Metzler matrix that is block decomposed:*

$$M = \begin{pmatrix} A & B \\ C & D \end{pmatrix}, \tag{33}$$

where A and D are square matrices. The matrix M is Metzler stable if and only if A and $D - CA^{-1}B$ are Metzler stable.

In our case, matrix M is represented by matrix A_3 in (32), so that

$$\begin{aligned} A &= \begin{pmatrix} -\mu_2 & 0 \\ 0 & -\left(\eta\dfrac{\lambda_z}{\delta_z} + \mu_4\right) \end{pmatrix}, \\ B &= \begin{pmatrix} \beta_s\dfrac{\lambda_h}{\mu_1} & 0 \\ 0 & \beta_r\dfrac{\lambda_r}{\mu_3} \end{pmatrix}, \\ C &= \begin{pmatrix} 0 & 0 \\ N\mu_2 & K\zeta\mu_4 \end{pmatrix} \text{ and} \\ D &= \begin{pmatrix} -\left(\beta_s\dfrac{\lambda_h}{\mu_1} + \delta_s\right) & 0 \\ 0 & -\left(\beta_r\dfrac{\lambda_r}{\mu_3} + \delta_m\right) \end{pmatrix}. \end{aligned} \tag{34}$$

Upon computation in Mathematica software, we obtain

$$D - CA^{-1}B = \begin{pmatrix} -\omega_1 & 0 \\ \omega_2 & -\omega_3 \end{pmatrix}, \tag{35}$$

where $\omega_1 = \delta_s + \beta_s(\lambda_h/\mu_1)$, $\omega_2 = N\beta_s\lambda_h/\mu_1$, and $\omega_3 = \delta_m + \beta_r\lambda_r(\eta\lambda_h + (1 - K\zeta)\delta_z\mu_4)/\mu_3(\eta\lambda_z + \delta_z\mu_4)$.

For the matrix $D - CA^{-1}B$ to be Metzler stable, ω_3 should be strictly nonnegative. Therefore, the expression in the numerator

$$\beta_r\lambda_r\left(\eta\lambda_h + (1 - K\zeta)\,\delta_z\mu_4\right) \geq 0. \tag{36}$$

Upon simplification of (36),

$$K\zeta\beta_r\lambda_r\delta_z\mu_4 \leq \beta_r\lambda_r\left(\eta\lambda_h + \delta_z\mu_4\right), \tag{37}$$

$$\begin{aligned} &\left(\frac{\beta_r\lambda_r + \delta_m\mu_3}{\beta_r\lambda_r}\right)\left(\frac{K\zeta\beta_r\lambda_r\delta_z\mu_4}{\left(\beta_r\lambda_r + \delta_m\mu_3\right)\left(\eta\lambda_z + \delta_z\mu_4\right)}\right) \\ &\quad \leq 1, \end{aligned} \tag{38}$$

$$\left(\frac{\beta_r\lambda_r + \delta_m\mu_3}{\beta_r\lambda_r}\right)R_0 \leq 1 \tag{39}$$

$$R_0 \leq \frac{\beta_r\lambda_r}{\beta_r\lambda_r + \delta_m\mu_3} < 1. \tag{40}$$

Clearly, matrix A in (34) is Metzler stable. However, the matrix $D - CA^{-1}B$ is Metzler stable if and only if $R_0 < 1$. From Lemma 3, we deduce the following theorem.

Theorem 4. *The malaria-free equilibrium $\mathscr{E}_0$ of model system (1) is globally asymptotically stable if the threshold quantity $R_0 < 1$.*

The above result is quite significant in malaria control. The global stability of the disease-free status would be guaranteed if and only if the in-host basic reproduction number R_0 is less than one. Malaria intervention should therefore focus on eliminating infected erythrocytes and/or malaria merozoites that are responsible for erythropoiesis cycle and invasions at the blood stage.

3.2. The Endemic Equilibrium Analysis. When $R_0 > 1$, the stability of the disease-free equilibrium (15) is violated. A different equilibrium state termed the endemic equilibrium is achieved. Equating to zero the RHS of system (1) and solving for the state variables R, H, Z, S, and M in terms of the infected states H_X and R_X, we obtain the endemic state $\mathscr{E}_1 = (H^*, H_X^*, R^*, R_X^*, Z^*, S^*, \mathrm{M}^*)$, where

$$\begin{aligned} H^* &= \frac{1}{\mu_1}\left\{\lambda_h + \frac{\rho_1 H_X^*}{\kappa_1 + H_X^*} - \mu_2 H_X^*\right\}, \\ S^* &= \frac{\mu_1\mu_2 H_X^*}{\beta_s\left(\lambda_h + \rho_1 H_X^*/\left(\kappa_1 + H_X^*\right) - \mu_2 H_X^*\right)}, \end{aligned} \tag{41}$$

$$\begin{aligned} R^* &= \frac{1}{\mu_3}\left\{\lambda_r + \frac{\rho_2 R_X^*}{\kappa_2 + R_X^*} - \mu_4 R_X^*\right\}, \\ M^* &= \mu_3\left(R_X^*\mu_4 + \frac{\eta R_X^*\left(\rho_3 R_X^*/\left(\kappa_3 + R_X^*\right) + \lambda_z\right)}{\mu_1}\right) \end{aligned} \tag{42}$$

$$Z^* = \frac{1}{\delta_z}\left\{\lambda_z + \frac{\rho_3 R_X^*}{\kappa_3 + R_X^*}\right\} \tag{43}$$

Substituting (41) into the 2^{nd} equation in (1) and simplifying, we obtain the following cubic equation:

$$\alpha_3 H_X^{*3} + \alpha_2 H_X^{*2} + \alpha_1 H_X^* + \alpha_0 = 0, \tag{44}$$

where

$$\begin{aligned} \alpha_3 &= \mu_2^2\beta_s > 0, \\ \alpha_2 &= \mu_2\left(\mu_1\left(-\delta_s\right) - \beta_s\left(\lambda_h - \kappa_1\mu_2 + \Lambda + \rho_1\right)\right), \\ \alpha_1 &= \beta_s\left(\lambda_h\left(\Lambda - \kappa_1\mu_2\right) + \Lambda\left(\rho_1 - \kappa_1\mu_2\right)\right) \\ &\quad - \kappa_1\mu_1\mu_2\delta_s, \text{ and} \\ \alpha_0 &= \kappa_1\Lambda\lambda_h\beta_s > 0. \end{aligned} \tag{45}$$

The number and nature of the roots of (44) are determined by the following discriminant:

$$\begin{aligned} \Delta = {} & 18\alpha_3\alpha_2\alpha_1\alpha_0 - 4{\alpha_2}^3\alpha_0 + {\alpha_2}^2{\alpha_1}^2 - 4\alpha_3{\alpha_1}^3 \\ & - 27{\alpha_3}^2{\alpha_0}^2. \end{aligned} \tag{46}$$

So

(i) if $\Delta = 0$, then (44) has multiple real roots and only one endemic equilibrium would exist,

(ii) if $\Delta < 0$, then (44) has 1 real root and a complex conjugate root and hence only one endemic equilibrium,

(iii) if $\Delta > 0$, then (44) has 3 distinct real roots and so there is more than one endemic equilibrium when $R_0 > 1$ for model system (1).

Analysis under (46) implies that, in the absence of external interventions in the form of antimalarial treatment, there will always be some infected hepatocytes during malaria infection. We then evaluate the possible values of the state variable R_X at equilibrium by substituting expressions in (42) and (43) into the 4^{th} equation in (1). After simplification in Mathematica software, we obtain the following cubic equation:

$$R_X^* \left(\theta_3 R_X^{*3} + \theta_2 R_X^{*2} + \theta_1 R_X^* + \theta_0\right) = 0, \tag{47}$$

where

$$\begin{aligned}
\theta_3 &= -\mu_4\beta_r\left(\mu_1\mu_4 + \eta\left(\rho_3 + \lambda_z\right)\right) < 0,\\
\theta_2 &= \eta\rho_3\left(\beta_r\left(-\kappa_2\mu_4 + \rho_2 + \lambda_r\right) - 1\right) + \left(\mu_1\mu_4 + \eta\lambda_z\right)\\
&\quad \cdot \left(\beta_r\left(-\left(\kappa_2 + \kappa_3\right)\mu_4 + \rho_2 + \lambda_r\right) - 1\right),\\
\theta_1 &= \eta\kappa_2\rho_3\left(\beta_r\lambda_r - 1\right) - \left(\mu_1\mu_4 + \eta\lambda_z\right)\left(\kappa_3\right.\\
&\quad \left. + \kappa_2\left(\beta_r\left(\kappa_3\mu_4 - \lambda_r\right) + 1\right) + \kappa_3\left(-\beta_r\right)\left(\rho_2 + \lambda_r\right)\right),\\
\theta_0 &= \kappa_2\kappa_3\left(\beta_r\lambda_r - 1\right)\left(\mu_1\mu_4 + \eta\lambda_z\right).
\end{aligned} \tag{48}$$

Clearly, $R_X^* = 0$ or

$$\theta_3 R_X^{*3} + \theta_2 R_X^{*2} + \theta_1 R_X^* + \theta_0 = 0. \tag{49}$$

The state $R_X^* = 0$ corresponds to a scenario in which there are no parasite-infected red blood cells. This could signify the liver stage of parasite development so that an endemic state $(H^{**}, H_X^{**}, R^{**}, 0, 0, S^{**}, 0)$ exists. Alternatively, $R_X^* = 0$ could correspond to the disease-free equilibrium point (15) for system (1).

The roots of the cubic equation (49) are given as

$$\begin{aligned}
R_{X1}^* &= -\frac{\kappa_3\left(\mu_1\mu_4 + \eta\lambda_z\right)}{\eta\rho_3 + \mu_1\mu_4 + \eta\lambda_z} < 0,\\
R_{X2,3}^* &= \frac{\left(\beta_r\lambda_r - \kappa_2\mu_4\beta_r + \rho_2\beta_r - 1\right) \pm \sqrt{\Theta}}{2\mu_4\beta_r},
\end{aligned} \tag{50}$$

where

$$\begin{aligned}
\Theta &= 4\mu_4\beta_r\left(\kappa_2\beta_r\lambda_r - \kappa_2\right)\\
&\quad + \left(\beta_r\lambda_r - \kappa_2\mu_4\beta_r + \rho_2\beta_r - 1\right)^2.
\end{aligned} \tag{51}$$

The root $R_{X1}^* < 0$ should be ignored, since all the model state variables are nonnegative for all time $t \geq 0$. This leaves $R_{X2,3}^*$ as the only two possible roots of (49).

From the above discussion, model (1) could experience a single endemic state or multiple endemic states subject to the roots of (44) and (47). If $R_{X2,3}^*$ are real and positive, then one or two endemic equilibrium points are possible for model (1). It is thus evident that the explicit form of the endemic equilibrium state for model (1) is cumbersome. We shall therefore show its existence numerically based on a certain choice of parameter values in Section 4. Note that case (iii) of (46) indicates the possibility of having multiple endemic equilibria and hence the likelihood of experiencing a backward bifurcation phenomenon. This will be investigated in another research paper.

4. Numerical Simulations and Discussions

In this section, we provide some numerical simulations to illustrate the behaviour of model system (1). We carry out model sensitivity analysis and investigate parameter influence on the dynamics of red blood cells, macrophages, and malaria parasites under different conditions on the in-host reproduction number, R_0.

4.1. Sensitivity Analysis. In epidemic modelling, sensitivity analysis is performed to investigate model parameters with significant influence on R_0 and hence on the transmission and the spread of the disease under study [43]. Following [44], the normalised forward-sensitivity index of a variable, $\triangle$, which depends differentially on a parameter, α, is defined as

$$\Upsilon_\alpha^{\triangle} = \frac{\partial\triangle}{\partial\alpha} \times \frac{\alpha}{\triangle}. \tag{52}$$

Using the formulation in (52) and the parameter values in Table 3, the local sensitivity indices (SI) of R_0 (see (20)) relative to the model parameters are calculated in Mathematica software and the results summarised in Table 4. Note that, due to limited data on in-host dynamics, all the parameter values used in evaluating the sensitivity indices are obtained from indicated past literature.

A positive sign on the SI indicates that an increase (decrease) in the value of such a parameter increases (decreases) the value of R_0 and hence the growth of malaria infection. On the other hand, a negative sign is indicative of a parameter that negatively affects R_0. In order to eliminate in-host malaria infection, the in-host reproduction number should be less than one, that is, $R_0 < 1$.

The average number of merozoites released per bursting infected erythrocyte K and the proportion of merozoites that cause secondary invasions at the blood phase ζ are the most sensitive parameters in determining the disease outcomes. They have the highest sensitivity indices of +1.0000. For instance, a 10% increase (decrease) ζ or K generates a 10% increase (decrease) on R_0 and hence malaria infection severity.

The parameters λ_z, η, μ_4, and δ_z occupy the second rank in influencing the model outcomes. An increase in the parameters μ_4 and δ_z is likely to increase the model R_0. On the other hand, an increase in λ_z and η has a direct negative influence on R_0. Macrophages are highly

Table 3: Parameter values used in the numerical simulation and demonstration of the existence of endemic equilibrium point. See Table 2 for detailed parameter descriptions.

Symbol	Interpretation	Value	Source
δ_z	Death rate of macrophages	0.05/day	[19]
δ_s	Death rate of sporozoites	1.2×10^{-11} /day	[20]
η	Elimination rate of IRBCs by macrophages	$10^{-10} cells\mu l^{-1}//day$	[19]
λ_h	Recruitment rate of H	$2.5 \times 10^8 cells/\mu l^{-1}/day$	[21]
ρ_1	Production rate of H due to H_X	$2.5 \times 10^{-5}/day$	[19]
μ_1	Death rate of H	0.029 /day	[20]
Λ	Rate of injection of sporozoites	20 sporozoites/day	[20]
ρ_2	Production rate of RBCs due to IRBCs	$2.5 \times 10^{-5}/day$	[19]
β_s	Hepatocyte invasion rate	$1.0 \times 10^{-6}/sporozoites/day$	[20]
ρ_3	Immunogenicity of IRBCs	$2.5 \times 10^{-5}/day$	[19]
μ_2	Death rate of infected hepatocytes	0.02/day	[20]
κ_1	Inhibition rate	$1\ cells/\mu l^{-1}$	[22]
λ_r	Recruitment rate of RBCs	$2.5 \times 10^8 cells/\mu l^{-1}/day$	[23]
ζ	Merozoites that cause secondary infections	0.726 (unitless)	[24]
μ_3	Death rate of healthy RBCs	0.0083/day	[23]
κ_2	Inhibition rate	$1\ cells/\mu l^{-1}$	[22]
β_r	Invasion rate of RBCs	$2.0 \times 10^{-9}/merozoites/day$	[23]
N	Merozoites per liver schizont	10000/day	[21]
μ_4	Death rate of infected RBCs	0.025/day	[19]
κ_3	Inhibition rate	$1\ cells/\mu l^{-1}$	[22]
δ_m	Death rate of merozoites	48/day	[23]
K	Merozoites per blood schizont	16	[21]
λ_z	Recruitment rate of macrophages	$30/\mu l^{-1}/day$	[19]

Table 4: Sensitivity indices of R_0 relative to the model parameters.

Parameter	SI	Parameter	SI
K	+1.0000	ζ	+1.0000
β_r	+0.920422	μ_3	-0.920422
λ_r	+0.920422	λ_z	-0.998585
μ_4	+0.998585	η	-0.998585
δ_z	+0.998585	δ_m	-0.920422

instrumental in malaria parasite clearance and should be preserved.

The rate of generation of macrophages from the bone marrow, λ_z, together with the rate of phagocytosis of infected red blood cells, η, is likely to decrease, proportionally, the disease progression when they are increased. With increased λ_z, there would be more macrophages to phagocytose and clear the rapidly growing density of blood schizonts. This would negatively affect the erythrocytic schizogony. Decreased clearance rate by macrophages would only guarantee successful multiplication of the merozoites through the erythrocytic schizogonic cycle. The subsequent result is increased concentration of merozoites in the host blood and disease progression to even deadly levels.

The parameters β_r and λ_r increase (or decrease) R_0 when they are increased (or decreased). Epidemiologically, an improved erythrocyte invasion rate, β_r, is likely to generate even more new blood schizonts. This increases parasitemia in the host. A 10% increase (decrease) in β_r would increase (decrease) the threshold parameter R_0 by about +9.2%.

Any therapeutic effort that clears the blood schizonts and the infectious merozoites at the blood stage would definitely guarantee immense reduction in model R_0. Therefore, an increase in the death rate of the infected red blood cells and that of the merozoites is likely to decrease significantly the in-host reproduction number R_0. This can be achieved through the use of effective antimalarials such as the use of artemisinin based combination therapy (ACT) in malaria treatment. Moreover, effective vaccines at the erythrocytic stage could greatly help minimize erythrocyte infection rate β_r.

Since the local sensitivity indices are relatively close, we carry out further investigation on parameter influence on disease progression by generating the partial rank correlation coefficients (PRCCs) for each parameter value in model R_0 in the following section.

4.1.1. Global Sensitivity Analysis. A global sensitivity analysis (GSA) is performed to examine the response of an epidemic model to parameter variation within a wider range of parameter space [45]. Applying the approach in [45], the PRCCs between the in-host basic reproduction number R_0 and each of the parameters in Table 2 are derived. Using 1000 simulations per run of the Latin Hypercube Sampling (LHS) scheme [46], the established PRCCs are derived and presented in Figure 2.

Unlike the results in Table 4, the model parameter with the highest influence on R_0 according to the PRCCs results shown in Figure 2 is the rate of invasion of red blood cells by merozoites, β_r. This is followed closely by the recruitment rate of susceptible red blood cells λ_r from the bone marrow. The second set of parameters that also increase (decrease) model R_0 when they are increased (decreased) are ζ, K, μ_3, and δ_z, respectively.

The merozoites' death rate δ_m, the death rate of IRBCs μ_4, and the rate of elimination of IRBCs by macrophages η are shown to have the highest negative influence on disease progression. Although an increase in μ_4 was shown to decrease disease progression in Table 4, the results from global sensitivity analysis are contradictory. An increase in the death rate of parasitized erythrocytes μ_4 decreases parasitemia and hence disease progression.

Based on these results of sensitivity analysis, we make the following remarks: (1) results of global sensitivity analysis are robust and a lot more realistic for implementation, (2) malaria control should target elimination of merozoites and infected red blood cells, (3) an effective and efficient malaria vaccine that deactivates infectious merozoites could be helpful in limiting erythrocyte invasion rate, and (4) a vaccine that is protective of susceptible erythrocytes could further ensure reduced density of second and future generation of merozoites that are responsible for disease progression.

4.2. Numerical Results. Model system (1) is solved numerically using the package scipy.integrate.odeint in Python language. The simulations are performed to illustrate the possible dynamics of the red blood cells, the malaria parasite, and macrophages. For purposes of these simulations, the initial conditions of the variables are hereby assumed. We note that different dynamics could be achieved for a different set of initial conditions.

For $R_0 < 1$ (see Figure 3), the density of susceptible hepatocyte initially declines as the density of infected hepatocytes rises due to invasion from sporozoites. The host's immune system responds to sporozoite invasion by increasing hepatocyte density that levels off at the disease-free equilibrium point $\mathscr{E}_0$ (see Figure 3(a)). As the sporozoites decline to near zero (see Figure 3(b)), infected hepatocytes decline and stabilize at $\mathscr{E}_0$ in (15).

At the blood stage, the rising density of infected erythrocytes declines in a similar fashion to that of the infective merozoites when $R_0 < 1$ (see Figure 3(c)). The densities of the infected erythrocytes and merozoites approach $\mathscr{E}_0$ asymptotically. On the other hand, we observe that the density of susceptible red blood cells initially diminishes due to infection by merozoites and later rises before it plateaus as shown in Figure 3(c).

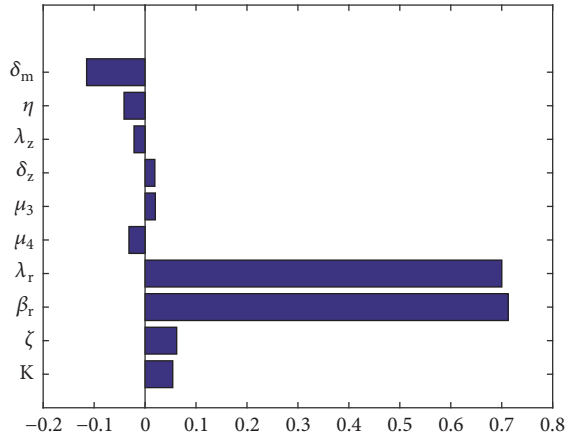

Figure 2: Tornado plots of PRCCs of parameters that influence model R_0 generated using parameter values in Table 3. Parameters with $PRCC > 0$ and $PRCC < 0$ increase and decrease model R_0, respectively.

When $R_0 > 1$, a sharp fall in the density of susceptible hepatocytes in the liver is observed (see Figure 4(a)). This is due to rapid invasion of hepatocytes by the sporozoites. An invasion on susceptible hepatocyte generates a corresponding steady rise in the density of infected hepatocytes (see Figure 4(b)). Owing to natural intervention by the immune system cells, the respective decline and rising levels of susceptible and infected hepatocytes level off and remain relatively constant after the third month. More liver cells are generated to replace infected ones. Figure 4(c) indicates a steady decline in sporozoite density at the liver stage during infections. Invaded hepatocytes burst open to produce merozoites instead of sporozoites and hence the steady decline in sporozoite levels.

Malaria infection dynamics are most rapid in the first 2 weeks within the host liver as illustrated in Figures 4(a), 4(b), and 4(c). This is similar to results in [22, 31]. In the absence of clinical intervention, some of the sporozoites may remain dormant in the human liver and could cause future malaria infections. As the liver schizonts release merozoites into host's blood stream, a rapid decline in the density of red blood cells is observed (see Figure 5(a)). However, the density of infected erythrocytes is noted to rise with equal proportion as shown in Figure 5(b).

An early sharp rise in the density of merozoites in the first one week of the blood stage is noted in Figure 5(c). The density remains high for several weeks and does not decline for the entire infection period of one month. A second-generation merozoite invades other sets of healthy erythrocytes within minutes, leading to an exponential growth in the density of blood schizonts and hence merozoites in the human blood. Without therapeutic intervention, the density of merozoites stabilizes several weeks after infection at the endemic equilibrium point. This is consistent with the findings in [19, 20, 23].

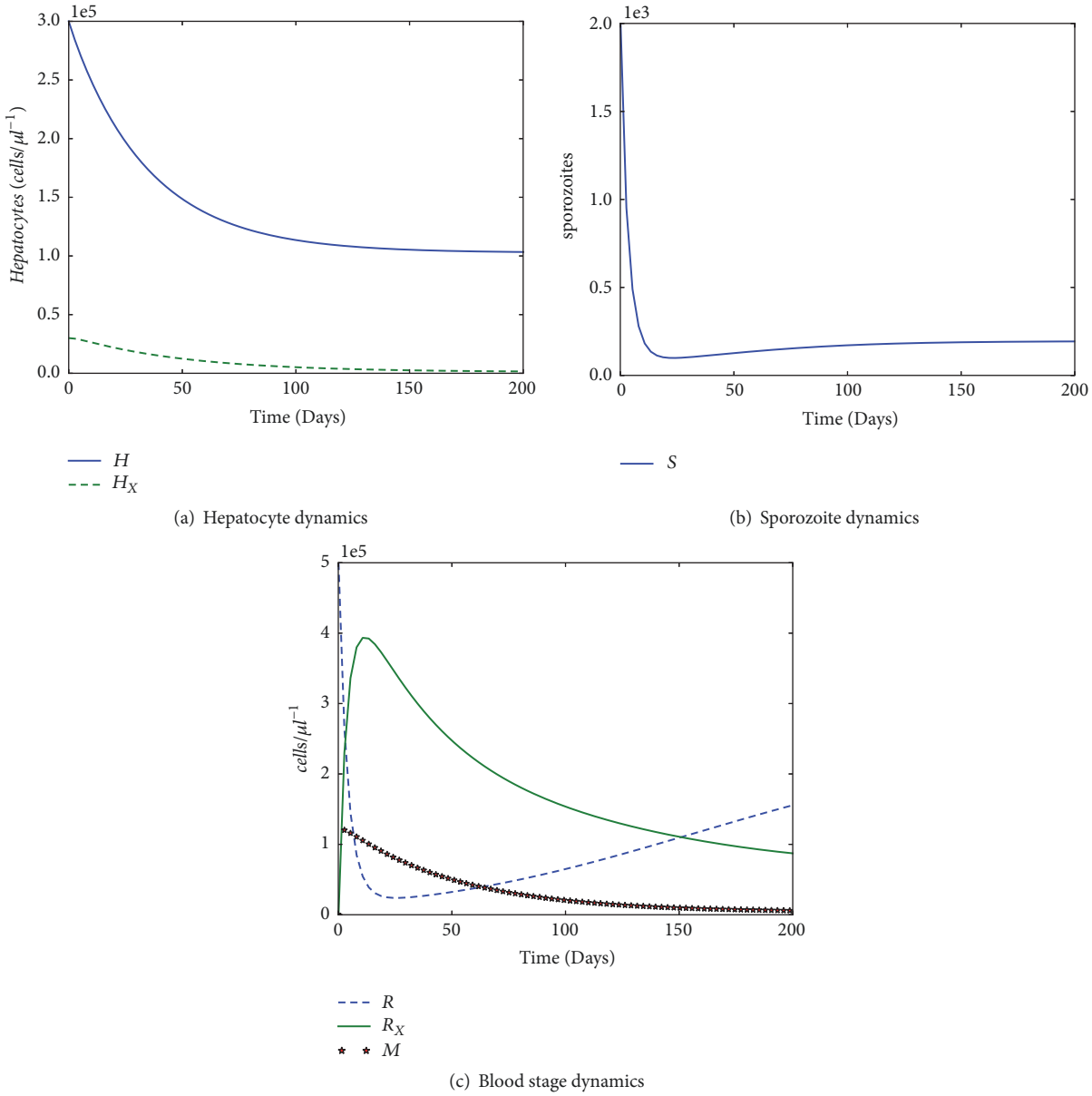

(a) Hepatocyte dynamics

(b) Sporozoite dynamics

(c) Blood stage dynamics

FIGURE 3: Graphs showing the simulation of in-host malaria model (1) when the model $R_0 = 0.22866 < 1$. Figures (a) and (b) show model dynamics at the liver stage. The chosen initial conditions are $H0 = 300000$, $H_X0 = 20000$, $R0 = 500000$, $R_X0 = 50$, $Z0 = 300000$, $S0 = 2000$, and $M = 70$. Used parameter values are given in Table 3.

The invasion of healthy erythrocytes prompts an immune response from host's macrophages. These macrophages phagocyte on the generated blood schizonts. At the onset of erythrocytic infection, several macrophages are generated. The rise in the density of macrophages is proportional to that of infected erythrocytes as shown in Figure 5(d). This rising density is shown to level off after about 16 days at the endemic equilibrium point. It remains high throughout the infection period.

From these discussions, we make the following observations: (1) if $R_0 < 1$, low level malaria infection can easily be contained by the host's defence mechanism and loss of life is less likely; (2) therapeutically, $R_0 < 1$ may be achieved through quick interventions targeting the blood schizonts and the merozoites responsible for secondary infections during the erythrocytic cycle; (3) Figures 4 and 5 prove the existence of malaria endemic equilibrium point.

Hematological parameters such as the density of healthy and infected erythrocytes in malaria hosts have considerable influence on malaria infection and possible impacts [47]. According to WHO [48], hyperparasitemia causes drastic reduction in concentrations of erythrocytes, leading to anaemia among malaria patients. The impacts of increasing the model parameters δ_m and β_r on healthy and infected red blood cells are as shown in Figures 6 and 7, respectively.

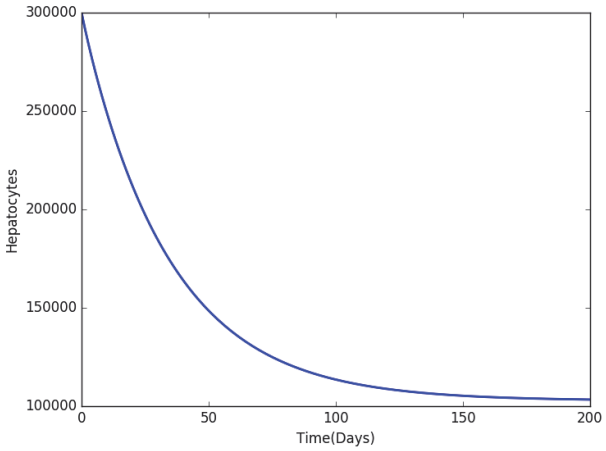

(a) Susceptible hepatocytes

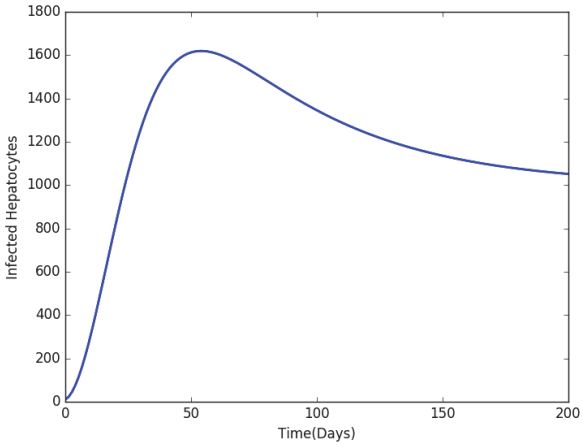

(b) Infected hepatocytes

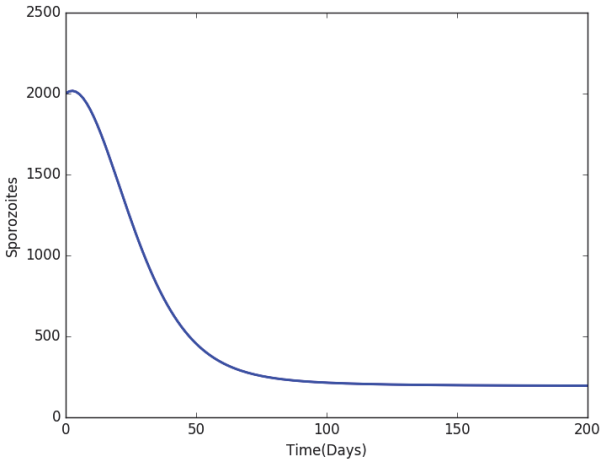

(c) Sporozoites

FIGURE 4: Graphs showing population dynamics of the liver hepatocytes and malaria sporozoites when $R_0 = 1.58690 > 1$. Used parameter values can be found in Table 3 with the chosen initial conditions described by $H0 = 300000$, $H_X0 = 10$, $R0 = 500000$, $R_X0 = 10$, $Z0 = 10$, $S0 = 2000$, and $M = 20$.

Observe that increased death rate of malaria merozoites δ_m decreases and increases the concentration of parasitized red blood cells and healthy red blood cells, respectively (see Figures 6(a) and 6(b)). Malaria control should thus target the infectious merozoites at the blood stage.

Results in Figure 7(a) indicate that an improved invasion rate by merozoites on susceptible red blood cells causes more loss in healthy erythrocytes. The reverse effect is observed in Figure 7(b), where an increase in the rate of infection of healthy erythrocytes produces a corresponding increase in the density of IRBCs. A keen look at Figure 7(b) reveals that the infected red blood cells begin to appear after about 10–15 days of initial infection. This is consistent with the incubation period of *Plasmodium falciparum* malaria [49].

The severity of malaria infection can easily increase if the density or production of macrophages is compromised [19]. Figure 8(b) shows a near direct relationship on the density of infected red blood cells R_X and the death rate of the macrophages δ_z. An increase in the death of macrophages would propel erythrocytic schizogony and hence increased merozoite numbers in the human blood. A high merozoite density increases the severity of malaria infection. This result is quite vital in malaria intervention, especially with respect to malaria patients who may be suffering from other infections that are deleterious to immune cells. Diseases such as HIV/AIDS greatly weaken the immune system of the patient as crucial immune cells such as macrophages are destroyed. Macrophages are important target cells for HIV-1 virus [50]. During malaria infections, such patients often suffer from severe malaria and should seek immediate medical attention.

Like the senescent red blood cells, aberrant infected erythrocytes formed during malaria infection are eliminated phagocytically by the host's macrophage cells in the red pulp of the spleen [51]. The phagocytic potential of the spleen is vital at the erythrocytic cycle. The higher the phagocytic behaviour of the macrophage, the lower the density of parasitized erythrocytes (see Figure 8(a)). The severity of

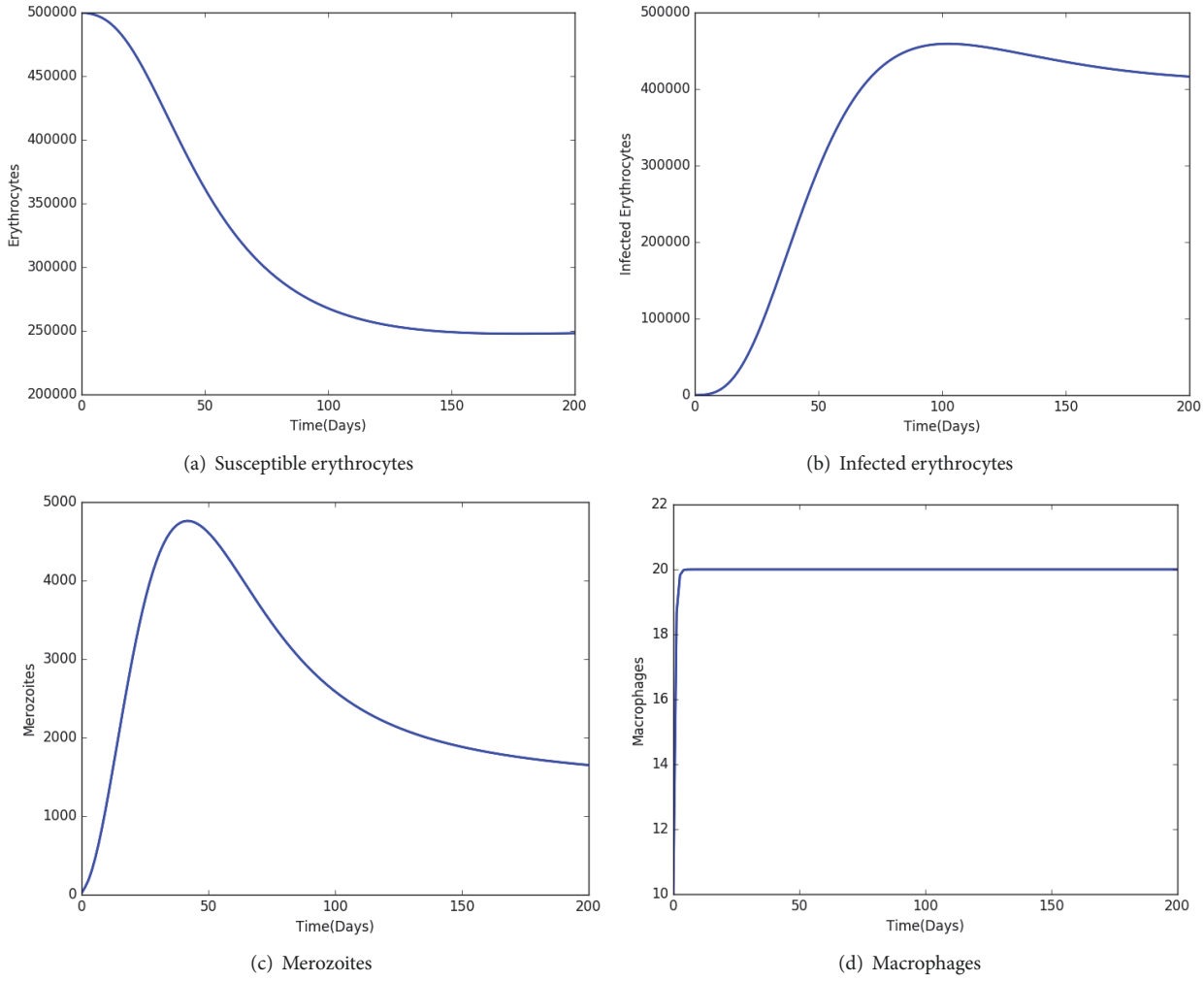

(a) Susceptible erythrocytes

(b) Infected erythrocytes

(c) Merozoites

(d) Macrophages

FIGURE 5: Graphs showing population dynamics of red blood cells, macrophages, and malaria merozoites when $R_0 = 1.58690 > 1$. Simulation parameter values are available in Table 3.

malaria infection increases with decreasing ability of the host's phagocytic merozoites to clear infected red blood cells from circulation during the erythrocytic cycle.

5. Conclusion and Discussion

In this paper, a mathematical model of in-host malaria infection in [21] is extended to include the liver stage of parasite development. Unlike the models in [19, 23, 30], we considered the macrophages as the most effective innate immune cells in eliminating malaria parasites from the human blood circulation. In addition, the liver hepatocytes are assumed to be generated from the bone marrow and through a process of self-regeneration from existing hepatocytes.

We proved that the formulated model is biologically and mathematically well posed in an invariant region Ω. The malaria-free equilibrium is shown to be locally asymptotically stable when the in-host reproduction number is less than unity. The global stability of the malaria-free state is only guaranteed if the threshold quantity R_0 is less than unity.

Our numerical results show that intervention during malaria infection should focus on minimizing merozoite invasion rate on healthy erythrocytes and the density of merozoites in circulation, which are responsible for secondary invasion at the blood stage. In the absence of malaria treatment, the immune cells (macrophages) are shown to be vital in eliminating infected red blood cells at the blood stage. The higher the rate of phagocytosis of infected erythrocytes by macrophages, the lower the density of infected red blood cells and hence malaria parasitemia. Patients suffering from such infections as HIV/AIDS and TB that have deleterious effect on the protective immune cells should seek immediate medical treatment when infected with malaria. Their compromised immune system exposes them to severe malaria attacks and possible untimely death.

For quick and timely reduction of parasitemia, an increased merozoite death rate using antimalarial drugs such as ACT would be necessary. This would further ensure reduced density of infected red blood cells and hence future generation merozoites. By killing a single blood schizont,

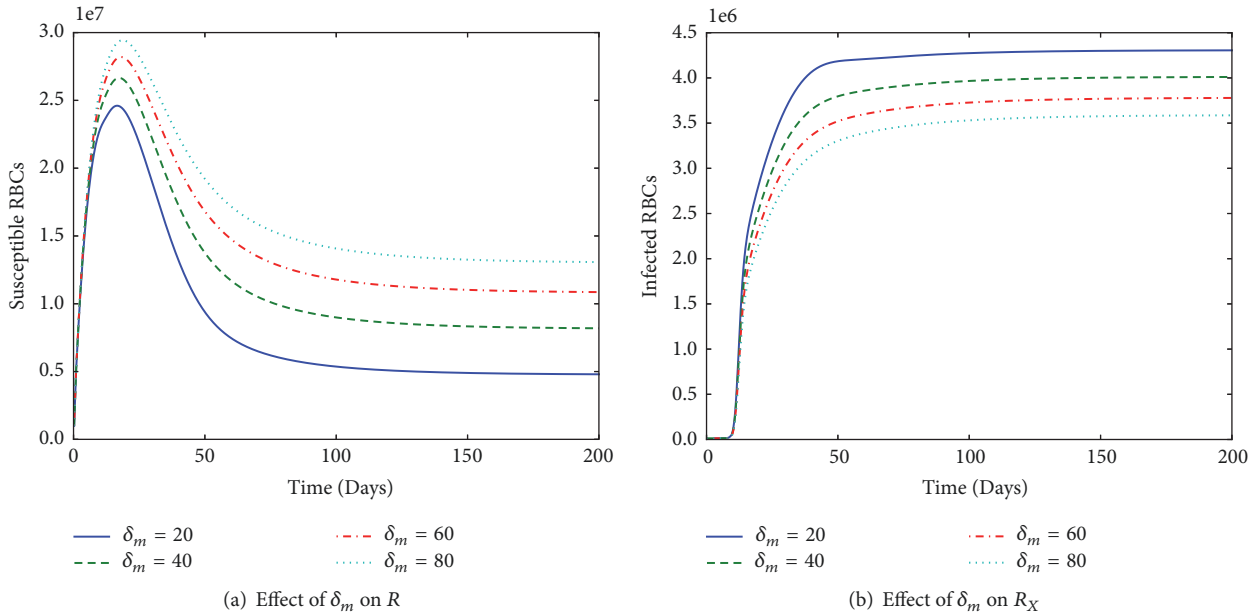

(a) Effect of δ_m on R (b) Effect of δ_m on R_X

FIGURE 6: Graphs showing the behaviour of (a) susceptible RBCs and (b) infected RBCs. They were obtained by varying the death rate of merozoites δ_m from 20 to 80 in steps of 20, while keeping the other parameters (see Table 3) constant.

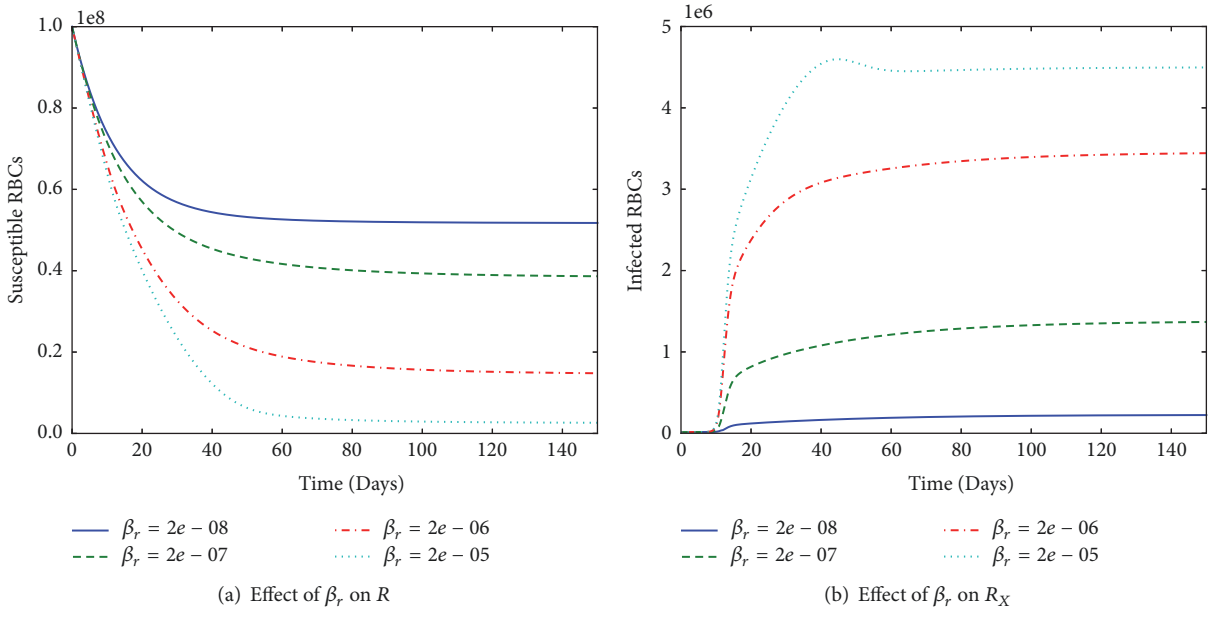

(a) Effect of β_r on R (b) Effect of β_r on R_X

FIGURE 7: Graphs showing the behaviour of (a) susceptible RBCs and (b) infected RBCs. They were obtained by varying the merozoite invasion rate β_r from 2×10^{-8} to 2×10^{-5} in steps of 10^{-1}, while keeping the other parameters in Table 3 constant.

we are likely to avoid the production of sixteen merozoites at maturity. Moreover, an appropriate vaccine that targets erythrocyte invasion process may equally guarantee minimal erythropoiesis. The erythrocyte invasion-avoidance vaccine would minimize the density of infected erythrocytes and hence malaria disease severity. This intervention could help terminate the erythrocytic schizont, leading to minimal parasite transmission to mosquito vector for further development and sexual reproduction.

In this study, drug resistance was not analyzed; this can be considered as a potential area for future investigation.

Conflicts of Interest

The authors declare that there are no conflicts of interest regarding the publication of this article.

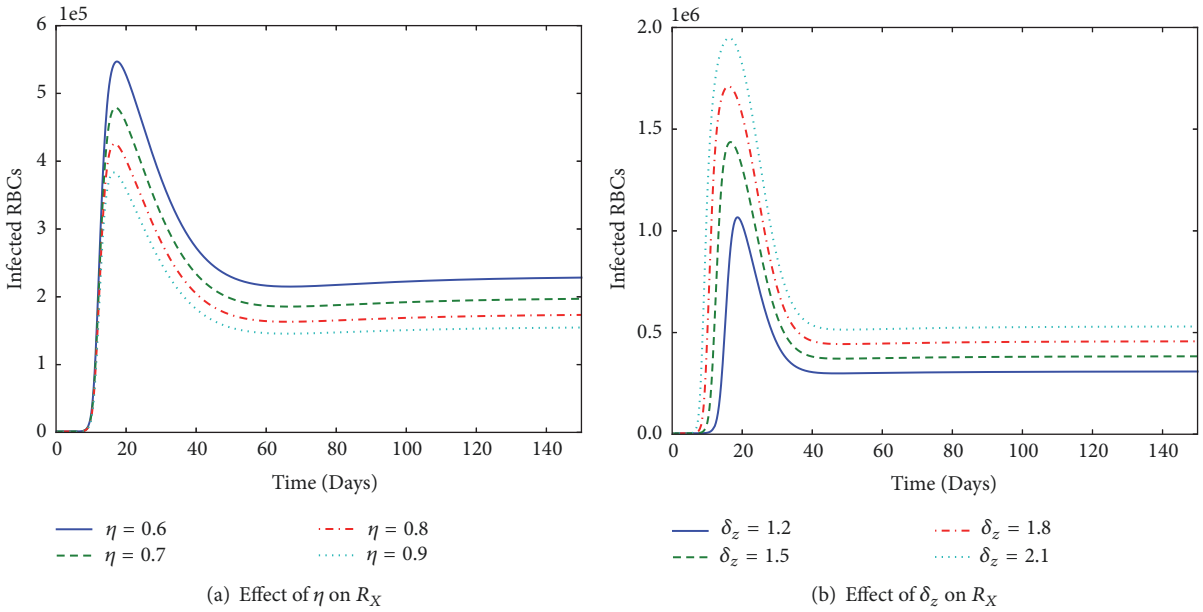

(a) Effect of η on R_X

(b) Effect of δ_z on R_X

FIGURE 8: Graphs showing the effect of varying the rate of phagocytosis of IRBCs by macrophages, η (in (a)), and the effect of increased decay rate of macrophages, δ_z (in (b)), on the behaviour of infected erythrocytes R_X. All parameter values are in Table 3.

Acknowledgments

The authors acknowledge with gratitude the support from the Institute of Mathematical Sciences, Strathmore University, and the National Research Fund (NRF), Kenya, for the production of this manuscript.

References

[1] WHO, *Global Health Observatory (GHO) data: Malaria*, 2017, http://www.who.int/gho/malaria/en/.

[2] WHO, "Fact sheet: World malaria report 2016," http://www.who.int/malaria/media/world-malaria-report-2016/en/.

[3] WHO, "Fact sheet: Malaria," http://www.who.int/mediacentre/factsheets/fs094/en/.

[4] WHO., "Achieving the malaria MDG target: Reversing the incidence of malaria 2000-2015," http://www.who.int/malaria/publications/atoz/9789241509442/en/.

[5] K. Mendis, B. J. Sina, P. Marchesini, and R. Carter, "The neglected burden of *Plasmodium vivax* malaria," *The American Journal of Tropical Medicine and Hygiene*, vol. 64, no. 1-2, supplement, pp. 97–106, 2001.

[6] N. T. Bailey, *The biomathematics of malaria*, Charles Griffin, 1982.

[7] M. M. Mota, G. Pradel, J. P. Vanderberg et al., "Migration of Plasmodium sporozoites through cells before infection," *Science*, vol. 291, no. 5501, pp. 141–144, 2001.

[8] A. M. Vaughan, A. S. I. Aly, and S. H. I. Kappe, "Malaria Parasite Pre-Erythrocytic Stage Infection: Gliding and Hiding," *Cell Host & Microbe*, vol. 4, no. 3, pp. 209–218, 2008.

[9] M. F. Good, H. Xu, M. Wykes, and C. R. Engwerda, "Development and regulation of cell-mediated immune responses to the blood stages of malaria: implications for vaccine research," *Annual Review of Immunology*, vol. 23, pp. 69–99, 2005.

[10] H. H. Diebner, M. Eichner, L. Molineaux, W. E. Collins, G. M. Jeffery, and K. Dietz, "Modelling the transition of asexual blood stages of Plasmodium falciparum to gametocytes," *Journal of Theoretical Biology*, vol. 202, no. 2, pp. 113–127, 2000.

[11] C. Chiyaka, "Using mathematics to understand malaria infection during erythrocytic stages," *NuSpace Institutional Repository*, 2010.

[12] S. H. I. Kappe, K. Kaiser, and K. Matuschewski, "The Plasmodium sporozoite journey: A rite of passage," *Trends in Parasitology*, vol. 19, no. 3, pp. 135–143, 2003.

[13] L. H. Miller, D. I. Baruch, K. Marsh, and O. K. Doumbo, "The pathogenic basis of malaria," *Nature*, vol. 415, no. 6872, pp. 673–679, 2002.

[14] A. D. Augustine, B. F. Hall, W. W. Leitner, A. X. Mo, T. M. Wali, and A. S. Fauci, "NIAID workshop on immunity to malaria: Addressing immunological challenges," *Nature Immunology*, vol. 10, no. 7, pp. 673–678, 2009.

[15] Q. Chen, A. Amaladoss, W. Ye et al., "Human natural killer cells control Plasmodium falciparum infection by eliminating infected red blood cells," *Proceedings of the National Acadamy of Sciences of the United States of America*, vol. 111, no. 4, pp. 1479–1484, 2014.

[16] B. S. Franklin, P. Parroche, M. A. Ataíde et al., "Malaria primes the innate immune response due to interferon-γ induced enhancement of toll-like receptor expression and function," *Proceedings of the National Acadamy of Sciences of the United States of America*, vol. 106, no. 14, pp. 5789–5794, 2009.

[17] D. Z. de Back, E. B. Kostova, M. van Kraaij, T. K. van den Berg, and R. van Bruggen, "Of macrophages and red blood cells; A complex love story," *Frontiers in Physiology*, vol. 5, article 9, 2014.

[18] K. Chotivanich, R. Udomsangpetch, R. McGready et al., "Central role of the spleen in malaria parasite clearance," *The Journal of Infectious Diseases*, vol. 185, no. 10, pp. 1538–1541, 2002.

[19] C. Chiyaka, W. Garira, and S. Dube, "Modelling immune response and drug therapy in human malaria infection," *Computational and Mathematical Methods in Medicine. An Interdisciplinary Journal of Mathematical, Theoretical and Clinical Aspects of Medicine*, vol. 9, no. 2, pp. 143–163, 2008.

[20] M. A. Selemani, L. S. Luboobi, and Y. Nkansah-Gyekye, "On stability of the in-human host and in-mosquito dynamics of malaria parasite," *Asian Journal of Mathematics and Applications*, 2016.

[21] J. Tumwiine, J. Y. Mugisha, and L. S. Luboobi, "On global stability of the intra-host dynamics of malaria and the immune system," *Journal of Mathematical Analysis and Applications*, vol. 341, no. 2, pp. 855–869, 2008.

[22] M. A. Selemani, L. S. Luboobi, and Y. Nkansah-Gyekye, "The in-human host and in-mosquito dynamics of malaria parasites with immune responses," *New Trends in Mathematical Sciences*, vol. 5, no. 3, pp. 182–207, 2017.

[23] Y. Li, S. Ruan, and D. Xiao, "The within-host dynamics of malaria infection with immune response," *Mathematical Biosciences and Engineering*, vol. 8, no. 4, pp. 999–1018, 2011.

[24] A. M. Talman, O. Domarle, F. E. McKenzie, F. Ariey, and V. Robert, "Gametocytogenesis: the puberty of *Plasmodium falciparum*," *Malaria Journal*, vol. 3, article 24, 2004.

[25] R. M. Anderson, R. M. May, and S. Gupta, "Non-linear phenomena in host-parasite interactions," *Parasitology*, vol. 99, pp. S59–S79, 1989.

[26] B. Hellriegel, "Modelling the immune response to malaria with ecological concepts: Short-term behaviour against long-term equilibrium," *Proceedings of the Royal Society B Biological Science*, vol. 250, no. 1329, pp. 249–256, 1992.

[27] J. Swinton, "The dynamics of blood-stage malaria: Modelling strain specific and strain transcending immunity. Models for Infectious Human Diseases," in *Their Structure and Relation to Data*, V. Isham and and G. Medley, Eds., pp. 210–212, Cambridge University Press, Cambridge, UK, 1996.

[28] A. M. Dondorp, S. Yeung, L. White et al., "Artemisinin resistance: current status and scenarios for containment," *Nature Reviews Microbiology*, vol. 8, no. 4, pp. 272–280, 2010.

[29] N. J. White, "Antimalarial drug resistance," *The Journal of Clinical Investigation*, vol. 113, no. 8, pp. 1084–1092, 2004.

[30] J. Tumwiine, S. D. Hove-Musekwa, and F. Nyabadza, "A Mathematical Model for the Transmission and Spread of Drug Sensitive and Resistant Malaria Strains within a Human Population," *ISRN biomathematics*, vol. 2014, Article ID 636973, pp. 1–12, 2014.

[31] Z. Tabo, L. S. Luboobi, and J. Ssebuliba, "Mathematical modelling of the in-host dynamics of malaria and the effects of treatment," *Journal of Mathematics and Computer Science*, vol. 17, no. 1, pp. 1–21, 2017.

[32] C. A. W. Bate, J. Taverne, and J. H. L. Playfair, "Malarial parasites induce TNF production by macrophages," *The Journal of Immunology*, vol. 64, no. 2, pp. 227–231, 1988.

[33] M. M. Elloso, H. C. Van Der Heyde, J. A. Vande Waa, D. D. Manning, and W. P. Weidanz, "Inhibition of Plasmodium falciparum in vitro by human $\gamma\delta$ T cells," *The Journal of Immunology*, vol. 153, no. 3, pp. 1187–1194, 1994.

[34] V. V. Ganusov, C. T. Bergstrom, and R. Antia, "Within-host population dynamics and the evolution of microparasites in a heterogeneous host population," *Evolution*, vol. 56, no. 2, pp. 213–223, 2002.

[35] I. M. Rouzine and F. E. McKenzie, "Link between immune response and parasite synchronization in malaria," *Proceedings of the National Acadamy of Sciences of the United States of America*, vol. 100, no. 6, pp. 3473–3478, 2003.

[36] N. J. White et al., "Malaria pathophysiology," *Malaria, parasite biology, pathogenesis and protection*, pp. 371–385, 1998.

[37] N. Fausto, J. S. Campbell, and K. J. Riehle, "Liver regeneration," *Hepatology*, vol. 43, no. 2, pp. S45–S53, 2006.

[38] N. Fausto, "Liver regeneration and repair: hepatocytes, progenitor cells, and stem cells," *Hepatology*, vol. 39, no. 6, pp. 1477–1487, 2004.

[39] J. Crutcher and S. Hoffman, *Malaria. Medical Microbiology*, University of Texas Medical Branch at Galveston, 4th edition, 1996.

[40] S. N. Wickramasinghe and S. H. Abdalla, "Blood and bone marrow changes in malaria," *Baillieres Best Practice and Research in Clinical Haematology*, vol. 13, no. 2, pp. 277–299, 2000.

[41] P. van den Driessche and J. Watmough, "Reproduction numbers and sub-threshold endemic equilibria for compartmental models of disease transmission," *Mathematical Biosciences*, vol. 180, pp. 29–48, 2002.

[42] J. C. Kamgang and G. Sallet, "Global asymptotic stability for the disease free equilibrium for epidemiological models," *Comptes Rendus Mathématique. Académie des Sciences. Paris*, vol. 341, no. 7, pp. 433–438, 2005.

[43] N. Chitnis, J. M. Hyman, and J. M. Cushing, "Determining important parameters in the spread of malaria through the sensitivity analysis of a mathematical model," *Bulletin of Mathematical Biology*, vol. 70, no. 5, pp. 1272–1296, 2008.

[44] L. Arriola and J. Hyman, "Lecture notes, forward and adjoint sensitivity analysis: with applications in dynamical systems," *Linear Algebra and Optimisation Mathematical and Theoretical Biology Institute*, 2005.

[45] J. Wu, R. Dhingra, M. Gambhir, and J. V. Remais, "Sensitivity analysis of infectious disease models: Methods, advances and their application," *Journal of the Royal Society Interface*, vol. 10, no. 86, article 1018, 2013.

[46] M. Stein, "Large sample properties of simulations using Latin hypercube sampling," *Technometrics. A Journal of Statistics for the Physical, Chemical and Engineering Sciences*, vol. 29, no. 2, pp. 143–151, 1987.

[47] L. M. Erhart, K. Yingyuen, N. Chuanak et al., "Hematologic and clinical indices of malaria in a semi-immune population of Western Thailand," *The American Journal of Tropical Medicine and Hygiene*, vol. 70, no. 1, pp. 8–14, 2004.

[48] WHO, "Severe and complicated malaria," *Transactions of the Royal Society of Tropical Medicine and Hygiene*, vol. 84, pp. 1–65, 1990.

[49] W. E. Collins and G. M. Jeffery, "Plasmodium malariae: Parasite and disease," *Clinical Microbiology Reviews*, vol. 20, no. 4, pp. 579–592, 2007.

[50] T. Shiri, W. Garira, and S. D. Musekwa, "A two-strain HIV-1 mathematical model to assess the effects of chemotherapy on disease parameters," *Mathematical Biosciences and Engineering*, vol. 2, no. 4, pp. 811–832, 2005.

[51] J. Krücken, L. I. Mehnert, M. A. Dkhil et al., "Massive destruction of malaria-parasitized red blood cells despite spleen closure," *Infection and Immunity*, vol. 73, no. 10, pp. 6390–6398, 2005.

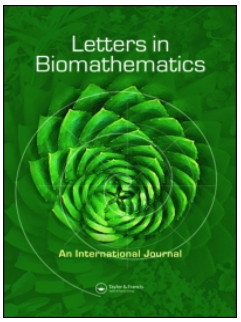

Letters in Biomathematics

ISSN: (Print) 2373-7867 (Online) Journal homepage: https://www.tandfonline.com/loi/tlib20

Mathematical model for the in-host malaria dynamics subject to malaria vaccines

Titus Okello Orwa, Rachel Waema Mbogo & Livingstone Serwadda Luboobi

To cite this article: Titus Okello Orwa, Rachel Waema Mbogo & Livingstone Serwadda Luboobi (2018) Mathematical model for the in-host malaria dynamics subject to malaria vaccines, Letters in Biomathematics, 5:1, 222-251, DOI: 10.1080/23737867.2018.1526132

To link to this article: https://doi.org/10.1080/23737867.2018.1526132

Published online: 29 Sep 2018.

LETTERS IN BIOMATHEMATICS
2018, VOL. 5, NO. 1, 222–251
https://doi.org/10.1080/23737867.2018.1526132

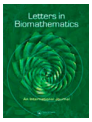

Taylor & Francis
Taylor & Francis Group

OPEN ACCESS Check for updates

Mathematical model for the in-host malaria dynamics subject to malaria vaccines

Titus Okello Orwa, Rachel Waema Mbogo and Livingstone Serwadda Luboobi

Institute of Mathematical Sciences, Strathmore University, Nairobi, Kenya

ABSTRACT

Despite the success of the existing malaria control strategies, reported malaria cases are still quite high. In 2016, the WHO reported about 216 million malaria cases; 90% of which occurred in the WHO African Region. In this paper, a mathematical model for the in-host *Plasmodium falciparum* malaria subject to malaria vaccines is formulated and analysed. An efficacious pre-erythrocytic vaccine is shown to greatly reduce the severity of clinical malaria. Based on the normalized forward sensitivity index technique, the average number of merozoites released per bursting blood schizont is shown to be the most sensitive parameter in the model. Numerical simulation results further suggest that an efficacious blood stage vaccine has the potential to reduce the burst size of the blood schizonts and maximize the rate of activation of CD8+ T cells during malaria infection. Moreover, vaccine combinations that are efficacious might help in achieving a malaria free population by the year 2030. This paper provides useful insights in malaria vaccine control and a unique opportunity to intensify support and funding for malaria vaccine development.

ARTICLE HISTORY
Received 22 June 2018
Accepted 14 September 2018

KEYWORDS
Malaria vaccines; vaccine efficacy; hepatocytes; CD8+ T cells; red blood cells; *Plasmodium falciparum*

1. Introduction

To date, the World Health Organization (WHO) considers effective vector control strategies such as long-lasting insecticidal nets (ITNs) and indoor residual spraying (IRS) as the main ways to prevent and reduce malaria transmission in communities with high malaria prevalence (Homan, 2016; WHO, 2017a). In addition, chemoprophylaxis and antimalarial drugs such as chloroquine and artemisinin-based combination therapy (ACT) are currently used to prevent and treat clinical malaria, respectively, in different parts of the world (Bhatt et al., 2015; WHO, 2015). These strategies have contributed to the substantial global decline in malaria mortality and morbidity (Negal, Alemu, & Tasew, 2016). However, despite the success of the existing malaria prevention and control strategies, reported malaria cases are still quite high. In 2016, the WHO reported about 216 million malaria cases; 90% of which occurred in the WHO African Region (WHO, 2017b). This represented an increase of 5 million malaria cases from the year 2015.

CONTACT Titus Okello Orwa torwa@strathmore.edu. Institute of Mathematical Sciences, Strathmore University, P.O. Box 59857-00200, Nairobi, Kenya

Malaria is a mosquito-borne infectious disease caused by an intracellular protozoan parasite of the genus *Plasmodium* (Liehl et al., 2015; Risco-Castillo et al., 2015). *Plasmodium falciparum* is the deadliest (Derbyshire, Mota, & Clardy, 2011) and predominant malaria parasite in sub-Saharan African and was responsible for 99% of all malaria cases in 2016 (WHO, 2017b). While probing for blood, female Anopheles mosquito inoculates sporozoites into the human dermis. The deposited parasites rapidly migrate to the liver, where they invade the hepatocytes with the formation of protective parasitophorous vacuole (Bertolino & Bowen, 2015; Ishino, Yano, Chinzei, & Yuda, 2004; Mota et al., 2001). During this pre-erythrocytic stage, the sporozoites undergo rapid asexual reproduction (White et al., 2014; White, 2017), develop and differentiate asymptomatically into thousands of erythrocytic forms called merozoites (Sturm et al., 2006). The cyclical erythrocytic stage begins when infected hepatocytes burst open, releasing infective-merozoites into the blood stream (Haldar, Murphy, Milner, & Taylor, 2007). The released merozoites quickly invade susceptible red blood cells leading to the formation of infected red blood cells (IRB) cells. The waves of bursting erythrocytes and invasions of fresh erythrocytes by secondary merozoites produce malaria characteristic symptoms such as chills and headache (Derbyshire et al., 2011). Some merozoites develop into sexual forms called gametocytes that are later sucked up by feeding mosquitoes for sexual reproduction and development within the mosquito gut (sporogonic stage). If left untreated, malaria patients may develop severe symptoms and progress to coma or death.

Parasite resistance to current antimalarial drugs (Dondorp et al., 2010; Maude et al., 2009; Sidhu, Verdier-Pinard, & Fidock, 2002; Wellems & Plowe, 2001) and vector insecticides (Alout, Labbé, Chandre, & Cohuet, 2017a; Alout, Roche, Dabiré, & Cohuet, 2017b; Soko, Chimbari, & Mukaratirwa, 2015) poses a serious threat to malaria control. To defeat the disease, many more tools with the potential to save lives today and in the future are needed (Birkett, 2016; Greenwood & Targett, 2009; MVI, 2018). An efficacious, safe and affordable malaria vaccine would help to bridge the control gap left by other intervention measures (MVI, 2018).

A malaria vaccination strategy is performed to either induce protective immune responses prior to malaria infection or to provide protection in case of malaria attack (Arama & Troye-Blomberg, 2014). Current malaria vaccines have shown minimal efficacy (Birkett, 2016; Birkett, Moorthy, Loucq, Chitnis, & Kaslow, 2013; Miura, 2016). In the completed phase III clinical testing, RTS,S/AS01 (which is the most advanced malaria vaccine to date) showed 36.3% vaccine efficacy in children and 25.9% in infants (Birkett, 2016; Miura, 2016). Although the results of phase 3 trials are promising, a more efficacious malaria vaccine is crucial if the 2030 goal of malaria eradication by WHO is to be accomplished (malERA Consultative Group on Vaccines et al., 2011).

Although there is no licensed vaccine against malaria today, many experts believe that a malaria vaccine is a necessary tool for successful malaria elimination (MVFG, 2018; Ouattara & Laurens, 2014). There are three categories of malaria vaccine candidates: pre-erythrocytic vaccines (PEV), blood stage vaccines (BSV) and transmission blocking vaccines (TBV) that target the parasite at different stages of its life cycle (see Figure 1). PEV are designed to prevent malaria infections in humans by inducing antibodies that block invasion of hepatocytes by sporozoites and/or cell-mediated immune responses that target infected hepatocytes (Duffy, Sahu, Akue, Milman, & Anderson, 2012). In this respect, PEVs

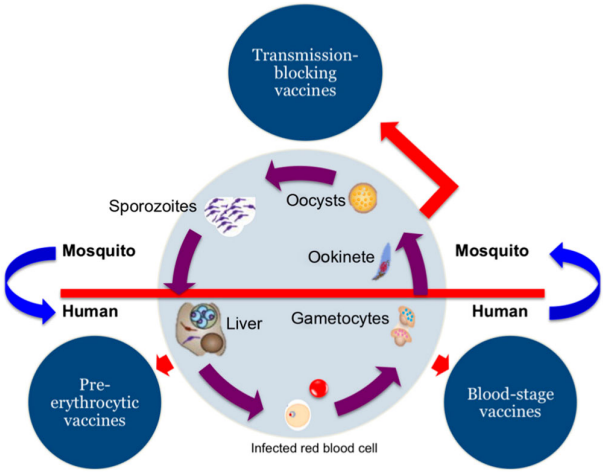

Figure 1. Target sites in the malaria life cycle that could be interrupted by pre-erythrocytic, blood-stage and transmission-blocking vaccines. Source: Arama and Troye-Blomberg (2014).

target malaria sporozoites thereby interrupting the life cycle of malaria parasite at an early stage (March et al., 2013). Several clinical trials (Abdulla et al., 2008; Alonso et al., 2004; Bojang et al., 2001; Polhemus et al., 2009) and (RTS, S. C. T. P., 2011) have shown the potential of RTS,S to prevent malaria infection and clinical disease in infants and young children living in sub-Saharan Africa (Birkett, 2016; Miura, 2016; RTS, S. C. T. P., 2012). PEV may also induce protection against clinical malaria at the blood stage by temporarily reducing the number of merozoites that emerge from the bursting infected liver cells (Alonso et al., 2004).

BSV on the other hand elicits anti-invasion and anti-disease responses at the blood stage (Moorthy, Good, & Hill, 2004). They, therefore, lower merozoites density and prevent clinical manifestations and hence severity of malaria infection in humans. Due to gene alteration and antigenic variation in malaria merozoites, BSV may not provide complete immunity to the host (Pandey et al., 2013). At present, merozoite surface protein 3 (MSP3) (Audran et al., 2005) and merozoite surface protein 1 (MSP1) (Ogutu et al., 2009) are the leading blood stage vaccine candidates for plasmodium malaria (Plowe, Alonso, & Hoffman, 2009).

The aim of TBV is to stop subsequent generation of infectious malaria sporozoites from the female anopheles mosquito vector. TBV induces antibodies against antigens on gametes, zygote and ookinetes, blocking ookinete to oocyst transition and hence stopping parasite development within the mosquito midgut (Carter, Mendis, Miller, Molineaux, & Saul, 2000). Consequently, the density of malaria sporozoites in the mosquito salivary glands is decreased. The leading malaria vaccine candidate in this category is the *Plasmodium falciparum* ookinete surface antigens (Pfs25) (Arevalo-Herrera et al., 2005; Hisaeda et al., 2000).

Due to intracellular infections, *P. falciparum* parasites are susceptible to immune-mediated control by CD8+ T cells, which target intracellular pathogens (Villarino, 2013). The CD8+ T cells have both direct and indirect effector pathways for parasite elimination

at the liver stage. The indirect mechanism includes the production of IFN-γ and TNF, whereas the direct mechanism involves the release of perforin and granzymes (Nganou-Makamdop, van Gemert, Arens, Hermsen, & Sauerwein, 2012). IFN-γ suppresses parasite development through direct impairment of parasite differentiation in hepatocytes (Mellouk et al., 1987). Moreover, IFN-γ increases the expression of nitric oxide synthase which leads to subsequent increase in nitric oxide that confers protection against *P. falciparum* (Seguin et al., 1994). Although CD8+ T cells are sufficiently primed during blood stage malaria, they offer very minimal contribution to protective immunity. It is thought in Villarino (2013) that vascular endothelial cells that acquire antigen from IRBCs stimulate CD8+ T cells to release perforin and granzyme B during blood stage malaria. The capacity of CD8+ T cells to eradicate malaria parasites and infected cells both at the liver stage and at the blood stage is therefore considered in this paper.

A lot of research has been carried on clinical malaria control (Austin, White, & Anderson, 1998; Hellriegel, 1992; Kamangira, Nyamugure, & Magombedze, 2014; Li, Ruan, & Xiao, 2011; Tumwiine, Hove-Musekwa, & Nyabadza, 2014). Some of these models have focussed on the role of the host's immune cells (Malaguarnera & Musumeci, 2002; Tumwiine et al., 2014) while others are based on the use of antimalarial drugs (Kamangira et al., 2014; Magombedze, Chiyaka, & Mukandavire, 2011) in controlling clinical malaria. In Chiyaka, Garira, and Dube (2008), both the immune cells and malaria chemotherapy controls are considered. In Rouzine and McKenzie (2003), the role of innate immunity in mediating synchronization between the replication cycles of parasites in different erythrocytes is explored. Kamangira et al. (2014) investigated erythrocytes–malaria parasite dynamics in the presence of immune response and/or drug intervention at the erythrocytic stage. Results in Nannyonga, Mwanga, Haario, Mbalawata, and Heilio (2014) showed that malaria merozoites can be absorbed in already IRB cells, leading to faster rapture of IRB cells and hence causing anaemia. Tabo, Luboobi, and Ssebuliba (2017) incorporated the liver stage in their model and investigated treatment as a control strategy for blood stage malaria. Results from their study showed that a treatment strategy using highly effective drugs targeting specific parameters can reduce malaria progression and control the disease in humans. The above research activities have been very insightful in understanding in-host malaria dynamics and control, however, none of these investigations has attempted to evaluate the possible impacts of malaria vaccines in controlling clinical *P. falciparum* malaria both at the liver stage and at the blood stage. In this study, we formulate a more detailed in-host malaria model that considers parasite–cell interactions at the liver stage and the blood stage subject to malaria vaccines. Our goals are to study the interacting cell-parasite populations through a mathematical model and to numerically investigate the possible impacts of malaria vaccines on the severity of *P. falciparum* malaria infection.

The rest of the paper is organized as follows. In the following section, we incorporate vaccination control to a formulated in-host malaria model and describe the corresponding model parameters and variables. The vaccine model is analysed and its vaccine reproductive number together with parameter sensitivity analysis is computed in Section 3. In Section 4, we investigate the effects of malaria vaccines and vaccine efficacy on malaria dynamics and malaria severity. A discussion and conclusion complete the paper in Sections 5 and 6, respectively.

2. Model formulation

We present a mathematical model of in-host *P. falciparum* malaria dynamics in the presence of malaria vaccines. The compartmental model is an extension of the hepatocytic–erythrocytic in-host malaria model in Orwa, Mbogo, and Luboobi (2018) in which two compartments of gametocytes $G(t)$ and CD8+ T cells $W(t)$ are added to capture the effects of the transmission blocking vaccines and the general effects of CD8+ T cells on the density of the IRB cells and hence malaria infection dynamics. The rest of the populations include susceptible liver hepatocytes $H(t)$, infected liver hepatocytes $X(t)$, malaria sporozoites $S(t)$, susceptible red blood cells $R(t)$, infected red blood cells (blood trophozoites) $T(t)$, infected red blood cells (blood schizonts) $C(t)$ and malaria merozoites $M(t)$.

During feeding, infected mosquito injects Λ sporozoites into the human skin. These sporozoites traverse Kupffer and endothelial cells and enter the liver hepatocytes. Susceptible liver hepatocytes are recruited by self-replication at a rate λ_h. Following invasion by sporozoites at the rate β_s, infected hepatocytes X progress to hepatic-schizont which eventual burst open at the rate μ_x to release merozoites into the blood stream. The initial recruitment of the merozoites is hence represented by the term $N\mu_x X$, where N is the number of merozoites released per bursting infected hepatocyte. The released merozoites invade and infect the host's red blood cells at a rate β_r and die naturally at the rate μ_m.

Based on their stage of infection, we classify IRB cells as either blood trophozoites (early stage of infection) or blood schizonts (late stage of infection). Susceptible RBCs are recruited at a constant rate λ_r from the bone marrow and their concentration decreases through natural death at the rate μ_r or due to invasion by the merozoites at the rate β_r. Following merozoite invasion, susceptible RBCs move to the class of infected red blood cells (blood trophozoites) T. The generated blood trophozoites decay naturally at a rate μ_t or progress into blood schozonts C class at the rate γ. Mature blood schizonts burst open to release more merozoites into blood stream. This is represented by the term $(P\mu_c C/1 + dW)$, where P denotes the number of merozoites released per bursting blood schizont and μ_c is the decay rate of the blood schizonts.

At the pre-erythrocytic stage, the malaria sporozoites are debilitated by vaccine-induced anti-CSP antibodies (PEV) as they molt through the tissues (Mellouk et al., 1990; Schwenk et al., 2003). This reduced invasion of hepatocytes by the malaria sporozoites is represented by the term $\beta_s(1-\nu)SH$, where $0 < \nu < 1$ is the efficacy of the pre-erythrocytic vaccine. Sporozoites that successfully invade the hepatocytes are, however, targeted by vaccine-induced CSP-specific CD8+ T cells (PEV). The CD8+ T cells kill the resulting infected hepatocyte (Renia et al., 1991; Sun et al., 2003; White et al., 2013). The killing of infected hepatocytes reduces the burst size N of the infected hepatocytes. This is represented by the term $(1-b)N$, where $0 < b < 1$ is the probability with which the vaccine inhibits merozoite emergence from infected hepatocyte.

An unbounded bilinear function rEI is considered in Anderson, May, and Gupta (1989), Niger and Gumel (2011) and Hetzel and Anderson (1996) to model the killing of infected cells I by the CD8+ T cells E. The simple mass-action term depends solely on the product of the concentration of the immune cells and the density of the infected cells. However, if we take into account the fact that cell proliferation can saturate then the nonlinear bounded

Michaelis–Menten–Monod function, presented in Equation (1) is most reasonable (Agur, Abiri, & Van der Ploeg, 1989; Antia, Levin, & May, 1994).

$$\nabla = \nabla_{\max} \frac{B}{K_b + B}, \tag{1}$$

where B is the concentration of substrate, ∇ is the growth rate of the microorganisms B, $\nabla_{\max}$ is the maximum specific growth rate of B and K_b is the half-velocity constant, $\nabla/\nabla_{\max}$.

In Pilyugin and Antia (2000), the nonlinear bounded Michaelis–Menten–Monod function (1) is used to model the handling time in immune response and their targets and how it affects the infection. In this paper, we adopt such a nonlinear bounded function $(p_1 IE/(1 + \beta I))$ in Chiyaka et al. (2008), where it is used to describe the killing of infected erythrocytes I by the immune cells E (CD8+ T cells, in our case). This formulation has also been used in Cai, Tuncer, and Martcheva (2017) and Selemani, Luboobi, and Nkansah-Gyekye (2017). The parameter p_1 describes the rate of removal of I by E and $1/\beta$ is the saturation constant that stimulates the proliferation of the CD8+ T cells to grow at half their maximum rate.

The effects of the BSV on merozoite invasion of the red blood cells are represented by the term $(((1 - \varrho)\beta_r RM)/1 + dW)$, where $0 < \varrho < 1$ is the efficacy of the BSV and $1/d$ is a saturation constant that stimulates CD8+ T cells to grow at half their maximum rate. In addition, BSV reduces the density of merozoites that are released per bursting blood schizont, so that the burst size P becomes $(1 - a)P$, where $0 < a < 1$ accounts for the vaccine-induced reduction of merozoites released per bursting IRB cell. BSV is further assumed to enhance the production of CD8+ T cells at a rate τ, where $\tau > 1$. For purposes of simulation, we assume $1 < \tau < 2$. Administered TBV is assumed to reduce the recruitment rate of the sporozoites Λ to $(1 - \chi)\Lambda$, where $0 < \chi < 1$ is the efficacy of the TBV. Moreover, the inoculated sporozoites are assumed to die naturally at the rate μ_s.

The immune cells (CD8+ T cells) are recruitment at a constant rate λ_w from the thymus. Furthermore, the presence of infected cells such as infected hepatocytes, blood trophozoites and blood schizonts stimulates the production of CD8+ T cells. The increased production of $W(t)$ due to $X(t)$, $T(t)$ and $C(t)$ is also modelled using the nonlinear bounded Michaelis–Menten–Monod function (1) and is represented by the terms $(\delta_x WX/1 + \varepsilon_0 X)$, $(\delta_t WT/1 + \varepsilon_1 T)$ and $(\delta_c WC/1 + \varepsilon_2 C)$, respectively. The parameter $\delta_i | i = \{x, t, c\}$ represents the immunogenecity of infected hepatocytes, blood trophozoites and blood schizonts respectively. On the other hand, the phagocytotic effects of CD8+ T cells on infected cells (X, T and C) are represented by the terms $(k_x(1 - \nu)WX/1 + \varepsilon_0 X)$, $(k_t(1 - \varrho)WT/1 + \varepsilon_1 T)$ and $(k_c(1 - \varrho)WC/1 + \varepsilon_2 C)$, where $k_j | j = \{x, t, c\}$ is the immunosensitivity of X,T and C, respectively.

The density of blood schizonts C decreases when they burst open to release merozoites into blood stream or when they die naturally at the rate μ_c. A proportion π of the released merozoites develops into gametocytes $G(t)$ whose natural decay rate is denoted by μ_g. Just like the susceptible hepatocytes whose natural mortality is at the rate μ_h, we assume a constant decay rates μ_t and μ_w for blood trophozoites and the CD8+ T cells respectively.

The descriptions of the variables and parameters used in the model are summarized in Tables 1 and 2 respectively.

Table 1. Description of variables.

Variable	Description
$H(t)$	Concentration of uninfected hepatocytes
$X(t)$	Concentration of infected hepatocytes
$R(t)$	Concentration of susceptible red blood cells
$T(t)$	Concentration of blood trophozoites
$C(t)$	Concentration of blood schizonts
$S(t)$	Concentration of sporozoites
$M(t)$	Concentration of merozoites in blood
$G(t)$	Concentration of gametocytes in blood
$W(t)$	Concentration of CD8+ T cells

Table 2. Description of parameters.

Parameter	Description
Λ	The rate of injection of sporozoites into liver due to mosquito bites
μ_s	The decay rate of sporozoites
λ_h	Rate of production of susceptible hepatocytes from the bone marrow
λ_r	Rate of production of susceptible RBC by the bone marrow
μ_h, μ_x	Death rate of susceptible hepatocyte and infected hepatocyte respectively
π	Proportion of parasites that become gametocytes per dying blood schizont
k_x, k_t, k_c	Immunosensitivity of infected hepatocytes, blood trophozoites and blood schizonts respectively
$\delta_x, \delta_t, \delta_c$	Immunogenecity of infected hepatocytes, blood trophozoites and blood schizonts respectively
β_s	Infection rate of hepatocytes by sporozoites
μ_r	The natural mortality rate of RBC
β_r	Rate of infection of RBCs by merozoites
μ_t, μ_c	The rate of decay of blood trophozoites and blood schizonts respectively
μ_m, μ_g	Decay rate of merozoites and gametocytes respectively
γ	Progression rate of IRB cells from trophozoite to schizont stage
χ	Efficacy of transmission blocking vaccine
ϱ	Efficacy of blood stage vaccine.
d	The rate of inhibition of immune response
λ_w	The rate of production of CD8+ T cells
$1/\varepsilon_0, 1/\varepsilon_1, 1/\varepsilon_2$	half saturation constants for infected hepatocytes, blood trophozoites and blood schizonts respectively
τ	A parameter that accounts for vaccine-induced enhanced production of CD8+ T cells
υ	Efficacy of pre-erythrocytic stage vaccine
μ_w	Decay rate of CD8+ T cells
b	A parameter that accounts for PEV-induced reduction of merozoites released per bursting infected hepatocyte
a	A parameter that accounts for BSV-induced reduction of merozoites released per bursting blood schizont
P	The average number of merozoites released per bursting blood schizont
N	The average number of merozoites released per bursting infected hepatocytes

The in-host malaria dynamics subject to vaccination is represented in the compartmental flow diagram in Figure 2. Based on the above model description and assumptions, the in-host malaria model that takes vaccines into account is formulated using a system of

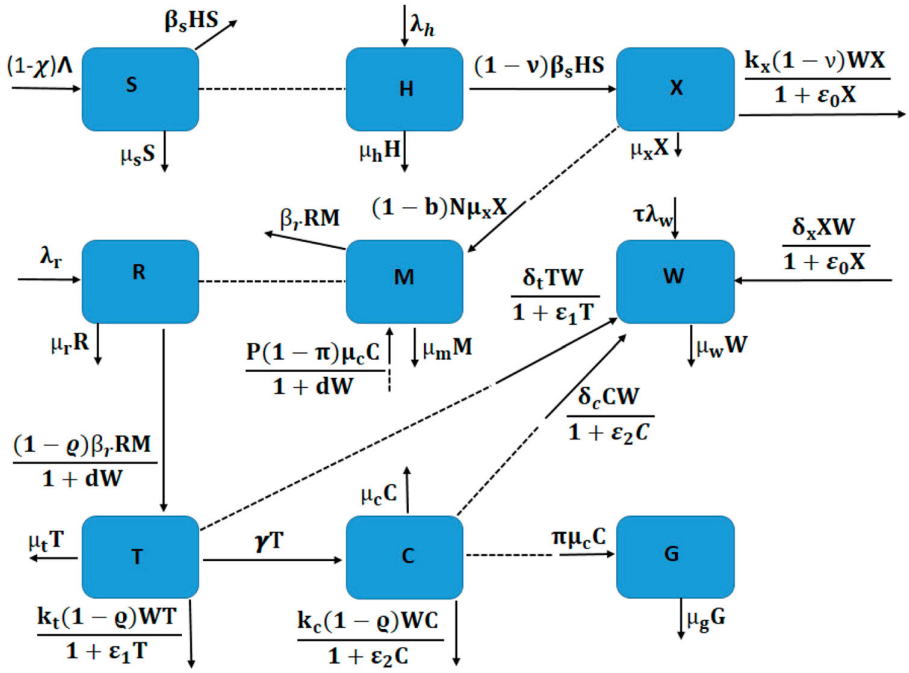

Figure 2. Schematic diagram for in-host malaria with vaccine therapy. The dotted lines without arrows indicate cell–parasite interaction and the solid lines show progression from one compartment to another.

nonlinear ordinary differential equations and presented as follows:

$$\left.\begin{aligned}
\frac{\mathrm{d}S}{\mathrm{d}t} &= (1-\chi)\Lambda - \mu_s S - \beta_s HS,\\
\frac{\mathrm{d}H}{\mathrm{d}t} &= \lambda_h - \mu_h H - \beta_s(1-\nu)HS,\\
\frac{\mathrm{d}X}{\mathrm{d}t} &= \beta_s(1-\nu)SH - \mu_x X - \frac{k_x(1-\nu)WX}{1+\varepsilon_0 X},\\
\frac{\mathrm{d}R}{\mathrm{d}t} &= \lambda_r - \frac{(1-\varrho)\beta_r RM}{1+dW} - \mu_r R,\\
\frac{\mathrm{d}T}{\mathrm{d}t} &= \frac{(1-\varrho)\beta_r RM}{1+dW} - \mu_t T - \gamma T - \frac{k_t(1-\varrho)WT}{1+\varepsilon_1 T},\\
\frac{\mathrm{d}C}{\mathrm{d}t} &= \gamma T - \mu_c C - \frac{k_c(1-\varrho)WC}{1+\varepsilon_2 C},\\
\frac{\mathrm{d}M}{\mathrm{d}t} &= (1-b)N\mu_x X + \frac{P(1-\pi)(1-a)\mu_c C}{1+dW} - \mu_m M - \beta_r RM,\\
\frac{\mathrm{d}G}{\mathrm{d}t} &= \pi\mu_c C - \mu_g G,\\
\frac{\mathrm{d}W}{\mathrm{d}t} &= \tau\lambda_w + W\left(\frac{\delta_x X}{1+\varepsilon_0 X} + \frac{\delta_t T}{1+\varepsilon_1 T} + \frac{\delta_c C}{1+\varepsilon_2 C}\right) - \mu_w W.
\end{aligned}\right\} \tag{2}$$

We assume that all the parameters used in the model are positive and the initial conditions for system (2) are: $H(0) \geq 0, X(0) \geq 0, S(0) \geq 0, R(0) \geq 0, T(0) \geq 0, C(0) \geq 0, M(0) \geq 0$, $G(0) \geq 0$, $W(0) \geq 0$.

3. Model analysis

3.1. Well-posedness of the model

We aim to evaluate the effects of the different vaccines on the concentration of infected hepatocytes and infected red blood cells. Therefore, the model should be biologically coherent. That is, all the state variables and their solutions must be non-negative and bounded, respectively, in the region Φ, where

$$\begin{aligned} \Phi = \left\{ (H, X, R, T, C, S, M, G, W) \in \mathbb{R}_+^9 : N_r(t) \leq \max\left\{ N_r(0), \frac{\lambda_r}{\mu_1} \right\}, \right. \\ N_h(t) \leq \max\left\{ N_h(0), \frac{\lambda_h}{\mu_2} \right\}, N_p(t) \leq \max\left\{ N_p(0), \frac{(1-\chi)\Lambda}{\mu_3} \right\}, \\ \left. W(t) \leq \max\left\{ W(0), \frac{\tau\lambda_w}{\mu_w} \right\} \right\}, \end{aligned} \tag{3}$$

and $N_r(t) = R(t) + T(t) + C(t)$, $N_h(t) = H(t) + X(t)$, $N_p(t) = S(t) + M(t) + G(t)$, $\mu_1 = \min\{\mu_r, \mu_t, \mu_c\}$, $\mu_2 = \min\{\mu_h, \mu_x\}$ and $\mu_3 = \min\{\mu_s, \mu_m, \mu_g\}$.

For the in-host malaria model (2) to be biologically meaningful, we prove the following theorem.

Theorem 3.1: *The region Φ is positively invariant with respect to the in-host malaria model (2), and a non-negative solution $(H(t), X(t), R(t), T(t), C(t), S(t), M(t), G(t), W(t))$ exists $\forall t \geq 0$.*

Proof: From the sporozoite compartment $S(t)$ in system (2), we have

$$\frac{\mathrm{d}S}{\mathrm{d}t} = (1-\chi)\Lambda - \mu_s S - \beta_s H S \geq -(\mu_s + \beta_s H)S. \tag{4}$$

Integrating (4) yields

$$S(t) \geq S(0)\exp\{-(\mu_s t + \beta_s \int_0^t H(n)\mathrm{d}n)\}. \tag{5}$$

This shows that in the absence of malaria interventions, $S(t) \geq 0$ for all time $t \geq 0$.

Using the same argument above, it is easy to see that

$$H(t) \geq H(0)\exp\{-(\mu_h t + \beta_s(1-\nu) \int_0^t S(n)\mathrm{d}n)\}. \tag{6}$$

This process can be repeated for all the state variables so that $S(t), H(t), X(t), R(t), T(t), C(t), M(t), G(t), W(t)$ are all positive for all $t \geq 0$. Thus the solutions of in-host malaria model (2) remain positive in Φ for all time $t \geq 0$. A quick guide on proof for positivity and

boundedness is available in Nyabadza, Njagarah, and Smith (2013) and Traoré, Sangaré, and Traoré (2017).

To show that the solutions of model system (2) are bounded, we let N_r be the total concentration of the red blood cells in the human host, that is $N_r(t) = R(t) + T(t) + C(t)$ and

$$\frac{\mathrm{d}N_r}{\mathrm{d}t} = \lambda_r - \mu_r R - \mu_t T - \mu_c C - \left(\frac{k_t(1-\varrho)WT}{1+\varepsilon_1 T} + \frac{k_c(1-\varrho)WC}{1+\varepsilon_2 C}\right), \tag{7}$$

$$\leq \lambda_r - \mu_1 N_r \quad \text{where} \quad \mu_1 = \min\{\mu_r, \mu_t, \mu_c\}. \tag{8}$$

Using the initial condition $N_r(0) = N_{r0} > 0$, Equation (8) is solved by integration into

$$N_r(t) \leq \frac{\lambda_r}{\mu_1} + \mathrm{e}^{-\mu_1 t}\left(N_r(0) - \frac{\lambda_r}{\mu_1}\right).$$

This implies that at any time t, $N_r(t) \leq \max\{N_r(0), \frac{\lambda_r}{\mu_1}\}$. This approach can similarly be applied to the population of hepatocytes $N_h = H(t) + X(t)$, population of parasites $N_p = S(t) + M(t) + G(t)$ and to the concentration of CD8+ T cells $W(t)$, so that we obtain

$$N_h(t) \leq \max\left\{N_h(0), \frac{\lambda_h}{\mu_2}\right\}, \quad \text{where } \mu_2 = \min\{\mu_h, \mu_x\};$$
$$N_p(t) \leq \max\left\{N_p(0), \frac{(1-\chi)\Lambda}{\mu_3}\right\}, \quad \text{where } \mu_3 = \min\{\mu_s, \mu_m, \mu_g\} \quad \text{and}$$
$$W(t) \leq \max\left\{W(0), \frac{\tau\lambda_w}{\mu_w}\right\}.$$

The above analysis shows that the region Φ is positively invariant and attracting for system (2) and the model is hence well posed for study. ■

3.2. Parasite free equilibrium and vaccination reproduction number

The parasite free equilibrium (PFE), E_v, depicts the absence of malaria parasites from the human host. The PFE of the in-host malaria model system (2) exists and is given by

$$E_v = (H^0, X^0, R^0, T^0, C^0, S^0, M^0, G^0, W^0) = \left(\frac{\lambda_h}{\mu_h}, 0, \frac{\lambda_r}{\mu_r}, 0, 0, 0, 0, 0, \frac{\tau\lambda_w}{\mu_w}\right). \tag{9}$$

The vaccination reproduction number (denoted by R_v), on the other hand, is a threshold quantity which governs the spread of the infection. It represents on average the number of new infected cells (RBCs or liver hepatocytes) generated by a single infectious merozoite (or sporozoites) at the blood (or liver) stage in the presence of malaria vaccines. Using the next generation matrix approach (Diekmann, Heesterbeek, & Metz, 1990; Van den Driessche & Watmough, 2002), the matrix $\mathcal{F}_1$ that represents the rate of appearance of new infections and the matrix $\mathcal{V}_1$ that denotes the transfer of infections from one compartment

to the other are respectively given as

$$\mathcal{F}_1 = \begin{pmatrix} \beta_s(1-\nu)SH \\ 0 \\ \dfrac{(1-\varrho)\beta_r RM}{1+dW} \\ 0 \\ 0 \\ 0 \end{pmatrix} \quad \text{and}$$

$$\mathcal{V}_1 = \begin{pmatrix} \mu_x X + \dfrac{k_x(1-\nu)WX}{1+\varepsilon_0 X} \\ -(1-\chi)\Lambda + \mu_s S + \beta_s SH \\ \mu_t T + \gamma T + \dfrac{k_t(1-\varrho)WT}{1+\varepsilon_1 T} \\ -\gamma T + \mu_c C + \dfrac{k_c(1-\varrho)WC}{1+\varepsilon_2 C} \\ -(1-b)N\mu_x X - \dfrac{P(1-\pi)(1-a)\mu_c C}{1+dW} + \mu_m M + \beta_r RM \\ -\pi\mu_c C + \mu_g G \end{pmatrix}. \tag{10}$$

Upon taking the partial derivatives of the terms in $\mathcal{F}_1$ and $\mathcal{V}_1$ and evaluating at the parasite free equilibrium E_v, we obtain a non-negative matrix F_1 and a non-singular matrix V_1 as follows.

$$\mathrm{F}_1 = \begin{pmatrix} 0 & \dfrac{(1-\nu)\beta_s\lambda_h}{\mu_h} & 0 & 0 & 0 & 0 \\ 0 & 0 & 0 & 0 & 0 & 0 \\ 0 & 0 & 0 & 0 & \dfrac{(1-e)\beta_r\lambda_r\mu_w}{\mu_r(d\tau\lambda_w+\mu_w)} & 0 \\ 0 & 0 & 0 & 0 & 0 & 0 \\ 0 & 0 & 0 & 0 & 0 & 0 \\ 0 & 0 & 0 & 0 & 0 & 0 \end{pmatrix} \tag{11}$$

and

$$\mathrm{V}_1 = \begin{pmatrix} V_a & 0 & 0 & 0 & 0 & 0 \\ 0 & \dfrac{\beta_s\lambda_h}{\mu_h} + \mu_s & 0 & 0 & 0 & 0 \\ 0 & 0 & V_b & 0 & 0 & 0 \\ 0 & 0 & -\gamma & \dfrac{(1-\varrho)\tau k_c\lambda_w}{\mu_w} + \mu_c & 0 & 0 \\ -(1-b)N\mu_x & 0 & 0 & -\dfrac{(1-a)P(1-\pi)\mu_c}{\dfrac{d\tau\lambda_w}{\mu_w}+1} & \dfrac{\beta_r\lambda_r}{\mu_r} + \mu_m & 0 \\ 0 & 0 & 0 & -\pi\mu_c & 0 & \mu_g \end{pmatrix}, \tag{12}$$

where $V_a = (((1-\varrho)\tau k_x\lambda_w)/\mu_w) + \mu_x$ and $V_b = \gamma + \mu_t + (((1-\varrho)\tau k_t\lambda_w)/\mu_w)$.

The vaccination reproduction number is the spectral radius of $(F_1V_1^{-1})$. That is,

$$R_v = \frac{P(1-\pi)(1-a)(1-\varrho)\gamma\beta_r\lambda_r\mu_c}{\mu_r\left(\frac{d\tau\lambda_w+\mu_w}{\mu_w}\right)^2\left(\mu_m+\frac{\beta_r\lambda_r}{\mu_r}\right)\left(\frac{(1-\varrho)\tau k_c\lambda_w}{\mu_w}+\mu_c\right)\left(\frac{(1-\varrho)\tau k_t\lambda_w}{\mu_w}+\gamma+\mu_t\right)}. \quad (13)$$

In the absence of malaria vaccines ($\chi = \varrho = \nu = a = b = 0, \tau = 1$), model (2) has a basic reproduction number R_m given by

$$R_m = \frac{P(1-\pi)\gamma\beta_r\lambda_r\mu_c}{\mu_r\left(\frac{d\lambda_w+\mu_w}{\mu_w}\right)^2\left(\frac{k_c\lambda_w}{\mu_w}+\mu_c\right)\left(\mu_m+\frac{\beta_r\lambda_r}{\mu_r}\right)\left(\gamma+\frac{k_t\lambda_w}{\mu_w}+\mu_t\right)}. \quad (14)$$

On comparing Equations (13) and (14), we deduce the following:

$$R_m = R_v \times \Theta^{**}, \quad (15)$$

where

$$\Theta^{**} = \frac{(1-a)(1-e)\left(\frac{d\lambda_w}{\mu_w}+1\right)(d\lambda_w+\mu_w)\left(\frac{k_c\lambda_w}{\mu_w}+\mu_c\right)\left(\gamma+\frac{k_t\lambda_w}{\mu_w}+\mu_t\right)}{\mu_w\left(\frac{d\tau\lambda_w}{\mu_w}+1\right)^2\left(\frac{(1-e)\tau k_c\lambda_w}{\mu_w}+\mu_c\right)\left(\gamma+\frac{(1-e)\tau k_t\lambda_w}{\mu_w}+\mu_t\right)}.$$

We observe from Equation (15) that in the absence of vaccination, $R_v = R_m$. However, the introduction of malaria vaccines reduces the basic reproduction number by a factor of $0 < \Theta^{**} < 1$. The use of efficacious malaria vaccines therefore has a great potential in reducing mortality due to *P. falciparum* malaria disease.

3.3. Sensitivity analysis

The main concern in the control of infectious diseases is the capacity of the infection to invade the population. The threshold quantity called the vaccine reproduction number provides a reasonable measure of the ability of the infective malaria parasites to invade the susceptible cell populations (Heesterbeek & Dietz, 1996). When $R_v < 1$, the infective parasites produce less than one new infection per infection period and the disease subsequently dies out. However, when $R_v > 1$, an infective parasite generates several infections leading to disease severity. In light of this, we carry out sensitivity analysis of model R_v in (13) so as to determine important parameters in the dynamics of *P. falciparum* malaria in the presence of vaccine controls. Following Arriola and Hyman (2007), the normalized forward sensitivity indices of R_v with respect to input parameters a, denoted by Γ_a, is given by

$$\Gamma_a = \frac{\partial R_v}{\partial a} \times \frac{a}{R_v}. \quad (16)$$

Based on the model R_v and the parameter values in Table 4, we derive the following analytical expressions for sensitivity indices of R_v with respect to parameters ϱ, P, π and τ. A part from the parameter P, whose sensitivity index does not depend on other parameter values, the rest of the expressions for the sensitivity indices are complex (see for instance

(18)–(20)). We therefore evaluate the sensitivity indices of R_v using the baseline parameter values in Table 4.

$$\Gamma_P = +1 \tag{17}$$

$$\Gamma_\varrho = \varrho\left(\tau\lambda_w\left(-\frac{k_c}{(\varrho-1)\tau k_c\lambda_w - \mu_c\mu_w} - \frac{k_t}{(\varrho-1)\tau k_t\lambda_w - \mu_w(\gamma+\mu_t)}\right) + \frac{1}{\varrho-1}\right) \tag{18}$$

$$\Gamma_\pi = -\frac{\Lambda}{1-\Lambda} \tag{19}$$

$$\Gamma_\tau = \tau\lambda_w\left(-\frac{(\varrho-1)k_c}{(\varrho-1)\tau k_c\lambda_w - \mu_c\mu_w} - \frac{2d}{d\tau\lambda_w + \mu_w} - \frac{(\varrho-1)k_t}{(\varrho-1)\tau k_t\lambda_w - \mu_w(\gamma+\mu_t)}\right). \tag{20}$$

Using Mathematica software, the sensitivity results for the 17 parameters in R_v are as shown in Table 3. The rate of merozoite invasion β_r, the rate of progression of infected red blood cells from the trophozoite state to blood schizonts γ and the average number of merozoites released per bursting blood schizont P increase (or decrease) the vaccine reproduction number when they are increased (or decreased) as shown in Table 3. Malaria vaccine development should target these parameters to reduce malaria disease progression in humans. On the other hand, the higher the efficacy of blood stage vaccine ϱ, the lower the value of R_v. A highly efficient erythrocytic vaccine has the potential to eradicate clinical malaria. The proportions of merozoites that development into gametocytes π is also shown to decrease the value of R_v when they are increased. The higher the concentration of gametocytes, the lower the density of merozoites in the host's blood. Although this would minimize secondary and subsequent erythrocytic invasions and hence malaria severity, it has the potential to enhance parasite transmission to the mosquito vector. This is due to increased concentration of gametocytes per blood sample per mosquito bite.

The density of merozoites released per bursting infected red blood cells and the efficacy of the blood stage vaccine are shown to be the most sensitive parameters in influencing in-host malaria progression. For example, a 10% increase (or decrease) on P will cause a 10% increase (or decrease) in R_v. These two parameters should hence be carefully estimated (Mikucki, 2012) and clinical malaria control using antimalarial drugs and malaria vaccines should target the two parameters. This is because a small variation in such a parameter will lead to large quantitative changes in R_v and hence on malaria disease progression.

Table 3. The sensitivity indices of R_v with respect model parameters.

Parameter	Sensitivity index	Parameter	Sensitivity index
P	+1	π	−0.25
a	−0.25	ϱ	−0.770486
γ	+0.293702	β_r	+0.0000663956
λ_r	+0.0000664	μ_c	+0.0000247494
μ_r	−0.000066396	d	−0.0222497
τ	−0.080544	λ_w	−0.080544
μ_w	+0.080	μ_m	−0.00006639
k_c	−0.0000247494	k_t	−0.0582696
μ_t	−0.235433		

3.4. Local stability of parasite free equilibrium

The local stability of E_v is investigated as follows. We begin by linearizing model system (2) around E_v so that we have the following Jacobian matrix J_1.

$$J_1 = \begin{pmatrix} -\mu_h & 0 & -A_0 & 0 & 0 & 0 & 0 & 0 & 0 \\ 0 & -A_1 & A_2 & 0 & 0 & 0 & 0 & 0 & 0 \\ 0 & 0 & -A_3 & 0 & 0 & 0 & 0 & 0 & 0 \\ 0 & 0 & 0 & -\mu_r & 0 & 0 & -A_4 & 0 & 0 \\ 0 & 0 & 0 & 0 & -A_5 & 0 & A_6 & 0 & 0 \\ 0 & 0 & 0 & 0 & \gamma & -A_7 & 0 & 0 & 0 \\ 0 & A_{11} & 0 & 0 & 0 & A_8 & -A_9 & 0 & 0 \\ 0 & 0 & 0 & 0 & 0 & \pi\mu_t & 0 & -\mu_g & 0 \\ 0 & \frac{\tau\delta_x\lambda_w}{\mu_w} & 0 & 0 & A_{10} & \frac{\tau\delta_c\lambda_w}{\mu_w} & 0 & 0 & -\mu_w \end{pmatrix} \tag{21}$$

where

$$A_0 = \frac{(1-\nu)\beta_s\lambda_h}{\mu_h}, A_1 = \frac{(1-\nu)\tau k_x\lambda_w}{\mu_w} + \mu_x, A_2 = \frac{(1-\nu)\beta_s\lambda_h}{\mu_h},$$

$$A_3 = \frac{\beta_s\lambda_h}{\mu_h} + \mu_s, A_4 = \frac{(1-\varrho)\beta_r\lambda_h}{\mu_h(\frac{d\tau\lambda_w}{\mu_w}+1)}, A_5 = \gamma + \mu_t + \frac{(1-\varrho)\tau k_t\lambda_w}{\mu_w},$$

$$A_6 = \frac{(1-\varrho)\beta_r\lambda_h}{\mu_h\left(\frac{d\tau\lambda_w}{\mu_w}+1\right)}, A_7 = \frac{(1-\varrho)\tau k_c\lambda_w}{\mu_w} + \mu_c, A_8 = \frac{(1-a)P(1-\pi)\mu_c}{\frac{d\tau\lambda_w}{\mu_w}+1},$$

$$A_9 = \frac{\beta_r\lambda_h}{\mu_h} + \mu_m, A_{10} = \frac{\tau\delta_t\lambda_w}{\mu_w} \quad \text{and} \quad A_{11} = (1-b)N\mu_x.$$

It is easy to see from matrix J_1 that the first eigenvalue, $\lambda_1 = -\mu_h < 0$. Upon deleting row 1 and column 1 from which λ_1 is placed, a new sub-matrix J_2 is produced.

$$J_2 = \begin{pmatrix} -A_1 & A_2 & 0 & 0 & 0 & 0 & 0 & 0 \\ 0 & -A_3 & 0 & 0 & 0 & 0 & 0 & 0 \\ 0 & 0 & -\mu_r & 0 & 0 & A_4 & 0 & 0 \\ 0 & 0 & 0 & -A_5 & 0 & A_6 & 0 & 0 \\ 0 & 0 & 0 & \gamma & -A_7 & 0 & 0 & 0 \\ A_{11} & 0 & 0 & 0 & A_8 & -A_9 & 0 & 0 \\ 0 & 0 & 0 & 0 & \pi\mu_t & 0 & -\mu_g & 0 \\ \frac{\tau\delta_x\lambda_w}{\mu_w} & 0 & 0 & A_{10} & \frac{\tau\delta_c\lambda_w}{\mu_w} & 0 & 0 & -\mu_w \end{pmatrix}. \tag{22}$$

On applying the above procedure to columns 3, 7 and 8 and their corresponding rows in matrix (22), we obtain the next three eigenvalues: $\lambda_2 = -\mu_r < 0$, $\lambda_3 = -\mu_g < 0$ and $\lambda_4 = -\mu_w < 0$. The resultant matrix J_3 is as follows:

$$J_3 = \begin{pmatrix} -A_1 & A_2 & 0 & 0 & 0 \\ 0 & -A_3 & 0 & 0 & 0 \\ 0 & 0 & -A_5 & 0 & A_6 \\ 0 & 0 & \gamma & -A_7 & 0 \\ A_{11} & 0 & 0 & A_8 & -A_9 \end{pmatrix}. \tag{23}$$

The rest of the eigenvalues are obtained by solving the characteristic equation of matrix J_3:

$$\lambda^5 + \beta_1\lambda^4 + \beta_2\lambda^3 + \beta_3\lambda^2 + \beta_4\lambda + \beta_5 = 0, \tag{24}$$

where

$$\beta_1 = A_1 + A_3 + A_5 + A_7 + A_9 > 0, \tag{25}$$

$$\begin{aligned}\beta_2 = {} & A_1A_3 + A_1A_5 + A_3A_5 + A_1A_7 + A_3A_7 + A_5A_7 \\ & + A_1A_9 + A_3A_9 + A_5A_9 + A_7A_9 > 0,\end{aligned} \tag{26}$$

$$\beta_3 = A_1A_3A_5 + A_1A_3A_7 + A_1A_5A_7 + A_3A_5A_7 + A_1A_3A_9 + A_1A_5A_9 + A_3A_5A_9 \tag{27}$$

$$+ A_1A_7A_9 + A_3A_7A_9 + A_5A_8A_9\left[(1 - R_v)\left(\frac{A_6^2A_7A_8}{\lambda_r}\right)\right], \tag{28}$$

$$\beta_4 = A_6A_8(A_1A_8)[(1 - R_v)] + A_1A_3A_5A_7 + A_1A_3A_5A_9 + A_1A_3A_7A_9 + A_1A_5A_7A_9 \tag{29}$$

$$\beta_5 = A_1A_3A_5A_7A_9\left[(1 - R_v)\frac{A_6}{\lambda_r}\right]. \tag{30}$$

Equation (24) has negative roots (eigenvalues) if all its coefficients terms are positive. That is, $\beta_1 > 0$, $\beta_2 > 0$, $\beta_3 > 0$, $\beta_4 > 0$ and $\beta_5 > 0$. We can clearly see from Equations (25) and (26) that β_1 and β_2 are positive terms. However, the coefficients β_3, β_4 and β_5 can only be positive if the vaccine reproduction number R_v is less than unity, $R_v < 1$.

Thus, using Theorem 2 in Van den Driessche and Watmough (2002), the following lemma is established.

Lemma 3.1: *The disease free equilibrium E_v is locally asymptotically stable if* $\mathrm{R}_v < 1$ *and unstable if* $\mathrm{R}_v > 1$.

Lemma 3.1 shows that if we are to eliminate the malaria parasite following malaria infection, then we have to administer a vaccine or combinations of vaccines that would guarantee the existence of a stable disease free equilibrium. Epidemiologically, when $R_v < 1$, we expect the parasites to decay off so that the severity of malaria infection is reduced to near zero or totally eliminated. On the other hand, if $R_v > 1$, the malaria infection persists within the human host; that is, more red blood cells and susceptible hepatocytes are infected. This implies that the vaccines may not be efficacious; their use do not eradicate malaria infection among infected individuals. The malaria parasites are therefore likely to persist at the erythrocytic stage in an infected individual and subsequently can be transmitted to other persons in close contact via the mosquito vector.

3.5. Critical efficacy of blood stage vaccine

Definition 1: Vaccine efficacy is interpreted as the proportionate reduction in malaria disease attack rate within a vaccinated person compared to an unvaccinated person (Small, Cheng, & Ten, 2010).

Generally, the vaccine efficacy V_E is expressed as follows (Orenstein, Wassilak, Strebel, Bernier, & Blackwelder, 1990):

$$V_E = \frac{ARU - ARV}{ARU} \times 100, \tag{31}$$

where ARU is the parasite attack rate of unvaccinated individual and ARV is the attack rate for vaccinated people. A critical vaccine efficacy therefore refers to the minimum efficacy value beyond which the vaccine is capable of eradicating the infection from the human host. To establish a critical malaria vaccine efficacy from the vaccine reproduction number (13), we assume that only the blood stage vaccine is administered to the individual. That is, $\nu = 0, b = 0, \chi = 0$. We then solve for ϱ from the equation $R_v = 1$ as follows:

$$\frac{P(1-\pi)(1-a)(1-\varrho)\gamma\beta_r\lambda_r\mu_c}{\left(\frac{(1-\varrho)\tau k_c\lambda_w}{\mu_w} + \mu_c\right)\left(\frac{(1-\varrho)\tau k_t\lambda_w}{\mu_w} + \gamma + \mu_t\right)} = \mu_r\left(\frac{d\tau\lambda_w + \mu_w}{\mu_w}\right)^2\left(\mu_m + \frac{\beta_r\lambda_r}{\mu_r}\right). \tag{32}$$

By simplification, Equation (32) reduces to

$$\frac{(1-\varrho)\mu_w^2}{(\mu_c\mu_w + (1-\varrho)\tau k_t\lambda_w)(\mu_w(\gamma+\mu_t) + (1-\varrho)\tau k_c\lambda_w)} = \Delta, \tag{33}$$

where

$$\Delta = \frac{\mu_r\left(\frac{d\tau\lambda_w}{\mu_w} + 1\right)(d\tau\lambda_w + \mu_w)\left(\mu_m + \frac{\beta_r\lambda_r}{\mu_r}\right)}{(1-\pi)(1-a)\gamma P\mu_c\beta_r\lambda_r\mu_w}. \tag{34}$$

Upon solving for $(1-\varrho)$ in (33) using the quadratic formula, we obtain

$$(1-\varrho) = \frac{-\mathcal{B}_1 \pm \sqrt{{\mathcal{B}_1}^2 - 4(\mathcal{B}_2\mathcal{B}_0)}}{2\mathcal{B}_2}, \tag{35}$$

where

$$\mathcal{B}_0 = -\Delta\mu_c(\gamma+\mu_t)\mu_w^2,\ \mathcal{B}_1 = -\mu_w(\Delta\tau k_c\lambda_w(\gamma+\mu_c+\mu_t) - \mu_w),\ \text{and}$$
$$\mathcal{B}_2 = -\Delta(\tau k_c\lambda_w)^2.$$

From Equation (35), the critical efficacy of the blood stage vaccine, $0 < \varrho_c < 1$, is

$$\varrho_c = 1 - \left(\frac{-\mathcal{B}_1 \pm \sqrt{{\mathcal{B}_1}^2 - 4(\mathcal{B}_2\mathcal{B}_0)}}{2\mathcal{B}_2}\right), \tag{36}$$

where $\mathcal{B}_i$, $i = \{0, 1, 2\}$, are as defined in Equation (35).

Equation (36) implies that for any blood stage vaccine to effectively control clinical malaria, then its efficacy must be higher than the stated critical vaccine efficacy.

Differentiating R_v with respect to vaccine efficacy ϱ yields

$$\begin{aligned}\frac{\partial R_v}{\partial \varrho} = &-\frac{P(1-\pi)(1-a)\beta_r\lambda_r\mu_c\gamma}{\mu_r\left(\mu_m+\frac{\beta_r\lambda_r}{\mu_r}\right)\left(\frac{(1-e)\tau k_c\lambda_w}{\mu_w}+\mu_c\right)\left(\frac{d\tau\lambda_w}{\mu_w}+1\right)^2\Psi_3}\\ &+\frac{P(1-\pi)(1-a)\beta_r\lambda_r\mu_c\gamma(1-e)\tau\lambda_w k_t}{\mu_r\mu_w\left(\mu_m+\frac{\beta_r\lambda_r}{\mu_r}\right)\left(\frac{(1-e)\tau k_c\lambda_w}{\mu_w}+\mu_c\right)\left(\frac{d\tau\lambda_w}{\mu_w}+1\right)^2{\Psi_3}^2}\\ &+\frac{P(1-\pi)(1-a)\beta_r\lambda_r\mu_c\gamma(1-e)\tau\lambda_w k_c}{\mu_r\mu_w\left(\mu_m+\frac{\beta_r\lambda_r}{\mu_r}\right)\left(\frac{(1-e)\tau k_c\lambda_w}{\mu_w}+\mu_c\right)^2\left(\frac{d\tau\lambda_w}{\mu_w}+1\right)^2\Psi_3},\end{aligned} \tag{37}$$

where $\Psi_3 = ((((1-\varrho)\tau k_t\lambda_w)/\mu_w)+\gamma+\mu_t)$.

We further simplify the right-hand side (RHS) of (37) by making the following representations: let $\Psi_1 = \mu_r(\mu_m + ((\beta_r\lambda_r)/\mu_r))$, $\Psi_2 = ((((1-\varrho)\tau k_c\lambda_w)/\mu_w)+\mu_c)$ and $\Psi_4 = (1+((d\tau\lambda_w)/\mu_w))$. This results in

$$\frac{\partial R_v}{\partial \varrho} = \frac{P(1-\pi)(1-a)\beta_r\lambda_r\mu_c\gamma(1-\varrho)\tau\lambda_w k_t k_c}{\Psi_1\Psi_2\Psi_3\Psi_4^2}\left\{\frac{1}{\mu_w k_c\Psi_3}+\frac{1}{\mu_w k_t{\Psi_2}^2}-\Gamma\right\}, \tag{38}$$

where $\Gamma = (1/(1-\varrho)\tau\lambda_w k_c k_t)$. We observe that $(\partial R_v/\partial\varrho) < 0$ when $\mu_c{\mu_w}^2(\gamma+\mu_t) > \tau k_c k_t{\lambda_w}^2(1-\varrho)$. R_v is therefore a decreasing function of the blood stage vaccine ϱ. This means that an efficacious BSV reduces the density of IRB cells within the human host. Figure 4 shows the profiles of the density of blood trophozoites and blood schizonts as a function of the efficacy of the BSV, ϱ. The concentration of infected erythrocytes decreases with increasing values of ϱ.

4. Numerical simulation

4.1. Vaccine efficacy

Lemma 4.1: *The vaccination threshold $R_v < 1$ whenever $\varrho > \varrho_c$*

When the efficacy of the BSV is higher than the critical vaccine efficacy ϱ_c, the merozoites are eradicated from the blood stream. Under this setting, the capacity of the blood stage vaccine to eradicate malaria parasites in the host's blood stream is guaranteed by Lemma 4.1. The results of Lemma 4.1 is shown numerically in Figure 3(a) and (b) using different values of ϱ. In Figure 3, a blood stage vaccine with a minimum efficacy of 94% is needed to control the blood stage parasites. Using the provided parameter values and expression (13), we observe that under this condition, R_v is less that unity. That is $R_v = 0.58 < 1$.

Lemma 4.2: *The vaccination threshold $R_v > 1$ whenever $\varrho < \varrho_c$*

When the efficacy of the blood stage vaccine is lower than the critical efficacy ($\varrho < \varrho_c$), the rate of infection of susceptible infected red blood cells is higher. This leads to increased density of infected red blood cells (blood trophozoites and blood schizonts) as shown in

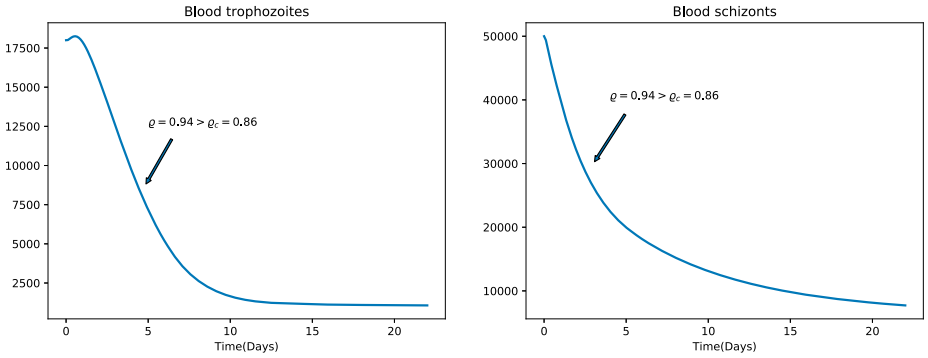

Figure 3. Graphs showing the density of (a) blood trophozoites $T(t)$ and (b) blood schizonts $C(t)$ when the blood stage vaccine efficacy, $\varrho = 0.94 > \varrho_c = 0.86$ and $R_v = 0.58 < 1$. The parameter values are available in Table 4.

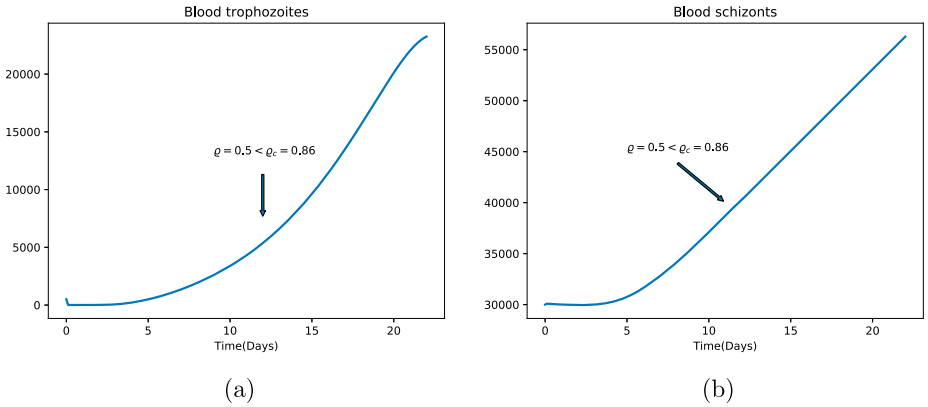

Figure 4. Graphs showing the density of (a) blood trophozoites $T(t)$ and (b) blood schizonts $C(t)$ when the efficacy of blood stage vaccine, $\varrho = 0.5 < \varrho_c = 0.86$ and $R_v = 1.27 > 1$. The used parameters values are available in Table 4.

Figure 4. Using the parameter values in Table 4 and the expression for the vaccine reproduction number, we observe that the above condition is only guaranteed when R_v is greater than unity. That is, $R_v = 1.27 > 1$.

Only a highly efficacious blood stage vaccine, ($\varrho > 90\%$) would guarantee the achievement of a malaria free equilibrium as shown in Figure 5. A blood stage vaccine with lower efficacy, ($\varrho < 50\%$) is likely to be less effective in clearing the malaria parasites. A malaria persistent steady state is hence probable (see Figure 5). The concentration of gametocytes in the blood stream is indirectly influenced by the blood stage vaccine. Higher vaccine efficacy minimizes the concentration of gametocytes that are later sucked up by feeding anopheles mosquitoes. As the efficacy of blood stage vaccine diminishes, higher concentration of gametocytes is observed in the blood stream as shown is Figure 6.

Table 4. Parameter values used in the numerical simulations and sensitivity analysis.

Parameter	Value	Range	Units	Source
P	16	(15–20)	/erythrocytes/day	Diebner et al. (2000)
k_x	0.01	(0.001–0.9)	/day	Chiyaka et al. (2008)
k_t	0.01	(0.001–0.9)	/day	Chiyaka et al. (2008)
k_c	0.000001	(0.001–0.9)	/day	Chiyaka et al. (2008)
μ_r	0.083	(0.05–0.1)	/day	Anderson et al. (1989)
β_r	2.0×10^{-1}	(0.07–0.3)	/mm^3/day	Dondorp, Kager, Vreeken, and White (2000)
β_s	1.0×10^{-3}	(0.001–0.2)	/mm^3/day	Selemani, Luboobi, and Nkansah-Gyekye (2016)
π	0.2	(0.1–0.9)	unitless	Talman, Domarle, McKenzie, Ariey, and Robert (2004)
μ_h	0.029	(0.01–0.5)	/day	Estimated
μ_x	0.02	(0.01–1)	/day	Selemani et al. (2016)
λ_r	3×10^3	$(3 \times 10^3 - 3 \times 10^8)$	cells/ml/day	Li et al. (2011)
λ_h	3×10^5	$(3 \times 10^5 - 3 \times 10^8)$	cells/μl^{-1}/day	Tumwiine, Mugisha, and Luboobi (2008)
λ_w	30	(10–40)	/μl^{-1}/day	Chiyaka, Garira, and Dube (2010)
μ_m	48	(46–50)	/day	Li et al. (2011)
Λ	30	(18–35)	sporozoites/day	Selemani et al. (2016)
μ_s	1.2	$(1.0 - 2.4)$	/day	Selemani et al. (2016)
μ_t	0.5	(0.01–0.8)	/day	Magombedze et al. (2011)
μ_c	0.5	(0.01–0.9)	/day	Magombedze et al. (2011)
μ_g	0.0000625	$(6.0 \times 10^{-5} - 7.0 \times 10^{-5})$	/day	Selemani et al. (2016)
μ_w	2	(0.05–3)	/day	Chiyaka et al. (2010)
δ_x	1e-5	(1e-5–1e-7)	mm^{-3}/day	Chiyaka et al. (2010)
δ_t	0.05	(0.01–0.08)	mm^{-3}/day	Chiyaka et al. (2010)
δ_c	0.05	(0.01–0.08)	mm^{-3}/day	Chiyaka et al. (2010)
γ	1.5	(0.1–2)	/day	Selemani et al. (2016)
χ	0.2	(0–1)	unitless	Assumed
ϱ	0.45	(0–1)	unitless	Birkett (2016)
ν	0.3	(0–1)	unitless	Assumed
τ	1.5	(1–2)	unitless	Niger and Gumel (2011)
b	0.2	(0–1)	unitless	Niger and Gumel (2011)
a	0.2	(0–1)	unitless	Niger and Gumel (2011)
d	0.0005	(0.00005–0.02)	unitless	Magombedze et al. (2011)
N	10,000	(8000–20,000)	/day	Tumwiine et al. (2014)

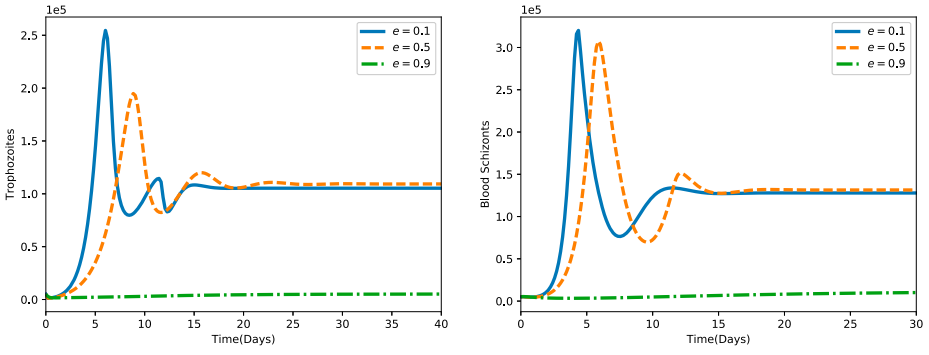

(a) (b)

Figure 5. Simulations showing the effect varying the parameter ϱ on the density of infected red blood cells. All other parameter values are in Table 4.

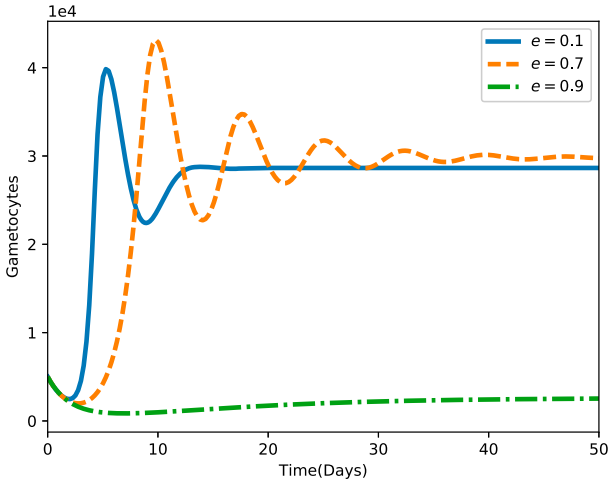

Figure 6. Simulations showing the effect varying the parameter ϱ on the concentration of gametocytes in blood. All other parameter values are in Table 4.

The effect of BSV-induced reduction of merozoites released per bursting blood schizont is monitored by differentiating R_v with respect to a. This gives

$$\frac{\partial R_v}{\partial a} = -\frac{(1-\pi)\gamma(1-\varrho)P\mu_c\beta_r\lambda_r}{\mu_r\left(\mu_m+\frac{\beta_r\lambda_r}{\mu_r}\right)\left(1+\frac{d\tau\lambda_w}{\mu_w}\right)^2\left(\frac{(1-\varrho)\tau k_c\lambda_w}{\mu_w}+\mu_c\right)\Psi_3} < 0,$$

where $\Psi_3 = ((((1-\varrho)\tau k_t\lambda_w)/\mu_w) + \gamma + \mu_t)$.

We make the following observations: the vaccine reproduction number R_v decreases with increasing value of a. As less blood schizonts burst, less merozoites are released and hence less secondary infections that increase the severity of the disease as displayed in Figure 7. This leads to the reduction in the vaccine reproduction number and hence the density of infected red blood cells in the blood stream.

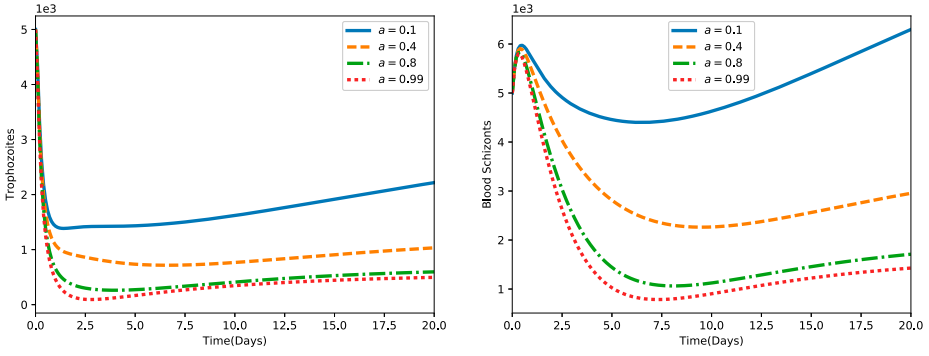

(a) (b)

Figure 7. Simulations showing the effect varying the parameter a on the density of (a) blood trophozoites $T(t)$ and (b) blood schizonts $C(t)$. All other parameter values are in Table 4.

The effect of the BSV-induced enhanced production of CD8+ T cells is monitored by the partial derivatives of R_v with respect to τ.

$$\begin{aligned}\frac{\partial R_v}{\partial \tau} = &-\frac{(1-\pi)(1-a)\gamma(1-e)^2 P k_c \mu_c \beta_r \lambda_r \lambda_w}{\mu_r \mu_w \left(\frac{d\tau\lambda_w}{\mu_w}+1\right)^2 \left(\mu_m + \frac{\beta_r \lambda_r}{\mu_r}\right)\left(\frac{(1-e)\tau k_c \lambda_w}{\mu_w}+\mu_c\right)^2 \Psi_3} \\ &- \frac{(1-\pi)(1-a)\gamma(1-e)^2 P k_t \mu_c \beta_r \lambda_r \lambda_w}{\mu_r \mu_w \left(\frac{d\tau\lambda_w}{\mu_w}+1\right)^2 \left(\mu_m + \frac{\beta_r \lambda_r}{\mu_r}\right)\left(\frac{(1-e)\tau k_c \lambda_w}{\mu_w}+\mu_c\right) {\Psi_3}^2} \\ &- \frac{2(1-\pi)(1-a)\gamma d(1-e) P \mu_c \beta_r \lambda_r \lambda_w}{\mu_r \mu_w \left(\frac{d\tau\lambda_w}{\mu_w}+1\right)^3 \left(\mu_m + \frac{\beta_r \lambda_r}{\mu_r}\right)\left(\frac{(1-e)\tau k_c \lambda_w}{\mu_w}+\mu_c\right) \Psi_3},\end{aligned} \tag{39}$$

where $\Psi_3 = ((((1-\varrho)\tau k_t \lambda_w)/\mu_w) + \gamma + \mu_t)$.

By applying the algebraic substitutions used in Equations (38) and (39) simplifies to

$$\frac{\partial R_v}{\partial \tau} = -\frac{\Theta^*}{\Psi_1 \Psi_2 \Psi_3 \Psi_4^2}\left(\frac{1}{dk_t \Psi_2} + \frac{1}{dk_c \Psi_3} + \frac{2}{(1-e)k_c k_t \Psi_4},\right) < 0, \tag{40}$$

where

$$\Theta^* = (1-\pi)(1-a)\gamma P(1-e)^2 d k_c k_t \mu_c \beta_r \lambda_r \lambda_w.$$

We observe from (40) that R_v decreases with increasing τ. As more CD8+ T cells are activated, more trophozoites and blood schizonts are killed through phagocytosis, leading to reduction in the severity of malaria infection as shown in Figure 8.

The effect of the BSV-induced reduction in the burst size P of infected red blood cells is shown by the following formula:

$$\frac{\partial R_v}{\partial P} = \frac{(1-\pi)(1-a)\gamma(1-e)\mu_c \beta_r \lambda_r \mu_c}{\mu_r \left(\frac{d\tau\lambda_w}{\mu_w}+1\right)(d\tau\lambda_w + \mu_w)\left(\mu_m + \frac{\beta_r \lambda_r}{\mu_r}\right)\left(\frac{(1-e)\tau k_c \lambda_w}{\mu_w}+\mu_c\right)\Psi_3},$$

where $\Psi_3 = ((((1-\varrho)\tau k_t \lambda_w)/\mu_w) + \gamma + \mu_t)$.

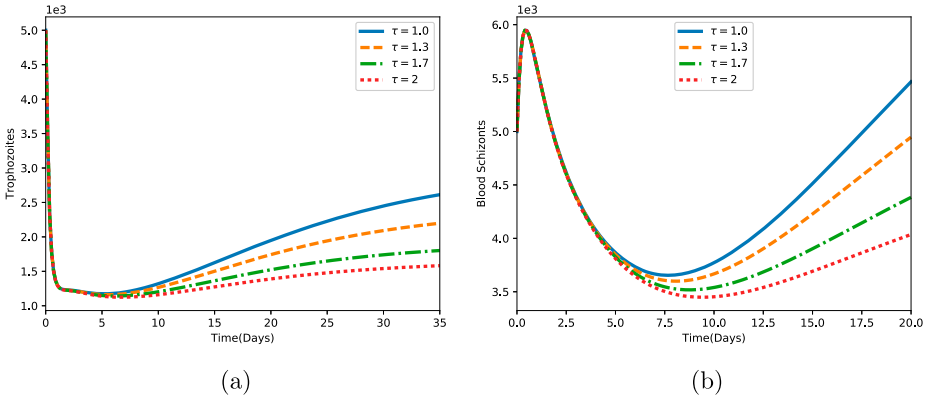

(a) (b)

Figure 8. Simulation showing the density of (a) blood trophozoites $T(t)$ and (b) blood schizonts $C(t)$ for varying values of blood stage vaccine-induced enhanced production parameter τ. All other parameter values are in Table 4.

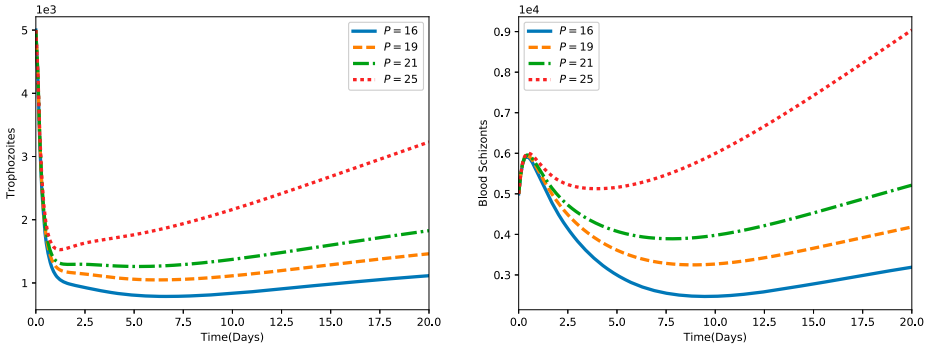

Figure 9. Simulations showing how the infected red blood cell burst size P affects the density of (a) blood trophozoites $T(t)$ and (b) blood schizonts $C(t)$. All other parameter values are in Table 4.

Note that $(\partial R_v/\partial P) > 0$ and R_v decreases (increases) with decreasing (increasing) value of P. The higher the density of released merozoites from bursting blood schizonts, the higher the rate of secondary invasions at the blood stage. The concentration of infected red blood cells in blood is observed to increase with increasing value of P as shown in Figure 9. An efficacious malaria vaccine would be necessary in minimizing secondary and future invasions that occur at the blood stage of malaria infection.

4.2. *Threshold analysis and vaccine impacts*

The Malaria Vaccine Technology Road map updated in November 2013 has two key strategic goals targeting *P. falciparum* and *P. vivax* malaria by the year 2030: (1) to develop vaccines with over 75% protective efficacy against clinical malaria and (2) to develop transmission blocking vaccines thereby reducing new cases of human malaria infections (MVFG, 2018). A combination of malaria vaccines (pre-erythrocytic, blood stage

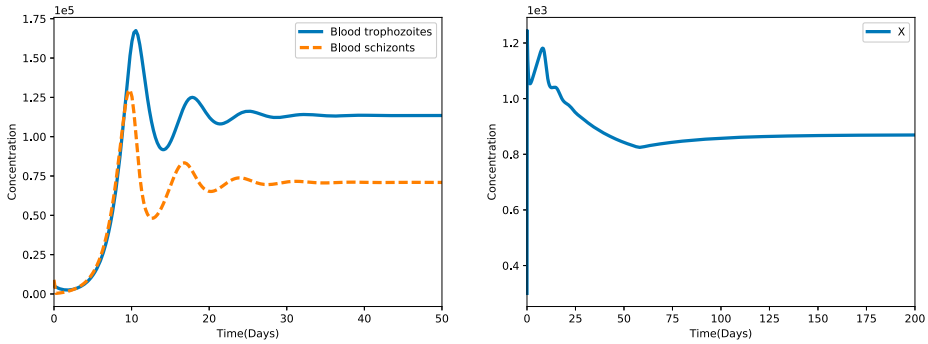

Figure 10. Time profile of the total concentration of infected red blood cells (a) and the concentration of infected liver hepatocytes (b) in the absence of malaria vaccines ($\varrho = \chi = \nu = 0$). All parameter values are in Table 4.

and transmission blocking vaccines) could help in achieving the over 75% strategic goal (Miura, 2016).

A highly efficacious blood stage vaccine has a potential to significantly reduce the numbers of gametocytes in the blood stream, thereby minimizing parasite transmission to mosquitoes and subsequently to other human beings. In the following section, we investigate the possible impacts of different malaria vaccine combinations with varying degrees of efficacy.

In the absence of malaria vaccines, $\varrho = \chi = \nu = 0$, we observe from Figure 13 that the concentration of infected red blood cells increases rapidly and settles at the parasite persistent equilibrium point. This trend is also observed with the infected liver hepatocytes (see Figure 10b). The concentration of infected liver hepatocytes rises due to invasion by

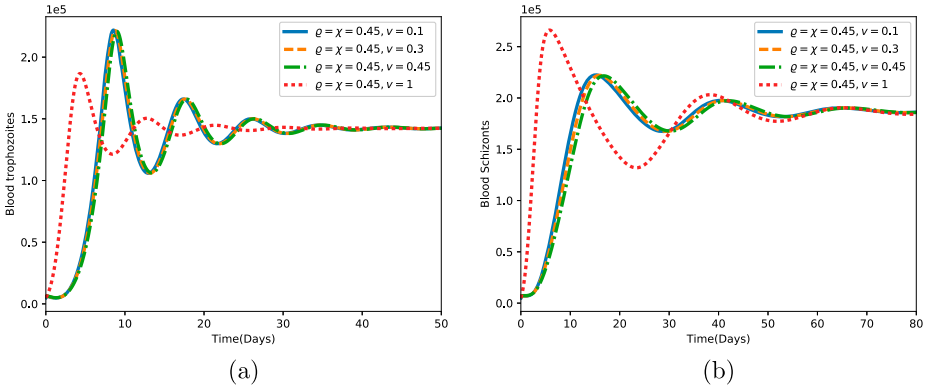

Figure 11. Time profile of the total concentration of (a) blood trophozoites and blood schizonts (b) for $\varrho = \chi = 0.45$ with varying efficacy of pre-erythrocytic vaccine ν. The set of parameter values is given in Table 4.

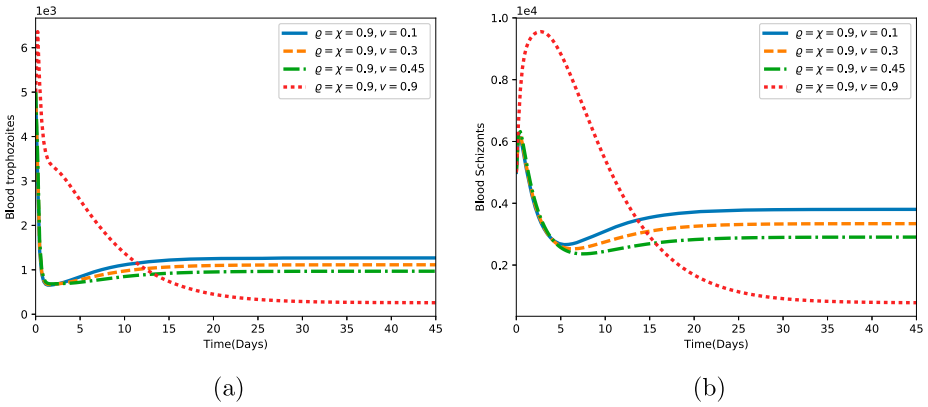

Figure 12. Time profile of the total concentration of (a) blood trophozoites and blood schizonts (b) for $\varrho = \chi = 0.9$ with varying efficacy of pre-erythrocytic vaccine ν. The set of parameter values is given in Table 4.

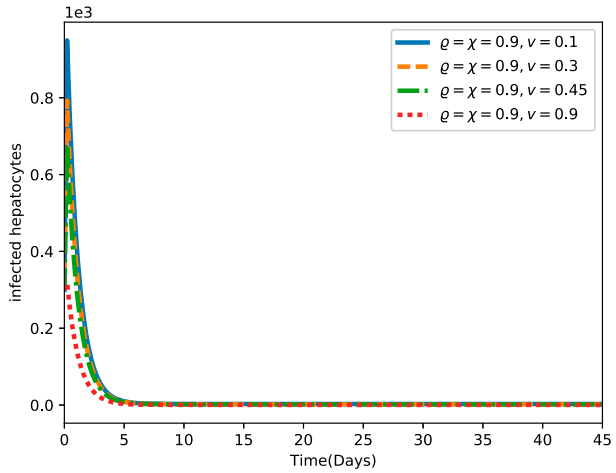

Figure 13. Simulation showing the profile of infected liver hepatocytes in the presence of perfect malaria vaccines ($\varrho = \chi = 0.9$). The efficacy of the pre-erythrocytic vaccine v is varied from 0 to 1. The set of parameter values is given in Table 4.

sporozoites for about a week. This is followed by a slight decline in density and subsequent persistent concentration at the liver stage.

A malaria vaccine with an efficacy of 45% may not be adequate in eliciting sufficient immune response to reduce and clear infections as shown in Figure 11. More plasmodium parasites are likely to persist in the blood stream, raising the severity of infections.

A combination of an imperfect blood stage vaccine (efficiency $\geq$ 90%) and an imperfect transmission blocking vaccine (efficiency $\geq$ 90%) is likely to result in rapid eradication of the infected infected red blood from the human host as displayed in Figure 12. Observe that the parasite free equilibrium is highly probable irrespective of the efficacy of the pre-erythrocytic vaccine in this context.

Similarly, the concentration of gametocytes in the blood stream is observed to diminish quickly in the presence of efficacious malaria vaccine combinations (see Figure 13).

5. Discussion

Using numerical simulation, we observe that the activated CD8+ T cells and malaria vaccines have a considerable effects on malaria control. Vaccination reduces the basic reproduction number by a constant factor. An imperfect blood stage vaccine with an efficacy of at least 90% is shown to be very effective in controlling in-host *P. falciparum* malaria.

We further observe that malaria vaccines that minimize the total number of merozoites released per bursting infected liver hepatocytes, reduce the concentrations of blood trophozoites and blood schizonts. Similarly, a highly efficacious vaccine greatly reduces the burst size of the blood schizonts, so that less merozoites are released from the infected red blood cells. This has the potential to reduce malaria severity and hence malaria transmission to the mosquito vector.

An efficacious blood stage vaccine should maximize the rate of activation of CD8+ T cells. We notice that the higher the vaccine potential to activate these immune cells, the lower the concentration of infected red blood cells in the host.

Our analysis further shows that different vaccine combinations yield different results. In the absence of vaccine therapy, the concentration of infected red blood cells (blood trophozoites and blood schizonts) is shown to increase and stabilize at the parasite persistent equilibrium. An imperfect pre-erythrocytic vaccine with an efficacy of at least 90% is also shown to guarantee the attainment of a parasite free equilibrium.

Like many other epidemic models, the presented in-host malaria model is formulated based on several model assumptions. The parameter values used in the study are also obtained from past literature. The results of our study should therefore be approached with some discretion. The presented model ignores the biology of CD8+ T activation and assumes constant parameter values. It would therefore be difficult to predict with higher accuracy, the optimal malaria vaccine efficacy. In spite of the stated shortcomings, the presented in-host malaria model provides useful insights on the need to improve the efficacy of current malaria vaccines in development and the need to try vaccine combinations in controlling clinical *P. falciparum* malaria infection.

Although the normalized forward sensitivity approach is helpful in identifying important parameters in the dynamics of the disease, it fails to explain the considerable uncertainties in estimating parameter values and hence parameter influences on specific output variables/states in the model. For future improvement of the above model, we recommend the inclusion uncertainty and sensitivity analysis with respect to infected cells of the in-host malaria model based on Latin Hypercube Sampling and Partial Rank Correlation Coefficient.

6. Conclusion

We have presented a mathematical model for in-host malaria dynamics subject to malaria vaccines. The analysed model provides useful insights in individual and combined vaccine impacts in reducing the severity of clinical malaria. The notion of critical vaccine efficacy is key in the development of malaria vaccines with the potential to eliminate or eradicate *P. falciparum* malaria in individuals infected with the disease.

In order to achieve a substantial reduction in malaria mortality and morbidity, the efficacy of the malaria vaccine should be higher than the corresponding critical vaccine efficacy. For instance, when the efficacy of the blood stage vaccine is lower than the critical efficacy ($\varrho < \varrho_c$), the rate of infection of susceptible infected red blood cells is higher and clinical malaria persists. However, the concentration of blood trophozoites and blood schizonts decreases drastically if the efficacy of the blood stage vaccine is higher than the critical blood stage vaccine efficacy.

The combined administration of malaria vaccines (Miura, 2016) and antimalarial drugs is likely to provide the much needed therapeutic control against *P. falciparum* malaria. The general and specific impacts generated by vaccine–WHO–antimalarial drugs combination will also form part of our future investigation.

Disclosure statement

No potential conflicts of interest are disclosed by the authors.

Funding

The authors acknowledge with gratitude the support from the Institute of Mathematical Sciences, Strathmore University, the National Research Fund (NRF) [NRF- Phd Grant Titus O.O.] Kenya and the DAAD [ST32 - PKZ: 91711149] in the production of this manuscript.

ORCID

Titus Okello Orwa http://orcid.org/0000-0002-0849-1663
Rachel Waema Mbogo http://orcid.org/0000-0003-1639-1360
Livingstone Serwadda Luboobi http://orcid.org/0000-0002-8256-8593

References

Abdulla, S., Oberholzer, R., Juma, O., Kubhoja, S., Machera, F., Membi, C., & Tanner, M.P.H. (2008). Safety and immunogenicity of RTS, S/AS02D malaria vaccine in infants. *New England Journal of Medicine*, *359*(24), 2533–2544.

Agur, Z., Abiri, D., Van der Ploeg (1989). Ordered appearance of antigenic variants of African trypanosomes explained in a mathematical model based on a stochastic switch process and immune-selection against putative switch intermediates. *Proceedings of the National Academy of Sciences*, *86*(23), 9626–9630.

Alonso, P. L., Sacarlal, J., Aponte, J. J., Leach, A., Macete, E., Milman, J., & Cohen, J. (2004). Efficacy of the RTS, S/AS02A vaccine against *Plasmodium falciparum* infection and disease in young African children: Randomised controlled trial. *The Lancet*, *364*(9443), 1411–1420.

Alout, H., Labbé, P., Chandre, F., & Cohuet, A. (2017a). Malaria vector control still matters despite insecticide resistance. *Trends in Parasitology*, *33*(8), 610–618.

Alout, H., Roche, B., Dabiré, R. K., & Cohuet, A. (2017b). Consequences of insecticide resistance on malaria transmission. *PLoS Pathogens*, *13*(9), e1006499.

Anderson, R., May, R., & Gupta, S. (1989). Non-linear phenomena in hostparasite interactions. *Parasitology*, *99*(S1), S59–S79.

Antia, R., Levin, B. R., & May, R. M. (1994). Within-host population dynamics and the evolution and maintenance of microparasite virulence. *The American Naturalist*, *144*(3), 457–472.

Arama, C., & Troye-Blomberg, M. (2014). The path of malaria vaccine development: Challenges and perspectives. *Journal of Internal Medicine*, *275*(5), 456–466.

Arevalo-Herrera, M., Solarte, Y., Yasnot, M. F., Castellanos, A., Rincon, A., Saul, A., & Herrera, S. (2005). Induction of transmission-blocking immunity in Aotus monkeys by vaccination with a *Plasmodium vivax* clinical grade pvs25 recombinant protein. *The American Journal of Tropical Medicine and hygiene*, *73*(5-suppl), 32–37.

Arriola, Leon M., & Hyman, James M. (2007). Being sensitive to uncertainty. *Computing in Science & Engineering*, *9*(2), 10–20.

Audran, R., Cachat, M., Lurati, F., Soe, S., Leroy, O., Corradin, G., & Spertini, F. (2005). Phase I malaria vaccine trial with a long synthetic peptide derived from the merozoite surface protein 3 antigen. *Infection and Immunity*, *73*(12), 8017–8026.

Austin, D., White, N., & Anderson, R. (1998). The dynamics of drug action on the within-host population growth of infectious agents: Melding pharmacokinetics with pathogen population dynamics. *Journal of Theoretical Biology*, *194*(3), 313–339.

Bertolino, P., & Bowen, D. G. (2015). Malaria and the liver: Immunological hide-and-seek or subversion of immunity from within? *Frontiers in Microbiology*, *6*, 41.

Bhatt, S., Weiss, D., Cameron, E., Bisanzio, D., Mappin, B., Dalrymple, U., & Wenger, E.A. (2015). The effect of malaria control on *Plasmodium falciparum* in Africa between 2000 and 2015. *Nature*, *526*(7572), 207.

Birkett, A. J. (2016). Status of vaccine research and development of vaccines for malaria. *Vaccine*, *34*(26), 2915–2920.

Birkett, A. J., Moorthy, V. S., Loucq, C., Chitnis, C. E., & Kaslow, D. C. (2013). Malaria vaccine R&D in the decade of vaccines: Breakthroughs, challenges and opportunities. *Vaccine*, *31*, B233–B243.

Bojang, K. A., Milligan, P. J., Pinder, M., Vigneron, L., Alloueche, A., Kester, K. E., & Yamuah, L. (2001). Efficacy of RTS, S/AS02 malaria vaccine against *Plasmodium falciparum* infection in semi-immune adult men in the gambia: A randomised trial. *The Lancet*, *358*(9297), 1927–1934.

Cai, L., Tuncer, N., & Martcheva, M. (2017). How does within-host dynamics affect population-level dynamics? Insights from an immuno-epidemiological model of malaria. *Mathematical Methods in the Applied Sciences*, *40*(18), 6424–6450.

Carter, R., Mendis, K. N., Miller, L. H., Molineaux, L., & Saul, A. (2000). Malaria transmission-blocking vaccines how can their development be supported? *Nature Medicine*, *6*(3), 241.

Chiyaka, C., Garira, W., & Dube, S. (2008). Modelling immune response and drug therapy in human malaria infection. *Computational and Mathematical Methods in Medicine*, *9*(2), 143–163.

Chiyaka, C., Garira, W., & Dube, S. (2010). Using mathematics to understand malaria infection during erythrocytic stages.

Derbyshire, E. R., Mota, M. M., & Clardy, J. (2011). The next opportunity in anti-malaria drug discovery: The liver stage. *PLoS Pathogens*, *7*(9), e1002178.

Diebner, H. H., Eichner, M., Molineaux, L., Collins, W. E., Jeffery, G. M., & Dietz, K. (2000). Modelling the transition of asexual blood stages of *Plasmodium falciparum* to gametocytes. *Journal of Theoretical Biology*, *202*(2), 113–127.

Diekmann, O., Heesterbeek, J. A. P., & Metz, J. A. (1990). On the definition and the computation of the basic reproduction ratio r 0 in models for infectious diseases in heterogeneous populations. *Journal of Mathematical Biology*, *28*(4), 365–382.

Dondorp, A. M., Kager, P. A., Vreeken, J., & White, N. J. (2000). Abnormal blood flow and red blood cell deformability in severe malaria. *Parasitology Today*, *16*(6), 228–232.

Dondorp, A. M., Yeung, S., White, L., Nguon, C., Day, N. P., Socheat, D., & Von Seidlein, L. (2010). Artemisinin resistance: Current status and scenarios for containment. *Nature Reviews Microbiology*, *8*(4), 272.

Duffy, P. E., Sahu, T., Akue, A., Milman, N., & Anderson, C. (2012). Pre-erythrocytic malaria vaccines: Identifying the targets. *Expert Review of Vaccines*, *11*(10), 1261–1280.

Greenwood, B., & Targett, G. (2009). Do we still need a malaria vaccine? *Parasite Immunology*, *31*(9), 582–586.

Haldar, K., Murphy, S. C., Milner Jr, D. A., & Taylor, T. E. (2007). Malaria: Mechanisms of erythrocytic infection and pathological correlates of severe disease. *Annual Review of Pathology: Mechanisms of Disease*, *2*, 217–249.

Heesterbeek, J., & Dietz, K. (1996). The concept of ro in epidemic theory. *Statistica Neerlandica*, *50*(1), 89–110.

Hellriegel, B. (1992). Modelling the immune response to malaria with ecological concepts: Short-term behaviour against long-term equilibrium. *Proceedings of the Royal Society of London B*, *250*(1329), 249–256.

Hetzel, C., & Anderson, R. (1996). The within-host cellular dynamics of bloodstage malaria: Theoretical and experimental studies. *Parasitology*, *113*(1), 25–38.

Hisaeda, H., Stowers, A. W., Tsuboi, T., Collins, W. E., Sattabongkot, J. S., Suwanabun, N., & Kaslow, D. C. (2000). Antibodies to malaria vaccine candidates pvs25 and pvs28 completely block the ability of *Plasmodium vivax* to infect mosquitoes. *Infection and Immunity*, *68*(12), 6618–6623.

Homan, T. (2016). *Impact of odour-baited mosquito traps for malaria control* (PhD thesis). Wageningen University.

Ishino, T., Yano, K., Chinzei, Y., & Yuda, M. (2004). Cell-passage activity is required for the malarial parasite to cross the liver sinusoidal cell layer. *PLoS Biology*, *2*(1), e4.

Kamangira, B., Nyamugure, P., & Magombedze, G. (2014). A theoretical mathematical assessment of the effectiveness of coartemether in the treatment of *Plasmodium falciparum* malaria infection. *Mathematical Biosciences*, *256*, 28–41.

Li, Y., Ruan, S., & Xiao, D. (2011). The within-host dynamics of malaria infection with immune response. *Mathematical Biosciences and Engineering*, *8*(4), 999–1018.

Liehl, P., Meireles, P., Albuquerque, I. S., Pinkevych, M., Baptista, F., Mota, M. M., & Prudêncio, M. (2015). Innate immunity induced by plasmodium liver infection inhibits malaria reinfections. *Infection and Immunity*, IAI 02796 IAI–02796 .

Magombedze, G., Chiyaka, C., & Mukandavire, Z. (2011). Optimal control of malaria chemotherapy. *Nonlinear Analysis: Modelling and Control*, *16*(4), 415–434.

Malaguarnera, L., & Musumeci, S. (2002). The immune response to *Plasmodium falciparum* malaria. *The Lancet Infectious Diseases*, *2*(8), 472–478.

malERA Consultative Group on Vaccines et al. (2011). A research agenda for malaria eradication: Vaccines. *PLoS Medicine*, *8*(1), e1000398.

March, S., Ng, S., Velmurugan, S., Galstian, A., Shan, J., Logan, D. J., & Hoffman, S. L. (2013). A microscale human liver platform that supports the hepatic stages of Plasmodium falciparum and vivax. *Cell Host & Microbe*, *14*(1), 104–115.

Maude, R. J., Pontavornpinyo, W., Saralamba, S., Aguas, R., Yeung, S., Dondorp, A. M., & White, L. J. (2009). The last man standing is the most resistant: Eliminating artemisinin-resistant malaria in Cambodia. *Malaria Journal*, *8*(1), 31.

Mellouk, S., Berbiguier, N., Druilhe, P., Sedegah, M., Galey, B., Yuan, L., & Hoffman, S. (1990). Evaluation of an in vitro assay aimed at measuring protective antibodies against sporozoites. *Bulletin of the World Health Organization*, *68*(Suppl), 52.

Mellouk, S., Maheshwari, R. K., Rhodes-Feuillette, A., Beaudoin, R. L., Berbiguier, N., Matile, H., & Chigot, J. P. (1987). Inhibitory activity of interferons and interleukin 1 on the development of *Plasmodium falciparum* in human hepatocyte cultures. *The Journal of Immunology*, *139*(12), 4192–4195.

Mikucki, M. A. (2012). *Sensitivity analysis of the basic reproduction number and other quantities for infectious disease models* (PhD thesis). Colorado State University. Libraries.

Miura, K. (2016). Progress and prospects for blood-stage malaria vaccines. *Expert Review of Vaccines*, *15*(6), 765–781.

Moorthy, V. S., Good, M. F., & Hill, A. V. (2004). Malaria vaccine developments. *The Lancet*, *363*(9403), 150–156.

Mota, M. M., Pradel, G., Vanderberg, J. P., Hafalla, J. C., Frevert, U., Nussenzweig, R. S., & Nussenzweig, V. (2001). Migration of plasmodium sporozoites through cells before infection. *Science*, *291*(5501), 141–144.

MVFG (2018). Malaria vaccine technology roadmap. Autoimmunity Research Foundation. Accessed 14/4/2018 from http ://www.who.int/immunization/topics/malaria/vaccine_roadmap/en/.

MVI (2018). Accelerating malaria vaccine development. Accessed 22/2/2018 from http://www.malariavaccine.org/malaria-and-vaccines/need-vaccine.

Nannyonga, B., Mwanga, G., Haario, H., Mbalawata, I. S., & Heilio, M. (2014). Determining parameter distribution in within-host severe *P. falciparum* malaria. *Bio Systems*, *126*, 76–84.

Negal, D., Alemu, A., & Tasew, G. (2016). Malaria vaccine development: Recent advances alongside the barriers. *Journal of Bacteriology and Parasitology*, *7*(6).

Nganou-Makamdop, K., van Gemert, G.-J., Arens, T., Hermsen, C. C., & R. W. Sauerwein (2012). Long term protection after immunization with *P. berghei* sporozoites correlates with sustained IFNγ responses of hepatic CD8+ memory T cells. *PLoS One*, *7*(5), e36508.

Niger, A. M., & Gumel, A. B. (2011). Immune response and imperfect vaccine in malaria dynamics. *Mathematical Population Studies*, *18*(2), 55–86.

Nyabadza, F., Njagarah, J. B., & Smith, R. J. (2013). Modelling the dynamics of crystal meth (tik) abuse in the presence of drug-supply chains in south africa. *Bulletin of Mathematical Biology*, *75*(1), 24–48.

Ogutu, B. R., Apollo, O. J., McKinney, D., Okoth, W., Siangla, J., Dubovsky, F., & Malkin, E. (2009). Blood stage malaria vaccine eliciting high antigen-specific antibody concentrations confers no protection to young children in Western Kenya. *PLoS One*, *4*(3), e4708.

Orenstein, W. A., Wassilak, S. G., Strebel, P. M., Bernier, R. H., & Blackwelder, W. C. (1990). Efficacy of pertussis vaccine. *The Journal of Pediatrics*, *117*(3), 508.

Orwa, T. O., Mbogo, R. W., & Luboobi, L. S. (2018). Mathematical model for hepatocytic-erythrocytic dynamics of malaria. *International Journal of Mathematics and Mathematical Sciences*, *2018*, Article ID 7019868, 18 pages, 2018. https://doi.org/10.1155/2018/7019868.

Ouattara, A., & Laurens, M. B. (2014). Vaccines against malaria. *Clinical Infectious Diseases*, *60*(6), 930–936.

Pandey, A. K., Reddy, K. S., Sahar, T., Gupta, S., Singh, H., Reddy, E. J., & More, K. R. (2013). Identification of a potent combination of key *Plasmodium falciparum* merozoite antigens that elicit strain-transcending parasite-neutralizing antibodies. *Infection and Immunity*, *81*(2), 441–451.

Pilyugin, S. S., & Antia, R. (2000). Modeling immune responses with handling time. *Bulletin of Mathematical Biology*, *62*(5), 869–890.

Plowe, C. V., Alonso, P., & Hoffman, S. L. (2009). The potential role of vaccines in the elimination of falciparum malaria and the eventual eradication of malaria.

Polhemus, M. E., Remich, S. A., Ogutu, B. R., Waitumbi, J. N., Otieno, L., Apollo, S., & Ofori-Anyinam, O. (2009). Evaluation of RTS, S/AS02A and RTS, S/AS01B in adults in a high malaria transmission area. *PLoS One*, *4*(7), e6465.

Renia, L., Marussig, M. S., Grillot, D., Pied, S., Corradin, G., Miltgen, F., Del Giudice, G., & Mazier, D. (1991). In vitro activity of CD4+ and CD8+ T lymphocytes from mice immunized with a synthetic malaria peptide. *Proceedings of the National Academy of Sciences*, *88*(18), 7963–7967.

Risco-Castillo, V., Topçu, S., Marinach, C., Manzoni, G., Bigorgne, A. E., Briquet, S., & Silvie, O. (2015). Malaria sporozoites traverse host cells within transient vacuoles. *Cell Host & Microbe*, *18*(5), 593–603.

Rouzine, I. M., & McKenzie, F. E. (2003). Link between immune response and parasite synchronization in malaria. *Proceedings of the National Academy of Sciences*, *100*(6), 3473–3478.

RTS, S. C. T. P. (2011). First results of phase 3 trial of RTS, S/AS01 malaria vaccine in African children. *New England Journal of Medicine*, *365*(20), 1863–1875.

RTS, S. C. T. P. (2012). A phase 3 trial of RTS, S/AS01 malaria vaccine in African infants. *New England Journal of Medicine*, *367*(24), 2284–2295.

Schwenk, R., Asher, L. V., Chalom, I., Lanar, D., Sun, P., White, K., & Krzych, U. (2003). Opsonization by antigen-specific antibodies as a mechanism of protective immunity induced by *Plasmodium falciparum* circumsporozoite protein-based vaccine. *Parasite Immunology*, *25*(1), 17–25.

Seguin, M. C., Klotz, F. W., Schneider, I., Weir, J. P., Goodbary, M., Slayter, M., & Green, S. J. (1994). Induction of nitric oxide synthase protects against malaria in mice exposed to irradiated *Plasmodium berghei* infected mosquitoes: Involvement of interferon gamma and CD8+ T cells. *Journal of Experimental Medicine*, *180*(1), 353–358.

Selemani, M. A., Luboobi, L. S., & Nkansah-Gyekye, Y. (2016). On stability of the in-human host and in-mosquito dynamics of malaria parasite. *Asian Journal of Mathematics and Applications*, *2016*, Article ID ama0353, 23 pages ISSN 2307-7743.

Selemani, M. A., Luboobi, L. S., & Nkansah-Gyekye, Y. (2017). The in-human host and in-mosquito dynamics of malaria parasites with immune responses. *New Trends in Mathematical Sciences*, *5*(3), 182–207.

Sidhu, A. B. S., Verdier-Pinard, D., & Fidock, D. A. (2002). Chloroquine resistance in *Plasmodium falciparum* malaria parasites conferred by pfcrt mutations. *Science*, *298*(5591), 210–213.

Small, D. S., Cheng, J., & Ten Have, T. R. (2010). Evaluating the efficacy of a malaria vaccine. *The International Journal of Biostatistics*, *6*(2).

Soko, W., Chimbari, M. J., & Mukaratirwa, S. (2015). Insecticide resistance in malaria-transmitting mosquitoes in Zimbabwe: A review. *Infectious Diseases of Poverty*, *4*(1), 46.

Sturm, A., Amino, R., Van de, Sand, Retzlaff, S., Rennenberg, A., Krueger, A., & V. T. Heussler (2006). Manipulation of host hepatocytes by the malaria parasite for delivery into liver sinusoids. *Science*, *313*(5791), 1287–1290.

Sun, P., Schwenk, R., White, K., Stoute, J. A., Cohen, J., Ballou, W. R., & Krzych, U. (2003). Protective immunity induced with malaria vaccine, RTS, S, is linked to *Plasmodium falciparum* circumsporozoite protein-specific CD4+ and CD8+ T cells producing IFN-γ. *The Journal of Immunology*, *171*(12), 6961–6967.

Tabo, Z., Luboobi, L. S., & Ssebuliba, J. (2017). Mathematical modelling of the in-host dynamics of malaria and the effects of treatment. *Journal of Mathematics and Computer Science*, *17*(1), 1–21.
Talman, A. M., Domarle, O., McKenzie, F. E., Ariey, F., & Robert, V. (2004). Gametocytogenesis: The puberty of Plasmodium falciparum. *Malaria Journal*, *3*(1), 24.
Traoré, B., Sangaré, B., & Traoré, S. (2017). A mathematical model of malaria transmission with structured vector population and seasonality. *Journal of Applied Mathematics*, *2017*, Article ID 6754097, 15 pages, 2017. https://doi.org/10.1155/2017/6754097
Tumwiine, J., Hove-Musekwa, S. D., & Nyabadza, F. (2014). A mathematical model for the transmission and spread of drug sensitive and resistant malaria strains within a human population. *ISRN Biomathematics*, *2014*, Article ID 636973, 12 pages, 2014. https://doi.org/10.1155/2014/636973
Tumwiine, J., Mugisha, J., & Luboobi, L. (2008). On global stability of the intra-host dynamics of malaria and the immune system. *Journal of Mathematical Analysis and Applications*, *341*(2), 855–869.
Van den Driessche, P., & Watmough, J. (2002). Reproduction numbers and sub-threshold endemic equilibria for compartmental models of disease transmission. *Mathematical Biosciences*, *180*(1), 29–48.
Villarino, N. (2013). CD8+ T cell responses to plasmodium and intracellular parasites. *Current Immunology Reviews*, *9*(3), 169–178.
Wellems, T. E., & Plowe, C. V. (2001). Chloroquine-resistant malaria. *The Journal of Infectious Diseases*, *184*(6), 770–776.
White, M. T., Bejon, P., Olotu, A., Griffin, J. T., Riley, E. M., Kester, K. E., & Ghani, A. C. (2013). The relationship between RTS,S vaccine-induced antibodies, CD4+ T cell responses and protection against *Plasmodium falciparum* infection. *PLoS One*, *8*(4), E61395.
White, N., Pukrittayakamee, S., Hien, T., Faiz, M., Mokuolu, O., & Dondorp, A. (2014). Malaria. *Lancet*, *383*, 723–35.
White, N. J. (2017). Malaria parasite clearance. *Malaria Journal*, *16*(1), 88.
WHO (2015). *World malaria report 2015*. Geneva: World Health Organization.
WHO (2017a). Malaria fact sheet; 2017. *WHO, Geneva*. Accessed 22/2/2017 from http://www.who.int/mediacentre/factsheets/fs094/en/.
WHO (2017b). *World malaria report 2017*. Geneva: World Health Organization.

Int. J. Appl. Comput. Math (2019) 5:73
https://doi.org/10.1007/s40819-019-0658-3

ORIGINAL PAPER

Uncertainty and Sensitivity Analysis Applied to an In-Host Malaria Model with Multiple Vaccine Antigens

Titus Okello Orwa[1] · Rachel Waema Mbogo[1] · Livingstone Serwadda Luboobi[1]

Abstract
Results of uncertainty and sensitivity analysis have significant epidemiological importance in malaria control. In this paper, the efficient technique of latin hypercube sampling (LHS) and partial rank correlation coefficient is applied to an in-host *Plasmodium falciparum* malaria model. Sensitivity indices of the basic reproduction number are derived using the normalised forward approach. By a theoretical analysis, we show the existence and stability of the model steady states based on threshold value R_0. Our results show that the in-host model is sensitive to variations in the efficacy of malaria vaccines. The rates of parasite to cell invasions, the density of merozoites released per bursting infected erythrocyte and the proportions of merozoites that become gametocytes are highly significant in determining the severity of malaria infection. Moreover, a highly effective vaccine combination is critical for malaria disease elimination goal. This study further shows that the long term precise predictions of the concentrations of infected cells during malaria infection would be difficult until these key parameters are correctly determined. These results are vital in the on-going malaria vaccine development.

Keywords Sensitivity analysis · Hepatocytes · Erythrocytes · *P. falciparum* · Vaccine combination

Introduction

During disease model formulation, we are bound to make simplifications and assumptions on the model itself and on the parameters that represent the different transitions and interactions in the model. Owing to uncertainty on parameter values, it is important to correctly understand the possible effects of the such parameter values to the anticipated model output [21,52]. Uncertainty in the set of parameter values generates variability in the model's predictive capabilities. The lower the number of uncertain parameters in a model, the lower the significance of variability introduced into a model. On the other hand, a higher number of uncertain parameters result into a higher significance of variability introduced [21].

Titus Okello Orwa
torwa@strathmore.edu

[1] Institute of Mathematical Sciences, Strathmore University, P.O Box 59857-00200, Nairobi, Kenya

In-host malaria transmission models have become very complex. Unlike simple models, complex models may best be understood by numerical analysis [8]. Uncertainty and sensitivity analysis are instrumental in analyzing the dynamics of such structurally complex models that experiences high levels of uncertainty in the estimation of their input parameter values. The concept of uncertainty analysis enables us to evaluate the variability in the output [30]. Conversely, a sensitivity analysis helps us to discern important parameters in the dynamics of infection under study. There are three techniques of uncertainty and sensitivity analysis [30]. These include: (i) latin hypercube sampling/partial rank correlation coefficient (LHS/PRCC), (ii) response surface methodology, and (3) differential analysis. The more sophisticated and efficient approach of LHS/PRCC [9,30] that permits synchronous variation of all input variables is considered in this study.

LHS/PRCC sensitivity analysis is a synergy of Latin Hypercube Sampling [38] and the Partial Rank Correlation Coefficient [26]. It aims to identify and rank pivotal model parameters whose uncertainties contribute to prediction imprecision [21]. In this paper, uncertainty and sensitivity analysis is applied to an in-host malaria model subject to malaria vaccines. We endevour to identify influential parameters in determining malaria disease progression and control within the human host. See [2,50] for a rigorous description of the different malaria vaccines.

Malaria is a mosquito-borne infectious disease caused by *Plasmodium* parasite. The disease is typically transmitted through the bite of an infected mosquito vector [20]. The injected sporozoites traverse host dermis and enter the liver hepatocytes for further asexual development. Hepatocite—invading sporozoites, grow, divide mitotically and differentiate into liver merozoites [12]. The release of these merozoites into blood stream marks the beginning of the blood stage cycle. The merozoites invade susceptible erythrocytes to feed on hemoglobin. Like the liver stage, the merozoites also differentiate, causing infected erythrocytes to burst open, releasing more merozoites into blood stream. Higher densities of blood merozoites increases the severity of clinical malaria. The daughter merozoites quickly invade other red blood cells to renew the cycle or develop into male or female gametocytes [13]. This cycle is associated with malaria characteristics symptoms [17,69]. See [6,49] for a detailed discussion on stages of malaria infection. Although malaria is both preventable and curable, severe malaria may lead to seizures, coma and death [22].

Currently, there are more than 30 malaria vaccine candidates under development [68]. These vaccines are generally categorised into: (1) pre-erythrocytic vaccines (PEV), (2) blood stage vaccines (BSV) and (3) transmission blocking vaccines (TBV) [6]. RTS,S/AS01 (also known as Mosquirix) is the only malaria vaccine that has received a positive scientific opinion from the European Medicines Agency (EMA) [18]. This pre-erythrocytic vaccine has been evaluated in large phase 3 trial in sub-Saharan Africa. The vaccine showed a 45.7% (95% CI, 41.7–49.5) efficacy against all episodes of clinical *P. falciparum* malaria across all sites in the 5–17 month age category [54]. Despite positive assessment from EMA, the World Health Organization (WHO) recomments further evaluation of RTS,S/AS01 in a series of pilot implementations before it can be introduced on a wide scale [70]. Nonetheless, an efficacious malaria vaccine forms a crucial component of future malaria control and elimination tool.

Several research studies [1,13,14,23,25,27,29,39–41,55] have focused on understanding the dynamics and control of *P. falciparum* infections. Although most of these models have investigated parameter importance in driving malaria infection, this is mainly based on the basic reproduction number of the model, which often do not have all the model parameters. Sensitivity analysis for the entire parameter space provides the right rigour for parameter evaluation in driving the disease progression. Previous studies [44,71], used parameter-driven LHS/PRCC procedure to ascertain important parameters and their relative importance in

the disease model output. In [21], LHS/PRCC procedure is coupled with the optimal control numerical procedure to simultaneously examine the effects parameters on the objective functional value. In this paper, the LHS/PRCC uncertainty and sensitivity analysis applied to an in-host *P. falciparum* malaria model with vaccine controls. Moreover, multi-component and multi-stage vaccine combinations is evaluated to establish optimal vaccine combinations.

This paper is organised as follows: we provide details of the in-host malaria transmission model and its properties such as non-negativity and boundedness of solutions in "The Model" section. We carry out model analysis including model steady states and their stability conditions in "Model Analysis" section. In "Uncertainty and Sensitivity Analysis" section, we derive sensitivity indices of the basic reproduction number relative to model parameters. We also perform uncertainty and sensitivity analysis of model parameters subject to infective and infected state variables. The existence of model equilibrium points is numerically demonstrated in "Numerical Simulation" section. Numerical evaluation of multi-component and multi-stage vaccine cocktail completes "Numerical Simulation" section. A discussion on epidemiological implications of uncertainty, sensitivity analysis and vaccine combinations completes the paper in "Epidemiological Implications and Conclusion" section.

The Model

We consider an in-host *P. falciparum* malaria model. The model anayses the dynamics of interactions between the human red blood cells (erythrocytes), the liver hepatocytes, the malaria parasite (*P. falciparum*) and the cytotoxic $CD8^+$ T-cells in the presence of multi-component and multi-stage vaccine antigens. The compartmental deterministic model is an extension of in-most malaria model by the authors in [49]. The model is thus composed of nine compartments: the malaria sporozoites $S(t)$, the susceptible hepatocytes $H(t)$, the infected hepatocytes $X(t)$, the susceptible erythrocytes $R(t)$, the infected red blood cells $T(t)$, the malaria gametocytes $G(t)$, the malaria merozoites $M(t)$, unactivated $CD8^+$ T-cells $W_n(t)$ and activated $CD8^+$ T-cells $W_a(t)$.

The activation of $CD8^+$ T-cells is caused by the presence of infected hepatocytes and infected erythrocytes only. This activation is further assumed to occur at a constant rate λ_w for both X and T. Unactivated $CD8^+$ T-cells are produced at a fixed rate Ω from the thymus. Unlike the model in [49], we have assumed that a proportion q of infected erythrocytes and a proportion ρ of infected hepatocytes get eradicated by the $CD8^+$ T-cells before they develop to the bursting stage. The rest of infected hepatocytes develop asexually and burst open to release blood stage merozoites. We assume that some of the newly generated merozoites develop into gametocytes. This proportion is denoted by the parameter π. The commitment to gametocytogenesis is presumably made during the immediately preceding cycle of blood schizogony [13]. These blood floating gametocytes are transmitted to the mosquito vector during feeding, marking the onset of the sporogonic cycle (not considered in this study).

During blood meal, infected mosquito injects Λ sporozoites into the skin of the human host. The sporozoites traverse the skin and invade the hepatocytes H at the rate β_s to generate infected hepatocytes X at the liver stage (see [64] for detailed description of the pre-erythrocytic stage infection). We assume a natural death rate of μ_s for malaria sporozoites. Although hepatocytes are generated at a rate λ_h from the bone marrow, we assume that both the infected and uninfected hepatocytes experience natural death at the rates μ_x and μ_h, respectively.

Three malaria vaccines are considered in this model to reduce the severity of *P. falciparum* malaria infection. These are: pre-erythrocytic vaccine (PEV) (see, [6,7,46]), blood stage

Table 1 Description of the state variables

Variable	Description
$W_n(t)$	Concentration unactivated CD8$^+$ T-cells
$W_a(t)$	Concentration activated CD8$^+$ T-cells
$H(t)$	Concentration of susceptible (uninfected) liver hepatocytes
$X(t)$	Concentration of infected hepatocytes
$S(t)$	Population of malaria sporozoites
$R(t)$	Concentration of susceptible (healthy) erythrocytes
$T(t)$	Concentration of infected erythrocytes
$M(t)$	Population of merozoites in blood
$G(t)$	Concentration of gemetocytes in blood

vaccine (BSV) (see [5,42,47]), and transmission blocking vaccines (TBV) (see [3,28]). The leading PEV, BSV and TBV considered in this study are RTS,S/AS01, merozoite surface protein 3 (MSP3), *P. falciparum* ookinete surface antigens (Pfs25), respectively. The PEV, BSV and TBV vaccines are assumed to posses efficacies denoted by ν, ϱ and χ, respectively, where $0 < \nu < 1$, $0 < \varrho < 1$ and $0 < \chi < 1$.

A summary of the descriptions of the state variables and model parameters is as shown in Tables 1 and 2 , respectively. Furthermore, the compartmental flow diagram for the in-host malaria model is provided in Fig. 1. We are motivated by the structural complexity of the in-host malaria model to apply LHS/PRCC technique for uncertainty and sensitivity analysis. The structural complexity in the model could lead to high levels of uncertainty in approximating the initial values of the input parameters.

Based on the dynamics described in Fig. 1, the following deterministic system describe the dynamics of the in-host malaria infections with multi-stage malaria vaccines:

$$\left.\begin{aligned}
\frac{\mathrm{d}S}{\mathrm{d}t} &= (1-\chi)\Lambda - \mu_s S - \beta_s S H,\\
\frac{\mathrm{d}H}{\mathrm{d}t} &= \lambda_h - \mu_h H - \frac{\beta_s(1-\nu)SH}{1+dW_a},\\
\frac{\mathrm{d}X}{\mathrm{d}t} &= \frac{\beta_s(1-\nu)SH}{1+dW_a} - \mu_x X - \frac{\rho X W_a}{1+\varepsilon_0 X},\\
\frac{\mathrm{d}R}{\mathrm{d}t} &= \lambda_r - \frac{(1-\varrho)\beta_r RM}{1+dW_a} - \mu_r R,\\
\frac{\mathrm{d}T}{\mathrm{d}t} &= \frac{(1-\varrho)\beta_r RM}{1+dW_a} - \mu_t T - \frac{qTW_a}{1+\varepsilon_1 T},\\
\frac{\mathrm{d}M}{\mathrm{d}t} &= \frac{P(1-q)(1-\pi)(1-a)\mu_t T}{1+dW_a} + (1-\rho)(1-b)N\mu_x X - \mu_m M - \beta_r RM,\\
\frac{\mathrm{d}G}{\mathrm{d}t} &= \frac{P(1-q)(1-a)\pi\mu_t T}{1+dW_a} - \mu_g G,\\
\frac{\mathrm{d}W_n}{\mathrm{d}t} &= \Omega - \tau\lambda_w(X+T)W_n - \mu_n W_n,\\
\frac{\mathrm{d}W_a}{\mathrm{d}t} &= \tau\lambda_w(X+T)W_n - \mu_a W_a,
\end{aligned}\right\} \quad (1)$$

Table 2 Table showing model parameters and their descriptions

Parameter symbol	Parameter description
P	Number of merozoites released per bursting erythrocyte
N	Number of merozoites released per bursting hepatocytes
Λ	Injection rate for sporozoites
μ_h	Death rate of susceptible liver hepatocytes
μ_x	Death rate of susceptible erythrocytes
μ_s μ_m	Death rates of sporozoites and merozoites respectively
λ_h	The recruitment rate of hepatocytes
λ_r	The recruitment rate of erythrocytes from the bone marrow
π	A proportion of merozoites that develop into gametocytes per dying infected red blood cell.
ρ	Immunosensitivity of infected hepatocytes
q	Immunosensitivity of infected erythrocytes
β_s, β_r	Rate of infection of hepatocytes and erythrocytes, respectively
b	A rate accounting for PEV-induced reduction of merozoites released per bursting infected hepatocyte
μ_r	Death rate of susceptible erythrocytes
μ_t	Mortality rate of infected erythrocytes
μ_g, μ_m	Mortality rate of gametocytes and merozoites, respectively
χ, ϱ, ν	Vaccine efficacies
d	Inhibition rate of $CD8^+$ T-cells response
Ω	Recruitment rate of unactivated $CD8^+$ T-cells from the thymus
λ_w	Immunogenicity of IRBCs and infected hepatocytes
$1/\varepsilon_0$	A saturation (half) constant for infected hepatocytes
$1/\varepsilon_1$	A saturation (half) constant for infected red blood cells
τ	A rate accounting for vaccine-induced increased generation of activated $CD8^+$T-cells
μ_n, μ_a	Death rates of unactivated and activated $CD8^+$ T-cells respectively
a	A rate accounting for BSV-induced reduction of merozoites released per bursting erythrocyte

with the general initial conditions:

$$S(0) \geq 0, \quad H(0) > 0, \quad X(0) \geq 0, \quad R(0) > 0, \quad T(0) \geq 0, \quad M(0) \geq 0,$$
$$G(0) \geq 0, \quad W_n(0) > 0, \quad W_a(0) \geq 0. \tag{2}$$

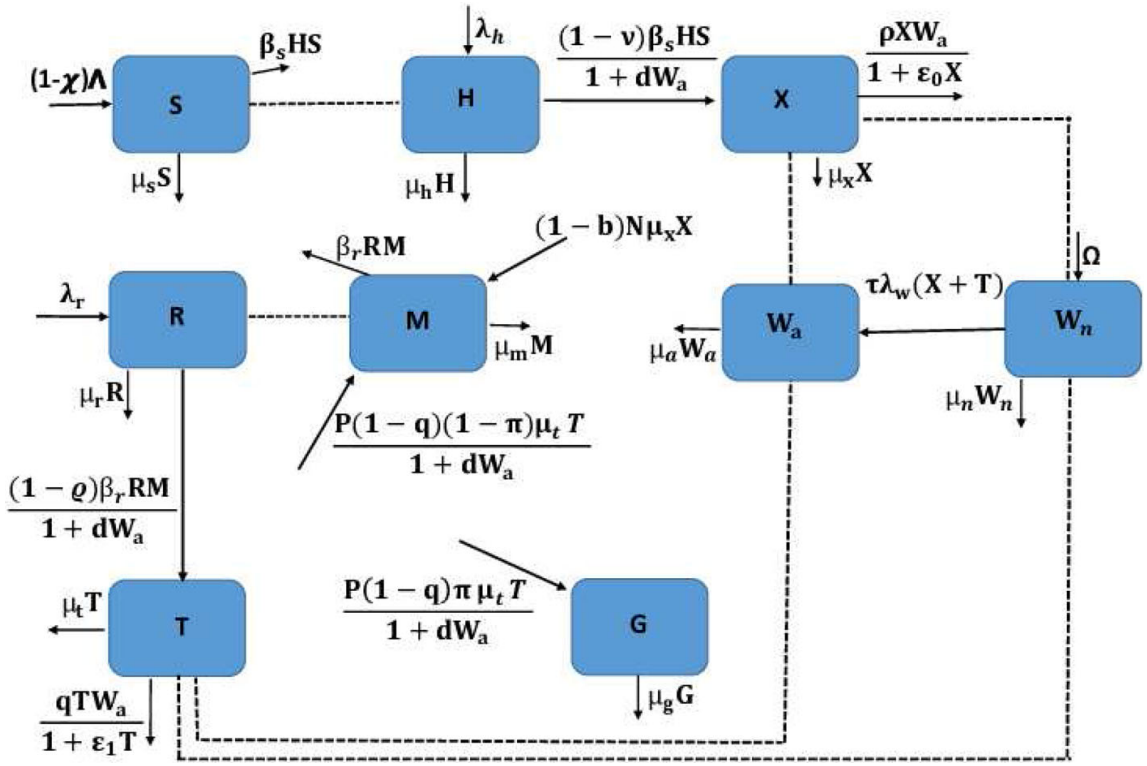

Fig. 1 A compartmental representation of the dynamics of in-host malaria infection with vaccine controls

Properties of the Model

Positivity of Solutions

The long term behaviour of any dynamical system is instrumental in the understanding of the system. The model system (1) monitors changes in the concentrations of blood cells, hepatocytes, malaria parasite and $CD8^+$ T-cells. To warrant biological sense, the state variables of system (1) should be non-negative. Specifically, we show that all solutions of model system (1) with non-negative initial conditions will remain non-negative for all time $t \geq 0$.

Theorem 1 *Given non-negative initial conditions in Eq. (2), the in-host model (1) has a non-negative solution* $(S(t), H(t), X(t), R(t), T(t), M(t), G(t), W_n(t), W_a(t))$*, for all time* $t \geq 0$.

Proof From the first equation in system (1), we can clearly see that

$$\frac{\mathrm{d}S}{\mathrm{d}t} \geq -(\mu_s + \beta_s H)S. \tag{3}$$

Upon integrating equation (3), we get

$$S(t) \geq S_0 \exp\left\{-\int_0^t (\mu_s + \beta_s H(s))\mathrm{d}s\right\}. \tag{4}$$

Therefore, $S(t) \geq 0$ for all $t \geq 0$. □

Similarly, from the last equation in system (1), we have

$$\frac{\mathrm{d}W_a}{\mathrm{d}t} \geq -\mu_a W_a. \tag{5}$$

Upon integrating the separable equation in (5), we obtain

$$W_a(t) = W_a(0)\exp(-\mu_a t) \geq 0.$$

Using the same argument, the rest of the state variables can similarly be shown to be non-negative for all time $t \geq 0$. That is, $H(t) > 0$, $X(t) \geq 0$, $R(t) > 0$, $T(t) \geq 0$, $M(t) \geq 0$, $G(t) \geq 0$ and $W_n(t) > 0\ \forall t \geq 0$. This completes the proof.

Boundedness of Solutions

The non-negative solutions to model system (1) must be well posed in regions of biological sense. We therefore prove that the solutions are bounded.

Let N_r be the sum of the density of susceptible and infected erythrocytes in the host. We thus have $N_r(t) = R(t) + T(t)$. Therefore,

$$\frac{\mathrm{d}N_r}{\mathrm{d}t} = \lambda_r - \mu_r R - \mu_t T - qTW_a, \tag{6}$$

$$\leq \lambda_r - \hat{\mu}N_r \quad \text{where} \quad \hat{\mu} = \min\{\mu_r, \mu_t\}. \tag{7}$$

Using the initial condition $N_r(0) = N_{r0} > 0$, Eq. (7) is solved by integration factor method to obtain

$$N_r(t) \leq \frac{\lambda_r}{\hat{\mu}} + e^{-\hat{\mu}t}\left(N_r(0) - \frac{\lambda_r}{\hat{\mu}}\right).$$

This implies that at any time t, $N_r(t) \leq \max\left\{N_r(0), \frac{\lambda_r}{\hat{\mu}}\right\}$.

Again, let $N_p(t) = S(t) + M(t) + G(t)$, be the sum of malaria parasites at any time t during clinical *P. falciparum* infection. So that,

$$\begin{aligned}\frac{\mathrm{d}N_p}{\mathrm{d}t} &= (1-\chi)\Lambda + \frac{P(1-q)(1-\pi)(1-a)\mu_t T}{1+dW_a} + (1-\rho)(1-b)N\mu_x X \\ &\quad + \frac{P(1-q)(1-a)\pi\mu_t T}{1+dW_a} - \mu_s S - \mu_m M - \mu_g G - \beta_s SH - \beta_r RM, \\ &\leq (1-\chi)\Lambda + \Psi_1(t) - \bar{\mu}N_p \quad \text{where} \quad \bar{\mu} = \min\{\mu_s, \mu_m, \mu_g\}, \quad \text{and} \end{aligned} \tag{8}$$

$$\begin{aligned}\Psi_1(t) &= \frac{P(1-q)(1-\pi)(1-a)\mu_t T}{1+dW_a} + (1-\rho)(1-b)N\mu_x X \\ &\quad + \frac{P(1-q)(1-a)\pi\mu_t T}{1+dW_a}.\end{aligned} \tag{9}$$

Upon solving (8), we obtain:

$$N_p(t) \leq \frac{(1-\chi)\Lambda}{\bar{\mu}} + e^{-\bar{\mu}t}\int_0^t e^{-\bar{\mu}t}\Psi_1(t)\mathrm{d}t + C_1 e^{-\bar{\mu}t},$$

where the constant of integration C_1 is given by,

$$C_1 = \left(N_P(0) - \frac{(1-\chi)\Lambda}{\bar{\mu}}\right) - \int_0^s \Psi_1(0)\mathrm{d}s.$$

Observe that $N_p(t) \leq \max\left\{N_p(0), \frac{(1-\chi)\Lambda}{\bar{\mu}}\right\}$. The above procedure can similarly be applied to the total concentrations of the liver hepatocytes $N_l(t) = H(t) + X(t)$ and that of $CD8^+$ T-cells $N_w(t) = W_a(t) + W_n(t)$ so that we arrive at:

$$\frac{\mathrm{d}N_l}{\mathrm{d}t} \leq \lambda_h - \mu^* N_l \quad \text{and} \quad \frac{\mathrm{d}N_w}{\mathrm{d}t} \leq \Omega - \mu_w N_w, \tag{10}$$

where $\mu^* = \min\{\mu_h, \mu_x\}$ and $\mu_w = \min\{\mu_a, \mu_n\}$.

Upon integrating and simplifying the equations in (10), we get,

$$N_l(t) \leq \max\left\{N_l(0), \frac{\lambda_h}{\mu^*}\right\} \quad \text{and} \quad N_w(t) \leq \max\left\{N_w(0), \frac{\Omega}{\mu_w}\right\} \quad \text{for all time} \quad t \geq 0.$$

Therefore, all feasible solutions of in-host malaria model (1) enter the region:

$$\begin{aligned}\mathcal{D} = \Bigg\{&(S, H, X, R, T, C, M, G, W) \in \mathbb{R}_+^9 : N_r(t) \leq \max\left\{N_r(0), \frac{\lambda_r}{\hat{\mu}}\right\} \\ &N_p(t) \leq \max\left\{N_p(0), \frac{(1-\chi)\Lambda}{\bar{\mu}}\right\}, \\ &N_l(t) \leq \max\left\{N_l(0), \frac{\lambda_h}{\mu^*}\right\}, N_w(t) \leq \max\left\{N_w(0), \frac{\Omega}{\mu_w}\right\}\Bigg\}.\end{aligned} \tag{11}$$

which is a positively invariant set of model system (1). This implies that all solutions in $\mathcal{D}$ remain in $\mathcal{D} \quad \forall t \geq 0$. It thus suffices to study the dynamics of model system (1) in $\mathcal{D}$.

Model Analysis

Existence and Stability Analysis of Disease-Free Equilibrium Point (DFE)

The disease-free equilibrium E_0 occurs when there is no *P. falciparum* infection within the human host. At E_0, $\Lambda = 0$ and there are no activated $CD8^+$-T cells; that is, $W_a = 0$. By setting the right hand-side of system (1) to zero, we obtain the following disease free equilibrium:

$$E_0 = (S^0, H^0, X^0, R^0, T^0, M^0, G^0, W_n^0, W_a^0) = \left(0, \frac{\lambda_h}{\mu_h}, 0, \frac{\lambda_r}{\mu_r}, 0, 0, 0, \frac{\Omega}{\mu_n}, 0\right). \tag{12}$$

The disease-free steady state is very crucial in the understanding of in-host malaria infection dynamics. In order to eradicate in-host malaria, we have to identify and establish necessary conditions for E_0 to be stable. This stability could be achieved through the use of effective anti-malarial drugs such as ACT or by using highly efficacious *Plasmodium falciparum* malaria vaccines.

Next, we apply the next generation matrix (NGM) approach (see [14,63] for detailed explanation of this technique) to compute the basic reproduction number R_0 of the in-host model (1). The NGM method presumes the local stability of E_0 for $R_0 < 1$ and instability for $R_0 > 1$. R_0 is the spectral radius of the next generation matrix (FV^{-1}) of system (1); that is, $R_0 = \rho(\mathrm{FV}^{-1})$. Adopting the matrix notations in [63], the matrices F and V are respectively given by:

$$\mathrm{F} = \begin{pmatrix} 0 & 0 & 0 & 0 & 0 & 0 & 0 \\ 0 & \frac{(1-\nu)\beta_s\lambda_h}{\mu_h} & 0 & 0 & 0 & 0 & 0 \\ 0 & 0 & 0 & \frac{(1-\varrho)\beta_r\lambda_r}{\mu_r} & 0 & 0 & 0 \\ 0 & 0 & 0 & 0 & 0 & 0 & 0 \\ 0 & 0 & 0 & 0 & 0 & 0 & 0 \\ 0 & 0 & 0 & 0 & 0 & 0 & 0 \\ 0 & 0 & 0 & 0 & 0 & 0 & 0 \end{pmatrix} \tag{13}$$

and

$$\mathrm{V} = \begin{pmatrix} \frac{\beta_s\lambda_h}{\mu_h} + \mu_s & 0 & 0 & 0 & 0 & 0 & 0 \\ 0 & \mu_x & 0 & 0 & 0 & 0 & 0 \\ 0 & 0 & \mu_t & 0 & 0 & 0 & 0 \\ 0 & -(1-\rho)(1-b)N\mu_x & \mathcal{A}_1 & \frac{\beta_r\lambda_r}{\mu_r} + \mu_m & 0 & 0 & 0 \\ 0 & 0 & -P\pi(1-a)(1-q)\mu_t & 0 & \mu_g & 0 & 0 \\ 0 & \frac{\tau\Omega\lambda_w}{\mu_n} & \frac{\tau\Omega\lambda_w}{\mu_n} & 0 & 0 & \mu_n & 0 \\ 0 & -\frac{\tau\Omega\lambda_w}{\mu_n} & -\frac{\tau\Omega\lambda_w}{\mu_n} & 0 & 0 & 0 & \mu_a \end{pmatrix}, \tag{14}$$

where $\mathcal{A}_1 = -P(1-\pi)(1-q)(1-a)\mu_t$.

Thus, the basic reproduction number R_0 is given by

$$R_0 = \rho(FV^{-1}) = \max\{R_{01}, R_{02}\}$$

where

$$\mathrm{R}_{01} = \frac{(1-\nu)\beta_s\lambda_h}{\mu_h\mu_x} \tag{15}$$

and

$$\mathrm{R}_{02} = \frac{P(1-\pi)(1-a)(1-\varrho)(1-q)\beta_r\lambda_r}{\beta_r\lambda_r + \mu_m\mu_r}. \tag{16}$$

Observe that R_{01} is the contribution of new cell invasions at the liver stage due to mortile sporozoites and R_{02} is the contributions of new cell invasions at the blood stage due to merozoite parasites. From Eqs. (15) and (16), it is evident that new cell invasions occur both at the liver stage (as depicted by R_{01}) and at the blood stage (as depicted by R_{02}). This implies that clinical control of *P. falciparum* malaria should target the parasite at both stages of its life cycle within the human host. An anti-malarial drug with the capacity to eradicate the sporozoites at the pre-erythrocytic stage and merozoites at the erythrocytic stage is most recommended. Furthermore, malaria vaccine development should equally focus on both stages of parasite development. A novel malaria vaccine should begin parasite eradication from the pre-erythrocytic stage and this should continue to the blood stage. This result is very important to the ongoing research and development of malaria vaccines.

The global stability of the disease-free equilibrium is established using a suitable Lyapunov candidate function [34,35,48]. We thus have the following theorem.

Theorem 2 *The disease-free equilibrium E_0 is globally asymptotically stable in R_+^9 if $R_0 < 1$.*

Proof Let $V(X, T, S, M, G) = \psi_1 X + \psi_2 T + \psi_3 S + \psi_4 M + \psi_5 G$ be a candidate Lyapunov function for some non-negative coefficients ψ_1, ψ_2, ψ_3, ψ_4 and ψ_5. The derivative of V with respect to time is by

$$
\begin{aligned}
\frac{\mathrm{d}V}{\mathrm{d}t} &= \psi_1\frac{\mathrm{d}X}{\mathrm{d}t} + \psi_2\frac{\mathrm{d}T}{\mathrm{d}t} + \psi_3\frac{\mathrm{d}S}{\mathrm{d}t} + \psi_4\frac{\mathrm{d}M}{\mathrm{d}t} + \psi_5\frac{\mathrm{d}G}{\mathrm{d}t},\\
&= \psi_1\left(\frac{\beta_s(1-\nu)SH}{1+dW_a} - \mu_x X - \frac{\rho X W_a}{1+\varepsilon_0 X}\right) + \psi_2\left(\frac{(1-\varrho)\beta_r RM}{1+dW_a} - \mu_t T - \frac{qTW_a}{1+\varepsilon_1 T}\right)\\
&\quad + \psi_3\left((1-\chi)\Lambda - \mu_s S - \beta_s SH\right)\\
&\quad + \psi_4\left(\frac{P(1-q)(1-\pi)(1-a)\mu_t T}{1+dW_a} + (1-\rho)(1-b)N\mu_x X - \mu_m M - \beta_r RM\right)\\
&\quad + \psi_5\left(\frac{P(1-q)(1-a)\pi\mu_t T}{1+dW_a} - \mu_g G\right),\\
&= \left(-\mu_x\left(N\psi_4(b(-\rho)+b+\rho-1)+\psi_1\right) - \frac{\Omega}{\mu_n}(\rho\psi_1+q\psi_2)\right)X\\
&\quad + \left(-\mu_t\left((a-1)P(q-1)\left((\pi-1)\psi_4 - \pi\psi_5\right)+\psi_2\right)\right)T\\
&\quad + \left(\psi_3(-\mu_s) - \frac{\lambda_h}{\mu_h}\left((\nu-1)\psi_1+\psi_3\right)\beta_s\right)S\\
&\quad + \left(\psi_4(-\mu_m) - \frac{\lambda_r}{\mu_r}\left((e-1)\psi_2+\psi_4\right)\beta_r\right)M\\
&\quad + (-\mu_g\psi_5)G.
\end{aligned}
$$

□

Setting the coefficients of X, T, S, M and G to zero and solving, we get

$$
\begin{aligned}
\psi_1 &= \frac{N(1-b)(1-\rho)\mu_x(1-\varrho)\beta_r\lambda_r\mu_a^2 - q\Omega(\beta_r\lambda_r+\mu_m\mu_r)\mu_a}{(1-\varrho)\beta_r\lambda_r\mu_a(\rho\Omega+\mu_x\mu_a)}\psi_4,\\
\psi_3 &= \frac{\frac{\lambda_h}{\mu_h}(1-\nu)\beta_s}{\frac{\lambda_h}{\mu_h}\beta_s+\mu_s}\left[\frac{N(1-b)(1-\rho)\mu_x(1-\varrho)\beta_r\lambda_r\mu_a^2 - q\Omega(\beta_r\lambda_r+\mu_m\mu_r)\mu_a}{(1-\varrho)\beta_r\lambda_r\mu_a(\rho\Omega+\mu_x\mu_a)}\right]\psi_4,\\
\psi_2 &= \left[\frac{\frac{\lambda_r}{\mu_r}\beta_r+\mu_m}{(1-\varrho)\frac{\lambda_r}{\mu_r}\beta_r}\right]\psi_4 \quad \text{and} \quad \psi_5 = \frac{\frac{1}{1-\varrho} - P(1-a)(1-\pi)(1-q) + \frac{\mu_m\mu_r}{\beta_r\lambda_r(1-\varrho)}}{\pi P(1-a)(1-q)}\psi_4.
\end{aligned}
$$

Using these coefficients, the time derivatives of the Lyapunov function is given as

$$
\begin{aligned}
\frac{\mathrm{d}V}{\mathrm{d}t} = &-\frac{(q+(1-b)(1-\varrho)N(1-\rho)\rho)\beta_r\lambda_r+q\mu_m\mu_r)(\mu_a+\mu_n)\mu_x}{(1-\varrho)\beta_r\lambda_r\mu_n(\rho\Omega+\mu_a\mu_x)}X\\
&-\frac{\mu_m\mu_r\mu_t(1+(1-\varrho)^2\lambda_r^2)}{(1-e)\beta_r\lambda_r}T - \frac{\mu_g(1-\varrho)\lambda_r\mu_m\mu_r}{\pi\beta_r(1-a)(1-q)}G(1-R_0).
\end{aligned}
\tag{17}
$$

If $R_0 < 1$ in (17) then $[\mu_g(1-\varrho)\lambda_r\mu_m\mu_r]/[\pi\beta_r(1-a)(1-q)](1-R_0) > 0$. We thus obtain $\frac{\mathrm{d}V}{\mathrm{d}t} \leq 0$. Furthermore, $\frac{\mathrm{d}V}{\mathrm{d}t} = 0$ if and only if $T = X = G = 0$. Therefore, V is a Lyapunov function in $\mathcal{D}$. Given that $\mathcal{D}$ is positively invariant and attracting, it follows that the maximum invariant set in $\{(S, H, X, R, T, M, G, W_n, W_a) \in \mathcal{D} : \dot{V} = 0\}$ is the singleton E_0. By LaSalle's Invariant principle [33], E_0 is globally asymptotically stable in $\mathcal{D}$ provided that $R_0 < 1$.

The Malaria Persistent Steady State

We establish the malaria persistent equilibrium E_p for model system (1) in the presence of $CD8^+$ T-cells by equating the right hand side of system (1) to zero. Using Mathematica software [31], model system (1), exhibits a malaria-persistent equilibrium point

$$E_p = (S^{\dagger}, H^*, X^*, R^*, T^*, M^*, G^*, W_n^*, W_a^*),$$

where

$$H^* = \frac{(1+dW_a^*)\lambda_h}{(1-\nu)\beta_s S^* + (1+dW_a^*)\mu_h}, \tag{18}$$

$$R^* = \frac{(1+dW_a^*)\lambda_r}{(1-\varrho)\beta_r M^* + (1+dW_a^*)\mu_r}, \tag{19}$$

$$W_n^* = \frac{\Omega}{\tau\lambda_w(X^*+T^*)+\mu_n}, \tag{20}$$

$$W_a^* = \frac{\tau\lambda_w(X^*+T^*)W_n^*}{\mu_a}, \tag{21}$$

$$G^* = \frac{P(1-q)(1-a)\pi\mu_t T^*}{\mu_g(1+dW_a^*)}, \tag{22}$$

$$M^* = \frac{(1+dW_a^*)[(1-b)^2(1-\varrho)NX^*\beta_r\mu_m\mu_x - (1+dW_a^*)\mu_r] \pm \sqrt{\Delta}}{2(1-\varrho)(1+dW_a^*)\beta_r}, \quad \text{where}$$

$$\begin{aligned}\Delta_m = (1+dW_a^*)\big\{&(-(e-1)\beta_r(-4(1-\pi)(1-a)P(1-q)T^*\mu_t \\ &+(1-b)^2NX^*(1+dW_a^*)\beta_r\mu_x(4(1+dW_a^*)\lambda_r + (1-b)^2(1-e)NX^*\mu_m^2\mu_x)) \\ &-2(1-b)^2(1-e)NX^*(1+dW_a^*)^2\mu_m\beta_r\mu_r\mu_x + (1+dW_a^*)^3\mu_r^2\big\},\end{aligned} \tag{23}$$

$$S^* = \frac{1}{-2(1-\nu)\beta_s\nu_s}\left\{-\Delta_s \pm \sqrt{\Delta_s^2 + 4((1-\nu)\beta_s\mu_s)((1-\chi)\Lambda(1+dW_a^*)\mu_h)}\right\},$$

$$\text{where} \quad \Delta_s = \beta_s(\Lambda(1-\chi)(1-\nu) - (1+dW_a^*)\lambda_h) - (1+dW_a^*)\mu_h\mu_s, \tag{24}$$

$$T^* = \frac{1}{-2\epsilon_1((1-\varrho)\beta_r M^* + (1+dW_a^*)\mu_r)\mu_t}\left\{-\Delta_t \pm \sqrt{\Delta_T^*}\right\},$$

$$\text{where} \quad \Delta_t = \beta_s(\Lambda(1-\chi)(1-\nu) - (1+dW_a^*)\lambda_h) - (1+dW_a^*)\mu_h\mu_s;$$

$$\Delta_T^* = \Delta_t^2 + 4\epsilon_1\mu_t((1-\varrho)\beta_r M^* + (1+dW_a^*)\mu_r)(\beta_r\lambda_r(1-\varrho)M^*) \quad \text{and} \tag{25}$$

$$X^* = \frac{\Delta_x \pm \sqrt{\Delta_x^2 + 4\epsilon_0((1-\nu)\beta_s S^* + (1+dW_a^*)\mu_h)\mu_x)(1-\nu)\beta_s\lambda_h S^*}}{2\epsilon_0((1-\nu)\beta_s S^* + (1+dW_a^*)\mu_h)\mu_x}, \quad \text{where}$$

$$\begin{aligned}\Delta_x = &(1-\nu)(\epsilon_0\lambda_h - \mu_x)\beta_s S^* - d\rho W_a^{*2}\mu_h - \mu_h\mu_x \\ &- W_a^*((1-\nu)\rho\beta_s S^* + \mu_h(\rho + d\mu_x)).\end{aligned} \tag{26}$$

Based on the formulated model in Eq. (1), the activated CD8$^+$ T-cells only exists due to the presence of infected erythrocytes and infected liver hepatocytes. Hence, in the absence of malaria infection ($X = T = 0$), $W_a = 0$. Moreover, non of the malaria parasites exists; that is $S^* = M^* = G^* = 0$. We further observe that when $S^* = M^* = X^* = T^* = W_a^* = 0$, the susceptible erythrocytes, susceptible hepatocytes and the unactivated CD8$^+$ T-cells become $H^* = \frac{\lambda_h}{\mu_h}$, $R^* = \frac{\lambda_r}{\mu_r}$ and $W_n^* = \frac{\Omega}{\mu_n}$ respectively. We thus arrive at an equilibrium point called the disease free equilibrium point of model (1) illustrated in Eq. (12). From the above computations, it is evident that the analytical expressions of E_p is too complex. We shall therefore provide a numerical illustration of the model equilibrium points in "Numerical Simulation" section.

Theorem 3 *The malaria persistent steady state E_p is locally asymptotically stable if $R_0 > 1$ in the interior of the biologically feasible region $\mathcal{D}$.*

Proof The stability of the malaria persistent equilibrium E_p (when $R_0 > 1$ but close to 1) is proved using the center manifold theory (CMT) presented by Castillo-Chavez and Song in [11]. Adopting the notations used in [11] and without re-stating the theorem, we calculate the values of arguments **a** and **b**. The signs (+ or −) of **a** and **b** determine the local dynamics of system (1) around E_p [66].

Suppose we consider β_* to be our bifurcation parameter, then at $R_0 = 1$, we have $\beta_* = \max\{\beta_s^*, \beta_r^*\}$, where

$$\beta_r^* = \frac{\mu_m \mu_r}{[P(1-q)(1-\pi)(1-\varrho)(1-a)-1]\lambda_r} \quad \text{and} \quad \beta_s^* = \frac{\mu_h \mu_x}{(1-\nu)\lambda_h}. \tag{27}$$

□

In applying the CMT, we begin by transforming the state variables $(S, H, X, R, T, M, G, W_n, W_a)$ into $(x_1, x_2, x_3, x_4, x_5, x_6, x_7, x_8, x_9)$ respectively. The model system (1), is hence represented as $\frac{dg}{dt} = g(\mathbf{x})$, where $\mathbf{x} = (x_1, x_2, x_3, x_4, x_5, x_6, x_7, x_8, x_9)$. The model system (1) thus becomes

$$\left.\begin{aligned}
\dot{x}_1 &= (1-\chi)\Lambda - \mu_s x_1 - \beta_s x_1 x_2,\\
\dot{x}_2 &= \lambda_h - \mu_h x_2 - \frac{\beta_s(1-\nu)x_1 x_2}{1+dx_9},\\
\dot{x}_3 &= \frac{\beta_s(1-\nu)x_1 x_2}{1+dx_9} - \mu_x x_3 - \frac{\rho x_3 x_9}{1+\varepsilon_0 x_3},\\
\dot{x}_4 &= \lambda_r - \frac{(1-\varrho)\beta_r x_4 x_6}{1+dx_9} - \mu_r x_4,\\
\dot{x}_5 &= \frac{(1-\varrho)\beta_r x_4 x_6}{1+dx_9} - \mu_t x_5 - \frac{q x_5 x_9}{1+\varepsilon_1 x_5},\\
\dot{x}_6 &= \frac{P(1-q)(1-\pi)(1-a)\mu_t x_5}{1+dx_9} + (1-\rho)(1-b)N\mu_x x_3 - \mu_m x_6 - \beta_r x_4 x_6,\\
\dot{x}_7 &= \frac{P(1-q)(1-a)\pi\mu_t x_5}{1+dx_9} - \mu_g x_7,\\
\dot{x}_8 &= \Omega - \tau\lambda_w(x_3+x_5)x_8 - \mu_n x_8,\\
\dot{x}_9 &= \tau\lambda_w(x_3+x_5)x_8 - \mu_a x_9,
\end{aligned}\right\} \tag{28}$$

such that;
$x_1(0) \geq 0, x_2(0) \geq 0, x_3(0) \geq 0, x_4(0) \geq 0, x_5(0) \geq 0, x_6(0) \geq 0, x_7(0) \geq 0, x_8(0) \geq 0, x_9(0) \geq 0$.

The new model system (28) with the bifurcation point β_* has a simple zero eigenvalue. This attribute enables us to use the CMT to analyze the stability of system (28) near $\beta_* = \max\{\beta_s^*, \beta_r^*\} = \max\{\beta_s, \beta_r\}$.

Therefore, a right eigenvector $w = [w_1, w_2, w_3, w_4, w_5, w_6, w_7, w_8, w_9]^T$ associated with the simple zero eigenvalue is obtained from the linearization matrix corresponding to the zero eigenvector as follows:

$$\begin{pmatrix} -A_2 & 0 & 0 & 0 & 0 & 0 & 0 & 0 & 0 \\ -A_3 & -\mu_h & 0 & 0 & 0 & 0 & 0 & 0 & \\ A_3 & 0 & -\mu_x & 0 & 0 & 0 & 0 & 0 & 0 \\ 0 & 0 & 0 & -\mu_r & 0 & -A_4 & 0 & 0 & 0 \\ 0 & 0 & 0 & 0 & -\mu_t & A_4 & 0 & 0 & 0 \\ 0 & 0 & 0 & 0 & A_0 & -A_5 & 0 & 0 & 0 \\ 0 & 0 & 0 & 0 & A_1 & 0 & -\mu_g & 0 & 0 \\ 0 & 0 & -\frac{\tau\Omega\lambda_w}{\mu_n} & 0 & -\frac{\tau\Omega\lambda_w}{\mu_n} & 0 & 0 & -\mu_n & 0 \\ 0 & 0 & \frac{\tau\Omega\lambda_w}{\mu_n} & 0 & \frac{\tau\Omega\lambda_w}{\mu_n} & 0 & 0 & 0 & -\mu_a \end{pmatrix} \begin{pmatrix} w_1 \\ w_2 \\ w_3 \\ w_4 \\ w_5 \\ w_6 \\ w_7 \\ w_8 \\ w_9 \end{pmatrix} = \begin{pmatrix} 0 \\ 0 \\ 0 \\ 0 \\ 0 \\ 0 \\ 0 \\ 0 \\ 0 \end{pmatrix} \tag{29}$$

where $A_0 = (1-a)P(1-\pi)(1-q)\mu_t$, $A_1 = (1-a)P\pi(1-q)\mu_t$, $A_2 = \left(\frac{\beta_s\lambda_h}{\mu_h} + \mu_s\right)$, $A_3 = \frac{(1-\nu)\beta_s\lambda_h}{\mu_h}$, $A_4 = \frac{(1-\varrho)\beta_r\lambda_r}{\mu_r}$ and $A_5 = \left(\frac{\beta_r\lambda_r}{\mu_r} + \mu_m\right)$.

Solving for the right eigenvectors, we obtain

$$w_5 = \frac{-\left(\frac{\beta_r\lambda_r}{\mu_r} + \mu_m\right)}{(1-a)P(1-\pi)(1-q)\mu_t}, \quad w_7 = \frac{-(1-a)P\pi(1-q)\mu_t}{\mu_g} + \frac{\left(\frac{\beta_r\lambda_r}{\mu_r} + \mu_m\right)}{(1-a)P(1-\pi)(1-q)\mu_t},$$

$$w_4 = -\frac{(1-\varrho)\beta_r\lambda_r}{\mu_r^2}, \quad w_8 = \frac{\tau\Omega\lambda_w}{(1-a)P(1-\pi)(1-q)\mu_t\mu_n^2}\left(\frac{\beta_r\lambda_r}{\mu_r} + \mu_m\right), w_6 = 1,$$

$$w_9 = -\frac{\tau\Omega\lambda_w}{\mu_a\mu_n}\left(\frac{\beta_r\lambda_r}{\mu_r} + \mu_m\right), \quad w_1 = w_2 = w_3 = 0.$$

Similarly, upon solving for the left eigenvector $v = [v_1, v_2, v_3, v_4, v_5, v_6, v_7, v_8, v_9]^T$ associated with the zero eigenvalue in system (28), we obtain

$$v_1 = v_2 = v_3 = v_4 = 0, \quad v_5 = P(1-a)(1-\pi)(1-q), v_6 = 1, v_7, v_8, v_9 = 0.$$

Next, we calculate the values of **a** and **b** as described in [11]. That is,

$$\mathbf{a} = \sum_{i,j,k=1}^{9} v_k w_i w_j \frac{\partial^2 g_k(\mathbf{O}, 0)}{\partial x_i \partial x_j} \quad \text{and} \quad \mathbf{b} = \sum_{i,k=1}^{9} v_k w_i \frac{\partial^2 g_k(\mathbf{O}, 0)}{\partial x_i \partial \beta_*}. \tag{30}$$

The non-zero partial derivatives of $g(x)$ in system (28) associated with the argument **a** are given as

$$\frac{\partial^2 g_1}{\partial x_1 \partial x_2} = -\beta_s, \quad \frac{\partial^2 g_2}{\partial x_1 \partial x_2} = -(1-\nu)\beta_s, \quad \frac{\partial^2 g_2}{\partial x_1 \partial x_9} = d(1-\nu)\frac{\lambda_h}{\mu_h}\beta_s,$$

$$\frac{\partial^2 g_4}{\partial x_4 \partial x_6} = -(1-\varrho)\beta_r,$$

$$\frac{\partial^2 g_4}{\partial x_6 \partial x_9} = \frac{d(1-\varrho)\beta_r\lambda_r}{\mu_r}, \quad \frac{\partial^2 g_5}{\partial x_5 \partial x_9} = -q, \quad \frac{\partial^2 g_5}{\partial x_4 \partial x_6} = (1-\varrho)\beta_r,$$

$$\frac{\partial^2 g_5}{\partial x_6 \partial x_9} = \frac{-d(1-\varrho)\beta_r\lambda_r}{\mu_r},$$

$$\frac{\partial^2 g_6}{\partial x_4 \partial x_6} = -\beta_r, \quad \frac{\partial^2 g_6}{\partial x_5 \partial x_9} = P(1-a)(1-\pi)(1-q)d\mu_t,$$

$$\frac{\partial^2 g_7}{\partial x_5 \partial x_9} = P\pi(1-a)(1-q), \quad \frac{\partial^2 g_8}{\partial x_3 \partial x_8} = \frac{\partial^2 g_8}{\partial x_5 \partial x_8} = -\tau\lambda_w,$$
$$\frac{\partial^2 g_9}{\partial x_3 \partial x_8} = \frac{\partial^2 g_9}{\partial x_5 \partial x_8} = \tau\lambda_w.$$

Thus, the expression for **a** is:

$$\begin{aligned}\mathbf{a} &= v_5 w_5 w_9 \frac{\partial^2 g_5}{\partial x_5 \partial x_9} + v_5 w_4 w_6 \frac{\partial^2 g_5}{\partial x_4 \partial x_6} + v_5 w_6 w_9 \frac{\partial^2 g_5}{\partial x_6 \partial x_9} + v_6 w_4 w_6 \frac{\partial^2 g_6}{\partial x_4 \partial x_6} \\ &\quad + v_6 w_5 w_9 \frac{\partial^2 g_6}{\partial x_5 \partial x_9} \\ &= -\left(\frac{\beta_r \lambda_r}{\mu_r} + \mu_m\right)\left(\frac{d(1-\varrho)\beta_r \lambda_r}{\mu_r}\right)\left(\frac{P(1-a)(1-\pi)(1-q)\mu_t \tau \Omega \lambda_w}{\mu_a \mu_t \mu_n}\right) < 0. \quad (31)\end{aligned}$$

We repeat the above procedure in computing the values of **b**. The non-zero partial derivatives of $g(x)$ associated with **b** are given by

$$\frac{\partial^2 g_1}{\partial x_1 \partial \beta_*} = -\frac{\lambda_h}{\mu_h}, \quad \frac{\partial^2 g_2}{\partial x_1 \partial \beta_*} = \frac{-(1-\nu)\lambda_h}{\mu_h}, \quad \frac{\partial^2 g_3}{\partial x_1 \partial \beta_*} = \frac{(1-\nu)\lambda_h}{\mu_h},$$
$$\frac{\partial^2 g_4}{\partial x_6 \partial \beta_*} = \frac{-(1-\varrho)\lambda_r}{\mu_r},$$
$$\frac{\partial^2 g_5}{\partial x_6 \partial \beta_*} = \frac{(1-\varrho)\lambda_r}{\mu_r}, \quad \frac{\partial^2 g_6}{\partial x_6 \partial \beta_*} = \frac{-\lambda_r}{\mu_r}.$$

Upon substituting these derivatives into Eq. (30), it follows that

$$\begin{aligned}\mathbf{b} &= v_5 w_6 \frac{\partial^2 g_5}{\partial x_6 \partial \beta_*} + v_6 w_6 \frac{\partial^2 g_6}{\partial x_6 \partial \beta_*} \\ &= \frac{\lambda_r}{\mu_r}\left(P(1-a)(1-\pi)(1-q)(1-\varrho) + 1\right) > 0. \quad (32)\end{aligned}$$

Thus, a is positive ($a > 0$) and b is negative ($b < 0$). Based on item (iv) of theorem 2 in [11], the malaria persistent equilibrium E_p is locally asymptotically stable for $R_0 > 1$, but close to 1.

Uncertainty and Sensitivity Analysis

Sensitivity Analysis of Infected and Infective States of the In-Host Malaria Model

The in-host malaria model in this paper has numerous unknown parameters, coupled with limited data. Therefore, there is a considerable uncertainty [9] in estimating the values of the 30 transmission parameters in model system (1). The uncertainty in the input values allows significant variability in the model predictions of the future malaria parasite density within the human host and the concentrations of the infected red blood cells and hence the severity of clinical *P. falciparum* malaria. Consequently, we perform the LHS/PRCC sensitivity analysis to evaluate variabilities in model predictions. With LHS/PRCC technique, we are able to explore the entire parameter space of model (1), with minimal computer simulation.

We simultaneously examine the effects of the LHS parameters on the two infected state variables: the infected liver hepatocytes $X(t)$ and the infected erythrocytes $T(t)$ and the

three infective parasite states: sporozoite $S(t)$, merozoites $M(t)$ and Gametocytes $G(t)$ in model system (1). The PRCCs are used to identify the key parameters contributing to the imprecision in predicting the future density of infected liver hepatocytes and infected red blood cells [9].

The process of performing LHS on disease models is described elsewhere [8,38] and references cited therein. Following PRCC methodology described in [52], we rank the LHS parameters in the LHS matrix together with the outcome measures: $T(t)$, $X(t)$, $M(t)$, $G(t)$ and $S(t)$. Two linear regression models are generated in response to each parameter and outcome measure. A Pearson rank correlation coefficient for the residuals from the two regression models gives the PRCC values for that specific parameter. Due to lack of data on the distribution function, we consider a uniform distribution for all model parameters in Table 3.

Results of Analyzing the LHS/PRCC for the In-Host Malaria Model

Using 1000 runs of Latin hypercube sampling, the PRCC and p value data from the 30 parameters in model system (1) are summarized in **Appendices A, B, C, D** and **E**. The PRCC and p values are computed based on the regression coefficient for outcome measures ($T(t)$, $X(t)$, $M(t)$, $S(t)$ and $G(t)$ and displayed in Tables 5, 6, 7 8 and 9 , respectively. The size of PRCC shows the importance of the uncertainty in estimating the value of the specific variable in contributing to the prediction imprecision [9]. The PRCC sign (+ or −), however, shows the qualitative relationship between the input parameter and the output variables. Parameters with large PRCC values (PRCC from 0.5 to 1 or PRCC from -1 to -0.5) coupled with a corresponding small p value (p value < 0.05) are considered as the most influential [21].

A slight change in a highly influential parameter is likely to produce a significant change in the outcome variable. The symbol $(*)$ indicates less influential parameters with p values < 0.05 and PRCC values in the range (-0.1 to -0.49 or 0.1 to 0.49). Further, the symbol $(**)$ is used to indicate moderately critical parameters in prediction imprecision, and have p value < 0.05 and PRCC values in the range (-0.5 to -0.79 or 0.5 to 0.79). Lastly, the symbol $(***)$ indicates the most critical and likely contributors to uncertainty, with PRCC values in the range (-0.8 to -0.99 or $+0.8$ to $+0.99$).

Results in Appendices A, B, C, D and E indicate that the rate of invasion by merozoites β_r, the rate of invasion of liver hepatocytes β_s, malaria vaccine efficacies (ϱ, ν, and χ) and the recruitment rates for the hepatocyte and erythrocytes λ_h and λ_r respectively are statistically significant in determining the variation of concentrations of erythrocytes, infected hepatocytes and the density of malaria parasites (sporozoites, merozoites and gametocytes). The infected erythocyte burst size P and the number of merozoites released per bursting sporozoite N is shown to significantly increase the the density of the merozoites and the concentration of infected red blood cells T in blood. Clinical malaria controls should thus target these infected cells for eradication before they mature to bursting stage.

Moreover, from Appendices A and D, the proportion of merozoites that develop into gametocytes per dying infected erythrocyte π and immunosensitivity of infected erythrocytes q are shown to have significant influence in determining the concentrations of gametocytes and merozoites, respectively, during clinical *P. falciparum* infection. An efficacious blood stage vaccine coupled with a transmission blocking vaccine antigens has the potential of reducing the density of gametocytes during clinical malaria. This reduces parasite transmission to mosquito vector.

Table 3 Table showing the numerical values of model parameter values used in sensitivity analysis and numerical simulations

Symbol	Value	Min	Max	Unit	Source
Λ	30	20	35	Sporozoites/day	[56]
μ_s	1.2	0.8	1.5	/day	[56]
λ_r	3E5	3E3	3E6	cells/ml/day	[36]
λ_h	3E5	3E3	3E6	cells/μl^{-1}/day	[61]
β_r	8E−5	8E−7	8E−3	/mm^3/day	[15]
β_s	5E−4	5E−5	5E−3	/mm^3/day	[56]
μ_h	0.029	0.01	0.03	/day	[49]
μ_x	0.02	0.01	0.05	/day	[56]
π	0.2	0.1	0.9	Unitless	[59]
μ_r	8.3E−5	8.3E−6	0.0001	/day	[1]
μ_m	48	46	49	/day	[36]
μ_t	0.7	0.5	0.8	/day	[37]
μ_g	0.0625	0.5	0.78	/day	[56]
χ	0.6	0	1	Unitless	Assumed
ϱ	0.45	0	1	Unitless	[6]
ν	0.7	0	1	Unitless	Assumed
d	5E−4	1E−4	0.001	Unitless	Assumed
τ	1.5	1.2	1.9	Unitless	[45]
λ_w	30	25	35	/unitless/day	[45]
b	0.17	0.2	0.5	Unitless	[45]
a	0.16	0.2	0.4	Unitless	[45]
P	16	13	20	/erythrocytes/day	[13]
N	10,000	8000	11,000	/day	[60]
ϵ_0	1E−5	1E−6	1E−4	/day	[60]
ϵ_1	1E−5	1E−6	1E−4	/day	[60]
q	0.01	0.001	0.02	Unitless	[45]
ρ	0.3	0.2	0.45	Unitless	[45]
μ_n	0.4	0.3	0.72	/day	[1]
μ_a	0.4	0.3	0.72	/day	[36]
Ω	30	24	33	Unitless	[37]

Figures 2 and 3 illustrates Monte Carlo simulations for some of the parameters with the greatest PRCC values against model R_0.

It is evident that a highly efficacious pre-erythrocytic vaccine such as RTS,S/SA01 (with efficacy ν) and blood stage vaccine such as MSP3 (with efficacy ε) could effectively help in reducing parasitemia and malaria severity during clinical *P. falciparum* infections. Sporozoite invasion rate β_s and the merozoite invasion parameter β_r are also shown to increase the model R_0 and hence the severity of the disease within the human host.

Although the LHS/PRCC technique is useful in identifying significant parameters in the in-host malaria model, it fails to rank the parameters in order of their contribution to variations and disease progression. This ranking is very crucial in the design of clinical interventions

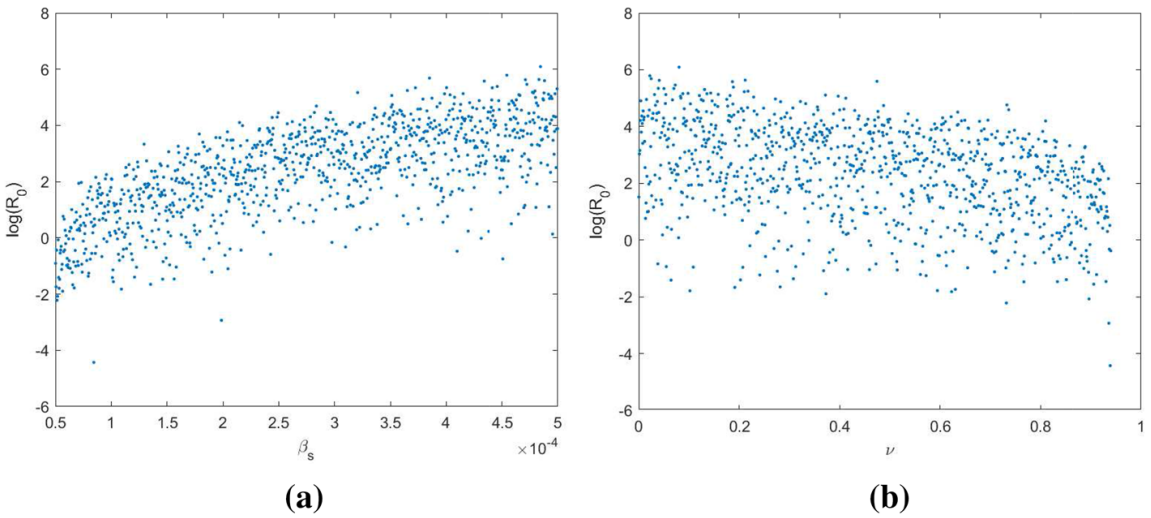

Fig. 2 The Monte Carlo simulations for some of the parameters with the greatest PRCC magnitudes, using values in Table 3 and 1000 simulations per run. The parameters are: **a** sporozoite invasion rate β_s and **b** efficacy of pre-erythrocytic vaccine ν

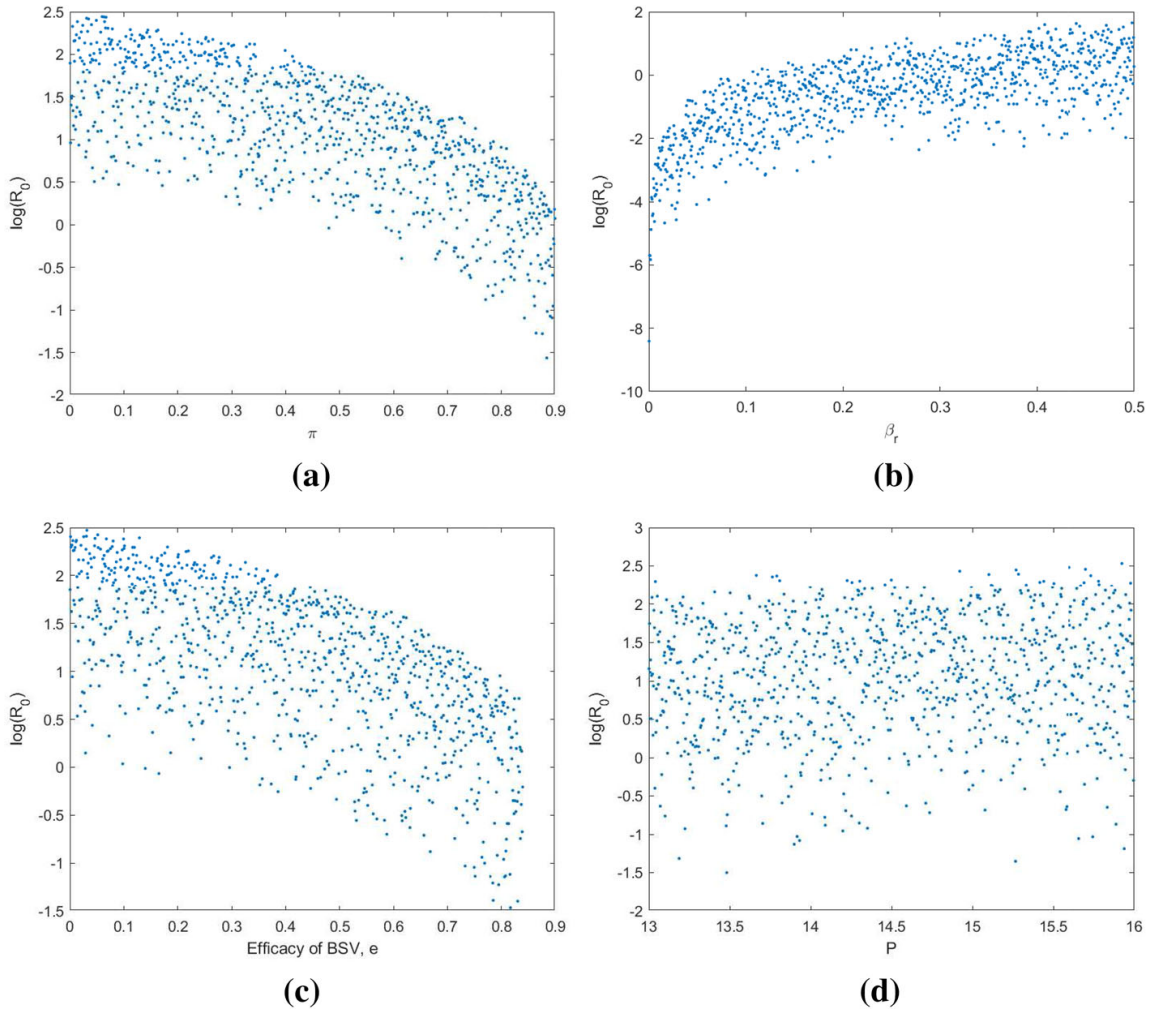

Fig. 3 The Monte Carlo simulations for some of the parameters with the greatest PRCC magnitudes, using values in Table 3 and 1000 simulations per run. They are: **a** proportion of parasites that become gametocytes π, **b** merozoite invasion rate β_r, **c** efficacy of blood stage vaccine e and **d** the number of merozoites produced per bursting blood schizont P

Table 4 The sensitivity results

Parameter	S.I	Parameter	S.I
P	+1	a	−0.785714
β_s	+1	π	−0.785714
λ_h	+1	β_r	+0.62402
μ_h	−1	λ_r	+0.62402
μ_x	−1	μ_m	−0.62406
ϱ	−0.785714	μ_r	−0.62406
ν	−0.785714	q	−0.428571

and in the development of malaria vaccines. In response, we consider the normalized forward sensitivity index of the model reproduction number in (15) and (16) against LHS parameters in Table 3 in the next section.

Sensitivity Analysis Based on Model R_0

We adopt the normalized forward sensitivity (NFS) index technique described in [4] to compute the sensitivity indices of the model R_0 with respect to input parameters $P, \beta_r, \beta_s, \lambda_h, \lambda_r, \mu_h, \mu_r, \mu_x, \mu_m, \varrho, a, \pi, \nu$ are presented in Table 4. The sensitivity indices (S.I) are evaluated in Mathematica software based on the baseline parameter values in Table 3.

From Table 4, we observe that the population of malaria merozoites that are released per bursting infected erythrocyte P, the rates of invasions of healthy erythrocytes β_r and hepatocytes β_s, the rate of recruitment of susceptible hepatocytes λ_h and erythrocytes λ_r have a direct effects on the severity of clinical malaria. A 10% increase (or decrease) in the magnitude of P, increase (or decrease) model R_0 by 10%. Clinical malaria control should aim at eradicating or reducing these parameters. On the other hand, malaria vaccines (ϱ and ν) are shown to reduce R_0 when their efficacies are improved. An increase (or decrease) in the immunosensitivity of infected red blood cells q is similarly shown to reduce (or increase) the model R_0. By rank, the parameters P, β_s, λ_h are the most influential in model (1), followed by the vaccine efficacies ϱ and ν. Clinical considerations should thus favour these parameters in the development of malaria vaccines.

In conclusion, the LHS/PRCC technique is robust and considers the entire parameter space in determining significant parameters in a disease model. However, it fails the ranking test. On the other hand, although the NFS index technique is beneficial in discerning and ranking significant parameters in a model, it does not explain the considerable uncertainties in estimating parameter values. It therefore fails to uncover parameter effects on particular variables or populations in the model. Due to the importance attached to the significance and rank of each parameter in the model, we advise that both approaches be used in future analysis of parameter uncertainty and sensitivity analysis in disease models.

Numerical Simulation

In this section, we illustrate numerically the dynamics of the in-host model system (1). When the basic reproduction number R_0 is less than unity, clinical *P. falciparum* malaria is observed to die out (see Figs. 4, 5) and the malaria-free state $E_0 = (0, 5 \times 10^5, 0, 0, 5 \times$

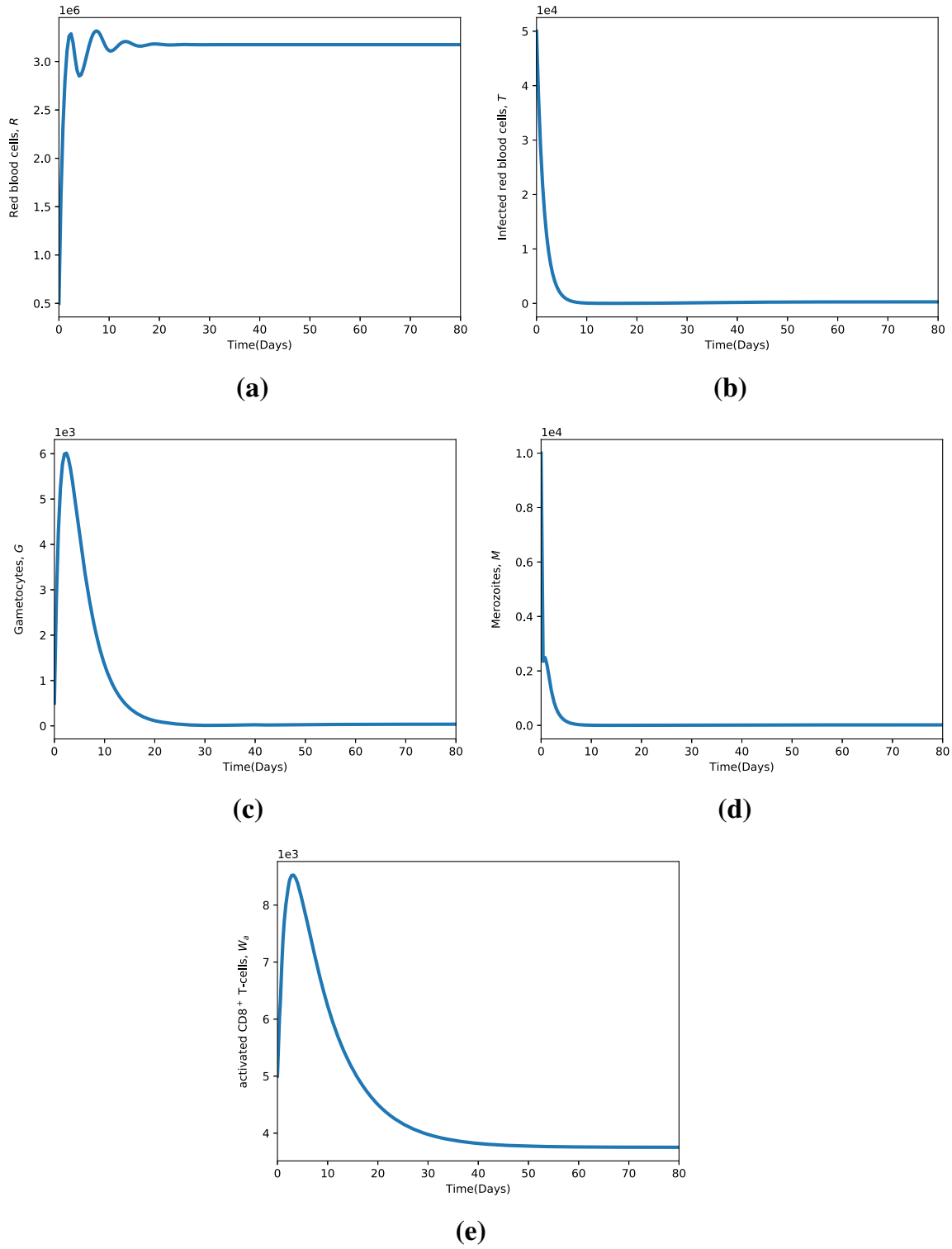

Fig. 4 The dynamics of model (1) when the basic reproduction number $R_0 = 0.8881 < 1$, the malaria-free equilibrium E_0 is globally asymptotically stable

$10^6, 0, 0, 0, 0, 0)$ is globally asymptotically stable. Additionally, only an efficacious BSV has the chance to totally eradicate the merozoites from the blood stream of the human host. Notice that even if R_0 is less than unity, some activated $CD8^+$ T-cells $W_a(t)$ still exists (see Fig. 4e). This shows that individual-level acquired immunity against malaria is maintained for some period of time even if all malaria parasites are eradicated from the host. All simulations are performed using parameter values in Table 3.

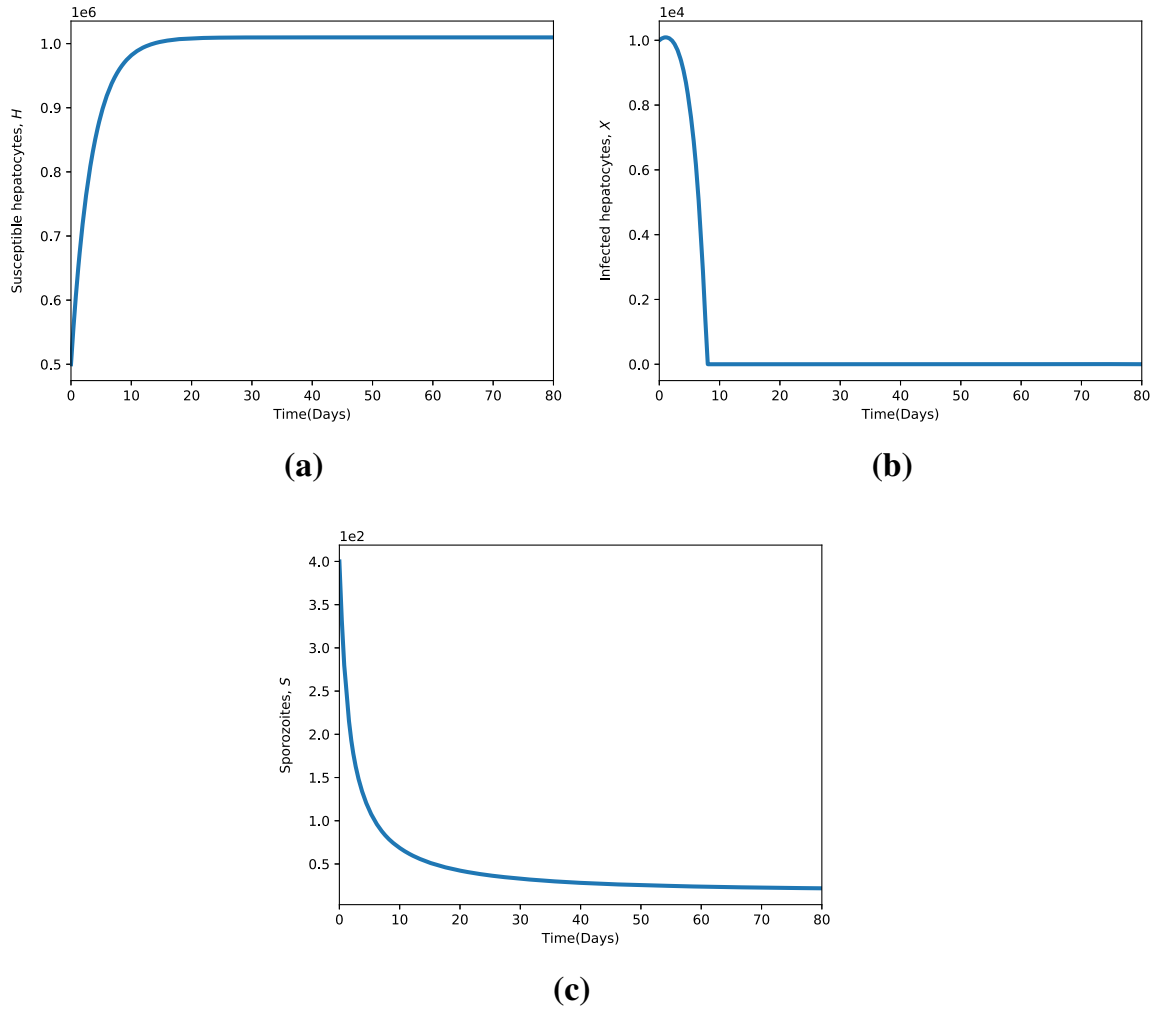

Fig. 5 Polulation dynamics of the liver hepatocytes and the sporozoites when the reproduction number $R_0 = 0.8881 < 1$. Parameter values are available in Table 3

Similarly, the density of sporozoites decline rapidly when $R_0 = R_{01} < 1$, leading to a corresponding decrease in the density of infected hepatocytes as shown in Fig. 5.

The persistent steady state, $E_p = (S^*, H^*, X^*, R^*, T^*, M^*, G^*, W_n^*, W_a^*) = (10^3, 3 \times 10^5, 3 \times 10^3, 5 \times 10^6, 5 \times 10^3, 10^3, 5 \times 10^2, 5 \times 10^3, 5 \times 10^3)$ is shown to be stable when R_0 is greater than unity, $R_0 = 1.3364 > 1$ (See Figs. 6, 7). We observe that the densities of sporozoites, merozoites, gametocytes, infected hepatocytes and infected erythrocytes grow and persists both at the pre-erythrocytic and blood stages of parasite development.

Multi-component and Multi-stage Vaccine Cocktail

Here, we illustrate the need to develop a multi-component and multi-stage *P. falciparum* malaria vaccines with sufficient prospect to minimize the severity of malaria infection from human host. Several strategies have been considered in the development of efficient multi-component and multi-stage *P. falciparum* vaccine formulations [16,51,53,57,58,67]. A synthetic peptide (SPf66) that combines antigens from the blood stages of malaria linked together with an antigen from the sporozoite stage reduced the number of first attacks with *P. falciparum* by 28% in South America [24]. High level of sterile efficacy and safety of combining pre-erythrocytic vaccine, RTS,S/AS01B with vectored vaccines are reported in [53].

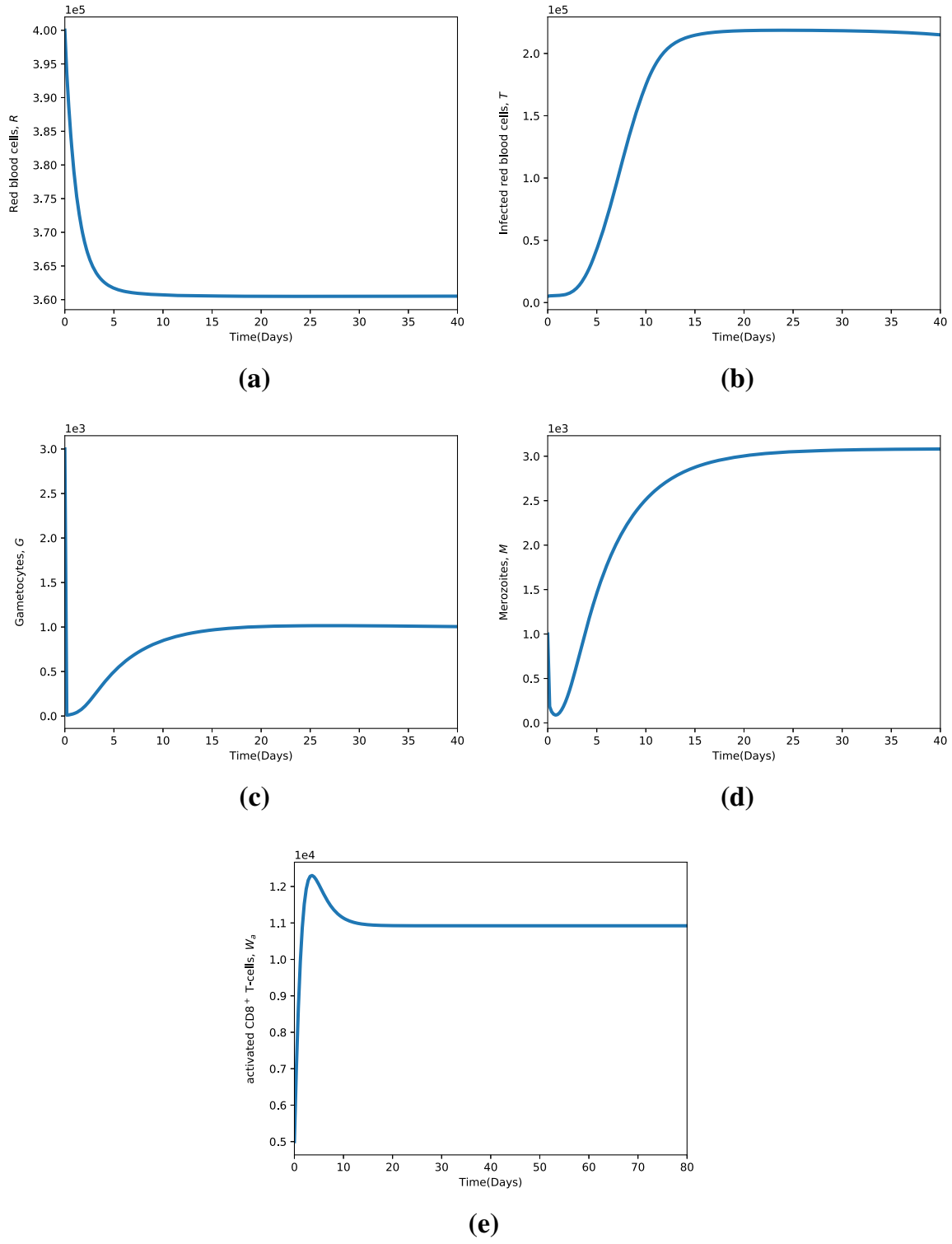

Fig. 6 When the reproduction number $R_0 = 1.3364 > 1$, the malaria-persistent equilibrium point E_p is stable for the chosen set of parameter values. The model parameter values are available in Table 3

Plasmodium falciparum chimeric protein 2.9 which is a combination of the C-terminal regions of domain III of AMA-1 and 19-kDa of MSP1 induced both anti-MSP1–19 and anti-AMA-1(III) Abs at levels 11- and 18-fold higher, respectively, than individual components did [51]. Studies in [19] have also shown that a combination of multiple vaccine candidates in fusion proteins may lead to improved characteristics of the vaccine.

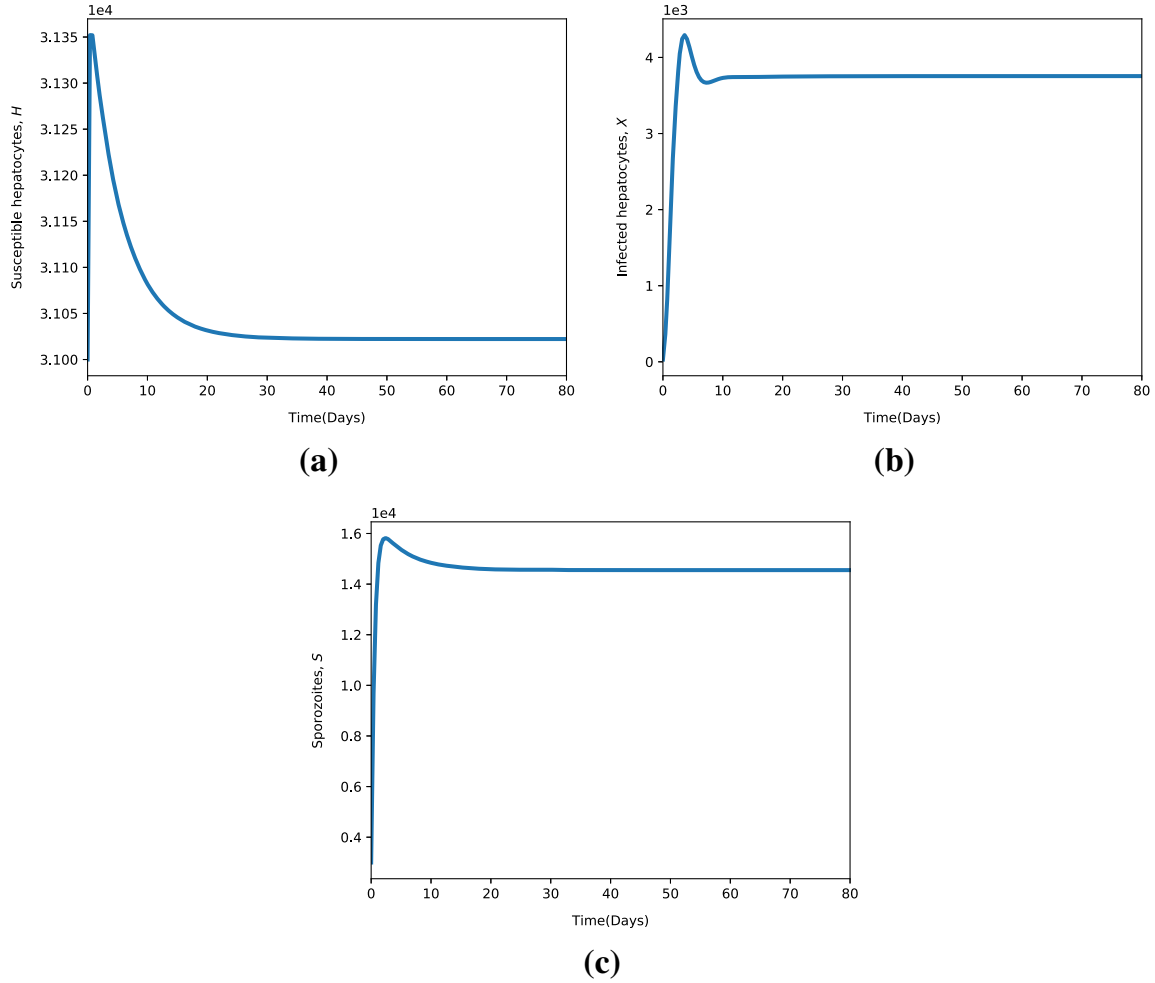

Fig. 7 When the reproduction number $R_0 = 1.3364 > 1$, the malaria-persistent equilibrium E_p is stable

Synergism from combination of transmission blocking vaccines is shown in [67] to confer protection by simultaneously inducing multiple, independent immune responses directed towards *P. falciparum* sporozoites. This ensures high levels of vaccine efficacy against the parasite. The need for multi-stage malaria vaccine is also emphasised in [16] where DNA vaccines are shown to have high capacity to induce CD8(+) cytotoxic T lymphocytes and interferon-gamma responses in humans during *P. falciparum* infection [62].

From these studies, it is evident that a multi-stage specific vaccine cocktail has the potential to prevent initial malaria infection at the pre-erythrocytic stage, reduce or eradicate clinical manifestation and prevent the transmission of gametocytes from infected human hosts to susceptible feeding female anopheles mosquito [10]. We therefore evaluate numerically the effects of malaria vaccine combinations on the severity of *P. falciparum* malaria infection. The vaccines are broadly categorized as: pre-erythrocytic vaccines, blood stage vaccines and transmission blocking vaccines. The vaccines are assumed to have an optimal efficacy of 75%. We chose this figure in consistency with the WHO strategic goal of developing a *P. falciparum* vaccine with atleast 75% efficacy [43].

Results in Fig. 8, shows the effects of all the three vaccines combined with a constant optimal efficacy of 75%. The density of infected erythrocytes T and infected hepatocytes X is shown to fall significantly. The severity of malaria infection is therefore highly reduced when the three vaccine antigens are combined.

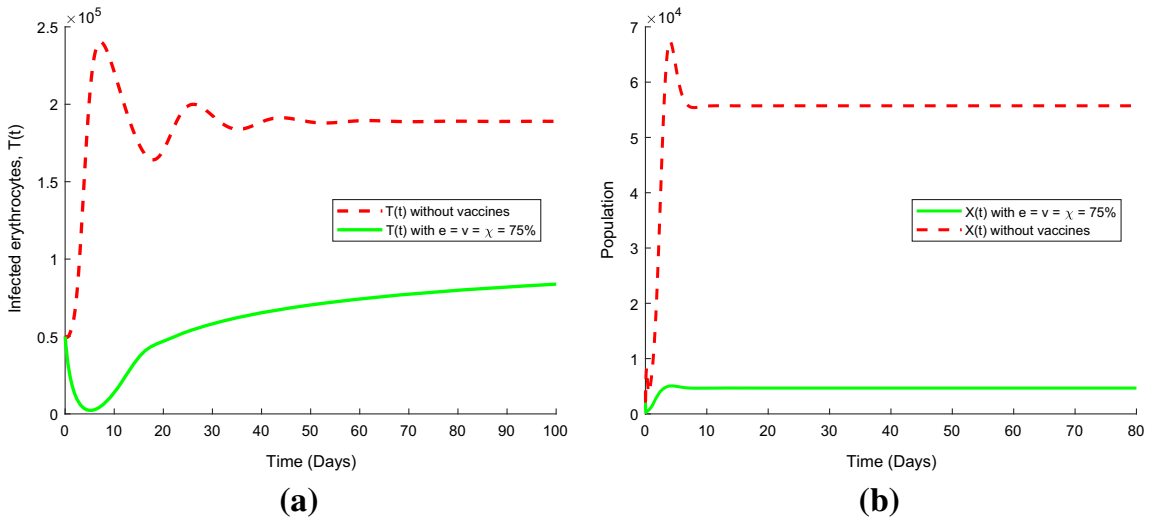

Fig. 8 Impact of a 75% efficacious combined malaria vaccines on the dynamics of infected red blood cells T and infected hepatocytes X. The simulations are performed when $R_{01} = 2.564 > 1$, and $R_{02} = 5.564 > 1$

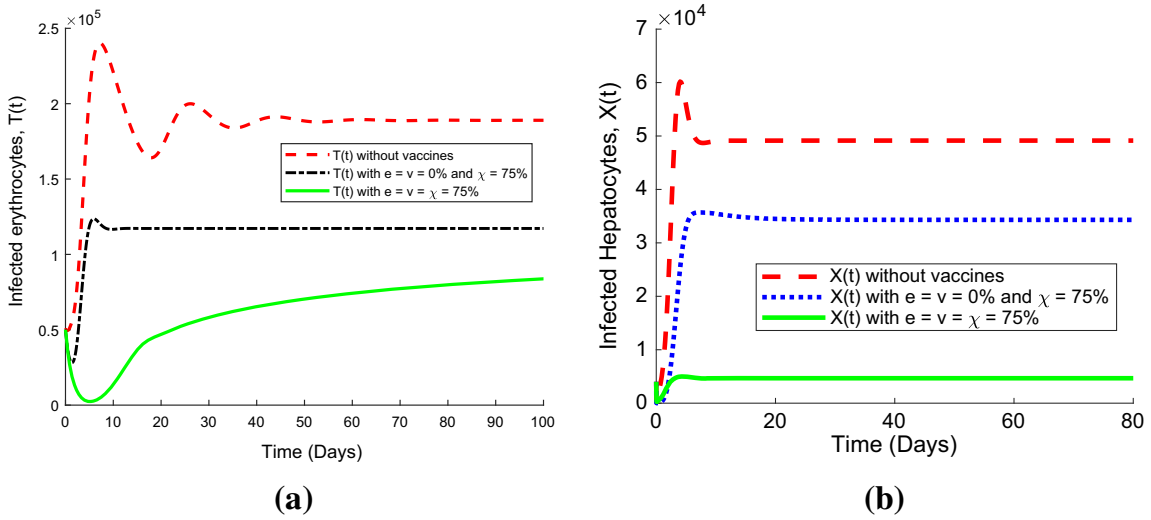

Fig. 9 Impact of a 75% efficacious transmission blocking vaccine on the dynamics of infected red blood cells and infected hepatocytes. The simulations are performed when $R_{01} = 2.564 > 1$, and $R_{02} = 5.564 > 1$

The use of only one vaccine is shown in Figs. 9, 10 and 11 to have minimal effects on the severity of malaria infection.

Finally, a combination of any two vaccines (with different antigens) is likely to moderately reduce the severity of malaria infection. The effects of paired—vaccine combinations are as shown in Figs. 12, 13 and 14. Unlike infected hepatocytes, transmission blocking vaccines are shown to have minimal effects on the density of infected red blood cells (see Fig. 10).

A combination of an efficacious pre-erythrocytic vaccine and an effective blood stage vaccine antigens has the potential to significantly reduce malaria severity as shown in Fig. 14. Moreover, a combination of antigens from transmission blocking vaccine and those of pre-erythrocytic vaccine at the liver stage, as shown in Fig. 12b, are very effective in suppressing the density of infected hepatocytes in the liver.

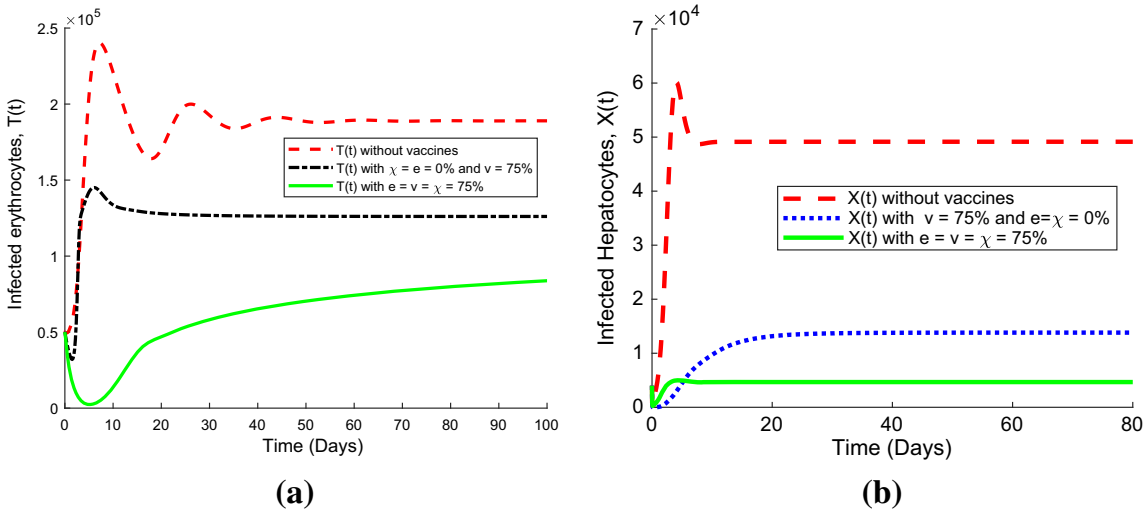

Fig. 10 Impact of a 75% efficacious pre-erythrocytic vaccine on the dynamics of infected red blood cells and infected hepatocytes. The simulations are performed when $R_{01} = 2.564 > 1$, and $R_{02} = 5.564 > 1$

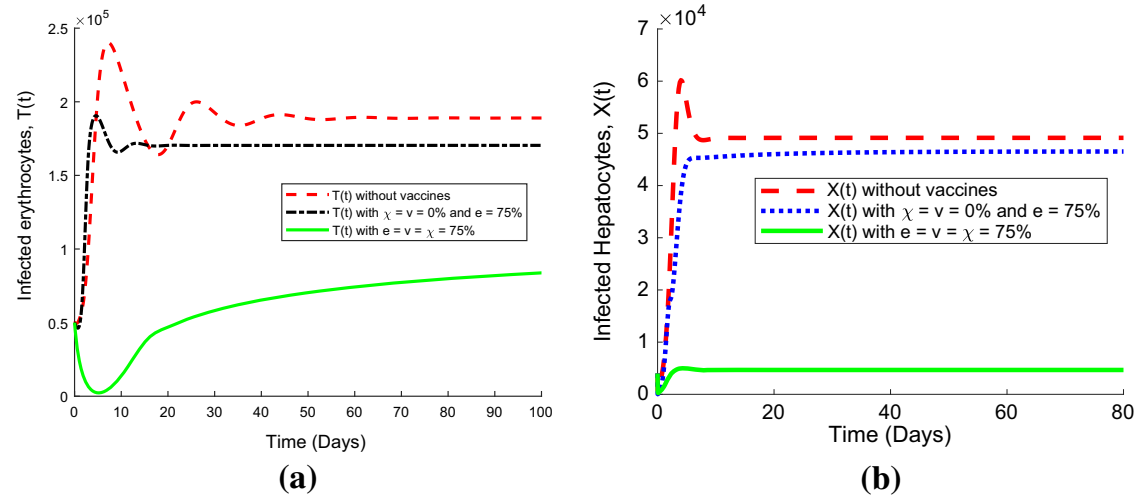

Fig. 11 Impact of a 75% efficacious blood stage vaccine on the dynamics of infected red blood cells and infected hepatocytes. The simulations are performed when $R_{01} = 2.564 > 1$, and $R_{02} = 5.564 > 1$

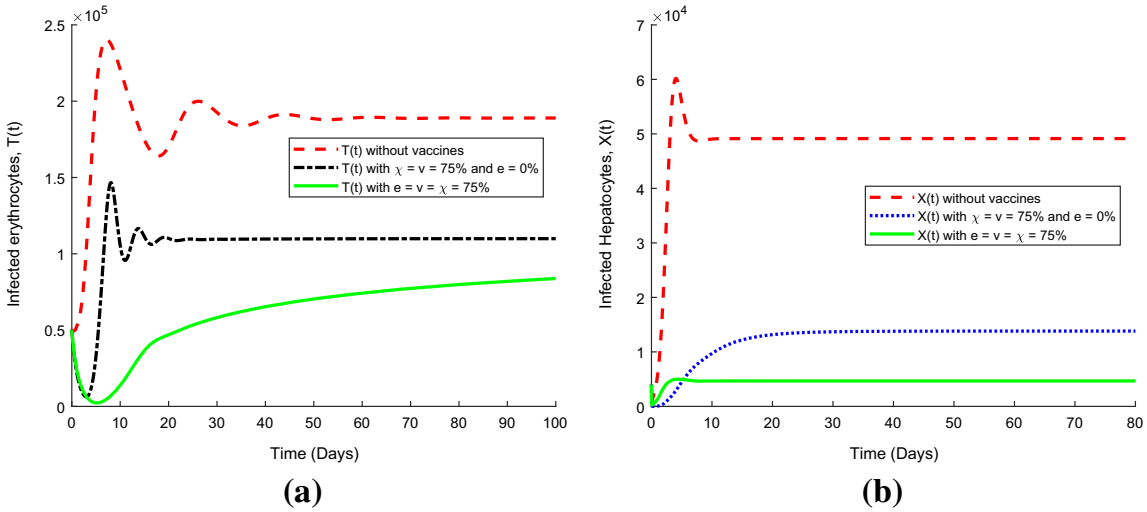

Fig. 12 The effect of combining a PEV and TBV that are both 75% efficacious on the dynamics of infected red blood cells and infected hepatocytes. The simulations are performed when $R_{01} = 2.564 > 1$, and $R_{02} = 5.564 > 1$

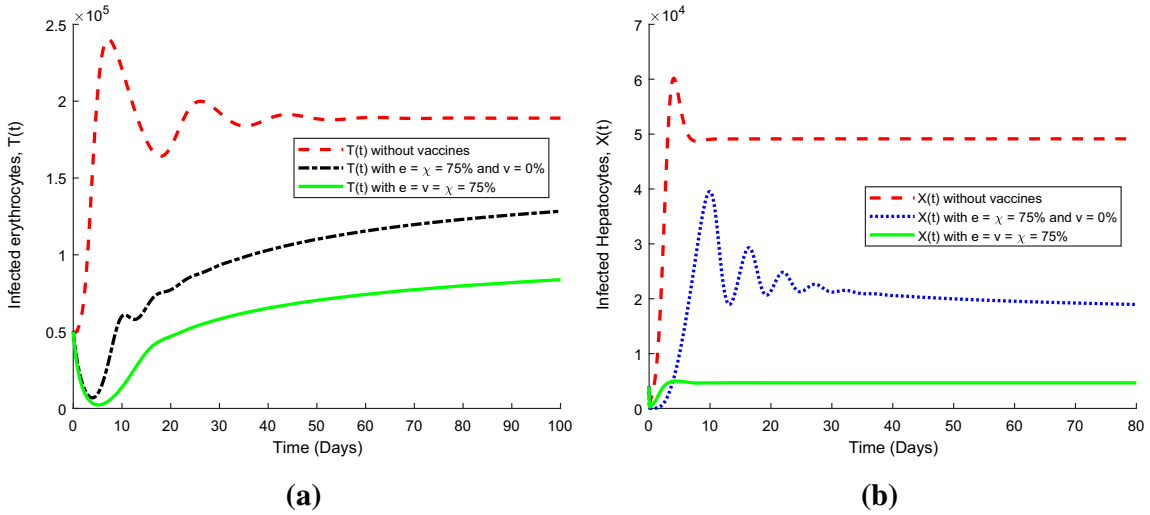

Fig. 13 The effect of combining a TBV and a PEV that are both 75% efficacious on the dynamics of infected red blood cells and infected hepatocytes. The simulations are performed when $R_{01} = 2.564 > 1$, and $R_{02} = 5.564 > 1$

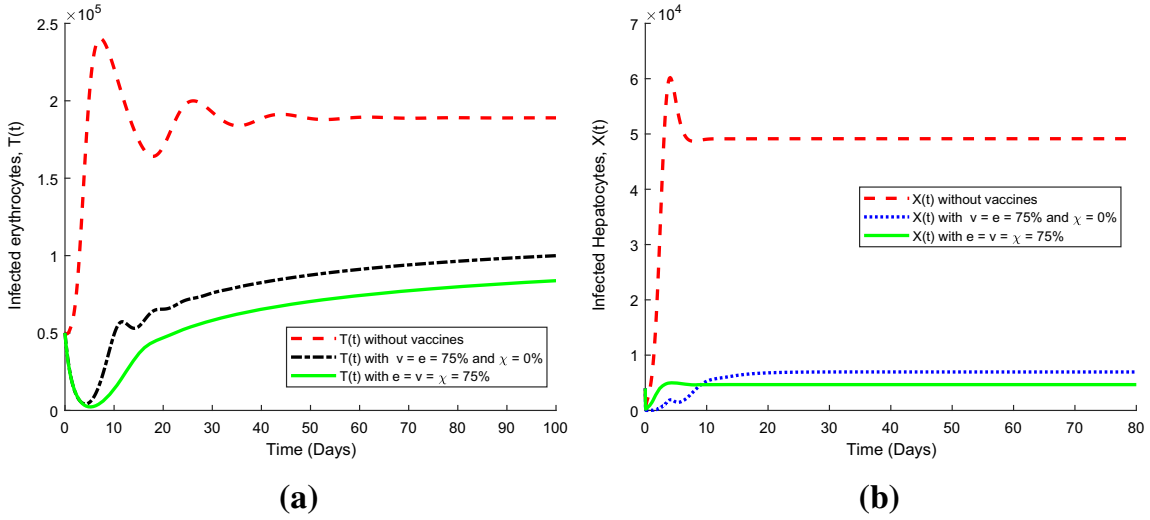

Fig. 14 The effect of combining a PEV and a BSV that are both 75% efficacious on the dynamics of infected red blood cells and infected hepatocytes. The simulations are performed when $R_{01} = 2.564 > 1$, and $R_{02} = 5.564 > 1$

Epidemiological Implications and Conclusion

Results of uncertainty and sensitivity analysis have significant epidemiological importance in malaria control. The presented model is shown to be sensitive to variations in vaccine efficacies χ, ϱ and ν. Only efficacious malaria vaccines have a chance to eradicate *P. falciparum* malaria or to reduce its severity, significantly, during clinical infection. Sensitivity indices based on the model reproduction number indicates that the rate of invasion of susceptible erythrocytes by merozoite parasites β_r and the rate of invasion of liver hepatocytes by the sporozoites β_s are highly sensitive to malaria disease progression. Malaria vaccines must therefore target and eradicate the infective parasites and infected cells. Other parameters such as the proportions of merozoites that become gametocytes per dying blood schizont π and the average number of merozoites released per bursting blood schizonts P are also shown to have a considerable impact on the model R_0 and hence the severity of infection.

A highly efficacious blood stage vaccine is necessary to lower the rate π. A reduction in the density of blood gametocytes has the potential of lowering malaria transmission from the human host to the mosquito vector.

Given the protective capacity of liver stage-specific $CD8^+$ T-cells [65], a lot more research that focuses on developing an efficacious blood stage vaccine that would prime blood trophozoite-specific $CD8^+$ T-cells is called for. The parameter τ which accounts for vaccine-induced production of $CD8^+$ T-cells is shown to have significant negative effects on the concentration of infected hepatocytes. The more efficient the pre-erythrocytic vaccine is, the lower the density of released merozoites into the host's blood. Moreover, a rapid eradication of parasitized liver hepatocytes is likely to result into less infected erythrocytes at the blood stage. An efficacious pre-erythrocytic vaccines has a potential to eradicate infected liver hepatocytes. Such efficacious liver stage vaccines may also reduce the overall burst size of an infected hepatocyte, leading to reduced erythrocytic schizonogy and hence the severity of clinical *P. falciparum* malaria.

Multiple combination of malaria vaccine antigen has a great potential in reducing the severity of malaria infections due to *P. falciparum* parasite. The synergy of combining pre-erythrocytic vaccines, blood stage vaccines and transmission blocking vaccines antigens induces multiple immune responses with the potential to prevent or eradicate malaria infection. As highlighted in [32], our study shows that a highly effective vaccine combination is critical for *P. falciparum* malaria disease elimination goal.

Although efficacious malaria vaccines are shown to be very effective in reducing severity of clinical malaria, our results further confirm the need to combine vaccine with existing anti-malarial therapy to achieve a complete eradication of the parasites from the host. Finally, the LHS/PRCC analysis revealed that the prediction imprecision was mainly due to certain key parameters. Long term precise predictions of the concentrations of infected liver hepatocytes and infected red blood cells would be difficult until these key parameters are correctly determined. A great understanding of parameter uncertainty and sensitivity analysis of in-host malaria in humans is necessary in order to develop effective vaccines against *P. falciparum* pathogen.

Acknowledgements The authors would like to thank the anonymous referees for their constructive comments. The authors also acknowledge with gratitude the support from the institute of Mathematical Sciences-Strathmore university.

Author contributions All authors contributed to all sections of this manuscript.

Funding The authors acknowledge with gratitude the financial support from the German Academic Exchange Service (DAAD) [ST32-PKZ:91711149] and the national Research Fund (NRF)-Kenya [NRF-Phd Grant Titus O.O], in the production of this manuscript.

Compliance with Ethical Standards

Conflict of interest The authors declare that there is no conflict of interest regarding the publication of this article.

Appendix A: PRCC Between Infected Red Blood Cells *T* and Each Parameter

See Table 5.

Table 5 PRCC between infected red blood cells T and each parameter

Parameter	PRCC	p value	Parameter	PRCC	p value
Λ	0.040124	0.69185	ν	−0.35423*	0.0001255
μ_s	0.092654	0.35921	d	−0.021968	0.82825
λ_h	0.16815	0.094459	λ_w	0.02639	0.79438
λ_r	0.99993***	1.2467E−191	τ	0.028815	0.77596
β_r	0.60394**	0.0030343	a	−0.033076	0.7439
β_s	−0.072861	0.47128	b	−0.037844	0.70854
μ_h	0.045043	0.65633	P	0.28652*	0.0038515
μ_x	0.022164	0.82674	N	0.50348**	0.0003056
π	0.24376	0.14528	ϵ_0	−0.050167	0.62012
μ_r	−0.54174**	5.8708E−9	ϵ_1	0.0092028	0.92759
μ_t	−0.043585	0.66677	ρ	0.087162	0.38852
μ_m	−0.08574	0.39634	q	−0.261905*	0.00154063
μ_g	−0.13006	0.19715	μ_n	−0.093091	0.35694
χ	−0.13607	0.17706	μ_a	−0.054864	0.58771
ϱ	−0.30701	0.0018909	Ω	0.041721	0.68024

The results are significant at the 0.05 level

Appendix B: PRCC Between Infected Hepatocytes *X* and Each Parameter

See Table 6.

Table 6 PRCC between infected hepatocytes X and each parameter

Parameter	PRCC	p value	Parameter	PRCC	p value
Λ	−0.034437	0.73375	ν	−0.307831*	0.00093836
μ_s	0.071002	0.48269	d	−0.1442	0.15231
λ_h	0.9749***	9.5419E−66	λ_w	−0.094174	0.35135
λ_r	0.06407	0.52654	τ	−0.20137*	0.000044531
β_r	−0.080809	0.42415	a	−0.075135	0.45751
β_s	0.53926**	0.00016701	b	0.061933	0.54045
μ_h	−0.87273***	2.7908E−23	P	0.076347	0.45026
μ_x	0.14762	0.14273	N	0.10516	0.29776
π	−0.045846	0.6506	ϵ_0	0.21125	0.034877
μ_r	0.094998	0.34713	ϵ_1	−0.16583	0.09918
μ_t	0.12588	0.21205	ρ	0.033235	0.74272
μ_m	0.13493	0.18073	q	0.095106	0.34658
μ_g	0.033064	0.74399	μ_n	0.039223	0.69843
χ	−0.28902	0.0035417	μ_a	−0.052237	0.60575
ϱ	−0.061742	0.5417	Ω	0.10411	0.30264

The results are significant at the 0.05 level

Appendix C: PRCC Between Merozoites *M* and Each Parameter

See Table 7.

Table 7 PRCC between merozoites M and each parameter

Parameter	PRCC	p value	Parameter	PRCC	p value
Λ	0.013086	0.89718	ν	−0.61866**	6.9194E−12
μ_s	0.12012	0.23389	d	0.12239	0.22509
λ_h	− 0.005884	0.95367	λ_w	−0.30208	0.0022545
λ_r	−0.78852**	2.0731E−22	τ	−0.11155	0.26918
β_r	−0.77199**	5.3565E−21	a	0.14416	0.15243
β_s	0.10834	0.28328	b	−0.18907	0.059575
μ_h	0.080773	0.42436	P	0.28652*	0.0038515
μ_x	0.46617*	1.0183E−06	N	−0.50348**	0.0003056
π	−0.29849	0.0025577	ϵ_0	−0.23892	0.01667
μ_r	0.060227	0.55168	ϵ_1	−0.057548	0.56955
μ_t	−0.05975	0.55485	ρ	−0.25708	0.0098207
μ_m	−0.090522	0.37042	q	−0.047855	0.63635
μ_g	0.18256	0.069072	μ_n	−0.0015737	0.9876
χ	−0.67251**	1.8298E−14	μ_a	0.1363	0.17632
ϱ	−0.024582	0.80818	Ω	−0.12172	0.22769

The results are significant at the 0.05 level

Appendix D: PRCC Between Gametocytes *G* and Each Parameter

See Table 8.

Table 8 PRCC between gametocytes G and each parameter

Parameter	PRCC	p value	Parameter	PRCC	p value
Λ	0.09861	0.32902	ν	−0.54919**	3.2858E−09
μ_s	−0.18356	0.067537	d	−0.33627	0.00062476
λ_h	0.16929	0.092216	λ_w	−0.14215	0.15831
λ_r	−0.79454***	5.8878E−23	τ	−0.080527	0.42578
β_r	−0.76958**	8.4228E−21	a	−0.16499	0.10092
β_s	−0.021251	0.83378	b	−0.31287	0.0015279
μ_h	0.060337	0.55095	P	0.059063	0.55941
μ_x	0.40198*	3.3899E−05	N	0.24601	0.013619
π	0.698883**	0.0032768	ϵ_0	−0.28727	0.0037563
μ_r	−0.022582	0.82353	ϵ_1	0.075806	0.45349
μ_t	0.075502	0.45531	ρ	−0.047433	0.63933
μ_m	0.067991	0.50149	q	0.12264	0.22416
μ_g	−0.084857	0.40124	μ_n	−0.12368	0.22021
χ	−0.55186**	2.6601E−09	μ_a	0.17443	0.082611
ϱ	−0.55799**	1.6273E−09	Ω	0.15261	0.12956

The results are significant at the 0.05 level

Appendix E: PRCC Between Sporozoites *S* and Each Parameter

See Table 9.

Table 9 PRCC between sporozoites S and each parameter

Parameter	PRCC	p value	Parameter	PRCC	p value
Λ	0.31314*	0.00097533	ν	0.0067811	0.94661
μ_s	−0.68707**	0.0094591	d	0.010905	0.91425
λ_h	−0.012635	0.90071	λ_w	0.0043436	0.96579
λ_r	0.03593	0.72266	τ	0.023508	0.81642
β_r	0.025432	0.80168	a	0.0065303	0.94859
β_s	−0.0091069	0.92835	b	−0.017604	0.86199
μ_h	0.022838	0.82156	P	−0.019561	0.84683
μ_x	0.0056574	0.95545	N	−0.015923	0.87505
π	−0.0047473	0.96261	ϵ_0	−0.00027845	0.99781
μ_r	0.00025243	0.99801	ϵ_1	−0.0003386	0.99733
μ_t	−0.011016	0.91338	ρ	−0.031317	0.75709
μ_m	0.0096995	0.9237	q	−0.0037326	0.9706
μ_g	−0.023075	0.81974	μ_n	0.030253	0.7651
χ	−0.699368*	0.0001184	μ_a	−0.0042258	0.96672
ϱ	0.01863	0.85403	Ω	−0.0052564	0.95861

The results are significant at the 0.05 level

References

1. Anderson, R., May, R., Gupta, S.: Non-linear phenomena in host–parasite interactions. Parasitology **99**(S1), S59–S79 (1989)
2. Arama, C., Troye-Blomberg, M.: The path of malaria vaccine development: challenges and perspectives. J. Intern. Med. **275**(5), 456–466 (2014)
3. Arevalo-Herrera, M., Solarte, Y., Yasnot, M.F., Castellanos, A., Rincon, A., Saul, A., Mu, J., Long, C., Miller, L., Herrera, S.: Induction of transmission-blocking immunity in Aotus monkeys by vaccination with a *Plasmodium vivax* clinical grade PVS25 recombinant protein. Am. J. Trop. Med. Hyg. **73**(5–Suppl), 32–37 (2005)
4. Arriola, L., Hyman, J.: Lecture notes, forward and adjoint sensitivity analysis: with applications in dynamical systems. Linear Algebra and Optimisation Mathematical and Theoretical Biology Institute, Summer (2005)
5. Audran, R., Cachat, M., Lurati, F., Soe, S., Leroy, O., Corradin, G., Druilhe, P., Spertini, F.: Phase i malaria vaccine trial with a long synthetic peptide derived from the merozoite surface protein 3 antigen. Infect. Immun. **73**(12), 8017–8026 (2005)
6. Birkett, A.J.: Status of vaccine research and development of vaccines for malaria. Vaccine **34**(26), 2915–2920 (2016)
7. Birkett, A.J., Moorthy, V.S., Loucq, C., Chitnis, C.E., Kaslow, D.C.: Malaria vaccine R&D in the decade of vaccines: breakthroughs, challenges and opportunities. Vaccine **31**, B233–B243 (2013)
8. Blower, S.M., Dowlatabadi, H.: Sensitivity and uncertainty analysis of complex models of disease transmission: an HIV model, as an example. Int. Stat. Rev. **62**(2), 229–243 (1994)
9. Blower, S.M., Hartel, D., Dowlatabadi, H., Anderson, R.M., May, R.M.: Drugs, sex and HIV: a mathematical model for New York city. Philos. Trans. R. Soc. Lond. B **331**(1260), 171–187 (1991)
10. Boes, A., Spiegel, H., Voepel, N., Edgue, G., Beiss, V., Kapelski, S., Fendel, R., Scheuermayer, M., Pradel, G., Bolscher, J.M., et al.: Analysis of a multi-component multi-stage malaria vaccine candidate–tackling the cocktail challenge. PLoS ONE **10**(7), e0131456 (2015)
11. Castillo-Chavez, C., Song, B.: Dynamical models of tuberculosis and their applications. Math. Biosci. Eng. **1**(2), 361–404 (2004)
12. Cowman, A.F., Crabb, B.S.: Invasion of red blood cells by malaria parasites. Cell **124**(4), 755–766 (2006)
13. Diebner, H.H., Eichner, M., Molineaux, L., Collins, W.E., Jeffery, G.M., Dietz, K.: Modelling the transition of asexual blood stages of *Plasmodium falciparum* to gametocytes. J. Theor. Biol. **202**(2), 113–127 (2000)
14. Diekmann, O., Heesterbeek, J.A.P., Metz, J.A.: On the definition and the computation of the basic reproduction ratio r0 in models for infectious diseases in heterogeneous populations. J. Math. Biol. **28**(4), 365–382 (1990)
15. Dondorp, A.M., Kager, P.A., Vreeken, J., White, N.J.: Abnormal blood flow and red blood cell deformability in severe malaria. Parasitol. Today **16**(6), 228–232 (2000)
16. Doolan, D.L., Hoffman, S.L.: Dna-based vaccines against malaria: status and promise of the multi-stage malaria DNA vaccine operation. Int. J. Parasitol. **31**(8), 753–762 (2001)
17. ECDC: Prevention and control measures for malaria (2018). http://ecdc.europa.eu/en/malaria/prevention-and-control. Retrieved June 2018
18. EMA: First malaria vaccine receives positive scientific opinion from EMA. European Medicines Agency (2015). https://www.ema.europa.eu/en/news/first-malaria-vaccine-receives-positive-scientific-opinion-ema. Accessed March 2019
19. Faber, B.W., Younis, S., Remarque, E.J., Garcia, R.R., Riasat, V., Walraven, V., van der Werff, N., van der Eijk, M., Cavanagh, D.R., Holder, A.A., et al.: Diversity covering AMA1-MSP119 fusion proteins as malaria vaccines. Infect. Immun. pages IAI–01267 (2013)
20. Frischknecht, F., Baldacci, P., Martin, B., Zimmer, C., Thiberge, S., Olivo-Marin, J.-C., Shorte, S.L., Ménard, R.: Imaging movement of malaria parasites during transmission by anopheles mosquitoes. Cell. Microbiol. **6**(7), 687–694 (2004)
21. Gomero, B.: Latin hypercube sampling and partial rank correlation coefficient analysis applied to an optimal control problem (2012)
22. Gomes, A.P., Vitorino, R.R., Costa, A.d P., Mendonça, E.G.d, Oliveira, M.G.d A., Siqueira-Batista, R.: Severe *Plasmodium falciparum* malaria. Rev. Bras. Terapia Intensiva **23**(3), 358–369 (2011)
23. Gravenor, M., Kwiatkowski, D.: An analysis of the temperature effects of fever on the intra-host population dynamics of *Plasmodium falciparum*. Parasitology **117**(2), 97–105 (1998)
24. Graves, P.M., Gelband, H.: Vaccines for preventing malaria (SPf66). Cochrane Database Syst. Rev. (2), CD005966 (2006). https://doi.org/10.1002/14651858.CD005966
25. Gurarie, D., McKenzie, F.E.: Dynamics of immune response and drug resistance in malaria infection. Malar. J. **5**(1), 86–101 (2006)

26. Hamby, D.: A review of techniques for parameter sensitivity analysis of environmental models. Environ. Monit. Assess. **32**(2), 135–154 (1994)
27. Hetzel, C., Anderson, R.: The within-host cellular dynamics of bloodstage malaria: theoretical and experimental studies. Parasitology **113**(1), 25–38 (1996)
28. Hisaeda, H., Stowers, A.W., Tsuboi, T., Collins, W.E., Sattabongkot, J.S., Suwanabun, N., Torii, M., Kaslow, D.C.: Antibodies to malaria vaccine candidates PVS25 and PVS28 completely block the ability of plasmodium vivax to infect mosquitoes. Infect. Immun. **68**(12), 6618–6623 (2000)
29. Hoshen, M., Heinrich, R., Stein, W., Ginsburg, H.: Mathematical modelling of the within-host dynamics of *Plasmodium falciparum*. Parasitology **121**(3), 227–235 (2000)
30. Iman, R.L., Helton, J.C.: An investigation of uncertainty and sensitivity analysis techniques for computer models. Risk Anal. **8**(1), 71–90 (1988)
31. Inc., W.R. SystemModeler, Version 5.1. Champaign, IL (2018)
32. Kumar, N.: A vaccine to prevent transmission of human malaria: a long way to travel on a dusty and often bumpy road. Current Sci. **92**, 1535–1544 (2007)
33. LaSalle, J.: The Stability of Dynamical Systems, Volume 25 of Regional Conference Series in Applied Mathematics. SIAM, Philadelphia (1976)
34. Li, M.Y., Muldowney, J.S.: Global stability for the seir model in epidemiology. Math. Biosci. **125**(2), 155–164 (1995)
35. Li, M.Y., Shu, H.: Global dynamics of an in-host viral model with intracellular delay. Bull. Math. Biol. **72**(6), 1492–1505 (2010)
36. Li, Y., Ruan, S., Xiao, D.: The within-host dynamics of malaria infection with immune response. Math. Biosci. Eng. **8**(4), 999–1018 (2011)
37. Magombedze, G., Chiyaka, C., Mukandavire, Z.: Optimal control of malaria chemotherapy. Nonlinear Anal. Modell. Control **16**(4), 415–434 (2011)
38. McKay, M.D., Beckman, R.J., Conover, W.J.: Comparison of three methods for selecting values of input variables in the analysis of output from a computer code. Technometrics **21**(2), 239–245 (1979)
39. McQueen, P.G., McKenzie, F.E.: Age-structured red blood cell susceptibility and the dynamics of malaria infections. Proc. Natl. Acad. Sci. USA **101**(24), 9161–9166 (2004)
40. Molineaux, L., Diebner, H., Eichner, M., Collins, W., Jeffery, G., Dietz, K.: *Plasmodium falciparum* parasitaemia described by a new mathematical model. Parasitology **122**(4), 379–391 (2001)
41. Molineaux, L., Dietz, K.: Review of intra-host models of malaria. Parassitologia **41**(1/3), 221–232 (1999)
42. Moorthy, V.S., Good, M.F., Hill, A.V.: Malaria vaccine developments. The Lancet **363**(9403), 150–156 (2004)
43. MVFG: Malaria vaccine technology roadmap. Autoimmunity Research Foundation (2018). Retrieved from http://www.who.int/immunization/topics/malaria/vaccine_roadmap/en/. Accessed Aug 2018
44. Neilan, R.L.M., Schaefer, E., Gaff, H., Fister, K.R., Lenhart, S.: Modeling optimal intervention strategies for cholera. Bull. Math. Biol. **72**(8), 2004–2018 (2010)
45. Niger, A.M., Gumel, A.B.: Immune response and imperfect vaccine in malaria dynamics. Math. Popul. Stud. **18**(2), 55–86 (2011)
46. Nunes, J.K., Woods, C., Carter, T., Raphael, T., Morin, M.J., Diallo, D., Leboulleux, D., Jain, S., Loucq, C., Kaslow, D.C.: Development of a transmission-blocking malaria vaccine: progress, challenges, and the path forward. Vaccine **32**(43), 5531–5539 (2014)
47. Ogutu, B.R., Apollo, O.J., McKinney, D., Okoth, W., Siangla, J., Dubovsky, F., Tucker, K., Waitumbi, J.N., Diggs, C., Wittes, J., et al.: Blood stage malaria vaccine eliciting high antigen-specific antibody concentrations confers no protection to young children in western Kenya. PLoS ONE **4**(3), e4708 (2009)
48. Omondi, E.O., Orwa, T.O., Nyabadza, F.: Application of optimal control to the onchocerciasis transmission model with treatment. Math. Biosci. **297**, 43–57 (2017)
49. Orwa, T.O., Mbogo, R.W., Luboobi, L.S.: Mathematical model for hepatocytic–erythrocytic dynamics of malaria. Int. J. Math. Math. Sci. **2018**, 7019868 (2018). https://doi.org/10.1155/2018/7019868
50. Orwa, T.O., Mbogo, R.W., Luboobi, L.S.: Mathematical model for the in-host malaria dynamics subject to malaria vaccines. Lett. Biomath. **5**(1), 222–251 (2018b)
51. Pan, W., Huang, D., Zhang, Q., Qu, L., Zhang, D., Zhang, X., Xue, X., Qian, F.: Fusion of two malaria vaccine candidate antigens enhances product yield, immunogenicity, and antibody-mediated inhibition of parasite growth in vitro. J. Immunol. **172**(10), 6167–6174 (2004)
52. Pereira, A., Broed, R.: Methods for uncertainty and sensitivity analysis: review and recomendations for implementation in ecolego. Fysikum, Stockholm (2006). http://urn.kb.se/resolve?urn=urn:nbn:se:su:diva-1079. Accessed Oct 2018
53. Rampling, T., Ewer, K.J., Bowyer, G., Bliss, C.M., Edwards, N.J., Wright, D., Payne, R.O., Venkatraman, N., de Barra, E., Snudden, C.M., et al.: Safety and high level efficacy of the combination malaria vaccine

regimen of RTS, S/AS01B with chimpanzee adenovirus 63 and modified vaccinia ankara vectored vaccines expressing me-trap. J. Infect. Dis. **214**(5), 772–781 (2016)
54. Rts, S.C.T.P.: Efficacy and safety of the RTS, S/AS01 malaria vaccine during 18 months after vaccination: a phase 3 randomized, controlled trial in children and young infants at 11 African sites. PLoS Med. **11**(7), e1001685 (2014)
55. Saul, A.: Models for the in-host dynamics of malaria revisited: errors in some basic models lead to large over-estimates of growth rates. Parasitology **117**(5), 405–407 (1998)
56. Selemani, M.A., Luboobi, L.S., Nkansah-Gyekye, Y.: On stability of the in-human host and in-mosquito dynamics of malaria parasite. Asian J. Math. Appl. **2016**, ama0353 (2016)
57. Stoute, J.A., Slaoui, M., Heppner, D.G., Momin, P., Kester, K.E., Desmons, P., Wellde, B.T., Garçon, N., Krzych, U., Marchand, M., et al.: A preliminary evaluation of a recombinant circumsporozoite protein vaccine against plasmodium falciparum malaria. New Engl. J. Med. **336**(2), 86–91 (1997)
58. Stowers, A.W., Kennedy, M.C., Keegan, B.P., Saul, A., Long, C.A., Miller, L.H.: Vaccination of monkeys with recombinant *Plasmodium falciparum* apical membrane antigen 1 confers protection against blood-stage malaria. Infect. Immun. **70**(12), 6961–6967 (2002)
59. Talman, A.M., Domarle, O., McKenzie, F.E., Ariey, F., Robert, V.: Gametocytogenesis: the puberty of *Plasmodium falciparum*. Malar. J. **3**(1), 24 (2004)
60. Tumwiine, J., Hove-Musekwa, S.D., Nyabadza, F.: A mathematical model for the transmission and spread of drug sensitive and resistant malaria strains within a human population. ISRN Biomathematics (2014)
61. Tumwiine, J., Mugisha, J., Luboobi, L.: On global stability of the intra-host dynamics of malaria and the immune system. J. Math. Anal. Appl. **341**(2), 855–869 (2008)
62. Tuteja, R.: DNA vaccine against malaria: a long way to go. Crit. Rev. Biochem. Mol. Biol. **37**(1), 29–54 (2002)
63. Van den Driessche, P., Watmough, J.: Reproduction numbers and sub-threshold endemic equilibria for compartmental models of disease transmission. Math. Biosci. **180**(1), 29–48 (2002)
64. Vaughan, A.M., Aly, A.S., Kappe, S.H.: Malaria parasite pre-erythrocytic stage infection: gliding and hiding. Cell Host Microbe **4**(3), 209–218 (2008)
65. Villarino, N., W Schmidt, N.: Cd8+ t cell responses to plasmodium and intracellular parasites. Curr. Immunol. Rev. **9**(3), 169–178 (2013)
66. White, E., Comiskey, C.: Heroin epidemics, treatment and ODE modelling. Math. Biosci. **208**(1), 312–324 (2007)
67. White, M.T., Smith, D.L.: Synergism from combinations of infection-blocking malaria vaccines. Malar. J. **12**(1), 280 (2013)
68. WHO: Tables of malaria vaccine projects globally. "The Rainbow Tables" (2015). World Health Organization. https://www.who.int/immunization/research/development/Rainbow_tables/en/. Accessed Mar 2019
69. WHO: Overview of malaria treatment (2017). http://www.who.int/gho/malaria/areas/treatment/overview/en/. Accessed Nov 2017
70. WHO: Malaria vaccine: WHO position paper, January 2016-recommendations. Vaccine **36**(25), 3576–3577 (2018)
71. Zhong, P.: Optimal theory applied in integrodifference equation models and in a cholera differential equation model. The University of Tennessee Knoxville (2011). https://trace.tennessee.edu/cgi/viewcontent.cgi?referer=https://www.google.com/&httpsredir=1&article=2287&context=utk_graddiss

Hindawi
Computational and Mathematical Methods in Medicine
Volume 2019, Article ID 9783986, 26 pages
https://doi.org/10.1155/2019/9783986

Research Article

Multiple-Strain Malaria Infection and Its Impacts on *Plasmodium falciparum* Resistance to Antimalarial Therapy: A Mathematical Modelling Perspective

Titus Okello Orwa, Rachel Waema Mbogo, and Livingstone Serwadda Luboobi

Institute of Mathematical Sciences, Strathmore University, P.O. Box 59857-00200, Nairobi, Kenya

Correspondence should be addressed to Titus Okello Orwa; torwa@strathmore.edu

Received 14 February 2019; Accepted 15 May 2019; Published 11 June 2019

Academic Editor: Konstantin Blyuss

The emergence of parasite resistance to antimalarial drugs has contributed significantly to global human mortality and morbidity due to malaria infection. The impacts of multiple-strain malarial parasite infection have further generated a lot of scientific interest. In this paper, we demonstrate, using the epidemiological model, the effects of parasite resistance and competition between the strains on the dynamics and control of *Plasmodium falciparum* malaria. The analysed model has a trivial equilibrium point which is locally asymptotically stable when the parasite's effective reproduction number is less than unity. Using contour plots, we observed that the efficacy of antimalarial drugs used, the rate of development of resistance, and the rate of infection by merozoites are the most important parameters in the multiple-strain *P. falciparum* infection and control model. Although the drug-resistant strain is shown to be less fit, the presence of both strains in the human host has a huge impact on the cost and success of antimalarial treatment. To reduce the emergence of resistant strains, it is vital that only effective antimalarial drugs are administered to patients in hospitals, especially in malaria-endemic regions. Our results emphasize the call for regular and strict surveillance on the use and distribution of antimalarial drugs in health facilities in malaria-endemic countries.

1. Introduction

The emergence of parasite resistance [1–4] to antimalarial drugs has contributed significantly to human mortality and morbidity due to malaria infection, worldwide [5–7]. A global malaria control strategy of 1992 [8] that advocated for early diagnosis and prompt treatment has been heavily compromised by the emergence of parasite resistance to antimalarial drugs. The evolution of parasite resistance has been described in [9] as an example of a Darwinian evolution. Parasites undergo mutations in their genome in response to the drug-treated human host. These mutations reduce the rate of parasite elimination from the host and increase their survival chances [9]. The most extensively used antimalarial drugs against the deadly *Plasmodium falciparum* malaria are chloroquine (CQ) and sulfadoxine-pyrimethamine (SP) [10, 11]. These drugs are cheap, easily available, and slowly eliminated from the human body [11]. However, the extensive use of CQ and SP has resulted in *P. falciparum* resistance. This has led to global increase in malaria cases and mortality [12]. In response, the World Health Organization (WHO) in 2006 recommended the use of artemisinin-based combination therapies (ACTs) as a first-line treatment for uncomplicated *P. falciparum* malaria [13]. Resistance to ACTs which are currently the standard treatment for *P. falciparum* is likely to cause global health crisis especially in African regions where *P. falciparum* malaria is endemic [11].

The emergence of parasite resistance to malaria therapy dates back to the 19th century. Quinine (1963) was the first-line antimalarial drug against *P. falciparum* [14]. High mortality cases coupled with high parasite resistance led to the introduction of a second drug, chloroquine (CQ), in 1934 [15]. A decade later, CQ was considered the first-line antimalarial drug by several countries until 1957, when the first focus of *P. falciparum* resistance was detected along the Thai-Cambodia border [16]. In Africa, *P. falciparum* resistance to CQ was first discovered among travelers from

Kenya to Tanzania [17]. By 1983, CQ resistance had spread to Sudan, Uganda [18], Zambia [19], and Malawi [20]. Unlike Africa, CQ was replaced for the first time with sulfadoxine-pyrimethamine (SP) as a first-line antimalarial drug in Thailand in 1967. Several other countries in Asia and South America followed thereafter [10]. Resistance to SP was, however, reported the same year [21] in the region. In 1988, CQ was replaced for the first time in Africa. KwaZulu-Natal Province of South Africa replaced CQ with SP [22]. In 1993, the Malawian government changed the treatment policy from CQ to SP. Other African countries followed thereafter: Kenya, South Africa, and Botswana (in 1998); Cameroon and Tanzania (in 2001); and Zimbabwe (in 2000) [23]. The effectiveness of SP was equally undermined by resistance. Unlike CQ, *P. falciparum* resistance to SP was mainly attributed to the long half-life of the drug [24]. Confirmed resistance to the artemisinin derivatives was first reported in Cambodia and Mekong regions in 2008 [25].

To leverage on parasite resistance, cost of treatment, and burden of malaria infection to communities and governments, the WHO recommends the use of artemisinin-based combination therapies (ACTs) as the first- and second-line treatment drugs for uncomplicated *P. falciparum* malaria [25]. ACT is a combination of artemisinin derivatives and a partner monotherapy drug. Artemisinin derivatives include artemether, artesunate, and dihydroartemisinin. These derivatives reduce the parasite biomass within the first three days of therapy, while the partner drug, with longer half-life, eliminates the remaining parasites [26]. The WHO currently recommends five different ACTs: (1) artesunate-amodiaquine (AS + AQ), (2) artesunate-mefloquine (AS + MQ), (3) artesunate + sulfadoxine-pyrimethamine (AS + SP), (4) artemether-lumefantrine (AM-LM), and (5) dihydroartemisinin-piperaquine (DHA + PPQ). Additionally, artesunate-pyronaridine may be used in regions where ACT treatment response is low [26]. Access to ACT has been tremendous in the last 8 years, with a recorded increase of 122 million procured treatment courses for the period 2010–2016. However, resistance to currently used ACTs has important public health consequences, especially in the African region, where resistant *P. falciparum* is predominant.

Numerous cross-sectional studies [27, 28] have revealed the possible impacts of multiple strains of *P. falciparum* on the development of resistance to ACTs. In [29] and citations therein, drug-sensitive parasites are shown to strongly suppress the growth and transmission of drug-resistant *P. falciparum* parasites. Although high-transmission settings such as sub-Saharan Africa account for about 90% of all global malaria deaths, resistance to antimalarial drugs has been shown to emerge from low-transmission settings, such as Southeast Asia and South America [29]. Causes of parasite resistance to ACTs are diverse. Historical studies [30, 31] indicate that antimalarial-resistant parasites could emerge from a handful of lineages. It is argued elsewhere [32, 33] that recombination during sexual reproduction in the mosquito vector could be responsible for the delayed appearance of multilocus resistance in high-transmission regions. Moreover, owing to repeated exposure for many years, individuals in high-transmission settings are likely to develop clinical immunity to malaria, leading to stronger selection for resistance [34]. Studies in [29] also support the hypothesis that in-host competition between drug-sensitive and drug-resistant parasites could inhibit the spread of resistance in high-transmission settings. Owing to their integral role in the recent success of global malaria control, the protection of efficacy of ACTs should be a global health priority [35].

Mathematical models of in-host malaria epidemiology and control constitute important tools in guiding strategies for malaria control [36, 37] and the associated financial planning [38]. While some researchers have focussed on probabilistic models [39, 40], others have investigated the effects of drug treatment and resistance development using dynamic models [41, 42]. A deterministic model by Esteva et al. [43] monitored the impact of drug resistance on the transmission dynamics of malaria in a human population. In [29], the impacts of within-host parasite competition are shown to inhibit the spread of resistance [44, 45]. On the contrary, some models [39, 46] have suggested that within-host competition is likely to speed up the spread of resistance in high-transmission settings due to a phenomenon called "competitive release." In this paper, we provide theoretical insights using mathematical modelling of the impacts of multiple-strain infections on resistance, dynamics, and antimalarial control of *P. falciparum* malaria.

The rest of the paper is organized as follows: In Section 2, we formulate the within-human malaria model that has both the drug-sensitive and drug-resistant *P. falciparum* parasite strains subject to antimalarial therapy. In Section 3, we analyze the model based on epidemiological theorems. Within-host competition between parasite strains and the effects of antimalarial drug efficacy on parasite clearance are discussed in Section 4. Sensitivity analysis and multiple-strain infection and its effects on resistance and malaria dynamics are demonstrated in Section 5. We conclude the paper in Section 6 by emphasizing the need for antimalarial therapy with the potential to eradicate multiple-strain infection due to *P. falciparum*.

2. Model Formulation

We present in this paper a deterministic model that describes the within-human-host competition and transmission dynamics of two strains of *P. falciparum* parasites during malaria infection. The compartmental model considers the coinfection and competition between the drug-sensitive (dss) and the drug-resistant (drs) *P. falciparum* strains in the presence of antimalarial therapy. The drs arise presumably from the dss. The rare mechanism here could possibly be due to single point mutation [47]. Both drs and dss initiate immune responses that follow density-dependent kinetics.

Our model is composed of eight compartments: susceptible/healthy/unparasitized erythrocytes (red blood cells) $X(t)$, parasitized/infected erythrocytes ($Y_r(t)$ and $Y_s(t)$), merozoites ($M_s(t)$ and $M_r(t)$), gametocytes ($G_s(t)$ and $G_r(t)$), and immune cells $W(t)$. The healthy erythrocytes

(RBCs) make up the resource for competition between the drug-resistant and drug-sensitive parasite strains. The infected red blood cells (IRBCs) and different erythrocytic parasite life cycles are categorized based on the strain of the infecting parasite. The merozoites are therefore categorized into drug-sensitive and drug-resistant strains, denoted by $M_s(t)$ and $M_r(t)$, respectively. The merozoites invade the healthy erythrocytes during the erythrocytic stage, leading to formation of infected erythrocytes. The variable $Y_s(t)$ denotes the red blood cells (RBCs) infected with drug-sensitive merozoites, whereas $Y_r(t)$ refers to the RBCs infected with drug-resistant merozoites. Similarly, the variables $G_s(t)$ and $G_r(t)$ represent drug-sensitive and drug-resistant gametocytes, respectively. Owing to saturation in cell and parasite growth, we consider the nonlinear Michaelis–Mented–Monod function described in [48, 49] and used in [50–53] to model the reductive effects of the immune cells on the parasite and infected-cell populations.

The density of the healthy RBCs is increased at the rate λ_x per healthy RBC per unit time from the host's bone marrow, and healthy RBCs die naturally at a rate μ_x. Following parasite invasion by free floating merozoites, the healthy erythrocytes get infected by both drug-sensitive and drug-resistant merozoite strains at the rates β and $\delta_r\beta$, respectively. The parameter δ_r (with $0 < \delta_r < 1$) accounts for the reduced fitness (infectiousness) of the resistant parasite strains in relation to the drug-sensitive strains. The destruction of the healthy red blood cells is however limited by the adaptive immune cells W. This is represented by the term $1/(1+\gamma W)$, where γ is a measure of the efficacy of the immune cells. The equation that governs the evolution of the healthy RBCs is hence given by

$$\frac{dX}{dt} = \lambda_x - \mu_x X - \frac{\beta X}{1+\gamma W}\left(M_s + \delta_r M_r\right). \tag{1}$$

The parasitized erythrocytes are generated through mass action contact (invasion) between the susceptible healthy erythrocytes X and the blood floating merozoites (M_r and M_s). The merozoites subdivide mitotically, within the infected erythrocytes, into thousands of other merozoites, leading to cell burst and emergence of characteristic symptoms of malaria. Additionally, a single infected erythrocyte undergoes hemolysis at the rate μ_{ys} to produce P secondary merozoites, sustaining the erythrocytic cycle. The drug-sensitive IRBCs (Y_s) burst open to generate more drug-sensitive merozoites or drug-sensitive gametocytes at the rate σ_s. Similar dynamics are observed with the drug-resistant IRBCs, where the drug-resistant gametocytes are generated at the rate σ_r from IRBCs. Treatment with ACT is assumed to disfranchise the development of the merozoite within the infected erythrocyte. The drug-infested erythrocytes are hence likely to die faster. This is represented by the term $(1-\omega_s)^{-1}$, where $0 < \omega_s < 1$ represents the antimalarial-specific treatment efficacy. In this paper and for purposes of illustration and simulations, ω_s corresponds to the efficacy of artemether-lumefantrine (AL), which is the recommended first-line antimalarial ACT drug for *P. falciparum* infection in Kenya. We assume that no treatment is available for erythrocytes infected with the resistant parasite strains. The time rate of change for Y_s and Y_r takes the following form:

$$\begin{aligned}
\frac{dY_s}{dt} &= \frac{\beta X M_s}{1+\gamma W} - \frac{k_y Y_s W}{1+aY_s} - \frac{1}{1-\omega_s}\mu_{ys} Y_s - \sigma_s Y_s,\\
\frac{dY_r}{dt} &= \frac{\delta_r \beta X M_r}{1+\gamma W} - \frac{k_y Y_r W}{1+aY_r} - \mu_{yr} Y_r - \sigma_r Y_r.
\end{aligned} \tag{2}$$

The drug-resistant merozoites M_r and the drug-resistant gametocytes G_r die naturally at the rates μ_{mr} and μ_{gr}, respectively. It is further assumed that drug-sensitive merozoites M_s and gametocytes G_s may develop into drug-resistant merozoites M_r and gametocytes G_r at the rates Ψ_1 and Ψ_2, respectively. The cost of resistance associated with AL is represented by the parameter α_s. Parasite resistance to antimalarial drugs exacerbates the erythrocytic cycle and increases the cost of treatment [54, 55]. The higher the resistance to antimalarial therapy, the higher the density of malarial parasites in blood. We therefore model this decline in drug effectiveness by rescaling the density of merozoites produced per bursting parasitized erythrocyte P by the factor $(1-\alpha_s)$, where $\alpha_s = 1$ implies no resistance; that is, the ACT is highly effective in eradicating the parasites. If $\alpha_s = 0$ corresponds to maximum resistance, the used ACT drug is least effective in treating the infection. The converse of these descriptions applies to the drug-resistant *P. falciparum* parasite strains. The equations that govern the rate of change of the infected red blood cells and the merozoites take the following form:

$$\begin{aligned}
\frac{dM_s}{dt} &= (1-\alpha_s)P\mu_{ys}Y_s - \frac{\beta M_s X}{1+\gamma W} - \frac{k_m M_s W}{1+aM_s} - (\Psi_1 + \mu_{ms} + \zeta)M_s,\\
\frac{dM_r}{dt} &= (1-\alpha_r)P\mu_{yr}Y_r + \Psi_1 M_s - \frac{\delta_r \beta M_r X}{1+\gamma W} - \frac{k_m M_r W}{1+aM_r} - \mu_{mr} M_r,\\
\frac{dG_s}{dt} &= \sigma_s Y_s - \frac{k_g W G_s}{1+aG_s} - (\Psi_2 + \mu_{gs} + \eta)G_s,\\
\frac{dG_r}{dt} &= \sigma_r Y_r + \Psi_2 G_s - \frac{k_g W G_r}{1+aG_r} - \mu_{gr} G_r.
\end{aligned} \tag{3}$$

Antimalarial therapy increases the rate of elimination of drug-sensitive merozoites and gametocytes. This is represented by the nonnegative enhancement parameters ζ and η, respectively.

Although the innate immunity is faster, it is often limited by the on and off rates in its response to invading pathogens [56, 57]. The adaptive immunity, on the contrary, is very slower at the beginning but lasts long enough to ensure no parasite growth in subsequent infections [27]. We assume an immune system that is independent of the invading parasite strain. For purposes of simplicity, we only consider the adaptive immune system, which is mainly composed of the CD8 + T cells [58]. We adopt the assumption that the background recruitment of immune cells is constant (at the rate λ_w). Additionally, the production of the immune cells is assumed to be boosted by the infective and infected cells (G_r, G_s), (M_r, M_s), and (Y_r, Y_s) at constant rates h_g, h_m, and h_y, respectively. Circulating gametocytes, infective

merozoites, and infected erythrocytes are removed phagocytotically by the immune cells at the rates $k_g W$, $k_m W$, and $k_y W$, respectively. The immune cells also get depleted through natural death at the rate μ_w. The equation for the immune cells takes the following form:

$$\frac{dW}{dt} = \lambda_w + \left\{\frac{h_g(G_s+G_r)}{G_s+G_r+e_g} + \frac{h_y(Y_s+Y_r)}{Y_s+Y_r+e_y} + \frac{h_m(M_s+M_r)}{M_s+M_r+e_m}\right\}W - \mu_w W. \tag{4}$$

Following invasion by the merozoites, the IRBCs either produce merozoites or differentiate into gametocytes upon bursting. The total erythrocyte population at any time t, denoted by $C(t)$, is therefore given by

$$C(t) = X(t) + Y_s(t) + Y_r(t). \tag{5}$$

Similarly, the sum total of *P. falciparum* parasites, denoted by $P(t)$, within the host at any time t is described by the following equation:

$$P(t) = M_s(t) + M_r(t) + G_s(t) + G_r(t). \tag{6}$$

The above dynamics can be represented by the schematic diagram in Figure 1. The list of model variables and model parameters is provided in Tables 1 and 2, respectively.

2.1. Model Equations. Based on the above model descriptions and schematic diagram shown in Figure 1, the model in this paper consists of the following nonlinear system of ordinary differential equations:

$$\frac{dX}{dt} = \lambda_x - \mu_x X - \frac{\beta X}{1+\gamma W}(M_s + \delta_r M_r), \tag{7}$$

$$\frac{dY_s}{dt} = \frac{\beta X M_s}{1+\gamma W} - \frac{k_y Y_s W}{1+aY_s} - \frac{1}{1-\omega_s}\mu_{ys} Y_s - \sigma_s Y_s, \tag{8}$$

$$\frac{dY_r}{dt} = \frac{\delta_r \beta X M_r}{1+\gamma W} - \frac{k_y Y_r W}{1+aY_r} - \mu_{yr} Y_r - \sigma_r Y_r, \tag{9}$$

$$\frac{dM_s}{dt} = (1-\alpha_s)P\mu_{ys}Y_s - \frac{\beta M_s X}{1+\gamma W} - \frac{k_m M_s W}{1+aM_s} - (\Psi_1 + \mu_{ms} + \zeta)M_s, \tag{10}$$

$$\frac{dM_r}{dt} = (1-\alpha_r)P\mu_{yr}Y_r + \Psi_1 M_s - \frac{\delta_r \beta M_r X}{1+\gamma W} - \frac{k_m M_r W}{1+aM_r} - \mu_{mr} M_r, \tag{11}$$

$$\frac{dG_s}{dt} = \sigma_s Y_s - \frac{k_g W G_s}{1+aG_s} - (\Psi_2 + \mu_{gs} + \eta)G_s, \tag{12}$$

$$\frac{dG_r}{dt} = \sigma_r Y_r + \Psi_2 G_s - \frac{k_g W G_r}{1+aG_r} - \mu_{gr} G_r, \tag{13}$$

$$\frac{dW}{dt} = \lambda_w + \left\{\frac{h_g(G_s+G_r)}{G_s+G_r+e_g} + \frac{h_y(Y_s+Y_r)}{Y_s+Y_r+e_y} + \frac{h_m(M_s+M_r)}{M_s+M_r+e_m}\right\}W - \mu_w W, \tag{14}$$

subject to the following initial conditions:

$$\begin{aligned} X(0) &> 0, \\ Y_i(0) &\geq 0, \\ M_i(0) &\geq 0, \\ G_i(0) &\geq 0, \\ W(0) &> 0, \quad \text{for } i = s, r. \end{aligned} \tag{15}$$

3. Model Analysis

3.1. Positivity and Uniqueness of Solutions. The consonance between a formulated epidemiological model and its biological reality is key to its usefulness. Given that all the model parameters and variables are nonnegative, it is only sound that the model solutions be nonnegative at any future time $t \geq 0$ within a given biological space.

Theorem 1. *The region $\mathbb{R}^8_+$ with solutions of system (7)–(14) is positively invariant under the flow induced by system (7)–(14).*

Proof. We need to show that every trajectory from the region $\mathbb{R}^8_+$ will always remain within it. By contradiction, assume $\exists t^*$ (where t^* refers to time) in the interval $[0, \infty)$, such that $X(t^*) = 0$, $X'(t^*) < 0$ but for $0 < t < t^*$, $X(t) > 0$, and $Y_i(t) > 0$, $M_i(t) > 0$, $G_i(t) > 0$, and $W_i(t) > 0$ for $i = \{r, s\}$. Notice that, at $t = t^*$, $X(t)$ is declining from the original zero value. If such an X exists, then it should satisfy the differential equation (7). That is,

$$\frac{dX}{dt} = \lambda_x - \mu_x X(t^*) - \frac{\beta X(t^*)}{1+\gamma W(t^*)}(M_s(t^*) + \delta_r M_r(t^*)) = \lambda_x > 0. \tag{16}$$

We arrive at a contradiction, i.e., $X'(t^*) > 0$. This shows the nonexistence of such t^*. This argument can be extended to all the remaining seven variables $(Y_s, Y_r, M_s, M_r, G_s, G_r, W)$. The process of verification is however simpler. We can follow the steps as presented in [59, 60]. Let the total erythrocyte population $C(t)$ evolve according to the following formulation:

$$\frac{dC}{dt} \leq \lambda_x - \mu_c C, \tag{17}$$

where $\mu_c = \min\{\mu_x, \mu_{ys}, \mu_{yr}\}$. Similarly, the total density of malarial parasites $P(t)$ is described by

$$\frac{dP}{dt} \leq P\{(1-\alpha_s)\mu_{ys}Y_s + (1-\alpha_r)\mu_{yr}Y_r\} + \sigma_s Y_s + \sigma_r Y_r - \mu_p P, \tag{18}$$

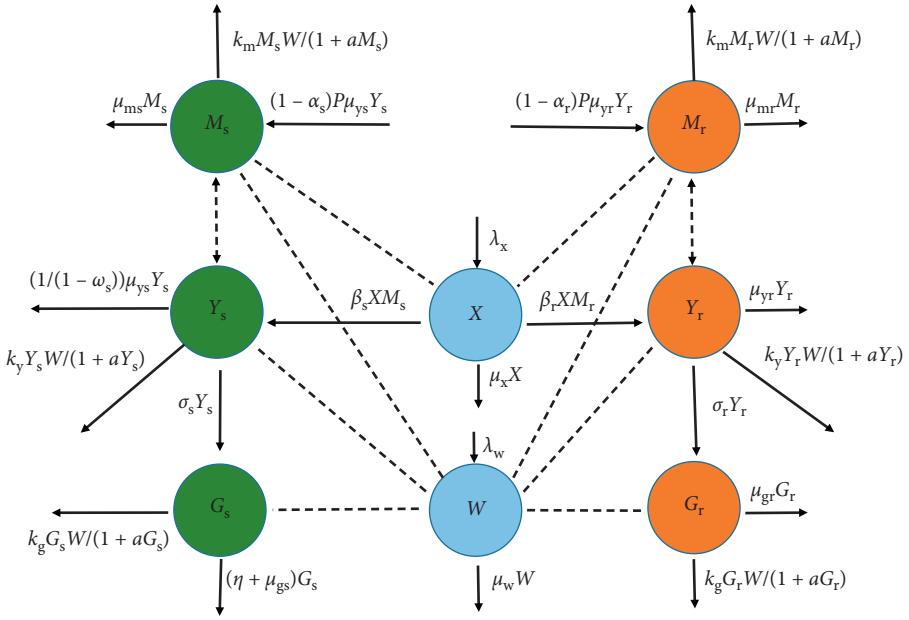

Figure 1: A model flow diagram. Drug-sensitive variables are shown in green colours while the drug-resistant variables are indicated in orange colours. Non-strain-specific variables like susceptible RBCs and immune cells are shown in blue colour. Solid lines indicate the movement of populations from one compartment to another. Dotted lines show possible interactions between the different populations.

Table 1: Description of the state variables of model system (11)–(18).

Variable	Description
X	Population of uninfected/unparasitized red blood cells (erythrocytes)
Y_s	Population of red blood cells infected by drug-sensitive merozoites
Y_r	Population of red blood cells infected by drug-resistant merozoites
M_s	Population of drug-sensitive merozoites
M_r	Population of drug-resistant merozoites
G_s	Population of drug-sensitive gametocytes
G_r	Population of drug-resistant gametocytes
W	Population of strain-independent immune cells

where $\mu_p = \min\{\mu_{ms}, \mu_{mr}, \mu_{gs}, \mu_{gr}\}$.

The solutions of equations (14), (17), and (18) are, respectively, given as

$$\begin{aligned} W(t) &\le \frac{\lambda_w}{\mu_w} + \left(W(0) - \frac{\lambda_w}{\mu_w}\right)e^{-\mu_w t}, \\ C(t) &\le \frac{\lambda_x}{\mu_c} + \left(C(0) - \frac{\lambda_x}{\mu_c}\right)e^{-\mu_c t}, \\ P(t) &\le \frac{\sigma_s \int_0^t Y_s(t)\Delta_{IF}dt + \sigma_r \int_0^t Y_r(t)\Delta_{IF}dt}{\Delta_{IF}} \\ &\quad + \left(P(0) - \frac{(\sigma_s+\sigma_r)\mu_p}{(1-\alpha_s)\mu_{ys} + (1-\alpha_r)\mu_{yr}}\right)\frac{1}{\Delta_{IF}}, \end{aligned} \tag{19}$$

where

$$\Delta_{IF} = \exp\left\{-\left((1-\alpha_s)\mu_{ys}\int_0^t Y_s(t)dt + (1-\alpha_r)\mu_{yr}\int_0^t Y_r(t)dt\right) - \int_0^t \mu_p dt\right\}. \tag{20}$$

Here, $C(0) = X(0) + Y_s(0) + Y_r(0)$ and $P(0) = M_s(0) + M_r(0) + G_s(0) + G_r(0)$ represent the initial total populations of erythrocytes and malarial parasites, respectively. We observe that all the solutions of equations (14), (17), and (18) remain nonnegative for all future time, $t \ge 0$. Moreover, the total populations are bounded: $0 \le C(t) \le \max\{C(0), (\lambda_x/\mu_c)\}$, $0 \le W(t) \le \max\{W(0), \lambda_w/\mu_w\}$ and $P(t) \le \max(P(0), ((\sigma_s+\sigma_r)\mu_p)/((1-\alpha_s)\mu_{ys} + (1-\alpha_r)\mu_{yr}))$. Thus, all the state variables of model system (7)–(14) and all their corresponding solutions are nonnegative and bounded in the phase space φ, where

$$\begin{aligned} \varphi = \Bigg[&(X, Y_s, Y_r, M_s, M_r, G_s, G_r, W) \in \mathbb{R}_+^8 : \\ &C(t) \le \max\left\{C(0), \frac{\lambda_x}{\mu_c}\right\}, \\ &W(t) \le \max\left\{W(0), \frac{\lambda_w}{\mu_w}\right\}, \\ &P(t) \le \max\left(P(0), \frac{(\sigma_s+\sigma_r)\mu_p}{(1-\alpha_s)\mu_{ys} + (1-\alpha_r)\mu_{yr}}\right)\Bigg]. \end{aligned} \tag{21}$$

Table 2: Description of model parameters.

Parameter	Description
λ_x	The rate of recruitment of red blood cells
ω_s	Antimalarial treatment efficacy
α_s, α_r	Parasite strain-specific fitness cost
λ_w	Background recruitment rate of immune cells
e_g, e_m, e_y	Hill parameters in G_i, M_i, and Y_i dynamics $(i = s, r)$
μ_x	Per capita natural mortality rate of unparasitized erythrocytes
μ_{ys}	Natural mortality rate of drug-sensitive IRBCs
μ_{yr}	Natural death rate of drug-resistant IRBCs
ζ, η	Rate of antimalarial eradication of merozoites and gametocytes, respectively
μ_{ms}	Death rate of drug-sensitive merozoites
μ_{mr}	Mortality rate of drug-resistant merozoites
μ_{gs}	Per capita mortality rate of drug-sensitive gametocytes
μ_{gr}	Mortality rate of drug-resistant gametocytes
μ_w	Natural mortality rate of immune cells (CD8 + T cells)
β	The rate of infection of susceptible RBCs by blood floating merozoites
σ_r, σ_s	Rate of formation of gametocytes from the infected RBCs
P	Number of merozoites produced per dying infected RBC
h_y	Immune cell proliferation rate due to IRBCs
h_m	Immune cell proliferation rate due to asexual merozoites
h_g	Immune cell proliferation rate due to gametocytes
k_y	Phagocytosis rate of IRBCs by immune cell
k_m	Phagocytosis rate of merozoites by immune cell
k_g	Phagocytosis rate of gametocytes by immune cell
Ψ_1	Rate of development of resistance by drug-sensitive merozoites
Ψ_2	Rate of development of resistance by drug-sensitive gametocytes
δ_r	Accounts for the reduced fitness of the resistant parasite strains
γ	Efficiency of immune effector to inhibit merozoite infection
$1/a$	Half-saturation constant for $Y(t)$, $M(t)$, and $G(t)$

It is obvious that φ is twice continuously differentiable function. That is, $\varphi_i \in \mathbb{C}^2$. This is because its components φ_i, $i = 1, 2, \ldots, 8$, are rational functions of state variables that are also continuously differentiable functions. We conclude that the domain φ is positively invariant. It is therefore feasible and biological meaningful to study model system (7)–(14).

Theorem 2. *The model system (7)–(14) has a unique solution.*

Proof. Let $\mathbf{x} = (X, Y_s, Y_r, M_s, M_r, G_s, G_r, W)^T \in \mathbb{R}^8_+$ so that $\mathbf{x}_1 = X$ and $\mathbf{x}_2 = Y_s$ as presented in system (7)–(14). Similarly, let $\mathbf{g}(\mathbf{x}) = (\mathbf{g}_i(\mathbf{x}),\ i = 1, \ldots, 8)^T$ be a vector defined in $\mathbb{R}^8_+$. The model system (7)–(14) can hence be written as

$$\frac{dx}{dt} = \mathbf{g}(\mathbf{x}), \quad \mathbf{x}(0) = \mathbf{x}_0, \tag{22}$$

where $\mathbf{x}$: $[0, \infty) \longrightarrow \mathbb{R}^8_+$ denotes a column vector of state variables and $\mathbf{g} : \mathbb{R}^8_+ \longrightarrow \mathbb{R}^8_+$ represents the right-hand side (RHS) of system (7)–(14). The result is as follows.

Lemma 1. *The function* $\mathbf{g}$ *is continuously differentiable in* $\mathbf{x}$.

Proof. All the terms in $\mathbf{g}$ are either linear polynomials or rational functions of nonvanishing polynomials. Since the state variables $(X, Y_s, Y_r, M_s, M_r, G_s, G_r, W)$ are all continuously differentiable functions of t, all the elements of vector $\mathbf{g}$ are continuously differentiable. Moreover, let $L(\mathbf{x}, \mathbf{n}, \theta) = \{\mathbf{x} + \theta(\mathbf{n} - \mathbf{x}) : 0 \le \theta \le 1\}$. By the mean value theorem,

$$\|\mathbf{g}(\mathbf{n}) - \mathbf{g}(\mathbf{x})\|_\infty = \|\mathbf{g}'(\mathbf{m}; \mathbf{n} - \mathbf{x})\|_\infty, \tag{23}$$

where $\mathbf{m} \in L(\mathbf{x}, \mathbf{n}, \theta)$ denotes the mean value point and $\mathbf{g}'$ the directional derivative of the function $\mathbf{g}$ at $\mathbf{m}$. However,

$$\begin{aligned} \|\mathbf{g}'(\mathbf{m}, \mathbf{n} - \mathbf{x})\|_\infty &= \left\| \sum_{i=1}^{8} (\nabla \mathbf{g}_i(\mathbf{m}) \cdot (\mathbf{n} - \mathbf{x})) e_i \right\|_\infty \\ &\le \left\| \sum_{i=1}^{8} (\nabla \mathbf{g}_i(\mathbf{m}) \right\|_\infty \|\mathbf{n} - \mathbf{x}\|_\infty, \end{aligned} \tag{24}$$

where e_i is the i^{th} coordinate unit in $\mathbb{R}^8_+$. We can clearly see that all the partial derivatives of $\mathbf{g}$ are bounded and that there exists a nonnegative U such that

$$\left\| \sum_{i=1}^{8} (\nabla \mathbf{g}_i(\mathbf{m}) \right\|_\infty \le U, \quad \text{for all } \mathbf{m} \in L. \tag{25}$$

Therefore, there exists $U > 0$ such that

$$\|\mathbf{g}(\mathbf{n}) - \mathbf{g}(\mathbf{x})\|_\infty \le U \|\mathbf{n} - \mathbf{x}\|_\infty. \tag{26}$$

This shows that the function $\mathbf{g}$ is Lipschitz continuous. Since $\mathbf{g}$ is Lipschitz continuous, model system (7)–(14) has a unique solution by the uniqueness theorem of Picard [61].

3.2. Stability Analysis of the Parasite-Free Equilibrium Point (PFE). The in-host malaria dynamics are investigated by studying the behaviour of the model at different model equilibrium points. Knowledge on model equilibrium points is useful in deriving parameters that drive the infection to different stability points. The model system (7)–(14) has a parasite-free equilibrium point $\mathbb{E}_0$ given by

$$\begin{aligned} \mathbb{E}_0 &= (X_*, Y_{s*}, Y_{r*}, M_{s*}, M_{r*}, G_{s*}, G_{r*}, W_*) \\ &= \left(\frac{\lambda_x}{\mu_x}, 0, 0, 0, 0, 0, 0, \frac{\lambda_w}{\mu_w} \right). \end{aligned} \tag{27}$$

Using the next-generation operator method by van den Driessche and Watmough [62] and matrix notations therein, we obtain a nonsingular matrix Q showing the terms of transitions from one compartment to the other and a nonnegative matrix F of new infection terms as follows:

$$F = \begin{pmatrix} 0 & 0 & \dfrac{\beta\lambda_x\mu_w}{(\gamma\lambda_w+\mu_w)\mu_x} & 0 & 0 & 0 \\ 0 & 0 & 0 & \dfrac{\delta_r\beta\lambda_x\mu_w}{(\gamma\lambda_w+\mu_w)\mu_x} & 0 & 0 \\ 0 & 0 & 0 & 0 & 0 & 0 \\ 0 & 0 & 0 & 0 & 0 & 0 \\ 0 & 0 & 0 & 0 & 0 & 0 \\ 0 & 0 & 0 & 0 & 0 & 0 \end{pmatrix}, \quad (28)$$

$$Q = \begin{pmatrix} \nu_1 & 0 & 0 & 0 & 0 & 0 \\ 0 & \nu_2 & 0 & 0 & 0 & 0 \\ -P(1-\alpha_s)\mu_{ys} & 0 & \nu_3 & 0 & 0 & 0 \\ 0 & -P(1-\alpha_r)\mu_{yr} & -\Psi_1 & \nu_4 & 0 & 0 \\ -\sigma_s & 0 & 0 & 0 & \nu_5 & 0 \\ 0 & -\sigma_r & 0 & 0 & -\Psi_2 & \nu_6 \end{pmatrix}, \quad (29)$$

where $\nu_1 = ((k_y\lambda_w/\mu_w) + \sigma_s + (\mu_{ys}/1-\omega_s))$, $\nu_2 = ((k_y\lambda_w/\mu_w) + \sigma_r + \mu_{yr})$, $\nu_4 = (\mu_{mr} + (k_m\lambda_w/\mu_w) + (\delta_r\beta\lambda_x\mu_w/(\gamma\lambda_w + \mu_w)\mu_x))$, $\nu_3 = (\zeta + \mu_{ms} + \Psi_1 + (k_m\lambda_w/\mu_w) + (\beta\lambda_x\mu_w/(\gamma\lambda_w + \mu_w)\mu_x))$, and $\nu_5 = (\eta + \mu_{gs} + (k_g\lambda_w/\mu_w) + \Psi_2)$, $\nu_6 = (\mu_{gr} + (k_g\lambda_w/\mu_w))$.

The effective reproduction number R_E of model system (7)–(14) associated with the parasite-free equilibrium is the spectral radius of the next-generation matrix FQ^{-1}, where

$$Q^{-1} = \begin{pmatrix} \dfrac{1}{\nu_1} & 0 & 0 & 0 & 0 & 0 \\ 0 & \dfrac{1}{\nu_2} & 0 & 0 & 0 & 0 \\ \dfrac{P(1-\alpha_s)\mu_{ys}}{\nu_1\nu_3} & 0 & \dfrac{1}{\nu_3} & 0 & 0 & 0 \\ \dfrac{P(1-\alpha_s)\mu_{ys}\Psi_1}{\nu_1\nu_3\nu_4} & \dfrac{P(1-\alpha_r)\mu_{yr}}{\nu_2\nu_4} & 0 & \dfrac{1}{\nu_4} & 0 & 0 \\ \sigma_s/\nu_1\nu_5 & 0 & 0 & 0 & \dfrac{1}{\nu_5} & 0 \\ \sigma_s\Psi_2/\nu_1\nu_5\nu_6 & \dfrac{\sigma_r}{\nu_2\nu_6} & 0 & 0 & \Psi_2/\nu_5\nu_6 & \dfrac{1}{\nu_6} \end{pmatrix}. \quad (30)$$

It follows that

$$R_E = \rho\left(FQ^{-1}\right) = \max\{R_s, R_r\}, \quad (31)$$

where

$$R_s = \frac{P(1-\alpha_s)\mu_{ys}\beta\lambda_x\mu_w}{\left(\left(k_y\lambda_w/\mu_w\right) + \sigma_s + \left(\mu_{ys}/1-\omega_s\right)\right)(\zeta + \mu_{ms} + (k_m\lambda_w/\mu_w) + \Psi_1 + (\beta\lambda_x\mu_x/(\gamma\lambda_w + \mu_w)\mu_x))(\gamma\lambda_w + \mu_w)\mu_x},$$

$$R_r = \frac{P(1-\alpha_r)\mu_{yr}\delta_r\beta\lambda_x\mu_w}{\left(\left(k_y\lambda_w/\mu_w\right) + \sigma_r + \mu_{yr}\right)(\mu_{mr} + (k_m\lambda_w/\mu_w) + (\delta_r\beta\lambda_x\mu_w/(\gamma\lambda_w + \mu_w)\mu_x))(\gamma\lambda_w + \mu_w)\mu_x}. \quad (32)$$

From equation (31), it is evident that, in a multiple-strain *P. falciparum* malaria infection, the progression of the disease depends on the reproduction number of different parasite strains. If the threshold quantity $R_s > R_r$, the drug-sensitive parasite strains will dominate the drug-resistant strains and hence the driver of the infection. To manage the infection in this case, the patient should be given antimalarials that can eradicate the drug-sensitive parasites. Conversely, if $R_r > R_s$, the infection is mainly driven by the drug-resistant parasite strains. In this scenario, the used antimalarial drugs should be highly efficacious and effective enough to kill both the drug-resistant and drug-sensitive parasite strains in the blood of the human host. This result is quite instrumental in improving antimalarial therapy for *P. falciparum* infections. The best antimalarials should be sufficient enough to eradicate both parasite strains within the human host.

Based on Theorem 2 in [63], we have the following lemma.

Lemma 2. *The parasite-free equilibrium point $\mathbb{E}_0$ is locally asymptotically stable if $R_E < 1$ ($R_s < 1$ and $R_r < 1$) and unstable otherwise.*

The Jacobian matrix associated with the in-host model system (7)–(14) at $\mathbb{E}_0$ is given by

$$J_{\mathbb{E}_0} = \begin{pmatrix} -\mu_x & 0 & 0 & \frac{-\beta\lambda_x\mu_w}{(\gamma\lambda_w+\mu_w)\mu_x} & \frac{-\delta_r\beta\lambda_x\mu_w}{(\gamma\lambda_w+\mu_w)\mu_x} & 0 & 0 & 0 \\ 0 & -\nu_1 & 0 & \frac{\beta\lambda_x\mu_w}{(\gamma\lambda_w+\mu_w)\mu_x} & 0 & 0 & 0 & 0 \\ 0 & 0 & -\nu_2 & 0 & \frac{\beta\lambda_x\mu_w}{(\gamma\lambda_w+\mu_w)\mu_x} & 0 & 0 & 0 \\ 0 & P(1-\alpha_s)\mu_{ys} & 0 & -\nu_3 & 0 & 0 & 0 & 0 \\ 0 & 0 & P(1-\alpha_r)\mu_{yr} & \Psi_1 & -\nu_4 & 0 & 0 & 0 \\ 0 & \sigma_s & 0 & 0 & 0 & -\nu_5 & 0 & 0 \\ 0 & 0 & \sigma_r & 0 & 0 & \Psi_2 & -\nu_6 & 0 \\ 0 & \frac{h_y\lambda_w}{e_y\mu_w} & \frac{h_y\lambda_w}{e_y\mu_w} & \frac{h_m\lambda_w}{e_m\mu_w} & \frac{h_m\lambda_w}{e_m\mu_w} & \frac{h_g\lambda_w}{e_g\mu_w} & \frac{h_g\lambda_w}{e_g\mu_w} & -\mu_w \end{pmatrix}, \tag{33}$$

where the terms $\nu_1, \ldots, \nu_6$ are as defined in (30). It is clear from matrix (33) that the first four eigenvalues are $-\mu_x$ (from column 1), $-\mu_w$ (from column 8), $-(\mu_{gr} + (k_g\lambda_w/\mu_w)) = -\nu_6$ (from column 7), and $-(\eta + \mu_{gs} + (k_g\lambda_w/\mu_w)) = -\nu_5$ (from column 6). They are all negative. The remaining four eigenvalues are obtained from the roots of the following quartic equation:

$$P(\lambda) = \lambda^4 + p_1\lambda^3 + p_2\lambda^2 + p_3\lambda + p_4, \tag{34}$$

where

$$p_1 = (\nu_1 + \nu_2 + \nu_3 + \nu_4) > 0, \tag{35}$$

$$\begin{aligned} p_2 = {} & \nu_3\nu_4 + \nu_2(\nu_3 + \nu_4) + \nu_1(\nu_2 + \nu_3 + \nu_4) \\ & - \frac{P\beta\lambda_x\mu_w}{(\gamma\lambda_w+\mu_w)\mu_x}\left((1-\alpha_s)\mu_{ys} - (1-\alpha_r)\mu_{yr}\delta_r\right), \end{aligned} \tag{36}$$

$$\begin{aligned} p_3 = {} & \frac{1}{K}\left[\nu_3\left(\nu_2\nu_4K - P(1-\alpha_r)\mu_{yr}\delta_r\beta\lambda_x\mu_w\right)\right] \\ & - \frac{1}{K}\left[P(1-\alpha_s)\mu_{ys}\beta\lambda_x\mu_w(\nu_2+\nu_4)\right. \\ & \left. + \frac{\nu_1}{K}\left[(\nu_3\nu_4) + \nu_2(\nu_3+\nu_4)\right]K - P(1-\alpha_r)\mu_{yr}\delta_r\beta\lambda_x\mu_w\right], \end{aligned} \tag{37}$$

$$p_4 = \frac{\left(\nu_2\nu_4K - P(1-\alpha_r)\mu_{yr}\delta_r\beta\lambda_x\mu_w\right)\left(\nu_1\nu_3K - P(1-\alpha_s)\mu_{ys}\beta\lambda_x\mu_w\right)}{K}. \tag{38}$$

Due to complexity in the coefficients of the polynomial (34), we shall rely on the Routh–Hurwitz stability criterion [64], which provides sufficient condition for the existence of the roots of the given polynomial on the left half of the plane.

Definition 1. The solutions of the quartic equation (34) are negative or have negative real parts provided that the determinants of all Hurwitz matrices are positive [64].

Based on the Routh–Hurwitz criterion, the system of inequalities that describe the stability region $\mathbb{E}_0$ is presented as follows:

(i) $p_1 > 0$
(ii) $p_3 > 0$
(iii) $p_4 > 0$
(iv) $p_1p_2p_3 > p_3^2 + p_1^2p_4$

From (35), it is clear that $p_1 > 0$. Upon simplifying p_2 in (36), we obtain

$$\begin{aligned} p_2 = {} & \nu_3\nu_4 + \nu_2\nu_3 + \nu_1\nu_2 + \nu_1\nu_4 + \left(\nu_1\nu_3 + \frac{\lambda_x\mu_w\beta B_1}{K}\right) \\ & + \left(\nu_2\nu_4 + \frac{\lambda_x\mu_w\delta_r\beta B_2}{K}\right), \end{aligned} \tag{39}$$

where $B_1 = -P(1-\alpha_s)\mu_{ys}$ and $B_2 = -P(1-\alpha_r)\mu_{yr}$.

Thus,

$$\begin{aligned} p_2 = {} & \nu_3\nu_4 + \nu_2\nu_3 + \nu_1\nu_2 + \nu_1\nu_4 + \nu_1\nu_3\left[1 - \frac{B_1\beta\lambda_x\mu_w}{\nu_1\nu_3K}\right] \\ & + \nu_2\nu_4\left[1 - \frac{B_2\delta_r\beta\lambda_x\mu_w}{\nu_2\nu_4K}\right] \\ = {} & (\nu_1+\nu_3)(\nu_2+\nu_4) + \nu_1\nu_3[1-R_s] \\ & + \nu_2\nu_4[1-R_r] > 0, \quad \text{if and only if } R_s, R_r < 1. \end{aligned} \tag{40}$$

Similarly, the expression for p_4 can be rewritten as follows:

$$\begin{aligned} p_4 &= \left[\nu_1\nu_3 + \frac{B_1\beta\lambda_x\mu_x}{K}\right]\left[\nu_2\nu_4 + \frac{B_2\delta_r\beta\lambda_x\mu_w}{K}\right] \\ &= \nu_1\nu_3\left[1 + \frac{B_1\beta\lambda_x\mu_w}{\nu_1\nu_3K}\right]\nu_2\nu_4\left[1 + \frac{B_2\delta_r\beta\lambda_x\mu_w}{\nu_2\nu_4K}\right] \\ &= \nu_1\nu_3\left[1 - R_s\right]\nu_2\nu_4\left[1 - R_r\right] > 0, \quad \text{if and only if } R_s, R_r < 1. \end{aligned} \tag{41}$$

Lastly, upon simplifying equation (37), we obtain

$$\begin{aligned} p_3 &= \nu_2\nu_3\nu_4 + \nu_1\nu_3\nu_4 + \nu_1\nu_2\left(\nu_3 + \nu_4\right) \\ &\quad + \frac{\beta B_1\lambda_x\mu_w\left(\nu_2 + \nu_4\right)}{K} \\ &\quad + \frac{\delta_r\beta B_2\lambda_x\mu_w\left(\nu_1 + \nu_3\right)}{K} \\ &= \nu_1\nu_2\nu_3\nu_4\left[\frac{1}{\nu_4}\left(1 + \frac{\beta B_1\lambda_x\mu_w}{\nu_1\nu_3K}\right) + \frac{1}{\nu_2}\left(1 + \frac{\beta B_1\lambda_x\mu_w}{\nu_1\nu_3K}\right)\right. \\ &\quad \left. + \frac{1}{\nu_1}\left(1 + \frac{\delta_r\beta B_2\lambda_x\mu_w}{\nu_2\nu_4K}\right) + \frac{1}{\nu_3}\left(1 + \frac{\delta_r\beta B_2\lambda_x\mu_w}{\nu_2\nu_4K}\right)\right] \\ &= \nu_1\nu_2\nu_3\nu_4\left[\frac{\nu_2 + \nu_4}{\nu_2\nu_4}\left(1 - R_s\right) + \frac{\nu_1 + \nu_3}{\nu_1\nu_3}\left(1 - R_r\right)\right] \\ &= \nu_1\nu_3\left(\nu_2 + \nu_4\right)\left[1 - R_s\right] + \nu_2\nu_4\left(\nu_1 + \nu_3\right)\left[1 - R_r\right] > 0, \\ &\qquad \text{if and only if } R_s, R_r < 1. \end{aligned} \tag{42}$$

Since all the coefficients of the quartic equation (34) are nonnegative, all its roots are therefore negative or have negative real parts. Hence, the Jacobian matrix (33) has negative eigenvalues or eigenvalues with negative real parts if and only if the effective reproduction number R_E is less than unity. Equilibrium point $\mathbb{E}_0$ is therefore locally asymptotically stable when $R_E < 1$ (when both $R_s < 1$ and $R_r < 1$). This implies that an effective antimalarial drug would cure the costrain infected human host, provided that the drug reduces the effective reproduction number to less than 1.

Lemma 2 shows that *P. falciparum* malaria can be eradicated/controlled within the human host if the initial parasite and cell populations are within the basin of attraction of the trivial equilibrium point $\mathbb{E}_0$. To be certain to eradicate/control the infection irrespective of the initial parasite and cell populations, we need to prove the global stability of the parasite-free equilibrium point. This is presented in the following section.

3.3. Global Asymptotic Stability Analysis of the Parasite-Free Equilibrium Point. Following the work by Kamgong and Sallet [65], we begin by rewriting system (7)–(14) in a pseudotriangular form:

$$\left.\begin{aligned} \dot{X}_1 &= D_1(X)\left(X - X_1^*\right) + D_2(X)X_2, \\ \dot{X}_2 &= D_3(X)X_2, \end{aligned}\right\}, \tag{43}$$

where X_1 is a vector representing the densities of noninfective population groups (unparasitized erythrocytes and immune cells) and X_2 represents the densities of infected/infective groups (infective *P. falciparum* parasites and/or infected host cells) that are responsible for disease transmissions. For purposes of clarity and simplicity to the reader, we shall represent $(X_1, 0)$ with X_1 and $(0, X_2)$ with X_2 in $\mathbb{R}_+^8 \times \mathbb{R}_+^8$. We assume the existence of a parasite-free equilibrium in φ: $X^* = (X_1^*, 0)$. Thus,

$$\begin{aligned} X &= \left(X_1, X_2\right), \\ X_1 &= (X, W), \\ X_2 &= \left(Y_s, Y_r, M_s, M_r, G_s, G_r\right), \\ X_1^* &= \left(\frac{\lambda_x}{\mu_x}, \frac{\lambda_w}{\mu_w}\right). \end{aligned} \tag{44}$$

We analyze system (43) based on the assumption that it is positively invariant and dissipative in φ. Moreover, the subsystem $\overline{X}_1$ is globally asymptotically stable at X_1^* on the projection of φ on $\mathbb{R}_+^8$. This implies that whenever there are no infective malarial parasites, all cell populations will settle at the parasite-free equilibrium point $\mathbb{E}_0$. Finally, D_2 in (43) is a Metzler matrix that is irreducible for any $X \in \varphi$. We assume adequate interactions between and among different parasites and cell compartments in the model.

The matrices $D_1(X)$ and $D_2(X)$ are easily computed from subsystem $\dot{X}_1$ in (43) so that we have

$$D_1(X) = \begin{pmatrix} -\mu_x & 0 \\ 0 & -\mu_w \end{pmatrix},$$

$$D_2(X) = \begin{pmatrix} 0 & 0 & \frac{-\beta\lambda_x\mu_w}{(\gamma\lambda_w+\mu_w)\mu_x} & \frac{-\delta_r\beta\lambda_x\mu_w}{(\gamma\lambda_w+\mu_w)\mu_x} & 0 & 0 \\ \frac{h_y\lambda_w}{e_y\mu_w} & \frac{h_y\lambda_w}{e_y\mu_w} & \frac{h_m\lambda_w}{e_m\mu_w} & \frac{h_m\lambda_w}{e_m\mu_w} & \frac{h_g\lambda_w}{e_g\mu_w} & \frac{h_g\lambda_w}{e_g\mu_w} \end{pmatrix}. \tag{45}$$

We can easily see that the eigenvalues of matrix D_1 are both real and negative ($-\mu_x < 0, -\mu_w < 0$). This shows that the subsystem $\dot{X}_1 = D_1(X)(X - X_1^*) + D_2(X)X_2$ is globally asymptotically stable at the trivial equilibrium X_1^*. Additionally, from subsystem $\dot{X}_2 = D_3(X)X_2$, we obtain the following matrix:

$$D_3(X) = \begin{pmatrix} -\nu_1 & 0 & \frac{\beta\lambda_x\mu_w}{(\gamma\lambda_w+\mu_w)\mu_x} & 0 & 0 & 0 \\ 0 & -\nu_2 & 0 & \frac{\beta\lambda_x\mu_w}{(\gamma\lambda_w+\mu_w)\mu_x} & 0 & 0 \\ P(1-\alpha_s)\mu_{ys} & 0 & -\nu_3 & 0 & 0 & 0 \\ 0 & P(1-\alpha_r)\mu_{yr} & \Psi_1 & -\nu_4 & 0 & 0 \\ \sigma_s & 0 & 0 & 0 & -\nu_5 & 0 \\ 0 & \sigma_r & 0 & 0 & \Psi_2 & -\nu_6 \end{pmatrix}. \tag{46}$$

Notice that all the off-diagonal entries of $D_3(X)$ are nonnegative (equal to or greater than zero), showing that $D_3(X)$ is a Metzler matrix. To show the global stability of the parasite-free equilibrium $\mathbb{E}_0$, we need to show that the square matrix $D_3(X)$ in (46) is Metzler stable. We therefore need to prove the following lemma.

Lemma 3. *Let K be a square Metzler matrix that is block decomposed:*

$$K = \begin{pmatrix} K_{11} & K_{12} \\ K_{21} & K_{22} \end{pmatrix}, \tag{47}$$

where K_{11} and K_{22} are square matrices. The matrix K is Metzler stable if and only if K_{11} and $K_{22} - K_{21}K_{11}^{-1}K_{12}$ are Metzler stable.

Proof. The matrix K in Lemma 3 refers to $D_3(X)$ in our case. We therefore let

$$K_{11} = \begin{pmatrix} -\nu_1 & 0 & \frac{\beta\lambda_x\mu_w}{(\gamma\lambda_w+\mu_w)\mu_x} \\ 0 & -\nu_2 & 0 \\ P(1-\alpha_s)\mu_{ys} & 0 & -\nu_3 \end{pmatrix},$$

$$K_{12} = \begin{pmatrix} 0 & 0 & 0 \\ \frac{\beta\lambda_x\mu_w}{(\gamma\lambda_w+\mu_w)\mu_x} & 0 & 0 \\ 0 & 0 & 0 \end{pmatrix},$$

$$K_{21} = \begin{pmatrix} 0 & P(1-\alpha_r)\mu_{yr} & \Psi_1 \\ \sigma_s & 0 & 0 \\ 0 & \sigma_r & 0 \end{pmatrix}, \tag{48}$$

$$K_{22} = \begin{pmatrix} -\nu_4 & 0 & 0 \\ 0 & -\nu_5 & 0 \\ 0 & \Psi_2 & -\nu_6 \end{pmatrix}.$$

Results from analytical computations based on Maple software give

$$K_{11}^{-1} = \begin{pmatrix} -\dfrac{\nu_3}{\nu_1\nu_3 + \left(P\beta(\alpha_s - 1)\lambda_x\mu_w\mu_{ys}\right)/\left((\gamma\lambda_w + \mu_w)\mu_x\right)} & 0 & -\dfrac{\beta\lambda_x\mu_w}{\nu_1\nu_3(\gamma\lambda_w + \mu_w)\mu_x + P\beta(\alpha_s - 1)\lambda_x\mu_w\mu_{ys}} \\ 0 & -\dfrac{1}{\nu_2} & 0 \\ \dfrac{P(\alpha_s - 1)(\gamma\lambda_w + \mu_w)\mu_x\mu_{ys}}{\nu_1\nu_3(\gamma\lambda_w + \mu_w)\mu_x + P\beta(\alpha_s - 1)\lambda_x\mu_w\mu_{ys}} & 0 & -\dfrac{\nu_1}{\nu_1\nu_3 + \left(P\beta(\alpha_s - 1)\lambda_x\mu_w\mu_{ys}\right)/\left((\gamma\lambda_w + \mu_w)\mu_x\right)} \end{pmatrix}, \tag{49}$$

$$K_{22} - K_{21}K_{11}^{-1}K_{12} = \begin{pmatrix} -\nu_4 & 0 & 0 \\ 0 & -\nu_5 & 0 \\ 0 & \Psi_2 & -\nu_6 \end{pmatrix}, \tag{50}$$

where $\nu_4 = (\mu_{mr} + (k_m\lambda_w/\mu_w) + (\delta_r\beta\lambda_x\mu_w/(\gamma\lambda_w + \mu_w)\mu_x))$, $\nu_5 = (\eta + \mu_{gs} + (k_g\lambda_w/\mu_w) + \Psi_2)$, and $\nu_6 = (\mu_{gr} + (k_g\lambda_w/\mu_w))$.

From equation (50), it is evident that all the diagonal elements of matrix $K_{22} - K_{21}K_{11}^{-1}K_{12}$ are negative and the rest of the elements in the matrix are nonnegative. This shows that matrix $K_{22} - K_{21}K_{11}^{-1}K_{12}$ is Metzler stable, and the parasite-free equilibrium point $\mathbb{E}_0$ is globally asymptotically stable in the biologically feasible region φ of model system (7)–(14). Epidemiologically, the above result implies that when there is no malaria infection, different cell populations under consideration will stabilize at the parasite-free equilibrium. However, if there exists a *P. falciparum* infection, then an appropriate control in forms of effective antimalarial drugs would be necessary to clear the parasites from the human blood and restore the system to the stable parasite-free equilibrium state.

3.4. Coexistence of Parasite-Persistent Equilibrium Point. The existence of a nontrivial equilibrium point represents a scenario in which the *P. falciparum* parasites are present within the host and the following conditions hold: $X^* > 0, Y_s^* \geq 0, Y_r^* \geq 0, M_s^* \geq 0, M_r^* \geq 0, G_s^* \geq 0, G_r^* \geq 0$, and $W^* > 0$. Upon equating the right-hand side of system (7)–(14) to zero and solving for the state variables, we obtain the parasite-persistent equilibrium point $\mathbb{E}_1 = (X^*, Y_s^*, Y_r^*, M_s^*, M_r^*, G_s^*, G_r^*, W^*)$, where

$$\begin{aligned} X^* &= \frac{(1 + \gamma W^*)\lambda_x}{\beta(M_s^* + \delta_r M_r^*) + (1 + \gamma W^*)\mu_x}, \\ Y_s^* &= \frac{\overline{b} + \sqrt{\overline{b}^2 - 4\overline{a}\overline{c}}}{-2\overline{a}}, \\ Y_r^* &= \frac{\underline{b} + \sqrt{\underline{b}^2 - 4\,\underline{a}\,\underline{c}}}{-2\,\underline{a}}, \end{aligned} \tag{51}$$

$$\overline{a} = -a\left((1 - \omega_s)\sigma_s + \mu_{ys}\right)(\beta M_s^* + \beta M_r^*\delta_r + (\gamma W^* + 1)\mu_x) < 0, \tag{52}$$

$$\begin{aligned} \overline{b} = {} & -\beta M_s^*\left(-a(1 - \omega_s)\lambda_x - \omega_s\sigma_s + \sigma_s + \mu_{ys}\right) \\ & - W^*(1 - \omega_s)k_y(\beta M_s^* + \beta M_r^*\delta_r \\ & + \gamma W^*\mu_x + \mu_x), \end{aligned} \tag{53}$$

$$\overline{c} = \beta M_s^*(1 - \omega_s)\lambda_x > 0, \tag{54}$$

$$\underline{a} = -a\left(\sigma_2 + \mu_{yr}\right)\left(\beta M_s^* + \beta M_r^*\delta_r + (\gamma W^* + 1)\mu_x\right) < 0, \tag{55}$$

$$\begin{aligned} \underline{b} = {} & \beta M_r^*\delta_r\left(a\lambda_x - \sigma_2 - \mu_{yr}\right) - W^*k_y(\beta M_s^* \\ & + \beta M_r^*\delta_r + \gamma W^*\mu_x + \mu_x) - \left(\sigma_2 + \mu_{yr}\right) \\ & \cdot (\beta M_s^* + \gamma W^*\mu_x + \mu_x), \end{aligned} \tag{56}$$

$$\underline{c} = \beta M_r^*\delta_r\lambda_x > 0, \tag{57}$$

$$\begin{aligned} G_s^* &= \frac{b_1 + \sqrt{b_1^2 - 4a_1c_1}}{-2a_1}, \\ G_r^* &= \frac{b_2 + \sqrt{b_2^2 - 4a_2c_2}}{-2a_2}, \end{aligned} \tag{58}$$

$$\begin{aligned} a_1 &= -a\left(\eta + \mu_{g1} + \Psi_2\right) < 0, \\ b_1 &= a\sigma_1Y_s^* - W^*k_g - \eta - \mu_{g1} - \Psi_2, \\ c_1 &= \sigma_1Y_s^* > 0, \end{aligned} \tag{59}$$

$$\begin{aligned} a_2 &= -a\mu_{g2} < 0, \\ b_2 &= aG_1\Psi_2 + a\sigma_2Y_r^* - W^*k_g - \mu_{g2}, \\ c_2 &= G_1\Psi_2 + \sigma_2Y_r^* > 0, \end{aligned} \tag{60}$$

$$\begin{aligned} M_s^* &= \frac{b_3 + \sqrt{b_3^2 - 4a_3c_3}}{-2a_3}, \\ M_r^* &= \frac{b_4 + \sqrt{b_4^2 - 4a_4c_4}}{-2a_4}, \end{aligned} \tag{61}$$

$$a_3 = -\left(a\beta M_r^* \delta_r (\zeta + \mu_{ms} + \Psi_1) + a\gamma W^* \mu_{ms}\mu_x + a\mu_{ms}\mu_x + a\beta P(1-\alpha_s)\mu_{ys}Y_s^* + \Psi_1 (a(\gamma W^* + 1)\mu_x + \beta) + a\gamma\zeta W^* \mu_x + a\beta\lambda_x + a\zeta\mu_x + \beta\zeta + \beta W^* k_m + \beta\mu_{ms}\right), \tag{62}$$

$$b_3 = -\beta M_r^* \delta_r \left(a(\alpha_s - 1)PY_s^* \mu_{ys} + \zeta + W^* k_m + \mu_{ms} + \Psi_1\right) - (\alpha_s - 1)\beta PY_s^* \mu_{ys} - \beta\lambda_x - (\gamma W^* + 1)\mu_x (a(\alpha_s - 1)PY_s^* \mu_{ys} + \zeta + W^* k_m + \mu_{ms} + \Psi_1), \tag{63}$$

$$c_3 = P(1-\alpha_s)Y_s^* \mu_{ys} (\beta M_r^* \delta_r + (\gamma W^* + 1)\mu_x) > 0, \tag{64}$$

$$a_4 = -(a\beta M_s^* (\Psi_1 \delta_r + \mu_{mr}) + \mu_{mr}(a(\gamma W^* + 1)\mu_x + \beta\delta_r) + a(1-\alpha_r)\beta PY_2 \delta_r \mu_{y2} + \beta W^* k_m \delta_r), \tag{65}$$

$$b_4 = a\beta M_s^{*2}\Psi_1 + M_s^* (-\beta(a\delta_r\lambda_x + \mu_{mr}) + a(1-\alpha_r)\beta PY_2\mu_{y2} + \Psi_1 (a(\gamma W^* + 1)\mu_x + \beta\delta_r)) + (1-\alpha_r)PY_2\mu_{y2} \cdot (a(\gamma W^* + 1)\mu_x + \beta\delta_r) - W^* k_m (\beta M_s^* + (\gamma W^* + 1)\mu_x) - \mu_{mr}(\gamma W^* + 1)\mu_x, \tag{66}$$

$$c_4 = \beta M_s^{*2}\Psi_1 + M_s^* ((1-\alpha_r)\beta PY_2\mu_{y2} + \beta\delta_r\lambda_x + \Psi_1 (\gamma W^* + 1)\mu_x) + (1-\alpha_r)PY_2 (\gamma W^* + 1)\mu_x\mu_{y2} > 0, \tag{67}$$

$$W^* = \frac{\Delta}{\mu_w \Delta - \left(h_g (G_s^* + G_r^*) + h_m (M_s^* + M_r^*) + h_y (Y_s^* + Y_r^*)\right)}, \tag{68}$$

where $\Delta = (e_g + G_s^* + G_r^*)(e_m + M_s^* + M_r^*)(e_y + Y_s^* + Y_r^*)$.

Using Descartes' "Rule of Signs" [66], it is evident that irrespective of the sign of $\overline{b}$ in (53), $\underline{b}$ in (56), b_1 in (59), b_2 in (60), b_3 in (63), and b_4 in (66), the state variables $Y_s^*, Y_r^*, M_s^*, M_r^*, G_s^*$, and G_r^* can only have one real positive solution. This shows that the model system (7)–(14) has a unique parasite-persistent equilibrium point $\mathbb{E}_1$.

3.5. Stability of the Coexistence of Parasite-Persistent Equilibrium Point. Here, we shall prove that the coexistence of parasite-persistent equilibrium $\mathbb{E}_1$ is locally asymptotically stable when $R_E > 1$ (or when $R_s > 1$ and $R_r > 1$). We shall follow the methodology by Esteva and Vargus presented in [67], which is based on the Krasnoselskii technique [68]. This methodology requires that we prove that the linearization of system (7)–(14) about the coexistence of parasite-persistent equilibrium does not have a solution of the form

$$\overline{S}(t) = \overline{S}_0 e^{\xi t}, \tag{69}$$

where $\overline{S}_0 = (S_1, S_2, \ldots, S_7)$, $(S_i, \xi) \in \mathbb{C}$, and the real part of ξ is nonnegative ($\mathrm{Re}(\xi) \geq 0$). Note that $\mathbb{C}$ is a set of complex numbers.

Next, we substitute a solution of the form (69) into the linearized system (7)–(14) about the coexistence of parasite-persistent equilibrium. We obtain

$$\begin{aligned}
\xi S_1 &= -\left(\frac{\beta M_s}{1+\gamma W} + \frac{k_y W}{1+\gamma W} + \frac{\mu_{ys}}{1-\omega_s} + \sigma_s\right) S_1 \\
&\quad - \frac{\beta M_s}{1+\gamma W} S_2 + \frac{\beta (C^* - Y_s - Y_r)}{1+\gamma W} S_3, \\
\xi S_2 &= -\frac{\delta_r \beta M_r}{1+\gamma W} S_1 - \left(\frac{\delta_r \beta M_r}{1+\gamma W} + \frac{k_y W}{1+aY_r} + \mu_{yr} + \sigma_r\right) S_2 \\
&\quad + \frac{\delta_r \beta (C^* - Y_s - Y_r)}{1+\gamma W} S_4, \\
\xi S_3 &= -\left(\frac{\beta M_s}{1+\gamma W} + P(1-\alpha_s)\mu_{ys}\right) S_1 + \frac{\beta M_s}{1+\gamma W} S_2 \\
&\quad - \left(\frac{k_m W}{1+aM_s} + \frac{\beta (C^* - Y_s - Y_r)}{1+\gamma W} + k_1\right) S_3, \\
\xi S_4 &= \Psi_1 S_3 + \left(\frac{\delta_r \beta M_r}{1+\gamma W} + P(1-\alpha_r)\mu_{yr}\right) S_2 \\
&\quad - \left(\frac{\delta_r \beta (C^* - Y_s - Y_r)}{1+\gamma W} + \frac{k_m W}{1+aM_r} + \mu_{mr}\right) S_4 + \frac{\delta_r \beta M_r}{1+\gamma W} S_1, \\
\xi S_5 &= \sigma_s S_1 - \left(\frac{k_g W}{1+aG_s} + k_2\right) S_5, \\
\xi S_6 &= \sigma_r S_2 + \Psi_2 S_4 - \left(\frac{k_g W}{1+aG_r} + \mu_{gr}\right) S_5, \\
\xi S_7 &= \lambda + \left(\frac{h_g (G_s + G_r)}{G_s + G_r + e_g} + \frac{h_y (Y_s + Y_r)}{Y_s + Y_r + e_y} + \frac{h_m (M_s + M_r)}{M_s + M_r + e_m}\right) S_7 \\
&\quad - \mu_w S_7,
\end{aligned} \tag{70}$$

where $(C^* - Y_s - Y_r) = X$, $k_1 = (\Psi_1 + \mu_{ms} + \zeta)$, and $k_2 = (\Psi_2 + \mu_{gs} + \eta)$.

Upon simplifying the equations in (70), we obtain

$$\begin{aligned}
\left[1 + \frac{(1+\gamma W)(1+aY_s)(1-\omega_s)}{\Delta_1}\xi\right]S_1 &= \frac{(1+\gamma W)(1+aY_s)(1-\omega_s)}{\Delta_1}\left(-\frac{\beta M_s}{1+\gamma W}S_2 + \frac{\beta(C^* - Y_s - Y_r)}{1+\gamma W}S_3\right),\\
\left[1 + \frac{\xi(1+\gamma W)(1+aY_r)}{\Delta_2}\right]S_2 &= \frac{(1+\gamma W)(1+aY_r)}{\Delta_2}\left(-\frac{\delta_r\beta M_r}{1+\gamma W}S_1 + \frac{\delta_r\beta(C^* - Y_s - Y_r)}{1+\gamma W}S_4\right),\\
\left[1 + \frac{(1+\gamma W)(1+aM_s)}{\Delta_3}\xi\right]S_3 &= \frac{(1+\gamma W)(1+aM_s)}{\Delta_3}\left(\frac{\beta M_s}{1+\gamma W} + P(1-\alpha_s)\mu_{ys}S_1 + \frac{\beta M_s}{1+\gamma W}S_2\right),\\
\left[1 + \frac{\xi(1+\gamma W)(1+aM_r)}{\Delta_4}\right]S_4 &= \frac{(1+\gamma W)(1+aM_r)}{\Delta_4}\left(\Psi_1 S_3 + \left(\frac{\delta_r\beta M_r}{1+\gamma W} + P(1-\alpha_r)\mu_{yr}\right)S_2 + \frac{\delta_r\beta M_r}{1+\gamma W}S_4\right),\\
\left[1 + \frac{(1+aG_s)}{k_g W + k_2}\xi\right]S_5 &= \frac{\sigma_s(1+aG_s)}{k_g W + k_2}S_1,\\
\left[1 + \frac{(1+aG_r)}{k_g W + \mu_{gr}}\xi\right]S_6 &= \frac{(1+aG_r)}{k_g W + \mu_{gr}}\{\sigma_r S_2 + \Psi_2 S_4\},\\
\left[1 + \frac{1}{\mu_w}\xi\right]S_7 &= \frac{\lambda_w}{\mu_w} + \frac{W}{\mu_w}\left(\frac{h_g(S_5+S_6)}{G_s+G_r+e_g} + \frac{h_y(S_1+S_2)}{Y_s+Y_r+e_y} + \frac{h_m(S_3+S_4)}{M_s+M_r+e_m}\right),
\end{aligned} \tag{71}$$

where

$$\begin{aligned}
\Delta_1 &= \beta M_s(1+aY_s)(1-\omega_s) + k_y W(1-\omega_s)(1+\gamma W)\\
&\quad + \mu_{ys}(1+aY_s)(1+\gamma W) + \sigma_s(1+aY_s)\\
&\quad (1-\omega_s)(1+\gamma W),\\
\Delta_2 &= \delta_r\beta M_r(1+aY_r) + k_y W(1+\gamma W)\\
&\quad + (\mu_{yr} + \sigma_r)(1+aY_r)(1+\gamma W),\\
\Delta_3 &= (1+aM_s)(\beta(C^* - Y_s - Y_r)) + k_m W(1+\gamma W)\\
&\quad + k_1(1+aM_s)(1+\gamma W),\\
\Delta_4 &= (1+aM_r)(\delta_r\beta(C^* - Y_s - Y_r))\\
&\quad + k_m W(1+\gamma W) + \mu_{mr}(1+aM_r)(1+\gamma W).
\end{aligned} \tag{72}$$

Separating the negative terms, we obtain the following system:

$$\left[1 + F_j(\xi)\right]S_j = (H\overline{S})_j, \quad \text{for } j = 1, 2, \ldots, 7, \tag{73}$$

where

$$\left.\begin{aligned}
F_1(\xi) &= \frac{(1+\gamma W)(1+aY_s)(1-\omega_s)}{\Delta_1}\xi,\\
F_2(\xi) &= \frac{\xi(1+\gamma W)(1+aY_r)}{\Delta_2},\\
F_3(\xi) &= \frac{(1+\gamma W)(1+aM_s)}{\Delta_3}\xi,\\
F_4(\xi) &= \frac{\xi(1+\gamma W)(1+aM_r)}{\Delta_4},\\
F_5(\xi) &= \frac{(1+aG_s)}{k_g W + k_2}\xi,\\
F_6(\xi) &= \frac{(1+aG_r)}{k_g W + \mu_{gr}}\xi,\\
F_7(\xi) &= \frac{1}{\mu_w}\xi,
\end{aligned}\right\} \tag{74}$$

with

$$H = \begin{pmatrix} 0 & 0 & \dfrac{\beta C^*}{1+\gamma w} & 0 & 0\ 0\ 0 \\ 0 & 0 & 0 & \dfrac{\delta_r \beta C^*}{1+\gamma W} & 0\ 0\ 0 \\ P(1-\alpha_s)\mu_{ys} & 0 & \dfrac{\beta C^*}{1+\gamma W} + k_1 & 0 & 0\ 0\ 0 \\ 0 & P(1-\alpha_r)\mu_{yr} & \Psi_1 & 0 & 0\ 0\ 0 \\ \sigma_s & 0 & 0 & 0 & 0\ 0\ 0 \\ 0 & \sigma_r & 0 & 0 & 0\ 0\ 0 \\ 0 & 0 & \lambda_w & 0 & 0\ 0\ 0 \end{pmatrix}. \tag{75}$$

Note that $X^* = C^* - Y_s^* - Y_r^*$ and all the elements in the square matrix H are nonnegative. The coordinates of $\mathbb{E}_1$ are all positive, and the j^{th} coordinate of the vector $H(\overline{S})$ is described by the notation $H(\overline{S})_j$ for $j = 1, \ldots, 7$. Additionally, the equilibrium $\mathbb{E}_1 = (Y_s^*, Y_r^*, M_s^*, M_r^*, G_s^*, G_r^*, W^*)$ satisfies $\mathbb{E}_1 = H\mathbb{E}_1$. If we assume, for example, that system (73) has a solution of the form $\overline{S}$, then there exists a small positive real number ϵ, such that $|\overline{S}| \le \epsilon \mathbb{E}_1$, where $|\overline{S}| = (|S_1|, |S_2|, \ldots, |S_7|)$. Note also that $|.|$ is a norm in the field of complex numbers.

Next, we show that $\mathrm{Re}(\xi) < 0$. To do so, we apply proof by contradiction. We let $\xi = 0$ and $\xi \neq 0$. For the case when $\xi = 0$, the determinant (∇) of (70) is given by

$$\nabla = \frac{\nu_5 \nu_6 \mu_w \left\{\nu_2 \nu_4 (\gamma\lambda_x + \mu_w)\mu_x + P\beta(1-\alpha_r)\lambda_x \mu_w \mu_{yr}\right\}\left\{\nu_1 \nu_3 (\gamma\lambda_x + \mu_w)\mu_x + P\beta(1-\alpha_s)\lambda_x \mu_w \mu_{ys}\right\}}{(\gamma\lambda_x + \mu_w)^2 \mu_x^2}, \tag{76}$$

where the positive terms $\nu_1, \ldots, \nu_6$ are as defined in matrix (29).

It is clear that the above determinant is nonnegative $(\nabla > 0)$. Consequently, the system (70) can only have the trivial solution $\overline{S} = (0, 0, 0, 0, 0, 0, \lambda_w/\mu_w)$. On the contrary, for $\xi \neq 0$, we assume $\mathrm{Re}(\xi) \ge 0$ and define $F(\xi) = \min|1 + F_j(\xi)|$, $j = 1, 2, \ldots, 7$. This implies that $F(\xi) > 1$ and $\epsilon/F(\xi) < \epsilon$. The minimality of ϵ means that $|\overline{S}| > \epsilon/F(\xi)\mathbb{E}_1$. While considering the nonnegativity property of H, if we assume the norms on the two sides of (73), we shall have

$$F(\xi)|\overline{S}| \le H|\overline{S}| \le \varepsilon H \mathbb{E}_1 = \varepsilon \mathbb{E}_1. \tag{77}$$

This implies that $|\overline{S}| \le \epsilon/F(\xi)\mathbb{E}_1 \le \epsilon\mathbb{E}_1$, which is a contradiction. Therefore, $\mathrm{Re}(\xi) < 0$ and $\mathbb{E}_1$ is locally asymptotically stable when $R_E > 1$.

4. Numerical Simulations

4.1. Boundary Equilibrium Points. In this section, we show by means of numerical simulation the existence and stability of a positive parasite-persistent equilibrium point that involves only one of the parasite strains under study.

4.1.1. Drug-Sensitive-Only Persistent Equilibrium Point E_s. This is an equilibrium point where only the drug-sensitive parasite strains are present in the infected human host. That is, the populations $Y_r = M_r = G_r = 0$. This steady state is only feasible if no resistant parasites emerge from infected red blood cells and the use of antimalarial treatment does not lead to resistance development; that is, $\Psi_1 = \Psi_2 = 0$. The original model (7)–(14) is thus reduced to

$$\left.\begin{aligned} \frac{dX}{dt} &= \lambda_x - \mu_x X - \frac{\beta X M_s}{1+\gamma W}, \\ \frac{dY_s}{dt} &= \frac{\beta X M_s}{1+\gamma W} - \frac{k_y Y_s W}{1+aY_s} - \frac{1}{1-\omega_s}\mu_{ys} Y_s - \sigma_s Y_s, \\ \frac{dM_s}{dt} &= (1-\alpha_s) P \mu_{ys} Y_s - \frac{\beta M_s X}{1+\gamma W} - \frac{k_m M_s W}{1+aM_s} - (\mu_{ms} + \zeta) M_s, \\ \frac{dG_s}{dt} &= \sigma_s Y_s - \frac{k_g W G_s}{1+aG_s} - (\mu_{gs} + \eta) G_s, \\ \frac{dW}{dt} &= \lambda_w + \left\{\frac{h_g(G_s)}{G_s + e_g} + \frac{h_y(Y_s)}{Y_s + e_y} + \frac{h_m(M_s)}{M_s + e_m}\right\} W - \mu_w W. \end{aligned}\right\} \tag{78}$$

Numerically, this equilibrium point is illustrated, as shown in Figure 2.

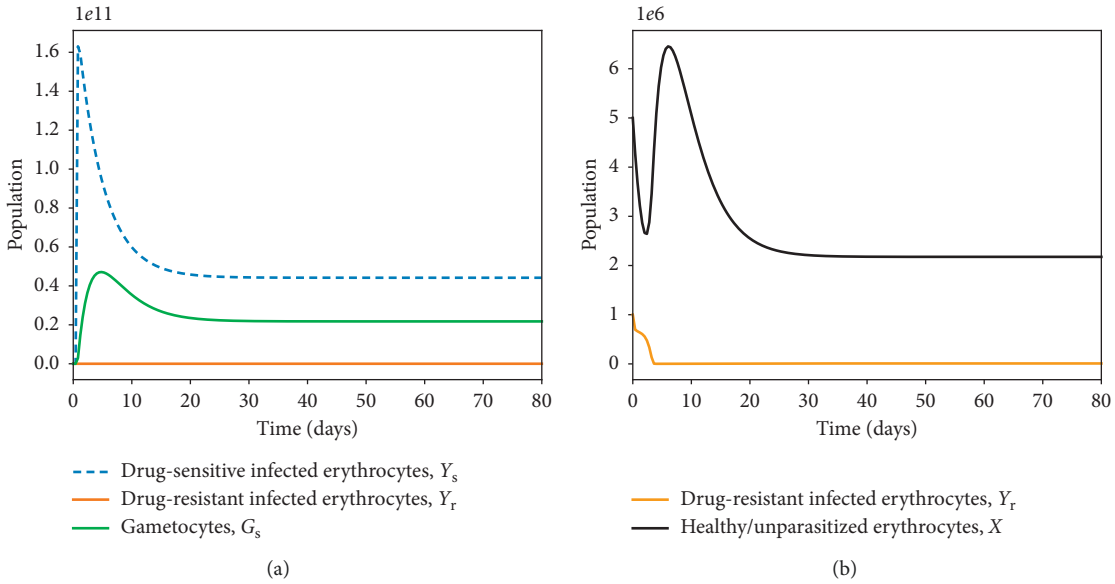

Figure 2: Simulations of model system (11)–(18) showing the existence of drug-sensitive-only equilibrium point. All parameter values are as presented in Table 3.

4.1.2. Drug-Resistant-Only Persistent Equilibrium Point E_r. In this case, the population of the drug-sensitive parasite strains declines to zero as the density of the resistant strains grows and stabilizes at an optimal population size. This is also illustrated numerically, as shown in Figure 3.

4.2. Within-Host Competition between Parasite Strains. We investigate the competitive exclusion principle by simulating the model system (7)–(14) under different values of the threshold quantities R_s and R_r in (31). Model (7)–(14) is simulated so that $R_s = 4.022$ and $R_r = 0.3131$, and we achieve a convergence to the drug-sensitive-only endemic equilibrium point E_s, as shown in Figure 4(a). Again, using the parameter values in Table 3 with $\Psi_1 = 0.9$ and ($R_s = 0.022$, $R_r = 3.0098$), the solutions of Y_s and Y_r converge to the drug-resistant-only endemic equilibrium point E_r (Figure 4(b)).

Provided that both R_s and R_r are greater than 1 (as shown in Figure 4(c)), the parasite-infected red blood cells remain persistent in the host. This implies that the merozoites (both drug-sensitive and drug-resistant) continue to multiply in the absence of antimalarial therapy, $\omega_s = 0$, or in the presence of ineffective antimalarial drugs. Similar results are observed in the dynamics of merozoites (M_s and M_r), as shown in Figure 5. It should be noted that the dominant merozoite strains are likely to drive the infection under these conditions. As the density of one strain increases, the population of the other strain is likely to decrease due to a phenomenon known as competitive exclusion principle. The most fit parasite strain survives as the weaker competitor dies out, as shown in Figure 5(a). Both drug-sensitive and drug-resistant merozoites would remain persistent if poor-quality antimalarial drugs are administered to *P. falciparum* malaria patients. Thus, in the absence of efficacious antimalarial drugs like ACTs with the potential to eradicate resistant merozoites, we are likely to experience an exponential growth in the density of drug-resistant merozoites, as displayed in Figure 5(b). This may lead to severe malaria and eventual death of the patient.

The bifurcation analysis of both scenarios is presented in Figure 6 (with and without competition between the parasite strains). When there is competition between the parasite strains, as shown in Figure 6(a), we observe that the strain with a higher threshold quantity R_0 would exclude the other strain. A decrease in the population of the drug-sensitive strain would pave way for a surge in the population of the drug-resistant strains, and vice versa. This is despite the fact that some drug-resistant strains emerge from the drug-sensitive strains as a result of mutation [77]. In Figure 6(b), we observe coexistence of the strains that do not compete with each other. Like the resistance strains, the sensitive strains are only present when their threshold quantity, R_s, is greater than unity. Both strains are however present when $R_r > 1$ and $R_s > 1$. Additionally, when $R_r < 1$ and $R_s < 1$, we arrive at the parasite-free equilibrium (PFE) point, as shown in Figures 6(a) and 6(b).

4.3. Antimalarial Drug Effects and Parasite Clearance. The effects of antimalarial drug treatment are monitored by establishing first and foremost that

$$\frac{\partial R_s}{\partial \omega_s} = -\frac{\beta\mu_1\mu_2 P(1-\alpha_s)\mu_w\lambda_x}{(1-\omega_s)^2\mu_x(\gamma\lambda_w+\mu_w)\left(\left(k_y\lambda_w/\mu_w\right)+\left(\mu_2/(1-\omega_1)\right)+\sigma_s\right)^2\left(\zeta+\left(k_m\lambda_w/\mu_w\right)+\mu_{ms}+\left(\beta\lambda_x\mu_x^2/(\gamma\lambda_w+\mu_w)\right)+\Psi_1\right)} < 0. \tag{79}$$

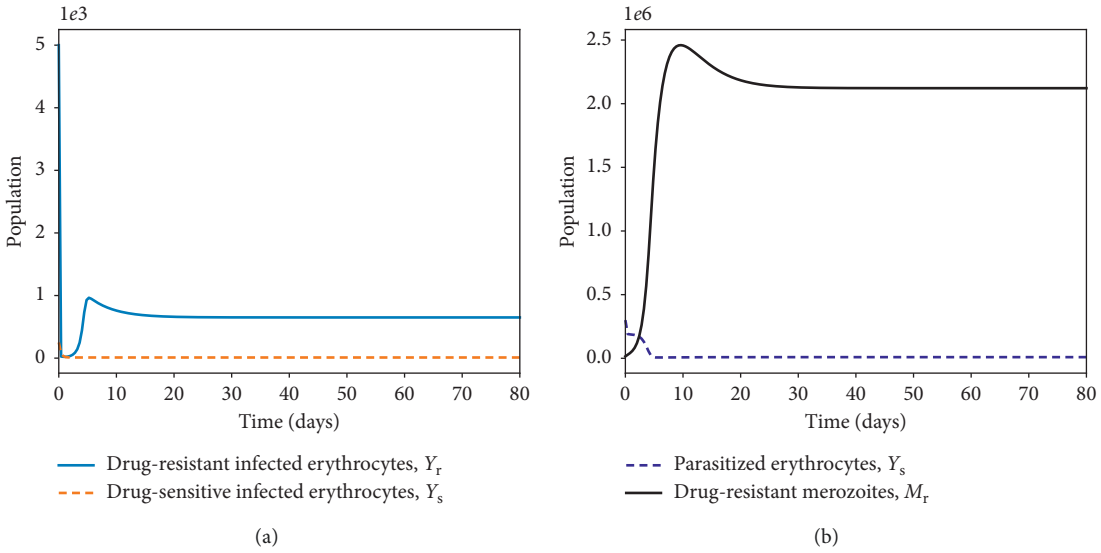

FIGURE 3: Simulations of model system (11)–(18) showing the existence of drug-resistant-only equilibrium point. All parameter values are as presented in Table 3.

Thus, R_s is a decreasing function of ω_s (the efficacy of the antimalarial drug used). Therefore, using a highly efficient antimalarial drug could lead to a scenario where $R_s < 1$ and $R_r < 1$ (disease-free state shown in Figure 7(c)). In Figure 7(a), model system (7)–(14) is simulated by varying the efficacy of the antimalarial drug ω_s and other model parameters chosen such that $R_r = 3.221$ and $R_s = 2.221$. The higher the efficacy of the used antimalarial, the lower the density of infected erythrocytes. Thus, governments and ministry of health officers should only roll out or permit the administration of antimalarials or ACTs that can eradicate (totally) both the drug-resistant and the drug-sensitive strains of *P. falciparum* parasites.

The rate of development of resistance by the drug-sensitive merozoites, Ψ_1, is shown to have very minimal impact on the dynamics of infected red blood cells Y_r as long as $R_s > 1$ and $R_r > 1$ (Figure 7(b)). Nevertheless, analytical results indicate that the higher the rate of development of resistance, the lower the severity of future malaria infections. This is presented as

$$\frac{\partial R_s}{\partial \Psi_1} = -\frac{\beta\mu_1 P(1-\alpha_s)\mu_w\lambda_x}{\mu_x(\gamma\lambda_w+\mu_w)\left(\left(k_y\lambda_w/\mu_w\right)+\left(\mu_2/(1-\omega_1)\right)+\sigma_s\right)\left(\zeta+\left(k_m\lambda_w/\mu_w\right)+\mu_{ms}+\left(\beta\lambda_x\mu_x^2/(\gamma\lambda_w+\mu_w)\right)+\Psi_1\right)^2} < 0. \tag{80}$$

Other parameters that have direct negative impacts on the progression of malaria infection are the efficacy of the immune effectors, γ, and the rate of therapeutic elimination of drug-sensitive merozoites, ζ:

$$\frac{\partial R_s}{\partial \zeta} = -\frac{\beta\mu_1 P(1-\alpha_s)\mu_w\lambda_x}{\mu_x(\gamma\lambda_w+\mu_w)\left(\left(k_y\lambda_w/\mu_w\right)+\left(\mu_2/(1-\omega_1)\right)+\sigma_s\right)\left(\zeta+\left(k_m\lambda_w/\mu_w\right)+\mu_{ms}+\left(\beta\lambda_x\mu_x^2/(\gamma\lambda_w+\mu_w)\right)+\Psi_1\right)^2} < 0, \tag{81}$$

$$\frac{\partial R_r}{\partial \gamma} = -\frac{\beta\mu_2 P(1-\alpha_r)\delta_r\lambda_w\mu_w^3\lambda_x\left(k_m\lambda_w+\mu_{mr}\mu_w\right)}{\mu_x\left(k_y\lambda_w+\mu_w\left(\mu_2+\sigma_r\right)\right)\left((\gamma\lambda_w+\mu_w)\left(k_m\lambda_w+\mu_{mr}\mu_w\right)+\beta\delta_r\mu_w\lambda_x\mu_x^2\right)^2} < 0. \tag{82}$$

Further simulations based on contour plots (see [78] for theory on contour plots) are used to ascertain the relational effects of selected pairs of model parameters on the disease threshold quantities R_s and R_r. In Figure 8(a), both β and μ_w increase the reproduction number due to drug-sensitive *P. falciparum* parasite strains. A direct relationship exists between the two parameters: the higher the decay rate of the immune cells, the higher the rate of infection of healthy erythrocytes.

In Figure 8(b), we observe the least increase in R_s with respect to an increase in ω_s relative to μ_{ys}. Antimalarial therapy is shown to be very effective in reducing the severity of *P. falciparum* infection. Conversely, the number of merozoites produced per dying blood schizont, P, is shown in Figure 8(c) to have a very high positive impact on R_s and hence on the severity of malaria infection due to drug-sensitive parasite strains. Clinical control should target and

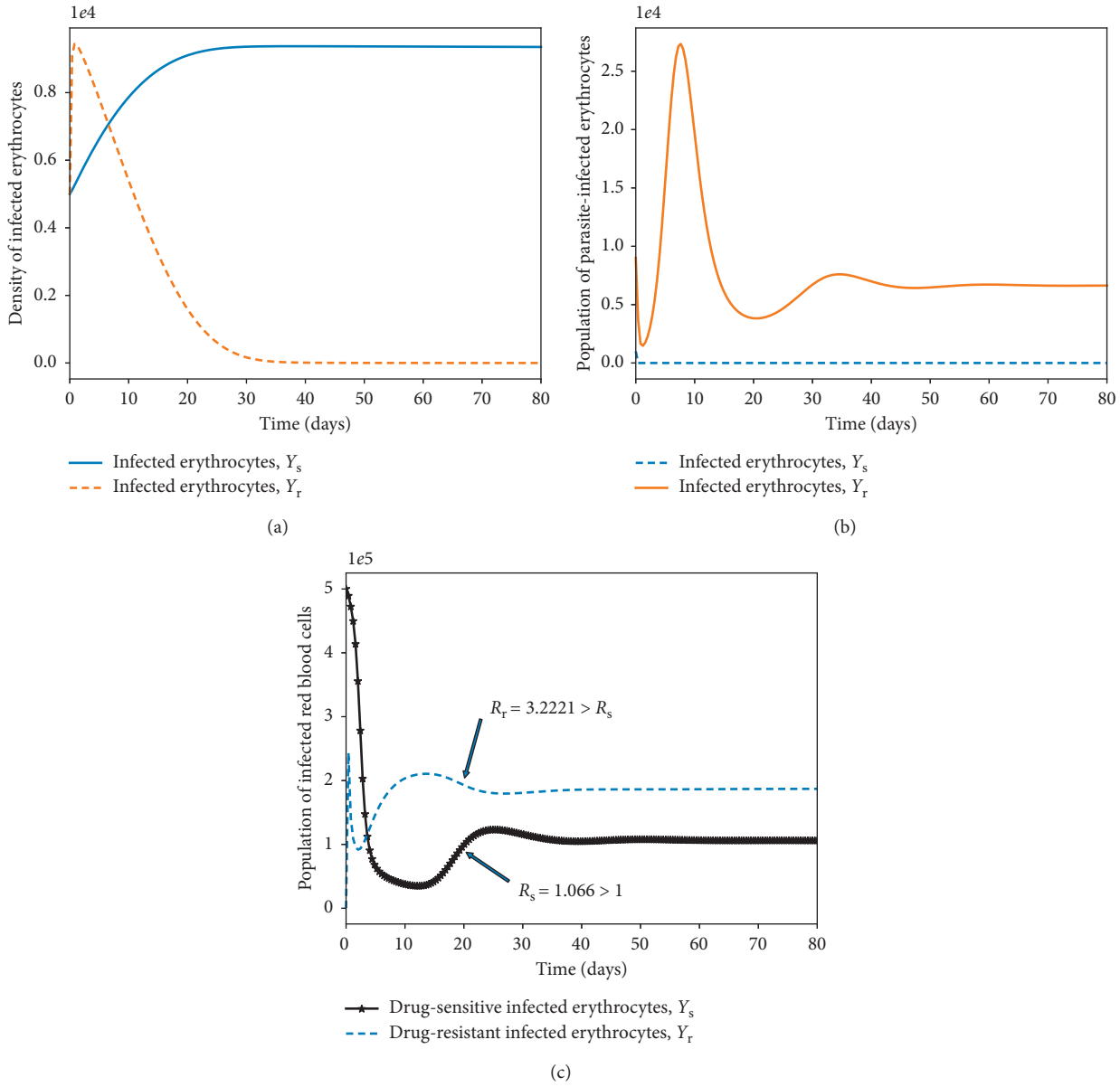

FIGURE 4: Simulations of model system (11)–(18). The figures show the dynamics of drug-sensitive and drug-resistant infected red blood cells under different conditions of the threshold values R_s and R_r. In Figure 4a, $R_s > R_r$. In Figure 4b, $R_r > R_s$, $\Psi_1 = 0$ and all other parameter values are as presented in Table 3.

eradicate infected red blood cells to diminish the erythrocytic cycles of infections.

We observe in Figure 9(b) that the rate at which merozoites develop resistance due to treatment failure has no resultant effects on the rate of formation of gametocytes that undergo sexual reproduction within the mosquito vector. The higher the value of R_r, the higher the cost of resistance, as shown in Figure 9(a). The higher the density of drug-resistant parasite strains, the higher the level of resistance and hence the cost of disease control. Unfortunately, highly effective antimalarial drugs (such as ACTs) that can eradicate both parasite strains are slightly expensive in several *P. falciparum* malaria-endemic regions [79]. Like the parameter P, the parasite infection rate β is shown to have a direct positive effect on the threshold quantity R_r (Figure 9(c)) due to drug-resistant parasite strains. Effective antimalarials should hence target new cell infections and eliminate recrudescence (by killing already infected erythrocytes).

5. Effects of Multiple-Strain Infection and Fitness Cost on Parasite Clearance

Numerous studies [27, 80] have suggested the negative impacts of drug resistance on the fitness and ability of the parasite to dominate the *P. falciparum* infection. Resistance to antimalarial drugs imposes fitness cost on the drug-resistant parasite. The drug-resistant parasite strains are thought to

Table 3: Baseline values and range for parameters of model (11)–(18).

Parameter	Value	Range	Units	Source
λ_x	3×10^3	$(3 \times 10^3 - 3 \times 10^8)$	Cells/μl^{-1}/day	[69]
λ_w	30	(10–40)	Cells/μl/day	[70]
ω_s	0.5	(0-1)	Unitless	Assumed
α_s	0.4	(0.1–1)	Unitless	Assumed
α_r	0.2	(0.01–1)	Unitless	Assumed
e_g, e_m, e_y	10^4	$(10^3–10^5)$	Unitless	[71]
μ_x	1/120	(0.05–0.1)	day^{-1}	[72]
μ_{ys}	0.5	(0.3–0.8)	day^{-1}	[73]
μ_{yr}	0.3	(0.3–0.8)	day^{-1}	Assumed
μ_{ms}, μ_{mr}	48	(46–50)	day^{-1}	[69]
μ_{gs}, μ_{gr}	0.0625	(0.05–0.1)	day^{-1}	[74]
μ_w	0.05	(0.02–0.08)	day^{-1}	[74]
δ_r	0.7	(0.01–0.99)	Unitless	Assumed
ζ, η	0.5	(0-1)	day^{-1}	[73]
P	16	(15–20)	Erythrocytes/day	[34]
β	6.5×10^{-7}	4.8×10^{-7}–6.8×10^{-7}	Merozoites/day	[75]
σ_r, σ_s	0.02	(0.01–0.03)	day^{-1}	[75]
h_y, h_m, h_g	0.05	(0.01–0.08)	mm^{-3}/day	[70]
k_y, k_m, k_g	0.000001	(0.001–0.9)	day^{-1}	[51]
Ψ_1	0.2	(0.01–2.2)	day^{-1}	Assumed
Ψ_2	0.01	(0.001–0.1)	day^{-1}	Assumed
δ_r	0.3	(0-1)	Unitless	Assumed
γ	0.5	(0-1)	Immune cell/μl	Assumed
$1/a$	0.2	(0-1)	Unitless	[76]

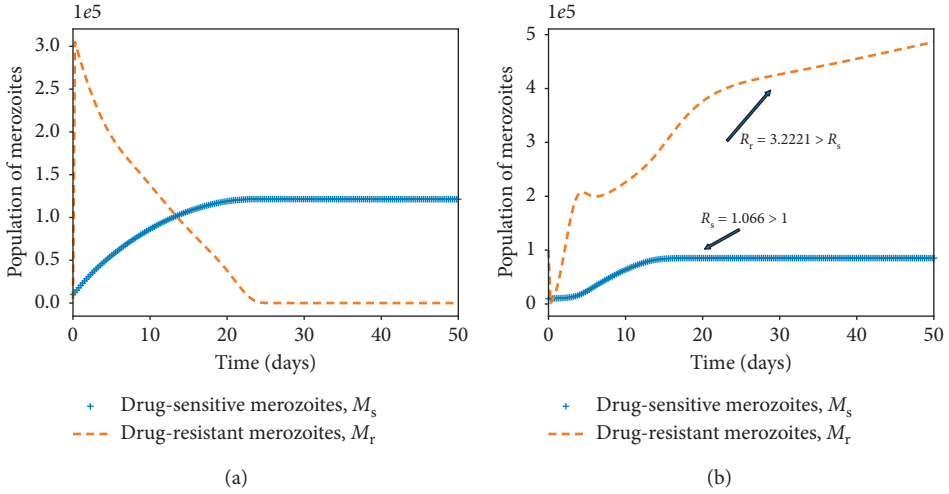

Figure 5: Simulations of model system (11)–(18). The figures show the dynamics of the merozoites under different conditions of the threshold values R_s and R_r. Competitive exclusion among the parasite strains is shown in (a). In (b), both parasite strains coexists and $R_r > R_s$, $\Psi_1 = 0$. Other parameter values are available in Table 3.

experience impaired growth within the human host [29]. The cost of resistance is further exacerbated due to the competition between parasite strains within an infected human host. In Figure 10(a), the area under the curve for the drug-resistant strain or the number of infected erythrocytes is lower than that of the drug-sensitive strains. However, in a multiple-strain infection (Figure 10(b)), the area difference is much bigger. This implies that competition between the parasite strains within the human host could result in elimination of one of the parasite strains provided that both R_s and R_r are less than unity.

The presence of multiple strains of *P. falciparum* parasites is likely to complicate and worsen the severity of malaria disease infection in humans. Figures 11 and 12 show the simulated model (7)–(14) for single- and multiple-strain infections, in the absence of preexisting immunity and antimalarial drugs. The persistence of gametocytes in Figures 11(b) and 12(b) is consistent with the actual observations of human malaria infection in the absence of antimalarial therapy [81]. Acquired immunity is shown in Figure 11(c) to increase and eventually level-off at higher levels to contain future infections.

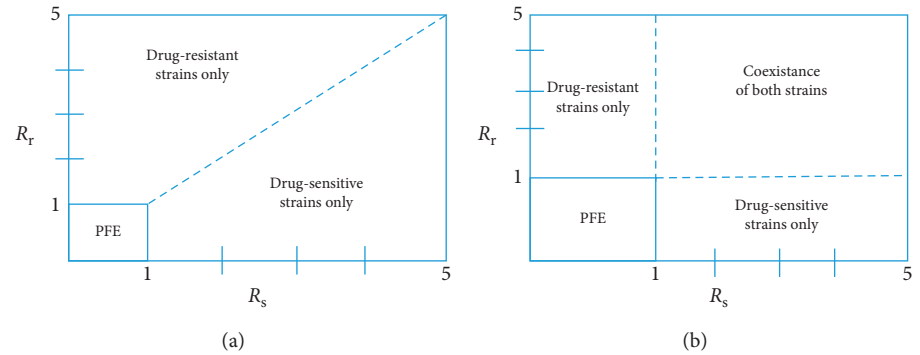

FIGURE 6: Bifurcation diagrams showing competitive exclusion (a) and coexistence equilibrium (b) for the drug-sensitive and drug-resistant *P. falciparum* parasite strains under different values of threshold quantities R_s and R_r. Both parasite strains coexists when $R_s > 1$ and $R_r > 1$ (see part (b)).

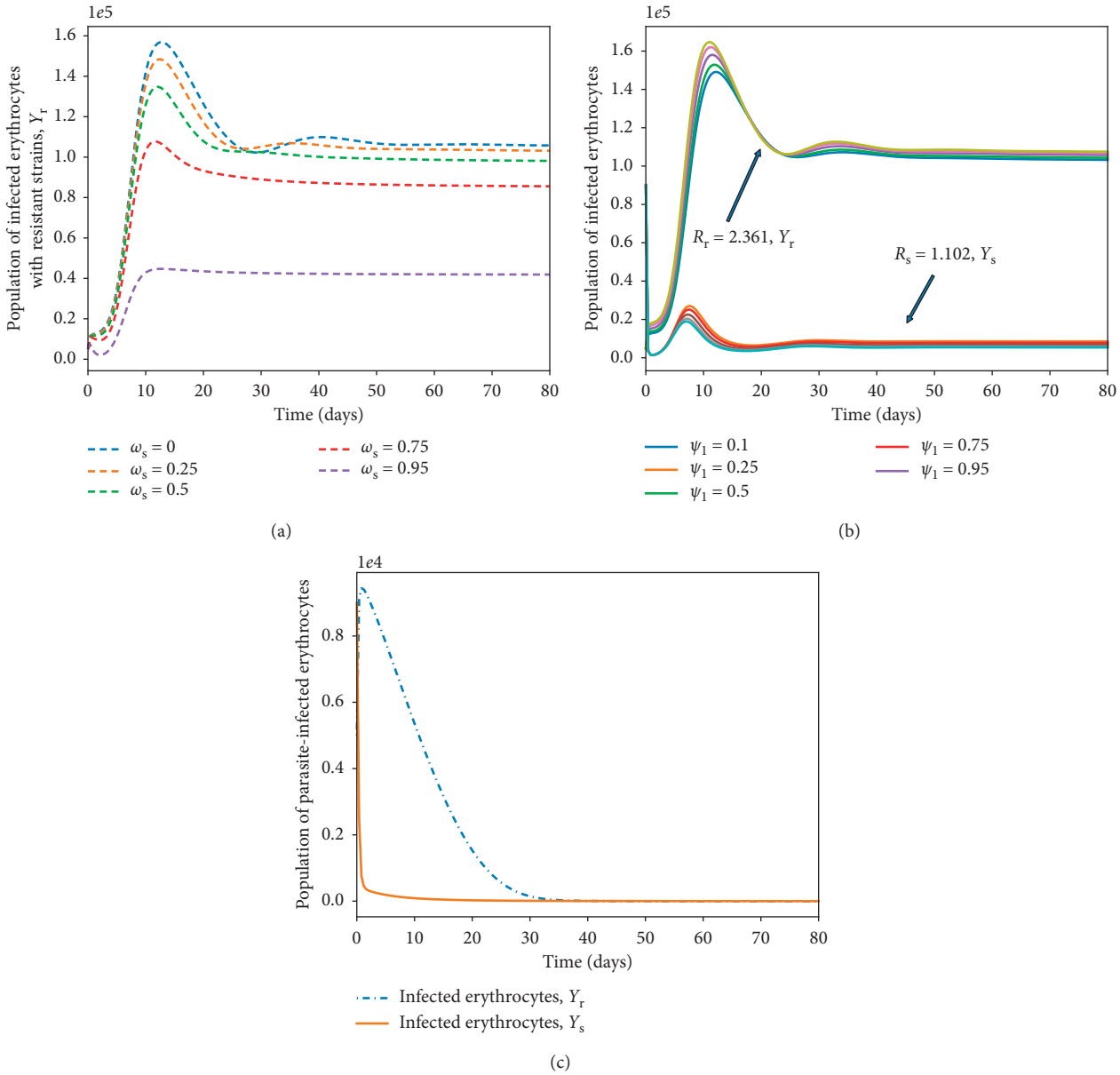

FIGURE 7: The effect of varying the efficacy of antimalarial drug used ω_s and the rate of development of resistance by the drug-sensitive merozoites Ψ_1, on the density of infected erythrocytes (Y_s, Y_r). The value of ω_s ranges from 0 to 1. The rest of the parameter values are available in Table 3. Figure (c) shows that in the absence of highly effective ACTs, drug-resistant parasite would take a longer time to eradicate.

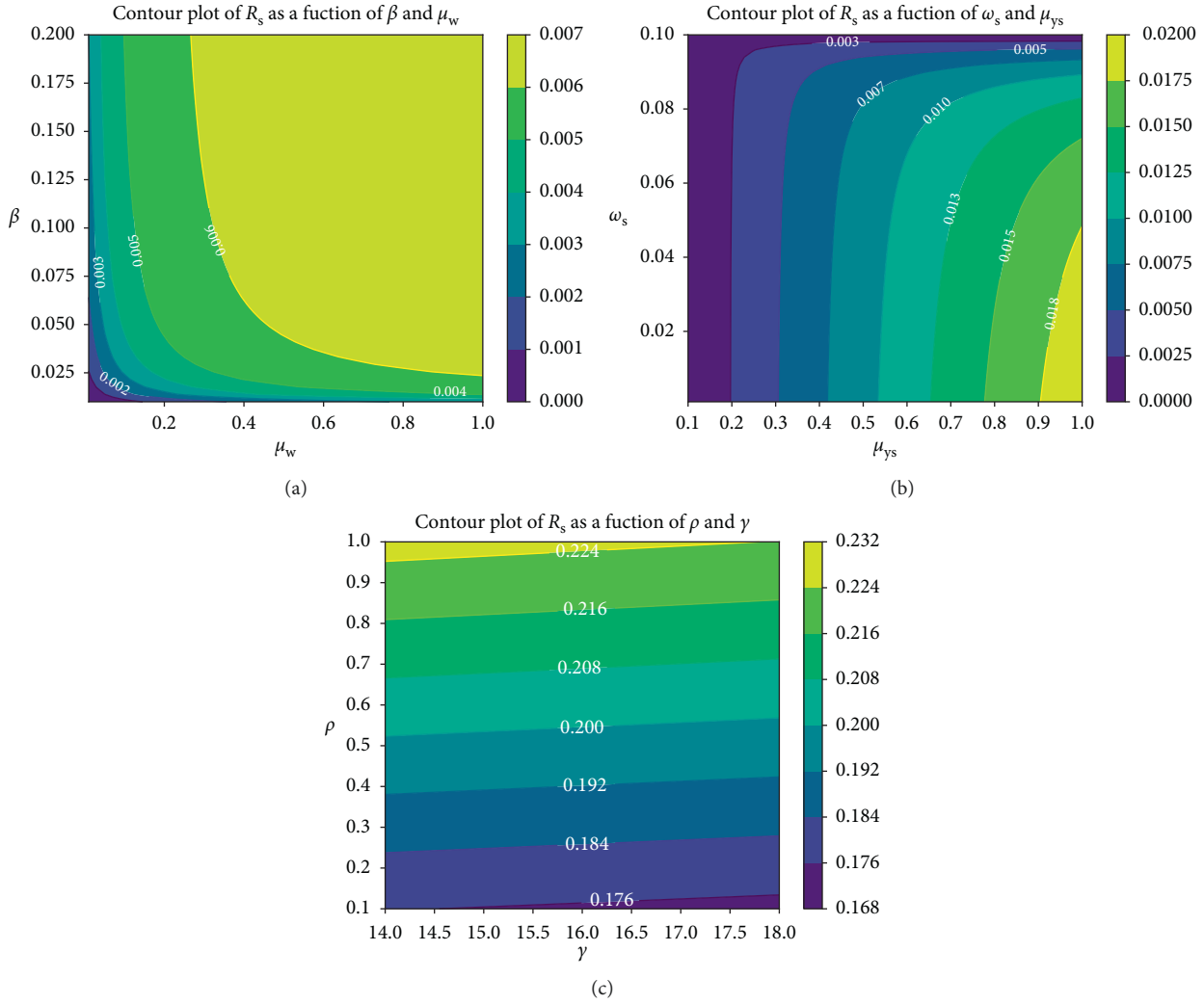

FIGURE 8: Contour plot of R_s as a function of (a) β and μ_w, (b) ω_s and μ_{ys}, (c) P and γ.

Although the aspect of timing is key in these multiple-strain infections, we assumed here that the two strains are introduced at the same time. In the long run, it is evident in Figures 10 and 12 that the sensitive strain overtakes the resistant strain. We argue that this could be as a result of strain-specific adaptive responses that symmetrically affect the sensitive parasites.

Unlike single-strain *P. falciparum* parasite infections, data on multiple-strain infections are not readily available. Nevertheless, a multiple-strain infection (drug-sensitive and drug-resistant) as presented in this paper is biologically reasonable and consistent with that of *P. Chabaudi* described in [82].

5.1. Sensitivity Analysis. In this paper, the primary model output of interest for the sensitivity analysis is the infected erythrocytes (Y_s, Y_r). However, the effective reproduction number R_E is a threshold quantity which represents on overage the number of secondary infected erythrocytes due to merozoite invasions. We can therefore measure the sensitivity indices of the effective reproduction number of model system (7)–(14) relative to model parameters. For example, the sensitivity of R_E relative to the parameter Ψ_1 is given by the following formulation:

$$\Upsilon_{\Psi_1} = \frac{\partial R_E}{\partial \Psi_1} \times \frac{\Psi_1}{R_E}. \tag{83}$$

Using the parameter values in Table 3, the expressions for sensitivity for all the parameters in R_E are evaluated and presented in Table 4. The higher the numerical value of the sensitivity index (S.I), the greater the variational impact of the parameter on the disease progression. A parameter with a negative index decreases the model R_E when they are increased. On the other hand, a parameter with a positive index would generate a proportional increase in R_E when they are magnified. Results shown in Table 4 indicate that the rate of infection of healthy erythrocytes by the merozoites β, the density of merozoites generated from each of the bursting schizonts P, the efficacy of antimalarial drug used ω_s, and the rate at which drug-sensitive merozoites develop resistance Ψ_1 are the four most influential parameters, in determining the disease dynamics as presented in model system (7)–(14).

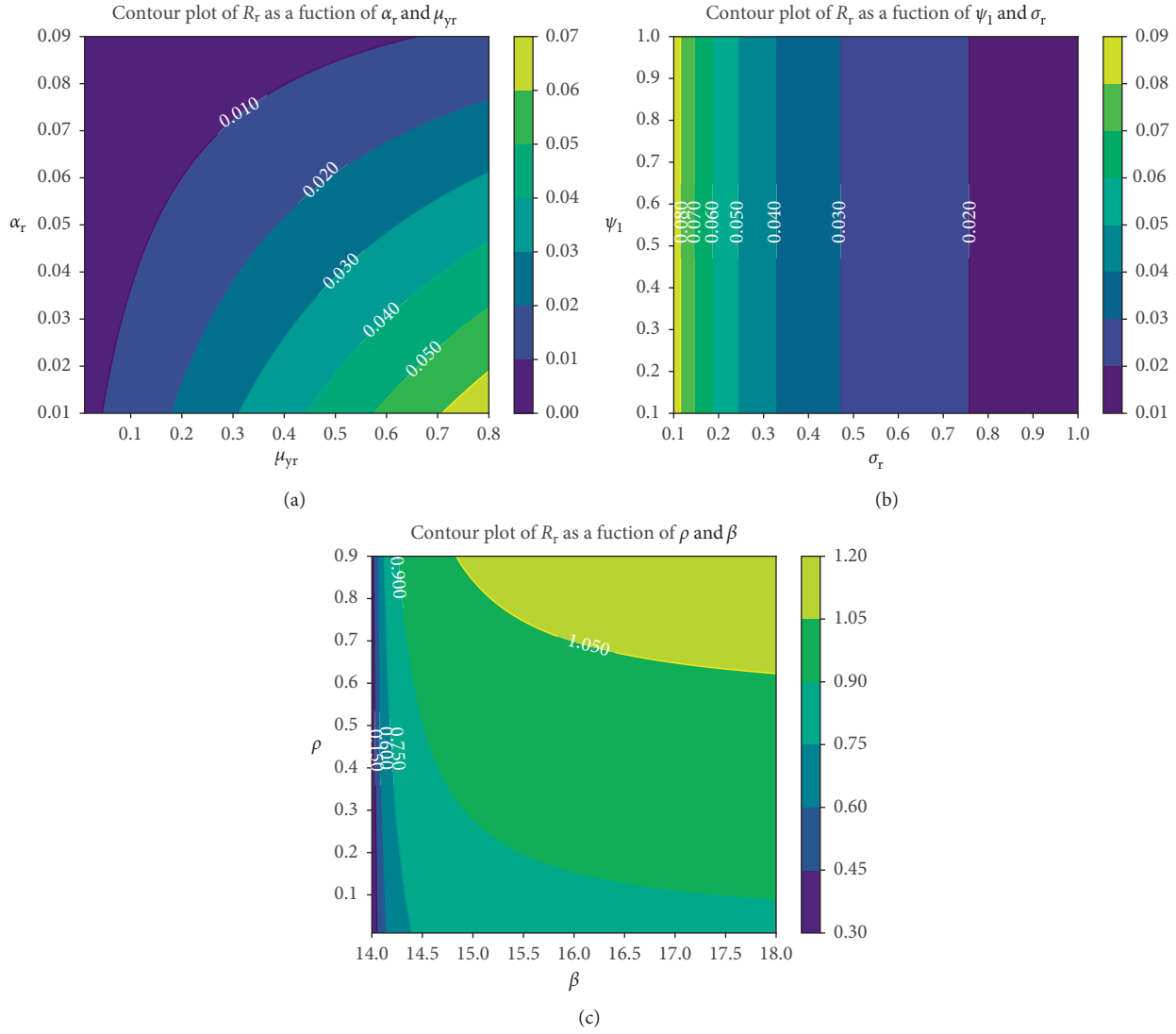

FIGURE 9: Contour plot of R_r as a function of (a) α_r and μ_{yr}, (b) Ψ_1 and σ_r, (c) P and β.

Results from sensitivity analysis emphasize the use of highly efficacious antimalarial drugs such as ACTs in malaria-endemic regions. This would mitigate the many cases of malaria in the region and further help to reduce emerging cases of parasite resistance to existing therapies. Drugs with a higher parasite clearance rate would greatly reduce resistance, which is associated with longer parasite exposure to antimalarial drugs. It is imperative, therefore, that governments and ministry of health personnel in malaria-endemic countries enforce the use of efficient antimalarial drugs that not only cure infected malaria patients but also eliminate the chance of *P. falciparum* parasites to develop resistance to existing therapy.

6. Conclusion

In this paper, a deterministic model of multiple-strain *P. falciparum* malaria infection has been formulated and analysed. The parasite strains are categorized as either drug-sensitive or drug-resistant. The infected erythrocytes and the malaria gametocytes are similarly grouped according to the strain of the parasite responsible for their existence. The immune cells are incorporated to reduce the invasive characteristic of the malaria merozoites. Antimalarial therapy is applied to the model but only targets red blood cells infected with drug-sensitive merozoites. Based on the next-generation matrix method, we computed the effective reproduction number R_E of the formulated model. Based on R_E, it is evident that the success of *P. falciparum* infection in the presence of multiple-parasite strains is directly dependent on the ability of the individual parasite strains to drive the infection. The parasite strain with a higher threshold value, R_0, is likely to dominate the infection. Prescribed antimalarial drugs should therefore be effective enough to eradicate both drug-sensitive and drug-resistant parasite strains in vivo. Linearization of the model at the parasite-free equilibrium reveals the local asymptotic stability of the trivial equilibrium point.

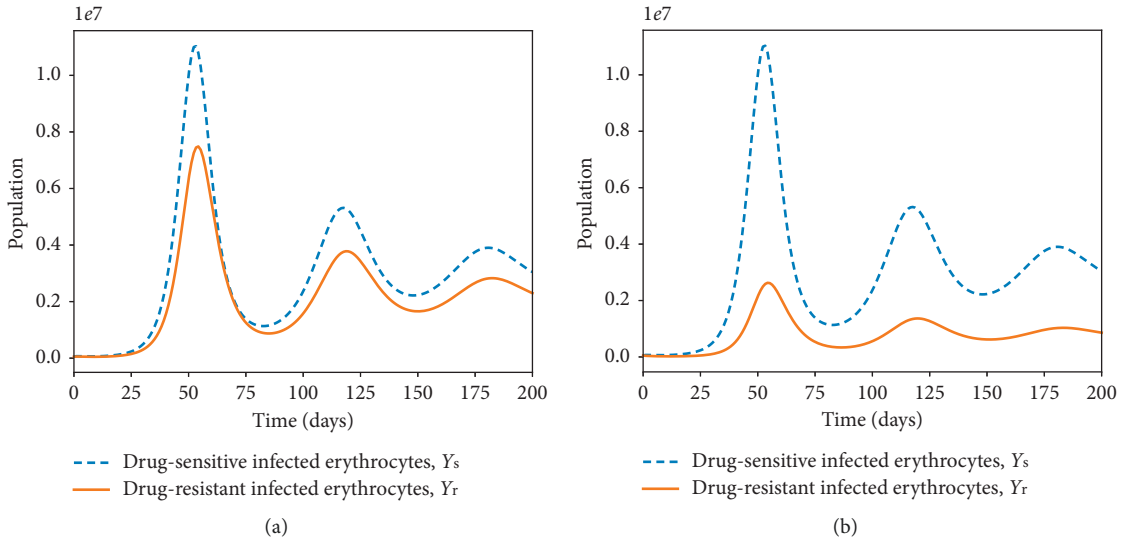

FIGURE 10: Dynamics of drug-sensitive (blue) and drug-resistant (orange) strains in a single infection (a) and in a multiple infection (b) in a naive human-host with no malaria therapy ($\omega_s = 0$). The density of the resistant strain is lower than that of drug-sensitive strain for $R_s = 2.123 > 1$ and $R_r = 1.912 > 1$ in a multiple-strain *P. falciparum* infection. The rest of the parameter values are as displayed in Table 3.

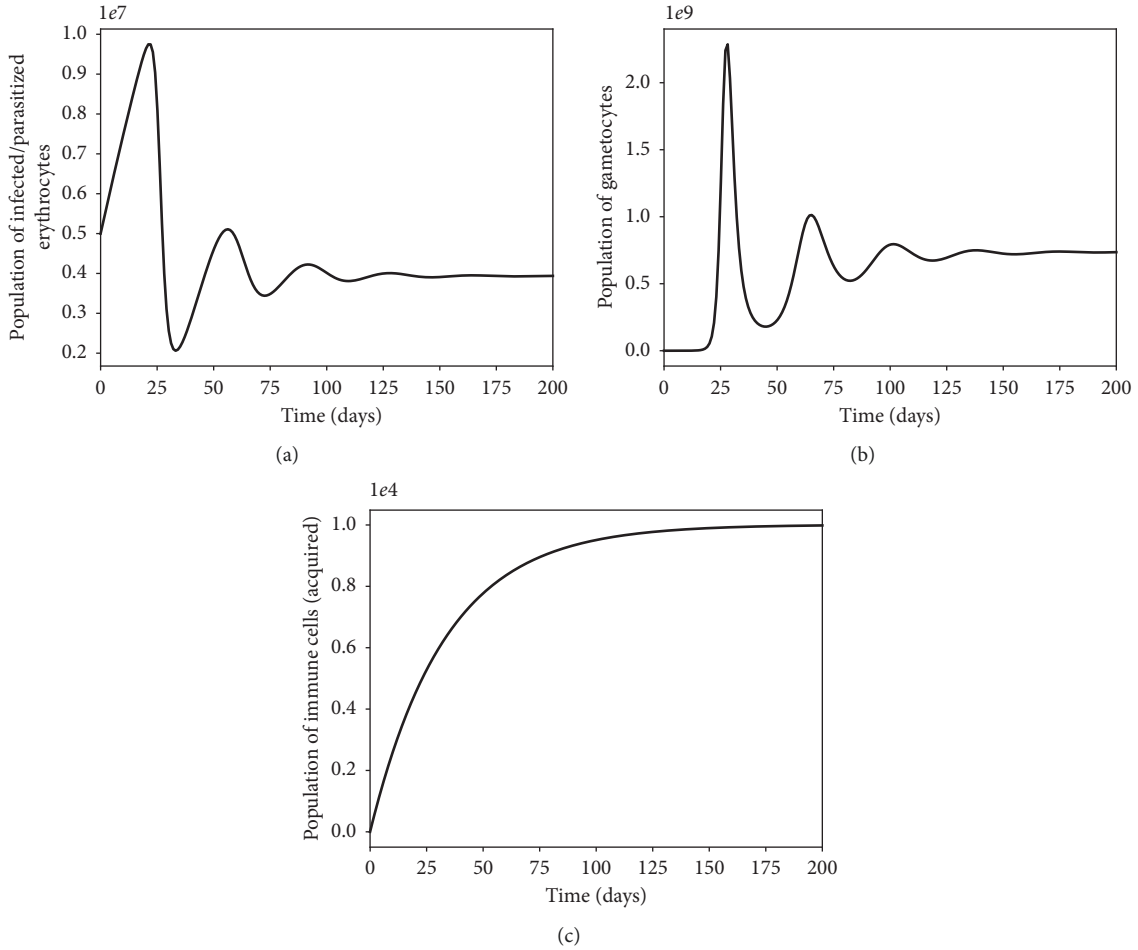

FIGURE 11: Dynamics of infected erythrocytes, gametocytes, and the immune cells with a single-strain *P. falciparum* infection. Here, we do not have preexisting immunity. The rest of the parameter values are as displayed in Table 3.

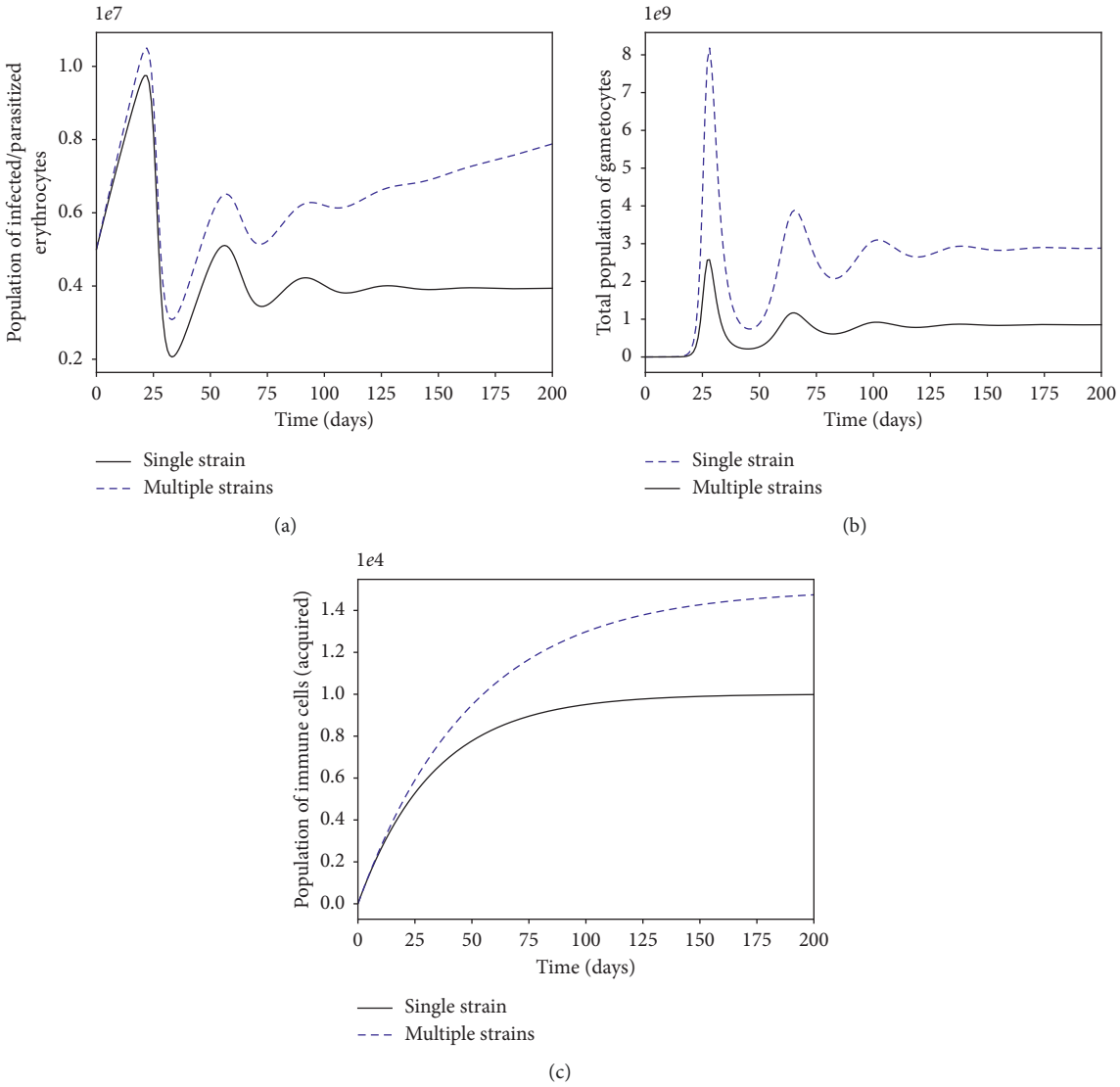

FIGURE 12: Within-human dynamics of single- and multiple-strain dynamics of infected erythrocytes, gametocytes, and the immune cells in the absence preexisting immunity and with no antimalarial treatment ($\omega_s = 0$). The rest of the model parameter values are in Table 3.

By rewriting the model in the pseudotriangular form, the parasite-free equilibrium is also shown to be globally asymptotically stable. Although the parasite-persistent equilibrium exists, its expression based on a single-model variable proved to be mathematically intractable. The use of antimalarial treatment may eradicate one parasite strain so that we arrive at either a drug-sensitive-only persistent equilibrium point or a drug-resistant-only persistent equilibrium point.

To assess the impacts of the different parasite strains to disease dynamics, the model is simulated for different values of the threshold quantities R_s and R_r. We observed that when $R_r > 1$ and $R_s > 1$, then both parasite strains are persistent and the infection becomes severe. If $R_r > 1$ and $R_s < 1$, then the drug-sensitive parasites would decline to zero as the drug-resistant strains continue to multiply and remain persistent, increasing the severity of infections. On the other hand, if $R_s > 1$ and $R_r < 1$, then the drug-resistant parasite strains would be eradicated. Moreover, provided that the threshold quantities R_s and R_r are less than unity, the use of an efficacious antimalarial drug would help eradicate *P. falciparum* infection.

The efficacy of antimalarial drug is shown to have direct negative impact on the density of infected red blood cells. The higher the efficacy of administered antimalarial drug, the lower the population of infective merozoites and the smaller the density of infected erythrocytes. This ensures prompt recovery from malaria infections. This result is consistent with that in [72, 83]. The efficacy of antimalarial drug is however shown to have least effect on the population of drug-resistant infected erythrocytes. The rate of development of resistance by drug-sensitive parasites is also shown to drive the infection due to resistant parasite strains. Using contour plots and results from sensitivity analysis, we observe that the efficacy of antimalarial drug used ω_s, the density of blood floating merozoites produced per infected

Table 4: Sensitivity indices of R_E relative to the model parameters.

Parameter	S.I
β	+0.9988
P	+1.0000
ω_s	−0.87513
λ_x	+0.7199
μ_x	−0.0016
k_y	−0.02701
σ_s	−0.7619
γ	−0.3333
μ_{mr}	−0.433
μ_{ms}	−0.52123
μ_{yr}	−0.232
Ψ_1	−0.77534
μ_{ys}	−0.492
λ_w	−0.3471
ζ	−0.0041
δ_r	+0.0023
k_m	−0.0020
σ_r	−0.541872
α_r	−0.1111
α_s	−0.09891
μ_w	0.3716

erythrocyte P, the rate of development of resistance Ψ_1, and the rate of infection by merozoites β are the most important parameters in the disease dynamics and control.

Finally, although the drug-resistant strain is shown to be less fit, the presence of both strains in the human host has a huge impact on the cost and success of antimalarial treatment. To reduce the emergence of resistant strains, it is vital that only effective antimalarial drugs are administered to patients in hospitals, especially in malaria-endemic regions. To improve malaria therapy and reduce cases of parasite resistance to existing therapy, our results call for regular and strict surveillance on antimalarial drugs in clinics and hospitals in malaria-endemic countries.

Data Availability

All data used in this study are included in this published article.

Conflicts of Interest

The authors declare that there are no conflicts of interest regarding the publication of this article.

Authors' Contributions

All authors contributed to all sections of this manuscript.

Acknowledgments

The authors are thankful to the anonymous referees for their constructive comments. The authors would also like to thank the Strathmore Institute of Mathematical Sciences for its support in the production of this manuscript. The authors acknowledge with gratitude the financial support from the German Academic Exchange Service (DAAD) (ST32-PKZ: 91711149) and the Kenya National Research Fund (NRF-Kenya) (NRF-Phd Grant Titus O.O), in the production of this manuscript.

References

[1] A. M. Dondorp, S. Yeung, L. White et al., "Artemisinin resistance: current status and scenarios for containment," *Nature Reviews Microbiology*, vol. 8, no. 4, pp. 272–280, 2010.

[2] R. J. Maude, W. Pontavornpinyo, S. Saralamba et al., "The last man standing is the most resistant: eliminating artemisinin-resistant malaria in Cambodia," *Malaria Journal*, vol. 8, no. 1, p. 31, 2009.

[3] A. B. S. Sidhu, D. Verdier-Pinard, and D. A. Fidock, "Chloroquine resistance in plasmodium falciparum malaria parasites conferred by pfcrt mutations," *Science*, vol. 298, no. 5591, pp. 210–213, 2002.

[4] T. E. Wellems and C. V. Plowe, "Chloroquine—resistant malaria," *Journal of Infectious Diseases*, vol. 184, no. 6, pp. 770–776, 2001.

[5] D. L. Smith, E. Y. Klein, F. E. McKenzie, and R. Laxminarayan, "Prospective strategies to delay the evolution of anti-malarial drug resistance: weighing the uncertainty," *Malaria Journal*, vol. 9, no. 217, 2010.

[6] R. W. Snow, J.-F. Trape, and K. Marsh, "The past, present and future of childhood malaria mortality in africa," *TRENDS in Parasitology*, vol. 17, no. 12, pp. 593–597, 2001.

[7] N. J. White, "Delaying antimalarial drug resistance with combination chemotherapy," *Parassitologia*, vol. 41, no. 1–3, pp. 301–308, 1999.

[8] WHO, *A Global Strategy for Malaria Control*, World Health Organization, Geneva, Switzerland, 1993.

[9] Y. Kim and K. A. Schneider, "Evolution of drug resistance in malaria parasite populations," *Nature Education Knowledge*, vol. 4, no. 8, pp. 6–16, 2013.

[10] A. O. Talisuna, P. Bloland, and U. D'Alessandro, "History, dynamics, and public health importance of malaria parasite resistance," *Clinical Microbiology Reviews*, vol. 17, no. 1, pp. 235–254, 2004.

[11] N. J. White and W. Pongtavornpinyo, "The de novo selection of drug-resistant malaria parasites," *Proceedings of the Royal Society of London. Series B: Biological Sciences*, vol. 270, no. 1514, pp. 545–554, 2003.

[12] J.-F. Trape, G. Pison, M.-P. Preziosi et al., "Impact of chloroquine resistance on malaria mortality," *Comptes Rendus de l'Académie des Sciences—Series III—Sciences de la Vie*, vol. 321, no. 8, pp. 689–697, 1998.

[13] WHO, *Guidelines for the Treatment of Malaria*, World Health Organization, Geneva, Switzerland, 2018.

[14] J. K. Baird, M. F. S. Nalim, H. Basri et al., "Survey of resistance to chloroquine by plasmodium vivax in Indonesia," *Transactions of the Royal Society of Tropical Medicine and Hygiene*, vol. 90, no. 4, pp. 409–411, 1996.

[15] P. E. Thompson and W. Leslie, "Antimalarial agents: chemistry and phamacology," in *Medicinal Chemistry*, G. de Stevens, Ed., Academic Press, New York, NY, USA, 1972.

[16] T. Harinasuta, P. Suntharasamai, and C. Viravan, "Chloroquine-resistant falciparum malaria in Thailand," *The Lancet*, vol. 286, no. 7414, pp. 657–660, 1965.

[17] S. Fogh, S. Jepsen, and P. Effersøe, "Chloroquine-resistant plasmodium falciparum malaria in Kenya," *Transactions of the Royal Society of Tropical Medicine and Hygiene*, vol. 73, no. 2, pp. 228-229, 1979.

[18] E. Onori, "The problem of plasmodium falciparum drug resistance in africa south of the sahara," *Bulletin of the World Health Organization*, vol. 62, pp. 55–62, 1984.

[19] J. M. Ekue, A. M. Ulrich, and E. K. Njelesani, "Plasmodium malaria resistant to chloroquine in a Zambian living in Zambia," *BMJ*, vol. 286, no. 6374, pp. 1315-1316, 1983.

[20] D. Overbosch, A. W. van den Wall Bake, P. C Stuiver, and H. J van der Kaay, "Chloroquine-resistant falciparum malaria from Malawi," *Tropical and Geographical Medicine*, vol. 36, no. 1, pp. 71-72, 1984.

[21] W. H. Wernsdorfer and D. Payne, "The dynamics of drug resistance in plasmodium falciparum," *Pharmacology & Therapeutics*, vol. 50, no. 1, pp. 95–121, 1991.

[22] B. L. Bredenkamp, B. L. Sharp, S. D. Mthembu, D. N. Durrheim, and K. I. Barnes, "Failure of sulphadoxine-pyrimethamine in treating plasmodium falciparum malaria in KwaZulu-Natal," *South African Medical Journal=Suid-Afrikaanse tydskrif vir geneeskunde*, vol. 91, no. 11, pp. 970–972, 2001.

[23] P. B. Bloland, E. M. Lackritz, P. N. Kazembe, J. B. O. Were, R. Steketee, and C. C. Campbell, "Beyond chloroquine: implications of drug resistance for evaluating malaria therapy efficacy and treatment policy in africa," *Journal of Infectious Diseases*, vol. 167, no. 4, pp. 932–937, 1993.

[24] S. J. Foote and A. F. Cowman, "The mode of action and the mechanism of resistance to antimalarial drugs," *Acta Tropica*, vol. 56, no. 2-3, pp. 157–171, 1994.

[25] WHO, *Artemisinin and Artemisinin-Based Combination Therapy Resistance. Global Malaria Programme*, World Health Organization, Geneva, Switzerland, 2016.

[26] WHO, *Q & A on Artemisinin Resistance*, World Health Organization, Geneva, Switzerland, 2018.

[27] M. Bushman, L. Morton, N. Duah et al., "Within-host competition and drug resistance in the human malaria parasite plasmodium falciparum," *Proceedings of the Royal Society B: Biological Sciences*, vol. 283, no. 1826, article 20153038, 2016.

[28] W. E. Harrington, T. K. Mutabingwa, A. Muehlenbachs et al., "Competitive facilitation of drug-resistant plasmodium falciparum malaria parasites in pregnant women who receive preventive treatment," *Proceedings of the National Academy of Sciences*, vol. 106, no. 22, pp. 9027–9032, 2009.

[29] M. Bushman, R. Antia, V. Udhayakumar, and J. C. de Roode, "Within-host competition can delay evolution of drug resistance in malaria," *PLoS biology*, vol. 16, no. 8, 2018.

[30] T. Mita, K. Tanabe, and K. Kita, "Spread and evolution of plasmodium falciparum drug resistance," *Parasitology International*, vol. 58, no. 3, pp. 201–209, 2009.

[31] S. Vinayak, M. T. Alam, T. Mixson-Hayden et al., "Origin and evolution of sulfadoxine resistant plasmodium falciparum," *PLoS Pathogens*, vol. 6, no. 3, article e1000830, 2010.

[32] I. M. Hastings and W. M. Watkins, "Intensity of malaria transmission and the evolution of drug resistance," *Acta Tropica*, vol. 94, no. 3, pp. 218–229, 2005.

[33] A. O. Talisuna, P. Langi, T. K. Mutabingwa et al., "Intensity of transmission and spread of gene mutations linked to chloroquine and sulphadoxine-pyrimethamine resistance in falciparum malaria," *International Journal for Parasitology*, vol. 33, no. 10, pp. 1051–1058, 2003.

[34] E. Y. Klein, D. L. Smith, M. F. Boni, and R. Laxminarayan, "Clinically immune hosts as a refuge for drug-sensitive malaria parasites," *Malaria Journal*, vol. 7, no. 67, 2008.

[35] WHO, *World Malaria Report 2017*, World Health Organization, Geneva, Switzerland, 2017.

[36] F. E. McKenzie, "Why model malaria?," *Parasitology Today*, vol. 16, no. 12, pp. 511–516, 2000.

[37] F. E. McKenzie and E. M. Samba, "The role of mathematical modeling in evidence-based malaria control," *American Journal of Tropical Medicine and Hygiene*, vol. 71, pp. 94–96, 2004.

[38] P. G. Coleman, S. Shillcutt, C. Morel, A. J. Mills, and C. Goodman, "A threshold analysis of the cost-effectiveness of artemisinin-based combination therapies in sub-Saharan Africa," *American Journal of Tropical Medicine and Hygiene*, vol. 71, pp. 196–204, 2004.

[39] I. M. Hastings, "A model for the origins and spread of drug-resistant malaria," *Parasitology*, vol. 115, no. 2, pp. 133–141, 1997.

[40] M. J. Mackinnon, "Drug resistance models for malaria," *Acta Tropica*, vol. 94, no. 3, pp. 207–217, 2005.

[41] S. J. Aneke, "Mathematical modelling of drug resistant malaria parasites and vector populations," *Mathematical Methods in the Applied Sciences*, vol. 25, no. 4, pp. 335–346, 2002.

[42] J. Koella and R. Antia, "Epidemiological models for the spread of anti-malarial resistance," *Malaria Journal*, vol. 2, no. 1, p. 3, 2003.

[43] L. Esteva, A. B. Gumel, and C. V. De Leó N, "Qualitative study of transmission dynamics of drug-resistant malaria," *Mathematical and Computer Modelling*, vol. 50, no. 3-4, pp. 611–630, 2009.

[44] E. Y. Klein, D. L. Smith, R. Laxminarayan, and S. Levin, "Superinfection and the evolution of resistance to antimalarial drugs," *Proceedings of the Royal Society B: Biological Sciences*, vol. 279, no. 1743, pp. 3834–3842, 2012.

[45] M. Legros and S. Bonhoeffer, "A combined within-host and between-hosts modelling framework for the evolution of resistance to antimalarial drugs," *Journal of the Royal Society Interface*, vol. 13, no. 117, article 20160148, 2016.

[46] A. R. Wargo, S. Huijben, J. C. De Roode, J. Shepherd, and A. F. Read, "Competitive release and facilitation of drug-resistant parasites after therapeutic chemotherapy in a rodent malaria model," *Proceedings of the National Academy of Sciences*, vol. 104, no. 50, pp. 19914–19919, 2007.

[47] P. A. zur Wiesch, R. Kouyos, J. Engelstädter, R. R. Regoes, and S. Bonhoeffer, "Population biological principles of drug-resistance evolution in infectious diseases," *The Lancet Infectious Diseases*, vol. 11, no. 3, pp. 236–247, 2011.

[48] Z. Agur, D. Abiri, and L. H. Van der Ploeg, "Ordered appearance of antigenic variants of african trypanosomes explained in a mathematical model based on a stochastic switch process and immune-selection against putative switch intermediates," *Proceedings of the National Academy of Sciences*, vol. 86, no. 23, pp. 9626–9630, 1989.

[49] R. Antia, B. R. Levin, and R. M. May, "Within-host population dynamics and the evolution and maintenance of microparasite virulence," *American Naturalist*, vol. 144, no. 3, pp. 457–472, 1994.

[50] L. Cai, N. Tuncer, and M. Martcheva, "How does within-host dynamics affect population-level dynamics? insights from an immuno-epidemiological model of malaria," *Mathematical Methods in the Applied Sciences*, vol. 40, no. 18, pp. 6424–6450, 2017.

[51] C. Chiyaka, W. Garira, and S. Dube, "Modelling immune response and drug therapy in human malaria infection," *Computational and Mathematical Methods in Medicine*, vol. 9, no. 2, pp. 143–163, 2008.

[52] S. Pilyugin and R. Antia, "Modeling immune responses with handling time," *Bulletin of Mathematical Biology*, vol. 62, no. 5, pp. 869–890, 2000.

[53] M. A. Selemani, L. S. Luboobi, and Y. Nkansah-Gyekye, "The in-human host and in-mosquito dynamics of malaria parasites with immune responses," *New Trends in Mathematical Sciences*, vol. 5, no. 3, pp. 182–207, 2017.

[54] J. C. de Roode, R. Culleton, A. S. Bell, and A. F. Read, "Competitive release of drug resistance following drug treatment of mixed plasmodium chabaudi infections," *Malaria Journal*, vol. 3, no. 1, 2004.

[55] R. Hayward, K. J. Saliba, and K. Kirk, "pfmdr1 mutations associated with chloroquine resistance incur a fitness cost in plasmodium falciparum," *Molecular Microbiology*, vol. 55, no. 4, pp. 1285–1295, 2005.

[56] D. L. Doolan, C. Dobano, and J. K. Baird, "Acquired immunity to malaria," *Clinical Microbiology Reviews*, vol. 22, no. 1, pp. 13–36, 2009.

[57] P. Liehl, P. Meireles, I. S. Albuquerque et al., "Innate immunity induced by plasmodium liver infection inhibits malaria reinfections," *Infection and Immunity*, vol. 83, no. 3, pp. 1172–1180, 2015.

[58] N. Villarino and N. W. Schmidt, "CD8+ T cell responses to plasmodium and intracellular parasites," *Current Immunology Reviews*, vol. 9, no. 3, pp. 169–178, 2013.

[59] T. O. Orwa, R. W. Mbogo, and L. S. Luboobi, "Mathematical model for hepatocytic-erythrocytic dynamics of malaria," *International Journal of Mathematics and Mathematical Sciences*, vol. 2018, Article ID 7019868, 18 pages, 2018.

[60] T. O. Orwa, R. W. Mbogo, and L. S. Luboobi, "Mathematical model for the in-host malaria dynamics subject to malaria vaccines," *Letters in Biomathematics*, vol. 5, no. 1, pp. 222–251, 2018.

[61] J. K. Hale, *Ordinary Differential Equations*, John Wiley & Sons, New York, NY, USA, 1969.

[62] P. van den Driessche and J. Watmough, "Reproduction numbers and sub-threshold endemic equilibria for compartmental models of disease transmission," *Mathematical Biosciences*, vol. 180, no. 1-2, pp. 29–48, 2002.

[63] K. S. Vannice, G. V. Brown, B. D. Akanmori, and V. S. Moorthy, "MALVAC 2012 scientific forum: accelerating development of second-generation malaria vaccines," *Malaria Journal*, vol. 11, no. 1, p. 372, 2012.

[64] L. J. Allen, *Introduction to Mathematical Biology*, Pearson/Prentice Hall, Upper Saddle River, NJ, USA, 2007.

[65] J. C. Kamgang and G. Sallet, "Global asymptotic stability for the disease free equilibrium for epidemiological models," *Comptes Rendus Mathematique*, vol. 341, no. 7, pp. 433–438, 2005.

[66] X. Wang, "A simple proof of Descartes's rule of signs," *The American Mathematical Monthly*, vol. 111, no. 6, pp. 525-526, 2004.

[67] L. Esteva and C. Vargas, "Influence of vertical and mechanical transmission on the dynamics of dengue disease," *Mathematical Biosciences*, vol. 167, no. 1, pp. 51–64, 2000.

[68] M. Krasnoselskii, *Positive Solutions of Operator Equations*, Noordhoff, Groningen, Netherlands, 1964.

[69] Y. Li, S. Ruan, and D. Xiao, "The within-host dynamics of malaria infection with immune response," *Mathematical Biosciences and Engineering*, vol. 8, no. 4, pp. 999–1018, 2011.

[70] C. Chiyaka, "Using mathematics to understand malaria infection during erythrocytic stages," *Zimbabwe Journal of Science and Technology*, vol. 5, pp. 1–11, 2010.

[71] C. Colijn and T. Cohen, "How competition governs whether moderate or aggressive treatment minimizes antibiotic resistance," *Elife*, vol. 4, 2015.

[72] R. M. Anderson, C. A. Facer, and D. Rollinson, "Research developments in the study of parasitic infections," *Parasitology*, vol. 99, no. S1, p. S1, 1989.

[73] A. Mohammed, A. Ndaro, A. Kalinga et al., "Trends in chloroquine resistance marker, Pfcrt-K76T mutation ten years after chloroquine withdrawal in Tanzania," *Malaria Journal*, vol. 12, no. 1, p. 415, 2013.

[74] A. Ofosu-Okyere, M. J. Mackinnon, M. P. K. Sowa et al., "Novel plasmodium falciparum clones and rising clone multiplicities are associated with the increase in malaria morbidity in ghanaian children during the transition into the high transmission season," *Parasitology*, vol. 123, no. 2, pp. 113–123, 2001.

[75] B. Hellriegel, "Modelling the immune response to malaria with ecological concepts: short-term behaviour against long-term equilibrium," *Proceedings of the Royal Society of London Series B*, vol. 250, no. 1329, pp. 249–256, 1992.

[76] A. M. Niger and A. B. Gumel, "Immune response and imperfect vaccine in malaria dynamics," *Mathematical Population Studies*, vol. 18, no. 2, pp. 55–86, 2011.

[77] E. A. Ashley, M. Dhorda, R. M. Fairhurst et al., "Spread of artemisinin resistance in plasmodium falciparum malaria," *New England Journal of Medicine*, vol. 371, no. 5, pp. 411–423, 2014.

[78] D. Lane, "Online statistics education: a multimedia course of study," in *Proceedings of the EdMedia: World Conference on Educational Media and Technology*, pp. 1317–1320, Association for the Advancement of Computing in Education (AACE), Rice Univesity, Houston, TX, USA, 2003.

[79] H. Gelband, C. B. Panosian, K. J. Arrow et al., *Saving Lives, Buying Time: Economics of Malaria Drugs in An Age of Resistance*, National Academies Press, Washington, DC, USA, 2004.

[80] H. A. Babiker, I. M. Hastings, and G. Swedberg, "Impaired fitness of drug-resistant malaria parasites: evidence and implication on drug-deployment policies," *Expert Review of Anti-Infective Therapy*, vol. 7, no. 5, pp. 581–593, 2009.

[81] B. Teun, O. Lucy, S. Seif et al., "Revisiting the circulation time of plasmodium falciparum gametocytes: molecular detection methods to estimate the duration of gametocyte carriage and the effect of gametocytocidal drugs," *Malaria Journal*, vol. 2, no. 9, p. 136, 2010.

[82] J. C. de Roode, M. E. H. Helinski, M. A. Anwar, and A. F. Read, "Dynamics of multiple infection and within—host competition in genetically diverse malaria infections," *American Naturalist*, vol. 166, no. 5, pp. 531–542, 2005.

[83] J. A. N. Filipe, E. M. Riley, C. J. Drakeley, C. J. Sutherland, and A. C. Ghani, "Determination of the processes driving the acquisition of immunity to malaria using a mathematical transmission model," *PLoS Computational Biology*, vol. 3, no. 12, p. e255, 2007.